UNIVERSITY OF SOUTHAMPTON

FACULTY OF ENGINEERING AND APPLIED SCIENCE

DEPARTMENT OF CIVIL ENGINEERING

Project Supervisor: Professor P.B. Morice

A STUDY OF TWO-SPAN PRESTRESSED CONCRETE SUSPENSION BRIDGES

by

Mohamed Hesham Abdul Haleem Nowera

THESIS PRESENTED FOR THE DEGREE OF

DOCTOR OF PHILOSOPHY

To my Mother, my Wife MONA
and Children SARAH and OMAR

UNIVERSITY OF SOUTHAMPTON
FACULTY OF ENGINEERING AND APPLIED SCIENCE
DEPARTMENT OF CIVIL ENGINEERING

DOCTOR OF PHILOSOPHY

A STUDY OF TWO-SPAN PRESTRESSED CONCRETE SUSPENSION BRIDGES

by

Mohamed Hesham Abdul Haleem Nowera

ABSTRACT

Prestressed concrete suspension bridges can be regarded as conventional prestressed concrete structures whose main girders are prestressed by cables which have large eccentricities. Alternatively, they are self-anchored suspension bridges with concrete superstructures which are prestressed by the horizontal component of the cable tension applied at their ends. Due to the possible large eccentricities, prestressed concrete suspension bridges can be used for long span crossings.

The aim of this study is to investigate the use of this type of bridge for medium length crossings in the form of a two-span prestressed concrete suspension bridge. Amongst the special problems studied in this thesis is the contribution of changing cable tension, due to live loading, to the stress state of the structure. As this effect can be significant, a new approach is developed which is based upon modifying earlier research carried out by Timoshenko to suit the requirements of prestressed concrete theory. Subsequently, the method is compared with the commonly used Steinman approach which was slightly altered to suit prestressed concrete suspension bridges. This leads to the formulation of a new analysis to describe the various characteristic features of structural behaviour.

Another problem is the influence of grouting the main cable in the regions where it passes within the suspended beam. This is also studied in the thesis as it causes modifications to the standard analysis. An important aspect of the behaviour of prestressed concrete suspension bridges is their mode of failure under excessive live load. A theory is proposed to analyse this condition. In addition, a new approach in prestressing the suspended beams by shortening their suspenders is suggested.

In order to verify the validity of these analyses, two tests have been carried out on model bridges in which measurements were made within both elastic and failure stages of the structure. In one case ungrouted main cable was used and in the other the cable was grouted for a proportion of the span length. The results of these experiments confirmed the applicability of the theories which had been developed and enabled the stresses and deflections to be predicted with acceptable accuracy. The theoretical analysis and the experimental results indicated the advantages which arise from the use of grouted main cables.

Although there was no opportunity to carry out prolonged tests, a theoretical study has been given for the time effects on the prestressing force which might be expected with this form of structure based upon well known concepts in the behaviour of standard prestressed concrete construction. The thesis also comments upon the practical problems of the construction of such bridges and draws attention to the similarities with the commonly used self-anchored suspension bridge system. Various systems of developing the prestressing force are described.

ACKNOWLEGEMENTS

In writing this thesis, I would like to acknowledge the great help given to me by Professor P.B. Morice through his strong support, excellent supervision and continuous encouragement. Also, I would like to express my deepest gratitude to Professor D. Vandepitte of the University of Gent, Belgium, for his constructive criticism and encouraging remarks.

I am especially grateful and indebted to Mr A. Rogerson and Mr M. Wagstaff from the Concrete Laboratory for their help and patience during the experimental stage.

I would also like to acknowledge the moral support given to me by my mother and my wife. Finally, I would like to express my greatest appreciation to Miss Debbie Taylor for her excellent typing of my thesis.

CONTENTS

LIST OF FIGURES

PAGE

LIST OF TABLES

LIST OF PLATES

LIST OF SYMBOLS

A	=	The cross sectional area of the suspended beam.
A_c	=	The cross sectional area of the cable.
A_{s1}, A_{s2}, A_{s3}	=	Areas of steel for the different layers of reinforcement of the cross section of the beam.
A_{su}, A_{sul}	=	The cross sectional area of the suspenders in the left and right hand spans.
A_T	=	The cross sectional area of the tower.
A_1, A_2	=	Constants which define the conditions of failure for the suspended beam.
a	=	The eccentricities at the ends of the main cable from the centre line.
B	=	The section modulus of the suspended beam.
b	=	The breadth of the web of the T-shaped cross section of the beam.
b_1	=	The breadth of the flange of the T-shaped cross section or the breadth of the rectangular cross section of the beam.
C, C_1	=	The slopes at the ends of the free ungrouted part of the cable for grouted suspended beams.
D	=	One of two constants governing the relationship between the initial and final values of the prestressing force as reduced by shrinkage, creep and relaxation of the different parts of the structure.
d, d_1	=	The spacing between the suspenders in left and right hand spans.
E, E_c, E_s, E_{su}, E_T	=	Young's modulus of elasticity for the suspended beam, the cable, the reinforcement of the beam, the suspenders and the tower respectively.
F, F_1	=	The cable slopes at the ends of the beam.
F_c	=	The compressive force in the concrete in the beam cross section at failure.
F_s	=	The sum of the reinforcement forces in the beam cross section at failure.
f, f_1	=	The cable sags in the left and right hand spans.

f_c = The maximum allowable stresses at the top or bottom fibre of the beam.

f_{ult} = The cube strength of the concrete suspended beam.

f_y = The yield stress of the reinforcement.

G = The second constant in the formula governing the relationship between the initial and final values of the prestressing force as reduced by time effects.

g, g_1 = The ratio of the grouted lengths to the span lengths in both left and right hand spans.

H_w = The preliminary value of the prestressing force.

H_i = The initial value of the prestressing force which the cable acquires by the prestressing operation.

H_f = The final magnitude of the prestressing force as reduced by time effects.

H_p = The change in the prestressing forces as a result of the interaction between cable and beam due to the applied live loading.

H = The total magnitude of the prestressing force.

H_1 = The total magnitude of the prestressing force at the time of the formation of the first plastic hinge.

H_2 = The total value of the prestressing force at failure.

h = The height of the tower above the centre line of the suspended beam.

I = The second moment of area of the suspended beam.

i = The total number of the suspenders in the left hand span.

j = The total number of the suspenders in the right hand span.

k_1 = The ratio of the depth of the neutral axis to the effective depth of the cross section of the beam.

k_2 = The ratio of the depth of the point of application of the compressive force in the concrete to the effective depth of the cross section of the beam.

l_{sm}, l_{slm} = The suspenders lengths in the left and right hand spans.

ℓ, ℓ_1 = The lengths of the left and right hand spans.

M_D = The bending moments due to the self-weight of the suspended beam.

M_x, M_{x1} = The bending moments at any position of the left and right hand spans.

$M_{x[n]}, M_{x1[n]}$ = The bending moments at regions number [n] in the left and right hand spans.

m_x, m_{x1} = The bending moments produced by a unit axial force and no live loading.

N_T = The axial force in the tower.

n, n_1 = The ratios of the cable sags to the span lengths in the left and right hand spans.

P, P_1 = Concentrated live loads applied in the left and right hand spans.

$P_{p.h}$ = The concentrated load required to cause the formation of the first plastic hinge.

P_s, P_{s1} = The forces of the suspenders in the left and right hand spans.

P_{ult} = The failure concentrated load.

Q_x, Q_{x1} = The shear forces at any position of the left and right hand spans.

q_c, q_{c1} = The upward forces exerted by the cable, via the suspenders.

q_{smax}, q_{s1max} = The maximum total forces in the suspenders in a distributed load form.

r = The ratio of the distance of the first plastic hinge from one of the end supports to the length of the span at which it forms.

S, S_1 = The total lengths of the cable in the left and right hand spans.

S_f, S_{f1} = The lengths of the free ungrouted parts of the cable in the left and right hand spans.

T, T_1 = The cable tension at the left and right hand span.

t, t_1 = The ratios of the distances between the concentrated live loads and the end supports to the span length where the live load is applied.

V, V_1 = The vertical components of the cable tension for the left and right hand spans at the tower

V_o, V_{o1} = The vertical component of the cable tension at the left and right hand end supports.

W, W_1 = The dead loads of the suspender beam in the left and right hand spans including the self-weight of the cable and suspenders per unit length.

x_m, x_{1m} = The distance between either left or right end support to each suspender in the respective span.

y, y_1 = The cable eccentricities from the centre line of the suspended beam in the left and right hand spans.

Z = The total depth of the suspended beam.

z = The distance between the top fibre and the bottom reinforcement of the suspended beam (the effective depth).

z_1, z_2 = The distances between the line of centroid and both top and bottom fibres of the beam.

z_1 = The ratio of the depth of the upper flange reinforcement to the effective depth of the beam.

z_2 = The ratio of the depth of the bottom flange reinforcement to the effective depth of the beam.

z_3 = The ratio of the flange thickness to the effective depth of the beam.

z_4 = The ratio of the total depth to the effective depth of the beam.

α, β = The distances of the boundaries of a general loading from the left end support when divided by the left hand span length.

α_1, β_1 = The distances of the boundaries of a general loading from the right end support when divided by the right hand span length.

α_c, α_s = The thermal coefficient of expansion for the concrete and steel.

$\Gamma_{bm}, \Gamma_{bn}, \Gamma_c, \Gamma_s, \Gamma_T$ = The gaps between the two cut ends of a severed cable which is generated due to bending moments of the beam, axial stresses in the beam, cable forces, suspenders forces and the tower force respectively when divided by $\left[\frac{H_i \ell}{EI}\right]$.

γ = The factor by which the preliminary prestressing force is increased to overcome the reduction produced by time effects.

Δ	=	The gap between the two cut ends of the imaginary severed cable produced by the live loads.
ΔH_P	=	The increase in the prestressing force after the formation of the first plastic hinge.
Δt	=	The different between the design temperature value, 20^oC, and the ambient temperature.
$\Delta\sigma$ (ΔP)	=	The load required to exceed the first plastic hinge load to cause the failure of the structure.
δ	=	The gap between the two cut ends of the imaginary severed cable produced by the forces in the various parts of the structure as a result of a unit prestressing force.
δ_c	=	The gap produced by the cable force in an ungrouted suspended beam and it represents also the flexibility of the cable.
δ_{cf}	=	The gap produced by the cable force in its free ungrouted part in a grouted suspended beam.
ε_c	=	The strain in the bottom flange fibre of the cross section of the beam.
ε_o	=	The initial plastic strain of the concrete
ε_s	=	The shrinkage strain in the concrete of the suspended beam.
ε_y	=	The yield strain of the reinforcement.
$\varepsilon_{s1}, \varepsilon_{s2}, \varepsilon_{s3}$	=	The strains in the three layers of reinforcement in the cross section of the beam.
η	=	The vertical deflection of the suspended beam (and the cable).
$\theta, \theta_1, \theta_g, \theta_{g1}$	=	Constants.
Λ	=	The ratio by which the suspenders are shortened to produce the initial prestressing force in the cable.
λ	=	The ratio between the length of the right hand span to the left hand span.
μ^2	=	The total prestressing force when divided by the flexural rigidity of the suspended beam.
$\nu, \nu_1, \nu_g, \nu_{g1}$	=	Constants.
ξ	=	The horizontal displacement of the cable.

ρ	=	The ratio of the change in the prestressing force produced by the live loading to the preliminary value of the prestressing force.
σ, σ_1	=	A uniformly distributed load (partial or continuous) which is called a general loading applied in the left or right hand spans.
$\sigma_{p.h}$	=	The load required to form the first plastic hinge.
σ_{ult}	=	The failure load.
τ	=	The factor γ as reduced by the time effects.
ϕ, ϕ_1	=	Constants.
Ψ, Ψ_c, Ψ_s	=	The coefficients by which Young's modulus of elasticity of the concrete, the main cable and the suspender decrease due to creep respectively.
Ω	=	The internal energy stored in the superstructure.
ω	=	The ratio of the dead loads in both right and left hand spans.

CHAPTER 1

1. Introduction

1.1 The Concept of Prestressed Concrete Suspension Bridges

It is well known that large gaps can be bridged by means of prestressed concrete structures. However, the span length of prestressed concrete beams is necessarily limited and the longest span so far constructed is about 114m, (30). The girders are very deep at the supports, about 6m, and the prestressing force needed is thousands of kilonewtons.

For long spans, the dead load is usually larger than the live load, which causes difficulty in keeping the cable within the space limited by the upper and lower fibres of the beam throughout its length. To achieve this, the designer often has to increase the depth of the beam beyond the value which the live load moments require, solely to accommodate the cable, (9) and (13).

However, increasing the depth of the beam can be avoided by simply abandoning the requirement to keep the cable within the beam section or, in other words, the cable will be allowed to exceed the normal upper and lower limits, (31 and 32). As a result of this, it would be possible to increase the range of spans available without the need to increase the beam depth. Moreover, the use of a smaller prestressing force would be possible due to the larger eccentricities and cables will therefore be cheaper. Figure (1.1a) shows a three-span continuous prestressed concrete beam where the cable has descended well below its lower fibre especially in the centre span. As it is essential to transmit the vertical reactions resulting from the cable curvature to the beam, vertical struts would need to be used, as shown in the figure.

Although this scheme appears to be perfectly rational from a theoretical point of view, it would most certainly prove to be impractical for many reasons. Firstly, the required clear height

under the beam would compel the designer to raise its elevation in a way which would rarely be compatible with the topography of the surroundings. Secondly, a complex bracing system would be necessary between cable and beam in order to prevent lateral movement of the highly tensioned cable. It would certainly be difficult to produce a stable system of struts between cable and beam.

These practical disadvantages can be eliminated by means of adding the linear transformation profile shown in Figure (1.1b) to the concordant profile of Figure (1.1a), which is obtained form the dead load bending moments. As a result of this, the cable profile will be transformed so that it ties wholly above the centroidal axis of the suspended beam in the manner shown in Figure (1.1c). This will not alter in any way the cable curvature within each span nor the distribution of prestress for the beam, (8, 10 and 11). Although the cable slopes at both ends of the beam have changed, the magnitude and point of application of the horizontal component of its tension, prestressing force, remains unaffected. The vertical components of the cable tension at the beam ends, although altered, do not contribute to the stress state of the beam as they are directly picked up by the end supports. Furthermore, the vertical forces that the struts transfer from cable to beam remain unchanged since they depend on the cable curvature and the horizontal component of the cable tension.

Naturally, in the process of displacing the cable, what had previously been struts between cable and beam, now become ties, suspenders. Moreover, the cable has now to be supported by columns, towers, above the intermediate supports where its slope changes and the vertical forces become concentrated. Thus, we obtain, in an entirely natural way, a suspended concrete beam which is prestressed by the main cable. This type of bridge can also be regarded as a conventional prestressed concrete bridge whose main beams are prestressed by cables which have large eccentricities, much larger, in fact, than the depth of the main beams themselves.

One can also arrive at the concept of prestressed concrete suspension bridges in another, but equally, natural way. Many self-anchored suspension bridges, with steel stiffening girders, have been constructed over the years, none of which had very long spans, (14 and 29). The reason for this is that due to increasing cable tension, the steel girders need larger cross sections, more than the bending moments alone would require, in order to prevent buckling of the whole span in the horizontal plane as well as local buckling. On the other hand, if the steel girders are replaced by concrete ones, the large compressive force can be employed as a prestressing force. Moreover, as concrete beams are generally designed with massive cross sections, larger than an equivalent steel section, buckling in the horizontal plane or local buckling is always a remote possibility.

1.2 Inherent Advantages of Prestressed Concrete Suspension Bridges with Respect to Alternative Structures

Prestressed concrete suspension bridges have some definite advantages when compared with alternative structures for bridging across the same appropriate gap. The cost of the superstructure for a prestressed concrete suspension bridge is cheaper than that of a conventional prestressed concrete structure due to shallower stiffening girders and a smaller cable which results from the possibility of using large eccentricities for the cable.

Furthermore, the live load moments in a prestressed suspended beam are smaller than those in a prestressed conventional one due to the interaction which takes place between the cable and the beam in the former type. Similarly to ordinary suspension bridges, when the live load deflects the suspended beam, the suspenders force the cable to deflect also, hence to elongate and increases its tension. This means that the cable directly carries part of the live load, thus partly relieving the beam. The importance of this effect increases with the span length as in the suspension bridge built at Merelbeke near Gent, Belgium, with a main span of 56m, the live load moments are reduced by about 10% but in another one, Mariakerke, which was also built near Gent with a main span of 100m, the decrease amounts

to 25%, (31 and 33). It is worth noting that interaction also exists theoretically in conventional prestressed concrete structures, but both the increase of cable tension and its lever arm with respect to the centre line of the beam are so small that the resulting relieving moment is entirely negligible.

If the alternate structure is ordinary steel suspension bridge, a prestressed concrete suspension bridge is more feasible for the following reasons. Firstly, the latter does not need external anchorages to resist the large horizontal tension of the cable like the former. Secondly, the concrete superstructure for our type of bridge is cheaper than the steel one in ordinary suspension bridges as the amount of steel used for the former, including the prestressing steel and suspenders, is considerably less than the latter. Finally, our type of bridge is generally much more rigid than an equivalent steel suspension bridge, provided that the spans are long enough, due to larger cross sections, (36).

The feasibility of our type of bridge increases even further, if a self-anchored steel suspension bridge is proposed. Although the latter does not need external anchorages, it still costs more than the former as it requires considerable amount of additional steel in order to avoid buckling, as mentioned before, and resist the increase in the live load moments due to thrust, (14).

Obviously, in order to decide the preference of a certain type of bridge with respect to others, an accurate cost analysis must be carried out for each one.

1.3 Disadvantage of Prestressed Concrete Suspension Bridges

Due to large eccentricities, prestressed concrete suspension bridges are only suitable for sufficiently long crossings. However, since the concrete superstructure is heavier than that used in ordinary steel suspension bridges, the former will most certainly need larger foundations to carry the vertical loads. This is regarded to be disadvantageous as foundation work is always

considered to be expensive, (32). It is worth noting that this disadvantage is also shared by conventional prestressed concrete structures.

As a result of the aforementioned transformation scheme the vertical components of the cable tension at the ends of the beam will have the tendency of lifting them above their design elevation, Figure (1.1b). This effect can be prevented by means of using weights at these ends exceeding the values of the upward forces. The cheapest solution for this problem was undertaken by employing heavy concrete boxes filled with sand as abutments for the bridge, (32 and 35), (Section 6.3) in order to keep the beam ends at the desired elevation by their sheer weight, Figure (1.2). For the same reason, ties are used to connect the suspended beam with the foundation at the tower position, Figure (6.9). This clearly represents one of the unique features of prestressed concrete suspension bridges and is, indeed, disadvantageous due to the additional costs of constructing these abutments.

Finally, some increased complexity of construction may arise due to the erection of the various parts of the bridge especially the placing of the main cable with the designed eccentricities. Such work requires skilled labour and expert supervision which always proved expensive. However, this disadvantage is also shared by ordinary suspension bridges.

1.4 Range of Application of Prestressed Concrete Suspension Bridges

From the preceeding sections, it is clear that a prestressed concrete suspended beam has some definite advantages over alternative structural systems and it therefore, can provide an economical solution to bridge problems. Three-span prestressed concrete suspension bridges are only feasible for crossings which lie in the range of 90 - 900m according to Vandepitte, (34).

These limitations do not reflect any technical impossibility to exceed the specified limits but derive from economical considerations. For example, it is not feasible to build a three-span prestressed concrete suspension bridge for a total length less than 90ms, as a continuous conventional prestressed concrete bridge would provide the best solution. Moreover, an ordinary steel suspension bridge is more appropriate for spans longer than 900m than our type of bridge due to foundation cost, as mentioned earlier.

Nevertheless, prestressed concrete suspension bridges can be feasible in the range 50 - 150m when using two-span suspended beams, Figure (1.3). The main concept of this type of bridge is, clearly, identical to that of the three-span type and they share the same advantages and disadvantages. However, the two-span type can be used more effciently in the aforementioned range of lengths than the three-span type. For example, if a two-span bridge was constructed at Merelbeke, (32), instead of the present three-span type, it would have certainly been more efficient and economical. As the total length is 92ms, the interaction between cable and beam could have produced about 35% reduction in the live load moments. Moreover, only one pier and tower are required for the two span type as well as a lesser prestressing force, Section (6.5).

1.5 The Main Objectives of this Thesis

Early research was carried out in this topic by the inventor of prestressed concrete suspension bridges, Professor Vandepitte, (29 - 36), of the University of Gent, Belgium. He developed the theory and design procedure for three-span suspension bridges as well as the time effects on the magnitude of its prestressing force. His theory is based on Steinman's approach, (20 and 21), in order to calculate the effect of the live loading on the prestressing force and to evaluate the internal forces of the structure (bending moments, deflections and shear forces). In doing so, the effect of the axial, prestressing, force was ignored, (29).

The first objective of this thesis is to present, in simple terms, an accurate and reliable procedure for the design and analysis of two-span prestressed concrete suspension bridges. In doing so, the effect of the axial, prestressing, force has been included in all stages of the calculations, Chapter 2. Furthermore, Steinman's approach, (20 and 21), has been modified to include this effect as well as to suit two-span bridges. In addition, a new approach to evaluate the change in the prestressing force due to the applied live loading is introduced. It is an expansion of earlier research carried out by Timoshenko, (23 - 28), which has been modified to suit two-span prestressed concrete suspended beams with its accuracy theoretically investigated. Thereafter, a comparison has been carried out to specify the preference of either of the two approaches for accurate application.

Figure (1.3) shows the cable passing through the ends of the suspended beam with the lengths $g\ell$ and $g_1\ell_1$. The second objective of this thesis is to investigate the effect of grouting these lengths on the performance of the structure. In doing so, this effect has been included in the computation for the cable deformations due to various effects, the interaction between cable and beam and the internal forces of the structure, Chapter 3. Thereafter, an approximate method is given to determine the failure loads for both ungrouted and grouted types of structure when a single loading is applied on either of its spans, Chapter 4. During this, an exact method to calculate the ultimate moment of resistance of a general cross section is introduced for both hogging and sagging moments.

The time effects, such as shrinkage, creep and relaxation of the different parts of the structure, on the magnitude of the prestressing force are investigated in Chapter 5. The theory used is similar to that used for three-span bridges, (34), but with the necessary modifications in order to suit two-span prestressed suspended beams. Moreover, the special features of the construction of this type of bridges are described in Chapter 6 as well as a new approach to prestress the suspended beam by shortening its suspenders. The idea behind this approach is inspired by the contribution of the suspenders in forcing the cable to deflect, as a

result of any applied live loading, and to change its tension. Hence, this effect, when controlled, can be used to produce the desired tension in the cable by virtue of geometrical calculations as will be shown in Chapter 6.

Two experiments have been performed in order to check the validity of the design equations in both elastic and plastic stages for ungrouted and grouted test beams, Chapter 7. Furthermore, the aforementioned new technique in prestressing suspended beams by shortening their suspenders has been examined. Each of the two experiments comprises two stages, the first is intended to simulate the service life of the bridge as loads less than half the failure loads have been applied. The second stage has been carried out by applying an increasing load on one of the spans until the failure of the structure. For both stages, the cable tension, deflections and stresses of the test beams were monitored and compared with the calculated ones.

As the analysis throughout the thesis has been introduced in the form of equations, it was necessary to write a computer program, Appendix 28, which is capable of analysing both ungrouted and grouted two-span prestressed concrete suspended beams under any form of loading. The program can also calculate the failure loads of both types of bridge when a single loading is applied on either of their spans.

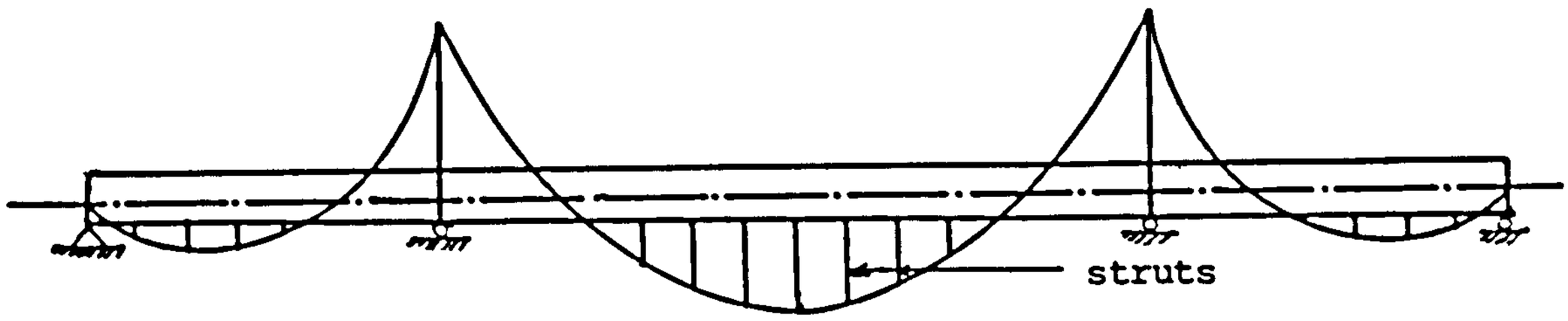

The initial cable eccentricities

(a)

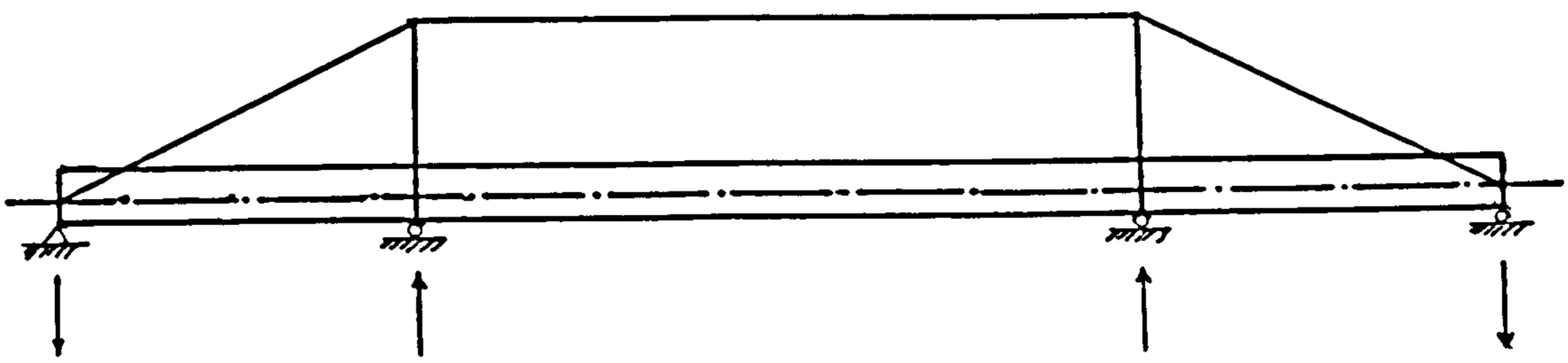

The linear transformation system

(b)

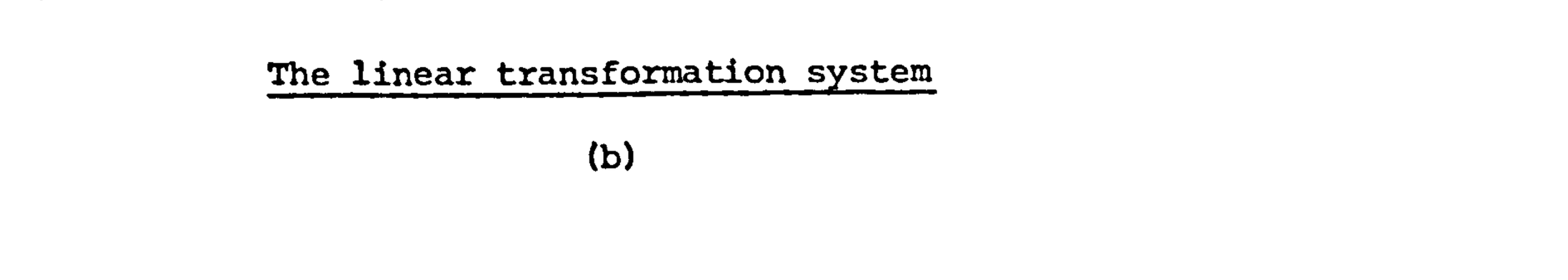

The final cable eccentricities

(c)

Figure (1.1)

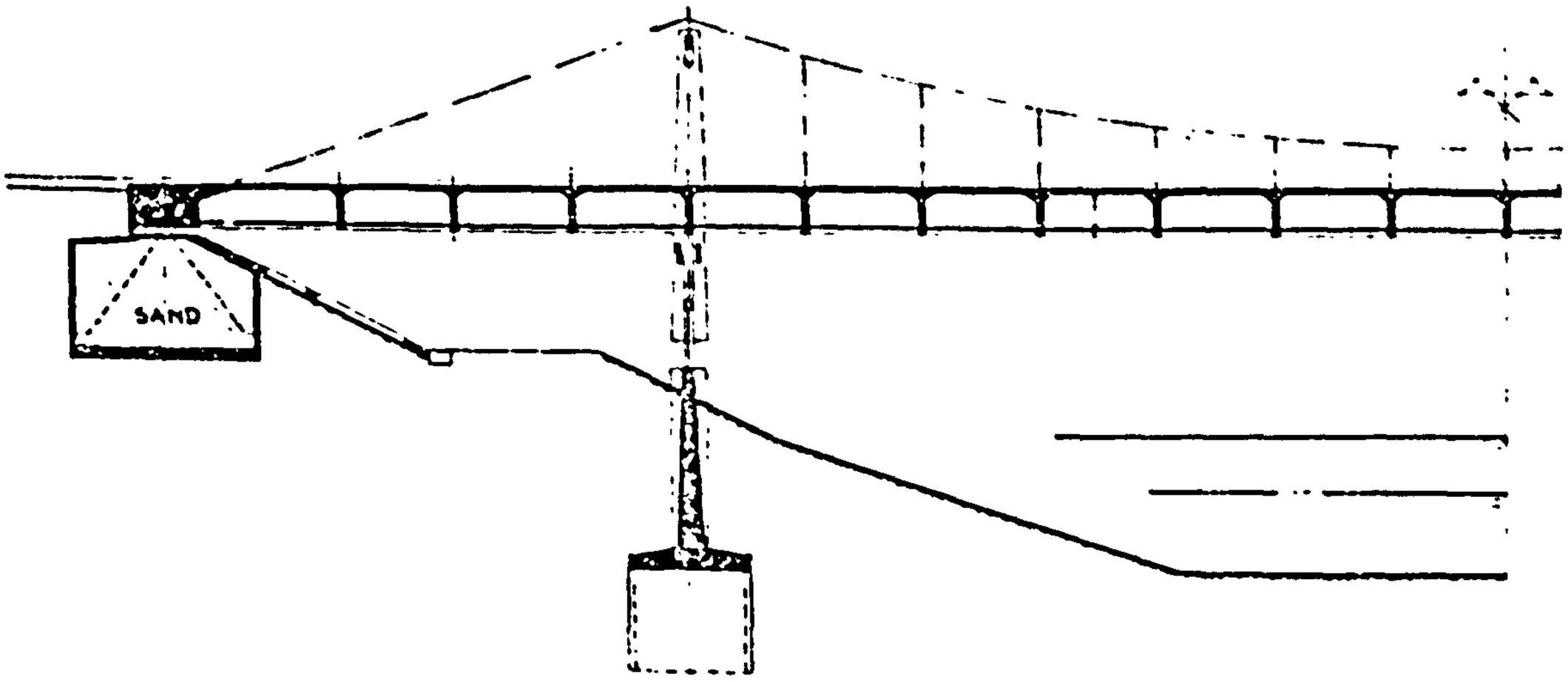

A half longitudual section of the Merelbeke bridge showing the concrete box at its left hand end

Figure (1.2)

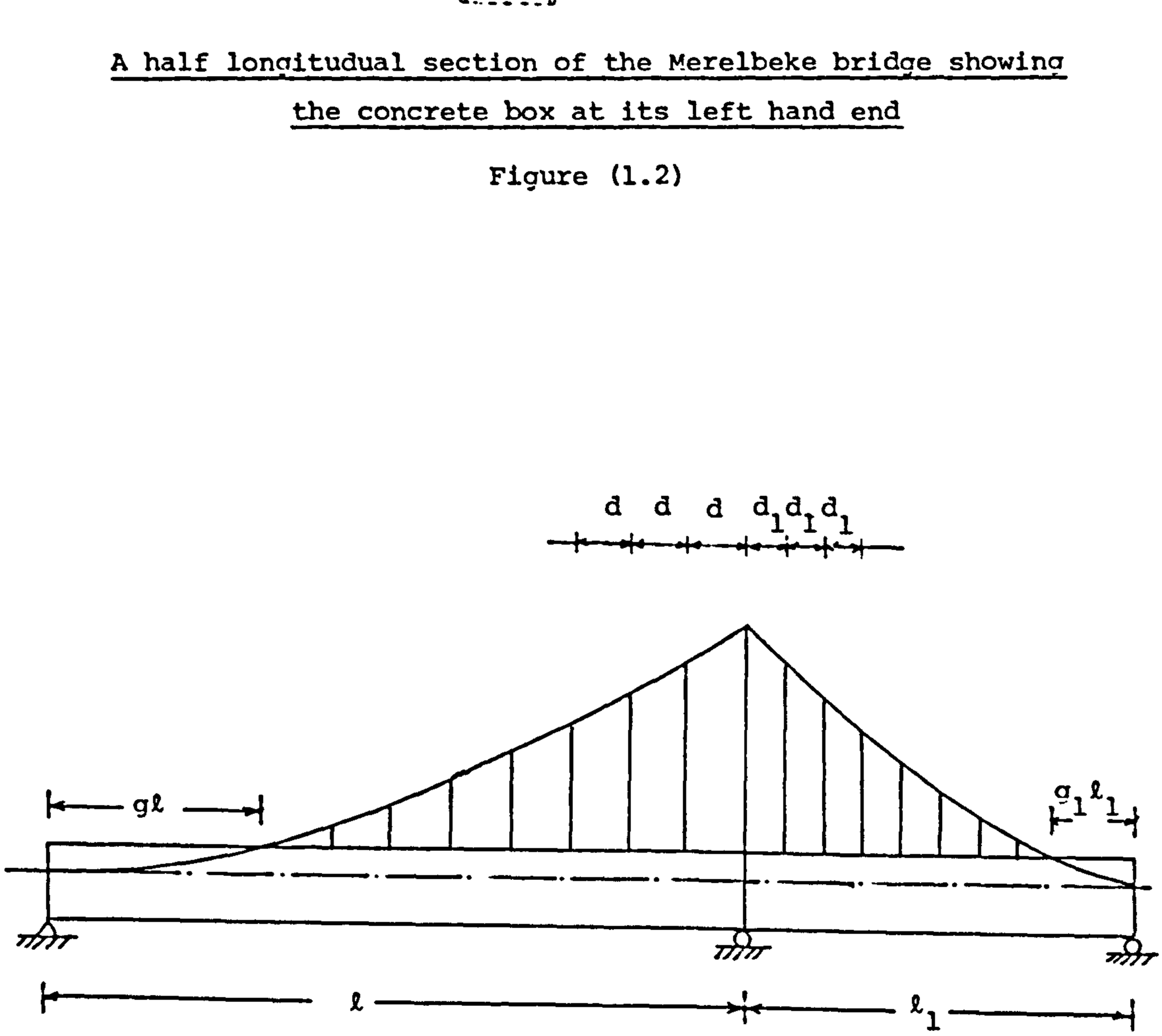

A Two-span prestressed concrete suspension bridge

Figure (1.3)

CHAPTER 2

2. Theory and Design of Two-Span Prestressed Concrete Suspension Bridges with Ungrouted Cables

2.1 Introduction

In this chapter, we give a complete solution for the design and analysis of this type of bridge. In the following chapter, the main differences between this type of bridge and prestressed concrete suspension bridge with grouted cables will be discussed.

The design procedure for both types of bridge is based upon the following realistic assumptions:

1. The spacing d and d_1 between the suspenders in the left and right hand spans is so small compared with the span lengths ℓ and ℓ_1, that the suspenders may be replaced by a membrane or screen without resistance to shear, i.e. the forces between the cable and the suspenders are assumed to be continuously distributed. (see Figure (1.3c)).

2. The cable curve is parabolic for the dead load and remains parabolic after the application of live load.

3. The extensions of the suspenders is ignored so that the downward displacement of the cable can be assumed to be equal to the beam deflection.

4. The deformation of the suspended beam due to shear may be ignored.

5. The flexural stiffness of the suspended beam EI is constant for both its spans.

The sign convention chosen will define a bending moment as positive when it tends to make the axis of the beam concave downwards, i.e. a hogging curveture. Consequently, the downward deflection and clockwise rotations are also defined as positive quantities. All the positive actions are shown in Figure (2.1).

The fundamental equations for the internal forces of the suspended beam can be written, as a result of the sign convention used, as follows:

$$M_x = + EI \frac{d^2\eta}{dx^2} \qquad (2.1a)$$

$$Q_x = - \frac{dM}{dx} = - EI \frac{d^3\eta}{dx^3} \qquad (2.1b)$$

$$q_x = - \frac{dQ}{dx} = + EI \frac{d^4\eta}{dx^4} \qquad (2.1c)$$

where I = The second moment of area of the cross section of the suspended beam

E = The modulus of elasticity for the concrete

η = The vertical deflection of the beam

M_x, Q_x = Bending moments and shear forces of the beam

q_x = Rate of loading of the beam.

2.2 The Evaluation of the Dimensions and the Preliminary Prestressing Force of the Prestressed Concrete Suspended Beam

The design of prestressed concrete suspended beams, as with conventional prestressed concrete beams, depends mainly on the moment conditions to which the beam will be subjected. More accurately, the range of moment variation is of greater importance than the absolute values of the bending moments themselves.

It is therefore convenient to start by defining certain moment conditions for any section of the beam. The dead load moment, denoted M_D, is a moment applied to the beam which remains of constant value and exists from the time of prestressing throughout the life of the beam. The dead loads are denoted by W and W_1 in the left and right hand span respectively. The dead load moments are usually much greater than the live load moments and therefore they are used to find the initial cable eccentricities, Figure (1.1a). After transforming the cable and finding its final eccentricities, Figure (1.1c), it will be proved that the cable at its present position is exerting upward forces exactly in balance with the dead loads and the beam does not experience any bending stresses, Figure (2.3a). Thus, similar to conventional prestressed beams, the section dimensions are determined to sustain the live load moments alone.

The extremes of bending moments due to live load are determined throughout the structure. In doing so, all the cases of live loading to which the suspended beam will be subjected must be considered. The maximum moment envelope is denoted M_1 and the minimum moment envelope M_2, with hogging moments considered positive. The variation of live load moments, $(M_1 - M_2)$, can then be established everywhere and the maximum value, M_L, determined as shown in Figure (2.2).

Assuming working stress limits of zero and f_c, compression, the minimum section modulus, B, is calculated from the expression, (see Figures (2.3)),

$$B_{min} = \frac{I}{Z_n} = \frac{M_L}{f_c} \tag{2.2}$$

where f_c is the maximum allowable stress and Z_n is the largest of the two quantities Z_1 and Z_2 which are the distances between the line of centroid and the upper and lower extreme fibres of the cross section of the suspended beam. Prestressed concrete suspension bridges can operate on low working stresses because of the possibility of having large cable eccentricities. Therefore, the maximum allowable working stress can be chosen as one half of that used in conventional prestressed concrete bridges. In other words, f_c can be chosen as one quarter of the cube strength of the concrete, f_{ult}.

From the chosen cross section satisfying the condition in Equation (2.2), it is possible to calculate I, A, Z_1 and Z_2 where A is the cross sectional area of the suspended beam. The required prestressing force H_w is then established from the expression,

$$H_w = \begin{cases} \frac{Z_1}{Z} f_c A & Z_1 < Z_2 \\ \frac{Z_2}{Z} f_c A & Z_1 > Z_2 \end{cases} \tag{2.3}$$

where H_w, the preliminary prestressing force, is also known as the horizontal tension as it is the horizontal component of the cable tension and Z is the total depth of the suspended beam (see Figure 2.3). It will be shown in Section 2.4 how to improve the stress distribution when the dead loads are applied in order to increase the efficiency of our structure.

2.3 The Parabolic Cable

2.3.1 Introduction

Similarly to ordinary suspension bridges, the cable eccentricities are obtained directly from the dead load bending moments. Usually the dead load is uniformly distributed which gives a parabolic bending moment diagram and consequently the cable geometry is also parabolic.

This section describes the properties of the parabolic cable in a series of formulae which are given in both exact and approximate version. Moreover, it discusses the effect of the cable deformation on its shape and tension.

2.3.2 The Properties of Parabolic Cables with No Eccentricities at their Ends

As mentioned in Chapter (1), the initial cable eccentricities are found by dividing the dead load bending moments M_D by the prestressing force H_w as shown in Figure (1.1a). Then, the shape is transformed by adding the linear system shown in Figure (1.1b) to the initial cable eccentricities. The final cable shape is shown in Figure (1.1c) for the whole length of the suspended beam.

Figure (2.4) shows the cable shape in the left hand span. In the figure we see that the cable is nearly coincident with the beam axis at the end support A, but has a finite eccentricity h at the intermediate support B. h can be defined as the height of the tower above the centre line of the beam.

Hence, the equation of the cable curve can be obtained as:

$$y' = \frac{M_D}{H_w}$$

and $$y = h\frac{x}{\ell} - |y'|$$

but since $$M_D = -\frac{1}{2} Wx(\ell - x)$$

The cable shape equation can be written as, (see Figure 2.4)

$$y = h\frac{x}{\ell} - \frac{Wx}{2H_w}(\ell - x) \qquad (2.4a)$$

Similarly for the right hand span,

$$y_1 = h\frac{x_1}{\ell_1} - \frac{W_1 x_1}{2H_w}(\ell_1 - x_1) \qquad (2.4b)$$

where W, W_1 are the self-weights of the suspended beam to which are added the weights of the main cable and the suspenders for both left and right hand spans. Equations (2.4) express the general formula for the parabolic cables with transformation. To find the cable sags f and f_1, see Figure (2.6), at the mid-points of the left and right hand spans we substitute

$x = \frac{\ell}{2}$ and $y = \frac{h}{2} - f$ in Equation (2.4a) and $x_1 = \frac{\ell_1}{2}$ and $y_1 = \frac{h}{2} - f_1$ in Equation (2.4b). This gives:

$$f = \frac{W\ell^2}{8H_w} \qquad (2.5a)$$

$$f_1 = \frac{W_1 \ell_1^2}{8H_w} \qquad (2.5b)$$

From Equations (2.5), it is evident that because of the equal horizontal tension of the cable in the two spans, we have:

$$\frac{W\ell^2}{8f} = \frac{W_1 \ell_1^2}{8f_1}$$

Consequently:

$$f_1 = \omega\lambda^2 f \qquad (2.6)$$

where $$\omega = \frac{W_1}{W} \tag{2.7}$$

and $$\lambda = \frac{\ell_1}{\ell} \tag{2.8}$$

Substituting from Equations (2.5) into Equations (2.4) we have, the following expressions for the cable shape:

$$y = h\,\frac{x}{\ell} - \frac{4f}{\ell^2}\,x\,(\ell - x)$$

$$y_1 = h\,\frac{x_1}{\ell_1} - \frac{4f_1}{\ell_1^2}\,x_1\,(\ell_1 - x_1)$$

Rearranging these expressions, we have:

$$y = F'x + \frac{4n}{\ell}\,x^2 \tag{2.9a}$$

$$y_1 = F_1'x_1 + \frac{4n_1}{\ell_1}\,x_1^2 \tag{2.9b}$$

where F' and F_1' are the cable slopes at the ends of the beam,

$$F' = \frac{h - 4f}{\ell} \tag{2.10a}$$

$$F_1' = \frac{h - 4f_1}{\ell_1} \tag{2.10b}$$

and $$n = \frac{f}{\ell} \tag{2.11a}$$

$$n_1 = \frac{f_1}{\ell_1} \tag{2.11b}$$

To check the validity of Expressions (2.9), we note that the bending moment produced by the cable forces M_c, is:

$$M_c = H_w y$$

Thus, from Equation (2.1c), the rate of loading for the cable forces can be obtained as,

$$q_c = + \frac{d^2 M_c}{dx^2} = + H_w \frac{d^2 y}{dx^2}$$

which yields:

$$q_c = - \frac{8f}{\ell^2} H_w = - W \qquad \text{for the left hand span}$$

and similarly $q_{c1} = - W_1$ for the right hand span

From the previous check, we deduce that by tensioning the cable by a force the horizontal component of which is H_w, the cable exerts upward uniformly distributed forces on the structure equal to the dead loads in both spans. To generalise the equations for the upward forces exerted by the cable, q_c and q_{c1}, in left and right hand spans, we have:

$$q_c = - \frac{8f}{\ell^2} H = - \frac{W}{H_w} H \qquad (2.12a)$$

$$q_{c1} = - \frac{8f_1}{\ell_1^2} H = - \frac{W_1}{H_w} H \qquad (2.12b)$$

where H is the horizontal component of the cable tension, the prestressing force at any time. From Equations (2.12), the ratio between the forces exerted by the cable in the left and right hand spans is:

$$\omega = \frac{q_{c1}}{q_c}$$

The tension, T or T_1, at any section of the cable in the left or right hand spans can be calculated from the expression obtained from studying the cable element shown in Figure (2.5):

$$T = H \frac{ds}{dx}$$

but $$\frac{ds}{dx} = \left[1 + \left(\frac{dy}{dx} \right)^2 \right]^{1/2}$$

which gives, from Equation (2.9):

$$T = H \left[1 + \left(F' + \frac{8n}{\ell} x \right)^2 \right]^{1/2} \qquad (2.13a)$$

$$T_1 = H \left[1 + \left(F_1' + \frac{8n_1}{\ell_1} x_1 \right)^2 \right]^{1/2} \qquad (2.13b)$$

From Equations (2.13), it is clear that T and T_1 are directly proportional to the cable slopes, $\left(\frac{dy}{dx}\right)$ and $\left(\frac{dy_1}{dx_1}\right)$. This means that T and T_1 are maximum at the top of the tower and minimum at the end supports.

The exact lengths of the cable S and S_1 for left and right hand spans can be calculated from the expression deduced from the cable element shown in Figure (2.5),

$$S = \int_0^{\ell} \left[1 + \left(\frac{dy}{dx} \right)^2 \right]^{1/2} dx$$

Carrying out this integration gives the exact lengths of the cable to be:

$$S = \frac{\ell}{16n} \left[\ln \left[\frac{(F'+8n)+[1+(F'+8n)^2]^{1/2}}{F' + [1+F'^2]^{1/2}} \right] + (F'+8n)[1+(F'+8n)^2]^{1/2} - F'[1+F'^2]^{1/2} \right] \qquad (2.14a)$$

for the left hand span and similarly,

$$S_1 = \frac{\ell_1}{16n_1} \left[\ln \left[\frac{(F_1'+8n_1)+[1+(F_1'+8n_1)^2]^{1/2}}{F_1' + [1+F_1'^2]^{1/2}} \right] + (F_1'+8n_1)[1+(F_1'+8n_1)^2]^{1/2} - F_1'[1+F_1'^2]^{1/2} \right] \qquad (2.14b)$$

for the right hand span. The derivation of the above formulae is given in Appendix 1, where F' & $(F'+8n)$ and F_1' & $(F_1'+8n_1)$ are the slopes

at the ends of the cable in each span and can be obtained from Equations (2.10) and (2.11). The magnitudes of these slopes are small due to the fact that the spans are usually long with respect to the height of the tower. This means that Formulae (2.14) can be simplified by series expansion, see Appendix 2. Thus, the approximate lengths of the flat cable can be written as:

$$S = \ell \left[1 + \frac{8}{15} n^2 (5-12n^2) + \frac{(F'+4n)^2}{8} [4-32n^2 - (F'+4n)^2] \right] \tag{2.15a}$$

for the left hand span and similarly,

$$S_1 = \ell_1 \left[1 + \frac{8}{15} n_1^2 (5-12n_1^2) + \frac{(F_1'+4n_1)^2}{8} [4-32n_1^2 - (F_1'+4n_1)^2] \right] \tag{2.15b}$$

for the right hand span.

2.3.3 The Properties of Parabolic Cables with Eccentricities at their Ends

The range of span application can be increased for our type of bridge by using eccentricities at the ends of the suspended beam. Figure (2.6) shows that these eccentricities, denoted 'a', introduce bending moments of opposite signs to those produced by the applied live loads. Therefore, their contribution in relieving the suspended beam is significant. The designer is free to choose the value of 'a' for which the suspended structure benefits most. Generally,'a' must be chosen to have the maximum possible value which is the downward core limit in order to avoid tensile stresses developing at a section of zero applied moment. Hence, we have:

$$a \leqslant \frac{I}{AZ_1} \tag{2.16}$$

To determine the effect of 'a' on the geometry of the parabolic cable, we have the cable shape in the left hand span, as shown in Figure (2.7). In the figure we see that the cable has a downward eccentricity, 'a', from the beam axis at the end support A

but has an upward finite eccentricity h to the top of the tower at the intermediate support B. Hence, following the aforementioned procedure we have:

$$y = \frac{h+a}{\ell} \; x \; - \left| y' \right|$$

$$\text{where} \quad y' = \frac{M_D}{H_w} = - \frac{W \; x}{2 \; H_w} \; (\ell - x)$$

Thus, we arrive at the final expression for the cable shape:

$$y = Fx + \frac{4n}{\ell} \; x^2 \tag{2.17a}$$

for the left hand span and similarly,

$$y_1 = F_1 x_1 + 4 \; \frac{n_1}{\ell_1} \; x_1^{\,2} \tag{2.17b}$$

for the right hand span where:

$$F = \frac{h+a \; - \; 4f}{\ell} \tag{2.18a}$$

$$F_1 = \frac{h+a \; - \; 4f_1}{\ell_1} \tag{2.18b}$$

and where n, n_1 can be obtained from Equations (2.11).

Obviously, Equations (2.17) and (2.18) are identical to Equations (2.9) and (2.10) when deleting the end eccentricities, a = o. Therefore, all the formulae used to determine the properties of the cable with no eccentricities at its ends, are applicable here when replacing F' and F_1' by F and F_1. Furthermore, we will consider the use of a cable with eccentricities at its ends as the general case on which the calculations will be based. Thus, a cable with no eccentricities at its ends will be regarded as a special case with a = o.

2.3.4 The Deformation of the Cable

The effect of the deformation of the cable on its tension is evaluated in this section. These deformations result from the following effects:

2.3.4.1 Tower Flexure

Tower flexure could be affected by powerful wind, earthquakes or imbalance of horizontal forces at the top of the tower. The latter could result from a cable slip at one of the anchorages at any of its ends.

As shown in Figure (2.8), tower flexure produces a change in the span length $\Delta\ell$ which forces the cable to change its length, shape and tension. The changes in the cable lengths ΔS and ΔS_1 can be found as follows:

$$\Delta S = \frac{\partial S}{\partial \ell} (\pm \Delta \ell)$$

$$\Delta S_1 = \frac{\partial S_1}{\partial \ell_1} (\mp \Delta \ell)$$

Obviously, if $\Delta\ell$ is produced when the tower bends to the left, this would mean a decrease in the left hand span length and an increase in the right hand span length and vice versa, see Figure (2.8). Thus, we have the exact change in the cable length as:

$$\Delta S = \frac{(\pm \Delta \ell)}{8n} \ln \left[\frac{(F+8n)+ [1+(F+8n)^2]^{1/2}}{F + [1+F^2]^{1/2}} \right] \qquad (2.19a)$$

$$\Delta S_1 = \frac{(\mp \Delta \ell)}{8n_1} \ln \left[\frac{(F_1+8n_1) + [1+(F_1+8n_1)^2]^{1/2}}{F_1 + [1+F_1^2]^{1/2}} \right] \qquad (2.19b)$$

for left and right hand spans respectively. Full derivation of these formulae is given in Appendix 3. For flat curves, approximate formulae have been derived as shown: (for details see Appendix 4)

$$\Delta S = \left[1 - \frac{8}{15} n^2(5-36n^2) - \frac{(F+4n)^2}{8}[4-96n^2-3(F+4n)^2] \right] (\pm\Delta\ell) \tag{2.20a}$$

$$\Delta S_1 = \left[1 - \frac{8}{15} n_1{}^2(5-36n_1{}^2) - \frac{(F_1+4n_1)^2}{8}[4-96n_1{}^2-3\ (F_1+4n_1)^2] \right] (\mp\Delta\ell) \tag{2.20b}$$

for left and right hand spans respectively.

The effect on the cable shape can be represented as the change in the cable sags Δf and Δf_1 for left and right hand spans, Figure (2.8). It can be proved that:

$$\frac{\partial S}{\partial f}\ \Delta f\ = \frac{\partial S}{\partial \ell}\ (\pm\ \Delta\ell)$$

Therefore, the relationship between Δf and $\Delta\ell$ is given as:

$$\Delta f = \frac{\partial S/\partial \ell}{\partial S/\partial f}\ (\pm\ \Delta\ell)$$

for the left hand span and similarly,

$$\Delta f_1 = \frac{\partial S_1/\partial \ell_1}{\partial S_1/\partial f_1}\ (\mp\ \Delta\ell)$$

for the right hand span.

Thus, carrying out these calculations, the final value for Δf and Δf_1 can be determined exactly as: (see Appendix 5)

$$\Delta f = \frac{2n}{\left[\left(\frac{(F+8n)\,[1+F^2]^{1/2} - F\,[1+(F+8n)^2]^{1/2}}{\ln\left[\frac{(F+8n)+[1+(F+8n)^2]^{1/2}}{F+[1+F^2]^{1/2}}\right]}\right)-1\right]}\ (\pm\Delta\ell) \qquad (2.21a)$$

$$\Delta f_1 = \frac{2n_1}{\left[\left(\frac{(F_1+8n_1)\,[1+F_1^2]^{1/2} - F_1\,[1+(F_1+8n_1)^2]^{1/2}}{\ln\left[\frac{(F_1+8n_1)+[1+(F_1+8n_1)^2]^{1/2}}{F_1+[1+F_1^2]^{1/2}}\right]}\right)-1\right]}\ (\mp\Delta\ell) \qquad (2.21b)$$

for left and right hand spans respectively. For flat curves, the approximate version of Formulae (2.21) are:

$$\Delta f = \frac{(\pm\Delta\ell)}{64n}\left[\left[\frac{120-64n^2(5-36n^2)-15\,(F+4n)^2[4-96n^2-3(F+4n)^2]}{[\,5\,[2-3\,(F+4n)^2]-48n^2\,]}\right]\right] \qquad (2.22a)$$

$$\Delta f_1 = \frac{(\mp\Delta\ell)}{64n_1}\left[\left[\frac{120-64n_1^2(5-36n_1^2)-15\,(F_1+4n_1)^2[4-96n_1^2-3(F_1+4n_1)^2]}{[\,5\,[2-3\,(F_1+4n_1)^2]-48n_1^2\,]}\right]\right] \qquad (2.22b)$$

for left and right hand spans respectively where F, F_1, n and n_1 can be computed from Equations (2.18) and (2.11). The derivation of Formulae (2.22) is given in Appendix 6.

Finally, the change in the cable tension ΔH corresponding to the variation of the cable lengths ΔS and ΔS_1 can be computed from Equation (2.35) as will be shown later in this section.

2.3.4.2 Construction Errors

The performance of the bridge depends on placing all of its elements correctly in the designed position. An error in the length of one, or more, of the suspenders could result in changing the

position of the cable with respect to the centre line of the beam and consequently affecting the bending moments produced by the cable tension. Therefore, it is essential to be able to calculate the effect of that error on the length, shape and tension of the cable (see Figure 2.9).

The lengths of the suspenders can be obtained from the following expressions which are deduced from Equations (2.17) and Figure (2.9):

$$l_{sm} = Fx_m + \frac{4n}{\ell} x^2_m - (a+Z_1) \qquad (2.23a)$$

$$l_{slm} = F_1 x_{1m} + \frac{4n_1}{\ell_1} x_1{}^2_m - (a+Z_1) \qquad (2.23b)$$

for suspenders in the left and right hand spans respectively where:

m is the suspender number, or numbers, at which the error took place.

l_{sm} and l_{slm} is the theoretical length of suspender number m in the left and right hand spans.

x_m and x_{1m} is the distance from the end supports to the faulty suspender in the left and right hand spans.

ϵ_m is the error in the faulty suspender length where:

ϵ_m = Actual Length - Theoretical Length.

Thus, from Equation (2.23a), we obtain the corresponding change in the cable sag:

$$\frac{\partial l_{sm}}{\partial f} = \frac{4}{\ell^2} \left[x^2_m - \ell x_m\right]$$

which yields,

$$\Delta f = - \frac{\ell^2}{4} \frac{\epsilon_m}{x_m \left[\ell - x_m\right]}$$

However, if there is more than one faulty suspender, the change in the cable sags can be obtained as:

$$\Delta f = -\frac{\ell^2}{4} \sum \frac{\epsilon_m}{x_m (\ell - x_m)} \qquad (2.24a)$$

$$\Delta f_1 = -\frac{\ell_1^2}{4} \sum \frac{\epsilon_{1m}}{x_{1m} (\ell_1 - x_{1m})} \qquad (2.24b)$$

for either, or both, the left and right hand spans respectively.

The corresponding changes in the cable lengths ΔS and ΔS_1 can be found exactly from the following relationships:

$$\Delta S = \frac{-\Delta f}{16n^2} \left[\ln \left[\frac{(F+8n) + [1+(F+8n)^2]^{1/2}}{F + [1+F^2]^{1/2}} \right] + F\,[1+(F+8n)^2]^{1/2} - (F+8n)[1+F^2]^{1/2} \right] \qquad (2.25a)$$

$$\Delta S_1 = \frac{-\Delta f}{16n_1^2} \left[\ln \left[\frac{(F_1+8n_1) + [1+(F_1+8n_1)^2]^{1/2}}{F_1 + [1+F_1^2]^{1/2}} \right] + F_1[1+(F_1+8n_1)^2]^{1/2} - (F_1+8n_1)[1+F_1^2]^{1/2} \right] \qquad (2.25b)$$

for the left and right hand spans respectively. The derivation of these formulae is given in Appendix 5. For flat curves, the approximate versions of these equations are found to be: (see Appendix 6)

$$\Delta S = \frac{8}{15} n\, \Delta f \left[5\,[2-3\,(F+4n)^2] - 48n^2 \right] \qquad (2.26a)$$

$$\Delta S_1 = \frac{8}{15} n_1\, \Delta f_1 \left[5\,[2-3\,(F_1+4n_1)^2] - 48n_1^2 \right] \qquad (2.26b)$$

for left and right hand span respectively where F, F_1, n and n_1 can be calculated from Equations (2.18) and (2.11).

Figure (2.10) shows that a construction error in the tower height Δh will also force the cable to change its length, shape and tension. The change in the cable lengths can be established from the following relationships:

$$\Delta S = \frac{\partial S}{\partial h} \Delta h$$

$$\Delta S_1 = \frac{\partial S_1}{\partial h} \Delta h$$

where Δh = Actual Height - Theoretical Height

Hence, calculating the quantities $\frac{\partial S}{\partial h}$ and $\frac{\partial S_1}{\partial h}$, see Appendix 7, we have:

$$\Delta S = \frac{\Delta h}{8n} \left[[1+ (F+8n)^2]^{1/2} - [1+F^2]^{1/2} \right] \qquad (2.27a)$$

$$\Delta S_1 = \frac{\Delta h}{8n_1} \left[[1+ (F_1+8n_1)^2]^{1/2} - [1+F_1^2]^{1/2} \right] \qquad (2.27b)$$

The effect on the cable shape can be represented, as mentioned earlier, as the change in the cable sags Δf and Δf_1. Similarly to the procedure followed in the preceeding section, we have:

$$\Delta f = \frac{\partial S/\partial h}{\partial S/\partial f} \Delta h$$

$$\Delta f_1 = \frac{\partial S_1/\partial h}{\partial S_1/\partial f} \Delta h$$

for left and right hand spans respectively. Hence, from Equations (2.25 and 2.27), we obtain the exact relationship between the change in the cable sags Δf & Δf_1 and the error in the tower height Δh as follows:

$$\Delta f = 2n\ \Delta h \frac{\left[\left[1 + F^2\right]^{1/2} - \left[1 + (F+8n)^2\right]^{1/2}\right]}{\left[\ln\left[\frac{(F+8n) + \left[1+(F+8n)^2\right]^{1/2}}{F + \left[1+F^2\right]^{1/2}}\right] + F\left[1+(F+8n)^2\right]^{1/2} - (F+8n)\left[1+F^2\right]^{1/2}\right]} \qquad (2.28a)$$

for the left hand span and similarly,

$$\Delta f_1 = 2n_1\ \Delta h \frac{\left[\left[1 + F_1^2\right]^{1/2} - \left[1 + (F_1+8n_1)^2\right]^{1/2}\right]}{\left[\ln\left[\frac{(F_1+8n_1) + \left[1+(F_1+8n_1)^2\right]^{1/2}}{F_1 + \left[1+F_1^2\right]^{1/2}}\right] + F_1\left[1+(F_1+8n_1)^2\right]^{1/2} - (F_1+8n_1)\left[1+F_1^2\right]^{1/2}\right]} \qquad (2.28b)$$

for the right hand span. For details see Appendix 5.

For flat curves, the above equations can be approximated to the following simplified versions:

$$\Delta f = 15\ \Delta h \frac{\left[\left[1+(F+8n)^2\right]^{1/2} - \left[1+F^2\right]^{1/2}\right]}{\left[5\left[2-3(F+4n)^2\right] - 48\ n^2\right]} \qquad (2.29a)$$

$$\Delta f_1 = 15\ \Delta h \frac{\left[\left[1+(F_1+8n)^2\right]^{1/2} - \left[1+F_1^2\right]^{1/2}\right]}{\left[5\left[2-3(F_1+4n_1)^2\right] - 48\ n_1^2\right]} \qquad (2.29b)$$

for left and right hand spans respectively where F, F_1, n and n_1 can be determined from Equations (2.18) and (2.11). (For details see Equations (2.26 & 2.27) and Appendix 6).

The corresponding change in the cable tension ΔH for all the aforementioned changes in the cable length ΔS and ΔS_1 can be evaluated from Equation (2.35) as will be mentioned later in this section.

2.3.4.3 The Temperature Effects

The effects of temperature changes, $\pm \Delta t$, on the stresses in this type of bridges will generally be small. However, the internal capacity and thermal conductivity of concrete differs considerably from that of the steel part of the structure. Hence, ambient temperature changes may lead to more significant stress changes than would arise in more conventional forms of structures constructed from homogeneous materials.

Starting with the suspended beam, the roller supports will force the total change in the beam length to take place in one of its spans. Denoting this change $\Delta \ell$, we have:

$$\Delta \ell = \pm \alpha_c \Delta t \ \ell \ (1+\lambda) \qquad (2.30)$$

where α_c is the thermal coefficient of expansion for the concrete,
$\simeq 0.0001$ per C°.

Thus, the corresponding change in the cable length and shape can be evaluated from Equations (2.19) and (2.21) for exact values or Equations (2.20) and (2.22) for approximate ones.

For the main cable, if the thermal coefficient of expansion for steel is denoted α_s, $\simeq 0.000011$ per C°, the change in the cable lengths for the left and right hand spans ΔS and ΔS_1 can be calculated as:

$$\Delta S = \pm \alpha_c \Delta t \ S \qquad (2.31a)$$

$$\Delta S_1 = \pm \alpha_c \Delta t \ S_1 \qquad (2.31b)$$

where S and S_1 can be calculated exactly from Equations (2.14) or approximately from Equations (2.15). The corresponding change in the cable sags Δf and Δf_1 can be evaluated from Equations (2.25) or (2.26).

Each suspender will respond to the temperature variations by elongating or contracting by amounts Δl_{sm} and Δl_{s1m}, where from Equations (2.23) we have:

$$\Delta l_{sm} = \pm \alpha_s \Delta t \left[F x_m + \frac{4n}{\ell} x^2_m - (a+Z_1)\right]$$

$$\Delta l_{s1m} = \pm \alpha_s \Delta t \left[F_1 x_{1m} + \frac{4n_1}{\ell_1} x^2_{1m} - (a+Z_1)\right]$$

for suspenders in the left and right hand spans respectively. Hence, assuming the total number of the suspenders to be equal to i and j for left and right hand spans respectively, the corresponding changes in the cable sags Δf and Δf_1 can be obtained from Equations (2.24) by replacing ϵ_m by Δl_{sm} and ϵ_{1m} by Δl_{s1m} (see Figure 2.9) which gives:

$$\Delta f = \mp \frac{\alpha_s \Delta t \ \ell^2}{4} \sum_{m=1}^{i} \frac{\left[F x_m + 4 \frac{n}{\ell} x^2_m - (a+Z_1)\right]}{\left[x_m (\ell - x_m)\right]} \qquad (2.32a)$$

$$\Delta f_1 = \mp \frac{\alpha_s \Delta t \ \ell_1^2}{4} \sum_{m=1}^{j} \frac{\left[F_1 x_{1m} + 4 \frac{n_1}{\ell_1} x^2_{1m} - (a+Z_1)\right]}{\left[x_{1m} (\ell_1 - x_{1m})\right]} \qquad (2.32b)$$

for the left and right hand spans respectively. Having found Δf and Δf_1, Equations (2.25) may be used to determine the corresponding change in the cable lengths ΔS and ΔS_1 due to the effect of temperature variation on the suspenders.

The temperature variation may force the tower to change its height by an amount Δh where: (assuming that the tower is made of concrete)

$$\Delta h = \pm \alpha_c \Delta t \ h \qquad (2.33)$$

The corresponding change in the cable lengths ΔS and ΔS_1 can directly be calculated from Equations (2.27). The change in the cable sags Δf and Δf_1 may be computed by using Equations (2.28) for exact values or Equations (2.29) for approximate ones.

It is worth noting that Equations (2.27 and 2.28) may be applied again to determine the effect of the elastic deformation of the tower on the behaviour of the cable. In other words, the tower may be subjected to some axial compression under the vertical force N_T, see Figure (2.15). This may result in a small change in its height which can be determined and substituted into Equations (2.27 and 2.28) to evaluate the effect on the cable lengths and shape.

The vertical force N_T is the sum of the vertical components, V and V_1, of the cable tensions for the left and right hand spans where:

$$N_T = V + V_1 = H \left[\frac{dy}{dx}\Big|_{x=\ell} + \frac{dy_1}{dx_1}\Big|_{x_1=\ell_1} \right]$$

which gives from Equations (2.17):

$$N_T = H \left[(F+8n) + (F_1+8n_1) \right] \qquad (2.34)$$

Finally, having found the total values of the change in the cable lengths ΔS and ΔS_1, the corresponding change in the cable tension ΔH can be evalulated from Equation (2.35) as will be shown in the following section.

2.3.4.4 The Effect of the Elastic Deformation of the Cable on its Tension

For the previous changes in the cable lengths, the cable is forced to change its tension by an amount ΔH. This change can be determined from the following formula, as derived in Appendix 8:

$$\Delta H = \frac{A_c E_c}{\ell} \left[\frac{\Delta S}{\left[1+F\ (F+8n) + \frac{64}{3} n^2\right]} + \frac{\Delta S_1}{\lambda\left[1+F_1\ (F_1+8n_1) + \frac{64}{3} n_1^{\,2}\right]} \right] \qquad (2.35)$$

where A_c and E_c are the cross sectional area and young's modulus of elasticity for the main cable respectively.

Equation (2.35) may be used to determine ΔH corresponding to a change, or changes, for the cable length, or lengths, which may occur in either, or both, of the left and right hand spans.

2.4 The Determination of the Initial Prestressing Force

From Equations (2.12), it can be seen that the preliminary prestressing force H_w produces upward distributed forces exactly in balance with the dead load in both left and right hand spans. Consequently, the suspended beam axis will be a straight line with zero bending stresses and axial compressive stresses $\frac{H_w}{A}$, Figure (2.3a). However, for loads of such long duration, the time effect such as shrinkage, creep and relaxation of the various parts of the structure will most certainly take place. Consequently, the prestressing force will decrease below the value of H_w and the suspended beam will deflect under the dead load alone and some tension stresses may develop.

For this reason, efficient design of prestressed concrete suspension bridges requires the prestressing force to be such that the upward forces exerted on the suspended structure exceed the self weight of that structure. In other words, the prestressing force must exceed H_w by an amount which ensures that it remains larger that H_w after the time effects take place. Thus, the initial prestressing force is assumed to be H_i, where:

$$H_i = H_w\ (1+y) \tag{2.36a}$$

and the final prestressing force, after the time effects take place, is H_f where:

$$H_f = H_w\ (1+\tau) \tag{2.36b}$$

and

$$y > \tau \tag{2.36c}$$

The value of the initial prestressing force H_i can be adjusted in order to increase the efficiency of the prestress distribution under the dead load, Figure (2.3a). Figure (2.11) shows the resultant of the upward forces exerted by the initial prestressing force, which are $W(1+y)$ and $W_1(1+y)$, and the dead loads in the left and right hand spans. The figure also shows the end moments $H_i a$ applied at both ends. Hence, by virtue of the three moments equation we have,

$$M_1 = \frac{H_i a}{2} + y \frac{W\ell^2}{8} e$$

where e is a constant which can be evaluated as follows:

$$e = \frac{(1 + \omega \lambda^3)}{(1 + \lambda)} \qquad (2.37)$$

and

$$M_2 = \frac{yW\ell^2}{128} (4-e)^2 + \frac{H_i a}{16} (4+3e)$$

at $x_2 = \frac{\ell}{8} [4-e]$

It can be proved that M_1 is the maximum moment and the critical section is located at the intermediate support B. Thus, the stresses of the cross section are as shown in Figure (2.12a), and must comply with the following conditions:

$$-\frac{H_i}{A} + \frac{M_1 Z_2}{I} \geqslant 0$$

$$-\frac{H_i}{A} - \frac{M_1 Z_1}{I} \leqslant -f_c$$

where f_c is the maximum allowable compressive stress, $\simeq \frac{1}{4} f_{ult}$. Hence, substituting for H_i and M_1, and rearranging the above equation, we have:

$$\frac{\left[\frac{I}{AZ_2} - \frac{a}{2}\right]}{\left[ef - \frac{I}{AZ_2} + \frac{a}{2}\right]} \leqslant y \leqslant \frac{\left[\frac{f_c I}{H_w Z_1} - \frac{I}{AZ_1} - \frac{a}{2}\right]}{\left[ef + \frac{I}{AZ_1} + \frac{a}{2}\right]}$$

where $f = \frac{W\ell^2}{8 H_w}$

The above equation gives the lower and upper limits for y. To ensure that no tension stresses will develop, under the dead load, after the time effects take place, the value of τ must comply with the following condition: (Equation (2.36c))

$$\tau \geqslant \frac{\left[\frac{I}{AZ_2} - \frac{a}{2}\right]}{\left[ef - \frac{I}{AZ_2} + \frac{a}{2}\right]} \qquad (2.38a)$$

Hence, y can be calculated from the following relationship:

$$\tau = Gy - D$$

where G and D are constants which can be evaluated from Formula (5.15) as will be discussed in Chapter (5). Then, the value of y must be checked to comply with the following condition, so that the compressive stresses will not exceed the maximum allowable stress f_c:

$$y \leqslant \frac{\left[\frac{f_c I}{H_w Z_1} - \frac{I}{AZ_1} - \frac{a}{2}\right]}{\left[ef + \frac{I}{AZ_1} + \frac{a}{2}\right]} \qquad (2.38b)$$

Figures (2.12) show the stress distribution under the dead load and maximum live load. They also show that the prestressed concrete suspended beam now operates in the most efficient and economical manner. It is worth noting that the prestressing force can be reduced, in order to employ a cheaper cable, when allowing for small tension stresses to develop, under the maximum live load, which can be sustained by the tensile reinforcement. However, such approach should be supported by sufficient investigation in all cases of live loading likely to affect the bridge in order to ensure that any tension stresses developing will remain less than the allowable ones.

2.5 The Behaviour of the Main Cable Under Applied Live Loading

2.5.1 Discussion

As mentioned in Chapter (1), the horizontal tension of the cable consists of two parts. The first part is the initial prestressing force H_i which is generated in the cable by means of hydraulic jack or any other method, as will be discussed later in Chapter (6). It independently exists to sustain the dead load as well as the time effects on its magnitude. The initial prestressing force indirectly sustains part of the applied live load through the upward forces it produces, as mentioned in the preceding section and it permanently remains in the structure for its entire working life.

The second part of the horizontal tension of the cable is denoted by H_p and it can be defined as the part which the horizontal tension of the cable gains or loses due to the application of live loading in any of the beam spans. As mentioned before, the suspenders force the main cable to deflect with the suspended beam and hence, elongate and increase its tension by the amount H_p. Obviously, H_p depends entirely on the type, location and magnitude of the applied live loading. It is also governed by the geometry of both the main cable and the prestressed concrete suspended beam. The value of H_p may contribute significantly to the stress state of the suspended structure providing that the spans are long enough. Therefore, it must be calculated with best possible accuracy.

Early research was undertaken in this field by Steinman and Timoshenko (20, 23, 25 and 26). However, their work was developed to cover ordinary suspension bridges which do not include the effect of the axial force. Therefore, it was essential to modify that work to suit prestressed concrete suspension bridges. Hence, two modified approaches will be described in this section to determine the change in the prestressing force H_p due to the applied live loading. Thereafter, a comparison will be carried out in order to decide upon the preference of either of them for best accuracy.

2.5.2 The Modified Steinman's Approach

2.5.2.1 The Principle Used

H_p is a statically indeterminate quantity. Hence, the required equation for its determination must therefore be deduced from the elastic deformation of the system.

We imagine the cable to be cut at a section close to one of its anchorages, see Figure (2.13). Then, with H_p = o, under the action of any load applied on the structure, the two cut ends would be separated by some horizontal distance Δ. If a unit horizontal force, H = 1, is applied between the cut ends, it would pull them back towards each other a small distance δ, Figure (2.14). Thus, the required change in the horizontal tension, H_p, would evidently be the ratio of these two imaginary displacements, or:

$$H_p = \frac{\Delta}{\delta} \tag{2.39}$$

The quantity Δ can be calculated directly by integrating the bending moments produced by the live loading M_x with the initial cable tension multiplied by the bending moments produced by a unit horizontal tension and no loading m_x over the two spans. Thus we have:

$$\Delta = - \sum \int \frac{M_x m_x}{EI} dx \tag{2.40}$$

where the negative sign is introduced as a result of the sign convention used as shown in Figure (2.1).

A similar procedure can be adopted to determine δ. It is defined as the change in the imaginary distance Δ produced by a unit horizontal tension and no loading is applied. Therefore, δ can directly be computed by virtue of Castigliano's first theorem (2) where it can be redefined as the derivative, with respect to H, of the internal energy Ω stored in the superstructure at H = 1. Thus we have:

$$\Omega = \frac{1}{2} \sum \int \frac{m_x^2}{EI} \, dx + \frac{1}{2} \sum \int \frac{N^2}{EA} \, dS$$

$$\delta = \frac{d\Omega}{dH} = \frac{1}{EI} \sum \int m_x \frac{dm_x}{dH} \, dx + \frac{1}{EA} \sum \int N \frac{dN}{dH} \, dS \qquad (2.41a)$$

where, N is The direct forces in the suspended beams, the main cable, the suspenders and the tower at H = 1 and no applied loading.

Hence, Equation (2.41a) can be rewritten as:

$$\delta = \delta_{bm} + \delta_{bn} + \delta_c + \delta_s + \delta_T \qquad (2.41b)$$

where, δ_{bm}, δ_{bn}, δ_c, δ_s and δ_T are the gaps produced by the moment of the suspended beam, the direct forces in the suspended beam, the main cable, the suspenders and the tower respectively at H = 1.

2.5.2.2 The Evaluation of the Total Gap δ

a) **The Determination of the Gap Produced by the Bending Moments of the Beam δ_{bm}**

From Equations (2.41):

$$\delta_{bm} = \frac{1}{EI} \sum \int m_x \frac{dm_x}{dH} \, dx$$

m_x is the bending moment produced by a unit prestressing force and no live loading is applied, see Figure (2.14).

Thus, ignoring the effect of unit axial force, the bending moment equations can be determined as;

$$m_x = \frac{dm_x}{dH} = a \left(1 - \frac{x}{\ell}\right) + \frac{4f}{\ell^2} x (\ell - x) - \bar{m} \frac{x}{\ell} \qquad (2.42a)$$

$$m_{x1} = \frac{dm_{x1}}{dH} = a\left(1 - \frac{x_1}{\ell_1}\right) + \frac{4f_1}{\ell_1^2} x_1 (\ell_1 - x_1) - \bar{m}\frac{x_1}{\ell_1} \qquad (2.42b)$$

for left and right hand spans where $\bar{m}$ is the moment at the intermediate support and can be calculated from the following expression:

$$\bar{m} = fe + \frac{a}{2} \qquad (2.42c)$$

and where e is a constant and can be determined from Equation (2.37).

Thus,

$$\delta_{bm} = \frac{1}{EI} \int m_x \frac{dm_x}{dH} dx = \sum \int \frac{m_x^2}{EI} dx \qquad \text{at } H = 1$$

Carrying out this integration, the final result is:

$$\delta_{bm} = \frac{\ell (1+\lambda)}{3EI} \left[\frac{8}{5} f^2 \frac{(1+\omega^2 \lambda^5)}{(1+\lambda)} - (fe - \frac{3}{2} a)(fe + \frac{a}{2}) \right] \qquad (2.43)$$

The full derivation of this formula is given in Appendix 9.

b) <u>The Determination of the Gaps Produced by the Axial Forces in the Various Parts of the Structure</u>

1. <u>The gap produced by the direct force in the suspended beam δ_{bn}</u>

The normal force in the suspended beam is obviously equal to the horizontal tension of the cable. Hence, we have

$$N = H \text{ and } \frac{dN}{dH} = 1$$

Thus we find:

$$\delta_{bn} = \frac{1}{EA} \sum \int N \frac{dN}{dH} dx = \frac{H}{EA} (\ell + \ell_1)$$

At H = 1, we obtain:

$$\delta_{bn} = \frac{\ell}{EA} (1 + \lambda) \qquad (2.44)$$

where $\lambda = \frac{\ell_1}{\ell}$

2. The gap produced by the direct force in the the main cable δ_c

From Figure (2.5),

$$N = T = H \frac{ds}{dx}$$

and

$$\frac{dN}{dH} = \frac{ds}{dx}$$

Hence, $\delta_c = \sum \frac{1}{A_c E_c} \int N \frac{dN}{dH} \, ds = \frac{H}{A_c E_c} \sum \int \left(\frac{ds}{dx} \right)^2 ds$

At H = 1, we find:

$$\delta_c = \frac{1}{A_c E_c} \sum \int \left(\frac{ds}{dx} \right)^3 dx$$

where A_c and E_c are The cross sectional area and young's modulus of elasticity of the main cable.

Thus by performing this integration, the following exact formula can be obtained: (see Appendix 10)

$$\delta_c = \frac{\ell}{64n \, A_c E_c} \Bigg[3 \, \ln \left[\frac{(F+8n) + [1+(F+8n)^2]^{1/2}}{F + [1+F^2]^{1/2}} \right] + (F+8n) \, [1+(F+8n)^2]^{1/2} [5+2(F+8n)^2]$$

$$- F \, [1+F^2]^{1/2} (5+2F^2) + \frac{1}{\omega} \left[3 \, \ln \left[\frac{(F_1+8n_1) + [1+(F_1+8n_1)^2]^{1/2}}{F_1 + [1+F_1^2]^{1/2}} \right] \right.$$

$$\left. + (F_1+8n_1) \, [1+(F_1+8n_1)^2]^{1/2} \, [5 + 2 \, (F_1+8n_1)^2] - F_1 \, [1+F_1^2]^{1/2} \, (5+2F^2) \right] \Bigg] \qquad (2.45)$$

where F, F_1, n and n_1 can be evaluated from Equations (2.18) and (2.11) respectively.

For flat curves, an approximate formula has been derived, see Appendix 11, to serve the same purpose:

$$\delta_c = \frac{\ell}{A_c E_c}\left[(1+\lambda)+\frac{3}{8}\frac{(F+4n)^2}{\lambda^3}\left[4\lambda^2(1+\lambda)+32\lambda^3 n^2(1+\omega^2\lambda)+(F+4n)^2\right.\right.$$

$$\left.\left.(1+\lambda^3)\right]+\frac{8}{5}n^2\left[5(1+\omega^2\lambda^3)+12n^2(1+\omega^4\lambda^5)\right]\right] \qquad (2.46)$$

where $\omega = \frac{W_1}{W}$ and $\lambda = \frac{\ell_1}{\ell}$

3. The gap produced by the direct forces in the suspenders δ_s

From Figures (2.9) and (2.14), it is clear that each suspender approximately carry a load equal to:

$$P_s = \frac{8f}{\ell^2}\ Hd \qquad \text{in the left hand span}$$

$$P_{s1} = \frac{8f_1}{\ell_1^{\,2}}\ Hd_1 \qquad \text{in the right hand span.}$$

Hence,

$$\delta_s = \sum \frac{1}{A_{su}E_{su}}\int N\frac{dN}{dH}\ ds = \sum \frac{1}{A_{su}E_{su}}\int P_s\frac{dP_s}{dH}\ ds$$

where $\frac{dP_s}{dH} = \frac{8f}{\ell^2}d = P_s$ at $H = 1$

$$\frac{dP_{s1}}{dH} = \frac{8f_1}{\ell_1^{\,2}}d_1 = P_{s1} \qquad \text{at } H = 1$$

Hence,

$$\delta_s = \frac{1}{E_{su}}\left(\frac{1}{A_{su}}\int_{\circ}^{1s} P_s^{\,2}\,ds + \frac{1}{A_{su1}}\int_{\circ}^{1s_1} P_{s1}^{\,2}\,ds_1\right)$$

where A_{su} and A_{sul} are the average cross sectional area of the suspenders in left and right hand spans respectively.

and E_{su} is Young's modulus of elasticity for the material of the suspenders.

Hence,

$$\delta_s = \frac{64f^2}{\ell^4} \frac{d}{A_{su}E_{su}} \sum ls + \frac{64f_1^2}{\ell_1^4} \frac{d_1}{A_{su}E_{su}} \sum ls_1$$

$$\delta_s = \frac{64f^2}{\ell^4 E_{su}} \left[\frac{d}{A_{su}} \sum ls + \frac{\omega^2 d_1}{A_{su1}} \sum ls_1 \right] \qquad (2.46a)$$

where $\sum ls$ and $\sum ls_1$ are The sum of the lengths of the suspenders in both left and right hand spans.

d and d_1 are The spacing between the suspenders in left and right hand respectively, see Figure (2.9).

$\sum ls$ and $\sum ls_1$ can be calculated directly by using Equations (2.23) which gives:

$$\sum l_s = \sum_{m=1}^{i} [Fx_m + \frac{4n}{\ell} x_m^2 - (a+z_1)] = F \left[\sum_{m=1}^{i} x_m \right] + \frac{4n}{\ell} \left[\sum_{m=1}^{i} x_m^2 \right] - i\,(a+z_1) \qquad (2.46b)$$

$$\sum ls_1 = \sum_{m=1}^{j} \left[F_1 x_{1m} + \frac{4n_1}{\ell_1} x_{1m}^2 - (a+Z_1) \right] = F_1 \left[\sum_{m=1}^{j} x_{1m} \right] + \frac{4n_1}{\ell_1} \left[\sum_{m=1}^{j} x_{1m}^2 \right] - j(a+Z_1) \qquad (2.46c)$$

where i and j are the total number of the suspenders in the left and right hand spans, Figure (2.9).

4. The gap produced by the direct force in the tower δ_T

As mentioned earlier, Equation (2.34), the total vertical force applied on the tower is found to be: (see Figure (2.15))

$$N_T = V + V_1 = H \left[(F+8n) + (F_1+8n_1) \right]$$

Hence $$\frac{dN_T}{dH} = \left[(F+8n) + (F_1+8n_1) \right]$$

Thus, $$\delta_T = \frac{1}{A_T E_T} \int_0^h N_T \frac{dN_T}{dH} \, ds$$

which at H = 1 yields:

$$\delta_T = \frac{h}{A_T E_T} \left[(F+8n) + (F_1+8n_1) \right]^2 \qquad (2.47)$$

where, h is The height of the tower above the axis of the suspended beam.

A_T and E_T are The average cross sectional area of the tower and the modulus of elasticity of the tower material (usually concrete).

Finally from Equation (2.41b), the total gap δ can be calculated. It can be proved that δ_{bn}, δ_s and δ_T are very small and may be ignored. Evidently, the cable behaviour under applied live loading is predominantly governed by the deformability of the cable δ_c and the rigidity of the suspended beam δ_{bm}. Nevertheless, δ_{bm} may also be ignored in most cases depending on the span length. We can generally calculate δ with sufficient accuracy as:

$$\delta = \delta_c + \delta_{bm} \qquad (2.48)$$

From Equations (2.45 or 2.46), it can be seen that the value of δ_c decreases with the increase of the span length. Consequently, the total value of δ decreases with the increase of the span length since it is dominated by δ_c. This will result in a larger H_p, see Equation (2.39), which explains why the interaction between the main cable and the prestressed cable suspended beam increases with the increase of the span length. In other words, δ_c can be redefined as the term which represents the flexibility of the cable. The more the span length is, the more rigid the cable becomes and accordingly the cable gains more force.

Finally, all formulae used to determine the total gap δ may be applied to cables with no eccentricities at their ends when substituting the end eccentricities zero, a = o.

2.5.2.3 The Evaluation of the Gap Δ

From Figure (2.13), the value of the gap Δ will differ according to the type, magnitude and location of the applied live loading. Therefore, it must be evaluated for each type of loading separately.

As mentioned in Section (2.4), the initial prestessing force H_i will exert upward forces which are equal, after substracting the dead loads, to γW and γW_1 in left and right hand spans. These forces are included in the calculation for Δ as their contribution can be significant to the change in the cable tension, H_p. In this section, the exact value of Δ is calculated for selected cases of loading.

a) A Concentrated Load

1. Applied in the left hand span

Figure (2.16a) shows a concentrated load P applied at a distance $t\ell$ from the left hand end support. Thus, Δ can be evaluated as: (Appendix 12)

$$\Delta = -\frac{a}{2}\left[1-\frac{(\nu_i+\nu_{1i})}{(\phi_i+\phi_{1i})}\right]\left[\frac{8f}{\ell^2}(\theta_i+\omega\theta_{1i})+a\,\mu_i^2\,[\ell(1+\lambda)+(\theta_i+\theta_{1i})]\right]$$

$$+\frac{2P}{H_i}\left[\frac{\sin\frac{\mu_i t\ell}{2}\sin\frac{\mu_i\ell}{2}(1-t)}{\cos\frac{\mu_i\ell}{2}}\left(\frac{8f}{\mu_i^2\ell^2}+a\right)-2ft(1-t)-\frac{\mu_i^2}{4}\frac{(\theta_i+\omega\theta_{1i})}{(\phi_i+\phi_{1i})}\right.$$

$$\left.\left[\frac{8f}{\mu_i^2\ell^2}+a\frac{[\ell(1+\lambda)+(\theta_i+\theta_{1i})]}{(\theta_i+\omega\theta_{1i})}\right]\left[\frac{\sin\mu_i t\ell}{\sin\mu_i\ell}-t\right]\right]-\frac{\gamma W}{H_i}\left[\frac{8f}{\ell^2}\left[\frac{1}{\mu_i^2}(\theta_i+\omega^2\theta_{1i})\right.\right.$$

$$\left.\left.-\frac{(\theta_i+\omega\theta_{1i})}{4(\phi_i+\phi_{1i})}-\frac{\ell^3}{12}(1+\omega^2\lambda^3)\right]+a(\theta_i+\omega\theta_{1i})\left[1-\frac{\mu_i^2}{4}\frac{[\ell(1+\lambda)+(\theta_i+\theta_{1i})]}{(\phi_i+\phi_{1i})}\right]\right] \tag{2.49}$$

where we have:

$$\mu_i^2 = \frac{H_i}{EI} \tag{2.50}$$

$$H_i = H_w(1+\gamma)$$

and where ν_i, ν_{1i}, ϕ_i, ϕ_{1i}, θ_i and θ_{1i} are constants which can be evaluated as follows:

$$\nu_i = \frac{1}{\ell}\left[\frac{\mu_i\ell}{\sin\mu_i\ell}-1\right] \quad , \nu_{1i} = \frac{1}{\ell_1}\left[\frac{\mu_i\ell_1}{\sin\mu_i\ell_1}-1\right] \tag{2.51a}$$

$$\phi_i = \frac{1}{\ell}\left[1-\frac{\mu_i\ell}{\tan\mu_i\ell}\right] \quad , \phi_{1i} = \frac{1}{\ell_1}\left[1-\frac{\mu_i\ell_1}{\tan\mu_i\ell_1}\right] \tag{2.51b}$$

$$\theta_i = \ell\left[\frac{\tan\frac{\mu_i\ell}{2}}{\frac{\mu_i\ell}{2}}-1\right] \quad , \theta_{1i} = \ell_1\left[\frac{\tan\frac{\mu_i\ell_1}{2}}{\frac{\mu_i\ell_1}{2}}-1\right] \tag{2.51c}$$

and where f, f_1, ω and λ can be computed from Equations (2.5), (2.7) and (2.8) respectively.

2. A concentrated load applied in the right hand span

Figure (2.16b) shows a concentrated load P_1 applied at a distance $t_1\ell_1$ from the right hand end support. Thus, Δ can be obtained from:

$$\Delta = -\frac{a}{2}\left[1-\frac{(\nu_i+\nu_{1i})}{(\phi_i+\phi_{1i})}\right]\left[\frac{8f}{\ell^2}(\theta_i+\omega\theta_{1i})+a\,\mu_i^{\,2}\,[\ell(1+\lambda)+(\theta_i+\theta_{1i})]\right]$$

$$+\frac{2P_1}{H_i}\left[\frac{\sin\frac{\mu_i t_1\ell_1}{2}\sin\frac{\mu_i\ell_1}{2}(1-t_1)}{\cos\frac{\mu_i\ell_1}{2}}\left(\frac{8f_1}{\mu_i^2\ell_1^{\,2}}+a\right)-2f_1t_1(1-t_1)-\frac{\mu_i^{\,2}}{4\omega}\frac{(\theta_i+\omega\theta_{1i})}{(\phi_i+\phi_{1i})}\right.$$

$$\left.\left[\frac{8f}{\mu_i^2\ell^2}+a\frac{[\ell\,(1+\lambda)+(\theta_i+\theta_{1i})]}{(\theta_i+\omega\theta_{1i})}\right]\left[\frac{\sin\mu_i t_1\ell_1}{\sin\mu_i\ell_1}-t_1\right]\right]-\frac{\gamma W}{H_i}\left[\frac{8f}{\ell^2}\left[\frac{1}{\mu_i^2}(\theta_i+\omega^2\theta_{1i})\right.\right.$$

$$\left.\left.-\frac{(\theta_i+\omega\theta_{1i})^2}{4\,(\phi_i+\phi_{1i})}-\frac{\ell^3}{12}\,(1+\omega^2\lambda^3)\right]+a\,(\theta_i+\omega\theta_{1i})\left[1-\frac{\mu_i^{\,2}}{4}\frac{[\ell(1+\lambda)+(\theta_i+\theta_{1i})]}{(\phi_i+\phi_{1i})}\right]\right] \qquad (2.52)$$

where Equations (2.50) and (2.51) apply.

b) A General Form of Loading

1. Applied at the left hand span

Figure (2.16c) shows a general loading σ occupying that part of the left hand span which is bounded by the distances $x = \beta\ell$ and $x = \alpha\ell$ from the left hand end support. Hence, Δ is found as: (Appendix 12)

$$\Delta = -\frac{a}{2}\left[1-\frac{(\nu_i+\nu_{1i})}{(\phi_i+\phi_{1i})}\right]\left[\frac{8f}{\ell^2}(\theta_i+\omega\theta_{1i})+a\,\mu_i^{\,2}\,[\ell(1+\lambda)+(\theta_i+\theta_{1i})]\right]$$

$$+ \frac{\sigma \ell}{H_i} \left[\left(\frac{8f}{\mu_i^2 \ell^2} + a \right) \left[\frac{[\sin \frac{\mu_i \ell}{2}(1-2\beta) - \sin \frac{\mu_i \ell}{2}(1-2\alpha)]}{\mu_i \ell \cos \frac{\mu_i \ell}{2}} - (\alpha-\beta) \right] - \frac{2}{3} f[\alpha^2(3-2\alpha) \right.$$

$$\left. - \beta^2(3-2\beta)] - \frac{\mu_i^2}{2} \frac{(\theta_i+\omega\theta_{1i})}{(\phi_i+\phi_{1i})} \left[\frac{8f}{\mu_i^2 \ell^2} + a \frac{[\ell\ (1+\lambda)+(\theta_i+\theta_{1i})]}{(\theta_i+\omega\theta_{1i})} \right] \left[\frac{(\cos\mu_i\beta\ell - \cos\mu_i\alpha\ell)}{\mu_i \ell \sin \mu_i \ell} \right. \right.$$

$$\left. \left. - \frac{1}{2} (\alpha^2-\beta^2) \right] \right] - \frac{yW}{H_i} \left[\frac{8f}{\ell^2} \left[\frac{1}{\mu_i^2} (\theta_i+\omega^2\theta_{1i}) - \frac{(\theta_i+\omega\theta_{1i})^2}{4\ (\phi_i+\phi_{1i})} - \frac{\ell^3}{12} (1+\omega^2\lambda^3) \right] \right.$$

$$\left. + a\ (\theta_i+\omega\theta_{1i}) \left[1 - \frac{\mu_i^2}{4} \frac{[\ell\ (1+\lambda) + (\theta_i+\theta_{1i})]}{(\phi_i+\phi_{1i})} \right] \right] \qquad (2.53)$$

where Equations (2.50) and (2.51) apply.

To evaluate the gap Δ for a continuous uniformly distributed load σ applied in the left hand span, we substitute $\alpha = 1$, and $\beta = o$ in the above equation.

2. <u>A general form of loading applied in the right hand span</u>

Figure (2.16d) shows a general loading σ_1 occupying that part of the right hand span which is bounded by the distances $x_1 = \beta_1 \ell_1$ and $x_1 = \alpha_1 \ell_1$ from the right hand end support. Thus, we have the gap Δ as follows:

$$\Delta = - \frac{a}{2} \left[1 - \frac{(\nu_i+\nu_{1i})}{(\phi_i+\phi_{1i})} \right] \left[\frac{8f}{\ell^2} (\theta_i+\omega\theta_{1i}) + a\ \mu_i^2\ [\ell(1+\lambda) + (\theta_i+\theta_{1i})] \right]$$

$$+ \frac{\sigma_1 \ell_1}{H_i} \left[\left(\frac{8f_1}{\mu_i^2 \ell_1^2} + a \right) \left[\frac{[\sin \frac{\mu_i \ell_1}{2}(1-2\beta_1) - \sin \frac{\mu_i \ell_1}{2}(1-2\alpha_1)]}{\mu_i \ell_1 \cos \frac{\mu_i \ell_1}{2}} - (\alpha_1-\beta_1) \right] \right.$$

$$- \frac{2}{3} f_1 \left[\alpha_1^2 (3-2\alpha_1) - \beta_1^2 (3-2\beta_1)\right] - \frac{\mu_i^2}{2\omega} \frac{(\theta_i+\omega\theta_{1i})}{(\phi_i+\phi_{1i})} \left[\frac{8f}{\mu_i^2 \ell^2} + a \right.$$

$$\left. \frac{[\ell(1+\lambda) + (\theta_i+\theta_{1i})]}{(\theta_i+\omega\theta_{1i})} \right] \left[\frac{(\cos \mu_i\beta_1\ell_1 - \cos \mu_i\alpha_1\ell_1)}{\mu_i\ell_1 \sin \mu_i\ell_1} - \frac{1}{2} (\alpha_1^2-\beta_1^2) \right] \Bigg]$$

$$- \frac{yW}{H_i} \left[\frac{8f}{\ell^2} \left[\frac{1}{\mu_i^2} (\theta_i+\omega^2\theta_{1i}) - \frac{(\theta_i+\omega\theta_{1i})^2}{4 (\phi_i+\phi_{1i})} - \frac{\ell^3}{12} (1+\omega^2\lambda^3) \right] + a (\theta_i+\omega\theta_{1i}) \right.$$

$$\left. \left[1 - \frac{\mu_i^2}{4} \frac{[\ell (1+\lambda) + (\theta_i+\theta_{1i})]}{(\phi_i+\phi_{1i})} \right] \right] \qquad (2.54)$$

where Equations (2.50) and (2.51) apply.

To evaluate Δ for a continuous uniformly distributed load σ_1 applied in the right hand span, we substitute $\alpha_1 = 1$ and $\beta_1 = o$ in the above equations. The derivation of Δ for a general case of loading is given in Appendix 12. Moreover, this expression is used to obtain Δ for a concentrated load in the same appendix.

As mentioned earlier, Formulae (2.49 - 2.54) are applicable to cables with no eccentricities at their ends when substituting a = o. Furthermore, H_p can be calculated after the time effects take place by replacing y by τ in the above formulae.

Finally, Formulae (2.49 - 2.54) can also be used to calculate H_p for practically every possible case of live loading. This can be achieved by using the principle of superposition for cases such as series of concentrated forces applied in both spans, different combinations of loading, ...etc.

2.5.3 The Modified Timoshenko's Approach

2.5.3.1 The Principle Used

Figure (2.17) shows an arbitrary element of the cable which has the length (ab = ds) before applying the live load. It elongates after applying the live load and its length becomes ($a'b'$ = ds+Δds). η and ξ are the vertical and horizontal displacements of point a.

The initial length of the element (ab) is obtained from the equation:

$$(ds)^2 = (dx)^2 + (dy)^2 \qquad \text{(i)}$$

The length of the same element after the application of live load is found from the equation:

$$(ds+\Delta ds)^2 = (dx+d\xi)^2 + (dy+d\eta)^2 \qquad \text{(ii)}$$

where Δds is the elongation of the element produced by live load and can be computed as follows, Figure (2.17):

$$\frac{\Delta ds}{ds} = \frac{T_p}{A_c E_c}$$

where T_p is the part of tensile force in the cable produced by live load.

Thus, similarly to Equations (2.13) we have:

$$T_p = H_p \left[1 + \left(\frac{dy}{dx} + \frac{d\eta}{dx} \right)^2 \right]^{1/2}$$

Neglecting the small change in the slopes of the cable produced by live load, $\frac{d\eta}{dx}$, (see Section 2.5.3.4) we have:

$$\Delta ds = \frac{H_p}{A_c E_c} \quad ds \, \frac{ds}{dx} \qquad \text{(iii)}$$

Since T_p is usually much smaller than T_i, = $H_i \frac{ds}{dx}$, the elongation

Δds is small and therefore $(\Delta ds)^2$ in Equation (ii) can be ignored. For the same reason, and from the fact that the cable exhibits a flat curve, we also neglect $(d\xi)^2$ in the same equation. Therefore, we obtain from Equations (i) and (ii):

$$ds\Delta ds = dx d\xi + dy d\eta + \frac{1}{2}(d\eta)^2$$

which yields:

$$d\xi = \frac{ds}{dx}\ \Delta ds - \frac{dy}{dx}\ d\eta + \frac{1}{2}\frac{d\eta}{dx}\ d\eta \qquad \text{(iv)}$$

Substituting from Equation (iii) in this equation and integrating, we obtain:

$$\xi = \frac{H_p}{A_c E_c}\int_o^x \left[\frac{ds}{dx}\right]^3 dx - \int_o^x \frac{dy}{dx}\frac{d\eta}{dx}\,dx + \frac{1}{2}\int_o^x \left[\frac{d\eta}{dx}\right]^2 dx \qquad (2.55)$$

If we perform this integration over the whole span length ℓ, ξ would vanish at the ends of the cable. Thus, we obtain:

$$\frac{H_p}{A_c E_c}\int_o^\ell \left[\frac{ds}{dx}\right]^3 dx = \int_o^\ell \frac{dy}{dx}\frac{d\eta}{dx}\,dx + \frac{1}{2}\int_o^\ell \left[\frac{d\eta}{dx}\right]^2 dx \qquad \text{(v)}$$

By making integration by parts to the first term of the right hand side of the equation, we have:

$$\int_o^\ell \frac{dy}{dx}\ \frac{d\eta}{dx}\,dx = \left[\frac{dy}{dx}\,\eta\right]_o^\ell - \int_o^\ell \frac{d^2y}{dx^2}\ \eta dx = +\frac{W}{H_w}\int_o^\ell \eta\,dx$$

where the deflection vanishes at the ends of the cable ($x = o, \ell$) and $\frac{d^2y}{dx^2} = -\frac{W}{H_w}$.

Hence, substituting back into equation (v) and by expanding it over both spans of the suspended beam we have:

$$\frac{H_p}{A_c E_c}\sum\int \left[\frac{ds}{dx}\right]^3 dx = \sum \frac{W}{H_w}\int \eta dx + \frac{1}{2}\ \sum\int \left[\frac{d\eta}{dx}\right]^2 dx \qquad (2.56)$$

As will be shown in Section 2.5.3.4, the magnitude of the second term of the right hand side of this equation is almost negligable when compared with the first term. Thus, we have the final expression for the change in the cable tension due to live load as:

$$\frac{H_p}{A_c E_c} \sum \int \left(\frac{ds}{dx} \right)^3 dx = \sum \frac{W}{H_w} \int \eta dx \qquad (2.57)$$

Obviously, the term of the left hand side of this equation is equal to $H_p \delta_c$ where,

$$\delta_c = \frac{1}{A_c E_c} \sum \int \left(\frac{ds}{dx} \right)^3 dx$$

and can be calculated directly by using Equation (2.45) for an exact value or Equation (2.46) for an approximate one.

2.5.3.2 The Evaluation of the term $\left(\sum \frac{W}{Hw} \int \eta dx \right)$

This term is calculated for both spans as,

$$\sum \frac{W}{H_w} \int \eta dx = \frac{W}{H_w} \left[\int_o^{\ell} \eta dx + \omega \int_o^{\ell_1} \eta_1 dx_1 \right] \qquad (2.58)$$

The prestressing force in the structure is equal to H after applying the live load where:

$$H = H_i + H_p = H_w (1 + \gamma) + H_p$$

For simplicity, let:

$$H = H_w (1 + \gamma + \rho) \qquad (2.59)$$

where $$\rho = \frac{H_p}{H_w} \qquad (2.60)$$

The total upward forces exerted on the suspended beam, after subtracting the dead loads, are $W\ (y+\rho)$ and $W_1\ (y+\rho)$ for left and right hand spans respectively. These forces must be included in the calculation as their contribution can be significant to the total value of the term $\left[\sum \frac{W}{H_w} \int \eta dx \right]$. In this section, the value of the term $\left[\sum \frac{W}{H_w} \int \eta dx \right]$ is given for selected cases of loading.

a. <u>A Concentrated Load</u>

1. <u>Applied in the left hand span</u>

Figure (2.18a) shows a concentrated load P applied at a distance $t\ell$ from the left hand end support. Thus the term $\left[\sum \frac{W}{H_w} \int \eta dx \right]$ is found as:

$$\sum \frac{W}{H_w} \int \eta dx = \frac{W}{H_w} \left[- \frac{a}{2} (\theta+\omega\theta_1) \left[1 - \frac{(\nu+\nu_1)}{(\phi+\phi_1)} \right] + \frac{2P}{H} \left[\frac{\sin \frac{\mu t \ell}{2} \sin \frac{\mu \ell}{2}(1-t)}{\mu^2 \cos \frac{\mu \ell}{2}} \right.\right.$$

$$\left. - \frac{t\ell^2}{4} (1-t) - \frac{(\theta+\omega\theta_1)}{4\ (\phi+\phi_1)} \left[\frac{\sin \mu t \ell}{\sin \mu \ell} - t \right] \right] - \frac{W\ (y+\rho)}{H} \left[\frac{1}{\mu^2} (\theta+\omega^2\theta_1) \right.$$

$$\left.\left. - \frac{(\theta+\omega\theta_1)^2}{4\ (\phi+\phi_1)} - \frac{\ell^3}{12} (1+\omega^2\lambda^3) \right] \right] \qquad (2.61)$$

where we have:

$$\mu^2 = \frac{H}{EI} \qquad (2.62)$$

$$H = H_w\ (1+y+\rho) \quad \text{and} \quad \rho = \frac{p}{H_w}$$

and where similarly to Equations (2.51), we have the constants ν, ν_1, ϕ, ϕ_1, θ and θ_1 as follows:

$$\nu = \frac{1}{\ell} \left[\frac{\mu \ell}{\sin \mu \ell} - 1 \right] \quad , \qquad \nu_1 = \frac{1}{\ell_1} \left[\frac{\mu \ell_1}{\sin \mu \ell_1} - 1 \right] \qquad (2.63a)$$

$$\phi = \frac{1}{\ell}\left[1 - \frac{\mu\ell}{\tan \mu\ell}\right] \quad , \quad \phi_1 = \frac{1}{\ell_1}\left[1 - \frac{\mu\ell_1}{\tan \mu\ell_1}\right] \tag{2.63b}$$

$$\theta = \ell\left[\frac{\tan \frac{\mu\ell}{2}}{\frac{\mu\ell}{2}} - 1\right] \quad , \quad \theta_1 = \ell_1\left[\frac{\tan \frac{\mu\ell_1}{2}}{\frac{\mu\ell_1}{2}} - 1\right] \tag{2.63c}$$

and where $\omega = \frac{W_1}{W}$ and $\lambda = \frac{\ell_1}{\ell}$

2. <u>A concentrated load applied in the right hand span</u>

Figure (2.18b) shows a concentrated load P_1 applied at a distance $t_1\ell_1$ from the right hand end support. Thus, we have:

$$\sum \frac{W}{H_w}\int \eta dx = \frac{W}{H_w}\left[-\frac{a}{2}(\theta+\omega\theta_1)\left[1 - \frac{(\nu+\nu_1)}{(\phi+\phi_1)}\right] + \frac{2\omega P_1}{H}\left[\frac{\sin \frac{\mu t_1\ell_1}{2} \sin \frac{\mu\ell_1}{2}(1-t_1)}{\mu^2 \cos \frac{\mu\ell_1}{2}}\right.\right.$$

$$\left. - \frac{t_1\ell_1^2}{4}(1-t) - \frac{(\theta+\omega\theta_1)}{4(\phi+\phi_1)}\left(\frac{\sin \mu t_1\ell_1}{\sin \mu\ell_1} - t\right)\right] - \frac{W(y+\rho)}{H}\left[\frac{1}{\mu^2}(\theta+\omega^2\theta_1)\right.$$

$$\left.\left. - \frac{(\theta+\omega\theta_1)^2}{4(\phi+\phi_1)} - \frac{\ell^3}{12}(1+\omega^2\lambda^3)\right]\right] \tag{2.64}$$

where Equations (2.62) and (2.63) apply.

b. <u>A General Form of Loading</u>

1. <u>Applied in the left hand span</u>

Figure (2.18c) shows a general load σ occupying that part of the left hand span which is bounded by the distances $x = \beta\ell$ and $x = \alpha\ell$ from the left hand end support. Thus, we have:

$$\sum \frac{W}{H_w}\int \eta dx = \frac{W}{H_w}\left[-\frac{a}{2}(\theta+\omega\theta_1)\left[1 - \frac{(\nu+\nu_1)}{(\phi+\phi_1)}\right] + \frac{\sigma\ell}{H}\left[\frac{1}{\mu^2}\left[\frac{[\sin \frac{\mu\ell}{2}(1-2\beta) - \sin \frac{\mu\ell}{2}(1-\alpha)]}{\mu\ell \cos \frac{\mu\ell}{2}}\right.\right.\right.$$

$$- (\alpha-\beta)\Big] - \frac{\ell^2}{12}\left[\alpha^2(3-2\alpha)-\beta^2(3-2\beta)\right] - \frac{(\theta+\omega\theta_1)}{4(\phi+\phi_1)}\left[\frac{2(\cos\mu\beta\ell - \cos\mu\alpha\ell)}{\mu\ell\sin\mu\ell}\right.$$

$$\left. - (\alpha^2-\beta^2)\right]\Big] - \frac{W(y+\rho)}{H}\left[\frac{1}{\mu^2}(\theta+\omega^2\theta_1) - \frac{(\theta+\omega\theta_1)^2}{4(\phi+\phi_1)} - \frac{\ell^3}{12}(1+\omega^2\lambda^3)\right]\Big] \tag{2.65}$$

where Equations (2.62) and (2.63) apply.

To evaluate the term $\left(\sum \frac{W}{H_w}\int \eta dx\right)$ for a continuous uniformly distributed load σ applied in the left hand span, we substitute $\alpha = 1$ and $\beta = o$ in the above equation.

2. A general load applied in the right hand span

Figure (2.18d) shows a general load σ_1 occupying that part of the right hand span which is bounded by the distances $x_1 = \beta_1\ell_1$ and $x_1 = \alpha_1\ell_1$ from the right hand end support. Thus, we have:

$$\sum \frac{W}{H_w}\int \eta dx = \frac{W}{H_w}\Bigg[- \frac{a}{2}(\theta+\omega\theta_1)\left[1 - \frac{(\nu+\nu_1)}{(\phi+\phi_1)}\right] + \frac{\omega\sigma_1\ell_1}{H}\left[\frac{1}{\mu^2}\left[\frac{[\sin\frac{\mu\ell}{2}1(1-2\beta_1) - \sin\frac{\mu\ell}{2}1(1-\alpha_1)]}{\mu\ell_1\cos\frac{\mu\ell}{2}1}\right.\right.$$

$$\left. - (\alpha_1-\beta_1)\right] - \frac{\ell_1^2}{12}\left[\alpha_1^2(3-2\alpha_1)-\beta_1^2(3-2\beta_1)\right] - \frac{(\theta+\omega\theta_1)}{4\omega(\phi+\phi_1)}\left[\frac{2(\cos\mu\beta_1\ell_1 - \cos\mu\alpha_1\ell_1)}{\mu\ell_1\sin\mu\ell_1}\right.$$

$$\left.\left. - (\alpha_1^2-\beta_1^2)\right]\right] - \frac{W(y+\rho)}{H}\left[\frac{1}{\mu^2}(\theta+\omega^2\theta_1) - \frac{(\theta+\omega\theta_1)^2}{4(\phi+\phi_1)} - \frac{\ell^3}{12}(1+\omega^2\lambda^3)\right]\Bigg] \tag{2.66}$$

where Equations (2.62) and (2.63) apply.

To evaluate the term $\left(\sum \frac{W}{H_w}\int \eta dx\right)$ for a continuous uniformly

distributed load σ_1 applied in the right hand span, substitute $\alpha_1 = 1$ and $\beta_1 = o$ in the above equation.

The derivation of the term $\left(\sum \frac{W}{H_w} \int \eta dx \right)$ is given for a general case of loading in Appendix 13. The case of a concentrated load is also shown in the same appendix as a special case to the general formula. Formulae (2.61 - 2.66) can be used to determine the term $\left(\sum \frac{W}{H_w} \int \eta dx \right)$ for any combination of live loading by using the principle of superposition The above formulae can also be used to evaluate this term for suspended beams with cables having no eccentricities at their ends, a = o.

Finally the term $\left(\sum \frac{W}{H_w} \int \eta dx \right)$, after the time effects take place, can be calculated when replacing y by τ in Formulae (2.61 - 2.66).

2.5.3.3 The Determination of the Change in the Cable Tension due to the Applied Live Load

H_p can be calculated from Equation (2.57), where:

$$H_p = \frac{1}{\delta_c} \sum \frac{W}{H_w} \int \eta dx$$

However, when substituting from Formulae (2.61 - 66), we will find that H_p appears on both sides of the equation and hence it can only be obtained by successive approximations. We start by neglecting H_p on the right hand side of the equation. Then, (ρ = o) and the quantities H, μ, ν, ν_1, ϕ, ϕ_1, θ and θ_1 will be equal to those quantities which can be found from Equations (2.50) and (2.51) respectively. This will give a value for H_p as the first approximation. Substituting this value is Equations (2.62) and (2.63), H can be found as well as μ, ν, ν_1, ϕ, ϕ_1, θ and θ_1. Consequently, a second value for H_p can be obtained which is usually accurate enough for practical applica-

tion. Nevertheless, if more accuracy is required, the whole procedure can be repeated and further approximations can be determined in the same manner.

2.5.3.4 The Accuracy of Timoshenko's Approach

In this section, we investigate the accuracy of Equations (2.56) and (2.57) and the magnitude of error caused by neglecting various small quantities during their derivation.

We begin with the discussion of the cable elongation. In the derivation of Expression (iii) of Section 2.5.3.1, the change in the cable slope produced by live load has been ignored. Taking it into account, we have:

$$\Delta ds = \frac{H_p ds}{A_c E_c} \left[1 + \left(\frac{dy}{dx} + \frac{d\eta}{dx} \right)^2 \right]^{1/2}$$

But since $\frac{dy}{dx}$ and $\frac{d\eta}{dx}$ are small quantities, hence:

$$\left[1 + \left(\frac{dy}{dx} + \frac{d\eta}{dx} \right)^2 \right]^{1/2} \approx 1 + \frac{1}{2} \left(\frac{dy}{dx} + \frac{d\eta}{dx} \right)^2 \approx \frac{ds}{dx} + \frac{dy}{dx}\frac{d\eta}{dx} + \frac{1}{2} \left(\frac{d\eta}{dx} \right)^2$$

(see Maclaurin's expansions in Appendix 2)

$$\text{Hence: } \Delta ds \approx \frac{H_p ds}{A_c E_c} \left[\frac{ds}{dx} + \frac{dy}{dx}\frac{d\eta}{dx} + \frac{1}{2} \left(\frac{d\eta}{dx} \right)^2 \right]$$

Using this more accurate expression for Δds we obtain, instead of Equation (2.56):

$$\frac{H_p}{A_c E_c} \sum \int \left(\frac{ds}{dx} \right)^3 dx = \sum \frac{W}{H_w} \int \eta dx + \frac{1}{2} \sum \int \left(\frac{d\eta}{dx} \right)^2 dx - \frac{H_p}{A_c E_c} \sum \int \left(\frac{ds}{dx} \right)^2 \left[\frac{dy}{dx}\frac{d\eta}{dx} + \frac{1}{2} \left(\frac{d\eta}{dx} \right)^2 \right] dx \qquad (2.67)$$

Where the last term on the right hand side of the equation represents the required correction. Since $\frac{H_p}{A_c E_c}$ is usually a very small quantity,

therefore we conclude that the error introduced by this term can be disregarded in a practical analysis.

We know that the horizontal displacement ξ of the cable does not affect the value of H_p because it vanishes when integrating its equation over the span length. However, ξ slightly affects the values of the bending moment within the span length. To determine this effect, it is shown in Figure (2.17) that the downward vertical displacement of point

'a' is actually $\left(\eta - \xi \frac{dy}{dx}\right)$. We also note that every element of loading transmitted to the cable is equal to $\left(H \frac{d^2y}{dx^2} dx\right)$. Hence, when displacing this element from its original position by a small distance ξ a small moment will be generated for each element which is $\left(\xi H \frac{d^2y}{dx^2} dx\right)$ Therefore, the additional bending moment equation moment produced by ξ is found to be:

$$M_\xi = H\xi \frac{dy}{dx} - \frac{WH}{H_w} \int_o^x \xi \, dx \qquad (2.68a)$$

$$M_{\xi 1} = H\xi_1 \frac{dy_1}{dx_1} - \frac{W_1 H}{H_w} \int_o^x \xi_1 \, dx_1 \qquad (2.68b)$$

for the left and right hand spans respectively. To take this additional moment into consideration, we must find the value of H_p from Equation (2.57) and then the deflection equations for the suspended beam can be written. Thus, by using Equation (2.55), the expressions for ξ and ξ_1 can be obtained for left and right hand spans. Substituting these expressions $\frac{dy}{dx}$ and $\frac{dy}{dx}$ into Equations (2.68) and knowing $M\xi$ and $M\xi_1$ can be obtained. However, these additional moments are very small, because of the flatness of the main cable, and can be ignored for practical analysis.

Finally, in Equation (2.57), the term $\frac{1}{2} \sum \int \left(\frac{d\eta}{dx}\right)^2 dx$ was

ignored. It is worth noting that this term represents the effect of the shortening of the beam length due to the applied axial, prestressing, force. The value of this term is given, Appendix 14, for a concnetrated load P applied in the left hand span as follows, Figure (2.18a):

$$\frac{1}{2} \sum \int \left(\frac{d\eta}{dx} \right)^2 dx = \frac{1}{4} \left(\frac{M^2}{H^2} + a^2 \right) \left[2 \left(\nu + \nu_1 \right) + \ell \left(\nu^2 + \lambda \nu_1^2 \right) - \left(\phi + \phi_1 \right) \right]$$

$$- \frac{Ma}{2H} \left[2 \left(\nu + \nu_1 \right) - \ell \left(\phi\nu + \lambda \phi_1 \nu_1 \right) - \left(\phi + \phi_1 \right) \right]$$

$$+ \frac{W (y+\rho)}{4H^2} \left(M + Ha \right) \left[\nu\ell(\ell+\theta) + \omega \nu_1 \ell_1 \left(\ell_1 + \theta_1 \right) - 2 \left(\theta + \omega\theta_1 \right) \right]$$

$$+ \frac{W^2 (y+\rho)^2}{24 \mu^2 H^2} \left[6 \nu\ell \left(\ell + \theta \right) + 6\omega^2 \nu_1 \ell_1 (\ell_1 + \theta_1) - 24(\theta + \omega^2 \theta_1) + \mu^2 \ell^3 \left(1 + \omega^2 \lambda^3 \right) \right]$$

$$+ \frac{2P\ell^4}{\pi E^2 I^2} \sum_{m=1,2,3}^{\infty} \frac{\sin m \pi t}{m \left[m^2\pi^2 - \mu^2\ell^2 \right]^2} \left[(-1)^m M - Ha - \frac{2W (y+\rho) \ell^2}{m^2\pi^2} \sin^2 \frac{m\pi}{2} \right.$$

$$\left. + \frac{P\ell}{2m\pi} \sin m\pi t \right] \qquad (2.69a)$$

where $$M = - Ha \frac{(\nu + \nu_1)}{(\phi + \phi_1)} + \frac{P}{(\phi + \phi_1)} \left[\frac{\sin \mu t \ell}{\sin \mu \ell} - t \right] - \frac{W}{2} (y+\rho) \frac{(\theta + \omega\theta_1)}{(\phi + \phi_1)}$$

(2.69b)

and Equations (2.62) and (2.63) can be used to find the quantities μ, ρ, ν, ν_1, ϕ, ϕ_1, θ and θ_1.

For a concentrated load P_1 applied in the right hand span, we have, Figure (2.18b):

$$\frac{1}{2} \sum \int \left(\frac{d\eta}{dx} \right)^2 dx = \frac{1}{4} \left(\frac{M^2}{H^2} + a^2 \right) \left[2 \left(\nu + \nu_1 \right) + \ell \left(\nu^2 + \lambda \nu_1^2 \right) - \left(\phi + \phi_1 \right) \right]$$

$$- \frac{Ma}{2H} \left[2 \left(\nu + \nu_1 \right) - \ell \left(\phi\nu + \lambda \phi_1 \nu_1 \right) - \left(\phi + \phi_1 \right) \right]$$

$$+ \frac{W\ (y+\rho)}{4H^2}\ (M+Ha)\ \left[\ \nu\ell\ (\ell+\theta) + \omega\ \nu_1\ell_1\ (\ell_1+\theta_1) - 2\ (\theta+\omega\theta_1)\ \right]$$

$$+ \frac{W^2(y+\rho)^2}{24\ \mu^2\ H^2}\ [6\ \nu\ell\ (\ell+\theta) + 6\omega^2\ \nu_1\ell_1\ (\ell_1+\theta_1) - 24(\theta+\omega^2\theta_1) + \mu^2\ell^3(1+\omega^2\lambda^3)]$$

$$+ \frac{2P_1\ell_1^4}{\pi\ E^2I^2} \sum_{m=1,2,3}^{\infty} \frac{\sin\ m\ \pi\ t_1}{m\ [m^2\pi^2 - \mu^2\ell_1^2\ ]^2}\ \left[\ (-1)^m\ M - Ha - \frac{2W_1(y+P)^2\ell_1}{m^2\pi^2} \sin^2\frac{m\pi}{2}\right.$$

$$\left. + \frac{P_1\ell_1}{2m\pi}\ \sin\ m\pi t_1\ \right] \qquad (2.70a)$$

$$\text{where } M = - Ha\ \frac{(\nu+\nu_1)}{(\phi+\phi_1)} + \frac{P_1}{(\phi+\phi_1)}\ \left[\ \frac{\sin\ \mu t_1\ell_1}{\sin\ \mu\ell_1} - t_1\right] - \frac{W}{2}\ (y+\rho)\ \frac{(\theta+\omega\theta_1)}{(\phi+\phi_1)} \qquad (2.70b)$$

For a general case of loading σ applied in the left hand span, we have as shown in Figure (2.18c):

$$\frac{1}{2}\ \sum \int \left(\frac{d\eta}{dx}\right)^2 dx = \frac{1}{4}\left[\ \frac{M^2}{H^2} + a^2\ \right]\ [2\ (\nu+\nu_1) + \ell\ (\nu^2+\lambda\nu_1^2\ ) - (\phi+\phi_1)\ ]$$

$$- \frac{Ma}{2H}\ \left[2\ (\nu+\nu_1) - \ell\ (\phi\nu+\lambda\phi_1\nu_1) - (\phi+\phi_1)\ \right]$$

$$+ \frac{W\ (y+\rho)}{4H^2}\ (M+Ha)\ \left[\ \nu\ell\ (\ell+\theta) + \omega\ \nu_1\ell_1\ (\ell_1+\theta_1) - 2\ (\theta+\omega\theta_1)\ \right]$$

$$+ \frac{W^2(y+\rho)^2}{24\ \mu^2\ H^2}\ [6\ \nu\ell\ (\ell+\theta) + 6\omega^2\ \nu_1\ell_1\ (\ell_1+\theta_1) - 24(\theta+\omega^2\theta_1) + \mu^2\ell^3(1+\omega^2\lambda^3)]$$

$$+ \frac{2\sigma\ell^5}{\pi^2E^2I^2} \sum_{m=1,2,3}^{\infty} \frac{(\cos\ m\pi\beta - \cos\ m\pi\alpha)}{m^2\left[m^2\pi^2 - \mu^2\ell^2\ \right]^2}\ \left[(-1)^m\ M - Ha - \frac{2W\ (y+\rho)\ell^2}{m^2\pi^2} \sin^2\frac{m\pi}{2}\right.$$

$$\left. + \frac{\sigma^2\ell}{2m^2\pi^2}\ \ (\cos\ m\pi\beta - \cos\ m\pi\alpha)\ \right] \qquad (2.71a)$$

$$\text{where } M = - Ha\ \frac{(\nu+\nu_1)}{(\phi+\phi_1)} + \frac{\sigma\ell}{2(\phi+\phi_1)}\ \left[\frac{2\ [\cos\ \mu\beta\ell - \cos\ \mu\alpha\ell]}{\mu\ell\ \sin\ \mu\ell} - (\alpha^2-\beta^2)\ \right].$$

$$- \frac{W}{2} (\gamma + \rho) \frac{(\theta+\omega\theta_1)}{(\phi+\phi_1)} \qquad (2.71b)$$

For a general loading σ_1 applied in the right hand span, we have as shown in Figure (2.18d):

$$\frac{1}{2} \sum \int \left(\frac{d\eta}{dx} \right)^2 dx = \frac{1}{4} \left[\frac{M^2}{H^2} + a^2 \right] \left[2 (\nu+\nu_1) + \ell (\nu^2+\lambda\nu_1^2) - (\phi+\phi_1) \right]$$

$$- \frac{Ma}{2H} \left[2 (\nu+\nu_1) - \ell (\phi\nu+\lambda\phi_1\nu_1) - (\phi+\phi_1) \right]$$

$$+ \frac{W (\gamma+\rho)}{4H^2} (M + Ha) \left[\nu\ell (\ell+\theta) + \omega \nu_1\ell_1 (\ell_1+\theta_1) - 2 (\theta+\omega\theta_1) \right]$$

$$+ \frac{W^2(\gamma+\rho)^2}{24 \mu^2 H^2} \left[6 \nu\ell (\ell+\theta) + 6\omega^2 \nu_1\ell_1 (\ell_1+\theta_1) - 24(\theta+\omega^2\theta_1) + \mu^2\ell^3(1+\omega^2\lambda^3)\right]$$

$$+ \frac{2\sigma\ell_1^5}{\pi^2E^2I^2} \sum_{m=1,2,3}^{\infty} \frac{(\cos m\pi\beta_1 - \cos m\pi\alpha_1)}{m^2\left[m^2\pi^2 - \mu^2\ell_1^2\right]^2} \left[(-1)^m M - Ha - \frac{2W_1(\gamma+\rho)\ell_1^2}{m^2\pi^2} \sin^2 \frac{m\pi}{2}\right.$$

$$\left. + \frac{\sigma_1\ell_1^2}{2m^2\pi^2} (\cos m\pi\beta_1 - \cos m\pi\alpha_1) \right] \qquad (2.72a)$$

where $M = - Ha \frac{(\nu+\nu_1)}{(\phi+\phi_1)} + \frac{\sigma_1\ell_1}{2(\phi+\phi_1)} \left[\frac{2 [\cos \mu\beta_1\ell_1 - \cos \mu\alpha_1\ell_1]}{\mu\ell_1 \sin \mu\ell_1} - (\alpha_1^2 - \beta_1^2) \right]$

$$- \frac{W}{2} (\gamma + \rho) \frac{(\theta+\omega\theta_1)}{(\phi+\phi_1)} \qquad (2.72b)$$

For a continuous uniformly distributed load σ applied in the left hand span, substitute $\alpha = 1$ and $\beta = o$ in Equations (2.71). Similarly, for a continuous uniformly distributed load σ_1 applied in the right hand span, substitute $\alpha_1 = 1$ and $\beta_1 = o$ in Equations (2.72).

The effect of the term $\left(\frac{1}{2} \sum \int \left(\frac{d\eta}{dx} \right)^2 dx \right)$ when included in the

calculation for H_p, does not exceed 5% and therefore, it may be ignored in a practical application.

2.5.4 Comparison Between the Steinman and Timoshenko Approaches

Starting with Steinman's approach, (20), we find that the method entirely ignores the effect of the change in the horizontal tension, H_p, on the stress state of the structure when computing H_p. This effect does change the upward forces by amounts ρW and ρW_1 in the left and right hand spans. It also changes the magnitude of the prestressing force which consequently affects its value.

One of the advantages of using Steinman's approach is that it takes into account the effect of the axial deformation of the suspended beam, the suspenders and the tower as well as the cable when calculating H_p. Moreover, a final answer can be obtained for the change in the prestressing force, H_p, without the need for any iterative methods.

Timoshenko's approach (23 - 26) however, takes into account the deformation of the cable alone when calculating H_p. This can be explained as the cable deformation is the dominating value compared with the negligible deformations of the rest of the structure. The method also takes into account the internal forces produced by H_p. The final value of the change in the prestressing force, H_p, is obtained after undertaking an iterative method as mentioned earlier.

The values of H_p when calculated for the test beams, Sections 7.5 and 7.6, have been found to be within 15% of the measured ones when using both approaches. However, Timoshenko's approach gave results in closer agreement with the experimental ones as shown in Figure (2.19). Moreover, when including the term $\left[\frac{1}{2}\sum\int\left(\frac{d\eta}{dx}\right)^2 dx\right]$ in the calculations, the calculated results came within about 9% of the measured ones.

Finally, we conclude that for prestressed concrete suspension bridges with short to medium spans, both approaches can be used to calculate the change in the cable tension, H_p, due to live loading with sufficient accuracy. However, for long and very long spans, only Timoshenko's approach can be applied due to the increased significance of the effect of the internal forces produced by H_p on the structural system.

2.6 Computation of the Internal Forces of the Structure

Having found the value of the change in the cable tension, H_p, due to live loading, it is easy to determine the internal forces for the various parts of the structure. In other words, the internal forces will be evaluated for the prestressed cable suspended beam, the suspenders and the tower in this section. For the prestressed cable suspended beam, the internal forces, which are the bending moments and the shear forces, are given in the form of equations covering any section of the beam in both spans. Furthermore, the deflection equations are also given so that the designer can check the value of deflections at any section of the prestressed cable suspended beam. Finally, these design equations are given in order of importance for the designer, i.e. bending moments, deflections and shear forces.

2.6.1 The Bending Moments, Deflections and Shear Forces of the Suspended Beam

In this section, the bending moments, deflections and shear forces equations have been derived for the same selected cases of loading shown in Section 2.5. The derivation is based on the fundamental relationships shown in Equations (2.1). In other words, the bending moments and shear forces equations have been formulated by using the obtained deflections equations as shown in Appendices 12 and 13.

2.6.1.1 For a Concentrated Load

a. Applied in the left hand span

For a concentrated load P applied at a distance tℓ from the left hand end support, see Figure (2.18a), the bending moment equations for the left hand span are:

$$M_{x(1)} = \frac{Ha}{\sin \mu\ell}\left[\sin \mu(\ell-x) - \frac{(\nu+\nu_1)}{(\phi+\phi_1)} \sin \mu x\right] - \frac{P}{\mu} \frac{\sin \mu x}{\sin \mu\ell}$$

$$\left[\sin \mu\ell(1-t) - \frac{\mu}{(\phi+\phi_1)}\left[\frac{\sin \mu t\ell}{\sin \mu\ell} - t\right]\right] + \frac{W(y+\rho)}{\mu^2 \sin \mu\ell}\left[\sin \mu x\right.$$

$$\left.\left[1 - \frac{\mu^2}{2} \frac{(\theta+\omega\theta_1)}{(\phi+\phi_1)}\right] + \sin \mu(\ell-x) - \sin \mu\ell\right] \qquad o \leqslant x \leqslant t\ell$$

(2.73a)

$$M_{x(2)} = \frac{Ha}{\sin \mu\ell}\left[\sin \mu(\ell-x) - \frac{(\nu+\nu_1)}{(\phi+\phi_1)} \sin \mu x\right] - \frac{P}{\mu \sin \mu\ell}\left[\sin \mu t\ell\right.$$

$$\sin \mu(\ell-x) - \frac{\mu}{(\phi+\phi_1)} \sin \mu x\left[\frac{\sin \mu t\ell}{\sin \mu\ell} - t\right]\left] + \frac{W(y+\rho)}{\mu^2 \sin \mu\ell}\right[\sin \mu x$$

$$\left[1 - \frac{\mu^2}{2} \frac{(\theta+\omega\theta_1)}{(\phi+\phi_1)}\right] + \sin \mu(\ell-x) - \sin \mu\ell\left] \qquad t\ell \leqslant x \leqslant \ell\right.$$

(2.73b)

and for the right hand span:

$$M_{x1} = \frac{Ha}{\sin \mu\ell_1}\left[\sin \mu(\ell_1-x_1) - \frac{(\nu+\nu_1)}{(\phi+\phi_1)} \sin \mu x_1\right] + \frac{P}{(\phi+\phi_1)} \frac{\sin \mu x_1}{\sin \mu\ell_1}$$

$$\left[\frac{\sin \mu t\ell}{\sin \mu\ell} - t\right] + \frac{W_1(y+\rho)}{\mu^2 \sin \mu\ell_1}\left[\sin \mu x_1\left[1 - \frac{\mu^2}{2\omega} \frac{(\theta+\omega\theta_1)}{(\phi+\phi_1)}\right]\right.$$

$$+ \sin \mu(\ell_1 - x_1) - \sin \mu \ell_1 \Bigg] \qquad 0 \leqslant x_1 \leqslant \ell_1$$

(2.73c)

where the constants ρ, μ, ν, ν_1, ϕ, ϕ_1, Θ and Θ_1 can be calculated from Equations (2.62) and (2.63). Hence, the values of the bending moments can then be used to evaluate the stresses at any section of the beam from the following equations:

$$f_c = -\frac{H}{A} \mp \frac{Mx}{I} \quad (Z_1 \text{ or } Z_2) \tag{2.74a}$$

$$f_{c1} = -\frac{H}{A} \mp \frac{Mx_1}{I} \quad (Z_1 \text{ or } Z_2) \tag{2.74b}$$

where f_c and f_{c1} are the stresses produced by the various loads applied on the beam at any section of the left and right hand spans respectively providing that plane sections remain plane after the application of these loads.

The deflections can be evaluated at any section of the left hand span from the following equations:

$$\eta_{(1)} = -a \left[\frac{x}{\ell} + \frac{\sin \mu(\ell - x)}{\sin \mu \ell} + \frac{(\nu+\nu_1)}{(\phi+\phi_1)} \left(\frac{x}{\ell} - \frac{\sin \mu x}{\sin \mu \ell} \right) - 1 \right]$$

$$+ \frac{P}{\mu H} \left[\frac{\sin \mu \ell (1-t)}{\sin \mu \ell} \sin \mu x - \mu x (1-t) + \frac{\mu}{(\phi+\phi_1)} \left(\frac{\sin \mu t \ell}{\sin \mu \ell} - t \right) \left(\frac{x}{\ell} \right.\right.$$

$$\left.\left. - \frac{\sin \mu x}{\sin \mu \ell} \right) \right] - \frac{W(y+\rho)}{\mu^2 H} \left[\frac{\sin \mu x}{\sin \mu \ell} \left[1 - \frac{\mu^2}{2} \frac{(\theta+\omega\theta_1)}{(\phi+\phi_1)} \right] + \frac{\sin \mu(\ell - x)}{\sin \mu \ell} \right.$$

$$\left. - 1 - \frac{\mu^2}{2} \frac{x}{\ell} \left[\ell(\ell - x) - \frac{(\theta+\omega\theta_1)}{(\phi+\phi_1)} \right] \right] \qquad 0 \leqslant x \leqslant t\ell$$

(2.75a)

$$\eta_{(2)} = -a\left[\frac{x}{\ell} + \frac{\sin\mu(\ell-x)}{\sin\mu\ell} + \frac{(\nu+\nu_1)}{(\phi+\phi_1)}\left\{\frac{x}{\ell} - \frac{\sin\mu x}{\sin\mu\ell}\right\} - 1\right] + \frac{P}{\mu H}$$

$$\left[\frac{\sin\mu t\ell}{\sin\mu\ell}\sin\mu(\ell-x) - \mu t(\ell-x) + \frac{\mu}{(\phi+\phi_1)}\left\{\frac{\sin\mu t\ell}{\sin\mu\ell} - t\right\}\left\{\frac{x}{\ell}\right.\right.$$

$$\left.\left. - \frac{\sin\mu x}{\sin\mu\ell}\right\}\right] - \frac{W(\gamma+\rho)}{\mu^2 H}\left[\frac{\sin\mu x}{\sin\mu\ell}\left[1 - \frac{\mu^2}{2}\frac{(\theta+\omega\theta_1)}{(\phi+\phi_1)}\right] + \frac{\sin\mu(\ell-x)}{\sin\mu\ell}\right.$$

$$\left. - 1 - \frac{\mu^2}{2}\frac{x}{\ell}\left[\ell(\ell-x) - \frac{(\theta+\omega\theta_1)}{(\phi+\phi_1)}\right]\right] \qquad t\ell \leqslant x \leqslant \ell$$

(2.75b)

and for the right hand span:

$$\eta_1 = -a\left[\frac{x_1}{\ell_1} + \frac{\sin\mu(\ell_1-x_1)}{\sin\mu\ell_1} + \frac{(\nu+\nu_1)}{(\phi+\phi_1)}\left\{\frac{x_1}{\ell_1} - \frac{\sin\mu x_1}{\sin\mu\ell_1}\right\} - 1\right] + \frac{P}{H(\phi+\phi_1)}$$

$$\left\{\frac{\sin\mu t\ell}{\sin\mu\ell} - t\right\}\left\{\frac{x_1}{\ell_1} - \frac{\sin\mu x_1}{\sin\mu\ell_1}\right\} - \frac{W_1(\gamma+\rho)}{\mu^2 H}\left[\frac{\sin\mu x_1}{\sin\mu\ell_1}\right.$$

$$\left.\left[1 - \frac{\mu^2}{2\omega}\frac{(\theta+\omega\theta_1)}{(\phi+\phi_1)}\right] + \frac{\sin\mu(\ell_1-x_1)}{\sin\mu\ell_1} - 1 - \frac{\mu^2}{2}\frac{x_1}{\ell_1}\left[\ell_1(\ell_1-x_1) - \frac{(\theta+\omega\theta_1)}{\omega(\phi+\phi_1)}\right]\right]$$

$$0 \leqslant x_1 \leqslant \ell_1$$

(2.75c)

The shear forces can be obtained at any section of the left hand span from the following equations:

$$Q_{x(1)} = \frac{\mu H a}{\sin\mu\ell}\left[\cos\mu(\ell-x) + \frac{(\nu+\nu_1)}{(\phi+\phi_1)}\cos\mu x\right] + P\frac{\cos\mu x}{\sin\mu\ell}$$

$$\left[{}^{\circ}\sin\mu\ell(1-t) - \frac{\mu}{(\phi+\phi_1)}\left\{\frac{\sin\mu t\ell}{\sin\mu\ell} - t\right\}\right] - \frac{W(\gamma+\rho)}{\mu\sin\mu\ell}\left[\cos\mu x\right.$$

$$\left[1 - \frac{\mu^2}{2} \frac{(\theta+\omega\theta_1)}{(\phi+\phi_1)}\right] - \cos \mu(\ell-x) \Bigg] \qquad o \leqslant x \leqslant t\ell$$

(2.76a)

$$Q_{x(2)} = \frac{\mu Ha}{\sin \mu\ell}\left[\cos \mu(\ell-x) + \frac{(\nu+\nu_1)}{(\phi+\phi_1)} \cos \mu x\right] - \frac{P}{\sin \mu\ell}$$

$$\left[\sin \mu t\ell \cos \mu(\ell-x) + \frac{\mu}{(\phi+\phi_1)} \cos \mu x \left\{\frac{\sin \mu t\ell}{\sin \mu\ell} - t\right\}\right] - \frac{W(y+\rho)}{\mu \sin \mu\ell}$$

$$\left[\cos \mu x \left[1 - \frac{\mu^2}{2\omega} \frac{(\theta+\omega\theta_1)}{(\phi+\phi_1)}\right] - \cos \mu(\ell-x)\right] \qquad t\ell \leqslant x \leqslant \ell$$

(2.76b)

and for the right hand span:

$$Q_{x1} = \frac{\mu Ha}{\sin \mu\ell}\left[\cos \mu(\ell_1-x_1) + \frac{(\nu+\nu_1)}{(\phi+\phi_1)} \cos \mu x_1\right] - \frac{\mu P}{(\phi+\phi_1)} \frac{\cos \mu x_1}{\sin \mu\ell_1}$$

$$\left(\frac{\sin \mu t\ell}{\sin \mu\ell} - t\right) - \frac{W_1(y+\rho)}{\mu \sin \mu\ell_1}\left[\cos \mu x_1 \left[1 - \frac{\mu^2}{2\omega} \frac{(\theta+\omega\theta_1)}{(\phi+\phi_1)}\right]\right.$$

$$\left. - \cos \mu(\ell_1-x_1)\right] \qquad o \leqslant x_1 \leqslant \ell_1$$

(2.76c)

b. <u>A concentrated load applied in the right hand span</u>

For a concentrated load P_1 applied at a distance $t_1\ell_1$ from the right hand end support, see Figure (2.18b), the bending moment equations for the left hand span is:

$$M_x = \frac{Ha}{\sin \mu\ell}\left[\sin \mu(\ell-x) - \frac{(\nu+\nu_1)}{(\phi+\phi_1)} \sin \mu x\right] + \frac{P_1}{(\phi+\phi_1)} \frac{\sin \mu x}{\sin \mu\ell}$$

$$\left(\frac{\sin \mu t_1\ell_1}{\sin \mu\ell_1} - t_1\right) + \frac{W(y+\rho)}{\mu^2 \sin \mu\ell}\left[\sin \mu x \left[1 - \frac{\mu^2}{2} \frac{(\theta+\omega\theta_1)}{(\phi+\phi_1)}\right] + \sin \mu(\ell-x)\right.$$

$$- \sin \mu \ell \Bigg]$$

$$0 \leqslant x \leqslant \ell \qquad (2.77a)$$

and for the right hand span;

$$M_{x(1)} = \frac{Ha}{\sin \mu \ell_1}\left[\sin \mu(\ell_1 - x_1) - \frac{(\nu+\nu_1)}{(\phi+\phi_1)} \sin \mu x_1 \right] - \frac{P_1}{\mu} \frac{\sin \mu x_1}{\sin \mu \ell_1}$$

$$\left[\sin \mu \ell_1(1-t_1) - \frac{\mu}{(\phi+\phi_1)} \left(\frac{\sin \mu t_1 \ell_1}{\sin \mu \ell_1} - t_1 \right) \right] + \frac{W_1 (\gamma+\rho)}{\mu^2 \sin \mu \ell_1}$$

$$\left[\sin \mu x_1 \left[1 - \frac{\mu^2}{2\omega} \frac{(\theta+\omega\theta_1)}{(\phi+\phi_1)} \right] + \sin \mu(\ell_1 - x_1) - \sin \mu \ell_1 \right]$$

$$0 \leqslant x_1 \leqslant t_1 \ell_1 \qquad (2.77b)$$

$$M_{x(2)} = \frac{Ha}{\sin \mu \ell_1}\left[\sin \mu(\ell_1 - x_1) - \frac{(\nu+\nu_1)}{(\phi+\phi_1)} \sin \mu x_1 \right] - \frac{P_1}{\mu \sin \mu \ell_1}$$

$$\left[\sin \mu t_1 \ell_1 \sin \mu(\ell_1 - x_1) - \frac{\mu}{(\phi+\phi_1)} \sin \mu x_1 \left(\frac{\sin \mu t_1 \ell_1}{\sin \mu \ell_1} - t_1 \right) \right]$$

$$+ \frac{W_1 (\gamma+\rho)}{\mu^2 \sin \mu \ell_1} \left[\sin \mu x_1 \left[1 - \frac{\mu^2}{2\omega} \frac{(\theta+\omega\theta_1)}{(\phi+\phi_1)} \right] + \sin \mu(\ell_1 - x_1) - \sin \mu \ell_1 \right]$$

$$t_1 \ell_1 \leqslant x \leqslant \ell_1 \qquad (2.77c)$$

The stresses can be calculated at any section from Equations (2.74).

The deflections can be computed at any section of the left hand span from the following equation:

$$\eta = - a \left[\frac{x}{\ell} + \frac{\sin \mu(\ell - x)}{\sin \mu \ell} + \frac{(\nu+\nu_1)}{(\phi+\phi_1)} \left(\frac{x}{\ell} - \frac{\sin \mu x}{\sin \mu \ell} \right) - 1 \right]$$

$$+\frac{P_1}{H\ (\phi+\phi_1)}\left[\frac{\sin\mu t_1\ell_1}{\sin\mu\ell_1}-t_1\right]\left[\frac{x}{\ell}-\frac{\sin\mu x}{\sin\mu\ell}\right]-\frac{W\ (y+\rho)}{\mu^2 H}\left[\frac{\sin\mu x}{\sin\mu\ell}\right.$$

$$\left.\left[1-\frac{\mu^2}{2}\ \frac{(\theta+\omega\theta_1)}{(\phi+\phi_1)}\right]+\frac{\sin\mu(\ell-x)}{\sin\mu\ell}-1-\frac{\mu^2}{2}\frac{x}{\ell}\left[\ell(\ell-x)-\frac{(\theta+\omega\theta_1)}{(\phi+\phi_1)}\right]\right]$$

$$o \leqslant x \leqslant \ell$$

(2.78a)

and for the right hand span:

$$\eta_{1(1)}=-a\left[\frac{x_1}{\ell_1}+\frac{\sin\mu(\ell_1-x_1)}{\sin\mu\ell_1}+\frac{(\nu+\nu_1)}{(\phi+\phi_1)}\left[\frac{x_1}{\ell_1}-\frac{\sin\mu x_1}{\sin\mu\ell_1}\right]-1\right]$$

$$+\frac{P_1}{\mu H}\left[\frac{\sin\mu\ell_1(1-t_1)}{\sin\mu\ell_1}\sin\mu x_1-\mu x_1(1-t_1)+\frac{\mu}{(\phi+\phi_1)}\left[\frac{\sin\mu t_1\ell_1}{\sin\mu\ell_1}\right.\right.$$

$$\left.\left.-t_1\right)\left[\frac{x_1}{\ell_1}-\frac{\sin\mu x_1}{\sin\mu\ell_1}\right]\right]-\frac{W_1\ (y+\rho)}{\mu^2\ H}\left[\frac{\sin\mu x_1}{\sin\mu\ell_1}\left[1-\frac{\mu^2}{2\omega}\ \frac{(\theta+\omega\theta_1)}{(\phi+\phi_1)}\right]\right.$$

$$\left.+\frac{\sin\mu(\ell_1-x_1)}{\sin\mu\ell_1}-1-\frac{\mu^2}{2}\frac{x_1}{\ell_1}\left[\ell_1(\ell_1-x_1)-\frac{(\theta+\omega\theta_1)}{\omega(\phi+\phi_1)}\right]\right]$$

$$o \leqslant x_1 \leqslant t_1\ell_1$$

(2.78b)

$$\eta_{1(2)}=-a\left[\frac{x_1}{\ell_1}+\frac{\sin\mu(\ell_1-x_1)}{\sin\mu\ell_1}+\frac{(\nu+\nu_1)}{(\phi+\phi_1)}\left[\frac{x_1}{\ell_1}-\frac{\sin\mu x_1}{\sin\mu\ell_1}\right]-1\right]$$

$$+\frac{P_1}{\mu H}\left[\frac{\sin\mu t_1\ell_1}{\sin\mu\ell_1}\sin\mu(\ell_1-x_1)-\ \mu t_1(\ell_1-x_1)+\frac{\mu}{(\phi+\phi_1)}\right.$$

$$\left.\left(\frac{\sin\mu t_1\ell_1}{\sin\mu\ell_1}-t_1\right)\left[\frac{x_1}{\ell_1}-\frac{\sin\mu x_1}{\sin\mu\ell_1}\right]\right]-\frac{W_1\ (y+\rho)}{\mu^2 H}\left[\frac{\sin\mu x_1}{\sin\mu\ell_1}\left[1-\right.\right.$$

$$\frac{\mu^2}{2\omega}\ \frac{(\theta+\omega\theta_1)}{(\phi+\phi_1)}\ \Big] + \frac{\sin\mu(\ell_1-x_1)}{\sin\mu\ell_1} - 1 - \frac{\mu^2}{2}\frac{x_1}{\ell_1}\left[\ell_1(\ell_1-x_1) - \frac{(\theta+\omega\theta_1)}{\omega(\phi+\phi_1)}\right]\Bigg]$$

$$t_1\ell_1 \leqslant x_1 \leqslant \ell_1$$

(2.78c)

The shear forces can be determined at any section of the left hand span from the following equation:

$$Q_x = \frac{\mu Ha}{\sin\mu\ell}\left[\cos\mu(\ell-x) + \frac{(\nu+\nu_1)}{(\phi+\phi_1)}\cos\mu x\right] - \frac{\mu P_1}{(\phi+\phi_1)}\ \frac{\cos\mu x}{\sin\mu\ell}\left[\frac{\sin\mu t_1\ell_1}{\sin\mu\ell_1}\right.$$

$$\left. - t_1\right] - \frac{W\ (y+\rho)}{\mu\sin\mu\ell}\left[\cos\mu x\left[1 - \frac{\mu^2}{2}\ \frac{(\theta+\omega\theta_1)}{(\phi+\phi_1)}\right] - \cos\mu(\ell-x)\right]$$

$$o \leqslant x \leqslant \ell$$

(2.79a)

and for the right hand span;

$$Q_{x1(1)} = \frac{\mu Ha}{\sin\mu\ell_1}\left[\cos\mu(\ell_1-x_1) + \frac{(\nu+\nu_1)}{(\phi+\phi_1)}\cos\mu x_1\right] + P_1\frac{\cos\mu x_1}{\sin\mu\ell_1}$$

$$\left[\sin\mu\ell_1(1-t_1) - \frac{\mu}{(\phi+\phi_1)}\left[\frac{\sin\mu t_1\ell_1}{\sin\mu\ell_1} - t_1\right]\right] - \frac{W_1\ (y+\rho)}{\mu\sin\mu\ell_1}$$

$$\left[\cos\mu x_1\left[1 - \frac{\mu^2}{2\omega}\ \frac{(\theta+\omega\theta_1)}{(\phi+\phi_1)}\right] - \cos\mu(\ell_1-x_1)\right]$$

$$o \leqslant x_1 \leqslant t_1\ell_1$$

(2.79b)

$$Q_{x1(2)} = \frac{\mu Ha}{\sin\mu\ell_1}\left[\cos\mu(\ell_1-x_1) + \frac{(\nu+\nu_1)}{(\phi+\phi_1)}\cos\mu x_1\right] - \frac{P_1}{\sin\mu\ell_1}$$

$$\left[\sin\mu t_1\ell_1\cos\mu(\ell_1-x_1) + \frac{\mu}{(\phi+\phi_1)}\ \cos\mu x_1\left[\frac{\sin\mu t_1\ell_1}{\sin\mu\ell_1} - t_1\right]\right]$$

$$- \frac{W_1\ (\gamma+\rho)}{\mu \sin \mu \ell_1} \left[\cos \mu x_1 \left[1 - \frac{\mu^2}{2\omega} \frac{(\theta+\omega\theta_1)}{(\phi+\phi_1)} \right] - \cos \mu(\ell_1 - x_1) \right]$$

$$t_1 \ell_1 \leqslant x_1 \leqslant \ell_1 \qquad (2.79c)$$

2.6.1.2 For a General Case Loading

a. Applied at the left hand span

For a general loading σ which occupies that part of the left hand span which is bounded by the distances $x = \beta\ell$ and $x = \alpha\ell$ from the left hand end support, Figure (2.18c), the bending moment equations for the left hand span are:

$$M_{x(1)} = \frac{Ha}{\sin \mu\ell} \left[\sin \mu(\ell - x) - \frac{(\nu+\nu_1)}{(\phi+\phi_1)} \sin \mu x \right] - \frac{\sigma}{\mu^2} \frac{\sin \mu x}{\sin \mu\ell}$$

$$\left[\cos \mu\ell(1-\alpha) - \cos \mu\ell(1-\beta) - \frac{\mu^2 \ell}{2\ (\phi+\phi_1)} \left[\frac{2\ [\cos \mu\beta\ell - \cos \mu\alpha\ell]}{\mu\ell \sin \mu\ell} - (\alpha^2 - \beta^2) \right] \right]$$

$$+ \frac{W\ (\gamma+\rho)}{\mu^2 \sin \mu\ell} \left[\sin \mu x \left[1 - \frac{\mu^2}{2} \frac{(\theta+\omega\theta_1)}{(\phi+\phi_1)} \right] + \sin \mu(\ell - x) - \sin \mu\ell \right]$$

$$o \leqslant x \leqslant \beta\ell \qquad (2.80a)$$

$$M_{x(2)} = \frac{Ha}{\sin \mu\ell} \left[\sin \mu(\ell - x) - \frac{(\nu+\nu_1)}{(\phi+\phi_1)} \sin \mu x \right] - \frac{\sigma}{\mu^2 \sin \mu\ell} \left[\sin \mu x \right.$$

$$\cos \mu\ell(1-\alpha) + \sin \mu(\ell - x) \cos \mu\beta\ell - \sin \mu\ell - \frac{\mu^2 \ell}{2\ (\phi+\phi_1)}$$

$$\left. \left[\frac{2\ [\cos \mu\beta\ell - \cos \mu\alpha\ell]}{\mu\ell \sin \mu\ell} - (\alpha^2 - \beta^2) \right] \sin \mu x \right] + \frac{W\ (\gamma+\rho)}{\mu^2 \sin \mu\ell} \left[\sin \mu x \right.$$

$$\left[1 - \frac{\mu^2}{2}\ \frac{(\theta+\omega\theta_1)}{(\phi+\phi_1)}\right] + \sin\mu(\ell-x) - \sin\mu\ell\Bigg] \qquad \beta\ell \leqslant x \leqslant \alpha\ell$$

(2.80b)

$$M_{x(3)} = \frac{Ha}{\sin\mu\ell}\left[\sin\mu(\ell-x) - \frac{(\nu+\nu_1)}{(\phi+\phi_1)}\sin\mu x\right] - \frac{\sigma}{\mu^2\sin\mu\ell}\Bigg[[\cos\mu\beta\ell$$

$$- \cos\mu\alpha\ell]\sin\mu(\ell-x) - \frac{\mu^2\ell}{2\ (\phi+\phi_1)}\left[\frac{2\ [\cos\mu\beta\ell - \cos\mu\alpha\ell]}{\mu\ell\sin\mu\ell} - (\alpha^2-\beta^2)\right]$$

$$\sin\mu x\Bigg] + \frac{W\ (y+\rho)}{\mu^2\sin\mu\ell}\Bigg[\sin\mu x\left[1 - \frac{\mu^2}{2}\frac{(\theta+\omega\theta_1)}{(\phi+\phi_1)}\right] + \sin\mu(\ell-x)$$

$$- \sin\mu\ell\Bigg] \qquad \alpha\ell \leqslant x \leqslant \ell$$

(2.80c)

and for the right hand span;

$$M_{x1} = \frac{Ha}{\sin\mu\ell_1}\left[\sin\mu(\ell_1-x_1) - \frac{(\nu+\nu_1)}{(\phi+\phi_1)}\sin\mu x_1\right] + \frac{\sigma\ell}{2(\phi+\phi_1)}\frac{\sin\mu x_1}{\sin\mu\ell_1}$$

$$\left[\frac{2\ [\cos\mu\beta\ell - \cos\mu\alpha\ell]}{\mu\ell\sin\mu\ell} - (\alpha^2-\beta^2)\right] + \frac{W_1\ (y+\rho)}{\mu^2\sin\mu\ell_1}\Bigg[\sin\mu x_1\left[1 - \frac{\mu^2}{2\omega}\right.$$

$$\left.\frac{(\theta+\omega\theta_1)}{(\phi+\phi_1)}\right] + \sin\mu(\ell_1-x_1) - \sin\mu\ell_1\Bigg] \qquad 0 \leqslant x_1 \leqslant \ell_1$$

(2.80d)

where ρ, μ, ν, ν_1, ϕ, ϕ_1, θ and θ_1 can be obtained from Equations (2.62) and (2.63). The stresses can be computed at any section from Equations (2.74).

The deflections can be evaluated at any section of the left hand span from the following equations:

$$\eta_{(1)} = -a\left[\frac{x}{\ell} + \frac{\sin\mu(\ell-x)}{\sin\mu\ell} + \frac{(\nu+\nu_1)}{(\phi+\phi_1)}\left(\frac{x}{\ell} - \frac{\sin\mu x}{\sin\mu\ell}\right) - 1\right] + \frac{\sigma}{\mu^2 H}$$

$$\left[\left[\cos \mu\ell(1-\alpha) - \cos \mu\ell(1-\beta)\right] \frac{\sin \mu x}{\sin \mu\ell} - \frac{\mu^2\ell^2}{2} (\alpha - \beta) \left[2 - (\alpha+\beta) \right] \right.$$

$$\left. \frac{x}{\ell} + \frac{\mu^2\ell}{2\ (\phi+\phi_1)} \left[\frac{2\ (\cos \mu\beta\ell - \cos \mu\alpha\ell)}{\mu\ell \sin \mu\ell} - (\alpha^2-\beta^2) \right] \left[\frac{x}{\ell} - \frac{\sin \mu x}{\sin \mu\ell} \right] \right]$$

$$- \frac{W\ (y+\rho)}{\mu^2 H} \left[\frac{\sin \mu x}{\sin \mu\ell} \left[1 - \frac{\mu^2}{2} \frac{(\theta+\omega\theta_1)}{(\phi+\phi_1)} \right] + \frac{\sin \mu(\ell-x)}{\sin \mu\ell} - 1 - \frac{\mu^2}{2} \frac{x}{\ell} \right.$$

$$\left. \left[\ell(\ell-x) - \frac{(\theta+\omega\theta_1)}{(\phi+\phi_1)} \right] \right] \qquad 0 \leqslant x \leqslant \beta\ell$$

(2.81a)

$$\eta_{(2)} = - a \left[\frac{x}{\ell} + \frac{\sin \mu(\ell-x)}{\sin \mu\ell} + \frac{(\nu+\nu_1)}{(\phi+\phi)} \left[\frac{x}{\ell} - \frac{\sin \mu x}{\sin \mu\ell} \right] - 1 \right] + \frac{\sigma}{\mu^2 H}$$

$$\left[\cos \mu\ell(1-\alpha) \frac{\sin \mu x}{\sin \mu\ell} + \cos \mu\beta\ell \frac{\sin \mu(\ell-x)}{\sin \mu\ell} - 1 - \frac{\mu^2\ell^2}{2} \right.$$

$$\left[(\alpha-\beta)[2- (\alpha + \beta)] \frac{x}{\ell} - (\frac{x}{\ell} - \beta)^2\right] + \frac{\mu^2\ell}{2\ (\phi+\phi_1)} \left[\frac{2\ (\cos \mu\beta\ell - \cos \mu\alpha\ell)}{\mu\ell \sin \mu\ell} \right.$$

$$\left. - (\alpha^2-\beta^2) \right] \left[\frac{x}{\ell} - \frac{\sin \mu x}{\sin \mu\ell} \right] \Bigg] - \frac{W\ (y+\rho)}{\mu^2 H} \left[\frac{\sin \mu x}{\sin \mu\ell} \left[1 - \frac{\mu^2}{2} \frac{(\theta+\omega\theta_1)}{(\phi+\phi_1)} \right] \right.$$

$$\left. + \frac{\sin \mu(\ell-x)}{\sin \mu\ell} - 1 - \frac{\mu^2}{2} \frac{x}{\ell} \left[\ell(\ell-x) - \frac{(\theta+\omega\theta_1)}{(\phi+\phi_1)} \right] \right] \qquad \beta\ell \leqslant x \leqslant \alpha\ell$$

(2.81b)

$$\eta_{(3)} = - a \left[\frac{x}{\ell} + \frac{\sin \mu(\ell-x)}{\sin \mu\ell} + \frac{(\nu+\nu_1)}{(\phi+\phi_1)} \left[\frac{x}{\ell} - \frac{\sin \mu x}{\sin \mu\ell} \right] - 1 \right]$$

$$+ \frac{\sigma}{\mu^2 H} \left[\frac{\sin \mu(\ell-x)}{\sin \mu\ell} (\cos \mu\beta\ell - \cos \mu\alpha\ell) - \frac{\mu^2\ell^2}{2} (\alpha^2-\beta^2) (1 - \frac{x}{\ell}) \right.$$

$$+ \frac{\mu^2 \ell}{2\ (\phi+\phi_1)} \left[\frac{2\ (\cos \mu\beta\ell - \cos \mu\alpha\ell)}{\mu\ell \sin \mu\ell} - (\alpha^2-\beta^2) \right] \left[\frac{x}{\ell} - \frac{\sin \mu x}{\sin \mu\ell} \right] \Bigg]$$

$$- \frac{W\ (y+\rho)}{\mu^2 H} \left[\frac{\sin \mu x}{\sin \mu\ell} \left[1 - \frac{\mu^2}{2} \frac{(\theta+\omega\theta_1)}{(\phi+\phi_1)} \right] + \frac{\sin \mu(\ell-x)}{\sin \mu\ell} - 1 \right.$$

$$\left. - \frac{\mu^2}{2} \frac{x}{\ell} \left[\ell(\ell-x) - \frac{(\theta+\omega\theta_1)}{(\phi+\phi_1)} \right] \right] \qquad \alpha\ell \leqslant x \leqslant \ell$$

(2.81c)

and for the right hand span,

$$\eta_1 = - a \left[\frac{x_1}{\ell_1} + \frac{\sin \mu(\ell_1-x_1)}{\sin \mu\ell_1} + \frac{(\nu+\nu_1)}{(\phi+\phi_1)} \left(\frac{x_1}{\ell_1} - \frac{\sin \mu x_1}{\sin \mu\ell_1} \right) - 1 \right]$$

$$+ \frac{\sigma\ell}{2H\ (\phi+\phi_1)} \left[\frac{2\ (\cos \mu\beta\ell - \cos \mu\alpha\ell)}{\mu\ell \sin \mu\ell} - (\alpha^2-\beta^2) \right] \left(\frac{x_1}{\ell_1} - \frac{\sin \mu x_1}{\sin \mu\ell_1} \right)$$

$$- \frac{W_1\ (y+\rho)}{\mu^2 H} \left[\frac{\sin \mu x_1}{\sin \mu\ell_1} \left[1 - \frac{\mu^2}{2\omega} \frac{(\theta+\omega\theta_1)}{(\phi+\phi_1)} \right] + \frac{\sin \mu(\ell_1-x_1)}{\sin \mu\ell_1} - 1 \right.$$

$$\left. - \frac{\mu^2}{2} \frac{x_1}{\ell_1} \left[\ell_1(\ell_1-x_1) - \frac{(\theta+\omega\theta_1)}{\omega(\phi+\phi_1)} \right] \right] \qquad o \leqslant x_1 \leqslant \ell_1$$

(2.81d)

The shear forces can be calculated at any section of the left hand span from the following equations:

$$Q_{x(1)} = \frac{\mu H a}{\sin \mu\ell} \left[\cos \mu(\ell-x) + \frac{(\nu+\nu_1)}{(\phi+\phi_1)} \cos \mu x \right] + \frac{\sigma}{\mu} \frac{\cos \mu x}{\sin \mu\ell} \left[\cos \mu\ell(1-\alpha) \right.$$

$$\left. - \cos \mu\ell(1-\beta) - \frac{\mu^2 \ell}{2\ (\phi+\phi_1)} \left[\frac{2\ (\cos \mu\beta\ell - \cos \mu\alpha\ell)}{\mu\ell \sin \mu\ell} - (\alpha^2-\beta^2) \right] \right]$$

$$- \frac{W\,(y+\rho)}{\mu \sin \mu\ell} \left[\cos \mu x \left[1 - \frac{\mu^2}{2} \frac{(\theta+\omega\theta_1)}{(\phi+\phi_1)} \right] - \cos \mu(\ell-x) \right]$$

$$0 \leqslant x \leqslant \beta\ell$$

(2.82a)

$$Q_{x(2)} = \frac{\mu Ha}{\sin \mu\ell} \left[\cos \mu(\ell-x) + \frac{(\nu+\nu_1)}{(\phi+\phi_1)} \cos \mu x \right] + \frac{\sigma}{\mu \sin \mu\ell} \left[\cos \mu x \right.$$

$$\cos \mu\ell(1-\alpha) - \cos \mu(\ell-x) \cos \mu\beta\ell - \frac{\mu^2\ell}{2\,(\phi+\phi_1)} \left[\frac{2\,(\cos \mu\beta\ell - \cos \mu\alpha\ell)}{\mu\ell \sin \mu\ell} \right.$$

$$\left. \left. -(\alpha^2 - \beta^2) \right] \cos \mu x \right] - \frac{W\,(y+\rho)}{\mu \sin \mu\ell} \left[\cos \mu x \left[1 - \frac{\mu^2}{2} \frac{(\theta+\omega\theta_1)}{(\phi+\phi_1)} \right] - \cos \mu(\ell-x) \right]$$

$$\beta\ell \leqslant x \leqslant \alpha\ell$$

(2.82b)

$$Q_{x(3)} = \frac{\mu Ha}{\sin \mu\ell} \left[\cos \mu(\ell-x) + \frac{(\nu+\nu_1)}{(\phi+\phi_1)} \cos \mu x \right] - \frac{\sigma}{\mu \sin \mu\ell} \left[[\cos \mu\beta\ell \right.$$

$$- \cos \mu\alpha\ell] \cos \mu(\ell-x) + \frac{\mu^2\ell}{2\,(\phi+\phi_1)} \left[\frac{2\,(\cos \mu\beta\ell - \cos \mu\alpha\ell)}{\mu\ell \sin \mu\ell} \right.$$

$$\left. \left. -(\alpha^2 - \beta^2) \right] \cos \mu x \right] - \frac{W\,(y+\rho)}{\mu \sin \mu\ell} \left[\cos \mu x \left[1 - \frac{\mu^2}{2} \frac{(\theta+\omega\theta_1)}{(\phi+\phi_1)} \right] - \cos \mu(\ell-x) \right]$$

$$\alpha\ell \leqslant x \leqslant \ell$$

(2.82c)

and for the right hand span,

$$Q_{x1} = \frac{\mu Ha}{\sin \mu\ell_1} \left[\cos \mu(\ell_1 - x_1) + \frac{(\nu+\nu_1)}{(\phi+\phi_1)} \cos \mu x_1 \right] - \frac{\mu\sigma\ell}{2\,(\phi+\phi_1)} \frac{\cos \mu x_1}{\sin \mu\ell_1}$$

$$\left[\frac{2\,(\cos \mu\beta\ell - \cos \mu\alpha\ell)}{\mu\ell \sin \mu\ell} - (\alpha^2 - \beta^2) \right] - \frac{W_1(y+\rho)}{\mu \sin \mu\ell_1}$$

$$\left[\cos \mu x_1 \left[1 - \frac{\mu^2}{2\omega} \frac{(\theta+\omega\theta_1)}{(\phi+\phi_1)} \right] - \cos \mu(\ell_1-x_1) \right] \qquad o \leqslant x_1 \leqslant \ell_1$$

(2.82d)

The bending moments, deflections and shear forces equations can be written for a continuous uniformly distributed load σ applied in the left hand span, when substituting $\alpha = 1$ and $\beta = o$ in Equations (2.80 - 2.82).

b. <u>A general loading applied in the right hand span</u>

For a general loading σ_1 which occupies that part of the right hand span which is bounded by the distances $x_1 = \beta_1 \ell_1$ and $x_1 = \alpha_1 \ell_1$ from the right hand end support, Figure (2.18d), the bending moment equation for the left hand span is:

$$M_x = \frac{Ha}{\sin \mu\ell} \left[\sin \mu(\ell-x) - \frac{(\nu+\nu_1)}{(\phi+\phi_1)} \sin \mu x \right] + \frac{\sigma_1 \ell_1}{2\,(\phi+\phi_1)} \frac{\sin \mu x}{\sin \mu\ell}$$

$$\left[\frac{2\,[\cos \mu\beta_1\ell_1 - \cos \mu\alpha_1\ell_1\,]}{\mu\ell_1 \sin \mu\ell_1} - (\alpha_1^2-\beta_1^2) \right] + \frac{W\,(\gamma+\rho)}{\mu^2 \sin \mu\ell} \left[\sin \mu x \left[1 - \frac{\mu^2}{2} \right. \right.$$

$$\left. \left. \frac{(\theta+\omega\theta_1)}{(\phi+\phi_1)} \right] + \sin \mu(\ell-x) - \sin \mu\ell \right] \qquad o \leqslant x \leqslant \ell$$

(2.83a)

and for the right hand span,

$$M_{x1(1)} = \frac{Ha}{\sin \mu\ell_1} \left[\sin \mu(\ell_1-x_1) - \frac{(\nu+\nu_1)}{(\phi+\phi_1)} \sin \mu x_1 \right] - \frac{\sigma_1}{\mu^2} \frac{\sin \mu x_1}{\sin \mu\ell_1} \left[\cos \mu\ell_1(1-\alpha_1) \right.$$

$$\left. - \cos \mu\ell_1(1-\beta_1) - \frac{\mu^2\ell_1}{2\,(\phi+\phi_1)} \left[\frac{2\,[\cos \mu\beta_1\ell_1 - \cos \mu\alpha_1\ell_1\,]}{\mu\ell_1 \sin \mu\ell_1} - (\alpha_1^2-\beta_1^2) \right] \right]$$

$$+ \frac{W_1\ (y+\rho)}{\mu^2 \sin \mu\ell_1}\left[\sin \mu x_1 \left[1 - \frac{\mu^2}{2\omega}\frac{(\theta+\omega\theta_1)}{(\phi+\phi_1)}\right] + \sin \mu(\ell_1-x_1) - \sin \mu\ell_1\right]$$

$$0 \leqslant x \leqslant \beta_1\ell_1 \qquad (2.83b)$$

$$M_{x1(2)} = \frac{Ha}{\sin \mu\ell_1}\left[\sin \mu(\ell_1-x_1) - \frac{(\nu+\nu_1)}{(\phi+\phi_1)} \sin \mu x_1\right] - \frac{\sigma_1}{\mu^2 \sin \mu\ell_1}\left[\sin \mu x_1\right.$$

$$\cos \mu\ell_1(1-\alpha_1) + \sin \mu(\ell_1-x_1) \cos \mu\beta_1\ell_1 - \sin \mu\ell_1 - \frac{\mu^2\ell_1}{2\ (\phi+\phi_1)}$$

$$\left[\frac{2\ [\cos \mu\beta_1\ell_1 - \cos \mu\alpha_1\ell_1\ ]}{\mu\ell_1 \sin \mu\ell_1} - \left(\alpha_1^2-\beta_1^2\right)\right] \sin \mu x_1\Bigg] + \frac{W_1(y+\rho)}{\mu^2 \sin \mu\ell_1}$$

$$\left[\sin \mu x_1 \left[1 - \frac{\mu^2}{2\omega}\frac{(\theta+\omega\theta_1)}{(\phi+\phi_1)}\right] + \sin \mu(\ell_1-x_1) - \sin \mu\ell_1\right]$$

$$\beta_1\ell_1 \leqslant x_1 \leqslant \alpha_1\ell_1 \qquad (2.83c)$$

$$M_{x1(3)} = \frac{Ha}{\sin \mu\ell_1}\left[\sin \mu(\ell_1-x_1) - \frac{(\nu+\nu_1)}{(\phi+\phi_1)} \sin \mu x_1\right] - \frac{\sigma_1}{\mu^2 \sin \mu\ell_1}\left[\left[\cos \mu\beta_1\ell_1\right.\right.$$

$$\left.- \cos \mu\alpha_1\ell_1\right] \sin \mu(\ell_1-x_1) - \frac{\mu^2\ell_1}{2\ (\phi+\phi_1)}\left[\frac{2\ [\cos \mu\beta_1\ell_1 - \cos \mu\alpha_1\ell_1\ ]}{\mu\ell_1 \sin \mu\ell_1} -\right.$$

$$\left.\left(\alpha_1^2-\beta_1^2\right)\right] \sin \mu x_1\Bigg] + \frac{W_1\ (y+\rho)}{\mu^2 \sin \mu\ell_1}\left[\sin \mu x_1 \left[1 - \frac{\mu^2}{2\omega}\frac{(\theta+\omega\theta_1)}{(\phi+\phi_1)}\right]\right.$$

$$\left. + \sin \mu(\ell_1-x_1) - \sin \mu\ell_1\right] \qquad \alpha_1\ell_1 \leqslant x_1 \leqslant \ell_1$$

(2.83d)

The stresses can be evaluated at any section from Equations (2.74).

The deflections can directly be calculated for the left hand span from the following equation:

$$\eta = - a \left[\frac{x}{\ell} + \frac{\sin \mu(\ell-x)}{\sin \mu\ell} + \frac{(\nu+\nu_1)}{(\phi+\phi_1)} \left(\frac{x}{\ell} - \frac{\sin \mu x}{\sin \mu\ell} \right) - 1 \right]$$

$$+ \frac{\sigma_1 \ell_1}{2H\ (\phi+\phi_1)} \left[\frac{2\left(\cos \mu\beta_1\ell_1 - \cos \mu\alpha_1\ell_1\right)}{\mu\ell_1 \sin \mu\ell_1} - \left(\alpha_1^2-\beta_1^2\right) \right] \left(\frac{x}{\ell} - \frac{\sin \mu x}{\sin \mu\ell} \right)$$

$$- \frac{W\ (y+\rho)}{\mu^2 H} \left[\frac{\sin \mu x}{\sin \mu\ell} \left[1 - \frac{\mu^2}{2} \frac{(\theta+\omega\theta_1)}{(\phi+\phi_1)} \right] + \frac{\sin \mu(\ell-x)}{\sin \mu\ell} - 1 - \frac{\mu^2}{2} \frac{x}{\ell} \right.$$

$$\left. \left[\ell(\ell-x) - \frac{(\theta+\omega\theta_1)}{(\phi+\phi_1)} \right] \right] \qquad o \leqslant x \leqslant \ell$$

(2.84a)

and for the right hand span;

$$\eta_{1(1)} = - a \left[\frac{x_1}{\ell_1} + \frac{\sin \mu(\ell_1-x_1)}{\sin \mu\ell_1} + \frac{(\nu+\nu_1)}{(\phi+\phi_1)} \left(\frac{x_1}{\ell_1} - \frac{\sin \mu x_1}{\sin \mu\ell_1} \right) - 1 \right]$$

$$+ \frac{\sigma_1}{\mu^2 H} \left[\left[\cos \mu\ell_1(1-\alpha_1) - \cos \mu\ell_1(1-\beta_1)\right] \frac{\sin \mu x_1}{\sin \mu\ell_1} - \frac{\mu^2 \ell_1^{\,2}}{2} (\alpha_1-\beta_1) \right.$$

$$[2 - (\alpha_1+\beta_1)] \frac{x_1}{\ell_1} + \frac{\mu^2 \ell_1}{2\ (\phi+\phi_1)} \left[\frac{2\ (\cos \mu\beta_1\ell_1 - \cos \mu\alpha_1\ell_1)}{\mu\ell_1 \sin \mu\ell_1} - \left(\alpha_1^2-\beta_1^2\right) \right]$$

$$\left. \left(\frac{x_1}{\ell_1} - \frac{\sin \mu x_1}{\sin \mu\ell_1} \right) \right] - \frac{W_1\ (y+\rho)}{\mu^2 H} \left[\frac{\sin \mu x_1}{\sin \mu\ell_1} \left[1 - \frac{\mu^2}{2\omega} \frac{(\theta+\omega\theta_1)}{(\phi+\phi_1)} \right] \right.$$

$$\left. + \frac{\sin \mu(\ell_1-x_1)}{\sin \mu\ell_1} - 1 - \frac{\mu^2}{2} \frac{x_1}{\ell_1} \left[\ell_1(\ell_1-x_1) - \frac{(\theta+\omega\theta_1)}{\omega(\phi+\phi_1)} \right] \right]$$

$$o \leqslant x_1 \leqslant \beta_1\ell_1$$

(2.84b)

$$\eta_{1(2)} = -a\left[\frac{x_1}{\ell_1} + \frac{\sin\mu(\ell_1-x_1)}{\sin\mu\ell_1} + \frac{(\nu+\nu_1)}{(\phi+\phi_1)}\left(\frac{x_1}{\ell_1} - \frac{\sin\mu x_1}{\sin\mu\ell_1}\right) - 1\right]$$

$$+\frac{\sigma_1}{\mu^2 H}\left[\cos\mu\ell_1(1-\alpha_1)\frac{\sin\mu x_1}{\sin\mu\ell_1} + \cos\mu\beta_1\ell_1\frac{\sin\mu(\ell_1-x_1)}{\sin\mu\ell_1} - 1\right.$$

$$-\frac{\mu^2\ell_1^2}{2}\left[(\alpha_1-\beta_1)[2-(\alpha_1+\beta_1)]\frac{x_1}{\ell_1} - \left(\frac{x_1}{\ell_1}-\beta_1\right)^2\right] + \frac{\mu^2\ell_1}{2(\phi+\phi_1)}$$

$$\left[\frac{2(\cos\mu\beta_1\ell_1 - \cos\mu\alpha_1\ell_1)}{\mu\ell_1\sin\mu\ell_1} - (\alpha_1^2-\beta_1^2)\right]\left[\frac{x_1}{\ell_1} - \frac{\sin\mu x_1}{\sin\mu\ell_1}\right] - \frac{W_1(\gamma+\rho)}{\mu^2 H}\left[\frac{\sin\mu x_1}{\sin\mu\ell_1}\right.$$

$$\left.\left.\left[1 - \frac{\mu^2}{2\omega}\frac{(\theta+\omega\theta_1)}{(\phi+\phi_1)}\right] + \frac{\sin\mu(\ell_1-x_1)}{\sin\mu\ell_1} - 1 - \frac{\mu^2}{2}\frac{x_1}{\ell_1}\left[\ell_1(\ell_1-x_1) - \frac{(\theta+\omega\theta_1)}{\omega(\phi+\phi_1)}\right]\right]\right.$$

$$\beta_1\ell_1 \leq x_1 \leq \alpha_1\ell_1 \qquad (2.84c)$$

$$\eta_{1(3)} = -a\left[\frac{x_1}{\ell_1} + \frac{\sin\mu(\ell_1-x_1)}{\sin\mu\ell_1} + \frac{(\nu+\nu_1)}{(\phi+\phi_1)}\left(\frac{x_1}{\ell_1} - \frac{\sin\mu x_1}{\sin\mu\ell_1}\right) - 1\right]$$

$$+\frac{\sigma_1}{\mu^2 H}\left[\frac{\sin\mu(\ell_1-x_1)}{\sin\mu\ell_1}(\cos\mu\beta_1\ell_1 - \cos\mu\alpha_1\ell_1) - \frac{\mu^2\ell_1^2}{2}(\alpha_1^2-\beta_1^2)\right.$$

$$\left.\left(1-\frac{x_1}{\ell_1}\right) + \frac{\mu^2\ell_1}{2(\phi+\phi_1)}\left[\frac{2(\cos\mu\beta_1\ell_1 - \cos\mu\alpha_1\ell_1)}{\mu\ell_1\sin\mu\ell_1} - (\alpha_1^2-\beta_1^2)\right]\left[\frac{x_1}{\ell_1} - \frac{\sin\mu x_1}{\sin\mu\ell_1}\right]\right]$$

$$-\frac{W_1(\gamma+\rho)}{\mu^2 H}\left[\frac{\sin\mu x_1}{\sin\mu\ell_1}\left[1 - \frac{\mu^2}{2\omega}\frac{(\theta+\omega\theta_1)}{(\phi+\phi_1)}\right] + \frac{\sin\mu(\ell_1-x_1)}{\sin\mu\ell_1} - 1\right.$$

$$- \frac{\mu^2}{2} \frac{x_1}{\ell_1} \left[\ell_1(\ell_1 - x_1) - \frac{(\theta+\omega\theta_1)}{\omega(\phi+\phi_1)} \right] \Bigg] \qquad \alpha_1\ell_1 \leqslant x_1 \leqslant \ell_1$$

(2.84d)

The shear forces can be calculated at any section of the left hand span from the following equation:

$$Q_x = \frac{\mu Ha}{\sin \mu\ell} \left[\cos \mu(\ell - x) + \frac{(\nu+\nu_1)}{(\phi+\phi_1)} \cos \mu x \right] - \frac{\mu\, \sigma_1 \ell_1}{2\,(\phi+\phi_1)} \frac{\cos \mu x}{\sin \mu\ell}$$

$$\left[\frac{2\,(\cos \mu\beta_1\ell_1 - \cos \mu\alpha_1\ell_1)}{\mu\ell_1 \sin \mu\ell_1} - (\alpha_1^2 - \beta_1^2) \right] - \frac{W\,(\gamma+\rho)}{\mu \sin \mu\ell} \left[\cos \mu x \left[1 - \right. \right.$$

$$\left. \left. \frac{\mu^2}{2} \frac{(\theta+\omega\theta_1)}{(\phi+\phi_1)} \right] - \cos \mu(\ell - x) \right] \qquad o \leqslant x \leqslant \ell$$

(2.85a)

and for the right hand span;

$$Q_{x1(1)} = \frac{\mu Ha}{\sin \mu\ell_1} \left[\cos \mu(\ell_1 - x_1) + \frac{(\nu+\nu_1)}{(\phi+\phi_1)} \cos \mu x_1 \right] + \frac{\sigma_1}{\mu} \frac{\cos \mu x_1}{\sin \mu\ell_1}$$

$$\left[\cos \mu\ell_1(1-\alpha_1) - \cos \mu\ell_1(1-\beta_1) - \frac{\mu^2\ell_1}{2\,(\phi+\phi_1)} \left[\frac{2\,(\cos \mu\beta_1\ell_1 - \cos \mu\alpha_1\ell_1)}{\mu\ell_1 \sin \mu\ell_1} \right. \right.$$

$$\left. \left. - (\alpha_1^2 - \beta_1^2) \right] \right] - \frac{W_1\,(\gamma+\rho)}{\mu \sin \mu\ell_1} \left[\cos \mu x_1 \left[1 - \frac{\mu^2}{2\omega} \frac{(\theta+\omega\theta_1)}{(\phi+\phi_1)} \right] - \cos \mu(\ell_1 - x_1) \right]$$

$$o \leqslant x_1 \leqslant \beta_1\ell_1$$

(2.85b)

$$Q_{x1(2)} = \frac{\mu Ha}{\sin \mu\ell_1} \left[\cos \mu(\ell_1 - x_1) + \frac{(\nu+\nu_1)}{(\phi+\phi_1)} \cos \mu x_1 \right] + \frac{\sigma_1}{\mu \sin \mu\ell_1} \left[\cos \mu x_1 \right.$$

$$\cos \mu\ell_1(1-\alpha_1) - \cos \mu(\ell_1-x_1) \cos \mu\beta_1\ell_1 - \frac{\mu^2\ell_1}{2\ (\phi+\phi_1)}\Bigg[\frac{2\ (\cos \mu\beta_1\ell_1-\cos \mu\alpha_1\ell_1)}{\mu\ell_1 \sin \mu\ell_1}$$

$$- \left(\alpha_1^2-\beta_1^2\right)\Bigg] \cos \mu x_1\Bigg] - \frac{W_1(y+\rho)}{\mu \sin \mu\ell_1}\left[\cos \mu x_1\left[1 - \frac{\mu^2}{2\omega}\frac{(\theta+\omega\theta_1)}{(\phi+\phi_1)}\right] - \cos \mu(\ell_1-x_1)\right]$$

$$\beta_1\ell_1 \leqslant x_1 \leqslant \alpha_1\ell_1 \qquad (2.85c)$$

$$Q_{x1(3)} = \frac{\mu Ha}{\sin \mu\ell_1}\left[\cos \mu(\ell_1-x_1) + \frac{(\nu+\nu_1)}{(\phi+\phi_1)} \cos \mu x_1\right] - \frac{\sigma_1}{\mu \sin \mu\ell_1}\Bigg[[\cos \mu\beta_1\ell_1$$

$$- \cos \mu\alpha_1\ell_1] \cos \mu(\ell_1-x_1) + \frac{\mu^2\ell_1}{2\ (\phi+\phi_1)}\Bigg[\frac{2\ (\cos \mu\beta_1\ell_1-\cos \mu\alpha_1\ell_1)}{\mu\ell_1 \sin \mu\ell_1}$$

$$- \left(\alpha_1^2-\beta_1^2\right)\Bigg] \cos \mu x_1\Bigg] - \frac{W_1(y+\rho)}{\mu \sin \mu\ell_1}\left[\cos \mu x_1\left[1 - \frac{\mu^2}{2\omega}\frac{(\theta+\omega\theta_1)}{(\phi+\phi_1)}\right]\right.$$

$$\left. - \cos \mu(\ell_1-x_1)\right] \qquad \alpha_1\ell_1 \leqslant x_1 \leqslant \ell_1$$

(2.85d)

The bending moments, deflections and shear forces equations can be written for a continuous uniformly distributed load σ_1 applied in the right hand span, when substituting $\alpha_1 = 1$ and $\beta_1 = o$ in Equations (2.83 - 2.85).

2.6.2 The Forces in the Suspenders

As mentioned in Section 2.1, the suspenders have been replaced by a continuous screen or membrane and their forces are represented in the calculations as upward uniformly distributed forces. The suspenders should be designed to sustain maximum forces. To calculate these forces, we use the fictitious system shown in Figure (2.20) which comprises a fictitious beam with fictitious supports

which represent the suspenders. $g\ell$ and $g_1\ell_1$ denote the lengths which the cable passes through the left and right hand spans of the suspended beam respectively.

The maximum upward forces result from having the maximum increase in the horizontal tension, H_p, due to live loading. Knowing H_{pmax}, the maximum value of the upward forces can be exactly evaluated from the following equations:-

$$q_{smax} = - W\ (1+\gamma + \rho_{max})\ \left[\ 1 + \frac{\theta}{\ell}\ \right]\ \left[1 - \frac{\mu^2}{4}\ \frac{(\theta+\omega\theta_1)}{(\phi+\phi_1)}\ \right] \qquad (2.86a)$$

$$q_{s1max} = - W_1\ (1+\gamma + \rho_{max})\ \left[\ 1 + \frac{\theta_1}{\ell_1}\ \right]\ \left[1 - \frac{\mu^2}{4\omega}\ \frac{(\theta+\omega\theta_1)}{(\phi+\phi_1)}\ \right] \qquad (2.86b)$$

where $\rho_{max} = \dfrac{H_{pmax}}{H_w}$

for left and right hand spans respectively. The derivation of these formulae is given in Appendix 15.

The approximate values for the maximum upward forces is found by simply ignoring the effect of the axial force which gives:

$$q_{smax} = - W\ (1 + \gamma + \rho_{max}) \qquad (2.87a)$$

$$q_{s1max} = - W_1\ (1 + \gamma + \rho_{max}) \qquad (2.87b)$$

The forces in the suspenders can then be obtained, as mentioned earlier, by calculating the reactions in the fictitious system shown in Figure (2.20). For simplicity, the suspenders forces can be calculated as: (Similar to part 3 of Section 2.5.2.2)

$$P_{smax} = q_{smax}\ d \qquad (2.88a)$$

$$P_{s1max} = q_{s1max}\ d_1 \qquad (2.88b)$$

for left and right hand spans respectively.

It is worth noting that the elongation in each suspender must be checked to ensure that it remains less than 10% of the average deflection of the beam at its position for any case of loading, (19). The reason for this is that as the cable has been assumed to deflect by equal amounts to the beam deflections, assumption (3). Thus, any excessive elongations in the suspenders would decrease the cable deflections and consequently, its interaction with the beam due to live loading, (26).

2.6.3 The Tower Force

For suspension bridges generally, the towers are usually portal frames of great height. The main considerations in their design are stability against the vertical cable forces and wind. This is why the towers are built with large cross sections which sustain the vertical forces applied by the cable and resist the wind by their sheer weight.

From Figure (2.15) and Equation (2.34), we have the maximum vertical force applied on the tower:

$$N_{T\ max} = H_w \ (1 + \gamma + \rho_{max}) \left[(F + 8n) + (F_1 + 8n_1) \right] \quad (2.89)$$

Hence, the wind forces in addition to N_{Tmax} can be used to calculate the internal forces of the tower depending, of course, on the nature of each particular bridge.

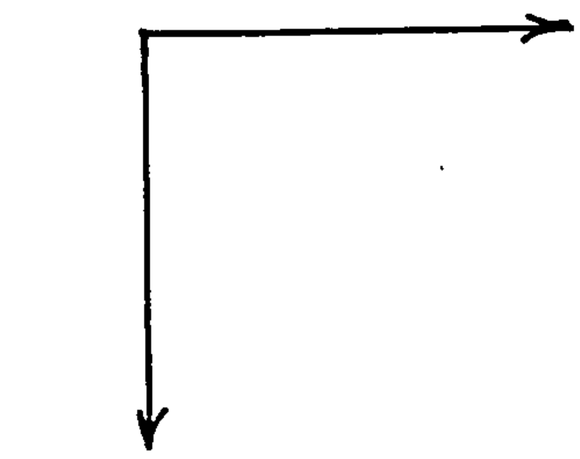

Positive Coordinates

Positive Deflection η

Positive rotation (slope)η'

Positive curvature (moment) M

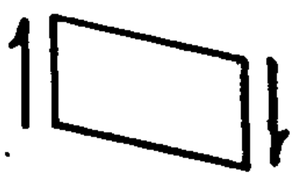

Positive shear forces Q

Positive loading q

The Sign Convention

Figure (2.1)

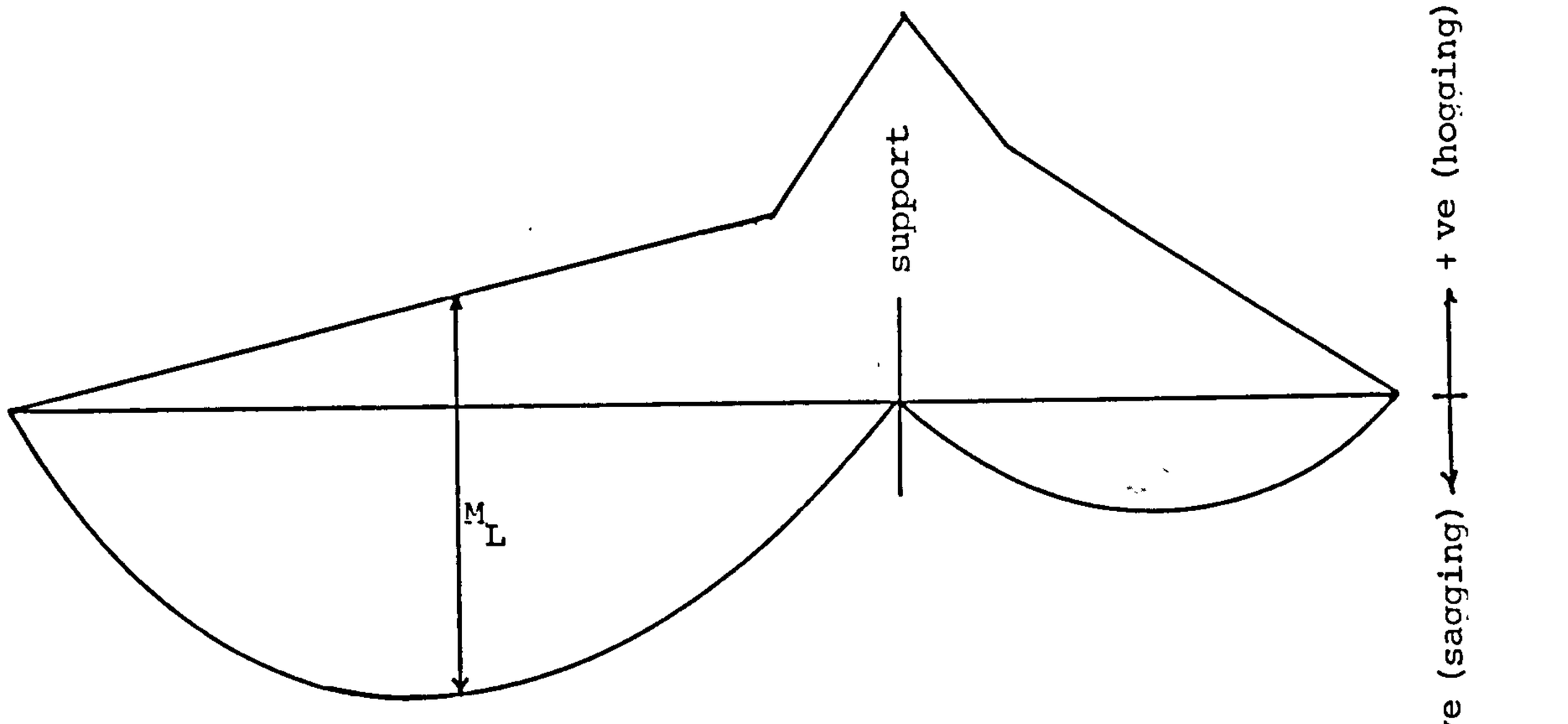

The maximum bending moment envelop

Figure (2.2)

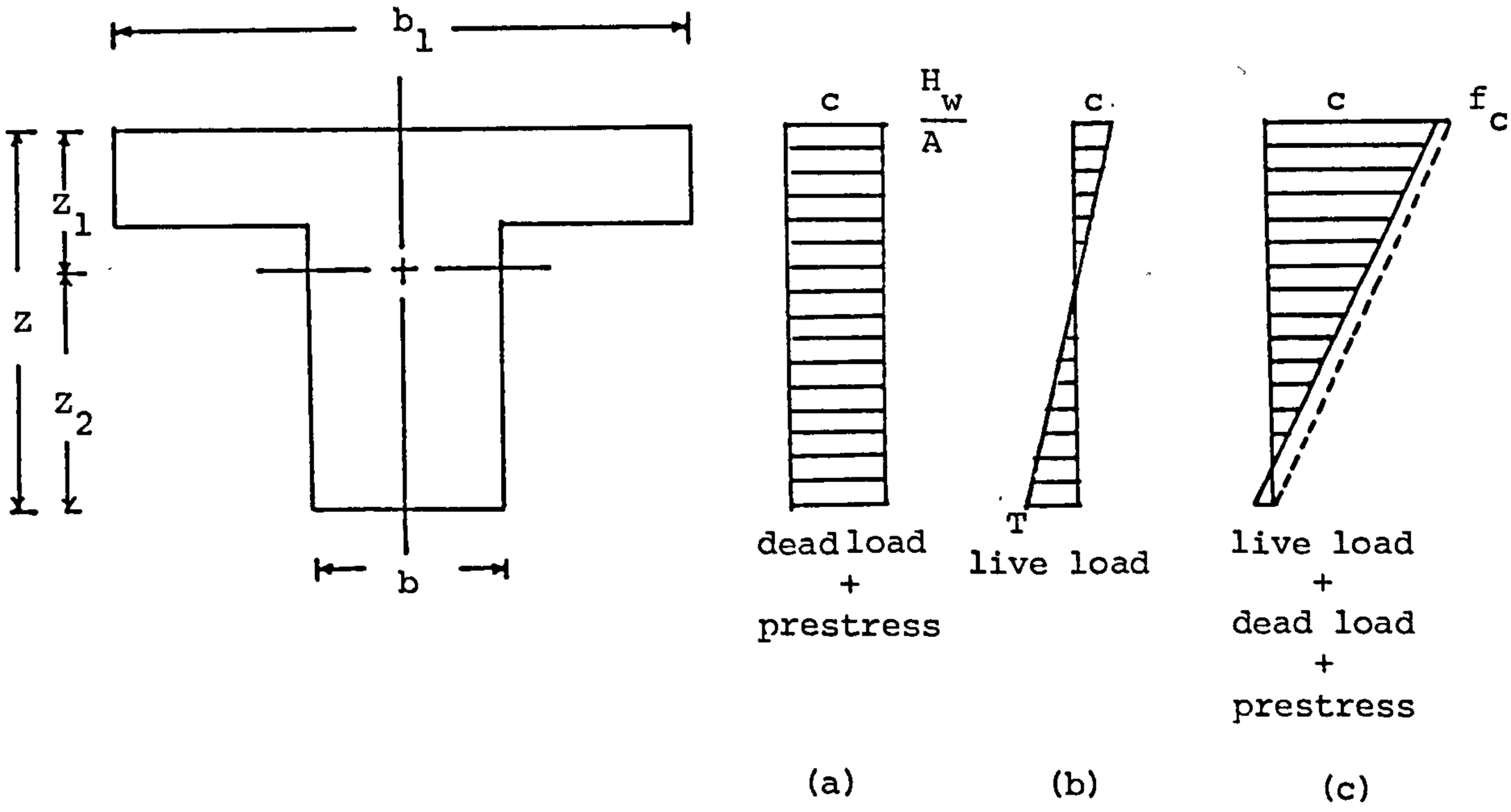

The stress distribution of the cross section of the beam when the preliminary prestressing force is applied

Figure (2.3)

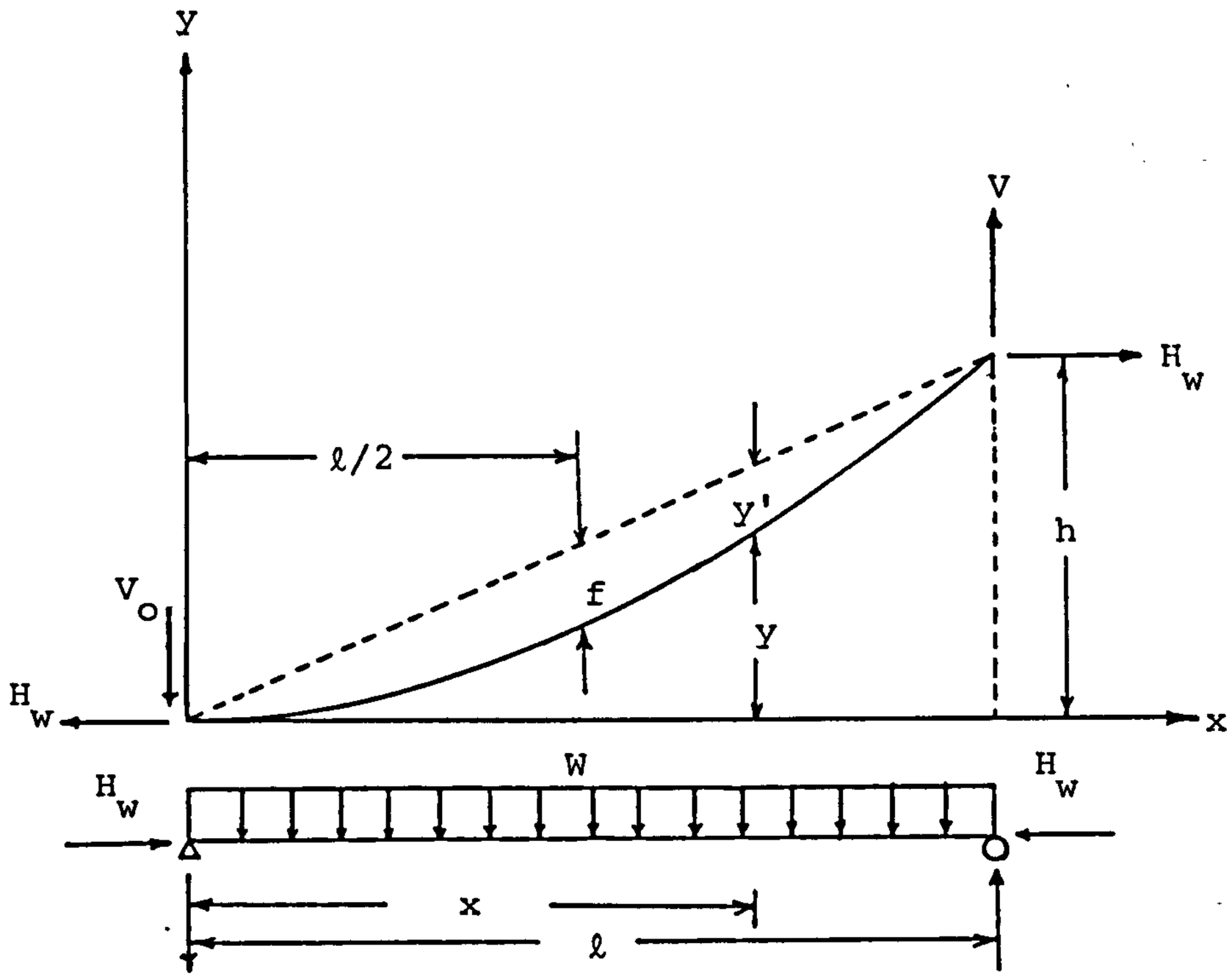

The cable shape in the left hand span without eccentricities at its ends

Figure (2.4)

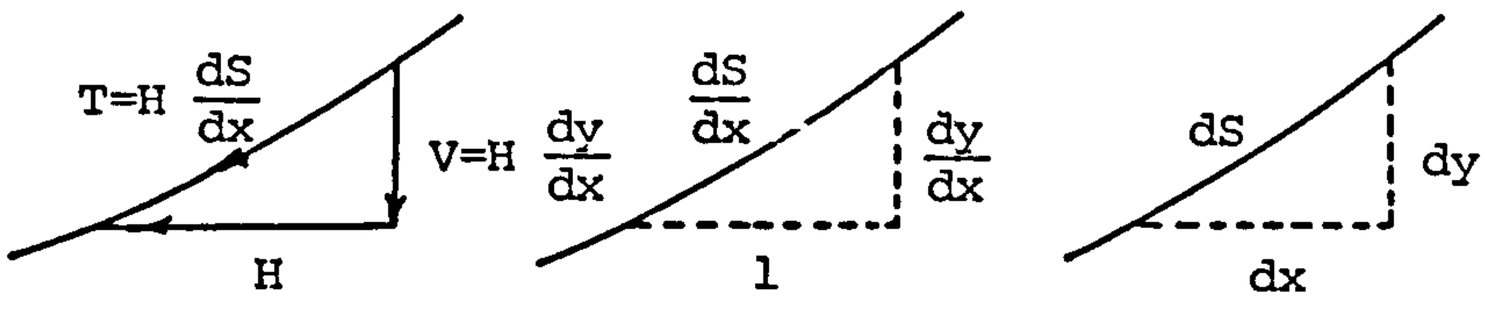

A cable element

Figure (2.5)

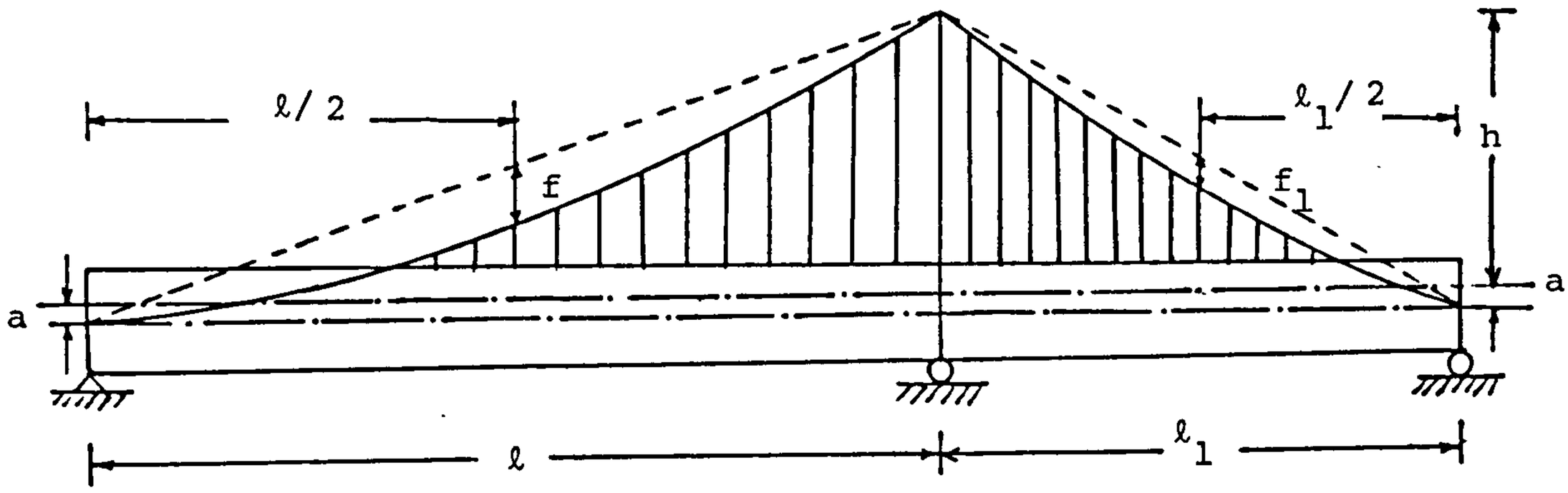

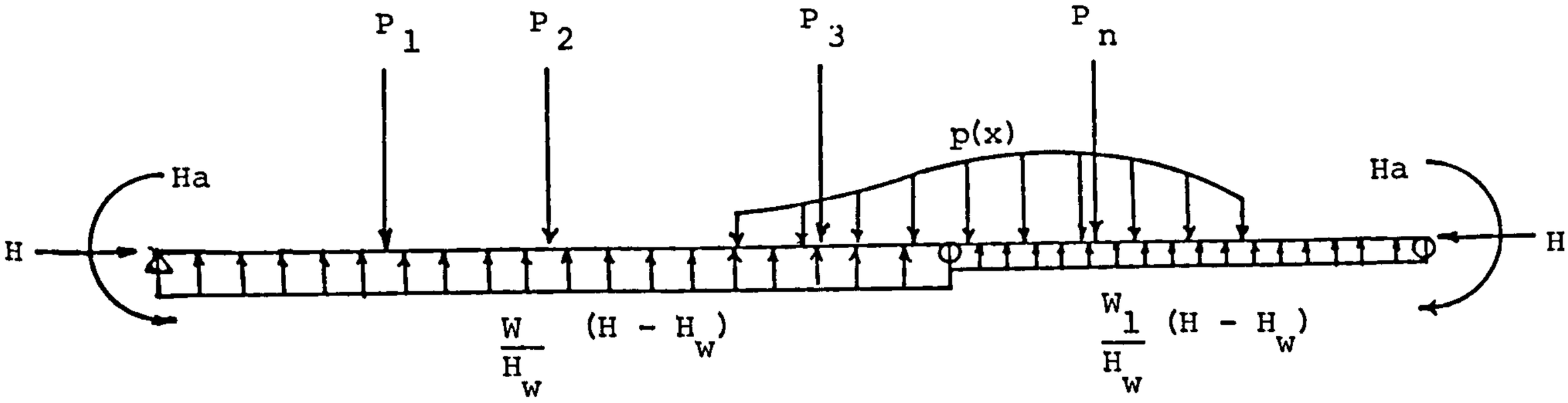

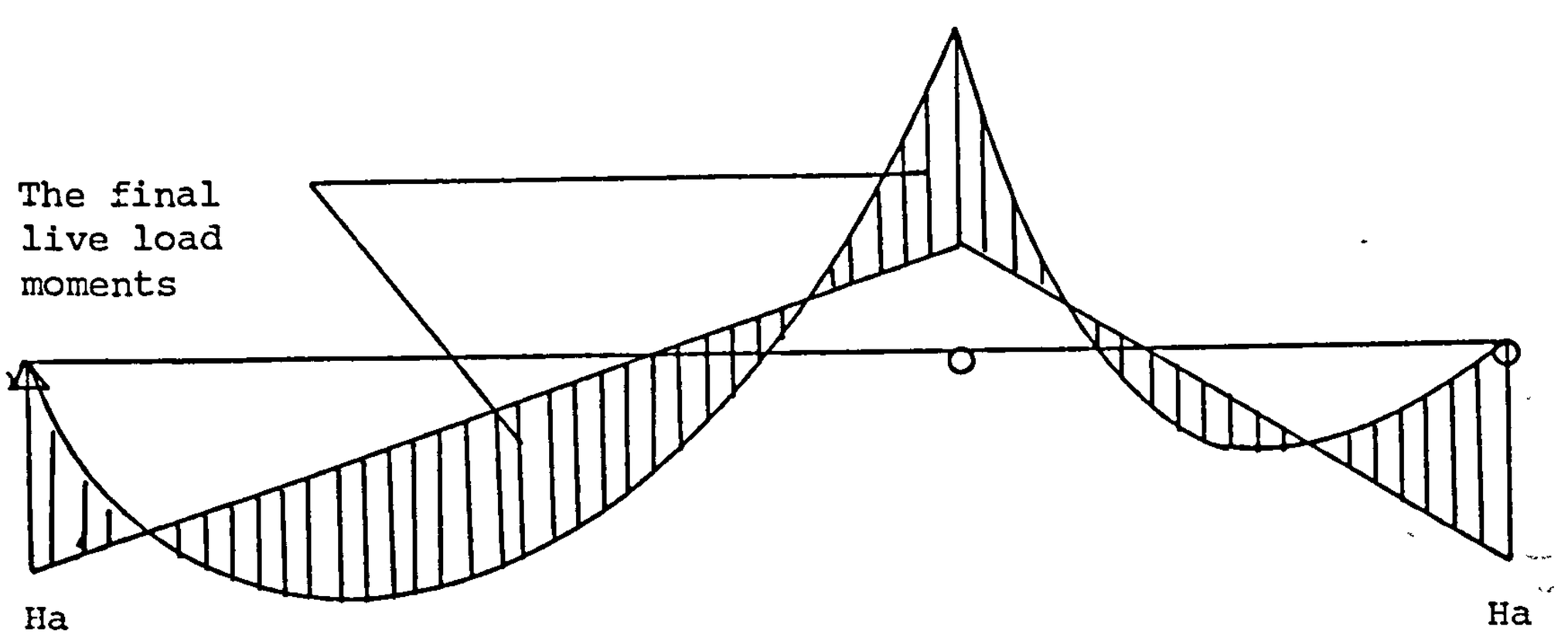

The reduction in the live load moments as a result of the eccentricities at the ends of the cable

Figure (2.6)

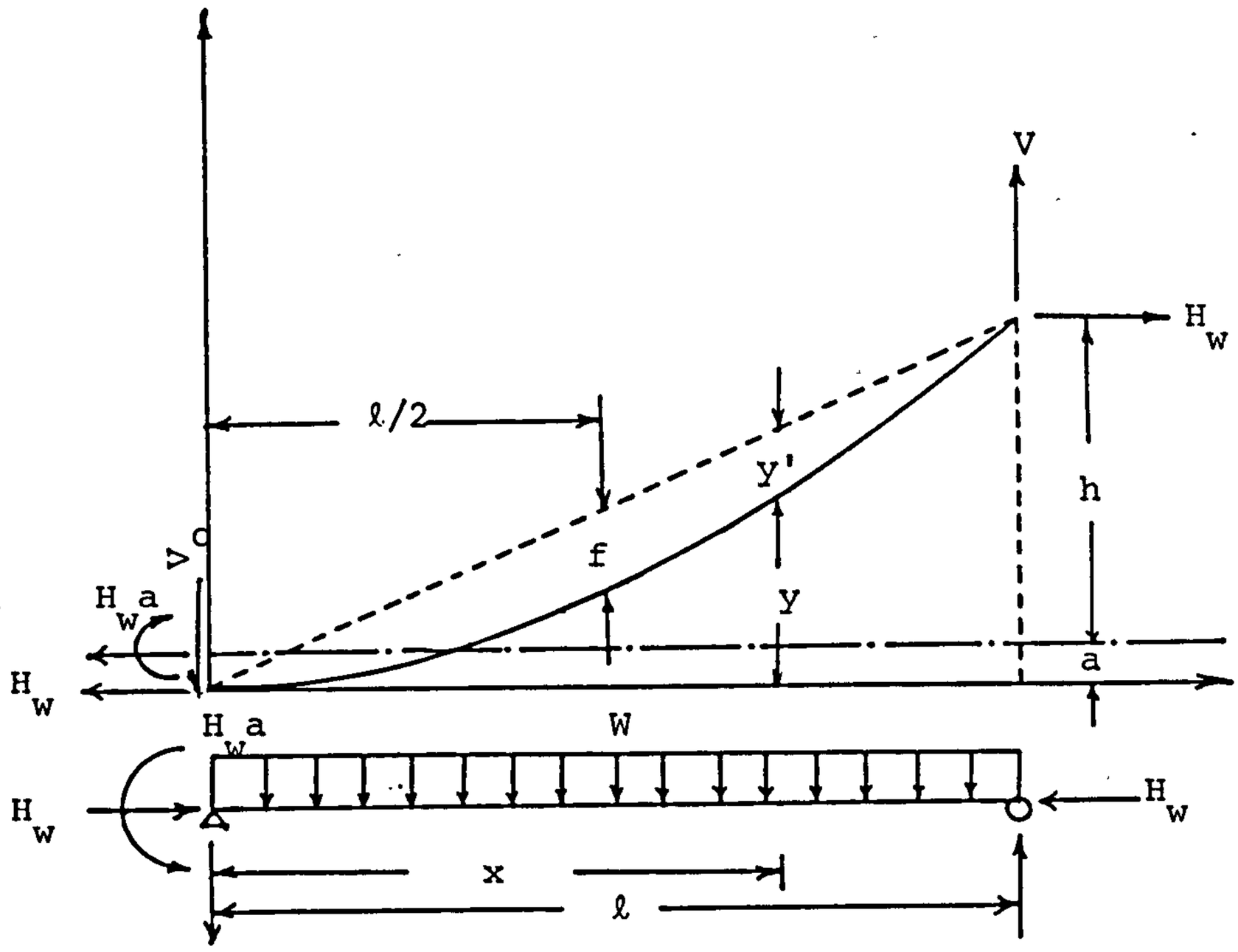

The cable shape in the left hand span with eccentricities at its ends

Figure (2.7)

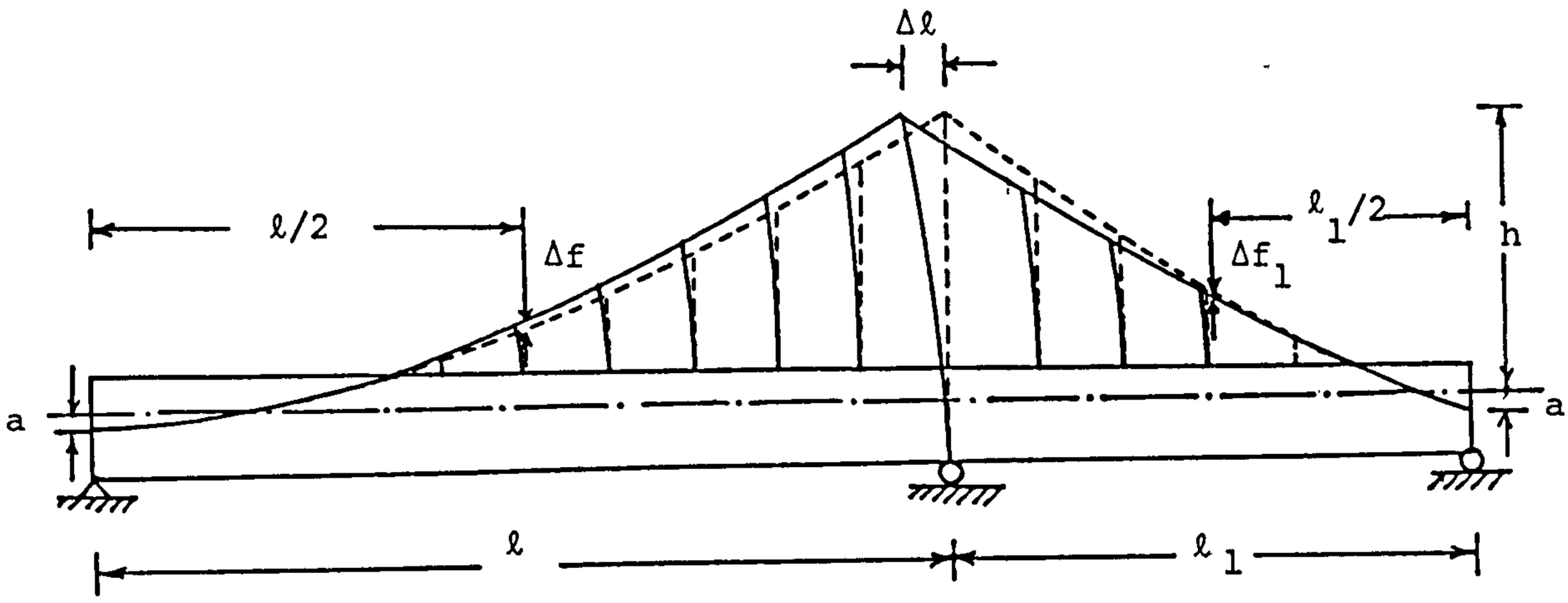

The main cable as affected by tower flexure

Figure (2.8)

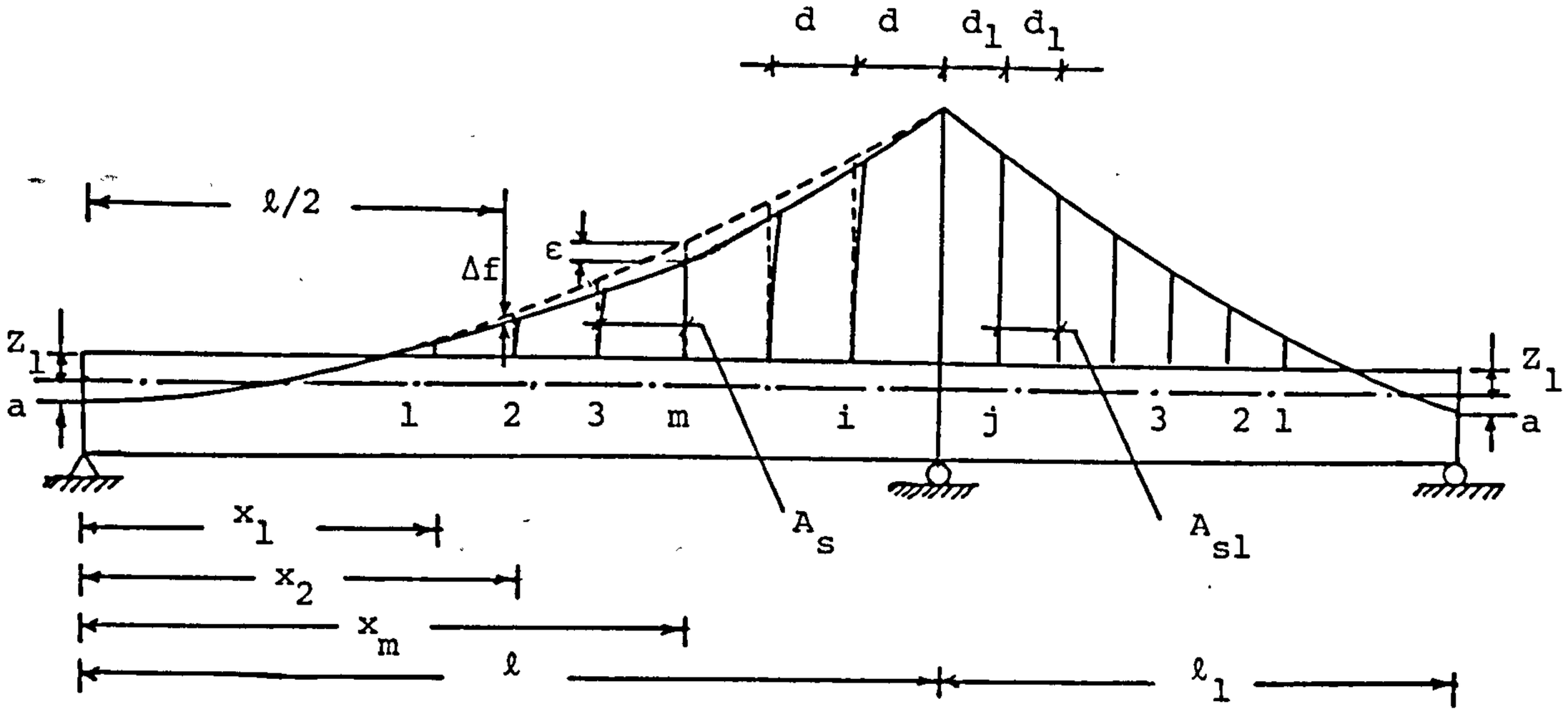

The main cable as affected by a construction error in one of the suspender lengths in the left hand span

Figure (2.9)

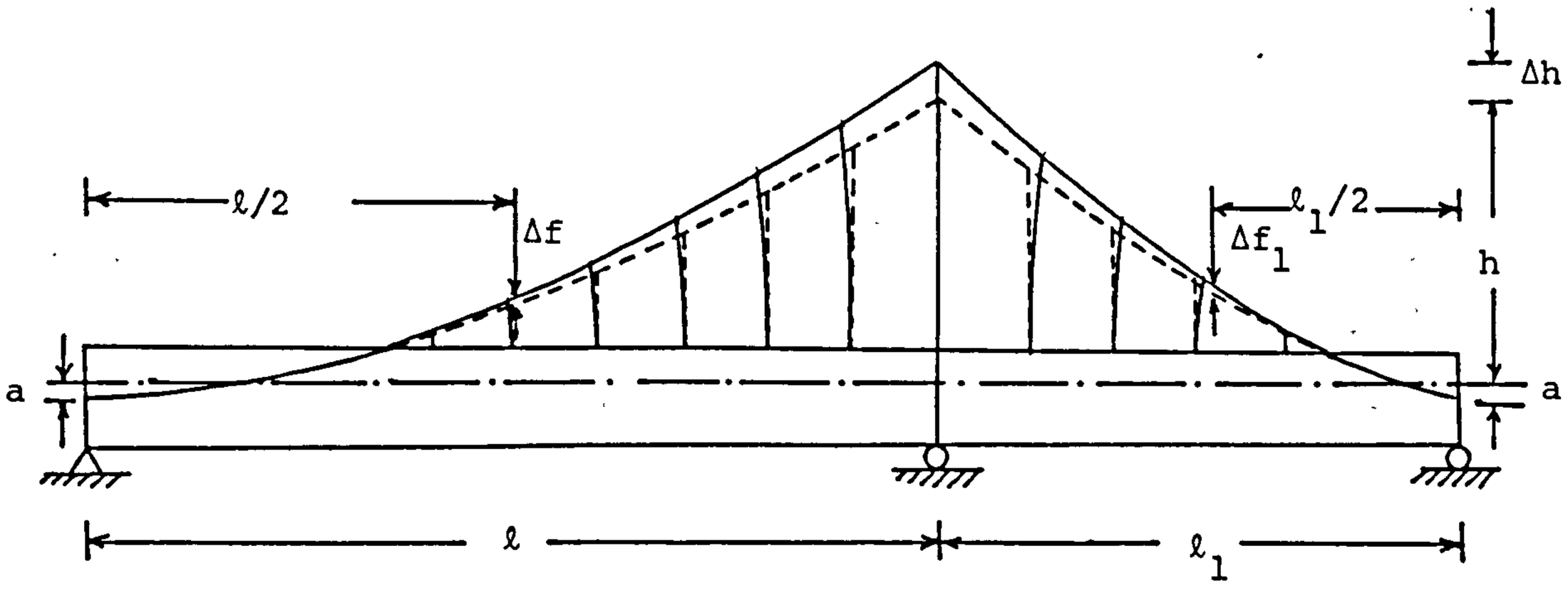

The main cable as affected by the expansion of the tower due to temperature rise

Figure (2.10)

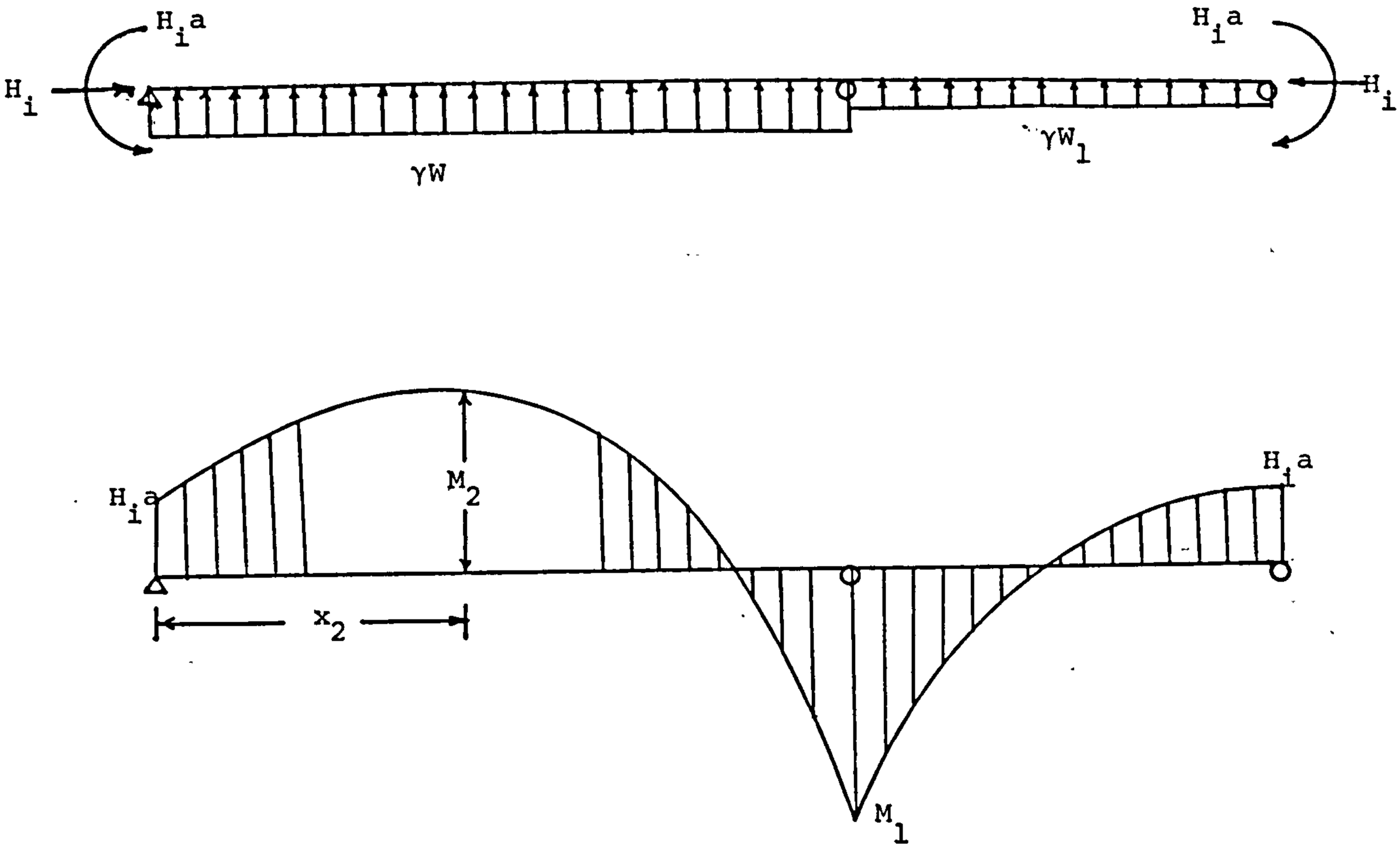

The bending moment diagram resulting from the combinations of the dead loads and the forces produced by the main cable

Figure (2.11)

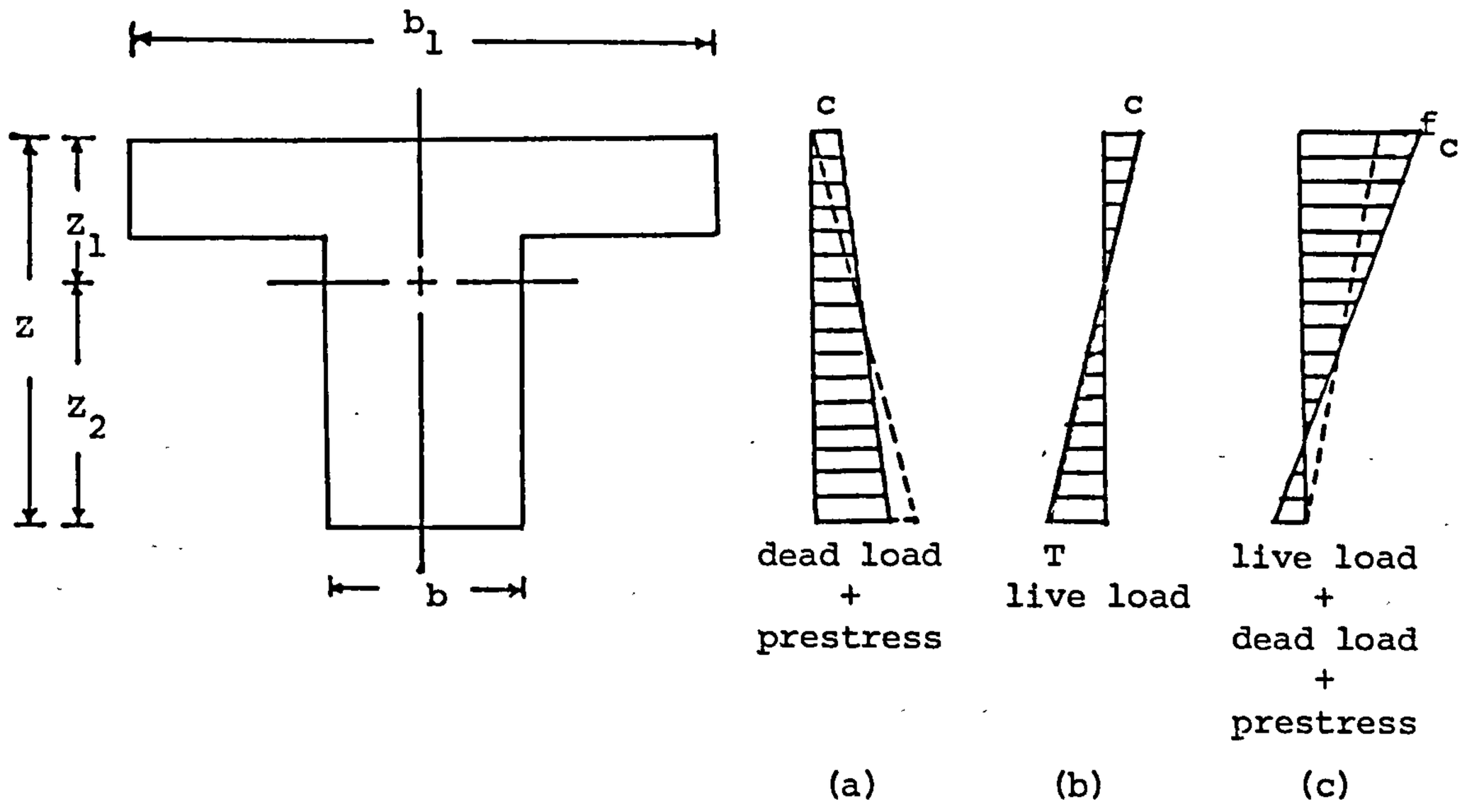

The stress distribution of the cross section of the beam when the initial prestressing force is applied

Figure (2.12)

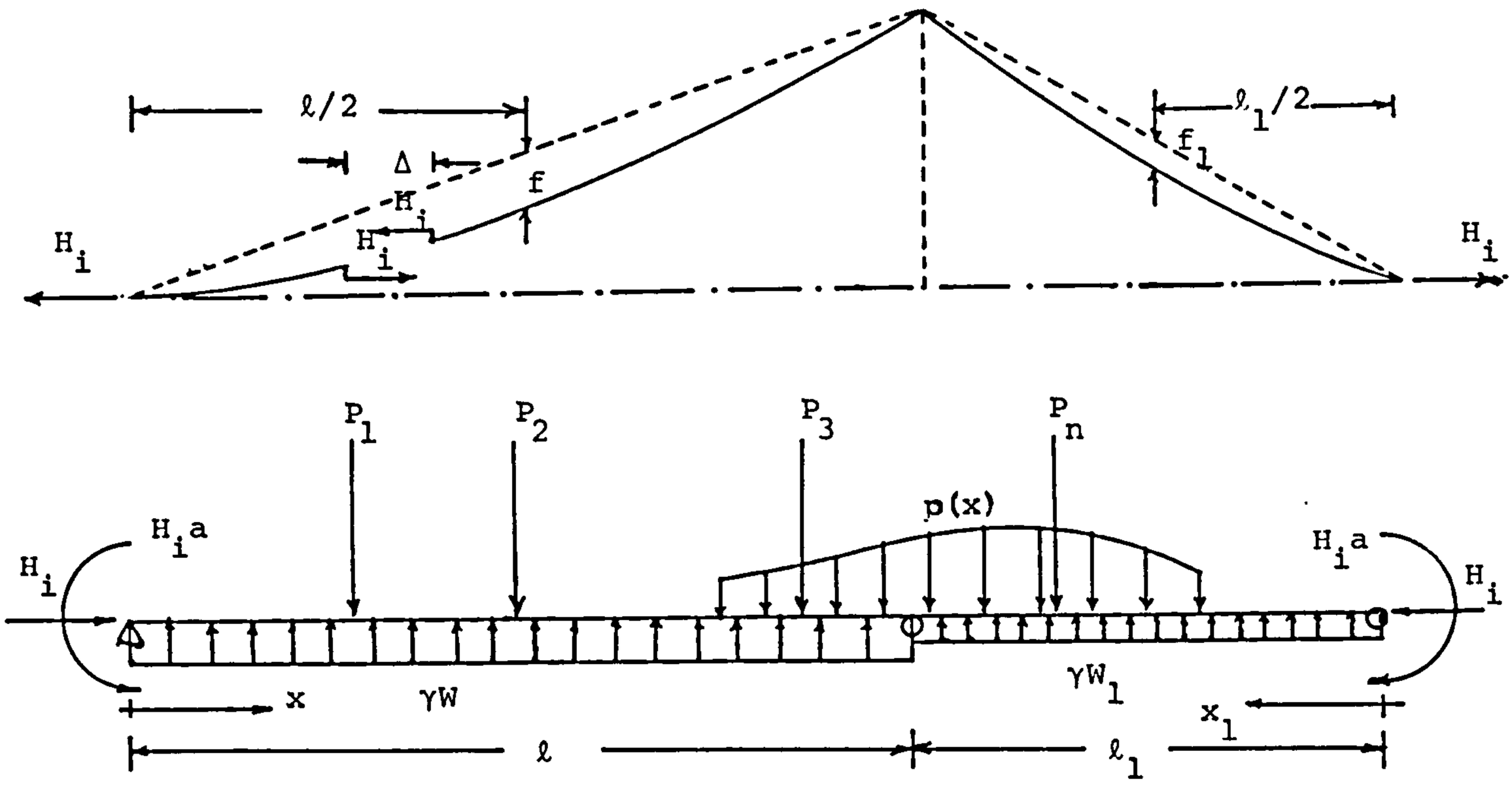

The gap Δ as produced by arbitrary live loads

Figure (2.13)

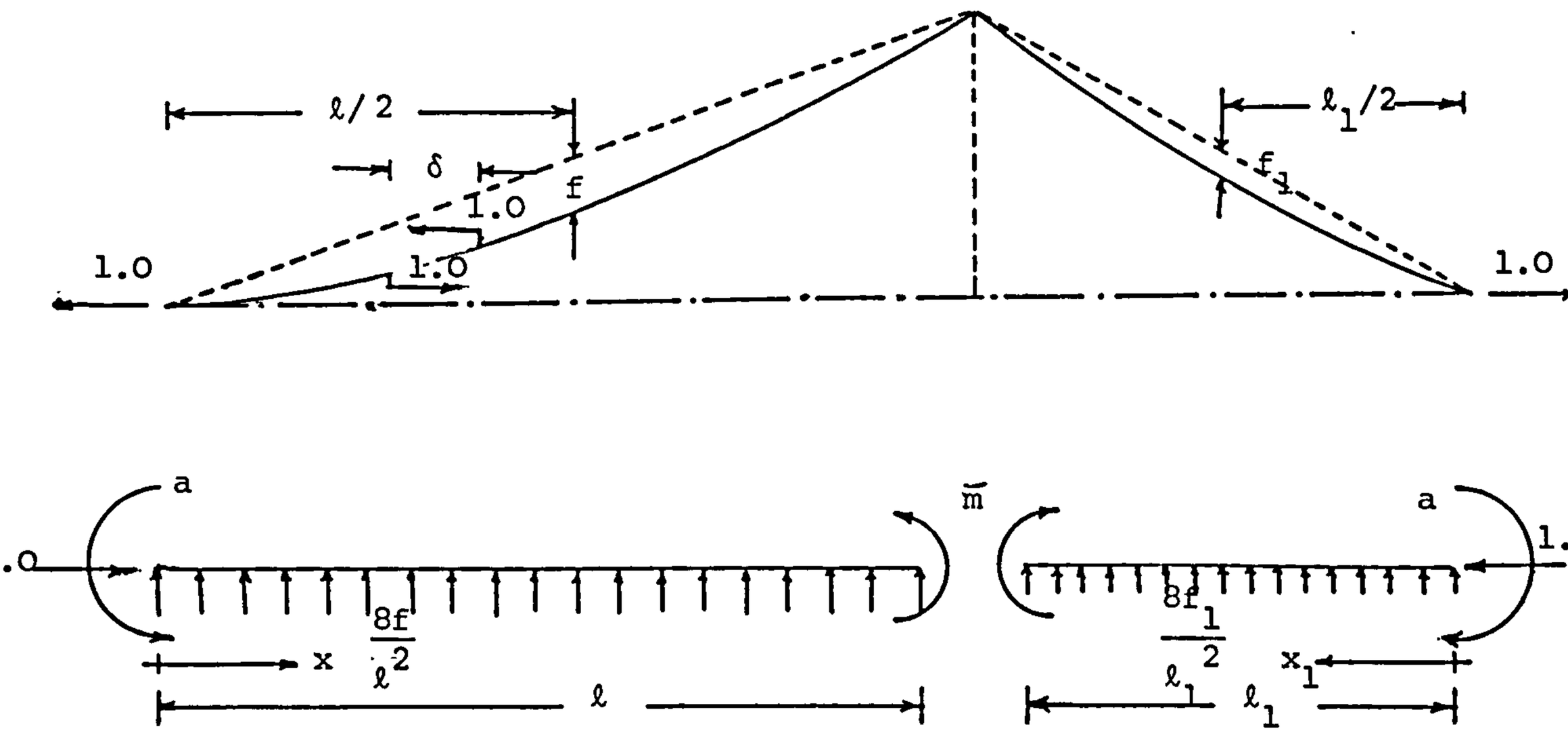

The gap δ as produced by a unit prestressing force

Figure (2.14)

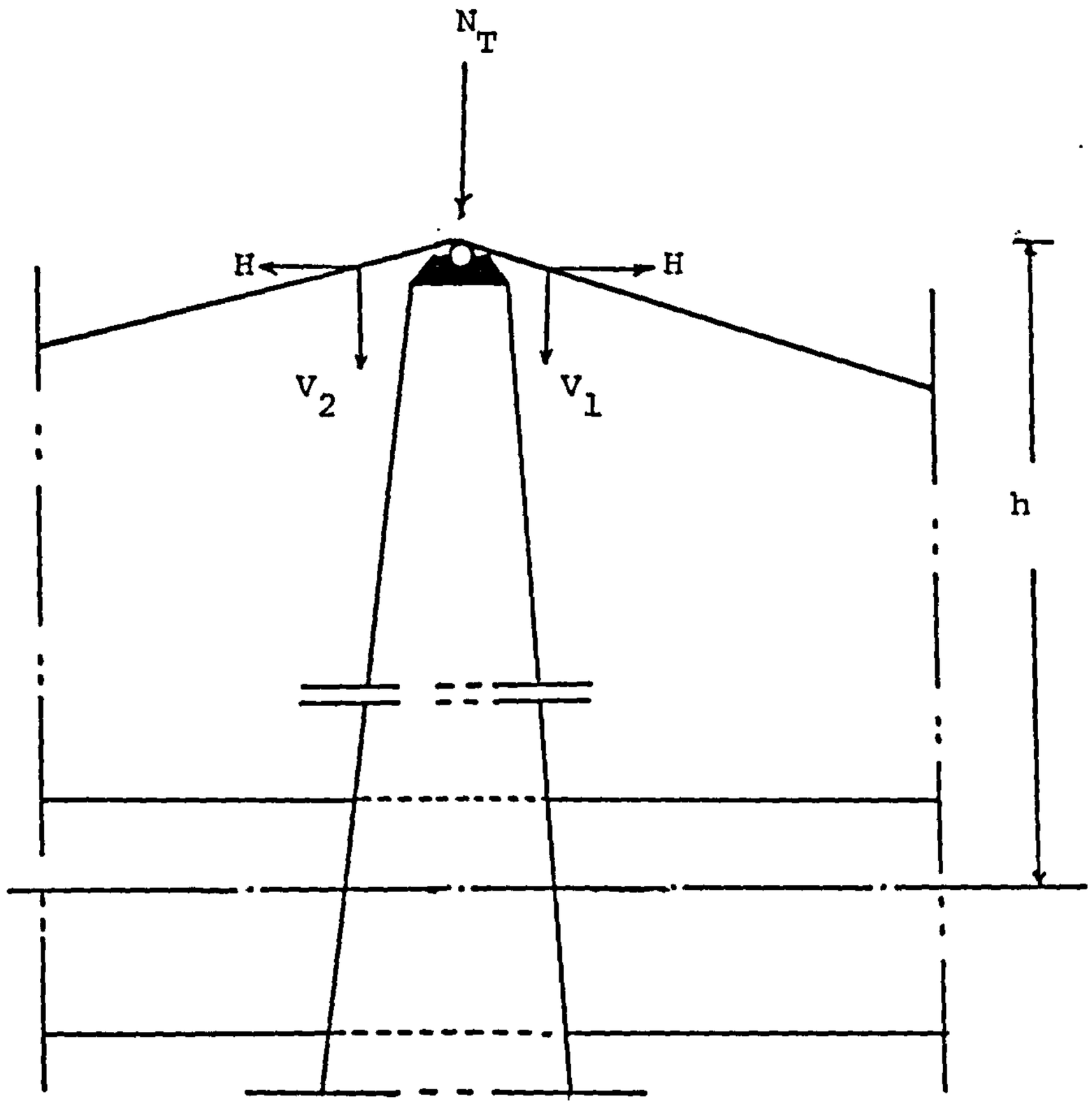

The Tower Force

Figure (2.15)

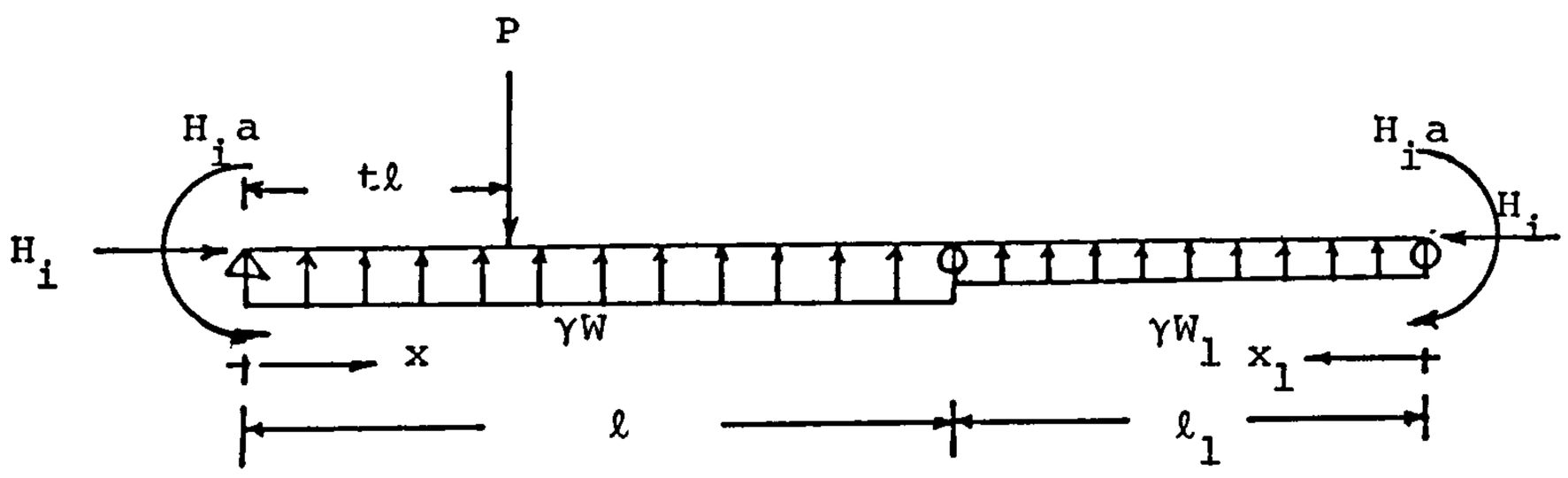

(a)

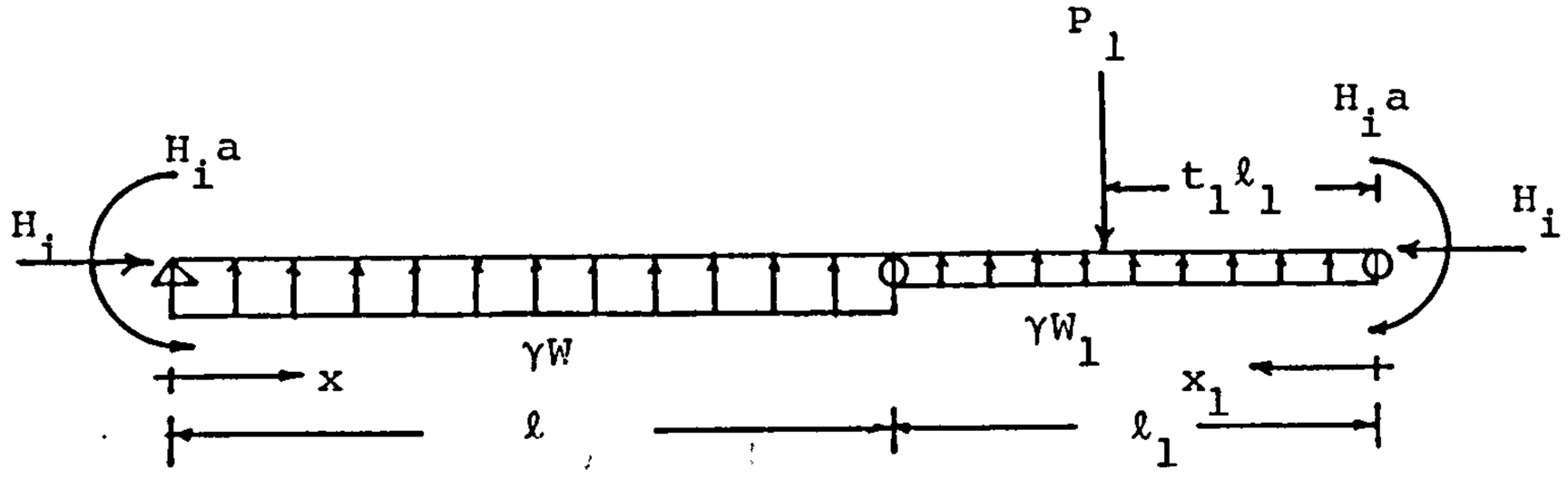

(b)

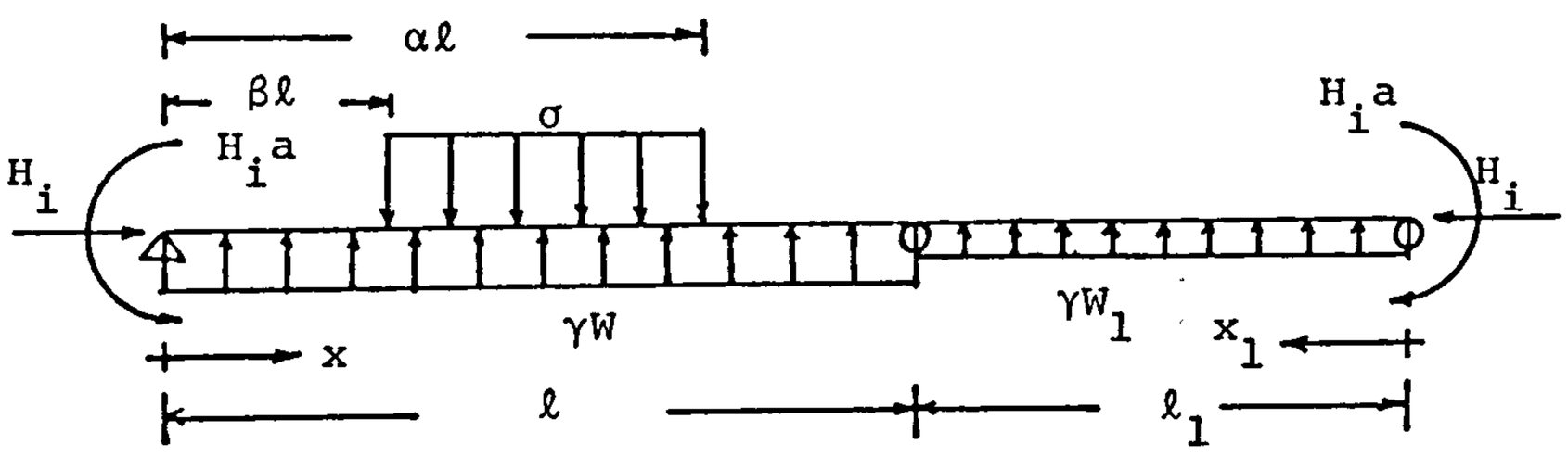

(c)

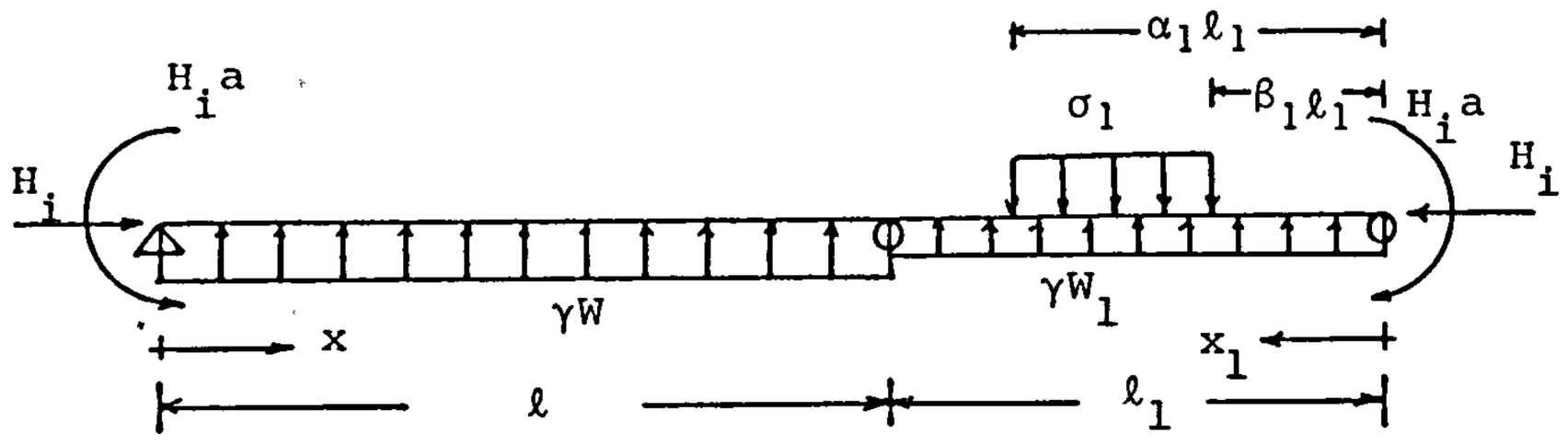

(d)

The suspended beam under various cases of live loading and the initial prestressing force is applied

Figure (2.16)

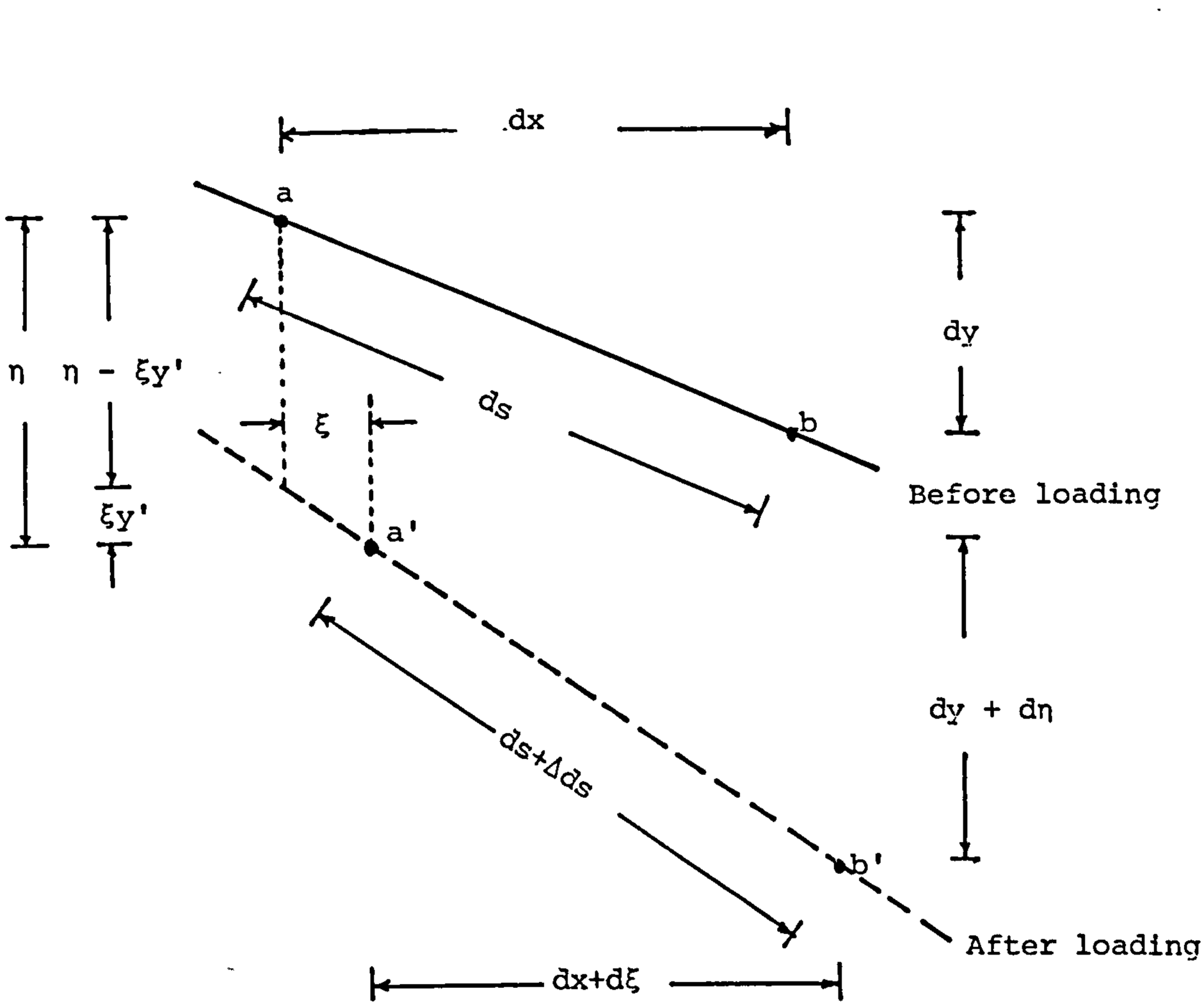

A cable element as affected by live loading

Figure (2.17)

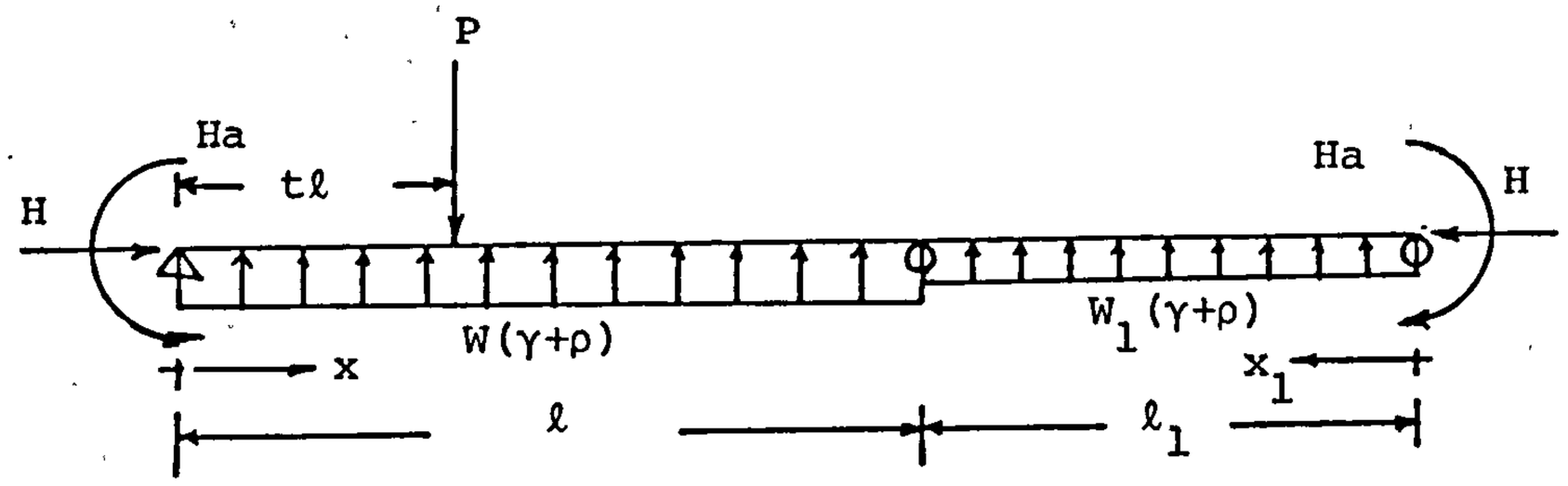

(a)

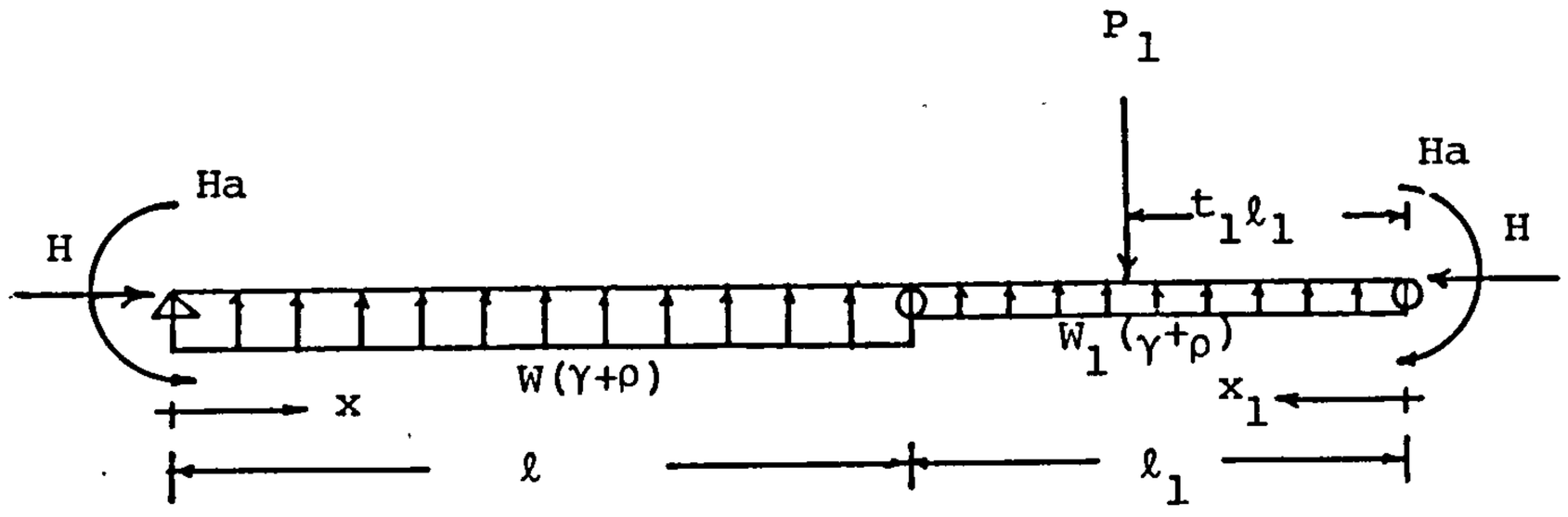

(b)

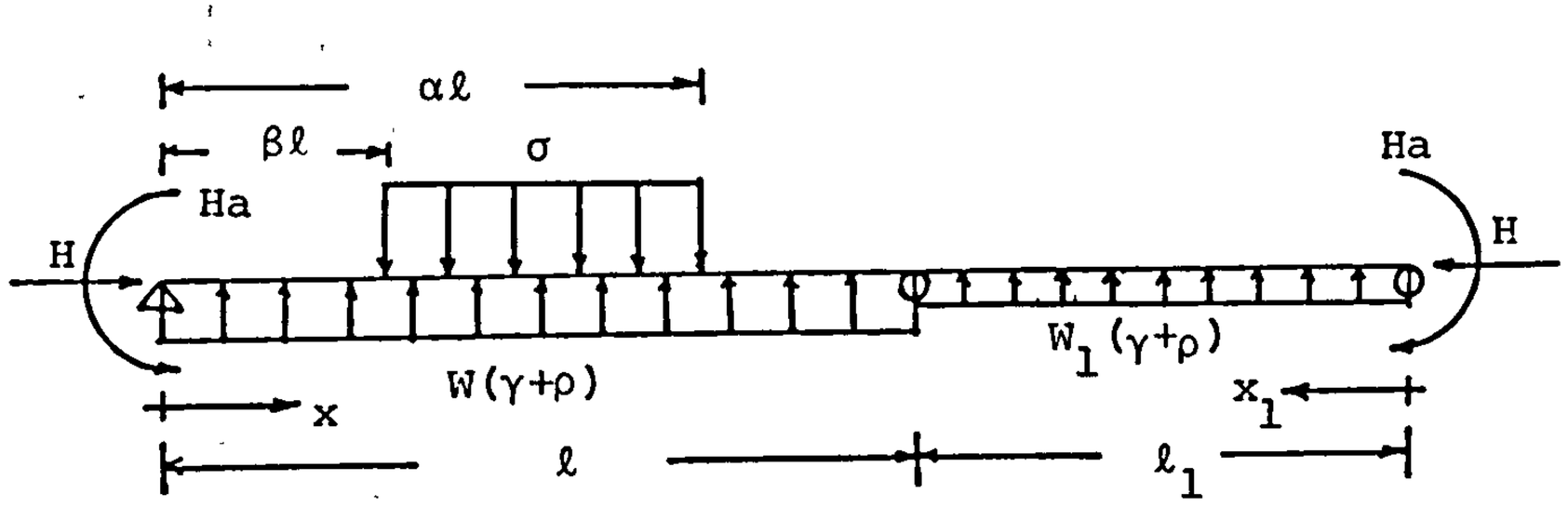

(c)

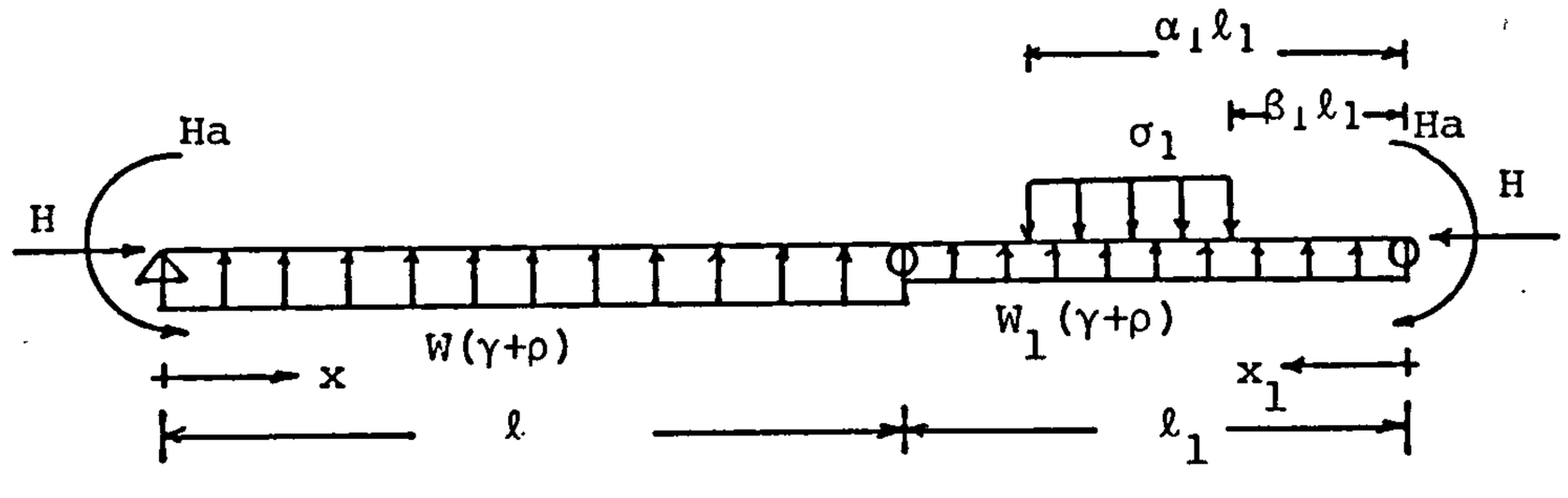

(d)

The suspended beam under various cases of live loading and the total prestressing force is applied

Figure (2.18)

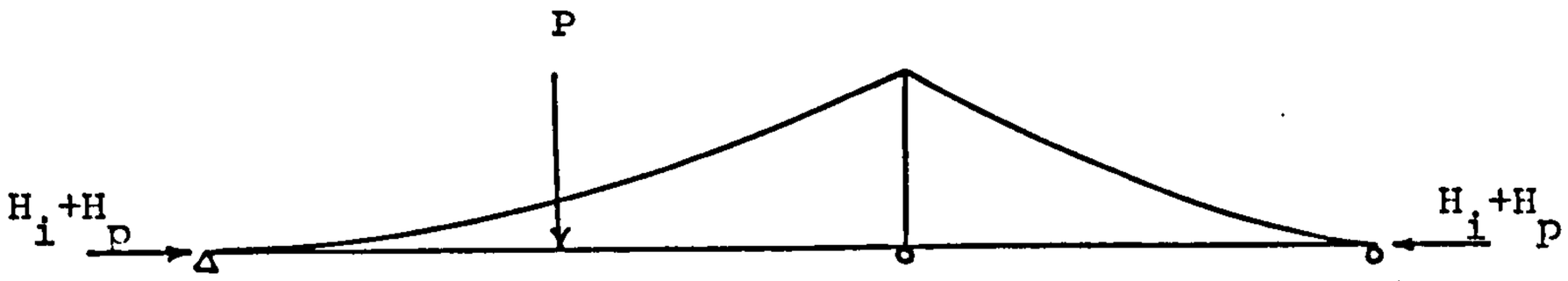

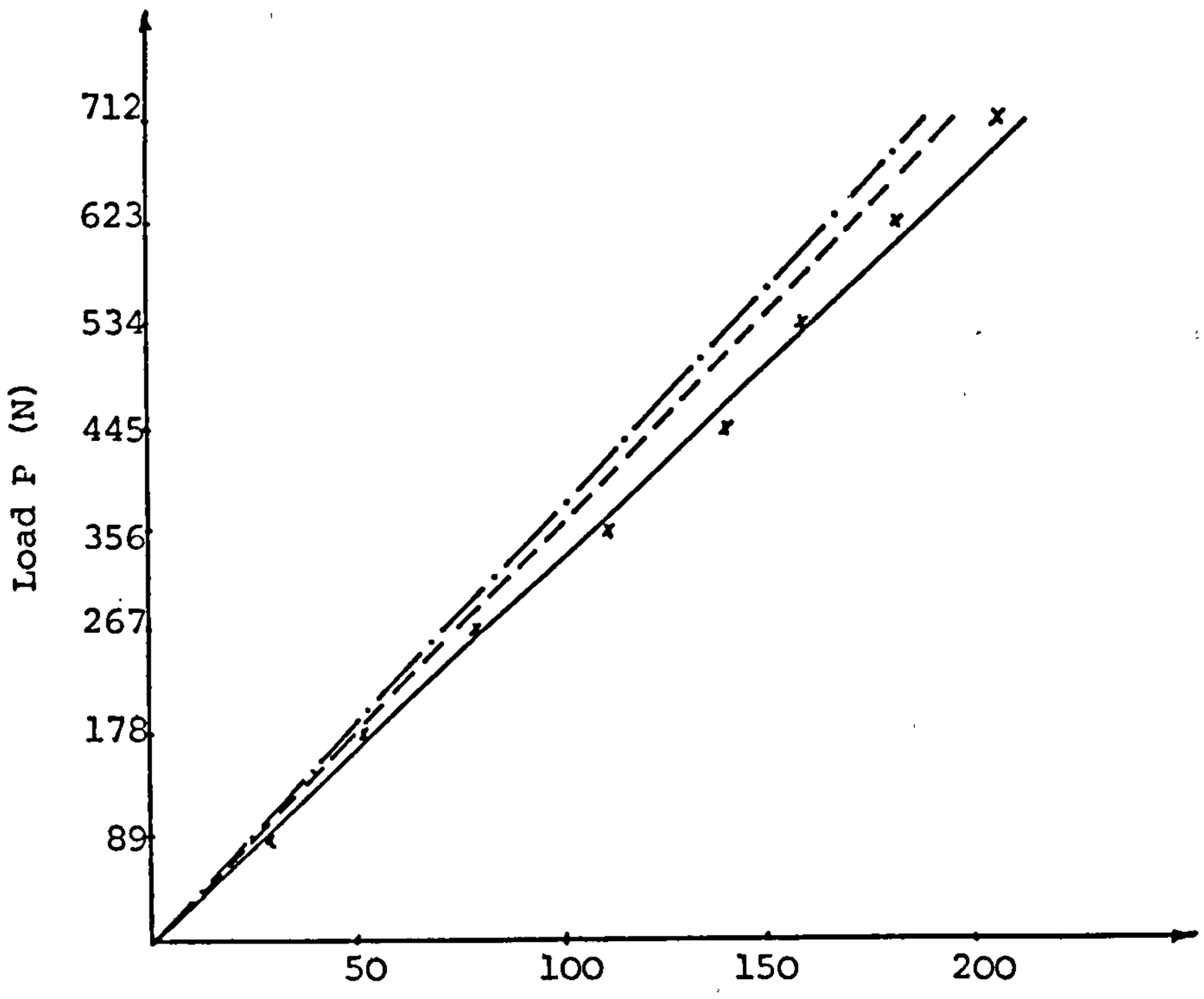

———— Measured

-------- Calculated by Timoshenko's approach

—·—·— Calculated by Steinman's approach

A comparison between the different approaches to evaluate the change in the prestressing force due to any applied live loading

Figure (2.19)

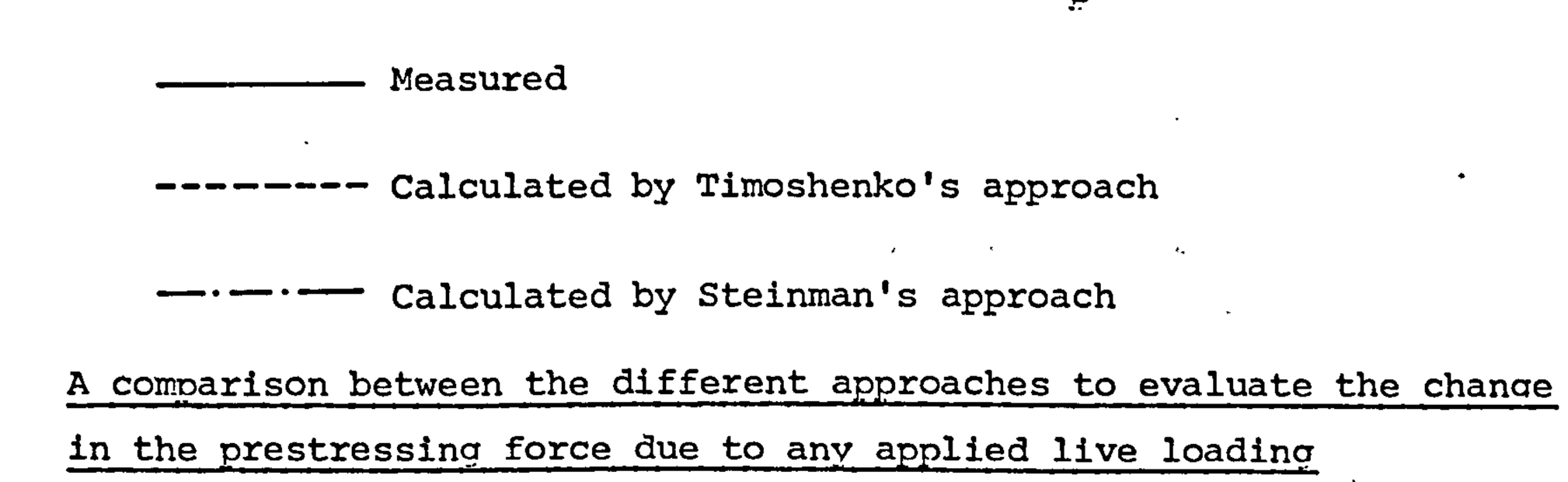

The system used to calculate the suspender forces

Figure (2.20)

CHAPTER 3

3. Theory and Design of Two-Span Prestressed Concrete Suspension Bridges with Grouted Cables

3.1 Introduction

In the following, we give a description of the grouted type of bridge and the effect of grouting on the forces of the structure.

Figure (3.1a) shows the grouted lengths of the cable denoted $g\ell$ and $g_1\ell_1$ for the left and right hand spans respectively. The initial prestressing force H_i remains effectively unchanged throughout the grouted lengths after the application of live loading. However, there will be a change in the cable tension, T_p, of the free ungrouted part of the cable due to the application of live loading, as shown in Figure (3.1b). The horizontal component of T_p is H_p in both spans and the vertical components are C H_p and C_1H_p in the left and right hand spans respectively.

Figure (3.1c) shows all the forces on the suspended beam when arbitrary live loads are applied. We have, similarly to the ungrouted type, continuous upward uniformly distributed loads, yW and yW_1, which result when subtracting the upward forces produced by the initial prestressing force, H_i, and the dead loads of the structure W and W_1 in the left and right hand spans. Furthermore, with the axial forces transferred to the centre line of the suspended beam, we have to add the end moments H_ia to account for the end eccentricities of the cable. We also have concentrated moments H_pZ_1, which are generated by the change in the horizontal tension H_p and applied at distances $g\ell$ and $g_1\ell_1$ from the end supports in the left and right hand spans. As mentioned earlier, Z_1 is the distance between the centre line and the top fibre of the suspended beam, see Figure (3.1a).

In addition, similarly to the ungrouted case, we have the partial upward uniformly distributed forces ρW and ρW_1 which are also generated by the increase in the prestressing force H_p and applied at the free ungrouted lengths of the cable, i.e. $g\ell \leqslant x \leqslant \ell$ and $g_1\ell_1 \leqslant x_1 \leqslant \ell_1$, in the left and right hand spans. ρ is the ratio of H_p to the preliminary value of the prestressing force H_w, see Section 2.2.

Obviously, the case of loading shown in Figure (3.1c) is extremely complicated especially because of the existence of the change in the prestressing force H_p within the span lengths. An analytical solution is possible but only with an enormous amount of labour and time consuming computer programming. Nevertheless, the system can be simplified by adding H_p to the initial prestressing force H_i throughout the beam length. In other words, the system will have only one axial force which will be applied at its ends, which is $H, = H_i + H_p$.

This approximation seems to be reasonable when considering the fact that the grouted lengths $g\ell$ and $g_1\ell_1$ never exceed 10% of the span lengths ℓ and ℓ_1 in full size bridges. Moreover, using H as the only axial force will undoubtedly give relatively greater values for moments, deflections ... etc, than the actual ones. Consequently, basing the design of the structure on those greater values will give an acceptable margin of safety.

The procedures of dimensioning the prestressed cable suspended beam and evaluating its initial prestressing force for maximum efficiency, H_i, are identical to those used for prestressed concrete suspension bridges with ungrouted cables (see Sections 2.2 and 2.4). Therefore, we will start this chapter by discussing the properties of the main cable and its deformation when subjected to different effects.

3.2 The Properties of the Parabolic Cable

Figure (3.2) shows the main cable in the left hand span. Clearly, its geometry is identical to that used in prestressed concrete suspension bridges with ungrouted cables. Therefore, Formulae (2.4 - 2.18) of the preceding chapter are applicable in this case and can be used to determine the required properties.

Figure (3.2) also shows the grouted length $g\ell$. g can be defined as the ratio of the grouted length of the left hand span to the entire length of the same span. Similar definition can be written for g_1 of the right hand span.

The grouted lengths ratios g and g_1 can be calculated by using Equations (2.17), where $x = g\ell$ at $y = Z_1+a$ which gives:

$$Z_1+a = F\ \ell\ g + 4\ n\ \ell\ g^2$$

$$g^2 + \frac{F\ell}{4f}\ g - \frac{(Z_1+a)}{4f} = o$$

Rejecting the negative solution, we have for the left hand span:

$$g = \left[\left(\frac{F\ell}{8f}\right)^2 + \left(\frac{Z_1+a}{4f}\right)\right]^{1/2} - \left(\frac{F\ell}{8f}\right) \qquad (3.1a)$$

Similarly, for the right hand span:

$$g_1 = \left[\left(\frac{F_1\ell_1}{8\ f_1}\right)^2 + \left(\frac{Z_1+a}{4\ f_1}\right)\right]^{1/2} - \left(\frac{F_1\ell_1}{8\ f_1}\right) \qquad (3.1b)$$

where f and f_1 are the cable sags in the left and right hand spans and can be calculated from Equation (2.5). Moreover, F and F_1 are the cable slopes at the left and right hand ends of the suspended beam which can be evaluated from Equations (2.18).

From Figure (3.1b), C and C_1 can be defined as the slopes of the main cable at the ends of the free ungrouted parts in the left and right hand spans respectively. In other words, from Equations (2.17) we have the cable slope equations:

$$\frac{dy}{dx} = F + \frac{8n}{\ell} x$$

$$\frac{dy_1}{dx} = F_1 + \frac{8n_1}{\ell_1} x_1$$

Hence, at $x = g\ell$ and $x_1 = g_1\ell_1$ we have:

$$C = F + 8\, n\, g \tag{3.2a}$$

$$C_1 = F_1 + 8\, n_1 g_1 \tag{3.2b}$$

where $n = \frac{f}{\ell}$ and $n_1 = \frac{f_1}{\ell_1}$.

From Equations (2.14), we see that the exact lengths of the ungrouted cable in the left and right hand spans have been expressed in terms of the slopes at their ends, F' & $(F'+8n)$ and F_1' & $(F_1'+8n_1)$ respectively. Taking advantage of that, the exact lengths of the free ungrouted parts of the main cable S_f and S_{f1} can be determined by replacing F' by C and F_1' by C_1 in Equations (2.14) for left and right hand spans respectively. Thus, we obtain:

$$S_f = \frac{\ell}{16n}\left[\ln\left[\frac{(F+8n) + [1+(F+8n)^2]^{1/2}}{C + [1+C^2]^{1/2}}\right] + (F+8n)[1+(F+8n)^2]^{1/2} - C\,[1+C^2]^{1/2}\right] \tag{3.3a}$$

$$S_{f1} = \frac{\ell_1}{16n_1}\left[\ln\left[\frac{(F_1+8n_1) + [1+(F_1+8n_1)^2]^{1/2}}{C_1 + [1+C_1^2]^{1/2}}\right] + (F_1+8n_1)[1+(F_1+8n_1)^2]^{1/2} - C_1\,[1+C_1^2]^{1/2}\right] \tag{3.3b}$$

The values of the end slopes [C, C_1, (F+8n) and (F_1+8n_1)] are usually small due to the fact that the spans are long with respect to the tower height. Therefore, Equations (3.3) can be approximated by using series expansion, see Appendix 16, which gives:

$$S_f = \frac{\ell}{48n} \left[(F+8n)\ [6+(F+8n)^2] - C\ [6+C^2] \right] \tag{3.4a}$$

$$S_{f1} = \frac{\ell_1}{48n_1} \left[(F_1+8n_1)\ [6+(F_1+8n_1)^2] - C_1\ [6+C_1^2] \right] \tag{3.4b}$$

for the left and right hand spans respectively.

The lengths of the grouted parts of the main cable S_g and S_{g1} can simply be calculated as follows:

$$S_g = S - S_f \tag{3.5a}$$

$$S_{g1} = S_1 - S_{f1} \tag{3.5b}$$

for the left and right hand spans respectively. Exact values can be obtained when substituting S, S_1, S_f and S_{f1} from Equations (2.14) and (3.3) or Equations (2.15) and (3.4) for approximate ones.

3.3 The Deformation of the Parabolic Cable

In this section, we discuss the deformability of the cable due to tower flexure, construction errors and temperature effects. Exact formulae as well as approximate ones are given to enable the designer to take into account these effects.

3.3.1 Tower Flexure

The causes for this effect are described in Section 2.3.4.1 and shown in Figure (2.8). Tower flexure can affect the main cable by causing it to change its length, shape and tension.

Starting with the changes in the main cable lengths ΔS_f and ΔS_{f1}, it is clear that they can only take place in the free ungrouted parts of the main cable for left and right hand spans respectively. Furthermore, they are governed by the following relationships:

$$\Delta S_f = \frac{\partial S_f}{\partial \ell} \quad (\pm \Delta \ell)$$

$$\Delta S_{f1} = \frac{\partial S_{f1}}{\partial \ell_1} \quad (\mp \Delta \ell)$$

Thus, by performing these derivations or by simply replacing F by C and F_1 by C_1 in Equations (2.19), we find:

$$\Delta S_f = \frac{(\pm \Delta \ell)}{8n} \ln \left[\frac{(F+8n) + [1+(F+8n)^2]^{1/2}}{C + [1+C^2]^{1/2}} \right] \qquad (3.6a)$$

$$\Delta S_{f1} = \frac{(\mp \Delta \ell)}{8n_1} \ln \left[\frac{(F_1+8n_1) + [1+(F_1+8n_1)^2]^{1/2}}{C_1 + [1+C_1^2]^{1/2}} \right] \qquad (3.6b)$$

for left and right hand spans respectively.

Approximate formulae are derived to give simplified versions of Equations (3.6) providing that the slopes are small enough, see Appendix 17. Hence, we have:

$$\Delta S_f = \frac{(\pm \Delta \ell)}{48n} \left[(F+8n)[6-(F+8n)^2] - C\,[6-C^2] \right] \qquad (3.7a)$$

$$\Delta S_{f1} = \frac{(\mp \Delta \ell)}{48n_1} \left[(F_1+8n_1)[6-(F_1+8n_1)^2] - C_1\,[6-C_1^2] \right] \qquad (3.7b)$$

for left and right hand spans respectively where F, F_1, C and C_1 can be found from Equations (2.18) and (3.2).

The effect on the cable shape can be represented as the change in the cable sags Δf and Δf_1 for left and right hand spans (see Figure 2.8). Following the same scheme of calculations shown in Section 2.4.3.1, or by simply replacing F by C and F_1 by C_1 in Equations (2.21), we arrive at the exact relationships between Δf, Δf_1 and $\Delta \ell$ as follows:

$$\Delta f = \frac{2n}{\left[\left[\frac{(F+8n)\,[1+C^2]^{1/2} - C\,[1+(F+8n)^2]^{1/2}}{\ln\left[\frac{(F+8n)+[1+(F+8n)^2]^{1/2}}{C+[1+C^2]^{1/2}}\right]}\right]-1\right]} (\pm \Delta\ell) \qquad (3.8a)$$

$$\Delta f_1 = \frac{2n_1}{\left[\left[\frac{(F_1+8n_1)\,[1+C_1^2]^{1/2} - C_1\,[1+(F_1+8n_1)^2]^{1/2}}{\ln\left[\frac{(F_1+8n_1)+[1+(F_1+8n_1)^2]^{1/2}}{C_1+[1+C_1^2]^{1/2}}\right]}\right]-1\right]} (\mp \Delta\ell) \qquad (3.8b)$$

for the left and right hand spans respectively.

The approximate forms of these relationships are, as derived in Appendix 18:

$$\Delta f = 2n\,\frac{[(F+8n)[6-(F+8n)^2] - C[6-C^2]\,]}{[(F+8n)^3 - C^3 - 3C(F+8n)[(F+8n)-C]]} (\pm \Delta\ell) \qquad (3.9a)$$

for the left hand span and:

$$\Delta f_1 = 2n_1\,\frac{[(F_1+8n_1)[6-(F_1+8n_1)^2] - C_1[6-C_1^2]]}{[(F_1+8n_1)^3 - C^3 - 3\,C_1(F_1+8n_1)[(F_1+8n_1)-C_1]]} (\mp \Delta\ell) \qquad (3.9b)$$

for the right hand span.

The corresponding change in the horizontal tension ΔH of the cable can be calculated from Equation (3.16) as will be shown later in Section (3.3.4)

3.3.2 Construction Errors

A construction error in one, or more, of the lengths of the suspenders will change the cable sag, or sags, Δf or Δf_1 by an amount which can be directly calculated from Equations (2.24), see Figure (2.9), for left or right hand spans.

The corresponding change in the cable length can be obtained when substituting the calculated value of the change in the cable sag, or sags, in the following exact equations: (similar to Equations (2.25))

$$\Delta S_f = - \frac{\Delta f}{16n^2} \left[\ln \left[\frac{(F+8n)+ [1+(F+8n)^2]^{1/2}}{C + [1+C^2]^{1/2}} \right] + C[1+(F+8n)^2]^{1/2} - (F+8n)[1+C^2]^{1/2} \right] \qquad (3.10a)$$

for the left hand span and:

$$\Delta S_{f1} = - \frac{\Delta f_1}{16n_1^2} \left[\ln \left[\frac{(F_1+8n_1)+ [1+(F_1+8n_1)^2]^{1/2}}{C_1 + [1+C_1^2]^{1/2}} \right] + C_1[1+(F_1+8n_1)^2]^{1/2} - (F_1+8n_1)[1+C_1^2]^{1/2} \right] \qquad (3.10b)$$

for the right hand span as shown in Appendix 18. The Appendix 18 also gives the approximate forms of these equations, providing that the cable slopes are small, as follows:

$$\Delta S_f = \frac{\Delta f}{96n^2} \left[[(F+8n)^3 - C^3] - 3C (F+8n)[(F+8n)-C] \right] \qquad (3.11a)$$

$$\Delta S_{f1} = \frac{\Delta f_1}{96n_1^2} \left[[(F_1+8n_1)^3 - C_1^3] - 3C_1 (F_1+8n_1)[(F_1+8n_1) - C_1] \right] \qquad (3.11b)$$

for the left and right hand spans respectively where F, F_1, C and C_1 can be evaluated from Equations (2.18) and (3.2). The corresponding change in the cable tension ΔH can be calculated from Equation (3.16) as will be shown later in Section (3.3.4).

Finally, for a construction error in the height of the tower Δh, see Figure (2.10), the corresponding change in the cable lengths ΔS_f and ΔS_{f1} can be obtained from the relationships:

$$\Delta S_f = \frac{\partial S_f}{\partial h} \Delta h$$

and,

$$\Delta S_{f1} = \frac{\partial S_{f1}}{\partial h} \Delta h$$

where Δh = Actual Height - Theoretical Height.

The relationship between ΔS_f, ΔS_{f1} and Δh can be directly established when replacing F by C and F_1 by C_1 in Equations (2.27) which gives:

$$\Delta S_f = \frac{\Delta h}{8n} \left[[1+(F+8n)^2]^{1/2} - [1 + C^2]^{1/2} \right] \qquad (3.12a)$$

$$\Delta S_{f1} = \frac{\Delta h}{8n_1} \left[[1+(F_1+8n_1)^2]^{1/2} - [1 + C_1^2]^{1/2} \right] \qquad (3.12b)$$

for left and right hand spans respectively.

Figure (2.10) also shows that the cable sags alter by amounts Δf and Δf_1 from the design values. These alterations can be calculated from the following relationships:

$$\frac{\partial S_f}{\partial f} \Delta f = \frac{\partial S_f}{\partial h} \Delta h$$

$$\frac{\partial S_{f1}}{\partial f_1} \Delta f_1 = \frac{\partial S_{f1}}{\partial h} \Delta h$$

Thus, from Equations (3.10) and (3.12), Δf and Δf_1 can exactly be evaluated as follows:

$$\Delta f = 2n \frac{\left[[1 + C^2]^{1/2} - [1+(F+8n)^2]^{1/2}\right]}{\left[\ln\left[\frac{(F+8n)+[1+(F+8n)^2]^{1/2}}{C+ [1+C^2]^{1/2}}\right] + C[1+(F+8n)^2]^{1/2} - (F+8n)[1+C^2]^{1/2}\right]} \Delta h \qquad (3.13a)$$

for the left hand span and,

$$\Delta f_1 = 2n_1 \frac{\left[[1 + C_1^2]^{1/2} - [1 + (F_1+8n_1)^2]^{1/2}\right]}{\left[\ln\left[\frac{(F_1+8n_1)+ [1+(F_1+8n_1)^2]^{1/2}}{C_1+ [1+C_1^2]^{1/2}}\right] + C_1[1+(F_1+8n_1)^2]^{1/2} - (F_1+8n_1)[1+C_1^2]^{1/2}\right]} \qquad (3.13b)$$

for the right hand span.

The approximate versions of these equations can be found from Equations (3.11) and (3.12) where we have:

$$\Delta f = 12n \frac{\left[[+(F+8n)^2]^{1/2} - [1 + C^2]^{1/2}\right]}{\left[[(F+8n)^3 - C^3] - 3C(F+8n)[(F+8n) - C]\right]} \Delta h \qquad (3.14a)$$

$$\Delta f_1 = 12n_1 \frac{\left[[1+(F_1+8n_1)^2]^{1/2} - [1 + C^2]^{1/2}\right]}{\left[[(F_1+8n_1)^3 - C_1^3] - 3C_1(F_1+8n_1)[(F_1+8n_1) - C_1]\right]} \Delta h \qquad (3.14b)$$

for left and right hand spans respectively where F, F_1, C and C_1 are the cable slopes and they can be determined from Equations (2.18) and (3.2).

The corresponding change in the cable tension ΔH can be computed from Equation (3.16) as will be shown later in Section (3.3.4).

3.3.3 The Temperature Effect

As mentioned earlier, in this form of construction the steel and concrete posts are separated and therefore, ambient temperature changes, $\pm\Delta t$, may lead to more significant stress changes than would arise in more conventional forms of structures.

Thus, starting with the suspended beam, the effect of temperature changes on its length is identical to that of the suspended beam with ungrouted cables. Therefore, Equation (2.30) may be used to determine the change in the length $\Delta\ell$. Then, the corresponding changes in the cable lengths ΔS_f and ΔS_{f1} and shape, Δf and Δf_1, can be determined by substituting $\Delta\ell$ into Equations (3.6) and (3.8) respectively for exact values or Equations (3.7) and (3.9) for approximate ones.

For the main cable, similar to Equations (2.31), the corresponding change in the cable lengths ΔS_f and ΔS_{f1} can be calculated as follows:

$$\Delta S_f = \pm \alpha_s \Delta t \, S_f \tag{3.15a}$$

$$\Delta S_{f1} = \pm \alpha_s \Delta t \, S_{f1} \tag{3.15b}$$

for the left and right hand spans respectively where α_s is the thermal coefficient of expansion for steel, $\simeq 0.000011$ per C°. The corresponding change in the cable sags Δf and Δf_1 can be evaluated from Equations (3.10) or (3.11).

The suspenders will respond to the temperature changes by elongating or contracting and consequently the cable sags will change by amounts Δf and Δf_1 which are governed by Equations (2.32). Thus, the corresponding changes in the cable lengths ΔS_f and ΔS_{f1} can then be calculated by substituting Δf and Δf_1 in Equations (3.10) for the exact values or Equations (3.11) for the approximate ones.

The height of the tower will also be affected by the change in the temperature. It will be altered by an amount Δh which can be calculated from Equation (2.33). Thus, the corresponding change in the cable lengths ΔS_f and ΔS_{f1} as well as the changes in the cable shape Δf and Δf_1 can be calculated from Equations (3.12) and (3.13) respectively.

Finally, the total change in the cable lengths can be evaluated and then, the corresponding change in the horizontal tension ΔH of the cable can be computed from Equation (3.16) as will be shown in the following section.

3.3.4 The Effect of the Elastic Deformation of the Cable on its Tension

For the previous changes in the cable lengths ΔS_f and ΔS_{f1} which result from the aforementioned effects, there will be a corresponding change in the cable tension ΔH which can be evaluated from the following equation: (see Appendix 19)

$$\Delta H = \frac{A_c E_c}{\ell}\left[\frac{\Delta S_f}{\left[(1-g)\left[1+F(C+8n)\right]+\frac{64}{3}n^2(1-g^3)\right]} + \frac{\Delta S_{f1}}{\lambda\left[(1-g_1)\left[1+F_1(C_1+8n_1)\right]+\frac{64}{3}n_1^2(1-g_1^3)\right]}\right] \tag{3.16}$$

where $\lambda = \frac{\ell_1}{\ell}$ and where A_c and E_c are the cross sectional area and Young's modulus of elasticity for the main cable. The quantities n, n_1, g and g_1 can be computed from Equations (2.11) and (3.1) respectively.

Equation (3.16) may be applied to determine the change in the horizontal tension ΔH of the cable corresponding to a change, or changes, which might occur in the cable length, or lengths, in either one or both spans of the suspended beam.

Finally, Formulae (3.1 - 3.16) are applicable to suspended beams with grouted cables and no eccentricities at their ends when substituting these eccentricities zero, a = o. Consequently, this

will change the cable slopes F, F_1, C and C_1, Equation (2.18) and (3.2), and the new values can be substituted into the above formulae. Moreover, it can be proved that the above formula are applicable to ungrouted cables when substituting the grouted lengths by zero, g = g_1 = o.

3.4 The Behaviour of the Main Cable Under Applied Live Loading

3.4.1 Discussion

As mentioned in Section 3.1, the free ungrouted part of the main cable will respond to the applied live loading by changing its tension an amount T_p, Figure (3.1b). The horizontal and vertical components of T_p will then act as external forces applied at distances $g\ell$ and $g_1\ell_1$ from the end supports of the left and right hand spans respectively. As a result of effectively transferring the horizontal component H_p to the centre line of the structure, external concentrated moments H_pZ_1 will have to be added at the same positions for both spans.

The change in the horizontal tension H_p will also generate upward uniformly distributed forces ρW and ρW_1 which will operate in the ungrouted regions, $g\ell \leqslant x \leqslant \ell$ and $g_1\ell_1 \leqslant x_1 \leqslant \ell_1$, for the left and right hand spans respectively, Figure (3.1c). It has also been mentioned that the system is simplified by adding the horizontal component of the change in the cable tension, H_p, to the axial forces at the ends of the beam.

Clearly, when applying Steinman's approach, (20) and (21), to evaluate H_p, the problem is transformed to be identical to that of the two-span prestressed concrete suspension bridges with ungrouted cables and therefore, Formulae (2.39 - 2.54) may be applied without any alterations. The reason for this is that the method entirely ignores the change in the horizontal tension H_p as well as the forces it produces. To some extent, the method gives results with sufficient accuracy for suspended beams with ungrouted cables providing

that the spans are not too long. However, for suspended beams with grouted cables, the change in the horizontal tension H_p produced by the live loading is usually of greater value. Consequently, the forces it generates may be of significant values and therefore can not be ignored.

For the above reasons, Timoshenko's approach, (25) and (26), is the only method which can be used in this case to determine H_p and Equation (2.57) may be applied again where:

$$\frac{H_p}{A_c E_c} \sum \int \left(\frac{dS_f}{dx} \right)^3 dx = \sum \frac{W}{H_w} \int \eta dx \qquad (3.17)$$

or simply:

$$H_p \, \delta_{cf} = \sum \frac{W}{H_w} \int \eta dx \qquad (3.18a)$$

where,

$$\delta_{cf} = \frac{1}{A_c E_c} \sum \int \left(\frac{dS_f}{dx} \right)^3 dx \qquad (3.18b)$$

Hence, we start this section by evaluating the different quantities of Equation (3.18).

3.4.2 The Determination of the Term δ_{cf}

As mentioned earlier, only the free ungrouted part of the main cable will respond to the applied live loading by changing its tensions for both left and right hand spans. Therefore, the integration of Equation (3.18b) must only be performed for the regions $g\ell \leqslant x \leqslant \ell$ and $g_1\ell_1 \leqslant x_1 \leqslant \ell_1$ for the left and right hand spans respectively. Hence, δ_{cf} can be calculated from the following equations:

$$\delta_{cf} = \frac{1}{A_c E_c} \left[\int_{g\ell}^{\ell} \left(\frac{dS_f}{dx} \right)^3 dx + \int_{g_1\ell_1}^{\ell_1} \left(\frac{dS_{f1}}{dx_1} \right)^3 dx_1 \right]$$

From Equation (2.45), the value of the term δ_c is expressed in terms of the slopes at the ends of the cable. Taking advantage of that, δ_{cf} can be directly obtained by replacing F by C and F_1 by C_1 in this Equation which gives:

$$\delta_{cf} = \frac{\ell}{64\ n\ A_c E_c}\left[3\ \ln\left[\frac{(F+8n)+[1+(F+8n)^2]^{1/2}}{C+[1+C^2]^{1/2}}\right]+(F+8n)[1+(F+8n)^2]^{1/2}[5+2(F+8n)^2]\right.$$

$$-C\,[1+C^2]^{1/2}(5+2C^2)+\frac{1}{\omega}\left[3\ \ln\left[\frac{(F_1+8n_1)+[1+(F_1+8n_1)^2]^{1/2}}{C_1+[1+C_1^2]^{1/2}}\right]\right.$$

$$\left.\left.+(F_1+8n_1)[1+(F_1+8n_1)^2]^{1/2}[5+2(F_1+8n_1)^2]-C_1[1+C_1^2]^{1/2}(5+2C_1^2)\right]\right] \qquad (3.19)$$

where $\omega = \frac{W_1}{W}$.

For flat curves, Equation (3.19) can be approximated, see Appendix 20, to give a simpler version for the determination of δ_{cf} as follows:

$$\delta_{cf} = \frac{\ell}{16\ n\ A_c E_c}\left[(F+8n)[2+(F+8n)^2]-C\,[2+C^2]+\frac{1}{\omega}\left[(F_1+8n_1)[2+(F_1+8n_1)^2]\right.\right.$$

$$\left.\left.-C_1[2+C_1^2]\right]\right] \qquad (3.20)$$

where F, F_1, C and C_1 can be computed from Equations (2.18) and (3.2) respectively.

Clearly, the value of δ_{cf} is less than δ_c, as can be seen from Equation (2.45) and (3.19), depending on the grouted lengths $g\ell$ and $g_1\ell_1$. This means that the change in the horizontal tension H_p of the cable will have a greater value than that of a suspended beam with ungrouted cables when live load is applied, see Equations

(3.18). Consequently, there will be an improvement in the interaction between the main cable and the suspended beam as will be discussed later in this chapter.

3.4.3 The Evaluation of the Term $\sum \frac{W}{H_w} \int \eta dx$

From Figure (3.1c), it can be seen that the applied forces on the prestressed cable suspended beam can be divided into two groups. The first group is that of the forces which do not change their type or location throughout the life of the bridge. It comprises the two upward continuous uniformly distributed loads γW & γW_1, the two upward partial uniformly distributed loads ρW & ρW_1, the two upward concentrated forces CH_p & C_1H_p, the two concentrated moments H_pZ_1 and the two end moments $H_i a$ for left and right hand spans respectively. The second group comprises the live loads which are applied to the structure.

For simplicity, the term $\sum \frac{W}{H_w} \int \eta dx$ will be evaluated separately for each group of forces. Obviously, it will remain unchanged for the first group of forces and change its value according to the type and location of the live loading for the second group of forces. The principle of superposition can then be used to determine the final value of the term $\sum \frac{W}{H_w} \int \eta dx$ for each case of loading.

For the first group of forces, the subscript 1 will be used i.e. $\left[\sum \frac{W}{H_w} \int \eta dx \right]_1$, to denote the required quantity. Thus, from Appendix 21, it can be evaluated as:

$$\left[\sum \frac{W}{H_w} \int \eta dx \right]_1 = - \frac{W}{H_w} \left[\frac{\gamma W}{H} \left[\frac{1}{\mu^2} (\theta+\omega^2\theta_1) - \frac{(\theta+\omega\theta_1)^2}{4(\phi+\phi_1)} - \frac{\ell^3}{12} (1+\omega^2\lambda^3) \right] \right.$$

$$+ \frac{\rho W}{H} \left[\frac{\ell}{\mu^2} \left(\frac{\cos \frac{\mu g \ell}{2} \sin \frac{\mu \ell}{2}(1-g)}{\frac{\mu \ell}{2} \cos \frac{\mu \ell}{2}} - (1-g) \right) + \frac{\omega^2 \ell_1}{\mu^2} \right.$$

$$\left[\frac{\cos \frac{\mu g_1 \ell_1}{2} \sin \frac{\mu \ell_1}{2}(1-g_1)}{\frac{\mu \ell_1}{2} \cos \frac{\mu \ell_1}{2}} - (1-g_1) \right] - (\theta+\omega\theta_1) \frac{(\theta_g+\omega\theta_{g1})}{4(\phi+\phi_1)}$$

$$- \frac{\ell^3}{12} \left[[1-g^2(3-2g)] + \omega^2\lambda^3 [1-g_1^2 (3-2g_1)] \right] \Bigg] + \frac{H_p}{\mu^2 H}$$

$$\Bigg[C \left[\frac{2 \sin \frac{\mu g \ell}{2} \sin \frac{\mu \ell}{2}(1-2g)}{\cos \frac{\mu \ell}{2}} - \frac{\mu^2 \ell^2 g}{2} (1-g) - \frac{\mu^2}{2} \frac{(\theta+\omega\theta_1)}{(\phi+\phi_1)} \right.$$

$$\left. \left[\frac{\sin \mu g \ell}{\sin \mu \ell} - g \right] \right] + \omega C_1 \left[\frac{2 \sin \frac{\mu g_1 \ell_1}{2} \sin \frac{\mu \ell_1}{2}(1-2g_1)}{\cos \frac{\mu \ell_1}{2}} \right.$$

$$- \frac{\mu^2 \ell_1^2}{2} g_1 (1-g_1) - \frac{\mu^2}{2} \frac{(\theta+\omega\theta_1)}{(\phi+\phi_1)} \left[\frac{\sin \mu g_1 \ell_1}{\sin \mu \ell_1} - g_1 \right] \Bigg] \Bigg]$$

$$- \frac{H_p Z_1}{2H} \Bigg[\ell \left[\frac{\sin \frac{\mu \ell}{2}(1-2g)}{\frac{\mu \ell}{2} \cos \frac{\mu \ell}{2}} - (1-2g) \right] + \omega \ell_1$$

$$\left[\frac{\sin \frac{\mu \ell_1}{2}(1-2g_1)}{\frac{\mu \ell_1}{2} \cos \frac{\mu \ell_1}{2}} - (1-2g_1) \right] - (\theta+\omega\theta_1) \frac{(\nu_g+\nu_{g1})}{(\phi+\phi_1)} \Bigg]$$

$$+ \frac{H_i a}{2H} (\theta+\omega\theta_1) \left[1 - \frac{(\nu+\nu_1)}{(\phi+\phi_1)} \right] \Bigg] \qquad (3.21)$$

in which $\omega = \frac{W_1}{W}$

$$\mu^2 = \frac{2H}{EI}$$

$$H = H_i + H_p = H_w (1+y+\rho),$$

$$\rho = \frac{H_p}{H_w},$$

and where,

$$\nu = \frac{1}{\ell}\left[\frac{\mu\ell}{\sin\mu\ell} - 1\right] \quad , \quad \nu_1 = \frac{1}{\ell_1}\left[\frac{\mu\ell_1}{\sin\mu\ell_1} - 1\right]$$

$$\phi = \frac{1}{\ell}\left[1 - \frac{\mu\ell}{\tan\mu\ell}\right] \quad , \quad \phi_1 = \frac{1}{\ell_1}\left[1 - \frac{\mu\ell_1}{\tan\mu\ell_1}\right]$$

$$\theta = \ell\left[\frac{\tan\frac{\mu\ell}{2}}{\frac{\mu\ell}{2}} - 1\right] \quad , \quad \theta_1 = \ell_1\left[\frac{\tan\frac{\mu\ell_1}{2}}{\frac{\mu\ell_1}{2}} - 1\right]$$

As given in Equations (2.62) and (2.63). Some of the above used parameters have been extended to include the effect of grouting restraint as follows:

$$\nu_g = \frac{1}{\ell}\left[\frac{\mu\ell}{\sin\mu\ell}\cos\mu g\ell - 1\right] \quad , \quad \nu_{g1} = \frac{1}{\ell_1}\left[\frac{\mu\ell_1}{\sin\mu\ell_1}\cos\mu g_1\ell_1 - 1\right] \tag{3.22a}$$

$$\theta_g = \ell\left[\frac{(\cos\mu g\ell - \cos\mu\ell)}{\frac{\mu\ell}{2}\sin\mu\ell} - (1-g^2)\right], \theta_{g1} = \ell_1\left[\frac{(\cos\mu g_1\ell_1 - \cos\mu\ell_1)}{\frac{\mu\ell_1}{2}\sin\mu\ell_1} - (1-g_1^2)\right] \tag{3.22b}$$

We note that θ_g, θ_{g1}, ν_g and ν_{g1} become equal to θ, θ_1, ν and ν_1 respectively when the cable is ungrouted, i.e. g, g_1 = o in Equations (3.22).

Having found the term $\left[\sum \frac{W}{H_w}\int \eta dx\right]_1$, the total value of the term on the right hand side of Equation (3.18) can then be evaluated as follows for the shown selected cases of loading, Figure (3.3). It is worth noting that the term $\sum \frac{W}{H_w}\int\eta dx$ for the live loads has been obtained as derived in Appendix 13.

1. For a Concentrated Load

a. Applied in the Left Hand Span

For a concentrated load P applied at a distance $t\ell$ from the left hand end support, Figure (3.3a), we have:

$$\sum \frac{W}{H_w} \int \eta dx = \left[\sum \frac{W}{H_w} \int \eta dx \right]_1 + \frac{2 W P}{H H_w} \left[\frac{\sin \frac{\mu t \ell}{2} \sin \frac{\mu \ell}{2}(1-t)}{\mu^2 \cos \frac{\mu \ell}{2}} - \frac{t \ell^2}{4} (1-t) \right.$$

$$\left. - \frac{(\theta+\omega\theta_1)}{4(\phi+\phi_1)} \left[\frac{\sin \mu t \ell}{\sin \mu \ell} - t \right] \right] \qquad (3.23)$$

where $\left[\sum \frac{W}{H_w} \int \eta dx \right]_1$ can be determined from Equation (3.21).

b. Applied in the Right Hand Span

For a concentrated load P_1 applied at a distance $t_1 \ell_1$ from the right hand end support, Figure (3.3b), we have:

$$\sum \frac{W}{H_w} \int \eta dx = \left[\sum \frac{W}{H_w} \int \eta dx \right]_1 + \frac{2 W_1 P_1}{H H_w} \left[\frac{\sin \frac{\mu t_1 \ell_1}{2} \sin \frac{\mu \ell_1}{2}(1-t_1)}{\mu^2 \cos_2 \frac{\mu \ell_1}{}} - \frac{t_1 \ell_1^2}{4} (1-t_1) \right.$$

$$\left. - \frac{(\theta+\omega\theta_1)}{4\omega(\phi+\phi_1)} \left[\frac{\sin \mu t_1 \ell_1}{\sin \mu \ell_1} - t_1 \right] \right] \qquad (3.24)$$

2. A General Case of Loading

a. Applied in the Left Hand Span

For a general loading σ which occupies that part of the left hand span which is bounded by the distances $x = \beta\ell$ and $x = \alpha\ell$ from the left hand end support as shown in Figure (3.3c), we have:

$$\sum \frac{W}{H_w} \int \eta dx = \left[\sum \frac{W}{H_w} \int \eta dx \right]_1 + \frac{W \sigma \ell}{H H_w} \left[\frac{1}{\mu^2} \left[\frac{\left(\sin \frac{\mu \ell}{2}(1-2\beta) - \sin \frac{\mu \ell}{2}(1-2\alpha) \right)}{\mu \ell \cos \frac{\mu \ell}{2}} \right. \right.$$

$$\left. - (\alpha - \beta) \right] - \frac{\ell^2}{12} \left[\alpha^2(3-2\alpha) - \beta^2(3-2\beta) \right] - \frac{(\theta + \omega\theta_1)}{4(\phi + \phi_1)}$$

$$\left. \left[\frac{2 \left(\cos \mu\beta\ell - \cos \mu\alpha\ell \right)}{\mu \ell \sin \mu \ell} - (\alpha^2 - \beta^2) \right] \right] \qquad (3.25)$$

where $\left[\sum \frac{W}{H_w} \int \eta dx \right]_1$ can be calculated from Equation (3.21).

b. <u>Applied in the Right Hand Span</u>

For a general loading σ_1 which occupies that part of the right hand span which is bounded the distances by $x_1 = \beta_1 \ell_1$ and $x_1 = \alpha_1 \ell_1$ from the right hand end support as shown in Figure (3.3d), we have:

$$\sum \frac{W}{H_w} \int \eta dx = \left[\sum \frac{W}{H_w} \int \eta dx \right]_1 + \frac{W_1 \sigma_1 \ell_1}{H H_w} \left[\frac{1}{\mu^2} \left[\frac{\left[\sin \frac{\mu \ell}{2}{}_1(1-2\beta_1) - \sin \frac{\mu \ell}{2}{}_1(1-2\alpha_1) \right]}{\mu \ell_1 \cos \frac{\mu \ell_1}{2}} \right. \right.$$

$$\left. - (\alpha_1 - \beta_1) \right] - \frac{\ell_1^2}{12} \left[\alpha_1^2(3-2\alpha_1) - \beta_1^2(3-2\beta_1) \right] - \frac{(\theta + \omega\theta_1)}{4\omega(\phi + \phi_1)}$$

$$\left. \left[\frac{2 \left(\cos \mu\beta_1 \ell_1 - \cos \mu\alpha_1 \ell_1 \right)}{\mu \ell_1 \sin \mu \ell_1} - (\alpha_1^2 - \beta_1^2) \right] \right] \qquad (3.26)$$

The term $\sum \frac{W}{H_w} \int \eta dx$ can be evaluated for a continuous uniformly distributed load for either left or right hand span by substituting $\alpha = 1$ and $\beta = o$ or $\alpha_1 = 1$ and $\beta_1 = o$ in Equation (3.25) or (3.26).

Formulae (3.23 - 3.26) can be used to evaluate the term $\sum \frac{W}{H_w} \int \eta dx$

for any combinations of live loading such as a series of concentrated force, different loading in both spans .... etc, by the principle of superposition. Furthermore, the above formulae can also be used to evaluate this term for suspended beams whose cables are grouted and have no eccentricities at their ends, a = o. In addition, the term $\sum \frac{W}{H_w} \int \eta dx$ can be computed after the time effects take place by replacing γ by τ in Equation (3.21) and then substituting in Formulae (3.23-3.26). As mentioned in Section 2.4, γ is the factor used to increase the initial prestressing force to overcome the time effects as well as to adjust the stresses in the beam for maximim efficiency and τ is the value of γ reduced by the time effects.

Finally, the change in cable tension H_p, due to the applied live loading, can be determined by successive approximations. The method used is identical to that described in Section 2.5.3.3. It is worth noting that the above formulae are applicable for ungrouted bridges when omitting the contribution of grout, $g = g_1 = o$.

3.5 The Determination of the Internal Forces in the Structure

Having found the change in the cable tension, H_p, due to the applied live loading, the internal forces can then be evaluated for the suspended beam, the suspenders and the tower.

3.5.1 The Internal Forces of the Suspended Beam

3.5.1.1 Description of the Method of Analysis

As mentioned earlier, the bending moments, deflections and shear forces for the suspended beam are given in the form of equations which cover all sections of the left and right hand spans of the structure. The derivation of these equations is based on the fundamental relationships: (see Equation 2.1)

$$M_x = EI \frac{d^2\eta}{dx^2}$$

$$Q_x = - EI \frac{d^3\eta}{dx^3}$$

In other words, the bending moments and shear force equations have been formulated by using the deflection equations obtained as shown in Appendices 12 and 22. Due to the number of external forces applied on the structure, we will divide them into two groups, as before, and find the total internal forces from the algebric sum of each of them. A subscript 1 will denote the bending moments, deflections and shear forces produced by the first group of forces,

i.e. $[M_{x_1}]$, $[\eta_1]$ and $[Q_{x_1}]$.

Due to the number of forces applied on the structure, it was inevitable to use large and several equations for the determination of the internal forces for different cases of live loading.

3.5.1.2 For the First Group of Forces

The bending moment equations for the left hand span are, Appendix 22, as follows:

$$[M_{x(1)}]_1 = \frac{yW}{\mu^2 \sin \mu\ell} \left[\sin \mu x \left[1 - \frac{\mu^2}{2} \frac{(\theta+\omega\theta_1)}{(\phi+\phi_1)} \right] + \sin \mu(\ell-x) - \sin \mu\ell \right]$$

$$+ \frac{\rho W}{\mu^2} \frac{\sin \mu x}{\sin \mu\ell} \left[[1 - \cos \mu\ell(1-g)] - \frac{\mu^2}{2} \frac{(\theta_g+\omega\theta_{g1})}{(\phi+\phi_1)} \right]$$

$$- \frac{H_p}{(\phi+\phi_1)} \frac{\sin \mu x}{\sin \mu\ell} \left[C \left(\frac{\sin \mu g\ell}{\sin \mu\ell} - g \right) + C_1 \left(\frac{\sin \mu g_1 \ell_1}{\sin \mu \ell_1} - g_1 \right) \right]$$

$$+ \frac{C H_p}{\mu} \frac{\sin \mu\ell(1-g)}{\sin \mu\ell} \sin \mu x + H_p Z_1 \frac{\sin \mu x}{\sin \mu\ell} \left[\cos \mu\ell(1-g) \right.$$

$$+ \frac{(\nu_g+\nu_{g1})}{(\phi+\phi_1)} \Big] + \frac{H_i a}{\sin \mu\ell} \Big[\sin \mu(\ell-x) - \frac{(\nu+\nu_1)}{(\phi+\phi_1)} \sin \mu x \Big]$$

$$0 \leqslant x \leqslant g\ell$$

(3.27a)

$$\left[M_{x(2)}\right]_1 = \frac{yW}{\mu^2 \sin \mu\ell} \Big[\sin \mu x \Big[1 - \frac{\mu^2}{2} \frac{(\theta+\omega\theta_1)}{(\phi+\phi_1)} \Big] + \sin \mu(\ell-x) - \sin \mu\ell \Big]$$

$$+ \frac{\rho W}{\mu^2 \sin \mu\ell} \Big[\sin \mu x \Big[1 - \frac{\mu^2}{2} \frac{(\theta_g+\omega\theta_{g1})}{(\phi+\phi_1)} \Big] + \cos \mu g\ell \sin \mu(\ell-x) - \sin \mu\ell \Big]$$

$$- \frac{H_p}{(\phi+\phi_1)} \frac{\sin \mu x}{\sin \mu\ell} \Big[C \Big(\frac{\sin \mu g\ell}{\sin \mu\ell} - g \Big) + C_1 \Big(\frac{\sin \mu g_1 \ell_1}{\sin \mu \ell_1} - g_1 \Big) \Big]$$

$$+ \frac{C H_p}{\mu} \frac{\sin \mu g\ell}{\sin \mu\ell} \sin \mu(\ell-x) + \frac{H_p Z_1}{\sin \mu\ell} \Big[\sin \mu x \frac{(\nu_g+\nu_{g1})}{(\phi+\phi_1)}$$

$$- \cos \mu g\ell \sin \mu(\ell-x) \Big] + \frac{H_i a}{\sin \mu\ell} \Big[\sin \mu(\ell-x) - \frac{(\nu+\nu_1)}{(\phi+\phi_1)} \sin \mu x \Big]$$

$$g\ell \leqslant x \leqslant \ell$$

(3.27b)

and for the right hand span,

$$\left[M_{x1(1)}\right]_1 = \frac{yW_1}{\mu^2 \sin \mu\ell_1} \Big[\sin \mu x_1 \Big[1 - \frac{\mu^2}{2\omega} \frac{(\theta+\omega\theta_1)}{(\phi+\phi_1)} \Big] + \sin \mu(\ell_1-x_1) - \sin \mu\ell_1 \Big]$$

$$+ \frac{\rho W_1}{\mu^2} \frac{\sin \mu x_1}{\sin \mu\ell_1} \Big[\Big[1 - \cos \mu\ell_1(1-g_1) \Big] - \frac{\mu}{2\omega} \frac{2\ (\theta_g+\omega\theta_{g1})}{(\phi+\phi_1)} \Big] \frac{H_p}{(\phi+\phi_1)}$$

$$\frac{\sin \mu x_1}{\sin \mu\ell_1} \Big[C \Big(\frac{\sin \mu g\ell}{\sin \mu\ell} - g \Big) + C_1 \Big(\frac{\sin \mu g_1 \ell_1}{\sin \mu\ell_1} - g_1 \Big) \Big]$$

$$+ \frac{C_1 H_p}{\mu} \frac{\sin \mu\ell_1(1-g_1)}{\sin \mu\ell_1} \sin \mu x_1 + H_p Z_1 \frac{\sin \mu x_1}{\sin \mu\ell_1} \Big[\cos \mu\ell_1(1-g_1)$$

$$+ \frac{(\nu_g+\nu_{g1})}{(\phi+\phi_1)} \Big] + \frac{H_i a}{\sin \mu\ell_1} \Big[\sin \mu(\ell_1-x_1) - \frac{(\nu+\nu_1)}{(\phi+\phi_1)} \sin \mu x_1 \Big]$$

$$0 \leqslant x_1 \leqslant g_1\ell_1$$

(3.27c)

$$[M_{x1(2)}]_1 = \frac{yW_1}{\mu^2 \sin \mu\ell_1} \Big[\sin \mu x_1 \Big[1 - \frac{\mu^2}{2\omega} \frac{(\theta+\omega\theta_1)}{(\phi+\phi_1)} \Big] + \sin \mu(\ell_1-x_1) - \sin \mu\ell_1 \Big]$$

$$+ \frac{\rho W_1}{\mu^2 \sin \mu\ell_1} \Big[\sin \mu x_1 \Big[1 - \frac{\mu^2}{2\omega} \frac{(\theta_g+\omega\theta_{g1})}{(\phi+\phi_1)} \Big] + \cos \mu g_1\ell_1 \sin \mu(\ell_1-x_1)$$

$$- \sin \mu\ell_1 \Big] - \frac{H_p}{(\phi+\phi_1)} \frac{\sin \mu x_1}{\sin \mu\ell_1} \Big[C\Big(\frac{\sin \mu g\ell}{\sin \mu\ell} - g \Big) + C_1 \Big[\frac{\sin \mu g_1\ell_1}{\sin \mu\ell_1} - g_1 \Big] \Big]$$

$$+ \frac{C_1 H_p}{\mu} \frac{\sin \mu g_1\ell_1}{\sin \mu\ell_1} \sin \mu(\ell_1-x_1) + \frac{H_p Z_1}{\sin \mu\ell_1} \Big[\sin \mu x_1 \frac{(\nu_g+\nu_{g1})}{(\phi+\phi_1)}$$

$$- \cos \mu g_1\ell_1 \sin \mu(\ell_1-x_1) \Big] + \frac{H_i a}{\sin \mu\ell_1} \Big[\sin \mu(\ell_1-x_1) - \frac{(\nu+\nu_1)}{(\phi+\phi_1)}$$

$$\sin \mu x_1 \Big] \qquad g_1\ell_1 \leqslant x_1 \leqslant \ell$$

(3.27d)

where μ, H, ν, ν_1, ϕ, ϕ_1, θ and θ_1 can be calculated from Equations (2.62) and (2.63) and where ν_g, ν_{g1}, θ_g and θ_{g1} can be evaluated from Equations (3.22).

The deflection equations for the first group of forces are found, Appendix 22, for the left hand span as follows:

$$[\eta_{(1)}]_1 = - \frac{yW}{\mu^2 H} \Big[\frac{\sin \mu x}{\sin \mu\ell} \Big[1 - \frac{\mu^2}{2} \frac{(\theta+\omega\theta_1)}{(\phi+\phi_1)} \Big] + \frac{\sin \mu(\ell-x)}{\sin \mu\ell} - 1 - \frac{\mu^2}{2} \frac{x}{\ell}$$

$$\Big[\ell(\ell-x) - \frac{(\theta+\omega\theta_1)}{(\phi+\phi_1)} \Big] \Big] - \frac{\rho W}{\mu^2 H} \Big[\frac{\sin \mu x}{\sin \mu\ell} \Big[[1 - \cos \mu\ell(1-g)] - \frac{\mu^2}{2} \frac{(\theta_g+\omega\theta_{g1})}{(\phi+\phi_1)} \Big]$$

$$- \frac{\mu^2}{2} \frac{x}{\ell} \left[\ell^2(1-g)^2 - \frac{(\theta_g + \omega\theta_{g1})}{(\phi+\phi_1)} \right] \Bigg] - \frac{H_p}{H(\phi+\phi_1)} \left[C \left(\frac{\sin \mu g\ell}{\sin \mu\ell} - g \right) \right.$$

$$\left. + C_1 \left(\frac{\sin \mu g_1 \ell_1}{\sin \mu \ell_1} - g_1 \right) \right] \left[\frac{x}{\ell} - \frac{\sin \mu x}{\sin \mu \ell} \right] - \frac{C\, H_p}{\mu\, H} \left[\sin \mu\ell(1-g) \frac{\sin \mu x}{\sin \mu \ell} \right.$$

$$\left. - \mu x(1-g) \right] + \frac{H_p Z_1}{H} \left[\frac{x}{\ell} \left(1 + \frac{(\nu_g + \nu_{g1})}{(\phi+\phi_1)} \right) - \frac{\sin \mu x}{\sin \mu \ell} \left(\cos \mu\ell(1-g) \right. \right.$$

$$\left. \left. + \frac{(\nu_g + \nu_{g1})}{(\phi+\phi_1)} \right) \right] - \frac{H_i a}{H} \left[\frac{x}{\ell} + \frac{\sin \mu(\ell-x)}{\sin \mu\ell} + \frac{(\nu+\nu_1)}{(\phi+\phi_1)} \left[\frac{x}{\ell} - \frac{\sin \mu x}{\sin \mu \ell} \right] - 1 \right]$$

$$0 \leqslant x \leqslant g\ell$$

(3.28a)

$$\left[\eta_{(2)}\right]_1 = - \frac{yW}{\mu^2 H} \left[\frac{\sin \mu x}{\sin \mu \ell} \left[1 - \frac{\mu^2}{2} \frac{(\theta+\omega\theta_1)}{(\phi+\phi_1)} \right] + \frac{\sin \mu(\ell-x)}{\sin \mu\ell} - 1 - \frac{\mu^2}{2} \frac{x}{\ell} \right.$$

$$\left. \left[\ell(\ell-x) - \frac{(\theta+\omega\theta_1)}{(\phi+\phi_1)} \right] \right] - \frac{\rho W}{\mu^2 H} \left[\frac{\sin \mu x}{\sin \mu \ell} \left[1 - \frac{\mu^2}{2} \frac{(\theta_g + \omega\theta_{g1})}{(\phi+\phi_1)} \right] \right.$$

$$+ \cos \mu g\ell \frac{\sin \mu(\ell-x)}{\sin \mu\ell} - 1 - \frac{\mu^2}{2} \left[\frac{x}{\ell} \left[\ell^2(1-g)^2 - \frac{(\theta_g + \omega\theta_{g1})}{(\phi+\phi_1)} \right] \right.$$

$$\left. \left. - (x-g\ell)^2 \right] \right] - \frac{H_p}{H(\phi+\phi_1)} \left[C \left(\frac{\sin \mu g\ell}{\sin \mu\ell} - g \right) + C_1 \left(\frac{\sin \mu g_1 \ell_1}{\sin \mu \ell_1} - g_1 \right) \right]$$

$$\left[\frac{x}{\ell} - \frac{\sin \mu x}{\sin \mu \ell} \right] - \frac{C\, H_p}{\mu H} \left[\frac{\sin \mu g\ell}{\sin \mu\ell} \sin \mu(\ell-x) - \mu g(\ell-x) \right]$$

$$+ \frac{H_p Z_1}{H} \left[\frac{x}{\ell} \left(1 + \frac{(\nu_g + \nu_{g1})}{(\phi+\phi_1)} \right) - 1 - \frac{\sin \mu x}{\sin \mu \ell} \frac{(\nu_g + \nu_{g1})}{(\phi+\phi_1)} + \cos \mu g\ell \right.$$

$$\frac{\sin \mu(\ell-x)}{\sin \mu\ell}\Bigg] - \frac{H_i a}{H}\left[\frac{x}{\ell} + \frac{\sin \mu(\ell-x)}{\sin \mu\ell} + \frac{(\nu+\nu_1)}{(\phi+\phi_1)}\left[\frac{x}{\ell} - \frac{\sin \mu x}{\sin \mu\ell}\right] - 1\right]$$

$$g\ell \leqslant x \leqslant \ell$$

(3.28b)

and for the right hand span:

$$[\eta_{1(1)}]_1 = -\frac{\gamma W_1}{\mu^2 H}\left[\frac{\sin \mu x_1}{\sin \mu\ell_1}\left[1 - \frac{\mu^2}{2\omega}\frac{(\theta+\omega\theta_1)}{(\phi+\phi_1)}\right] + \frac{\sin \mu(\ell_1-x_1)}{\sin \mu\ell_1} - 1 - \frac{\mu^2}{2}\frac{x_1}{\ell_1}\right.$$

$$\left.\left[\ell_1(\ell_1-x_1) - \frac{(\theta+\omega\theta_1)}{\omega(\phi+\phi_1)}\right]\right] - \frac{\rho W_1}{\mu^2 H}\left[\frac{\sin \mu x_1}{\sin \mu\ell_1}\left[[1 - \cos \mu\ell_1(1-g_1)] - \frac{\mu^2}{2\omega}\frac{(\theta_g+\omega\theta_{g1})}{(\phi+\phi_1)}\right]\right.$$

$$\left. - \frac{\mu^2}{2}\frac{x_1}{\ell_1}\left[\ell_1^2(1-g_1)^2 - \frac{(\theta_g+\omega\theta_{g1})}{\omega(\phi+\phi_1)}\right]\right] - \frac{H_p}{H(\phi+\phi_1)}\left[C\left[\frac{\sin \mu g\ell}{\sin \mu\ell} - g\right]\right.$$

$$\left. + C_1\left[\frac{\sin \mu g_1\ell_1}{\sin \mu\ell_1} - g_1\right]\right]\left[\frac{x_1}{\ell_1} - \frac{\sin \mu x_1}{\sin \mu\ell_1}\right] - \frac{C_1 H_p}{\mu H}\left[\sin \mu\ell_1(1-g_1)\frac{\sin \mu x_1}{\sin \mu\ell_1}\right.$$

$$\left. - \mu x_1(1-g_1)\right] + \frac{H_p Z_1}{H}\left[\frac{x_1}{\ell_1}\left[1 + \frac{(\nu_g+\nu_{g1})}{(\phi+\phi_1)}\right] - \frac{\sin \mu x_1}{\sin \mu\ell_1}\left[\cos \mu\ell_1(1-g_1)\right.\right.$$

$$\left.\left. + \frac{(\nu_g+\nu_{g1})}{(\phi+\phi_1)}\right]\right] - \frac{H_i a}{H}\left[\frac{x_1}{\ell_1} + \frac{\sin \mu(\ell_1-x_1)}{\sin \mu\ell_1} + \frac{(\nu+\nu_1)}{(\phi+\phi_1)}\left[\frac{x_1}{\ell_1} - \frac{\sin \mu x_1}{\sin \mu\ell_1}\right] - 1\right]$$

$$o \leqslant x_1 \leqslant g_1\ell_1$$

(3.28c)

$$[\eta_{1(2)}]_1 = -\frac{\gamma W_1}{\mu^2 H}\left[\frac{\sin \mu x_1}{\sin \mu\ell_1}\left[1 - \frac{\mu^2}{2\omega}\frac{(\theta+\omega\theta_1)}{(\phi+\phi_1)}\right] + \frac{\sin \mu(\ell_1-x_1)}{\sin \mu\ell_1} - 1 - \frac{\mu^2}{2}\frac{x_1}{\ell_1}\right.$$

$$\left.\left[\ell_1(\ell_1-x_1) - \frac{(\theta+\omega\theta_1)}{\omega(\phi+\phi_1)}\right]\right] - \frac{\rho W_1}{\mu^2 H}\left[\frac{\sin \mu x_1}{\sin \mu\ell_1}\left[1 - \frac{\mu^2}{2\omega}\frac{(\theta_g+\omega\theta_{g1})}{(\phi+\phi_1)}\right]\right.$$

$$\left. + \cos \mu g_1\ell_1 \frac{\sin \mu(\ell_1-x_1)}{\sin \mu\ell_1} - 1 - \frac{\mu^2}{2}\left[\frac{x_1}{\ell_1}\left[\ell_1^2(1-g_1)^2 - \frac{(\theta_g+\omega\theta_{g1})}{\omega(\phi+\phi_1)}\right]\right.\right.$$

$$- (x_1 - g_1 \ell_1)^2 \Big] \Big] - \frac{H_p}{H(\phi+\phi_1)} \left[C \left(\frac{\sin \mu g \ell}{\sin \mu \ell} - g \right) + C_1 \left(\frac{\sin \mu g_1 \ell_1}{\sin \mu \ell_1} - g_1 \right) \right]$$

$$\left[\frac{x_1}{\ell_1} - \frac{\sin \mu x_1}{\sin \mu \ell_1} \right] - \frac{C_1 H_p}{\mu H} \left[\frac{\sin \mu g_1 \ell_1}{\sin \mu \ell_1} \sin \mu(\ell_1 - x_1) - \mu g_1 (\ell_1 - x_1) \right]$$

$$+ \frac{H_p Z_1}{H} \left[\frac{x_1}{\ell_1} \left(1 + \frac{(\nu_g + \nu_{g1})}{(\phi+\phi_1)} \right) - 1 - \frac{\sin \mu x_1}{\sin \mu \ell_1} \frac{(\nu_g + \nu_{g1})}{(\phi+\phi_1)} + \cos \mu g_1 \ell_1 \right.$$

$$\left. \frac{\sin \mu(\ell_1 - x_1)}{\sin \mu \ell_1} \right] - \frac{H_i a}{H} \left[\frac{x_1}{\ell_1} + \frac{\sin \mu(\ell_1 - x_1)}{\sin \mu \ell_1} + \frac{(\nu+\nu_1)}{(\phi+\phi_1)} \left[\frac{x_1}{\ell_1} - \frac{\sin \mu x_1}{\sin \mu \ell_1} \right] - 1 \right]$$

$$g_1 \ell_1 \leqslant x_1 \leqslant \ell_1$$

(3.28d)

Finally, the shear forces equations can be written, for the first group of forces, Appendix 22, for the left hand span as follows:

$$[Q_{x(1)}]_1 = - \frac{yW}{\mu \sin \mu \ell} \left[\cos \mu x \left[1 - \frac{\mu^2}{2} \frac{(\theta+\omega\theta_1)}{(\phi+\phi_1)} \right] - \cos \mu(\ell - x) \right]$$

$$- \frac{\rho W}{\mu} \frac{\cos \mu x}{\cos \mu \ell} \left[[1 - \cos \mu \ell(1-g)] - \frac{\mu^2}{2} \frac{(\theta_g + \omega\theta_{g1})}{(\phi+\phi_1)} \right] + \mu \frac{H_p}{(\phi+\phi_1)}$$

$$\frac{\cos \mu x}{\sin \mu \ell} \left[C \left(\frac{\sin \mu g \ell}{\sin \mu \ell} - g \right) + C_1 \left(\frac{\sin \mu g_1 \ell_1}{\sin \mu \ell_1} - g_1 \right) \right] - C H_p$$

$$\frac{\sin \mu \ell(1-g)}{\sin \mu \ell} \cos \mu x - \mu H_p Z_1 \frac{\cos \mu x}{\sin \mu \ell} \left[\cos \mu \ell(1-g) + \frac{(\nu_g + \nu_{g1})}{(\phi+\phi_1)} \right]$$

$$+ \mu \frac{H_i a}{\sin \mu \ell} \left[\cos \mu(\ell - x) + \frac{(\nu+\nu_1)}{(\phi+\phi_1)} \cos \mu x \right] \qquad o \leqslant x \leqslant g\ell$$

(3.29a)

$$[Q_{x(2)}]_1 = - \frac{yW}{\mu \sin \mu \ell} \left[\cos \mu x \left[1 - \frac{\mu^2}{2} \frac{(\theta+\omega\theta_1)}{(\phi+\phi_1)} \right] - \cos \mu(\ell - x) \right]$$

$$- \frac{\rho W}{\mu \sin \mu \ell} \left[\cos \mu x \left[1 - \frac{\mu^2}{2} \frac{(\theta_g + \omega\theta_{g1})}{(\phi+\phi_1)} \right] - \cos \mu g \ell \cos \mu(\ell - x) \right]$$

$$+ \mu \frac{H_p}{(\phi+\phi_1)} \frac{\cos \mu x}{\sin \mu \ell} \left[C \left[\frac{\sin \mu g \ell}{\sin \mu \ell} - g \right] + C_1 \left[\frac{\sin \mu g_1 \ell_1}{\sin \mu \ell_1} - g_1 \right] \right]$$

$$+ C H_p \frac{\sin \mu g \ell}{\sin \mu \ell} \cos \mu(\ell - x) - \mu \frac{H_p Z_1}{\sin \mu \ell} \left[\cos \mu x \frac{(\nu_g + \nu_{g1})}{(\phi+\phi_1)} \right.$$

$$\left. + \cos \mu g \ell \cos \mu(\ell - x) \right] + \mu \frac{H_i a}{\sin \mu \ell} \left[\cos \mu(\ell - x) + \frac{(\nu+\nu_1)}{(\phi+\phi_1)} \cos \mu x \right]$$

$$g\ell \leqslant x \leqslant \ell$$

(3.29b)

and for the right hand span:

$$\left[Q_{x1(1)}\right]_1 = - \frac{yW_1}{\mu \sin \mu \ell_1} \left[\cos \mu x_1 \left[1 - \frac{\mu^2}{2\omega} \frac{(\theta+\omega\theta_1)}{(\phi+\phi_1)} \right] - \cos \mu(\ell_1 - x_1) \right]$$

$$- \frac{\rho W_1}{\mu} \frac{\cos \mu x_1}{\sin \mu \ell_1} \left[\left[1 - \cos \mu \ell_1 (1 - g_1) \right] - \frac{\mu^2}{2\omega} \frac{(\theta_g + \omega\theta_{g1})}{(\phi+\phi_1)} \right]$$

$$+ \mu \frac{H_p}{(\phi+\phi_1)} \frac{\cos \mu x_1}{\sin \mu \ell_1} \left[C \left[\frac{\sin \mu g \ell}{\sin \mu \ell} - g \right] + C_1 \left[\frac{\sin \mu g_1 \ell_1}{\sin \mu \ell_1} - g_1 \right] \right]$$

$$- C_1 H_p \frac{\sin \mu \ell_1 (1 - g_1)}{\sin \mu \ell_1} \cos \mu x_1 - \mu H_p Z_1 \frac{\cos \mu x_1}{\sin \mu \ell_1} \left[\cos \mu \ell_1 (1 - g_1) \right.$$

$$\left. + \frac{(\nu_g + \nu_{g1})}{(\phi+\phi_1)} \right] + \mu \frac{H_i a}{\sin \mu \ell_1} \left[\cos \mu(\ell_1 - x_1) + \frac{(\nu+\nu_1)}{(\phi+\phi_1)} \cos \mu x_1 \right]$$

$$0 \leqslant x_1 \leqslant g_1 \ell_1$$

(3.29c)

$$\left[Q_{x1(2)}\right]_1 = - \frac{yW_1}{\mu \sin \mu \ell_1} \left[\cos \mu x_1 \left[1 - \frac{\mu^2}{2\omega} \frac{(\theta+\omega\theta_1)}{(\phi+\phi_1)} \right] - \cos \mu(\ell_1 - x_1) \right]$$

$$- \frac{\rho W_1}{\mu \sin \mu \ell_1} \left[\cos \mu x_1 \left[1 - \frac{\mu^2}{2\omega} \frac{(\theta_g + \omega\theta_{g1})}{(\phi+\phi_1)} \right] - \cos \mu g_1 \ell_1 \cos \mu(\ell_1 - x_1) \right]$$

$$+ \mu \frac{H_p}{(\phi+\phi_1)} \frac{\cos \mu x_1}{\sin \mu \ell_1} \left[C \left(\frac{\sin \mu g \ell}{\sin \mu \ell} - g \right) + C_1 \left(\frac{\sin \mu g_1 \ell_1}{\sin \mu \ell_1} - g_1 \right) \right]$$

$$+ C_1 H_p \frac{\sin \mu g_1 \ell_1}{\sin \mu \ell_1} \cos \mu(\ell_1 - x_1) - \mu \frac{H_p Z_1}{\sin \mu \ell_1} \left[\cos \mu x_1 \frac{(\nu_g + \nu_{g1})}{(\phi+\phi_1)} \right.$$

$$\left. + \cos \mu g_1 \ell_1 \cos \mu(\ell_1 - x_1) \right] + \mu \frac{H_i a}{\sin \mu \ell_1} \left[\cos \mu(\ell_1 - x_1) + \frac{(\nu+\nu_1)}{(\phi+\phi_1)} \cos \mu x_1 \right]$$

$$g_1 \ell_1 \leqslant x_1 \leqslant \ell_1$$

(3.29d)

Having found the internal forces of the first group of forces, the total internal forces can then be obtained as will be shown in the following section.

3.5.1.3 The Total Internal Forces for Selected Cases of Loading

1. For a concentrated load

a. If $t < g$

For a concentrated load P applied at a distance $t\ell$ from the left hand end support, Figure (3.3a), we have the bending moment equations for the left hand span as follows:

$$M_{x(1)} = \left[M_{x(1)}\right]_1 - \frac{P}{\mu} \frac{\sin \mu x}{\sin \mu \ell} \left[\sin \mu \ell(1-t) - \frac{\mu}{(\phi+\phi_1)} \left(\frac{\sin \mu t \ell}{\sin \mu \ell} - t \right) \right]$$

$$o \leqslant x \leqslant t\ell$$

(3.30a)

$$M_{x(2)} = \left[M_{x(1)}\right]_1 - \frac{P}{\mu \sin \mu \ell} \left[\sin \mu t \ell \sin \mu(\ell - x) - \frac{\mu \sin \mu x}{(\phi+\phi_1)} \left(\frac{\sin \mu t \ell}{\sin \mu \ell} - t \right) \right]$$

$$t\ell \leqslant x \leqslant g\ell$$

(3.30b)

$$M_{x(3)} = \left[M_{x(2)}\right]_1 - \frac{P}{\mu \sin \mu\ell}\left[\sin \mu t\ell \sin \mu(\ell-x) - \frac{\mu \sin \mu x}{(\phi+\phi_1)}\left[\frac{\sin \mu t\ell}{\sin \mu\ell} - t\right]\right]$$

$$g\ell \leqslant x \leqslant \ell$$

(3.30c)

where $\left[M_{x(1)}\right]_1$ and $\left[M_{x(2)}\right]_1$ can be determined from Equations (3.27a & b)

and for the right hand span;

$$M_{x1(1)} = \left[M_{x1(1)}\right]_1 + \frac{P}{(\phi+\phi_1)} \frac{\sin \mu x_1}{\sin \mu\ell_1}\left[\frac{\sin \mu t\ell}{\sin \mu\ell} - t\right] \qquad o \leqslant x_1 \leqslant g_1\ell_1$$

(3.30d)

$$M_{x1(2)} = \left[M_{x1(2)}\right]_1 + \frac{P}{(\phi+\phi_1)} \frac{\sin \mu x_1}{\sin \mu\ell_1}\left[\frac{\sin \mu t\ell}{\sin \mu\ell} - t\right] \qquad g_1\ell_1 \leqslant x_1 \leqslant \ell_1$$

(3.30e)

where $\left[M_{x1(1)}\right]_1$ and $\left[M_{x1(2)}\right]_1$ can be determined from Equations (3.27c & d).

The stresses at any section of the beam can be calculated from Equations (2.74). The deflection equations for the left hand span are:

$$\eta_{(1)} = \left[\eta_{(1)}\right]_1 + \frac{P}{\mu H}\left[\frac{\sin \mu\ell(1-t)}{\sin \mu\ell}\sin \mu x - \mu x(1-t) + \frac{\mu}{(\phi+\phi_1)}\left[\frac{\sin \mu t\ell}{\sin \mu\ell} - t\right]\left[\frac{x}{\ell} - \frac{\sin \mu x}{\sin \mu\ell}\right]\right]$$

$$o \leqslant x \leqslant t\ell$$

(3.31a)

$$\eta_{(2)} = \left[\eta_{(1)}\right]_1 + \frac{P}{\mu H}\left[\frac{\sin \mu t\ell}{\sin \mu\ell}\sin \mu(\ell-x) - \mu t(\ell-x) + \frac{\mu}{(\phi+\phi_1)}\left[\frac{\sin \mu t\ell}{\sin \mu\ell} - t\right]\left[\frac{x}{\ell} - \frac{\sin \mu x}{\sin \mu\ell}\right]\right]$$

$$t\ell \leqslant x \leqslant g\ell$$

(3.31b)

$$\eta_{(3)} = \left[\eta_{(2)}\right]_1 + \frac{P}{\mu H}\left[\frac{\sin \mu t\ell}{\sin \mu\ell}\sin \mu(\ell-x) - \mu t(\ell-x) + \frac{\mu}{(\phi+\phi_1)}\left[\frac{\sin \mu t\ell}{\sin \mu\ell} - t\right]\left[\frac{x}{\ell} - \frac{\sin \mu x}{\sin \mu\ell}\right]\right]$$

$$g\ell \leqslant x \leqslant \ell$$

(3.31c)

where $[\eta_{(1)}]_1$ and $[\eta_{(2)}]_1$ can be evaluated from Equations (3.28a & b).
Hence, for the right hand span:

$$\eta_{1(1)} = [\eta_{1(1)}]_1 + \frac{P}{H(\phi+\phi_1)} \left[\frac{\sin \mu t\ell}{\sin \mu\ell} - t \right] \left[\frac{x_1}{\ell_1} - \frac{\sin \mu x_1}{\sin \mu \ell_1} \right]$$

$$o \leqslant x_1 \leqslant g_1 \ell_1$$

(3.31d)

$$\eta_{1(2)} = [\eta_{1(2)}]_1 + \frac{P}{H(\phi+\phi_1)} \left[\frac{\sin \mu t\ell}{\sin \mu\ell} - t \right] \left[\frac{x_1}{\ell_1} - \frac{\sin \mu x_1}{\sin \mu \ell_1} \right]$$

$$g_1 \ell_1 \leqslant x_1 \leqslant \ell_1$$

(3.31e)

where $[\eta_{1(1)}]_1$ and $[\eta_{1(2)}]_1$ can be evaluated from Equations (3.27c & d).

The shear forces can be determined at any section of the prestressed cable suspended beam from the following equations for the left hand span:

$$Q_{x(1)} = [Q_{x(1)}]_1 + P \frac{\cos \mu x}{\sin \mu \ell} \left[\sin \mu\ell(1-t) - \frac{\mu}{(\phi+\phi_1)} \left[\frac{\sin \mu t\ell}{\sin \mu\ell} - t \right] \right]$$

$$o \leqslant x \leqslant t\ell$$

(3.32a)

$$Q_{x(2)} = [Q_{x(1)}]_1 - \frac{P}{\sin \mu\ell} \left[\sin \mu t\ell \cos \mu(\ell-x) + \frac{\mu \cos \mu x}{(\phi+\phi_1)} \left[\frac{\sin \mu t\ell}{\sin \mu\ell} - t \right] \right]$$

$$t\ell \leqslant x \leqslant g\ell$$

(3.32b)

$$Q_{x(3)} = [Q_{x(2)}]_1 - \frac{P}{\sin \mu\ell} \left[\sin \mu t\ell \cos \mu(\ell-x) + \frac{\mu \cos \mu x}{(\phi+\phi_1)} \left[\frac{\sin \mu t\ell}{\sin \mu\ell} - t \right] \right]$$

$$g\ell \leqslant x \leqslant \ell$$

(3.32c)

where $[Q_{x(1)}]_1$ and $[Q_{x(2)}]_1$ can be evaluated from Equations (3.29a & b).
For the right hand span:

$$Q_{x1(1)} = [Q_{x1(1)}]_1 - \frac{\mu P}{(\phi+\phi_1)} \frac{\cos \mu x_1}{\sin \mu \ell_1} \left[\frac{\sin \mu t \ell}{\sin \mu \ell} - t \right] \qquad o \leqslant x_1 \leqslant g_1 \ell_1$$

(3.32d)

$$Q_{x1(2)} = [Q_{x1(2)}]_1 - \frac{\mu P}{(\phi+\phi_1)} \frac{\cos \mu x_1}{\sin \mu \ell_1} \left[\frac{\sin \mu t \ell}{\sin \mu \ell} - t \right] \qquad g_1 \ell_1 \leqslant x_1 \leqslant \ell_1$$

(3.32e)

where $[Q_{x1(1)}]_1$ and $[Q_{x1(2)}]_1$ can be calculated from Equations (3.29c & d).

b. <u>If $t \geqslant g$</u> (see Figure 3.3a)

The bending moment equations for the left hand span are:

$$M_{x(1)} = [M_{x(1)}]_1 - \frac{P}{\mu} \frac{\sin \mu x}{\sin \mu \ell} \left[\sin \mu \ell(1-t) - \frac{\mu}{(\phi+\phi_1)} \left[\frac{\sin \mu t \ell}{\sin \mu \ell} - t \right] \right]$$

$$o \leqslant x \leqslant g\ell$$

(3.33a)

$$M_{x(2)} = [M_{x(2)}]_1 - \frac{P}{\mu} \frac{\sin \mu x}{\sin \mu \ell} \left[\sin \mu \ell(1-t) - \frac{\mu}{(\phi+\phi_1)} \left[\frac{\sin \mu t \ell}{\sin \mu \ell} - t \right] \right]$$

$$g\ell \leqslant x \leqslant t\ell$$

(3.33b)

$$M_{x(3)} = [M_{x(2)}]_1 - \frac{P}{\mu \sin \mu \ell} \left[\sin \mu t \ell \sin \mu(\ell-x) - \frac{\mu \sin \mu x}{(\phi+\phi_1)} \left[\frac{\sin \mu t \ell}{\sin \mu \ell} - t \right] \right]$$

$$t\ell \leqslant x \leqslant \ell$$

(3.33c)

where $[M_{x(1)}]_1$ and $[M_{x(2)}]_1$, can be evaluated from Equations (3.27a & b).

The bending moment equations for the right hand span are identical to Equations (3.30d & e). The stresses can be evaluated at any section of the beam from Equations (2.74).

The deflections can be computed at any section of the prestressed cable suspended beam from the following equations for the left hand span:

$$\eta_{(1)} = [\eta_{(1)}]_1 + \frac{P}{\mu H}\left[\frac{\sin \mu\ell(1-t)}{\sin \mu\ell}\sin \mu x - \mu x(1-t) + \frac{\mu}{(\phi+\phi_1)}\left[\frac{\sin \mu t\ell}{\sin \mu\ell} - t\right]\right.$$

$$\left.\left[\frac{x}{\ell} - \frac{\sin \mu x}{\sin \mu\ell}\right]\right] \qquad o \leqslant x \leqslant g\ell$$

(3.34a)

$$\eta_{(2)} = [\eta_{(2)}]_1 + \frac{P}{\mu H}\left[\frac{\sin \mu\ell(1-t)}{\sin \mu\ell}\sin \mu x - \mu x(1-t) + \frac{\mu}{(\phi+\phi_1)}\left[\frac{\sin \mu t\ell}{\sin \mu\ell} - t\right]\right.$$

$$\left.\left[\frac{x}{\ell} - \frac{\sin \mu x}{\sin \mu\ell}\right]\right] \qquad g\ell \leqslant x \leqslant t\ell$$

(3.34b)

$$\eta_{(3)} = [\eta_{(2)}]_1 + \frac{P}{\mu H}\left[\frac{\sin \mu t\ell}{\sin \mu\ell}\sin \mu(\ell-x) - \mu t(\ell-x) + \frac{\mu}{(\phi+\phi_1)}\left[\frac{\sin \mu t\ell}{\sin \mu\ell} - t\right]\right.$$

$$\left.\left[\frac{x}{\ell} - \frac{\sin \mu x}{\sin \mu\ell}\right]\right] \qquad t\ell \leqslant x \leqslant \ell$$

(3.34c)

where $[\eta_{(1)}]_1$ and $[\eta_{(2)}]_1$ can be evaluated from Equations (3.28a & b).

The deflections can be calculated at any section of the right hand span from Equations (3.31d & e).

The shear forces equations for the left hand span are:

$$Q_{x(1)} = [Q_{x(1)}]_1 + P\frac{\cos \mu x}{\sin \mu\ell}\left[\sin \mu\ell(1-t) - \frac{\mu}{(\phi+\phi_1)}\left[\frac{\sin \mu t\ell}{\sin \mu\ell} - t\right]\right]$$

$$o \leqslant x \leqslant g\ell$$

(3.35a)

$$Q_{x(2)} = [Q_{x(2)}]_1 + \frac{P \cos \mu x}{\sin \mu\ell}\left[\sin \mu\ell(1-t) - \frac{\mu}{(\phi+\phi_1)}\left[\frac{\sin \mu t\ell}{\sin \mu\ell} - t\right]\right]$$

$$g\ell \leqslant x \leqslant t\ell$$

(3.35b)

$$Q_{x(3)} = [Q_{x(2)}]_1 - \frac{P}{\sin \mu\ell}\left[\sin \mu t\ell \cos \mu(\ell-x) + \frac{\mu}{(\phi+\phi_1)} \cos \mu x\left(\frac{\sin \mu t\ell}{\sin \mu\ell} - t\right)\right]$$

$$t\ell \leqslant x \leqslant \ell$$

(3.35c)

where $[Q_{x(1)}]_1$ and $[Q_{x(2)}]_1$ can be computed from Equations (3.29a & b).

As before, the shear forces can be evaluated at any section of the right hand span from Equations (3.32d & e).

2. <u>A concentrated load applied in the right hand span</u>

a. <u>If $t_1 \leqslant g_1$</u>

For a concentrated load P_1 applied at a distance $t_1\ell_1$ from the right hand end support, see Figure (3.3b), we have the bending moment equations for the left hand span as follows:

$$M_{x(1)} = [M_{x(1)}]_1 + \frac{P_1}{(\phi+\phi_1)} \frac{\sin \mu x}{\sin \mu\ell}\left(\frac{\sin \mu t_1\ell_1}{\sin \mu\ell_1} - t_1\right) \qquad o \leqslant x \leqslant g\ell$$

(3.36a)

$$M_{x(2)} = [M_{x(2)}]_1 + \frac{P_1}{(\phi+\phi_1)} \frac{\sin \mu x}{\sin \mu\ell}\left(\frac{\sin \mu t_1\ell_1}{\sin \mu\ell_1} - t_1\right) \qquad g\ell \leqslant x \leqslant \ell$$

(3.36b)

where $[M_{x(1)}]_1$ and $[M_{x(2)}]_1$ can be calculated from Equations (3.27a & b) and for the right hand span:

$$M_{x1(1)} = [M_{x1(1)}]_1 - \frac{P_1}{\mu} \frac{\sin \mu x_1}{\sin \mu\ell_1}\left[\sin \mu\ell_1(1-t_1) - \frac{\mu}{(\phi+\phi_1)}\left(\frac{\sin \mu t_1\ell_1}{\sin \mu\ell_1} - t_1\right)\right]$$

$$o \leqslant x_1 \leqslant t_1\ell_1$$

(3.36c)

$$M_{x1(2)} = [M_{x1(1)}]_1 - \frac{P_1}{\mu \sin \mu\ell_1}\left[\sin \mu t_1\ell_1 \sin \mu(\ell_1-x_1) - \frac{\mu \sin \mu x_1}{(\phi+\phi_1)}\right.$$

$$\left(\frac{\sin \mu t_1 \ell_1}{\sin \mu \ell_1} - t_1 \right) \Bigg] \qquad t_1 \ell_1 \leqslant x_1 \leqslant g_1 \ell_1$$

(3.36d)

$$M_{x1(3)} = \left[M_{x1(2)}\right]_1 - \frac{P_1}{\mu \sin \mu \ell_1} \left[\sin \mu t_1 \ell_1 \sin \mu(\ell_1 - x_1) - \frac{\mu \sin \mu x_1}{(\phi+\phi_1)} \right.$$

$$\left(\frac{\sin \mu t_1 \ell_1}{\sin \mu \ell_1} - t_1 \right) \Bigg] \qquad g_1 \ell_1 \leqslant x_1 \leqslant \ell_1$$

(3.36e)

where $\left[M_{x1(1)}\right]_1$ and $\left[M_{x1(2)}\right]_1$ can be evaluated from Equations (3.27c & d) The stresses can be evaluated at any section of the beam from Equations (2.74).

The deflections can be evaluated at any section of the left hand span from the following equations:

$$\eta_{(1)} = \left[\eta_{(1)}\right]_1 + \frac{P_1}{H(\phi+\phi_1)} \left(\frac{\sin \mu t_1 \ell_1}{\sin \mu \ell_1} - t_1 \right) \left(\frac{x}{\ell} - \frac{\sin \mu x}{\sin \mu \ell} \right) \quad o \leqslant x \leqslant g\ell$$

(3.37a)

$$\eta_{(2)} = \left[\eta_{(2)}\right]_1 + \frac{P_1}{H(\phi+\phi_1)} \left(\frac{\sin \mu t_1 \ell_1}{\sin \mu \ell_1} - t_1 \right) \left(\frac{x}{\ell} - \frac{\sin \mu x}{\sin \mu \ell} \right) \quad g\ell \leqslant x \leqslant \ell$$

(3.37b)

where $\left[\eta_{(1)}\right]_1$ and $\left[\eta_{(2)}\right]_1$, can be computed from Equations (3.28a & b).
For the right hand span, the deflection equations are:

$$\eta_{1(1)} = \left[\eta_{1(1)}\right]_1 + \frac{P_1}{\mu H} \left[\frac{\sin \mu \ell_1 (1-t_1)}{\sin \mu \ell_1} \sin \mu x_1 - \mu x_1 (1-t_1) + \frac{\mu}{(\phi+\phi_1)} \right.$$

$$\left(\frac{\sin \mu t_1 \ell_1}{\sin \mu \ell_1} - t_1 \right) \left(\frac{x_1}{\ell_1} - \frac{\sin \mu x_1}{\sin \mu \ell_1} \right) \Bigg] \qquad o \leqslant x_1 \leqslant t_1 \ell_1$$

(3.37c)

$$\eta_{1(2)} = \left[\eta_{1(1)}\right]_1 + \frac{P_1}{\mu H} \left[\frac{\sin \mu \ell_1 (1-t_1)}{\sin \mu \ell_1} \sin \mu x_1 - \mu x_1 (1-t_1) + \frac{\mu}{(\phi+\phi_1)} \right.$$

$$\left[\frac{\sin \mu t_1 \ell_1}{\sin \mu \ell_1} - t_1\right]\left[\frac{x_1}{\ell_1} - \frac{\sin \mu x_1}{\sin \mu \ell_1}\right]\Bigg] \qquad t_1\ell_1 \leqslant x_1 \leqslant g_1\ell_1$$

(3.37d)

$$\eta_{1(3)} = \left[\eta_{1(2)}\right]_1 + \frac{P_1}{\mu H}\left[\frac{\sin \mu t_1 \ell_1}{\sin \mu \ell_1} \sin \mu(\ell_1 - x_1) - \mu t_1(\ell_1 - x_1) + \frac{\mu}{(\phi+\phi_1)}\right.$$

$$\left[\frac{\sin \mu t_1 \ell_1}{\sin \mu \ell_1} - t_1\right]\left[\frac{x_1}{\ell_1} - \frac{\sin \mu x_1}{\sin \mu \ell_1}\right]\Bigg] \qquad g_1\ell_1 \leqslant x_1 \leqslant \ell_1$$

(3.37e)

where $\left[\eta_{1(1)}\right]_1$ and $\left[\eta_{1(2)}\right]_1$ can be obtained from Equations (3.28c & d).

The shear forces can be evaluated at any section of the left hand span from the following equations:

$$Q_{x(1)} = \left[Q_{x(1)}\right]_1 - \frac{\mu P_1}{(\phi+\phi_1)} \frac{\cos \mu x}{\sin \mu \ell}\left[\frac{\sin \mu t_1 \ell_1}{\sin \mu \ell_1} - t_1\right] \qquad o \leqslant x \leqslant g\ell$$

(3.38a)

$$Q_{x(2)} = \left[Q_{x(2)}\right]_1 - \frac{\mu P_1}{(\phi+\phi_1)} \frac{\cos \mu x}{\sin \mu \ell}\left[\frac{\sin \mu t_1 \ell_1}{\sin \mu \ell_1} - t_1\right] \qquad g\ell \leqslant x \leqslant \ell$$

(3.38b)

where $\left[Q_{x(1)}\right]_1$ and $\left[Q_{x(2)}\right]_1$ can be evaluated from Equations (3.29a & b).

The shear forces for the right hand span can be evaluated from the following equations:

$$Q_{x1(1)} = \left[Q_{x1(1)}\right]_1 + P_1 \frac{\cos \mu x_1}{\cos \mu \ell_1}\left[\sin \mu \ell_1(1-t_1) - \frac{\mu}{(\phi+\phi_1)}\left[\frac{\sin \mu t_1 \ell_1}{\sin \mu \ell_1} - t_1\right]\right]$$

$$o \leqslant x_1 \leqslant t_1\ell_1$$

(3.38c)

$$Q_{x1(2)} = \left[Q_{x1(1)}\right]_1 + P_1 \frac{\cos \mu x_1}{\cos \mu \ell_1}\left[\sin \mu \ell_1(1-t_1) - \frac{\mu}{(\phi+\phi_1)}\left[\frac{\sin \mu t_1 \ell_1}{\sin \mu \ell_1} - t_1\right]\right]$$

$$t_1\ell_1 \leqslant x_1 \leqslant g_1\ell_1$$

(3.38d)

$$Q_{x1(3)} = [Q_{x1(2)}]_1 - \frac{P_1}{\sin \mu \ell_1}\left[\sin \mu t_1 \ell_1 \cos \mu(\ell_1 - x_1) + \frac{\mu \cos \mu x_1}{(\phi+\phi_1)}\left(\frac{\sin \mu t_1 \ell_1}{\sin \mu \ell_1} - t_1\right)\right] \qquad g_1\ell_1 \leqslant x_1 \leqslant \ell_1$$

(3.38e)

where $[Q_{x1(1)}]_1$ and $[Q_{x1(2)}]_1$ can be calculated from Equations (3.29c & d).

b. <u>If $t_1 \geqslant g_1$</u> (see Figure 3.3b)

The bending moment equations for the left hand span will be identical to Equations (3.36a & b). Hence, for the right hand span, the bending moment equations are:

$$M_{x1(1)} = [M_{x1(1)}]_1 - \frac{P_1}{\mu}\frac{\sin \mu x_1}{\sin \mu \ell_1}\left[\sin \mu \ell_1(1-t_1) - \frac{\mu}{(\phi+\phi_1)}\left(\frac{\sin \mu t_1 \ell_1}{\sin \mu \ell_1} - t_1\right)\right] \qquad o \leqslant x_1 \leqslant g_1\ell_1$$

(3.39a)

$$M_{x1(2)} = [M_{x1(2)}]_1 - \frac{P_1}{\mu}\frac{\sin \mu x_1}{\sin \mu \ell_1}\left[\sin \mu \ell_1(1-t_1) - \frac{\mu}{(\phi+\phi_1)}\left(\frac{\sin \mu t_1 \ell_1}{\sin \mu \ell_1} - t_1\right)\right] \qquad g_1\ell_1 \leqslant x_1 \leqslant t_1\ell_1$$

(3.39b)

$$M_{x1(3)} = [M_{x1(2)}]_1 - \frac{P_1}{\mu \sin \mu \ell_1}\left[\sin \mu t_1 \ell_1 \sin \mu(\ell_1 - x_1) - \frac{\mu \sin \mu x_1}{(\phi+\phi_1)}\left(\frac{\sin \mu t_1 \ell_1}{\sin \mu \ell_1} - t_1\right)\right] \qquad t_1\ell_1 \leqslant x_1 \leqslant \ell_1$$

(3.39c)

where $[M_{x1(1)}]_1$ and $[M_{x1(2)}]_1$ can be found from Equations (3.27c & d). The stresses can be evaluated at any section of the beam from Equations (2.74).

The deflections for the left hand span can be obtained from Equations (3.37a & b). For the right hand span, the deflections can be evaluated from the following equations:

$$\eta_{1(1)} = [\eta_{1(1)}]_1 + \frac{P_1}{\mu H}\left[\frac{\sin \mu \ell_1(1-t_1)}{\sin \mu \ell_1} \sin \mu x_1 - \mu x_1(1-t_1) + \frac{\mu}{(\phi+\phi_1)}\right.$$

$$\left.\left(\frac{\sin \mu t_1 \ell_1}{\sin \mu \ell_1} - t_1\right)\left(\frac{x_1}{\ell_1} - \frac{\sin \mu x_1}{\sin \mu \ell_1}\right)\right] \qquad o \leqslant x_1 \leqslant g_1 \ell_1$$

(3.40a)

$$\eta_{1(2)} = [\eta_{1(2)}]_1 + \frac{P_1}{\mu H}\left[\frac{\sin \mu \ell_1(1-t_1)}{\sin \mu \ell_1} \sin \mu x_1 - \mu x_1(1-t_1) + \frac{\mu}{(\phi+\phi_1)}\right.$$

$$\left.\left(\frac{\sin \mu t_1 \ell_1}{\sin \mu \ell_1} - t_1\right)\left(\frac{x_1}{\ell_1} - \frac{\sin \mu x_1}{\sin \mu \ell_1}\right)\right] \qquad g_1 \ell_1 \leqslant x_1 \leqslant t_1 \ell_1$$

(3.40b)

$$\eta_{1(3)} = [\eta_{1(2)}]_1 + \frac{P_1}{\mu H}\left[\frac{\sin \mu t_1 \ell_1}{\sin \mu \ell_1} \sin \mu(\ell_1 - x_1) - \mu t_1(\ell_1 - x_1) + \frac{\mu}{(\phi+\phi_1)}\right.$$

$$\left.\left(\frac{\sin \mu t_1 \ell_1}{\sin \mu \ell_1} - t_1\right)\left(\frac{x_1}{\ell_1} - \frac{\sin \mu x_1}{\sin \mu \ell_1}\right)\right] \qquad t_1 \ell_1 \leqslant x_1 \leqslant \ell_1$$

(3.40c)

where $[\eta_{1(1)}]_1$ and $[\eta_{1(2)}]_1$ can be evaluated from Equations (3.28c & d).

The shear forces at any section of the left hand span can directly be evaluated from Equations (3.38a & b). For the right hand span, the shear forces equations are:

$$Q_{x1(1)} = [Q_{x1(1)}]_1 + P_1 \frac{\cos \mu x_1}{\sin \mu \ell_1}\left[\sin \mu \ell_1(1-t_1) - \frac{\mu}{(\phi+\phi_1)}\left(\frac{\sin \mu t_1 \ell_1}{\sin \mu \ell_1} - t_1\right)\right]$$

$$o \leqslant x_1 \leqslant g_1 \ell_1$$

(3.41a)

$$Q_{x1(2)} = \left[Q_{x1(2)}\right]_1 + P_1 \frac{\cos \mu x_1}{\sin \mu \ell_1} \left[\sin \mu \ell_1 (1-t_1) - \frac{\mu}{(\phi+\phi_1)} \left(\frac{\sin \mu t_1 \ell_1}{\sin \mu \ell_1} - t_1 \right)\right]$$

$$g_1 \ell_1 \leqslant x_1 \leqslant t_1 \ell_1$$

(3.41b)

$$Q_{x1(3)} = \left[Q_{x1(2)}\right]_1 - \frac{P_1}{\sin \mu \ell_1} \left[\sin \mu t_1 \ell_1 \cos \mu(\ell_1 - x_1) + \frac{\mu \cos \mu x_1}{(\phi+\phi_1)} \left(\frac{\sin \mu t_1 \ell_1}{\sin \mu \ell_1} - t_1 \right)\right]$$

$$t_1 \ell_1 \leqslant x_1 \leqslant \ell_1$$

(3.41c)

where $\left[Q_{x1(1)}\right]_1$ and $\left[Q_{x1(2)}\right]_1$ can be computed from Equations (3.29c & d).

For the preceding formulae for the internal forces of the beam, under a concentrated load the constants μ, H, ϕ, ϕ_1, θ and θ_1 can be determined from Equations (2.62) and (2.63).

3. A general case of loading

a. Applied in the left hand span

For a general loading σ which occupies that part of the left hand span which is bounded by $x = \beta\ell$ and $x = \alpha\ell$, see Figure (3.3c), we have the following cases:

1. If $\beta \geqslant g$

The bending moments can be calculated at any section of the left hand span from the following equations:

$$M_{x(1)} = \left[M_{x(1)}\right]_1 - \frac{\sigma}{\mu^2} \frac{\sin \mu x}{\sin \mu \ell} \left[\cos \mu \ell(1-\alpha) - \cos \mu \ell(1-\beta) - \frac{\mu^2 \ell}{2(\phi+\phi_1)}\right.$$

$$\left[\frac{2(\cos \mu\beta\ell - \cos \mu\alpha\ell)}{\mu\ell \sin \mu\ell} - (\alpha^2-\beta^2) \right] \Bigg] \qquad o \leqslant x \leqslant g\ell$$

(3.42a)

$$M_{x(2)} = \left[M_{x(2)}\right]_1 - \frac{\sigma}{\mu^2} \frac{\sin \mu x}{\sin \mu\ell} \Bigg[\cos \mu\ell(1-\alpha) - \cos \mu\ell(1-\beta) - \frac{\mu^2\ell}{2(\phi+\phi_1)}$$

$$\left[\frac{2(\cos \mu\beta\ell - \cos \mu\alpha\ell)}{\mu\ell \sin \mu\ell} - (\alpha^2-\beta^2) \right] \Bigg] \qquad g\ell \leqslant x \leqslant \beta\ell$$

(3.42b)

$$M_{x(3)} = \left[M_{x(2)}\right]_1 - \frac{\sigma}{\mu^2 \sin \mu\ell} \Bigg[\sin \mu x \cos \mu\ell(1-\alpha) + \sin \mu(\ell-x) \cos \mu\beta\ell$$

$$- \sin \mu\ell - \frac{\mu^2\ell}{2(\phi+\phi_1)} \sin \mu x \left[\frac{2(\cos \mu\beta\ell - \cos \mu\alpha\ell)}{\mu\ell \sin \mu\ell} - (\alpha^2-\beta^2) \right] \Bigg]$$

$$\beta\ell \leqslant x \leqslant \alpha\ell$$

(3.42c)

$$M_{x(4)} = \left[M_{x(2)}\right]_1 - \frac{\sigma}{\mu^2 \sin \mu\ell} \Bigg[(\cos \mu\beta\ell - \cos \mu\alpha\ell) \sin \mu(\ell-x) - \frac{\mu^2\ell}{2(\phi+\phi_1)}$$

$$\sin \mu x \left[\frac{2(\cos \mu\beta\ell - \cos \mu\alpha\ell)}{\mu\ell \sin \mu\ell} - (\alpha^2-\beta^2) \right] \Bigg] \qquad \alpha\ell \leqslant x \leqslant \ell$$

(3.42d)

where $\left[M_{x(1)}\right]_1$ and $\left[M_{x(2)}\right]_1$ can be evaluated from Equations (3.27a & b).

For the right hand span, we have:

$$M_{x1(1)} = \left[M_{x1(1)}\right]_1 + \frac{\sigma\ell}{2(\phi+\phi_1)} \frac{\sin \mu x_1}{\sin \mu\ell_1} \left[\frac{2(\cos \mu\beta\ell - \cos \mu\alpha\ell)}{\mu\ell \sin \mu\ell} - (\alpha^2-\beta^2) \right]$$

$$o \leqslant x_1 \leqslant g_1\ell_1$$

(3.42e)

$$M_{x1(2)} = \left[M_{x1(2)}\right]_1 + \frac{\sigma \ell}{2(\phi+\phi_1)} \frac{\sin \mu x_1}{\sin \mu \ell_1} \left[\frac{2(\cos \mu\beta\ell - \cos \mu\alpha\ell)}{\mu\ell \sin \mu\ell} - (\alpha^2-\beta^2) \right]$$

$$\varepsilon_1 \ell_1 \leqslant x_1 \leqslant \ell_1$$

(3.42f)

where $\left[M_{x1(1)}\right]_1$ and $\left[M_{x1(2)}\right]_1$ can be evaluated from Equations (3.27c & d). The stresses can be evaluated at any section of the beam from Equations (2.74).

The deflections can be determined for the left hand span from the following equations:

$$\eta_{(1)} = \left[\eta_{(1)}\right]_1 + \frac{\sigma}{\mu^2 H} \left[[\cos \mu\ell(1-\alpha) - \cos \mu\ell(1-\beta)] \frac{\sin \mu x}{\sin \mu\ell} - \frac{\mu^2\ell^2}{2} (\alpha-\beta) \right.$$

$$[2 - (\alpha+\beta)] \frac{x}{\ell} + \frac{\mu^2\ell}{2(\phi+\phi_1)} \left[\frac{2(\cos \mu\beta\ell - \cos \mu\alpha\ell)}{\mu\ell \sin \mu\ell} - (\alpha^2-\beta^2) \right]$$

$$\left. \left(\frac{x}{\ell} - \frac{\sin \mu x}{\sin \mu\ell} \right) \right] \qquad o \leqslant x \leqslant g\ell$$

(3.43a)

$$\eta_{(2)} = \left[\eta_{(2)}\right]_1 + \frac{\sigma}{\mu^2 H} \left[[\cos \mu\ell(1-\alpha) - \cos \mu\ell(1-\beta)] \frac{\sin \mu x}{\sin \mu\ell} - \frac{\mu^2\ell^2}{2} (\alpha-\beta) \right.$$

$$[2 - (\alpha+\beta)] \frac{x}{\ell} + \frac{\mu^2\ell}{2(\phi+\phi_1)} \left[\frac{2(\cos \mu\beta\ell - \cos \mu\alpha\ell)}{\mu\ell \sin \mu\ell} - (\alpha^2-\beta^2) \right]$$

$$\left. \left(\frac{x}{\ell} - \frac{\sin \mu x}{\sin \mu\ell} \right) \right] \qquad g\ell \leqslant x \leqslant \beta\ell$$

(3.43b)

$$\eta_{(3)} = \left[\eta_{(2)}\right]_1 + \frac{\sigma}{\mu^2 H} \left[\cos \mu\ell(1-\alpha) \frac{\sin \mu x}{\sin \mu\ell} + \cos \mu\beta\ell \frac{\sin \mu(\ell-x)}{\sin \mu\ell} - 1 - \frac{\mu^2\ell^2}{2} \right.$$

$$\left[(\alpha-\beta)[2-(\alpha+\beta)]\,\frac{x}{\ell}-\left(\frac{x}{\ell}-\beta\right)^2\right]+\frac{\mu^2\ell}{2(\phi+\phi_1)}\left[\frac{2(\cos\mu\beta\ell-\cos\mu\alpha\ell)}{\mu\ell\sin\mu\ell}-(\alpha^2-\beta^2)\right]\left[\frac{x}{\ell}-\frac{\sin\mu x}{\sin\mu\ell}\right]\right]$$

$$\beta\ell\leqslant x\leqslant\alpha\ell \qquad (3.43c)$$

$$\eta_{(4)}=\left[\eta_{(2)}\right]_1+\frac{\sigma}{\mu^2H}\left[(\cos\mu\beta\ell-\cos\mu\alpha\ell)\frac{\sin\mu(\ell-x)}{\sin\mu\ell}-\frac{\mu^2\ell^2}{2}(\alpha^2-\beta^2)\right.$$

$$\left.(1-\frac{x}{\ell})+\frac{\mu^2\ell}{2(\phi+\phi_1)}\left[\frac{2(\cos\mu\beta\ell-\cos\mu\alpha\ell)}{\mu\ell\sin\mu\ell}-(\alpha^2-\beta^2)\right]\left[\frac{x}{\ell}-\frac{\sin\mu x}{\sin\mu\ell}\right]\right]$$

$$\alpha\ell\leqslant x\leqslant\ell \qquad (3.43d)$$

where $\left[\eta_{(1)}\right]_1$ and $\left[\eta_{(2)}\right]_1$, can be computed from Equations (3.28a & b).

For the right hand span, we have:

$$\eta_{1(1)}=\left[\eta_{1(1)}\right]_1+\frac{\sigma\ell}{2H(\phi+\phi_1)}\left[\frac{2(\cos\mu\beta\ell-\cos\mu\alpha\ell)}{\mu\ell\sin\mu\ell}-(\alpha^2-\beta^2)\right]\left[\frac{x_1}{\ell_1}-\frac{\sin\mu x_1}{\sin\mu\ell_1}\right]$$

$$0\leqslant x_1\leqslant g_1\ell_1 \qquad (3.43e)$$

$$\eta_{1(2)}=\left[\eta_{1(2)}\right]_1+\frac{\sigma\ell}{2H(\phi+\phi_1)}\left[\frac{2(\cos\mu\beta\ell-\cos\mu\alpha\ell)}{\mu\ell\sin\mu\ell}-(\alpha^2-\beta^2)\right]\left[\frac{x_1}{\ell_1}-\frac{\sin\mu x_1}{\sin\mu\ell_1}\right]$$

$$g_1\ell_1\leqslant x_1\leqslant\ell_1 \qquad (3.43f)$$

where $\left[\eta_{1(1)}\right]_1$ and $\left[\eta_{1(2)}\right]_1$ can be calculated from Equations (3.28c & d).

The shear forces can be computed at any section of the left hand span from the following equations:

$$Q_{x(1)} = [Q_{x(1)}]_1 + \frac{\sigma}{\mu}\frac{\cos \mu x}{\sin \mu \ell}\left[\cos \mu\ell(1-\alpha) - \cos \mu\ell(1-\beta) - \frac{\mu^2 \ell}{2(\phi+\phi_1)}\right.$$

$$\left.\left[\frac{2(\cos \mu\beta\ell - \cos \mu\alpha\ell)}{\mu\ell \sin \mu\ell} - (\alpha^2-\beta^2)\right]\right] \qquad 0 \leqslant x \leqslant g\ell$$

(3.44a)

$$Q_{x(2)} = [Q_{x(2)}]_1 + \frac{\sigma}{\mu}\frac{\cos \mu x}{\sin \mu \ell}\left[\cos \mu\ell(1-\alpha) - \cos \mu\ell(1-\beta) - \frac{\mu^2 \ell}{2(\phi+\phi_1)}\right.$$

$$\left.\left[\frac{2(\cos \mu\beta\ell - \cos \mu\alpha\ell)}{\mu\ell \sin \mu\ell} - (\alpha^2-\beta^2)\right]\right] \qquad g\ell \leqslant x \leqslant \beta\ell$$

(3.44b)

$$Q_{x(3)} = [Q_{x(2)}]_1 + \frac{\sigma}{\mu \sin \mu \ell}\left[\cos \mu x \cos \mu\ell(1-\alpha) - \cos \mu(\ell-x) \cos \mu\beta\ell\right.$$

$$\left.- \frac{\mu^2 \ell}{2(\phi+\phi_1)} \cos \mu x \left[\frac{2(\cos \mu\beta\ell - \cos \mu\alpha\ell)}{\mu\ell \sin \mu\ell} - (\alpha^2-\beta^2)\right]\right]$$

$$\beta\ell \leqslant x \leqslant \alpha\ell$$

(3.44c)

$$Q_{x(4)} = [Q_{x(2)}]_1 - \frac{\sigma}{\mu \sin \mu \ell}\left[(\cos \mu\beta\ell - \cos \mu\alpha\ell) \cos \mu(\ell-x) + \frac{\mu^2 \ell}{2(\phi+\phi_1)}\right.$$

$$\left.\cos \mu x \left[\frac{2(\cos \mu\beta\ell - \cos \mu\alpha\ell)}{\mu\ell \sin \mu\ell} - (\alpha^2-\beta^2)\right]\right] \qquad \alpha\ell \leqslant x \leqslant \ell$$

(3.44d)

where $[Q_{x(1)}]_1$ and $[Q_{x(2)}]_1$ can be evaluated from Equations (3.29a & b).

For the right hand span, we have:

$$Q_{x1(1)} = [Q_{x1(1)}]_1 - \frac{\mu\sigma\ell}{2(\phi+\phi_1)} \frac{\cos \mu x_1}{\sin \mu\ell_1} \left[\frac{2(\cos \mu\beta\ell - \cos \mu\alpha\ell)}{\mu\ell \sin \mu\ell} - (\alpha^2-\beta^2) \right]$$

$$o \leqslant x_1 \leqslant g_1\ell_1$$

(3.44e)

$$Q_{x1(2)} = [Q_{x1(2)}]_1 - \frac{\mu\sigma\ell}{2(\phi+\phi_1)} \frac{\cos \mu x_1}{\sin \mu\ell_1} \left[\frac{2(\cos \mu\beta\ell - \cos \mu\alpha\ell)}{\mu\ell \sin \mu\ell} - (\alpha^2-\beta^2) \right]$$

$$g_1\ell_1 \leqslant x_1 \leqslant \ell_1$$

(3.44f)

where $[Q_{x1(1)}]_1$ and $[Q_{x1(2)}]_1$ can be obtained from Equations (3.29c & d).

2. <u>If $\beta < g < \alpha$</u>

The bending moments can be evaluated at any section of the left hand span from the following equations:

$$M_{x(1)} = [M_{x(1)}]_1 - \frac{\sigma}{\mu^2} \frac{\sin \mu x}{\sin \mu\ell} \left[\cos \mu\ell(1-\alpha) - \cos \mu\ell(1-\beta) - \frac{\mu^2\ell}{2(\phi+\phi_1)} \right.$$

$$\left. \left[\frac{2(\cos \mu\beta\ell - \cos \mu\alpha\ell)}{\mu\ell \sin \mu\ell} - (\alpha^2-\beta^2) \right] \right] \qquad o \leqslant x \leqslant \beta\ell$$

(3.45a)

$$M_{x(2)} = [M_{x(1)}]_1 - \frac{\sigma}{\mu^2 \sin \mu\ell} \left[\sin \mu x \cos \mu\ell(1-\alpha) + \sin \mu(\ell-x) \cos \mu\beta\ell \right.$$

$$\left. - \sin \mu\ell - \frac{\mu^2\ell}{2(\phi+\phi_1)} \sin \mu x \left[\frac{2(\cos \mu\beta\ell - \cos \mu\alpha\ell)}{\mu\ell \sin \mu\ell} - (\alpha^2-\beta^2) \right] \right]$$

$$\beta\ell \leqslant x \leqslant g\ell$$

(3.45b)

$$M_{x(3)} = [M_{x(2)}]_1 - \frac{\sigma}{\mu^2 \sin \mu\ell} \left[\sin \mu x \cos \mu\ell(1-\alpha) + \sin \mu(\ell-x) \cos \mu\beta\ell \right.$$

$$- \sin \mu\ell - \frac{\mu^2\ell}{2(\phi+\phi_1)} \sin \mu x \left[\frac{2(\cos \mu\beta\ell - \cos \mu\alpha\ell)}{\mu\ell \sin \mu\ell} - (\alpha^2-\beta^2) \right] \Bigg]$$

$$g\ell \leqslant x \leqslant \alpha\ell \qquad (3.45c)$$

$$M_{x(4)} = \left[M_{x(2)}\right]_1 - \frac{\sigma}{\mu^2 \sin \mu\ell} \left[(\cos \mu\beta\ell - \cos \mu\alpha\ell) \sin \mu(\ell-x) - \frac{\mu^2\ell}{2(\phi+\phi_1)} \right.$$

$$\left. \sin \mu x \left[\frac{2(\cos \mu\beta\ell - \cos \mu\alpha\ell)}{\mu\ell \sin \mu\ell} - (\alpha^2-\beta^2) \right] \right] \qquad \alpha\ell \leqslant x \leqslant \ell$$

(3.45d)

where $\left[M_{x(1)}\right]_1$ and $\left[M_{x(2)}\right]_1$ can be obtained from Equations (3.27a & b). For the right hand span, the bending moments can be directly computed, at any section, from Equations (3.42e & f). The stresses can be evaluated at any section of the beam from Equations (2.74).

The deflections can be calculated at any section of the left hand span from the following equations:

$$\eta_{(1)} = \left[\eta_{(1)}\right]_1 + \frac{\sigma}{\mu^2 H} \left[[\cos \mu\ell(1-\alpha) - \cos \mu\ell(1-\beta)] \frac{\sin \mu x}{\sin \mu\ell} - \frac{\mu^2\ell^2}{2} (\alpha-\beta) \right.$$

$$[2 - (\alpha+\beta)] \frac{x}{\ell} + \frac{\mu^2\ell}{2(\phi+\phi_1)} \left[\frac{2(\cos \mu\beta\ell - \cos \mu\alpha\ell)}{\mu\ell \sin \mu\ell} - (\alpha^2-\beta^2) \right]$$

$$\left. \left(\frac{x}{\ell} - \frac{\sin \mu x}{\sin \mu\ell} \right) \right] \qquad 0 \leqslant x \leqslant \beta\ell$$

(3.46a)

$$\eta_{(2)} = \left[\eta_{(1)}\right]_1 + \frac{\sigma}{\mu^2 H} \left[\cos \mu\ell(1-\alpha) \frac{\sin \mu x}{\sin \mu\ell} + \cos \mu\beta\ell \frac{\sin \mu(\ell-x)}{\sin \mu\ell} - 1 - \frac{\mu^2\ell^2}{2} \right.$$

$$\left. \left[(\alpha-\beta)[2 - (\alpha+\beta)] \frac{x}{\ell} - \left(\frac{x}{\ell} - \beta \right)^2 \right] + \frac{\mu^2\ell}{2(\phi+\phi_1)} \left[\frac{2(\cos \mu\beta\ell - \cos \mu\alpha\ell)}{\mu\ell \sin \mu\ell} - (\alpha^2-\beta^2) \right] \right.$$

$$\left[\frac{x}{\ell} - \frac{\sin \mu x}{\sin \mu \ell} \right] \Bigg] \qquad \beta\ell \leqslant x \leqslant g\ell$$

(3.46b)

$$\eta_{(3)} = [\eta_{(2)}]_1 + \frac{\sigma}{\mu^2 H} \Bigg[\cos \mu\ell(1-\alpha) \frac{\sin \mu x}{\sin \mu \ell} + \cos \mu\beta\ell \frac{\sin \mu(\ell-x)}{\sin \mu \ell} - 1 - \frac{\mu^2 \ell^2}{2}$$

$$\left[(\alpha-\beta)[2 - (\alpha+\beta)] \frac{x}{\ell} - \left(\frac{x}{\ell} - \beta \right)^2 \right] + \frac{\mu^2 \ell}{2(\phi+\phi_1)} \left[\frac{2(\cos \mu\beta\ell - \cos \mu\alpha\ell)}{\mu\ell \sin \mu\ell} \right.$$

$$\left. - (\alpha^2-\beta^2) \right] \left[\frac{x}{\ell} - \frac{\sin \mu x}{\sin \mu \ell} \right] \Bigg] \qquad g\ell \leqslant x \leqslant \alpha\ell$$

(3.46c)

$$\eta_{(4)} = [\eta_{(2)}]_1 + \frac{\sigma}{\mu^2 H} \left[\frac{\sin \mu(\ell-x)}{\sin \mu \ell} (\cos \mu\beta\ell - \cos \mu\alpha\ell) - \frac{\mu^2 \ell^2}{2} (\alpha^2-\beta^2)\left(1 - \frac{x}{\ell}\right) \right.$$

$$\left. + \frac{\mu^2 \ell}{2(\phi+\phi_1)} \left[\frac{2(\cos \mu\beta\ell - \cos \mu\alpha\ell)}{\mu\ell \sin \mu\ell} - (\alpha^2-\beta^2) \right] \left[\frac{x}{\ell} - \frac{\sin \mu x}{\sin \mu \ell} \right] \right]$$

$$\alpha\ell \leqslant x \leqslant \ell$$

(3.46d)

where $[\eta_{(1)}]_1$ and $[\eta_{(2)}]_1$ can be evaluated from Equations (3.28a & b). For the right hand span, the deflections can be computed, at any section, from Equations (3.43e & f).

The shear forces can be found at any section of the left hand span from the following equations:

$$Q_{x(1)} = [Q_{x(1)}]_1 + \frac{\sigma}{\mu} \frac{\cos \mu x}{\sin \mu \ell} \left[\cos \mu\ell(1-\alpha) - \cos \mu\ell(1-\beta) - \frac{\mu^2 \ell}{2(\phi+\phi_1)} \right.$$

$$\left. \left[\frac{2(\cos \mu\beta\ell - \cos \mu\alpha\ell)}{\mu\ell \sin \mu\ell} - (\alpha^2-\beta^2) \right] \right] \qquad o \leqslant x \leqslant \beta\ell$$

(3.47a)

$$Q_{x(2)} = [Q_{x(1)}]_1 + \frac{\sigma}{\mu \sin \mu\ell} \left[\cos \mu x \cos \mu\ell(1-\alpha) - \cos \mu(\ell-x) \cos \mu\beta\ell \right.$$

$$\left. - \frac{\mu^2\ell}{2(\phi+\phi_1)} \cos \mu x \left[\frac{2(\cos \mu\beta\ell - \cos \mu\alpha\ell)}{\mu\ell \sin \mu\ell} - (\alpha^2-\beta^2) \right] \right] \quad \beta\ell \leqslant x \leqslant g\ell$$

(3.47b)

$$Q_{x(3)} = [Q_{x(2)}]_1 + \frac{\sigma}{\mu \sin \mu\ell} \left[\cos \mu x \cos \mu\ell(1-\alpha) - \cos \mu(\ell-x) \cos \mu\beta\ell \right.$$

$$\left. - \frac{\mu^2\ell}{2(\phi+\phi_1)} \cos \mu x \left[\frac{2(\cos \mu\beta\ell - \cos \mu\alpha\ell)}{\mu\ell \sin \mu\ell} - (\alpha^2-\beta^2) \right] \right]$$

$$g\ell \leqslant x \leqslant \alpha\ell$$

(3.47c)

$$Q_{x(4)} = [Q_{x(2)}]_1 - \frac{\sigma}{\mu \sin \mu\ell} \left[(\cos \mu\beta\ell - \cos \mu\alpha\ell) \cos \mu(\ell-x) + \frac{\mu^2\ell}{2(\phi+\phi_1)} \right.$$

$$\left. \cos \mu x \left[\frac{2(\cos \mu\beta\ell - \cos \mu\alpha\ell)}{\mu\ell \sin \mu\ell} - (\alpha^2-\beta^2) \right] \right] \qquad \alpha\ell \leqslant x \leqslant \ell$$

(3.47d)

where $[Q_{x(1)}]_1$ and $[Q_{x(2)}]_1$ can be evaluated from Equations (3.29a & b). For the right hand span, the shear forces can directly be calculated, at any section, from Equations (3.44e & f).

3. <u>If $g \geqslant \alpha$</u>

The bending moments can be determined at any section of the left hand span from the following equations:

$$M_{x(1)} = [M_{x(1)}]_1 - \frac{\sigma}{\mu^2} \frac{\sin \mu x}{\sin \mu\ell} \left[\cos \mu\ell(1-\alpha) - \cos \mu\ell(1-\beta) - \frac{\mu^2\ell}{2(\phi+\phi_1)} \right.$$

$$\left[\frac{2(\cos \mu\beta\ell - \cos \mu\alpha\ell)}{\mu\ell \sin \mu\ell} - (\alpha^2-\beta^2) \right] \Bigg] \qquad 0 \leqslant x \leqslant \beta\ell$$

(3.48a)

$$M_{x(2)} = \left[M_{x(1)}\right]_1 - \frac{\sigma}{\mu^2 \sin \mu\ell} \Bigg[\sin \mu x \cos \mu\ell(1-\alpha) + \sin \mu(\ell-x) \cos \mu\beta\ell$$

$$- \sin \mu\ell - \frac{\mu^2\ell}{2(\phi+\phi_1)} \sin \mu x \left[\frac{2(\cos \mu\beta\ell - \cos \mu\alpha\ell)}{\mu\ell \sin \mu\ell} - (\alpha^2-\beta^2) \right] \Bigg]$$

$$\beta\ell \leqslant x \leqslant \alpha\ell$$

(3.48b)

$$M_{x(3)} = \left[M_{x(1)}\right]_1 - \frac{\sigma}{\mu^2 \sin \mu\ell} \Bigg[(\cos \mu\beta\ell - \cos \mu\alpha\ell) \sin \mu(\ell-x) - \frac{\mu^2\ell}{2(\phi+\phi_1)}$$

$$\sin \mu x \left[\frac{2(\cos \mu\beta\ell - \cos \mu\alpha\ell)}{\mu\ell \sin \mu\ell} - (\alpha^2-\beta^2) \right] \Bigg]$$

$$\alpha\ell \leqslant x \leqslant g\ell$$

(3.48c)

$$M_{x(4)} = \left[M_{x(2)}\right]_1 - \frac{\sigma}{\mu^2 \sin \mu\ell} \Bigg[(\cos \mu\beta\ell - \cos \mu\alpha\ell) \sin \mu(\ell-x) - \frac{\mu^2\ell}{2(\phi+\phi_1)}$$

$$\sin \mu x \left[\frac{2(\cos \mu\beta\ell - \cos \mu\alpha\ell)}{\mu\ell \sin \mu\ell} - (\alpha^2-\beta^2) \right] \Bigg] \qquad g\ell \leqslant x \leqslant \ell$$

(3.48d)

where $\left[M_{x(1)}\right]_1$ and $\left[M_{x(2)}\right]_1$ can be computed from Equations (3.27a & b). For the right hand span, the bending moments can be evaluated, at any section, from Equations (3.42e & f). The stresses at any section of the beam can be found from Equations (2.74).

The deflections can be obtained at any section of the left hand span from the following equations:

$$\eta_{(1)} = [\eta_{(1)}]_1 + \frac{\sigma}{\mu^2 H}\left[[\cos\ \mu\ell(1-\alpha) - \cos\ \mu\ell(1-\beta)]\ \frac{\sin\ \mu x}{\sin\ \mu\ell} - \frac{\mu^2\ell^2}{2}\ (\alpha-\beta)\right.$$

$$[2 - (\alpha+\beta)]\ \frac{x}{\ell} + \frac{\mu^2\ell}{2(\phi+\phi_1)}\left[\ \frac{2(\cos\ \mu\beta\ell - \cos\ \mu\alpha\ell)}{\mu\ell\ \sin\ \mu\ell} - (\alpha^2-\beta^2)\right]$$

$$\left.\left(\ \frac{x}{\ell} - \frac{\sin\ \mu x}{\sin\ \mu\ell}\ \right)\right] \qquad 0 \leqslant x \leqslant \beta\ell$$

(3.49a)

$$\eta_{(2)} = [\eta_{(1)}]_1 + \frac{\sigma}{\mu^2 H}\left[\ \cos\ \mu\ell(1-\alpha)\ \frac{\sin\ \mu x}{\sin\ \mu\ell} + \cos\ \mu\beta\ell\ \frac{\sin\ \mu(\ell-x)}{\sin\ \mu\ell} - 1 - \frac{\mu^2\ell^2}{2}\right.$$

$$[(\alpha-\beta)[2 - (\alpha+\beta)]\ \frac{x}{\ell} - (\ \frac{x}{\ell} - \beta)^2] + \frac{\mu^2\ell}{2(\phi+\phi_1)}\left[\ \frac{2(\cos\ \mu\beta\ell - \cos\ \mu\alpha\ell)}{\mu\ell\ \sin\ \mu\ell}\right.$$

$$\left.\left.- (\alpha^2-\beta^2)\right]\left(\ \frac{x}{\ell} - \frac{\sin\ \mu x}{\sin\ \mu\ell}\ \right)\right] \qquad \beta\ell \leqslant x \leqslant \alpha\ell$$

(3.49b)

$$\eta_{(3)} = [\eta_{(1)}]_1 + \frac{\sigma}{\mu^2 H}\left[\ \frac{\sin\ \mu(\ell-x)}{\sin\ \mu\ell}\ (\cos\ \mu\beta\ell - \cos\ \mu\alpha\ell) - \frac{\mu^2\ell^2}{2}\ (\alpha^2-\beta^2)(1 - \frac{x}{\ell}\ )\right.$$

$$\left.+ \frac{\mu^2\ell}{2(\phi+\phi_1)}\left[\ \frac{2(\cos\ \mu\beta\ell - \cos\ \mu\alpha\ell)}{\mu\ell\ \sin\ \mu\ell} - (\alpha^2-\beta^2)\right]\left(\ \frac{x}{\ell} - \frac{\sin\ \mu x}{\sin\ \mu\ell}\ \right)\right]$$

$$\alpha\ell \leqslant x \leqslant g\ell$$

(3.49c)

$$\eta_{(4)} = [\eta_{(2)}]_1 + \frac{\sigma}{\mu^2 H}\left[\ \frac{\sin\ \mu(\ell-x)}{\sin\ \mu\ell}\ (\cos\ \mu\beta\ell - \cos\ \mu\alpha\ell) - \frac{\mu^2\ell^2}{2}\ (\alpha^2-\beta^2)(1 - \frac{x}{\ell}\ )\right.$$

$$\left.+ \frac{\mu^2\ell}{2(\phi+\phi_1)}\left[\frac{2(\cos\ \mu\beta\ell - \cos\ \mu\alpha\ell)}{\mu\ell\ \sin\ \mu\ell} - (\alpha^2-\beta^2)\right]\left(\ \frac{x}{\ell} - \frac{\sin\ \mu x}{\sin\ \mu\ell}\ \right)\right]$$

$$g\ell \leqslant x \leqslant \ell$$

(3.49d)

where $[\eta_{(1)}]_1$ and $[\eta_{(2)}]_1$ can be found from Equations (3.28a & b). For the right hand span, the deflections can be evaluated, at any section, from Equations (3.43e & f).

The shear forces can be determined at any section of the left hand span from the following equations:

$$Q_{x(1)} = [Q_{x(1)}]_1 + \frac{\sigma}{\mu} \frac{\cos \mu x}{\sin \mu \ell} \left[\cos \mu \ell(1-\alpha) - \cos \mu \ell(1-\beta) - \frac{\mu^2 \ell}{2(\phi+\phi_1)} \left[\frac{2(\cos \mu\beta\ell - \cos \mu\alpha\ell)}{\mu \ell \sin \mu \ell} - (\alpha^2-\beta^2) \right] \right] \qquad o \leqslant x \leqslant \beta\ell$$

(3.50a)

$$Q_{x(2)} = [Q_{x(1)}]_1 + \frac{\sigma}{\mu \sin \mu \ell} \left[\cos \mu x \cos \mu \ell(1-\alpha) - \cos \mu(\ell-x) \cos \mu\beta\ell - \frac{\mu^2 \ell}{2(\phi+\phi_1)} \cos \mu x \left[\frac{2(\cos \mu\beta\ell - \cos \mu\alpha\ell)}{\mu \ell \sin \mu \ell} - (\alpha^2-\beta^2) \right] \right] \qquad \beta\ell \leqslant x \leqslant \alpha\ell$$

(3.50b)

$$Q_{x(3)} = [Q_{x(1)}]_1 - \frac{\sigma}{\mu \sin \mu \ell} \left[(\cos \mu\beta\ell - \cos \mu\alpha\ell) \cos \mu(\ell-x) + \frac{\mu^2 \ell}{2(\phi+\phi_1)} \cos \mu x \left[\frac{2(\cos \mu\beta\ell - \cos \mu\alpha\ell)}{\mu \ell \sin \mu \ell} - (\alpha^2-\beta^2) \right] \right] \qquad \alpha\ell \leqslant x \leqslant g\ell$$

(3.50c)

$$Q_{x(4)} = [Q_{x(2)}]_1 - \frac{\sigma}{\mu \sin \mu \ell} \left[(\cos \mu\beta\ell - \cos \mu\alpha\ell) \cos \mu(\ell-x) + \frac{\mu^2 \ell}{2(\phi+\phi_1)} \cos \mu x \left[\frac{2(\cos \mu\beta\ell - \cos \mu\alpha\ell)}{\mu \ell \sin \mu \ell} - (\alpha^2-\beta^2) \right] \right] \qquad g\ell \leqslant x \leqslant \ell$$

(3.50d)

where $[Q_{x(1)}]_1$ and $[Q_{x(2)}]_1$ can be determined from Equations (3.29a & b). For the right hand span, the shear forces can directly be computed from Equations(3.44e & f).

Finally, the bending moments, deflections and shear forces equations can be written for a continuous uniformly distributed load applied in the left hand span when substituting $\alpha = 1$ and $\beta = o$ in the equations given for the case when $\beta < g < \alpha$.

b. A general loading applied in the right hand span

For a general loading σ_1 which occupies that part of the right hand span which is bounded by the distances $x_1 = \beta_1 \ell_1$ and $x_1 = \alpha_1 \ell_1$ from the right hand end support, see Figure (3.3d), we have the following cases:

1. If $\beta_1 \geqslant g_1$

The bending moments can be evaluated at any section of the left hand span from the following equations:

$$M_{x(1)} = [M_{x(1)}]_1 + \frac{\sigma_1 \ell_1}{2(\phi+\phi_1)} \frac{\sin \mu x}{\sin \mu \ell} \left[\frac{2(\cos \mu\beta_1 \ell_1 - \cos \mu\alpha_1 \ell_1)}{\mu \ell_1 \sin \mu \ell_1} - (\alpha_1^2 - \beta_1^2) \right]$$

$$o \leqslant x \leqslant g\ell \qquad (3.51a)$$

$$M_{x(2)} = [M_{x(2)}]_1 + \frac{\sigma_1 \ell_1}{2(\phi+\phi_1)} \frac{\sin \mu x}{\sin \mu \ell} \left[\frac{2(\cos \mu\beta_1 \ell_1 - \cos \mu\alpha_1 \ell_1)}{\mu \ell_1 \sin \mu \ell_1} - (\alpha_1^2 - \beta_1^2) \right]$$

$$g\ell \leqslant x \leqslant \ell \qquad (3.51b)$$

where $[M_{x(1)}]_1$ and $[M_{x(2)}]_1$ can be found from Equations (3.27a & b).

For the right hand span, we have:

$$M_{x1(1)} = [M_{x1(1)}]_1 - \frac{\sigma_1}{\mu^2} \frac{\sin \mu x_1}{\sin \mu \ell_1} \left[\cos \mu \ell_1 (1-\alpha_1) - \cos \mu \ell_1 (1-\beta_1) - \frac{\mu^2 \ell_1}{2(\phi+\phi_1)} \right.$$

$$\left[\frac{2(\cos \mu\beta_1 \ell_1 - \cos \mu\alpha_1 \ell_1)}{\mu \ell_1 \sin \mu \ell_1} - (\alpha_1^2 - \beta_1^2)\right] \qquad 0 \leqslant x_1 \leqslant g_1 \ell_1$$

(3.51c)

$$M_{x1(2)} = [M_{x1(2)}]_1 - \frac{\sigma_1}{\mu^2} \frac{\sin \mu x_1}{\sin \mu \ell_1} \left[\cos \mu \ell_1 (1-\alpha_1) - \cos \mu \ell_1 (1-\beta_1) - \frac{\mu^2 \ell_1}{2(\phi+\phi_1)}\right.$$

$$\left[\frac{2(\cos \mu\beta_1 \ell_1 - \cos \mu\alpha_1 \ell_1)}{\mu \ell_1 \sin \mu \ell_1} - (\alpha_1^2 - \beta_1^2)\right] \qquad g_1 \ell_1 \leqslant x_1 \leqslant \beta_1 \ell_1$$

(3.51d)

$$M_{x1(3)} = [M_{x1(2)}]_1 - \frac{\sigma_1}{\mu^2 \sin \mu \ell_1} \left[\sin \mu x_1 \cos \mu \ell_1 (1-\alpha_1) + \sin \mu (\ell_1 - x_1)\right.$$

$$\cos \mu\beta_1 \ell_1 - \sin \mu \ell_1 - \frac{\mu^2 \ell_1}{2(\phi+\phi_1)} \sin \mu x_1 \left[\frac{2(\cos \mu\beta_1 \ell_1 - \cos \mu\alpha_1 \ell_1)}{\mu \ell_1 \sin \mu \ell_1}\right.$$

$$\left.\left. - (\alpha_1^2 - \beta_1^2)\right]\right] \qquad \beta \ell_1 \leqslant x_1 \leqslant \alpha \ell_1$$

(3.51e)

$$M_{x1(4)} = [M_{x1(2)}]_1 - \frac{\sigma_1}{\mu^2 \sin \mu \ell_1} \left[(\cos \mu\beta_1 \ell_1 - \cos \mu\alpha_1 \ell_1) \sin \mu (\ell_1 - x_1)\right.$$

$$\left. - \frac{\mu^2 \ell_1}{2(\phi+\phi_1)} \sin \mu x_1 \left[\frac{2(\cos \mu\beta_1 \ell_1 - \cos \mu\alpha_1 \ell_1)}{\mu \ell_1 \sin \mu \ell_1} - (\alpha_1^2 - \beta_1^2)\right]\right]$$

$$\alpha \ell_1 \leqslant x_1 \leqslant \ell_1$$

(3.51f)

where $[M_{x1(1)}]_1$ and $[M_{x1(2)}]_1$ can be found from Equations (3.27c & d). The stresses at any section of the beam can be determined from Equations (2.74).

The deflections can be obtained at any section of the left hand span from the following equations:

$$\eta_{(1)} = [\eta_{(1)}]_1 + \frac{\sigma_1 \ell_1}{2H(\phi+\phi_1)} \left[\frac{2(\cos \mu\beta_1\ell_1 - \cos \mu\alpha_1\ell_1)}{\mu\ell_1 \sin \mu\ell_1} - (\alpha_1^2-\beta_1^2) \right] \left(\frac{x}{\ell} - \frac{\sin \mu x}{\sin \mu\ell} \right)$$

$$o \leqslant x \leqslant g\ell$$

(3.52a)

$$\eta_{(2)} = [\eta_{(2)}]_1 + \frac{\sigma_1 \ell_1}{2H(\phi+\phi_1)} \left[\frac{2(\cos \mu\beta_1\ell_1 - \cos \mu\alpha_1\ell_1)}{\mu\ell_1 \sin \mu\ell_1} - (\alpha_1^2-\beta_1^2) \right] \left(\frac{x}{\ell} - \frac{\sin \mu x}{\sin \mu\ell} \right)$$

$$g\ell \leqslant x \leqslant \ell$$

(3.52b)

where $[\eta_{(1)}]_1$ and $[\eta_{(2)}]_1$ can be evaluated from Equations (3.28a & b).

For the right hand span, the deflection equations are:

$$\eta_{1(1)} = [\eta_{1(1)}]_1 + \frac{\sigma_1}{\mu^2 H} \left[[\cos \mu\ell_1(1-\alpha_1) - \cos \mu\ell_1(1-\beta_1)] \frac{\sin \mu x_1}{\sin \mu\ell_1} \right.$$

$$- \frac{\mu^2\ell_1^2}{2} (\alpha_1-\beta_1)[2 - (\alpha_1+\beta_1)] \frac{x_1}{\ell_1} + \frac{\mu^2\ell_1}{2(\phi+\phi_1)} \left[\frac{2(\cos \mu\beta_1\ell_1 - \cos \mu\alpha_1\ell_1)}{\mu\ell_1 \sin \mu\ell_1} \right.$$

$$\left. \left. - (\alpha_1^2-\beta_1^2) \right] \left(\frac{x_1}{\ell_1} - \frac{\sin \mu x_1}{\sin \mu\ell_1} \right) \right] \qquad o \leqslant x_1 \leqslant g_1\ell_1$$

(3.52c)

$$\eta_{1(2)} = [\eta_{1(2)}]_1 + \frac{\sigma_1}{\mu^2 H} \left[[\cos \mu\ell_1(1-\alpha_1) - \cos \mu\ell_1(1-\beta_1)] \frac{\sin \mu x_1}{\sin \mu\ell_1} \right.$$

$$- \frac{\mu^2\ell_1^2}{2} (\alpha_1-\beta_1)[2 - (\alpha_1+\beta_1)] \frac{x_1}{\ell_1} + \frac{\mu^2\ell_1}{2(\phi+\phi_1)} \left[\frac{2(\cos \mu\beta_1\ell_1 - \cos \mu\alpha_1\ell_1)}{\mu\ell_1 \sin \mu\ell_1} \right.$$

$$\left. \left. - (\alpha_1^2-\beta_1^2) \right] \left(\frac{x_1}{\ell_1} - \frac{\sin \mu x_1}{\sin \mu\ell_1} \right) \right] \qquad g_1\ell_1 \leqslant x_1 \leqslant \beta_1\ell_1$$

(3.52d)

$$\eta_{1(3)} = \left[\eta_{1(2)}\right]_1 + \frac{\sigma_1}{\mu^2 H}\left[\cos \mu\ell_1(1-\alpha_1)\frac{\sin \mu x_1}{\sin \mu\ell_1} + \cos \mu\beta_1\ell_1 \frac{\sin \mu(\ell_1-x_1)}{\sin \mu\ell_1} - 1\right.$$

$$\left. - \frac{\mu^2\ell_1^2}{2}\left[(\alpha_1-\beta_1)[2-(\alpha_1+\beta_1)]\frac{x_1}{\ell_1} - \left(\frac{x_1}{\ell_1}-\beta_1\right)^2\right] + \frac{\mu^2\ell_1}{2(\phi+\phi_1)}\right.$$

$$\left.\left[\frac{2(\cos \mu\beta_1\ell_1 - \cos \mu\alpha_1\ell_1)}{\mu\ell_1 \sin \mu\ell_1} - (\alpha_1^2-\beta_1^2)\right]\left(\frac{x_1}{\ell_1} - \frac{\sin \mu x_1}{\sin \mu\ell_1}\right)\right]$$

$$\beta_1\ell_1 \leqslant x_1 \leqslant \alpha_1\ell_1$$

(3.52e)

$$\eta_{1(4)} = \left[\eta_{1(2)}\right]_1 + \frac{\sigma_1}{\mu^2 H}\left[(\cos \mu\beta_1\ell_1 - \cos \mu\alpha_1\ell_1)\frac{\sin \mu(\ell_1-x_1)}{\sin \mu\ell_1} - \frac{\mu^2\ell_1^2}{2}\right.$$

$$\left.(\alpha_1^2-\beta_1^2)\left(1-\frac{x_1}{\ell_1}\right) + \frac{\mu^2\ell_1}{2(\phi+\phi_1)}\left[\frac{2(\cos \mu\beta_1\ell_1 - \cos \mu\alpha_1\ell_1)}{\mu\ell_1 \sin \mu\ell_1} - (\alpha_1^2-\beta_1^2)\right]\right.$$

$$\left.\left(\frac{x_1}{\ell_1} - \frac{\sin \mu x_1}{\sin \mu\ell_1}\right)\right] \qquad \alpha_1\ell_1 \leqslant x_1 \leqslant \ell_1$$

(3.52f)

where $\left[\eta_{1(1)}\right]_1$ and $\left[\eta_{1(2)}\right]_1$ can be evaluated from Equations (3.28c & d).

The shear foces can be determined at any section of the left hand span from the following equations:

$$Q_{x(1)} = \left[Q_{x(1)}\right]_1 - \frac{\mu\sigma_1\ell_1}{2(\phi+\phi_1)}\frac{\cos \mu x}{\sin \mu\ell}\left[\frac{2(\cos \mu\beta_1\ell_1 - \cos \mu\alpha_1\ell_1)}{\mu\ell_1 \sin \mu\ell_1} - (\alpha_1^2-\beta_1^2)\right]$$

$$o \leqslant x \leqslant g\ell$$

(3.53a)

$$Q_{x(2)} = \left[Q_{x(2)}\right]_1 - \frac{\mu\sigma_1\ell_1}{2(\phi+\phi_1)}\frac{\cos \mu x}{\sin \mu\ell}\left[\frac{2(\cos \mu\beta_1\ell_1 - \cos \mu\alpha_1\ell_1)}{\mu\ell_1 \sin \mu\ell_1} - (\alpha_1^2-\beta_1^2)\right]$$

$$g\ell \leqslant x \leqslant \ell$$

(3.53b)

where $[Q_{x(1)}]_1$ and $[Q_{x(2)}]_1$ can be evaluated from Equations (3.29a & b).

The shear forces equations for the right hand span are:

$$Q_{x1(1)} = [Q_{x1(1)}]_1 + \frac{\sigma_1}{\mu} \frac{\cos \mu x_1}{\sin \mu \ell_1} \left[\cos \mu \ell_1 (1-\alpha_1) - \cos \mu \ell_1 (1-\beta_1) - \frac{\mu^2 \ell_1}{2(\phi+\phi_1)} \right.$$

$$\left. \left[\frac{2(\cos \mu \beta_1 \ell_1 - \cos \mu \alpha_1 \ell_1)}{\mu \ell_1 \sin \mu \ell_1} - (\alpha_1^2 - \beta_1^2) \right] \right] \qquad 0 \leqslant x_1 \leqslant g_1 \ell_1$$

(3.53c)

$$Q_{x1(2)} = [Q_{x1(2)}]_1 + \frac{\sigma_1}{\mu} \frac{\cos \mu x_1}{\sin \mu \ell_1} \left[\cos \mu \ell_1 (1-\alpha_1) - \cos \mu \ell_1 (1-\beta_1) - \frac{\mu^2 \ell_1}{2(\phi+\phi_1)} \right.$$

$$\left. \left[\frac{2(\cos \mu \beta_1 \ell_1 - \cos \mu \alpha_1 \ell_1)}{\mu \ell_1 \sin \mu \ell_1} - (\alpha_1^2 - \beta_1^2) \right] \right] \qquad g_1 \ell_1 \leqslant x_1 \leqslant \beta_1 \ell_1$$

(3.53d)

$$Q_{x1(3)} = [Q_{x1(2)}]_1 + \frac{\sigma_1}{\mu \sin \mu \ell_1} \left[\cos \mu \ell_1 (1-\alpha_1) \cos \mu x_1 - \cos \mu \beta_1 \ell_1 \cos \mu (\ell_1 - x_1) \right.$$

$$\left. - \frac{\mu^2 \ell_1}{2(\phi+\phi_1)} \cos \mu x_1 \left[\frac{2(\cos \mu \beta_1 \ell_1 - \cos \mu \alpha_1 \ell_1)}{\mu \ell_1 \sin \mu \ell_1} - (\alpha_1^2 - \beta_1^2) \right] \right]$$

$$\beta_1 \ell_1 \leqslant x_1 \leqslant \alpha_1 \ell_1$$

(3.53e)

$$Q_{x1(4)} = [Q_{x1(2)}]_1 - \frac{\sigma_1}{\mu \sin \mu \ell_1} \left[(\cos \mu \beta_1 \ell_1 - \cos \mu \alpha_1 \ell_1) \cos \mu (\ell_1 - x_1) \right.$$

$$\left. + \frac{\mu^2 \ell_1}{2(\phi+\phi_1)} \cos \mu x_1 \left[\frac{2(\cos \mu \beta_1 \ell_1 - \cos \mu \alpha_1 \ell_1)}{\mu \ell_1 \sin \mu \ell_1} - (\alpha_1^2 - \beta_1^2) \right] \right]$$

$$\alpha_1 \ell_1 \leqslant x_1 \leqslant \ell_1$$

(3.53f)

where $[Q_{x1(1)}]_1$ and $[Q_{x1(2)}]_1$ can be calculated from Equations (3.29c & d).

2. <u>If $\beta_1 < g_1 < \alpha_1$</u>

The bending moments can be evaluated at any section of the left hand span by using Equations (3.51a & b). For the right hand span, the bending moment equations are:

$$M_{x1(1)} = [M_{x1(1)}]_1 - \frac{\sigma_1}{\mu^2}\frac{\sin \mu x_1}{\sin \mu \ell_1}\left[\cos \mu\ell_1(1-\alpha_1) - \cos \mu\ell_1(1-\beta_1) - \frac{\mu^2 \ell_1}{2(\phi+\phi_1)}\right.$$

$$\left.\left[\frac{2(\cos \mu\beta_1\ell_1 - \cos \mu\alpha_1\ell_1)}{\mu\ell_1 \sin \mu\ell_1} - (\alpha_1^2-\beta_1^2)\right]\right] \qquad o \leqslant x_1 \leqslant \beta_1\ell_1$$

(3.54a)

$$M_{x1(2)} = [M_{x1(1)}]_1 - \frac{\sigma_1}{\mu^2 \sin \mu\ell_1}\left[\cos \mu\ell_1(1-\alpha_1) \sin \mu x_1 + \cos \mu\beta_1\ell_1 \sin \mu(\ell_1-x_1)\right.$$

$$\left. - \sin \mu\ell_1 - \frac{\mu^2\ell_1}{2(\phi+\phi_1)} \sin \mu x_1 \left[\frac{2(\cos \mu\beta_1\ell_1 - \cos \mu\alpha_1\ell_1)}{\mu\ell_1 \sin \mu\ell_1} - (\alpha_1^2-\beta_1^2)\right]\right]$$

$$\beta_1\ell_1 \leqslant x_1 \leqslant g_1\ell_1$$

(3.54b)

$$M_{x1(3)} = [M_{x1(2)}]_1 - \frac{\sigma_1}{\mu^2 \sin \mu\ell_1}\left[\cos \mu\ell_1(1-\alpha_1) \sin \mu x_1 + \cos \mu\beta_1\ell_1 \sin \mu(\ell_1-x_1)\right.$$

$$\left. - \sin \mu\ell_1 - \frac{\mu^2\ell_1}{2(\phi+\phi_1)} \sin \mu x_1 \left[\frac{2(\cos \mu\beta_1\ell_1 - \cos \mu\alpha_1\ell_1)}{\mu\ell_1 \sin \mu\ell_1} - (\alpha_1^2-\beta_1^2)\right]\right]$$

$$g_1\ell_1 \leqslant x_1 \leqslant \alpha_1\ell_1$$

(3.54c)

$$M_{x1(4)} = [M_{x1(2)}]_1 - \frac{\sigma_1}{\mu^2 \sin \mu\ell_1}\left[(\cos \mu\beta_1\ell_1 - \cos \mu\alpha_1\ell_1) \sin \mu(\ell_1-x_1) - \frac{\mu^2\ell_1}{2(\phi+\phi_1)}\right.$$

$$\sin \mu x_1 \left[\frac{2(\cos \mu\beta_1 \ell_1 - \cos \mu\alpha_1 \ell_1)}{\mu \ell_1 \sin \mu \ell_1} - (\alpha_1^2 - \beta_1^2) \right] \qquad \alpha_1 \ell_1 \leq x_1 \leq \ell_1$$

(3.54d)

where $[M_{x1(1)}]_1$ and $[M_{x1(2)}]_1$ can be evaluated from Equations (3.27c & d). The stresses at any section of the beam can be determined from Equations (2.74).

The deflections can be computed at any section of the left hand span from Equations (3.52a & b). For the right hand span, the deflection equations are:

$$\eta_{1(1)} = [\eta_{1(1)}]_1 + \frac{\sigma_1}{\mu^2 H} \left[[\cos \mu\ell_1(1-\alpha_1) - \cos \mu\ell_1(1-\beta_1)] \frac{\sin \mu x_1}{\sin \mu \ell_1} \right.$$

$$- \frac{\mu^2 \ell_1^2}{2} (\alpha_1 - \beta_1)[2 - (\alpha_1 + \beta_1)] \frac{x_1}{\ell_1} + \frac{\mu^2 \ell_1}{2(\phi + \phi_1)} \left[\frac{2(\cos \mu\beta_1 \ell_1 - \cos \mu\alpha_1 \ell_1)}{\mu \ell_1 \sin \mu \ell_1} \right.$$

$$\left. \left. - (\alpha_1^2 - \beta_1^2) \right] \left(\frac{x_1}{\ell_1} - \frac{\sin \mu x_1}{\sin \mu \ell_1} \right) \right] \qquad 0 \leq x_1 \leq \beta_1 \ell_1$$

(3.55a)

$$\eta_{1(2)} = [\eta_{1(1)}]_1 + \frac{\sigma_1}{\mu^2 H} \left[\cos \mu\ell_1(1-\alpha_1) \frac{\sin \mu x_1}{\sin \mu \ell_1} + \cos \mu\beta_1 \ell_1 \frac{\sin \mu(\ell_1 - x_1)}{\sin \mu \ell_1} \right.$$

$$- 1 - \frac{\mu^2 \ell_1^2}{2} \left[(\alpha_1 - \beta_1)[2 - (\alpha_1 + \beta_1)] \frac{x_1}{\ell_1} - \left(\frac{x_1}{\ell_1} - \beta_1 \right)^2 \right] + \frac{\mu^2 \ell_1}{2(\phi + \phi_1)}$$

$$\left[\frac{2(\cos \mu\beta_1 \ell_1 - \cos \mu\alpha_1 \ell_1)}{\mu \ell_1 \sin \mu \ell_1} - (\alpha_1^2 - \beta_1^2) \right] \left(\frac{x_1}{\ell_1} - \frac{\sin \mu x_1}{\sin \mu \ell_1} \right) \Bigg]$$

$$\beta_1 \ell_1 \leq x_1 \leq g_1 \ell_1$$

(3.55b)

$$\eta_{1(3)} = [\eta_{1(2)}]_1 + \frac{\sigma_1}{\mu^2 H} \left[\cos \mu\ell_1(1-\alpha_1) \frac{\sin \mu x_1}{\sin \mu \ell_1} + \cos \mu\beta_1 \ell_1 \frac{\sin \mu(\ell_1 - x_1)}{\sin \mu \ell_1} - 1 \right.$$

$$- \frac{\mu^2 \ell_1^2}{2} \left[(\alpha_1-\beta_1)[2 - (\alpha_1+\beta_1)] \frac{x_1}{\ell_1} - \left(\frac{x_1}{\ell_1} - \beta_1 \right)^2 \right] + \frac{\mu^2 \ell_1}{2(\phi+\phi_1)}$$

$$\left[\frac{2(\cos \mu\beta_1 \ell_1 - \cos \mu\alpha_1 \ell_1)}{\mu \ell_1 \sin \mu \ell_1} - (\alpha_1^2-\beta_1^2) \right] \left[\frac{x_1}{\ell_1} - \frac{\sin \mu x_1}{\sin \mu \ell_1} \right] \Bigg]$$

$$g_1 \ell_1 \leqslant x_1 \leqslant \alpha_1 \ell_1$$

(3.55c)

$$\eta_{1(4)} = \left[\eta_{1(2)}\right]_1 + \frac{\sigma_1}{\mu^2 H} \left[(\cos \mu\beta_1 \ell_1 - \cos \mu\alpha_1 \ell_1) \frac{\sin \mu(\ell_1-x_1)}{\sin \mu \ell_1} - \frac{\mu^2 \ell_1^2}{2} \right.$$

$$(\alpha_1^2-\beta_1^2) \left(1 - \frac{x_1}{\ell_1} \right) + \frac{\mu^2 \ell_1}{2(\phi+\phi_1)} \left[\frac{2(\cos \mu\beta_1 \ell_1 - \cos \mu\alpha_1 \ell_1)}{\mu \ell_1 \sin \mu \ell_1} - (\alpha_1^2-\beta_1^2) \right]$$

$$\left. \left(\frac{x_1}{\ell_1} - \frac{\sin \mu x_1}{\sin \mu \ell_1} \right) \right] \qquad \alpha_1 \ell_1 \leqslant x_1 \leqslant \ell_1$$

(3.55d)

where $\left[\eta_{1(1)}\right]_1$ and $\left[\eta_{1(2)}\right]_1$ can be determined from Equations (3.28c & d).

The shear forces can be calculated at any section of the left hand span from Equations (3.53a & b). For the right hand span, the shear forces equations are:

$$Q_{x1(1)} = \left[Q_{x1(1)}\right]_1 + \frac{\sigma_1}{\mu} \frac{\cos \mu x_1}{\sin \mu \ell_1} \left[\cos \mu \ell_1(1-\alpha_1) - \cos \mu \ell_1(1-\beta_1) - \frac{\mu^2 \ell_1}{2(\phi+\phi_1)} \right.$$

$$\left. \left[\frac{2(\cos \mu\beta_1 \ell_1 - \cos \mu\alpha_1 \ell_1)}{\mu \ell_1 \sin \mu \ell_1} - (\alpha_1^2-\beta_1^2) \right] \right] \qquad 0 \leqslant x_1 \leqslant \beta_1 \ell_1$$

(3.56a)

$$Q_{x1(2)} = \left[Q_{x1(1)}\right]_1 + \frac{\sigma_1}{\mu \sin \mu \ell_1} \left[\cos \mu \ell_1(1-\alpha_1) \cos \mu x_1 - \cos \mu\beta_1 \ell_1 \cos \mu(\ell_1-x_1) \right.$$

$$- \frac{\mu^2 \ell_1}{2(\phi+\phi_1)} \cos \mu x_1 \left[\frac{2(\cos \mu\beta_1\ell_1 - \cos \mu\alpha_1\ell_1)}{\mu\ell_1 \sin \mu\ell_1} - (\alpha_1^2-\beta_1^2) \right] \Bigg]$$

$$\beta_1\ell_1 \leqslant x_1 \leqslant g_1\ell_1 \qquad (3.56b)$$

$$Q_{x1(3)} = [Q_{x1(2)}]_1 + \frac{\sigma_1}{\mu \sin \mu\ell_1} \left[\cos \mu\ell_1(1-\alpha_1) \cos \mu x_1 - \cos \mu\beta_1\ell_1 \cos \mu(\ell_1-x_1) \right.$$

$$- \frac{\mu^2 \ell_1}{2(\phi+\phi_1)} \cos \mu x_1 \left[\frac{2(\cos \mu\beta_1\ell_1 - \cos \mu\alpha_1\ell_1)}{\mu\ell_1 \sin \mu\ell_1} - (\alpha_1^2-\beta_1^2) \right] \Bigg]$$

$$g_1\ell_1 \leqslant x_1 \leqslant \alpha_1\ell_1 \qquad (3.56c)$$

$$Q_{x1(4)} = [Q_{x1(2)}]_1 - \frac{\sigma_1}{\mu \sin \mu\ell_1} \left[(\cos \mu\beta_1\ell_1 - \cos \mu\alpha_1\ell_1) \cos \mu(\ell_1-x_1) \right.$$

$$+ \frac{\mu^2 \ell_1}{2(\phi+\phi_1)} \cos \mu x_1 \left[\frac{2(\cos \mu\beta_1\ell_1 - \cos \mu\alpha_1\ell_1)}{\mu\ell_1 \sin \mu\ell_1} - (\alpha_1^2-\beta_1^2) \right] \Bigg]$$

$$\alpha_1\ell_1 \leqslant x_1 \leqslant \ell_1 \qquad (3.56d)$$

where $[Q_{x1(1)}]_1$ and $[Q_{x1(2)}]_1$ can be evaluated from Equations (3.29c & d).

3. <u>If $g_1 \geqslant \alpha_1$</u>

The bending moments can be determined at any section of the left hand span from Equations (3.51a & b). For the right hand span, the bending moment equations are:

$$M_{x1(1)} = [M_{x1(1)}]_1 - \frac{\sigma_1}{\mu^2} \frac{\sin \mu x_1}{\sin \mu\ell_1} \left[\cos \mu\ell_1(1-\alpha_1) - \cos \mu\ell_1(1-\beta_1) - \frac{\mu^2 \ell_1}{2(\phi+\phi_1)} \right.$$

$$\left[\frac{2(\cos \mu\beta_1\ell_1 - \cos \mu\alpha_1\ell_1)}{\mu\ell_1 \sin \mu\ell_1} - (\alpha_1^2-\beta_1^2)\right] \qquad 0 \leqslant x_1 \leqslant \beta_1\ell_1$$

(3.57a)

$$M_{x1(2)} = [M_{x1(1)}]_1 - \frac{\sigma_1}{\mu^2 \sin \mu\ell_1}\left[\cos \mu\ell_1(1-\alpha_1) \sin \mu x_1 + \cos \mu\beta_1\ell_1 \sin \mu(\ell_1-x_1)\right.$$

$$\left. - \sin \mu\ell_1 - \frac{\mu^2\ell_1}{2(\phi+\phi_1)} \sin \mu x_1 \left[\frac{2(\cos \mu\beta_1\ell_1 - \cos \mu\alpha_1\ell_1)}{\mu\ell_1 \sin \mu\ell_1} - (\alpha_1^2-\beta_1^2)\right]\right]$$

$$\beta_1\ell_1 \leqslant x_1 \leqslant \alpha_1\ell_1$$

(3.57b)

$$M_{x1(3)} = [M_{x1(1)}]_1 - \frac{\sigma_1}{\mu^2 \sin \mu\ell_1}\left[(\cos \mu\beta_1\ell_1 - \cos \mu\alpha_1\ell_1) \sin \mu(\ell_1-x_1)\right.$$

$$\left. - \frac{\mu^2\ell_1}{2(\phi+\phi_1)} \sin \mu x_1 \left[\frac{2(\cos \mu\beta_1\ell_1 - \cos \mu\alpha_1\ell_1)}{\mu\ell_1 \sin \mu\ell_1} - (\alpha_1^2-\beta_1^2)\right]\right]$$

$$\alpha_1\ell_1 \leqslant x_1 \leqslant g_1\ell_1$$

(3.57c)

$$M_{x1(4)} = [M_{x1(2)}]_1 - \frac{\sigma_1}{\mu^2 \sin \mu\ell_1}\left[(\cos \mu\beta_1\ell_1 - \cos \mu\alpha_1\ell_1) \sin \mu(\ell_1-x_1) - \frac{\mu^2\ell_1}{2(\phi+\phi_1)}\right.$$

$$\left. \sin \mu x_1 \left[\frac{2(\cos \mu\beta_1\ell_1 - \cos \mu\alpha_1\ell_1)}{\mu\ell_1 \sin \mu\ell_1} - (\alpha_1^2-\beta_1^2)\right]\right] \qquad g_1\ell_1 \leqslant x_1 \leqslant \ell_1$$

(3.57d)

where $[M_{x1(1)}]_1$ and $[M_{x1(2)}]_1$ can be determined from Equations (3.27c & d). The stresses at any section of the beam can be determined from Equations (2.74).

The deflections can be evaluated at any section of the left hand span from Equations (3.52a & b). For the right hand span, the deflection equations are:

$$\eta_{1(1)} = \left[\eta_{1(1)}\right]_1 + \frac{\sigma_1}{\mu^2 H}\left[\left[\cos \mu\ell_1(1-\alpha_1) - \cos \mu\ell_1(1-\beta_1)\right]\frac{\sin \mu x_1}{\sin \mu\ell_1}\right.$$

$$- \frac{\mu^2\ell_1^2}{2}(\alpha_1-\beta_1)[2-(\alpha_1+\beta_1)]\frac{x_1}{\ell_1} + \frac{\mu^2\ell_1}{2(\phi+\phi_1)}\left[\frac{2(\cos \mu\beta_1\ell_1 - \cos \mu\alpha_1\ell_1)}{\mu\ell_1 \sin \mu\ell_1}\right.$$

$$\left.\left. - (\alpha_1^2-\beta_1^2)\right]\left(\frac{x_1}{\ell_1} - \frac{\sin \mu x_1}{\sin \mu\ell_1}\right)\right] \qquad o \leqslant x_1 \leqslant \beta_1\ell_1$$

(3.58a)

$$\eta_{1(2)} = \left[\eta_{1(1)}\right]_1 + \frac{\sigma_1}{\mu^2 H}\left[\cos \mu\ell_1(1-\alpha_1)\frac{\sin \mu x_1}{\sin \mu\ell_1} + \cos \mu\beta_1\ell_1 \frac{\sin \mu(\ell_1-x_1)}{\sin \mu\ell_1}\right.$$

$$- 1 - \frac{\mu^2\ell_1^2}{2}\left[(\alpha_1-\beta_1)[2-(\alpha_1+\beta_1)]\frac{x_1}{\ell_1} - \left(\frac{x_1}{\ell} - \beta_1\right)^2\right] + \frac{\mu^2\ell_1}{2(\phi+\phi_1)}$$

$$\left[\frac{2(\cos \mu\beta_1\ell_1 - \cos \mu\alpha_1\ell_1)}{\mu\ell_1 \sin \mu\ell_1} - (\alpha_1^2-\beta_1^2)\right]\left(\frac{x_1}{\ell_1} - \frac{\sin \mu x_1}{\sin \mu\ell_1}\right)\Bigg]$$

$$\beta_1\ell_1 \leqslant x_1 \leqslant \alpha_1\ell_1$$

(3.58b)

$$\eta_{1(3)} = \left[\eta_{1(1)}\right]_1 + \frac{\sigma_1}{\mu^2 H}\left[(\cos \mu\beta_1\ell_1 - \cos \mu\alpha_1\ell_1)\frac{\sin \mu(\ell_1-x_1)}{\sin \mu\ell_1} - \frac{\mu^2\ell_1^2}{2}\right.$$

$$(\alpha_1^2-\beta_1^2)\left(1 - \frac{x_1}{\ell_1}\right) + \frac{\mu^2\ell_1}{2(\phi+\phi_1)}\left[\frac{2(\cos \mu\beta_1\ell_1 - \cos \mu\alpha_1\ell_1)}{\mu\ell_1 \sin \mu\ell_1} - (\alpha_1^2-\beta_1^2)\right]$$

$$\left.\left(\frac{x_1}{\ell_1} - \frac{\sin \mu x_1}{\sin \mu\ell_1}\right)\right] \qquad \alpha_1\ell_1 \leqslant x_1 \leqslant \varepsilon_1\ell_1$$

(3.58c)

$$\eta_{1(4)} = \left[\eta_{1(2)}\right]_1 + \frac{\sigma_1}{\mu^2 H}\left[(\cos \mu\beta_1\ell_1 - \cos \mu\alpha_1\ell_1)\frac{\sin \mu(\ell_1-x_1)}{\sin \mu\ell_1} - \frac{\mu^2\ell_1^2}{2}\right.$$

$$(\alpha_1^2-\beta_1^2)\left(1-\frac{x_1}{\ell_1}\right)+\frac{\mu^2\ell_1}{2(\phi+\phi_1)}\left[\frac{2(\cos\mu\beta_1\ell_1-\cos\mu\alpha_1\ell_1)}{\mu\ell_1\sin\mu\ell_1}-(\alpha_1^2-\beta_1^2)\right]$$

$$\left(\frac{x_1}{\ell_1}-\frac{\sin\mu x_1}{\sin\mu\ell_1}\right)\Bigg] \qquad \varepsilon_1\ell_1 \leqslant x_1 \leqslant \ell_1$$

(3.58d)

where $[\eta_{1(1)}]_1$ and $[\eta_{1(2)}]_1$ can be obtained from Equations (3.28c & d).

The shear forces can be determined at any section of the left hand span from Equations (3.54a & b). For the right hand span, the shear forces equations are:

$$Q_{x1(1)}=[Q_{x1(1)}]_1+\frac{\sigma_1}{\mu}\frac{\cos\mu x_1}{\sin\mu\ell_1}\left[\cos\mu\ell_1(1-\alpha_1)-\cos\mu\ell_1(1-\beta_1)-\frac{\mu^2\ell_1}{2(\phi+\phi_1)}\right.$$

$$\left.\left[\frac{2(\cos\mu\beta_1\ell_1-\cos\mu\alpha_1\ell_1)}{\mu\ell_1\sin\mu\ell_1}-(\alpha_1^2-\beta_1^2)\right]\right] \qquad 0 \leqslant x_1 \leqslant \beta_1\ell_1$$

(3.59a)

$$Q_{x1(2)}=[Q_{x1(1)}]_1+\frac{\sigma_1}{\mu\sin\mu\ell_1}\left[\cos\mu\ell_1(1-\alpha_1)\sin\mu x_1-\cos\mu\beta_1\ell_1\cos\mu(\ell_1-x_1)\right.$$

$$\left.-\frac{\mu^2\ell_1}{2(\phi+\phi_1)}\cos\mu x_1\left[\frac{2(\cos\mu\beta_1\ell_1-\cos\mu\alpha_1\ell_1)}{\mu\ell_1\sin\mu\ell_1}-(\alpha_1^2-\beta_1^2)\right]\right]$$

$$\beta_1\ell_1 \leqslant x_1 \leqslant \alpha_1\ell_1$$

(3.59b)

$$Q_{x1(3)}=[Q_{x1(1)}]_1-\frac{\sigma_1}{\mu\sin\mu\ell_1}\left[(\cos\mu\beta_1\ell_1-\cos\mu\alpha_1\ell_1)\cos\mu(\ell_1-x_1)\right.$$

$$+ \frac{\mu^2 \ell_1}{2(\phi+\phi_1)} \cos \mu x_1 \left[\frac{2(\cos \mu\beta_1 \ell_1 - \cos \mu\alpha_1 \ell_1)}{\mu \ell_1 \sin \mu \ell_1} - (\alpha_1^2 - \beta_1^2) \right] \Bigg]$$

$$\alpha_1 \ell_1 \leqslant x_1 \leqslant g_1 \ell_1 \qquad (3.59c)$$

$$Q_{x1(4)} = [Q_{x1(2)}]_1 - \frac{\sigma_1}{\mu \sin \mu \ell_1} \left[(\cos \mu\beta_1 \ell_1 - \cos \mu\alpha_1 \ell_1) \cos \mu(\ell_1 - x_1) \right.$$

$$+ \frac{\mu^2 \ell_1}{2(\phi+\phi_1)} \cos \mu x_1 \left[\frac{2(\cos \mu\beta_1 \ell_1 - \cos \mu\alpha_1 \ell_1)}{\mu \ell_1 \sin \mu \ell_1} - (\alpha_1^2 - \beta_1^2) \right] \Bigg]$$

$$g_1 \ell_1 \leqslant x_1 \leqslant \ell_1 \qquad (3.59d)$$

where $[Q_{x1(1)}]_1$ and $[Q_{x1(2)}]_1$ can be calculated from Equations (3.29c & d).

The bending moments, deflections and shear forces equations can be written for a continuous uniformly distributed load applied in the right hand span when substituting $\alpha_1 = 1$ and $\beta_1 = o$ in the equations given for the case when $\beta_1 < g_1 < \alpha_1$.

Finally, Formulae (3.27 - 59) can be used to determine the bending moments, deflections and shear forces for any different combinations of live loading by employing the principle of superposition. Furthermore, they can be used to find the internal forces for suspended beams with no eccentricities at the ends of their cable when substituting a = o in these formulae. In addition, Formulae (3.27 - 59) can also be used after the time effects take place by replacing γ by τ in Equations (3.27), (3.28) and (3.29). It is worth noting that these formulae can also be used for ungrouted beams when omitting the contribution of grout, $g = g_1 = o$.

3.5.2 The Forces in the Suspenders

Similar to Section 2.6.2, the forces in the suspenders must be evaluated for the maximum possible values. This can be achieved by knowing the maximal possible value of the increase in the prestressing force H_{pmax} which can be calculated when studying all possible cases of live loading to which the structure may be subjected. Hence, ρ_{max} can be determined from Equations (2.60), where:

$$\rho_{max} = \frac{H_{pmax}}{H_w}$$

From Appendix 23, the maximum suspenders load q_{smax} can be computed for the left hand span as follows:

$$q_{smax} = - W \left[(1+\gamma)(1+ \frac{\theta}{\ell}) \left[1 - \frac{\mu^2}{4} \frac{(\theta+\omega\theta_1)}{(\phi+\phi_1)} \right] + \frac{\rho_{max}}{2} \left[(1+ \frac{\theta}{\ell}) \left[1 - \frac{\mu^2}{2} \frac{(\theta_g+\omega\theta_{g1})}{(\phi+\phi_1)} \right] + \frac{\sin \frac{\mu\ell}{2}(1-2g)}{\frac{\mu\ell}{2} \cos \frac{\mu\ell}{2}} \right] \right] \quad (3.60a)$$

and for the right hand span, the maximum suspenders load is:

$$q_{s1max} = - W_1 \left[(1+\gamma)(1+ \frac{\theta_1}{\ell_1}) \left[1 - \frac{\mu^2}{4\omega} \frac{(\theta+\omega\theta_1)}{(\phi+\phi_1)} \right] + \frac{\rho_{max}}{2} \left[(1+ \frac{\theta_1}{\ell_1}) \left[1 - \frac{\mu^2}{2\omega} \frac{(\theta_g+\omega\theta_{g1})}{(\phi+\phi_1)} \right] + \frac{\sin \frac{\mu\ell_1}{2}(1-2g_1)}{\frac{\mu\ell_1}{2} \cos \frac{\mu\ell_1}{2}} \right] \right] \quad (3.60b)$$

where $\omega = \frac{W_1}{W}$ and where ϕ, ϕ_1, θ, θ_1, θ_g and θ_{g1} can be obtained from

Equations (2.63) and (3.22) respectively. It is worth mentioning that the suspenders load in this type of bridge becomes equal to that of the prestressed concrete suspension bridge with ungrouted cables when omitting the grout restraint, i.e. by substituting g, g_1 = o in Equations (3.60).

Finally, as shown in Figure (2.20), the forces in the suspenders, which are represented as the reactions in the fictitious supports of the system, can then be determined. For simplicity, the average force in each suspender can be obtained from Equations (2.88) for left and right hand spans. The extension in each suspender must be checked to ensure that it does not exceed 10% of the beam deflection at its position in order to prevent any reduction in the interaction between cable and beam as mentioned earlier.

3.5.3 The Tower Force

As mentioned in Section 2.6.4, the tower must be designed to sustain the maximum vertical tower force N_{Tmax} as well as the wind loads. Therefore, knowing ρ_{max}, as from the preceding section, the maximum vertical tower force is: (similar to Equation (2.89)).

$$N_{Tmax} = H_w (1+y+\rho_{max}) \left[(F+8n) + (F_1+8n_1)\right] \qquad (3.61)$$

Hence, the stability of the tower can be checked for different combinations of this force and the wind loads.

3.6 The Effect of Grouting on Prestressed Concrete Suspension Bridges

3.6.1 Introduction

In this section, we will discuss the main differences between prestressed concrete suspension bridges with ungrouted and grouted cables. To achieve the benefits of the comparison, we will consider

the effect of grouting on the behaviour of the main cable when subjected to the various effects, e.g. tower flexure, construction errors, ... etc, as well as due to live loading. Furthermore, we will also discuss the effect of grouting on the internal forces of the prestressed cable suspended beam, the suspenders and the tower.

Finally, basing our conclusion on the results obtained from both experiments, Chapter (7), we will be able to recommend the use of either types of bridge for practical application.

3.6.2 The Effect of Grouting on the Main Cable

3.6.2.1 The Deformations of the Main Cable

The effect of grouting is basically causing restraint to part of the length of the main cable in both spans and therefore, reducing its free lengths to S_f and S_{f1} in left and right hand spans respectively as can be seen from Equations (2.14) and (3.3). The value of this restraint depends on the lengths of the spans and the dimensions of the suspended beam as shown in Figure (3.2) and Equations (3.1). For short spans, the effect of the grouted lengths is greater and vice versa.

For the above reasons, tower flexure, construction errors or temperature changes have a lesser effect on the change in length and shape of the grouted main cable than the ungrouted one as can be deduced from Equations (3.6 - 15) and (2.19 - 33) respectively. However, for the grouted case, the corresponding change in the cable tension ΔH is greater as can be deduced when comparing Equations (2.35) and (3.16). This can be verified by the fact that the change in the cable tension ΔH is inversely proportional to the length function $\left(\frac{ds}{dx} \right)^2$ as shown in Appendices 8 & 19. Consequently, for the grouted case, a smaller free length of the cable means a more rigid cable and therefore the cable experiences larger changes of force.

Obviously, any increase in the cable tension is a bonus as it increases the prestressing force and consequently improves the performance of the entire system. Sometimes the change in the cable tension ΔH may be negative, e.g loose suspenders resulted from a construction error. This means that for the grouted case, more reduction in the prestressing force might take place than the ungrouted one. Even though the value of this reduction is usually insignificant, it will be always absorbed by the value of the initial prestressing force H_i, = H_w (1+y). In other words the value of y will overcome that reduction as well as the time effects.

3.6.2.2 The Behaviour of the Main Cable when Live Loading is Applied

As mentioned in the preceding section, the effect of grouting is basically to increase the rigidity of the main cable and make it capable of gaining more force. This is more obvious when comparing the values of δ_c and δ_{cf}, Equations (2.45) and (3.19), as these terms represent the flexibility of the main cable. The more the grouted lengths are, the less flexible the cable becomes and consequently the grouted main cable gains more force, H_p, due to the application of live loads.

From the observation of the two experiments, Sections 7.5 and 7.6, we measured more increase in the tension of the cable of the grouted case than the ungrouted one. A specimen of the results, when an increasing concentrated load P has been applied in the mid-point of the left hand span of the test beams, is plotted for both cases as shown in Figure (3.4). The figure clearly shows the difference in the rate of increase for the cable tension in both cases due to the applied load.

Therefore, we finally conclude that grouting the lengths through which the main cable passes within the prestressed cable suspended beam, undoubtedly improves the interaction between the cable and the beam. This can be considered as one of the advantages of grouting prestressed concrete suspension bridges.

3.6.3 The Effect of Grouting on the Internal Forces of the Suspended Beam

As a result of the greater value of the change in the cable tension H_p due to live loading, the prestressing force H will increase as well as the upward uniformly distributed forces ρW and ρW_1 in both spans. Accordingly, this will relieve the structure and therefore, reduce the bending moments, deflections and shear forces caused by the applied live loading.

The measured results of the two experiments confirmed this fact as lesser values for bending moments and deflections were recorded for the grouted test beam than the ungrouted one, Tables (7.1 - 20) This can be regarded as another advantage of grouting prestressed concrete suspension bridges.

3.6.4 The Effect of Grouting on the Suspenders Forces and the Tower Force

From Equations (2.86), (2.89), (3.60) and (3.61), it is clear that the greater value of H_p will most certainly increase both the suspenders forces and the tower force for the grouted case. Consequently, suspenders with larger diameters and towers with bigger cross sections will be needed to accommodate these extra forces.

This represents one disadvantage of grouting prestressed concrete suspension bridges as suspension bridges generally produce very large vertical forces on their towers.

3.6.5 Final Conclusion

From the previous analysis, we conclude that grouting prestressed cable suspension bridges redistributes the forces applied on that structure. It relieves the prestressed concrete suspended beam and accordingly increases the forces in both the suspenders and

the tower. Furthermore, more lifting forces will affect the two end supports and therefore, heavier concrete boxes of sand may be required (see Section 1.3).

Hence, the advantages of the method of grouting for prestressed concrete suspension bridges can be summarised as follows:

a. Tower flexure, construction errors and temperature changes have a lesser effect on the length and shape of the main cable but a favourable one to increase the cable tension.

b. Grouting improves the interaction between the main cable and the prestressed cable suspended beam which means that a greater part of the live loading is directly sustained by the main cable and consequently the beam will experience less internal stresses.

c. Grouting improves the overall rigidity of the structure and makes it more stable against wind and vibrations (see References (7), (8), (9) and and (22)).

The final decision whether to use grouting in prestressed concrete suspension bridges should be based on a cost analysis for each particular bridge and comparing the savings in the cost of the superstructure with the extra cost of the substructure to achieve the most economical design.

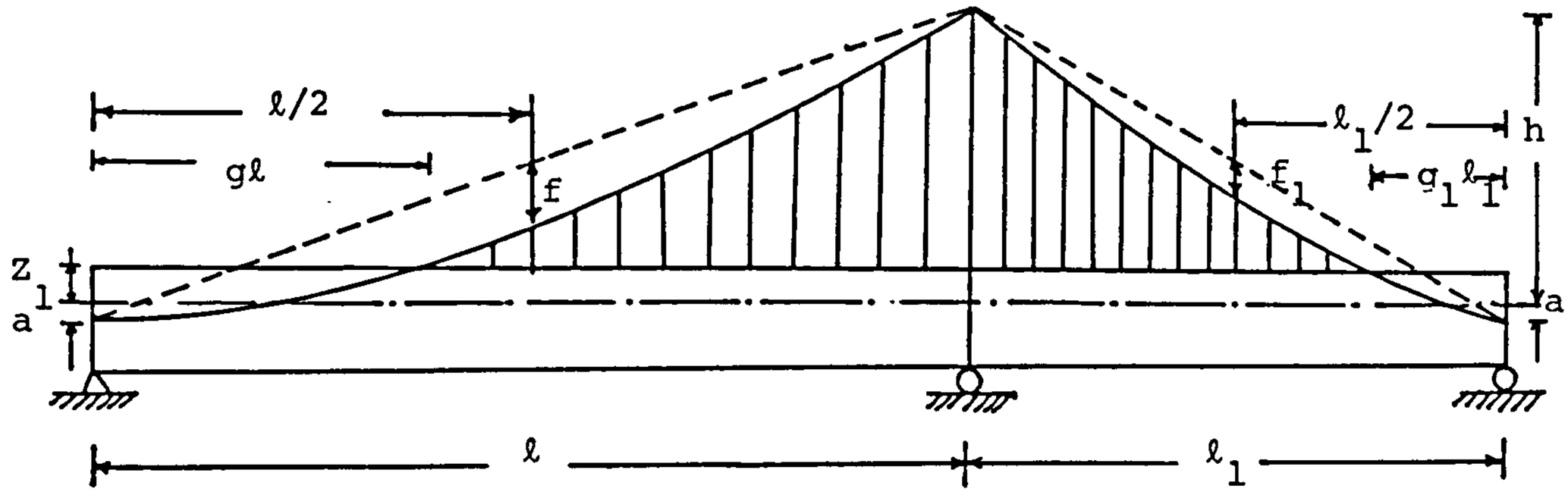

(a)

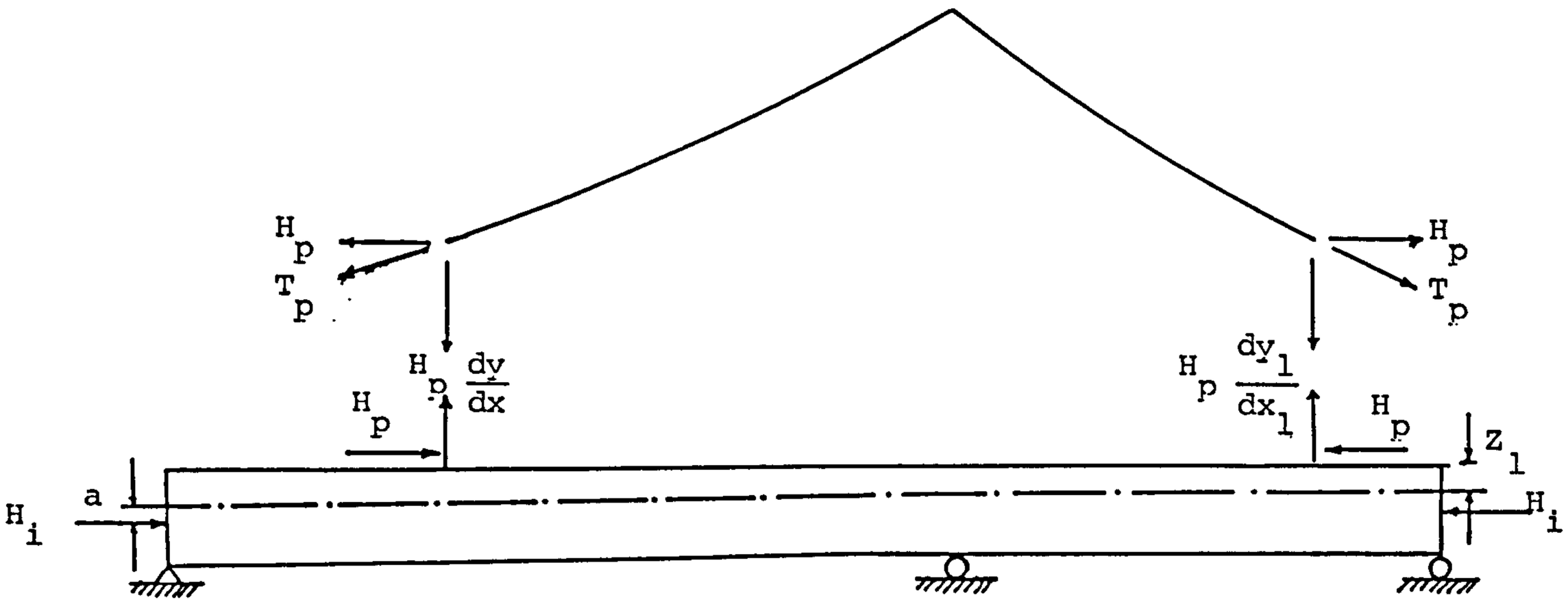

(b)

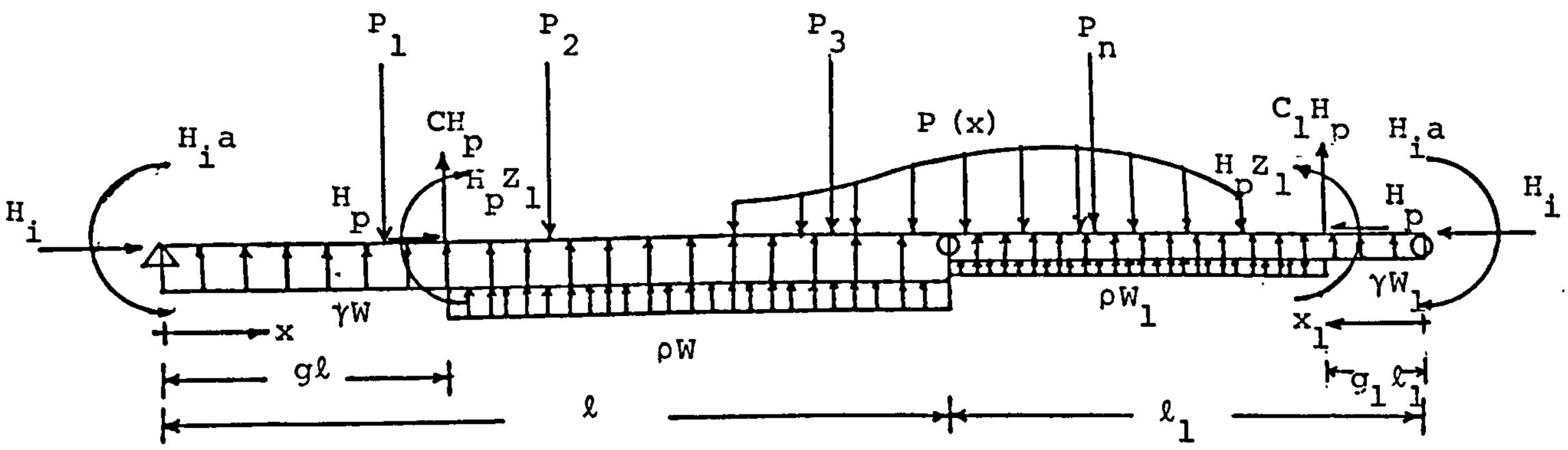

(c)

The forces in a grouted prestressed concrete suspended beam

Figure (3.1)

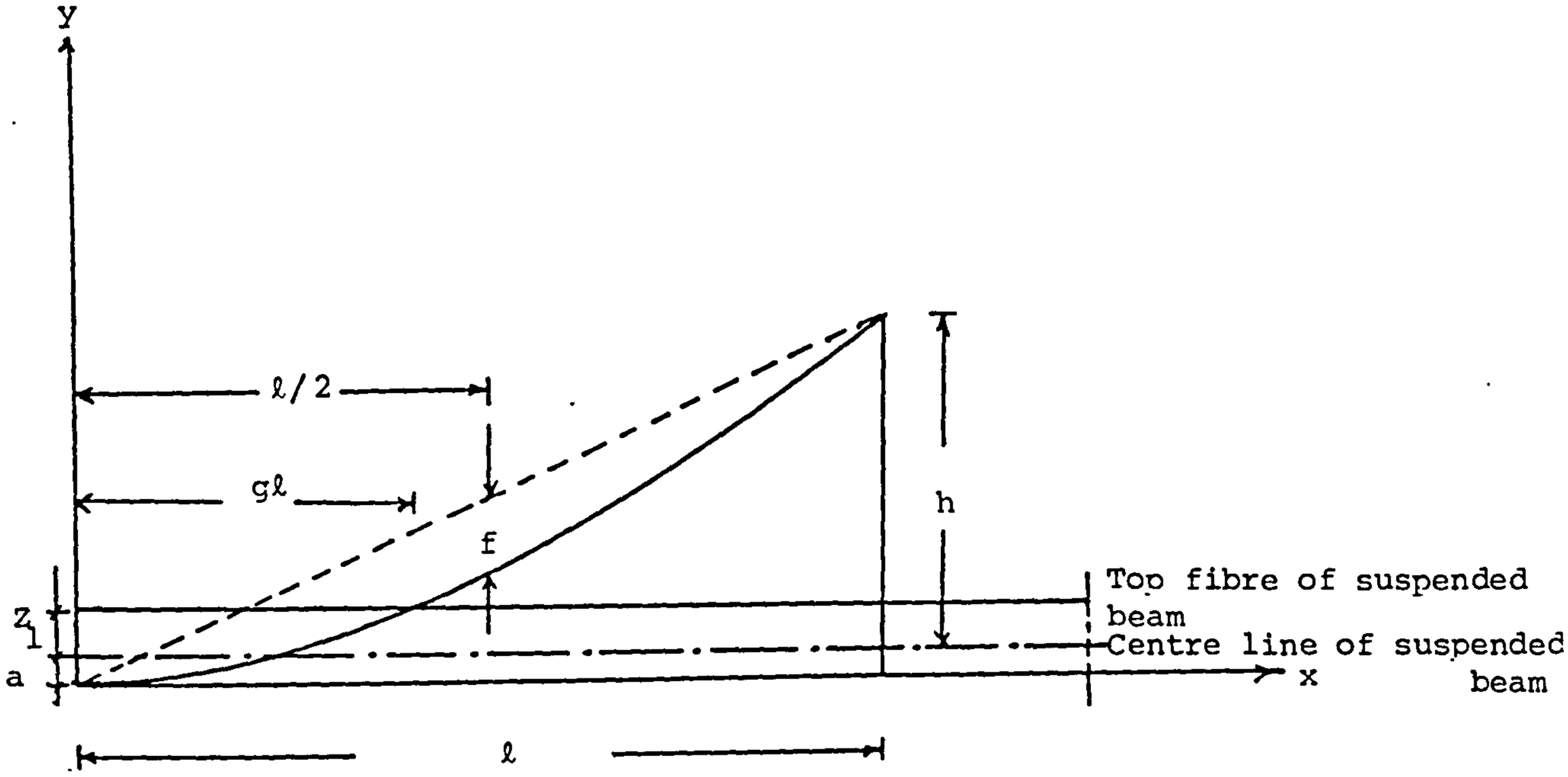

The grouted cable in the left hand span

Figure (3.2)

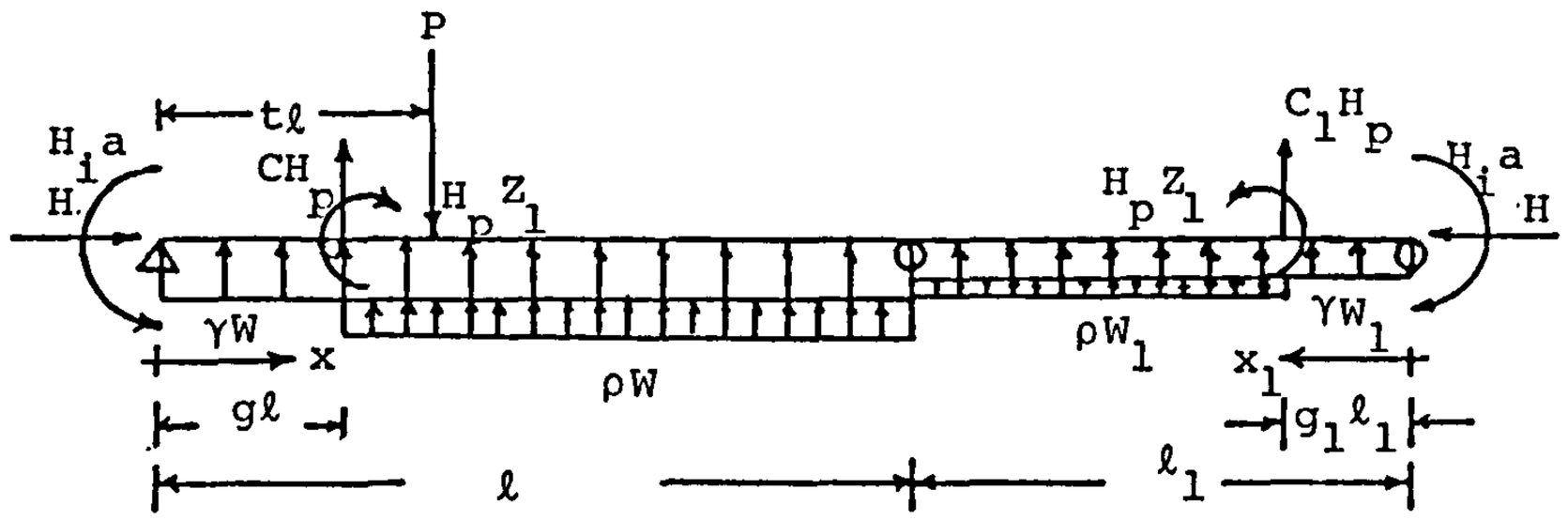

(a)

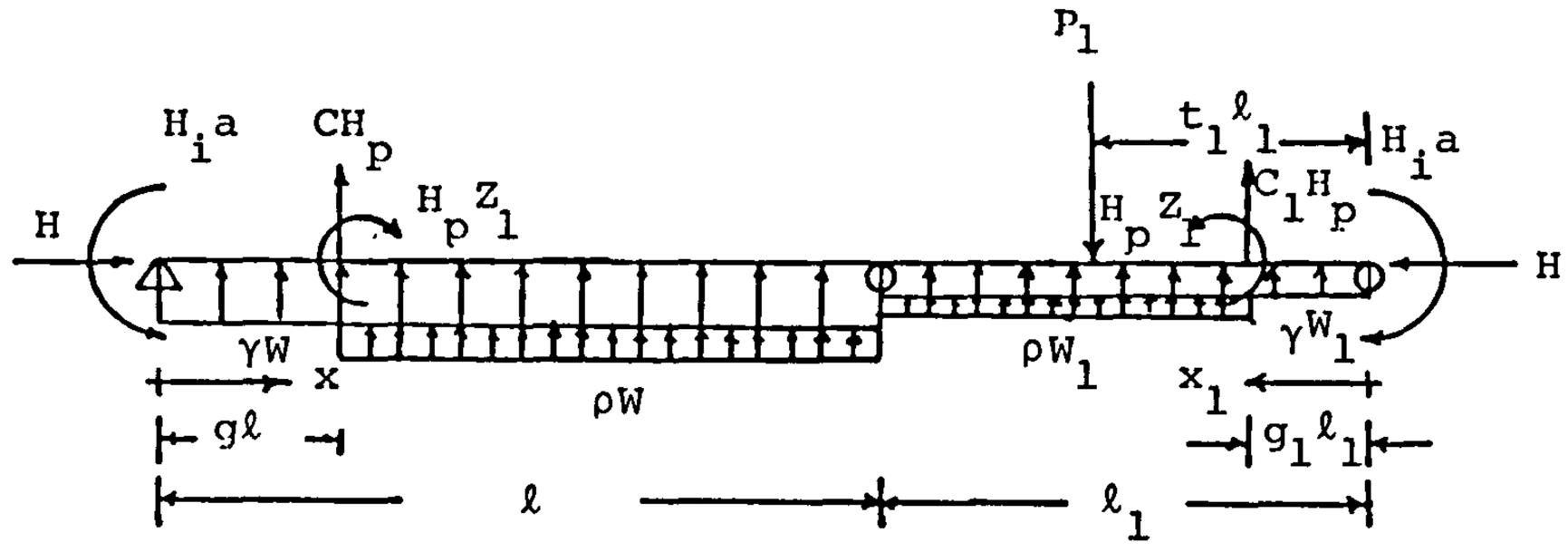

(b)

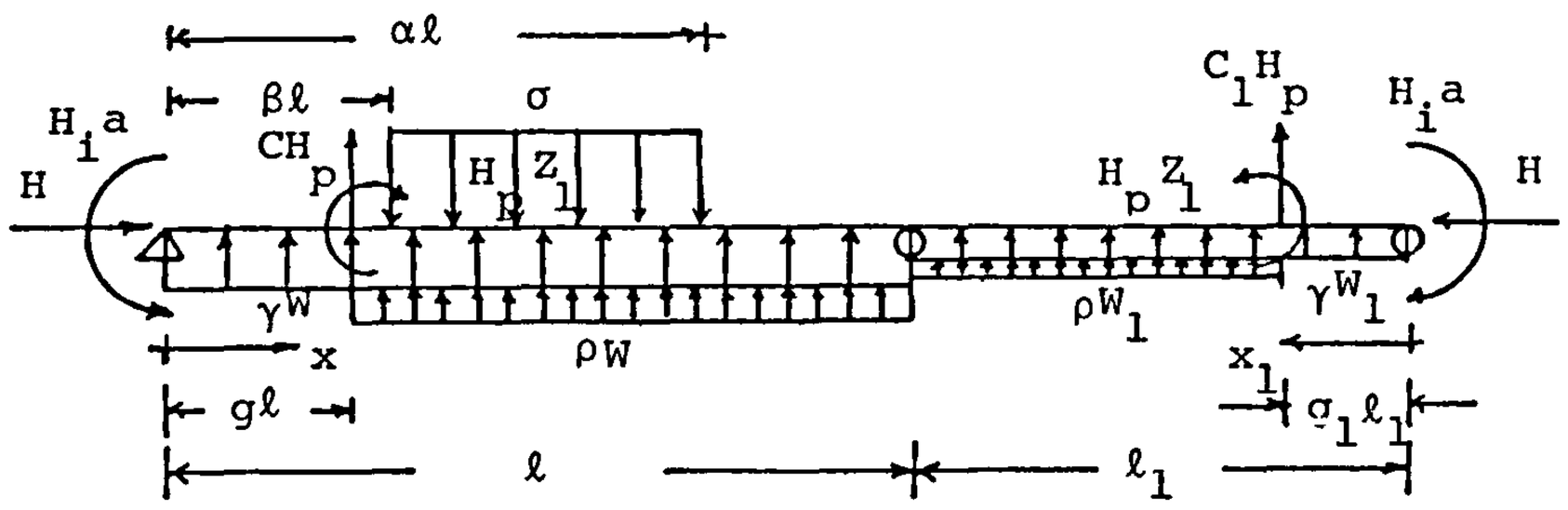

(c)

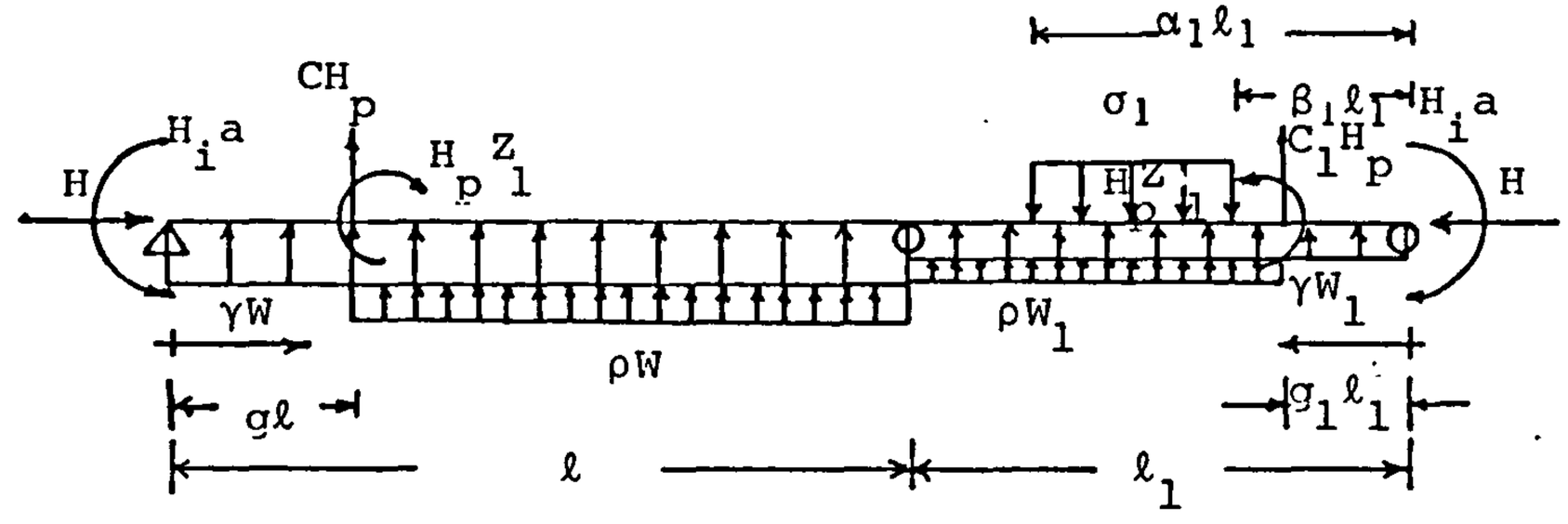

(d)

The grouted test beam under various cases of live loading

Figure (3.3)

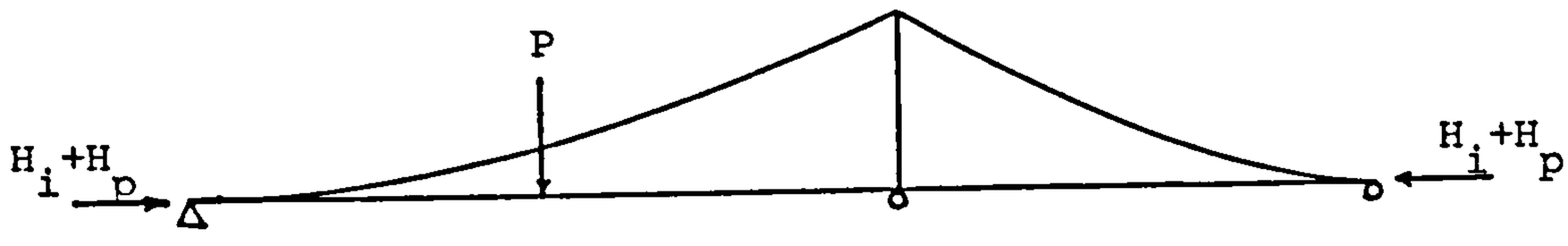

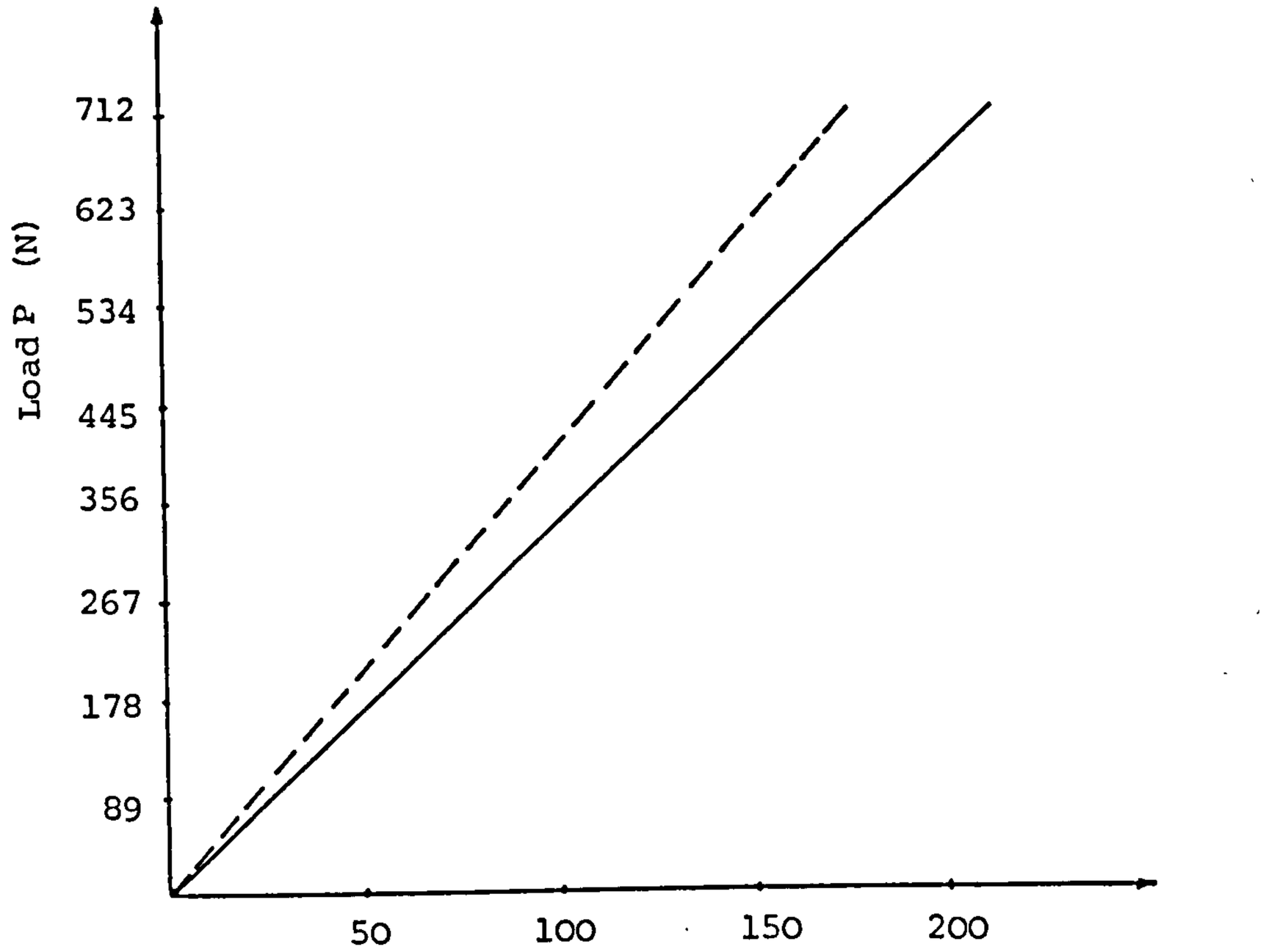

——— The grouted test beam

– – – – – The ungrouted test beam

The effect of grout on the increase in the prestressing force

Figure (3.4)

CHAPTER 4

4. The Failure Mechanisms and Loads of Two-Span Prestressed Concrete Suspension Bridges

4.1 Introduction

This chapter is concerned with the analysis of post-elastic behaviour of both grouted and ungrouted two-span prestressed concrete suspension bridges, and includes a comparison of the two systems.

As the bridges studied here are of a two-span continuous form, the formation of two plastic hinges will be needed to bring about complete failure, Figure (4.1). We shall base our analysis upon the concept of plastic hinges in which the ultimate moment of resistance of a concrete section, M_{ult}, is assumed to be sustained for a sufficient range of increasing curvature, Figure (4.2). Furthermore, we shall assume that the moment-curvature relationship of the cross section is linear up to this ultimate moment value so that our previously developed linear analysis of the two types of bridge may be used to determine the position of the first plastic hinge.

From the above, it is evident that loading in excess of that causing the development of the first plastic hinge, may be considered as being applied to a different structural system which will also be linear but significantly less stiff. In other words, the indeterminate structural system will become a determinate one due to the formation of the first plastic hinge. Thereafter, the internal stresses will develop for this system until the total moment at a second point of the structure reaches the ultimate value, M_{ult}, for that section. At this stage, the structure is converted to a mechanism, for any increased loading, and is considered to have collapsed.

Thus, the following assumptions have been made in the development of the analysis:

1. The suspended beam behaves linearly before and after the formation of the first plastic hinge noting that it becomes a determinate structure prior to its failure.

2. The connections between the suspenders and both of the main cable and the beam will not fail before the flexural failure of the suspended beam.

3. The cross section of the beam behaves in an under-reinforced fashion, i.e. the tensile reinforcement will yield before the concrete reaches its ultimate strain.

4. The reinforcement is made of a perfect mild-steel material which exhibits a distinct yield stress-strain pattern, Figure (4.3).

In the following section, we develop expressions from the ultimate moment of resistance, M_{ult}, for the cross sections of the beam which, for purpose of generality, are assumed to be of T-shaped sections and reinforced with three layers of mild steel.

4.2 The Determination of the Ultimate Moment of Resistance for the Cross Section of the Beam

4.2.1 For Sagging Moments (Top Fibre Lies in the Compression Stress Zone)

Figure (4.4a) shows the T-shaped cross section with all of its dimensions expressed in terms of its effective depth, Z', which can be defined as the distance between the top fibre and the main reinforcement, A_{s3}, of the beam. Figure (4.4b) indicates the stress distribution of the cross section where f_{s1} is the stress in the top flange reinforcement A_{s1}, at a depth z_1Z', and f_{s2} is the stress in the bottom flange reinforcement A_{s2}, at depth z_2Z'. The figure also shows the compressive force F_c in the concrete stress block which is effectively at a depth k_2Z' from the top fibre of the beam. In addi-

tion, we have the prestressing force H applied at the line of centroid of the cross section at a depth of Z_1 which can be evaluated from the following expression:

$$Z_1 = \frac{Z'}{2} \frac{(b_1-b)\ z_3^2 + bz_4^2}{(b_1-b)\ z_3 + bz_4} \qquad (4.1a)$$

where $z_4 = \frac{Z}{Z'}$ (4.1b)

and where z_3 is the ratio of the flange thickness to the effective depth. It is worth mentioning that for rectangular cross sections, the distance Z_1 is simply found as $\frac{Z}{2}$ which confirms the above expression $b_1 = b$.

Figure (4.4c) shows the strain distribution of the cross section where the strain at the top fibre is assumed to have reached the ultimate strain, 0.0035, B.S. (5) and (18). Meanwhile, from assumption (3), the strain at the main reinforcement is greater than the yield strain ε_y but its stress remains equal to the yield stress f_y, Figure (4.3). The figure also shows the axis of zero strain, natural axis, which is at a depth k_1Z' from the top fibre of the beam.

Hence, from Figure (4.4c), the strains at all of the top and bottom flange reinforcements as well as the bottom concrete fibre of the flange, ε_{s1}, ε_{s2} and ε_c, can be expressed in terms of the ultimate strain, by similar triangles, as follows:

$$\varepsilon_{s1} = \frac{k_1-z_1}{k_1}\ 0.0035 \qquad (4.2a)$$

$$\varepsilon_{s2} = \frac{k_1-z_2}{k_1}\ 0.0035 \qquad (4.2b)$$

$$\varepsilon_c = \frac{k_1-z_3}{k_1}\ 0.0035 \qquad (4.2c)$$

Thus, taking advantage of the linear stress-strain relationship for the reinforcement prior to yield, the stresses f_{s1} and f_{s2} can be evaluated as follows:

$$f_{s1} = \frac{k_1 - z_1}{k_1} 0.0035\ E_s \qquad (4.3a)$$

$$f_{s2} = \frac{k_1 - z_2}{k_1} 0.0035\ E_s \qquad (4.3b)$$

where E_s is Young's modulus of elasticity of the reinforcement.

The sum of the forces in the reinforcements, F_s, can then be obtained as follows:

$$F_s = A_{s3}\ f_y - A_{s1}\ f_{s1} - A_{s2}\ f_{s2}$$

which gives:

$$F_s = \frac{0.0035\ E_s}{k_1} \left[\left[A_{s3}\ \frac{\varepsilon_y}{0.0035} - A_{s1} - A_{s2} \right] k_1 + z_1 A_{s1} + z_2 A_{s2} \right] \qquad (4.4)$$

where $$\varepsilon_y = \frac{f_y}{E_s} \qquad (4.5)$$

Assuming that the depth of the neutral axis lies below the flange, i.e. $k_1 \geqslant z_3$, and by taking advantage of the similarity between the stress block of the concrete and its general stress-strain relationship, Figure (4.5), (as specified in B.S. (5) and (18)) the compressive force in the concrete, F_c, can be found as follows: (for details see Appendix 24)

$$F_c = \frac{2}{9} \frac{f_{ult}}{\gamma_m} \frac{z'}{k_1^2} \frac{0.0035}{\varepsilon_o} \left[\left[b_1 \frac{\varepsilon_o}{0.0035} \left(3 - \frac{\varepsilon_o}{0.0035}\right) - (b_1 - b) \left(3 - \frac{0.0035}{\varepsilon_o}\right) \right] \right.$$

$$\left. k_1^3 + (b_1 - b) \left[3z_3 \left(2 - \frac{0.0035}{\varepsilon_o}\right) k_1^2 - 3z_3^2 \left(1 - \frac{0.0035}{\varepsilon_o}\right) k_1 - z_3^3 \frac{0.0035}{\varepsilon_o} \right] \right]$$

$$k_1 \geqslant z_3 \qquad (4.6)$$

where ε_o is the initial plastic strain of the concrete, Figure (4.5), and can be calculated from the following expression: ((5) and (18))

$$\varepsilon_o = \frac{1}{4125}\sqrt{\frac{f_{ult}}{\gamma_m}} \tag{4.7}$$

where f_{ult} is the cube strength of the concrete (N/mm^2) and where γ_m is a partial factor of safety for the concrete and is taken as 1.3 for effects of excessive loads or damage, (5).

Hence, the following step is to consider the longitudinal equilibrium of the beam in which the effect of the prestressing force H must be included. However, for simplicity, we ignore the part of the prestressing force , H_p, which is generated as a result of the interaction between the main cable and beam. Thus, we have:

$$F_c - F_s - H_i = o \tag{4.8}$$

From Equations (4.4) and (4.6), we arrive at the following expression:

$$\frac{20}{117}\frac{f_{ult}}{E_s}\frac{Z'}{\varepsilon_o}\left[b_1\frac{\varepsilon_o}{0.0035}\left(3-\frac{\varepsilon_o}{0.0035}\right)-(b_1-b)\left(3-\frac{0.0035}{\varepsilon_o}\right)\right]k_1^3$$

$$+\left[\frac{20}{39}\frac{f_{ult}}{E_s}\frac{z_3 Z'}{\varepsilon_o}(b_1-b)\left(2-\frac{0.0035}{\varepsilon_o}\right)+A_{s1}+A_{s2}-\frac{1}{0.0035\,E_s}\left(A_{s3}f_y+H_i\right)\right]k_1^2$$

$$-\left[\frac{20}{39}\frac{f_{ult}}{E_s}\frac{z_3^2 Z'}{\varepsilon_o}(b_1-b)\left(1-\frac{0.0035}{\varepsilon_o}\right)+z_1A_{s1}+z_2A_{s2}\right]k_1-0.0006\frac{f_{ult}}{E_s}$$

$$\frac{z_3^3 Z'}{\varepsilon_o^2}(b_1-b)=o \qquad k_1 \geqslant z_3 \tag{4.9}$$

where the only unknown in this equation is the depth ratio, k_1, of the neutral axis. Thus, k_1 can be evaluated as well as the concrete force F_c and the top and bottom flange reinforcement forces $A_{s1}\,f_{s1}$ and $A_{s2}\,f_{s2}$, Equations (4.3) and (4.4).

Whence, the ultimate moment of resistance, M_{ult1}, of the cross section, when the top fibre lies in the compression stress zone, can be evaluated by taking the sum of the moments, for the internal forces of the cross section, about the tensile reinforcement. Thus, from Figure (4.4), we have:

$$M_{ult1} = F_c Z' (1-k_2) + A_{s1} f_{s1} Z'(1-z_1) + A_{s2} f_{s2} Z'(1-z_2) - H_i (Z'-Z_1) \qquad (4.10)$$

where the depth ratio, k_2, of the point of application of the concrete's compressive force, F_c, can be calculated from the following expression: (see Appendix 24)

$$k_2 = \frac{k_1}{4} \frac{\left[b_1 \left(\frac{0.021}{\varepsilon_o} + \frac{\varepsilon_o}{0.0035} - 4 \right) + (b_1-b) \frac{\varepsilon_c^2}{\varepsilon_o^2} \left[\frac{\varepsilon_c}{0.0035} \left(8-3 \frac{\varepsilon_c}{\varepsilon_o}\right) + 4 \frac{\varepsilon_c}{\varepsilon_o} - 12\right]\right]}{\left[b_1 \left(\frac{0.0105}{\varepsilon_o} - 1 \right) - (b_1-b) \frac{\varepsilon_c^2}{\varepsilon_o^2} \left(3 - \frac{\varepsilon_c}{\varepsilon_o}\right)\right]}$$

$$k_1 \geqslant z_3 \qquad (4.11)$$

where ε_c is the strain at the bottom fibre of the flange and can be evaluated from Equation (4.2c).

If the neutral axis is within the flange, i.e. $k_1 < z_3$, the contribution of the web to the values of F_c, k_1 and k_2 would have to be omitted. As Equations (4.6), (4.9) and (4.11) have been arranged in terms of the difference between the breadths of the flange and the web, this modification can be easily carried out when substituting $b = b_1$, which yields:

$$F_c = \frac{20}{117} f_{ult} b_1 Z' \left(3 - \frac{\varepsilon_o}{0.0035}\right) k_1 \qquad k_1 < z_3 \qquad (4.12)$$

$$\frac{20}{117} \frac{f_{ult}}{E_s} \frac{b_1 Z'}{0.0035} \left(3 - \frac{\varepsilon_o}{0.0035}\right) k_1^2 + \left[A_{s1} + A_{s2} - \frac{1}{0.0035\ E_s} (A_{s3} f_y + H_i)\right] k_1$$

$$- (z_1 A_{s1} + z_2 A_{s2}) = o \qquad k_1 < z_3 \qquad (4.13)$$

$$k_2 = \frac{k_1}{4} \frac{\left(\frac{0.021}{\varepsilon_o} + \frac{\varepsilon_o}{0.0035} - 4 \right)}{\left(\frac{0.0105}{\varepsilon_o} - 1 \right)} \qquad k_1 < z_3 \qquad (4.14)$$

Whence, the ultimate moment of resistance, M_{ult1}, can be evaluated when substituting these quantities into Expression (4.10). It is worth mentioning that the above formulae can also be used to calculate the ultimate moment of resistance for rectangular cross sections of breadth b_1 and with up to three layers of reinforcements.

4.2.2 For Hogging Moments (Top Fibre Lies in the Tensions Stress Zone)

Figures (4.6) show the stress and strain distributions for the cross section of the beam, where we see that the strain of the bottom fibre has reached its ultimate value, 0.0035, with the strain at tensile top flange reinforcement greater than the yield strain, ε_y. However, the stress there remains equal to the yield stress, f_y, for increasing values of the strain, Figure (4.3). Thus, from Figure (4.6c), the various strains of the cross section can be expressed in terms of the ultimate strain of the concrete, 0.0035, by virtue of similar triangles, which gives:

$$\varepsilon_{s2} = \frac{k_1 - z_2}{z_4 - k_1} 0.0035 \qquad < \varepsilon_y \qquad (4.15a)$$

$$\varepsilon_{s3} = \frac{1 - k_1}{z_4 - k_1} 0.0035 \qquad (4.15b)$$

where $z_4 = \frac{Z}{Z'}$

Hence, from assumption (3), the stresses in the bottom flange and bottom beam reinforcements, f_{s2} and f_{s3}, can be obtained as:

$$f_{s2} = \frac{k_1 - z_1}{z_4 - k_1} 0.0035 \; E_s \qquad < f_y \qquad (4.16a)$$

$$f_{s3} = \frac{1 - k_1}{z_4 - k_1} 0.0035\ E_s \qquad (4.16b)$$

The sum of the forces, F_s, in the reinforcements can then be obtained as:

$$F_s = A_{s1}\ f_y + A_{s2}\ f_{s2} - A_{s3}\ f_{s3}$$

which yields,

$$F_s = \frac{0.0035\ E_s}{(z_4 - k_1)} \left[\left[A_{s2} + A_{s3} - A_{s1}\ \frac{\varepsilon_y}{0.0035} \right] k_1 - z_2\ A_{s2} - A_{s3} + A_{s1}\ z_4\ \frac{\varepsilon_y}{0.0035} \right] \qquad (4.17)$$

where ε_y is the yield strain, Equation (4.5).

Thus, by taking advantage of the similarity between the concrete's stress block and its general stress-strain relationship, Figure (4.5), ((5) and (18)), the compressive force, F_c, can be expressed in the following equation: (see Appendix 25)

$$F_c = \frac{20}{117}\ f_{ult}\ bZ'\ \left(3 - \frac{\varepsilon_o}{0.0035}\right)(z_4 - k_1) \qquad (4.18)$$

where ε_o is the initial plastic strain of the concrete, Equation (4.7).

Whence, from the longitudinal equilibrium of the beam, Equation (4.8), the following formula can be obtained for the determination of the depth ratio, k_1, of the neutral axis:

$$\frac{20}{117}\ f_{ult}\ bZ'\ \left(3 - \frac{\varepsilon_o}{0.0035}\right) k_1^2 - \left[\frac{40}{117}\ f_{ult}\ bZ\ \left(3 - \frac{\varepsilon_o}{0.0035}\right) \right.$$

$$\left. + 0.0035\ E_s\ (A_{s2} + A_{s3}) - (A_{s1}\ f_y + H_i) \right] k_1 + \left[\frac{20}{117}\ f_{ult}\ z_4\ bZ\ \left(3 - \frac{\varepsilon_o}{0.0035}\right) \right.$$

$$\left. + 0.0035\ E_s\ (z_2\ A_{s2} + A_{s3}) - z_4\ (A_{s1}\ f_y + H_i) \right] = o \qquad (4.19)$$

For excessively under reinforced cross sections, the bottom flange reinforcement, A_{s2}, might yield as well. Therefore, to ensure the validity of the scheme of analysis, it is essential to compare

the value of the stress in this reinforcement, f_{s2}, with the yield stress, f_y. If $f_{s2} > f_y$, hence Equations (4.17) and (4.18) would have to be modified as a result of taking $f_{s2} = f_y$, Figure (4.3). Thus, we have:

$$F_s = \frac{1}{(z_4 - k_1)} \left[\left[0.0035\ E_s\ A_{s3} - (A_{s1} + A_{s2})\ f_y \right] k_1 + z_4\ (A_{s1} + A_{s2})\ f_y \right.$$

$$\left. - 0.0035\ E_s\ A_{s3} \right] \qquad (4.20)$$

and the expression for k_1 becomes:

$$\frac{20}{117}\ f_{ult}\ bZ'\ \left(3 - \frac{\varepsilon_o}{0.0035}\right) k_1^2 - \left[\frac{40}{117}\ f_{ult}\ bZ\ \left(3 - \frac{\varepsilon_o}{0.0035}\right) + 0.0035\ E_s \right.$$

$$A_{s3} - \left[(A_{s1} + A_{s2})\ f_y + H_i \right] \Big] k_1 + \left[\frac{20}{117}\ f_{ult}\ z_4\ bZ\ \left(3 - \frac{\varepsilon_o}{0.0035}\right) + 0.0035\ E_s \right.$$

$$\left. A_{s3} - z_4\ \left[(A_{s1} + A_{s2})\ f_y + H_i \right] \right] = o \qquad (4.21)$$

Having found the final value of the depth ratio, k_1, of the neutral axis, the compressive force, F_c, in the concrete as well as the forces, $A_{s2}\ f_{s2}$ and $A_{s3}\ f_{s3}$, in the reinforcements can be evaluated. Consequently, the ultimate moment of resistance, M_{ult2}, of the cross section, when the top fibre lies in the tension stress zone, can be obtained when taking the sum of the moments of the internal forces about the tensile reinforcement. Hence, from Figure (4.6), we have:

$$M_{ult2} = F_c Z'\ (k_2 - z_1) + A_{s3}\ f_{s3}\ Z'\ (1 - z_1) - A_{s2}\ f_{s2}\ Z'\ (z_2 - z_1) - H_i$$

$$(Z_1 - z_1 Z') \qquad f_{s2} < f_y \qquad (4.22a)$$

or alternatively:

$$M_{ult2} = F_c Z'\ (k_2 - z_1) + A_{s3}\ f_{s3}\ Z'\ (1 - z_1) - A_{s2}\ f_y\ Z'\ (z_2 - z_1) - H_i$$

$$(Z_1 - z_1 Z') \qquad f_{s2} \geqslant f_y \qquad (4.22b)$$

where the depth ratio, k_2, of the point of application of the concrete's compressive force, F_c, can be calculated as follows: (for details see Appendix 25)

$$k_2 = \frac{\left[k_1 \left[6 - \frac{\varepsilon_o}{0.0035} \left(4 - \frac{\varepsilon_o}{0.0035}\right)\right] + z_4\left[6 - \left(\frac{\varepsilon_o}{0.0035}\right)^2\right]\right]}{4\left(3 - \frac{\varepsilon_o}{0.0035}\right)} \qquad (4.23)$$

where ε_o is the initial plastic strain for the concrete, Figure (4.5) and Equation (4.7).

4.2.3 Comments

The effect of the axial (prestressing) force on the cross section of the beam, clearly increases its ultimate moment of resistance as can be deduced from Formulae (4.1 - 23), if H_i = o. Thus, as the loads increase, the strength of the beam, slightly, improves as a result of the interaction between the main cable and the suspended beam. This improvement can be considered in the calculations of the failure loads, as will be discussed in the following section.

Formulae (4.1 - 23) can be extended to evaluate the ultimate moment of resistance, M_{ult}, for I-shaped and rectangular cross sections exhibiting any arrangement of reinforcement layers. This is achieved by modifying the expression for the sum of the reinforcement forces, F_s, Equations (4.5), (4.17) or (4.20), to accommodate the required number of layers. Then, this modified expression can be included in the longitudinal equilibrium Equation (4.8), in which the term for the compressive force, F_c, of the concrete remains unchanged. Obviously, for symmetrical cross sections, with respect to their centre lines, the values of the ultimate moments of resistance are the same for either sagging or hogging moments.

4.3 The Determination of the Failure Loads for Two-Span Prestressed Concrete Suspension Bridges

4.3.1 Discussion

In this section, we describe the procedure for evaluating the failure loads when a single load is applied on either of the two spans of an ungrouted and grouted prestressed concrete suspension bridges.

As mentioned earlier, failure takes place in two stages, the first is when the value of the maximum moment, M_1, increases with the increase of the applied loading, σ, until it reaches the ultimate moment of resistance, M_{ult}, of the cross section at its position, Figure (4.7b). Therefore, from the first assumption, Section 4.1, the value of the first plastic hinge load $\sigma_{p.h}$, is directly obtained as follows:

$$\sigma_{p.h} = \frac{M_{ult}}{M_1} \sigma \qquad (4.24)$$

where the value of M_1 is calculated from the linear analysis described in the preceeding two chapters. A more accurate value for $\sigma_{p.h}$ is obtained when taking into account the contribution of the change in the prestressing force H_{pl}, which results from the first plastic hinge load, to the value of M_{ult}. To do so, we replace the initial prestressing force H_i, by the more accurate value of H_1, where:

$$H_1 = H_i + H_{pl} \qquad (4.25)$$

in the expressions for the ultimate moment of resistance M_{ult}, Formulae (4.1 - 23). Hence, a more accurate value for M_{ult} can be obtained and substituted in Equation (4.24) to find the final value of $\sigma_{p.h}$. This cycle of calculations can be repeated any number of times until exact values are obtained for the first plastic hinge load and

the ultimate moment of resistance. However, as the axial force effect on the value of M_{ult} is quite small, one cycle of calculations is sufficient for accurate results.

The second stage of failure, starts after the formation of the first plastic hinge as the suspended beam is still capable of sustaining more load in excess of $\sigma_{p.h}$. However, the structural system, as mentioned earlier, now behaves as a determinate one in its response to that load. Therefore, we can no longer use our previously derived formula, for linear analysis, to calculate the extra amount of load, $\Delta\sigma_{ult}$, required to bring about the complete failure of the structure. For this reason, the new structural system is analysed separately to determine its bending moments and change in the prestressing force, ΔH_p, which result for the loading $\Delta\sigma$, Figure (4.7c). Thus, the value and position of the maximum moment can be determined for this case of loading and consequently, the required loading $\Delta\sigma_{ult}$ is evaluated when the total value of this moment, when added to that corresponding to the first plastic hinge load, reaches the ultimate moment of resistance for the beam cross section at its position, Figure (4.7d). In doing so, the effect of ΔH_p must be included as well as the forces it generates as will be shown in the following section. Hence, the failure load σ_{ult} is found as follows:

$$\sigma_{ult} = \sigma_{p.h} + \Delta\sigma_{ult} \qquad (4.26)$$

To explain the above procedure further, we give in the following sections two examples for a general case of loading applied on the left hand span of an ungrouted and grouted T-shaped prestressed concrete suspended beams.

4.3.2 The Determination of the Failure Loads for a General Case of Loading Applied on the Left Hand Span of a T-Shaped Two-Span Ungrouted Prestressed Cable Suspended Beam

Figure (4.7a) shows a general loading σ which occupies the part of the left hand span that is bounded by the distances $x = \beta\ell$ and $x = \alpha\ell$ from the left end support. Clearly, the maximum absolute value of the bending moment, M_1, is expected to develop in the left hand span under the applied load, i.e. in the region $\beta\ell \leqslant x \leqslant \alpha\ell$. Figure (4.7b) shows the bending moment diagram where the position of the maximum moment, M_1, is marked by the distance $r\ell$ from the left end support. Thus, from Equation (2.80b) the value of M_1 can be found as follows:

$$M_1 = \frac{Ha}{\sin \mu\ell}\left[\sin \mu\ell(1-r) - \frac{(\nu+\nu_1)}{(\phi+\phi_1)} \sin \mu r\ell\right] - \frac{\sigma}{\mu^2 \sin \mu\ell}\left[\sin \mu r\ell \cos \mu\ell(1-\alpha)\right.$$

$$+ \sin \mu\ell(1-r) \cos \mu\beta\ell - \sin \mu\ell - \frac{\mu^2\ell}{2(\phi+\phi_1)}\left[\frac{2\,(\cos \mu\beta\ell - \cos \mu\alpha\ell)}{\mu\ell \sin \mu\ell}\right.$$

$$\left.\left. - (\alpha^2-\beta^2)\right] \sin \mu r\ell\right] + \frac{W(y+\rho)}{\mu^2 \sin \mu\ell}\left[\sin \mu r\ell \left(1 - \frac{\mu^2}{2}\frac{(\theta+\omega\theta_1)}{(\phi+\phi_1)}\right) - \sin \frac{\mu r\ell}{2}\right.$$

$$\left.\cos \frac{\mu\ell}{2}(1 - r)\right] \qquad (4.27)$$

where ρ, μ, ν, ν_1, ϕ, ϕ_1, θ and θ_1 can be determined from Equations (2.62) and (2.63) respectively. The distance $r\ell$ can be calculated from Equation (2.80b), as follows:

$$\tan \mu r\ell = \frac{1}{K}\left[\sigma\left[\cos \mu\ell(1-\alpha) - \frac{\mu^2\ell}{2(\phi+\phi_1)}\left[\frac{2(\cos \mu\beta\ell - \cos \mu\alpha\ell)}{\mu\ell \sin \mu\ell} - (\alpha^2-\beta^2)\right]\right]\right.$$

$$\left. + \mu^2 Ha \frac{(\nu+\nu_1)}{(\phi+\phi_1)} - W\,(y+\rho)\left[1 - \frac{\mu^2}{2}\frac{(\theta+\omega\theta_1)}{(\phi+\phi_1)}\right]\right] - \cot \mu\ell \qquad (4.28a)$$

where:

$$K = \sin \mu\ell \left[\sigma \cos \mu\beta\ell - \mu^2 Ha - W\,(y+\rho)\right] \qquad (4.28b)$$

The first plastic hinge load $\sigma_{p.h}$ can be evaluated when undertaking a trial and error approach, as mentioned in the preceding section. We begin by assuming any value for the first plastic hinge load, $\sigma_{p.h}$ and obtain the corresponding increase in the prestressing force H_{pl}, Formula (2.65). Consequently, the total prestressing force H_1, the distance $r\ell$ and the maximum bending moment M_1 can be evaluated by making use of Equations (4.25), (4.27) and (4.28) respectively. Thus, knowing the initial value for the ultimate moment of resistance M_{ult1}, Expression (4.10), when the top fibre lies in the compression stress zone, it will be possible to find an initial value of the first plastic hinge load $\sigma_{p.h}$, Equation (4.24) and Figure (4.7b). Whence, we can use this value as a start for another cycle of calculations to obtain new values for H_{pl} and M_1. Thus, the change in the prestressing force can be taken into account to find the ultimate moment of resistance M_{ult1} which is subsequently compared with the maximum bending moment M_1. No more than one cycle of the above calculations is necessary to evaluate the final first plastic hinge load $\sigma_{p.h}$ with sufficient accuracy.

Having found the first plastic hinge load $\sigma_{p.h}$ and the corresponding increase in the prestressing force H_{pl}, the total prestressing force, H_1, can be finally evaluated from Expression (4.25). The position of the second plastic hinge is obviously at the intermediate support where the value of the bending moment, M_2, can be calculated when substituting $x = \ell$ in Equation (2.80c), which gives: (see Figure 4.7b)

$$M_2 = - H_1 a \frac{(\nu+\nu_1)}{(\phi+\phi_1)} + \frac{\sigma_{p.h}\ell}{2(\phi+\phi_1)} \left[\frac{2(\cos \mu\beta\ell - \cos \mu\alpha\ell)}{\mu\ell \sin \mu\ell} - (\alpha^2-\beta^2) \right]$$

$$- \frac{W}{2} (y+\rho_1) \frac{(\theta+\omega\theta_1)}{(\phi+\phi_1)} \qquad (4.29)$$

where $\mu^2 = \dfrac{H_1}{EI}$,

$$\rho_1 = \frac{H_{p1}}{H_w} ,$$

and where the quantities ν, ν_1, ϕ, ϕ_1, θ and θ_1 can be computed from Equations (2.63).

Figure (4.7c) shows the loads applied on the structure after the formation of the first plastic hinge, where we have $\Delta\sigma$, which is the live loading exceeding $\sigma_{p.h}$, and the forces generated by the increase in the prestressing force, ΔH_p. These forces are the end moments $\Delta H_p a$ and the upward distributed forces $\Delta\rho W$ and $\Delta\rho W_1$ applied in both left and right hand spans. The value of the prestressing force now affecting the structure is:

$$H_2 = H_1 + \Delta H_p \qquad (4.30)$$

Hence, to evaluate the increase in the prestressing force ΔH_p, after the formation of the first plastic hinge, corresponding to the applied loads, we use Timoshenko's approach, (23), (25) and (26), which its general formula is:

$$\Delta H_p \ \delta_c = \sum \frac{W}{H_w} \int \eta \ dx$$

where δ_c can be determined from Formula (2.45) for an exact value or Formula (2.46) for an approximate one. Thus, from Appendix 26, we obtain the following expression:

$$\Delta H_p = \frac{W}{H_w \ \delta_c} \left[\frac{\Delta\sigma \ell^2}{2\mu \ H_2} \left[\left[2\alpha - (\alpha^2 - \beta^2) - \frac{1}{r} (r^2+\beta^2) \right] \right.\right.$$

$$\left[\frac{\cos \mu\ell(1+\lambda - \frac{r}{2}) - \cos \frac{\mu r \ell}{2} \left[\omega+(1-\omega) \cos \mu\ell_1\right]}{\sin \mu\ell_1 \ \cos \frac{\mu r \ell}{2}} + \frac{\mu\ell}{2} (1+\omega\lambda) \right]$$

$$\left.\left. + \frac{2 \sin \frac{\mu\ell}{2} \ \sin \frac{\mu\ell}{2}(1-r)}{\mu\ell_1 \cos \frac{\mu r \ell}{2}} \left[(1+\lambda)\left[2\alpha - \frac{1}{r} (r^2+\beta^2)\right] - \lambda (\alpha^2-\beta^2)\right] \right.\right.$$

$$- \frac{\mu\ell}{6}\left[\alpha^2\,(3-2\alpha) - \beta^2\,(3-2\beta)\right] + \frac{2}{\mu\ell}\left[\frac{\sin\frac{\mu\ell}{2}(2\alpha-r) - \sin\frac{\mu\ell}{2}(2\beta-r)}{\mu\ell\cos\frac{\mu r\ell}{2}}\right.$$

$$\left. - (\alpha-\beta)\right] + \frac{\Delta\rho W\ell^2}{2\mu H_2}\left[\frac{(1-r)}{\sin\mu\ell_1}\left[\cos\mu\ell_1 - \frac{\cos\mu\ell(1+\lambda-\frac{r}{2})}{\cos\frac{\mu r\ell}{2}}\right] - \frac{4\sin\frac{\mu\ell}{2}}{\mu^2\ell^2\cos\frac{\mu r\ell}{2}}\right.$$

$$\left[\cos\mu\ell(1-r) - \omega\tan\frac{\mu\ell_1}{2}\sin\frac{\mu\ell}{2}(1-r)\right] - \frac{2\sin\frac{\mu\ell}{2}\sin\frac{\mu\ell}{2}(1-r)}{\mu\ell_1\cos\frac{\mu r\ell}{2}}$$

$$\left[(1+\lambda)(1-r) + \lambda\,(1+\omega\lambda)\right] + \frac{\mu\ell}{6}\left[\frac{12}{\mu^2\ell^2}(1+\omega^2\lambda) + \omega\lambda\left[\omega\lambda^2 - 3(1-r)\right]\right.$$

$$\left. - (2-3r)\right] + \omega\tan\frac{\mu\ell_1}{2}\left[(1-r) - \frac{4\omega}{\mu^2\ell^2}\right]\Bigg] + \frac{\Delta H_p a}{\mu r H_2}\left[\frac{2\sin\frac{\mu\ell}{2}(1+2\lambda)\sin\frac{\mu\ell}{2}(1-r)}{\sin\mu\ell_1\cos\frac{\mu r\ell}{2}}\right.$$

$$+ \tan\frac{\mu r\ell}{2} - 2r\,\frac{\sin\frac{\mu\ell}{2}\cos\frac{\mu\ell}{2}(1+\lambda-r)}{\cos\frac{\mu\ell_1}{2}\cos\frac{\mu r\ell}{2}} - \frac{2(1+\lambda)}{\mu\ell_1}\frac{\sin\frac{\mu\ell}{2}\sin\frac{\mu\ell}{2}(1-r)}{\cos\frac{\mu r\ell}{2}}$$

$$\left.\left. + (1-2r)\left[\omega\tan\frac{\mu\ell_1}{2} - \frac{\mu\ell}{2}(1+\omega\lambda)\right]\right]\right] \qquad (4.31)$$

where $\mu^2 = \dfrac{H_2}{EI}$,

$\omega = \dfrac{W_1}{W}$,

$\Delta\rho = \dfrac{\Delta H_p}{H_w}$,

and where $\lambda = \dfrac{\ell_1}{\ell}$.

The new value of the moment at the intermediate support M_3, Figure (4.7d), can be calculated from the following expression, as derived in Appendix 26:

$$M_3 = \frac{\Delta\sigma \ell^2}{2} \left[2\alpha-(\alpha^2-\beta^2) - \frac{1}{r}(r^2+\beta^2)\right] - \frac{\Delta\rho}{2}\frac{(1-r)}{r}\left(Wr\ell^2 + 2H_w a\right) \qquad (4.32)$$

We notice from this equation that the axial, prestressing, force does not affect the value of the moment at the intermediate support. The reason for this is that, for determinate structures, secondary moments, developed by the axial force, are solely due to the deflections of the system noting that there is no deflection at the intermediate support.

To evaluate the part of the loading required to exceed the first plastic hinge load to cause the complete failure of the structure, $\Delta\sigma_{ult}$, we first calculate the ultimate moment of resistance, M_{ult2}, for the cross section above the intermediate support. This is carried out by using the more accurate value of H_1, which is now known, instead of H_i in Expression (4.22). Hence, considering the condition for failure, which is the total value of the moment at the intermediate support to reach the ultimate moment of resistance, M_{ult2}, Figure (4.7d), we obtain the following expression from Equation (4.32):

$$M_{ult2} = M_2 + M_3$$

which yields:

$$\Delta\sigma = A_1 + A_2 \Delta H_p \qquad (4.33a)$$

where A_1 and A_2 are the constants governing the failure condition and can be evaluated from the following expressions:

$$A_1 = \frac{2\left(M_{ult2} - M_2\right)}{\ell^2\left[2\alpha - (\alpha^2-\beta^2) - \frac{1}{r}(r^2+\beta^2)\right]} \qquad (4.33b)$$

$$A_2 = \frac{(1-r)(Wr\ell^2 + 2H_w a)}{r H_w \ell^2\left[2\alpha - (\alpha^2-\beta^2) - \frac{1}{r}(r^2+\beta^2)\right]} \qquad (4.33c)$$

and where M_2 can be calculated from Equation (4.29).

We start by assuming a value for $\Delta\sigma$ and from Formula (4.31), we determine the corresponding increase in the prestressing force, ΔH_p, by using the successive approximations procedure described in Section 2.5.3.3. Hence, assuming that the relationship between $\Delta\sigma$ and ΔH_p is linear, we plot a straight line using the obtained ΔH_p, and the point of origin, Figure (4.8). We also plot the other straight line relationship given in Equations (4.33) between ΔH_p and $\Delta\sigma$. The point of interception between the two straight lines is the required value for $\Delta\sigma_{ult}$ as shown in Figure (4.8). Whence, the failure load can be evaluated from Expression (4.26). A more accurate result can be obtained, when using the value of ΔH_{pult}, Figure (4.8), to calculate the total prestressing force at failure, Equation (4.30). This value can subsequently be used to determine another value for the ultimate moment of resistance, M_{ult2}, as mentioned earlier. Thus, following the above procedure, the two straight lines can be drawn and the failure load can be obtained.

The above procedure is a quick approximate solution to determine the failure load σ_{ult}. However, to determine the exact value of $\Delta\sigma_{ult}$, we continue assuming values for $\Delta\sigma$ and find the corresponding increase in the prestressing force ΔH_p, from Expression (4.31), until the condition in Equation (4.33) is satisfied. In doing so, we may also calculate the new values of M_{ult2} corresponding to the obtained values of the axial forces.

Formulae (4.24 - 33) can be used to determine the failure loads when a continuous uniformly distributed load is applied on the left hand span. This can be achieved by substituting $\alpha = 1$ and $\beta = o$ in all of these formulae and then following the aforementioned procedures. Furthermore, the above formulae can also be used to find the failure loads for a concentrated load P applied on the left hand span at a distance $t\ell$ from the left end support, Appendix 26. Clearly, the first plastic hinge will most certainly form under the applied load, i.e. $r = t$. Therefore, the maximum moment M_1 can directly be obtained from Equation (2.73a) as follows:

$$M_1 = \frac{Ha}{\sin \mu\ell}\left[\sin \mu\ell(1-t) - \frac{(\nu+\nu_1)}{(\phi+\phi_1)}\sin \mu t\ell\right] - \frac{P}{\mu}\frac{\sin \mu t\ell}{\sin \mu\ell}\left[\sin \mu\ell(1-t)\right.$$

$$- \frac{\mu}{(\phi+\phi_1)} \left[\frac{\sin \mu t\ell}{\sin \mu\ell} - t \right] \Bigg] + \frac{W(y+\rho)}{\mu^2 \sin \mu\ell} \left[\sin \mu t\ell \left[1 - \frac{\mu^2}{2} \frac{(\theta+\omega\theta_1)}{(\phi+\phi_1)} \right] \right.$$

$$\left. - 2 \sin \frac{\mu t\ell}{2} \cos \frac{\mu\ell}{2}(2-t) \right] \qquad (4.34)$$

We then apply the aforementioned procedure to determine the first plastic hinge load $P_{p.h}$ with the only difference of using Formula (2.61) instead of (2.65) to determine the change in the prestressing force, H_{p1}. Thus, we obtain the moment, M_2, at the intermediate support corresponding to the first plastic hinge load, $P_{p.h}$, as follows:

$$M_2 = - H_1 a \frac{(\nu+\nu_1)}{(\phi+\phi_1)} + \frac{P_{p.h}}{(\phi+\phi_1)} \left[\frac{\sin \mu t\ell}{\sin \mu\ell} - t \right] - \frac{W}{2} (y+\rho) \frac{(\theta+\omega\theta_1)}{(\phi+\phi_1)} \qquad (4.35)$$

Whence, the failure load can be determined, as before, by using the following formulae instead of Formulae (4.32 & 33): (full derivation is given in Appendix 26)

$$\Delta H_p = \frac{W}{H_w \delta_c} \left[\frac{\Delta P\ell}{\mu H_2} \left[(1-t) \left[\frac{\cos \mu\ell(1+\lambda-\frac{t}{2}) - \cos \frac{\mu t\ell}{2} [\omega+(1-\omega) \cos \mu\ell_1]}{\sin \mu\ell_1 \cos \frac{\mu t\ell}{2}} \right. \right. \right.$$

$$\left. \left. + \frac{\mu\ell}{2} (1+\omega\lambda) \right] + \frac{2[1+\lambda(1-t)]}{\mu\ell_1} \frac{\sin \frac{\mu\ell}{2} \sin \frac{\mu\ell}{2}(1-t)}{\cos \frac{\mu t\ell}{2}} - \frac{\mu t\ell}{2} (1-t) \right] + \frac{\Delta\rho W\ell^2}{2\mu H_2}$$

$$\left[\frac{(1-t)}{\sin \mu\ell_1} \left[\cos \mu\ell_1 - \frac{\cos \mu\ell(1+\lambda-\frac{t}{2})}{\cos \frac{\mu t\ell}{2}} \right] - \frac{4 \sin \frac{\mu\ell}{2}}{\mu^2\ell^2 \cos \frac{\mu t\ell}{2}} \left[\cos \mu\ell(1-t) \right. \right.$$

$$\left. \left. - \omega \tan \frac{\mu\ell_1}{2} \sin \frac{\mu\ell}{2}(1-t) \right] - \frac{2 \sin \frac{\mu\ell}{2} \sin \frac{\mu\ell}{2}(1-t)}{\mu\ell_1 \cos \frac{\mu t\ell}{2}} \left[(1+\lambda)(1-t) + \lambda \right. \right.$$

$$\left. \left. (1+\omega\lambda) \right] + \frac{\mu\ell}{6} \left[\frac{12}{\mu^2\ell^2} (1+\omega^2\lambda) + \omega\lambda \left[\omega\lambda^2 - 3(1-t) \right] - (2-3t) \right] + \omega \tan \frac{\mu\ell_1}{2} \right.$$

$$\left[(1-t) - \frac{4\omega}{\mu^2 \ell^2}\right]\Bigg] + \frac{\Delta H_p a}{\mu t\, H_2}\left[\frac{2 \sin\frac{\mu\ell}{2}(1+2\lambda)\, \sin\frac{\mu\ell}{2}(1-t)}{\sin \mu\ell_1 \cos\frac{\mu t\ell}{2}} + \tan\frac{\mu t\ell}{2} - 2t\right.$$

$$\frac{\sin\frac{\mu\ell}{2}\cos\frac{\mu\ell}{2}(1+\lambda-t)}{\cos\frac{\mu\ell_1}{2}\cos\frac{\mu t\ell}{2}} - \frac{2(1+\lambda)}{\mu\ell_1}\frac{\sin\frac{\mu\ell}{2}\sin\frac{\mu\ell}{2}(1-t)}{\cos\frac{\mu t\ell}{2}} + (1-2t)$$

$$\left.\left[\omega \tan\frac{\mu\ell_1}{2} - \frac{\mu\ell}{2}(1+\omega\lambda)\right]\right]\Bigg] \qquad (4.36)$$

where H_2 can be obtained from Equation (4.30). The new expression for the moment at the intermediate support, M_3, after the formation of the first plastic hinge is given as : (Appendix 26)

$$M_3 = \Delta P\ell(1-t) - \frac{\Delta\rho}{2t}(1-t)(Wt\ell^2 + 2H_w a) \qquad (4.37)$$

and the condition for failure is as follows:

$$M_{ult2} = M_2 + M_3$$

which gives:

$$\Delta P = A_1 + A_2\, \Delta H_p \qquad (4.38a)$$

where A_1 and A_2 are constants which can be evaluated from the following expressions:

$$A_1 = \frac{(M_{ult2} - M_2)}{\ell(1-t)} \qquad (4.38b)$$

$$A_2 = \frac{W\ell}{2H_w} + \frac{a}{t\ell} \qquad (4.38c)$$

where M_{ult2} and M_2 can be evaluated from Equations (4.22) and (4.35) respectively.

Finally, a similar approach can be adopted for the determination of the failure loads of any type of loading applied in the right hand span.

4.3.3 The Determination of the Failure Loads for a General Case of Loading Applied on the Left Hand Span of a T-Shaped Two-Span Grouted Prestressed Cable Suspended Beam

Figure (4.9a) shows a general loading σ which occupies the part of the left hand span that is bounded by $x = \beta\ell$ and $x = \alpha\ell$ from the left end support. The figure also shows the forces which result from combining the dead loads, W and W_1, of the beam with the forces and moments produced by the initial prestressing force H_i as well as its increase H_p, due to the applied general loading σ, in both left and right hand spans (see description of forces in Section 3.1).

For the case of loading shown, the maximum absolute bending moment M_1 is, again, expected to develop under the applied loading at a distance $r\ell$ from the left end support, Figure (4.9b). Thus, M_1 can be evaluated from Equation (3.42c) which gives:

$$M_1 = + \frac{H_i a}{\sin \mu\ell} \left[\sin \mu\ell(1-r) - \frac{(\nu+\nu_1)}{(\phi+\phi_1)} \sin \mu r\ell\right] - \frac{\sigma}{\mu^2 \sin \mu\ell} \left[\sin \mu r\ell \right.$$

$$\cos \mu\ell(1-\alpha) + \sin \mu\ell(1-r) \cos \mu\beta\ell - \sin \mu\ell - \frac{\mu^2 \ell}{2(\phi+\phi_1)} \sin \mu r\ell$$

$$\left[\frac{2 (\cos \mu\beta\ell - \cos \mu\alpha\ell)}{\mu\ell \sin \mu\ell} - (\alpha^2-\beta^2)\right]\Bigg] + \frac{\gamma W}{\mu^2 \sin \mu\ell} \left[\sin \mu r\ell \left[1 - \frac{\mu^2}{2}\right.\right.$$

$$\left.\left.\frac{(\theta+\omega\theta_1)}{(\phi+\phi_1)}\right] - 2 \sin \frac{\mu r\ell}{2} \cos \frac{\mu\ell}{2}(2-r)\right] + \frac{\rho W}{\mu^2 \sin \mu\ell} \left[\sin \mu r\ell \left[1 - \frac{\mu^2}{2} \frac{(\theta_g+\omega\theta_{g1})}{(\phi+\phi_1)}\right]\right.$$

$$\left. + \cos \mu g\ell \sin \mu\ell(1-r) - \sin \mu\ell\right] - \frac{H_p}{(\phi+\phi_1)} \frac{\sin \mu r\ell}{\sin \mu\ell} \left[C \left(\frac{\sin \mu g\ell}{\sin \mu\ell} - g\right)\right.$$

$$\left. + C_1 \left(\frac{\sin \mu g_1 \ell_1}{\sin \mu\ell_1} - g_1\right)\right] + \frac{C H_p}{\mu} \frac{\sin \mu g\ell}{\sin \mu\ell} \sin \mu\ell(1-r) + \frac{H_p Z_1}{\sin \mu\ell}$$

$$\left[\sin \mu r\ell \frac{(\nu_g+\nu_{g1})}{(\phi+\phi_1)} - \cos \mu g\ell \sin \mu\ell(1-r)\right] \qquad (4.39)$$

where ρ, μ, H, ν, ν_1, ϕ, ϕ_1, θ and θ_1 can be evaluated from Equations (2.62) and (2.63) and where ν_g, ν_{g1}, θ_g and θ_{g1} can be determined from Equations (3.22). g and g_1 can be defined as the ratios of the grouted lengths to the span lengths at left and right hand spans and can be evaluated from Equations (3.1). Moreover, C and C_1 are the slopes at the ends of the free ungrouted parts of the main cable at the left and right hand spans and can be evaluated from Equations (3.2).

The distance $r\ell$ can be determined by making use again of Equation (3.42c), which yields:

$$\tan \mu r\ell = \frac{1}{K} \Bigg[\sigma \cos \mu\ell(1-\alpha) - W(y+\rho) - \frac{\mu^2}{(\phi+\phi_1)} \Bigg[\frac{\sigma\ell}{2} \Bigg[\frac{2(\cos \mu\beta\ell - \cos \mu\alpha\ell)}{\mu\ell \sin \mu\ell}$$

$$- (\alpha^2-\beta^2)\Bigg] - W\left[y(\theta+\omega\theta_1) + \rho(\theta_g+\omega\theta_{g1})\right] - H_i a\,(\nu+\nu_1) - H_p$$

$$\Bigg[C\left[\frac{\sin \mu g\ell}{\sin \mu\ell} - g\right] + C_1\left[\frac{\sin \mu g_1 \ell_1}{\sin \mu\ell_1} - g_1\right]\Bigg] + H_p Z_1\,(\nu_g+\nu_{g1})\Bigg]\Bigg] - \cot \mu\ell$$

(4.40a)

where:

$$K = \sin \mu\ell \left[\sigma \cos \mu\beta\ell - W(y+\rho \cos \mu g\ell) - \mu^2 H_i a - \mu C H_p \sin \mu g\ell + \mu^2 H_p Z_1\right]$$

(4.40b)

We then apply the aforementioned procedure beginning by assuming a value for the first plastic hinge load $\sigma_{p.h}$ and obtain the corresponding increase in the prestressing force H_{p1}, Formula (3.25). Hence, the maximum bending moment M_1 can be evaluated as well as its distance, $r\ell$, from the left end support, Equations (4.39) and (4.40). Thus, knowing the ultimate moment of resistance, M_{ult1}, at this position of the beam, the initial value for the first plastic hinge load can be obtained, Equation (4.24). Whence, we can repeat this

scheme of calculation once more to evaluate more accurate values for H_{p1} and M_{ult1} until the value of the maximum moment, M_1, is precisely equal to M_{ult1}.

Having found the first plastic hinge load, $\sigma_{p.h}$, and the corresponding increase in the prestressing force, H_{p1}, we hence, calculate the final value of the total prestressing force, H_1, Equation (4.25). Whence, the corresponding bending moment M_2 at the intermediate support is found when substituting $x = \ell$ in Equation (3.42d), which gives:

$$M_2 = - H_i a \frac{(\nu+\nu_1)}{(\phi+\phi_1)} + \frac{\sigma_{p.h}\,\ell}{2(\phi+\phi_1)} \left[\frac{2(\cos \mu\beta\ell - \cos \mu\alpha\ell)}{\mu\ell \sin \mu\ell} - (\alpha^2-\beta^2) \right] - \frac{yW}{2}$$

$$\frac{(\theta+\omega\theta_1)}{(\phi+\phi_1)} - \frac{\rho_1 W}{2} \frac{(\theta_g+\omega\theta_{g1})}{(\phi+\phi_1)} - \frac{H_p}{(\phi+\phi_1)} \left[C \left(\frac{\sin \mu g\ell}{\sin \mu\ell} - g \right) + C_1 \left(\frac{\sin \mu g_1 \ell_1}{\sin \mu \ell_1} \right.\right.$$

$$\left.\left. - g_1 \right) \right] + H_p Z_1 \frac{(\nu_g+\nu_{g1})}{(\phi+\phi_1)} \qquad (4.41)$$

where $\mu^2 = \frac{H_1}{EI}$, $\rho_1 = \frac{H_{p1}}{H_w}$, and $\omega = \frac{W_1}{W}$

and where the quantities ν, ν_1, ϕ, ϕ_1, θ, θ_1, ν_g, ν_{g1}, θ_g and θ_{g1} can be evaluated from Equations (2.63) and (3.22) respectively.

The structure changes, as mentioned earlier, to become a determinate one in its response to the load $\Delta\sigma$ which exceeds the first plastic hinge load $\sigma_{p.h}$. Furthermore, the forces generated by the increase in the prestressing force ΔH_p, after the formation of the first plastic hinge, are affecting the new structural system, Figure (4.9c). These forces are the partial upward uniformly distributed forces, $\Delta\rho W$ and $\Delta\rho W_1$, which are applied in the ungrouted regions, $g\ell \leqslant x \leqslant \ell$ and $g_1 \leqslant x_1 \leqslant \ell_1$, and the concentrated moments $\Delta H_p Z_1$ in the left and right hand spans respectively. Z_1 can be defined as the distance between the top fibre and the line of centroid of the T-shaped cross section of the beam. In addition, we have the new value of the prestressing force, H_2, affecting the system where H_2 can be evaluated from Equations (4.30).

We now determine the value of the increase in the prestressing force ΔH_p for the case of loading shown in Figure (4.9c). In doing so, we once more make use of Timoshenko's Formula, (23) (25) and (26), where:

$$\Delta H_p = \frac{1}{\delta_{cf}} \sum \frac{W}{H_w} \int \eta \, dx$$

in which δ_{cf} can be evaluated from Formulae (3.19) or (3.20) for an exact or an approximate value. Hence, from Appendix 27, we have the following expression:

$$\Delta H_p = \frac{W}{H_w \, \delta_{cf}} \left[\frac{\Delta\sigma \ell^2}{2\mu \, H_2} \left[[2\alpha - (\alpha^2-\beta^2) - \frac{1}{r} (r^2+\beta^2)] \right.\right.$$

$$\left[\frac{\cos \mu\ell(1+\lambda-\frac{r}{2}) - \cos \frac{\mu r \ell}{2} [\omega + (1-\omega) \cos \mu\ell_1]}{\sin \mu\ell_1 \cos \frac{\mu r \ell}{2}} + \frac{\mu\ell}{2} (1+\omega\lambda) \right]$$

$$+ \frac{2 \sin \frac{\mu\ell}{2} \sin \frac{\mu\ell}{2}(1-r)}{\mu\ell_1 \cos \frac{\mu r \ell}{2}} [(1+\lambda)[2\alpha - \frac{1}{r} (r^2+\beta^2)] - \lambda (\alpha^2-\beta^2)] - \frac{\mu\ell}{6}$$

$$[\alpha^2(3-2\alpha) - \beta^2(3-2\beta)] + \frac{2}{\mu\ell} \left[\frac{\sin \frac{\mu\ell}{2}(2\alpha-r) - \sin \frac{\mu\ell}{2}(2\beta-r)}{\mu\ell \cos \frac{\mu r \ell}{2}} - (\alpha-\beta) \right] \Bigg]$$

$$+ \frac{\Delta\rho W \ell^2}{2r\mu \, H_2} \left[\frac{(1-r)(r-g)^2}{\sin \mu\ell_1} \left[\cos \mu\ell_1 - \frac{\cos \mu\ell(1+\lambda-\frac{r}{2})}{\cos \frac{\mu r \ell}{2}} \right] - \frac{2r}{\mu^2 \ell^2} \right.$$

$$\left[\frac{\sin \frac{\mu\ell}{2}(r-2g)}{\cos \frac{\mu r \ell}{2}} + \frac{\sin \frac{\mu\ell}{2}(2-r)}{\cos \frac{\mu r \ell}{2}} - 2\omega \frac{(\cos \mu g_1 \ell_1 - \cos \mu\ell_1)}{\sin \mu\ell_1 \cos \frac{\mu r \ell}{2}} \sin \frac{\mu\ell}{2} \right.$$

$$\left. \left. \sin \frac{\mu\ell}{2}(1-r) + 2\omega^2 \frac{\cos \frac{\mu g_1 \ell_1}{2}}{\cos \frac{\mu\ell_1}{2}} \sin \frac{\mu\ell_1}{2}(1-g_1) \right] - \frac{2 \sin \frac{\mu\ell}{2} \sin \frac{\mu\ell}{2}(1-r)}{\mu\ell_1 \cos \frac{\mu r \ell}{2}} \right.$$

$$\left[(r-g^2)(1+\lambda-r) + \lambda r(1-r) + \omega r\lambda^2(1-g_1^2)\right] + \frac{\mu\ell}{6}\left[\frac{12r}{\mu^2\ell^2}\left[(1-g) + \omega^2\lambda\right.\right.$$

$$(1-g_1)\Big] + 3\,(1+\omega\lambda)(r^2+g^2) - r\left[2+3\omega\lambda + g^2\,[3(2+\omega\lambda) - 2g] - \omega^2\lambda^3\,[1-3g_1^2\right.$$

$$\left.\left.\left. + 2g_1^3]\right]\right] + \omega\,(1-r)(r-g^2)\,\tan\frac{\mu\ell_1}{2}\Bigg] + \frac{2\,\Delta H_p}{\mu^2\,H_2}\left[C\left[\frac{\mu g\ell}{\sin\mu\ell_1}\,\frac{(1-r)}{2r}\right.\right.$$

$$\left[(1-\omega)\cos\mu\ell_1 + \omega\left[1 - \frac{\mu\ell_1}{2}\sin\mu\ell_1\right) - \frac{\cos\mu\ell(1+\lambda-\frac{r}{2})}{\cos\frac{\mu r\ell}{2}}\right] - \frac{\sin\frac{\mu g\ell}{2}}{\cos\frac{\mu r\ell}{2}}$$

$$\sin\frac{\mu\ell}{2}(r-g) - \frac{g}{\lambda r}\,(1+\lambda-r)\,\frac{\sin\frac{\mu\ell}{2}}{\cos\frac{\mu r\ell}{2}}\sin\frac{\mu\ell}{2}(1-r) - \frac{\mu^2\ell^2}{4r}\,g\,[1-r(2-g)]\Big]$$

$$+ C_1\left[\frac{\sin\frac{\mu\ell}{2}\sin\frac{\mu\ell}{2}(1-r)}{\sin\mu\ell_1\cos\frac{\mu r\ell}{2}}\left(\sin\mu g_1\ell_1 - g_1\sin\mu\ell_1\right) + \omega\,\frac{\mu^2\ell_1^2}{4}\,g_1(1-g_1)\right.$$

$$\left.\left. - \omega\,\frac{\sin\frac{\mu g_1\ell_1}{2}}{\cos\frac{\mu\ell_1}{2}}\,\sin\frac{\mu\ell_1}{2}(1-g_1)\right]\right] + \frac{\Delta H_p Z_1}{\mu\,H_2}\left[\frac{2(1+\lambda)}{\mu r\ell_1}\,\frac{\sin\frac{\mu\ell}{2}\sin\frac{\mu\ell}{2}(1-r)}{\cos\frac{\mu r\ell}{2}}\right.$$

$$+ \frac{\sin\frac{\mu\ell}{2}(r-2g)}{\cos\frac{\mu r\ell}{2}} - \frac{2\sin\frac{\mu\ell}{2}\cos\mu g_1\ell_1\sin\frac{\mu\ell}{2}(1-r)}{\sin\mu\ell_1\cos\frac{\mu r\ell}{2}} + \omega\,\frac{\sin\frac{\mu\ell_1}{2}(1-2g_1)}{\cos\frac{\mu\ell_1}{2}}$$

$$- \frac{(1-r)}{r}\,\frac{2\sin\frac{\mu\ell}{2}(1+2\lambda)\sin\frac{\mu\ell}{2}(1-r)+\sin\mu\ell_1\sin\frac{\mu r\ell}{2} + \omega\cos\frac{\mu r\ell}{2}\,(1-\cos\mu\ell_1)}{\sin\mu\ell_1\cos\frac{\mu r\ell}{2}}$$

$$\left.\left.\left. + \frac{\mu\ell}{2r}\,[1-2r(1-g) + \omega\lambda\,[1-2r(1-g_1)]]\right]\right] \qquad (4.42)$$

where $\mu^2 = \dfrac{H_2}{EI}$ and $\Delta\rho = \dfrac{\Delta H_p}{H_w}$

and where g, g_1, C and C_1 can be evaluated from Equations (3.1) and (3.2) respectively.

From Appendix 27, the value of the moment at the intermediate support M_3, after the formation of the first plastic hinge, can be computed as follows: (Figure 4.9d)

$$M_3 = \frac{\Delta\sigma \ell^2}{2} \left[2\alpha - (\alpha^2-\beta^2) - \frac{1}{r}(r^2+\beta^2)\right] - \frac{\Delta\rho}{2}\frac{(1-r)}{r}\left[W\ell^2 (r-g^2) + 2H_w (Cg\ell - Z_1)\right] \quad (4.43)$$

Thus, as before, considering the condition of failure for the structure, which is the total value of the bending moment at the intermediate support to reach the ultimate moment of resistance M_{ult2}, we find the following expression: (Figure (4.9d))

$$M_{ult2} = M_2 + M_3$$

which yields,

$$\Delta\sigma = A_1 + A_2 \Delta H_p \quad (4.44a)$$

where A_1 and A_2 are constants governing the failure condition and can be obtained from the following expressions:

$$A_1 = \frac{2 (M_{ult2} - M_2)}{\ell^2 \left[2\alpha - (\alpha^2-\beta^2) - \frac{1}{r}(r^2+\beta^2)\right]} \quad (4.44b)$$

$$A_2 = \frac{(1-r)\left[W\ell^2(r-g^2) + 2 H_w (Cg\ell - Z_1)\right]}{r H_w \ell^2 \left[2\alpha - (\alpha^2-\beta^2) - \frac{1}{r}(r^2+\beta^2)\right]} \quad (4.44c)$$

where the more accurate value of M_{ult2} can be evaluated from Equation (4.22) when replacing H_i by H_1.

Hence, as mentioned earlier, we assume a value for $\Delta\sigma$ and, from Expression (4.42), find the corresponding increase in the prestressing force ΔH_p. We then use these values to plot a straight line from the origin point which intercepts the other line drawn from

Equations (4.44), Figure (4.8). The point of interception gives the approximate value of the load $\Delta\sigma_{ult}$ required to cause the collapse of the structure. Consequently, the failure load σ_{ult} is:

$$\sigma_{ult} = \sigma_{p.h} + \Delta\sigma_{ult}$$

Alternatively, an exact value for the failure load σ_{ult} can be obtained when we continue assuming values for $\Delta\sigma$ and find the corresponding ΔH_p and M_{ult2}, until the condition in Equation (4.44) is satisfied.

Formulae (4.39 - 44) can be used to determine the failure loads for uniformly distributed and concentrated loads applied in the left hand span by performing the aforementioned modifications, Section 4.3.2. Furthermore, for loads applied in the right hand span, a similar approach can be adopted to find their failure values.

4.4 Comparison between the Behaviour of Ungrouted and Grouted Prestressed Concrete Suspension Bridges at Failure

From Section 4.3, it is obvious that the main cable behaves elastically (linearly) up to the formation of the first plastic hinge, as it steadily increases its tension, due to the applied live loading, according to the Formulae derived in Sections 2.5 and 3.4. Thereafter, the cable response to the increase in the live loading remains linear but at a much faster rate, Formulae (4.31) and (4.42), as a result of the loss in the stiffness of the structure due to the plastic hinge. Consequently, the forces generated by the increase in the cable tension will also increase and therefore, contribute significantly to the overall resistance of the suspended beam to the failure loads. Furthermore, the ultimate moments of resistance of the beam cross section at the different positions will increase as well, resulting into an additional improvement in the beam strength.

It has been established that grout increases the interaction between the main cable and the suspended beam. Consequently, we would intuitively expect grout to also improve the performance of the

suspended beam when failure load is applied. This has been clearly demonstrated during the test to failure stage of the experimental work. Figure (4.10) shows the relationships between the increase of the cable tension H_p and increasing concentrated loads P which have been applied in the mid-points of the left hand span of the ungrouted and grouted test beams. The figure clearly indicates the relatively slow increase in the cable tension, before the formation of the first plastic hinge, which is followed by a sharp rise, for both types of beam. The figure also shows that the grouted test beam gained more force than the ungrouted one all through the range of loading. Consequently, the former failed at a higher load than the latter. Furthermore, less bending moments, deflections and shear forces have been measured for the grouted beam, see experimental results. We therefore, conclude that at failure, grouting improves the interaction between cable and beam which results in a more rigid structure.

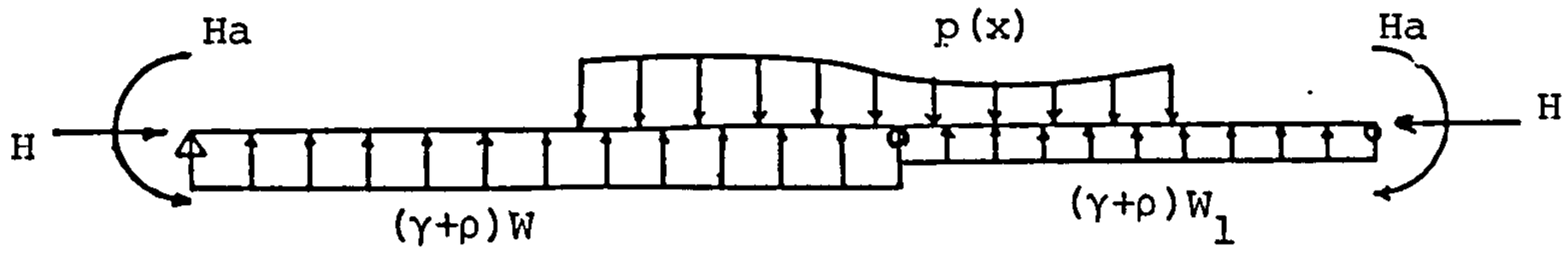

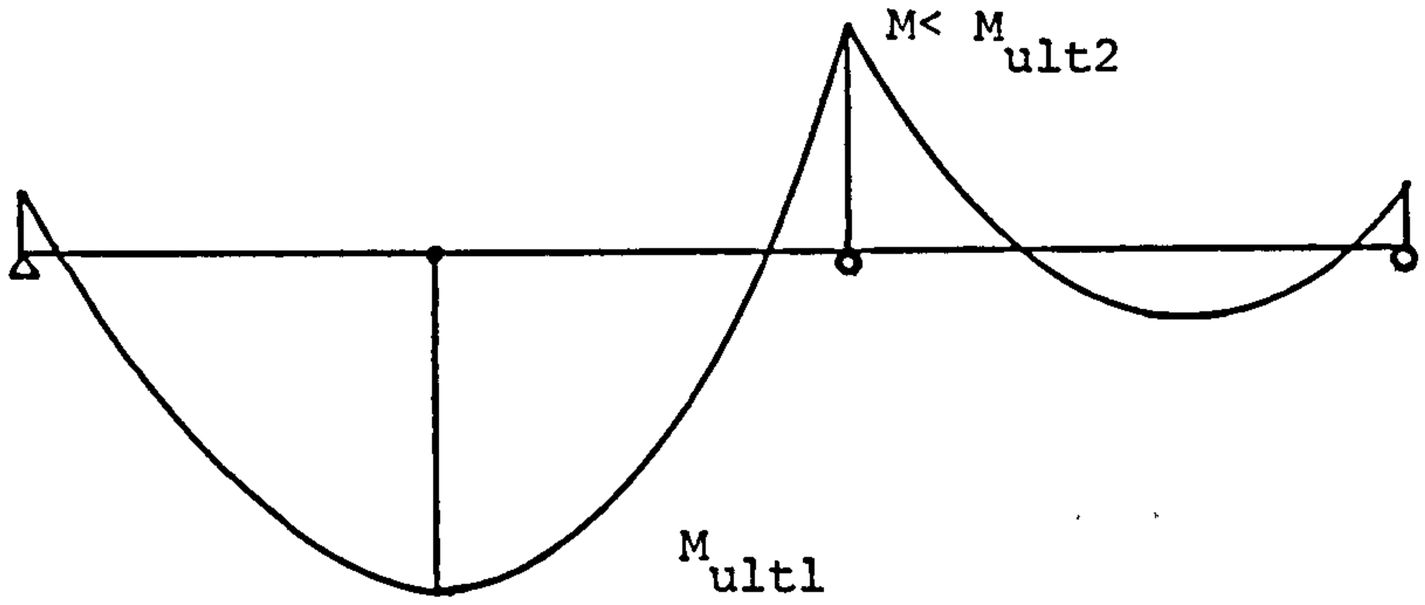

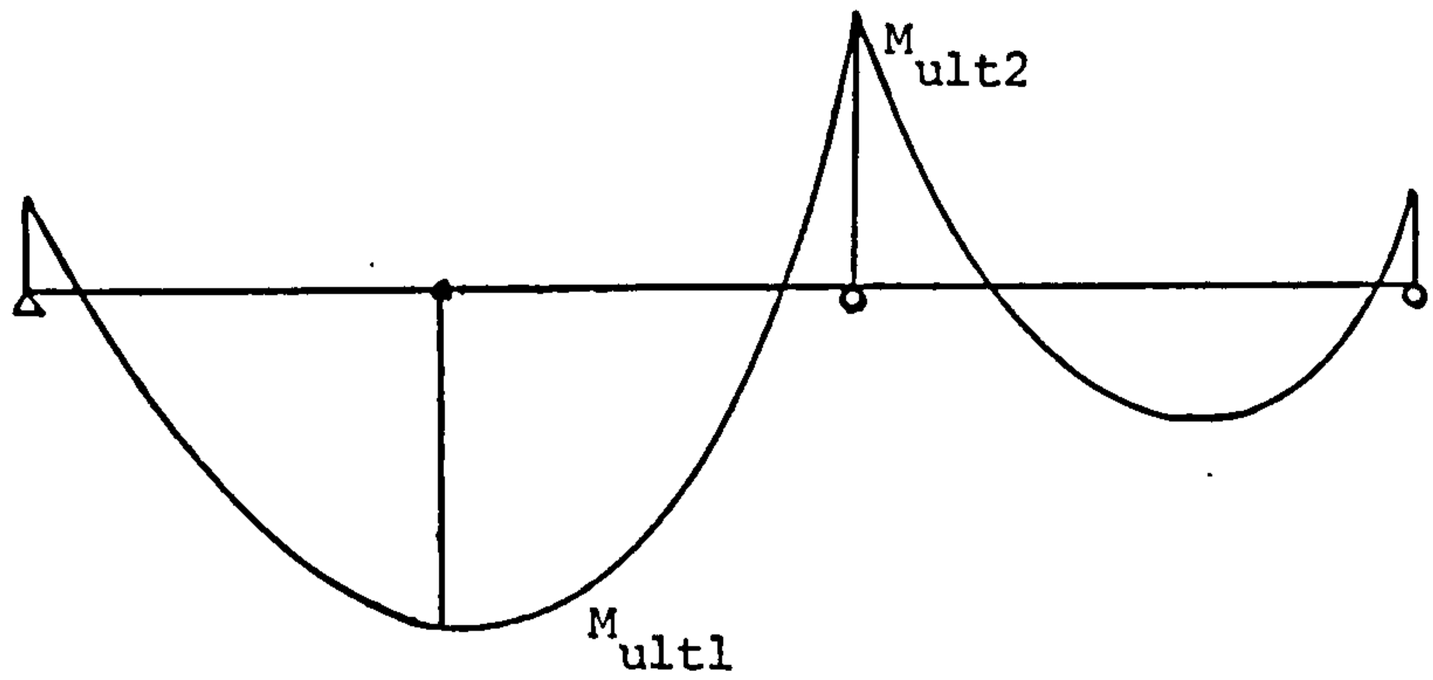

The failure stages of a prestressed concrete concrete suspended beam

Figure (4.1)

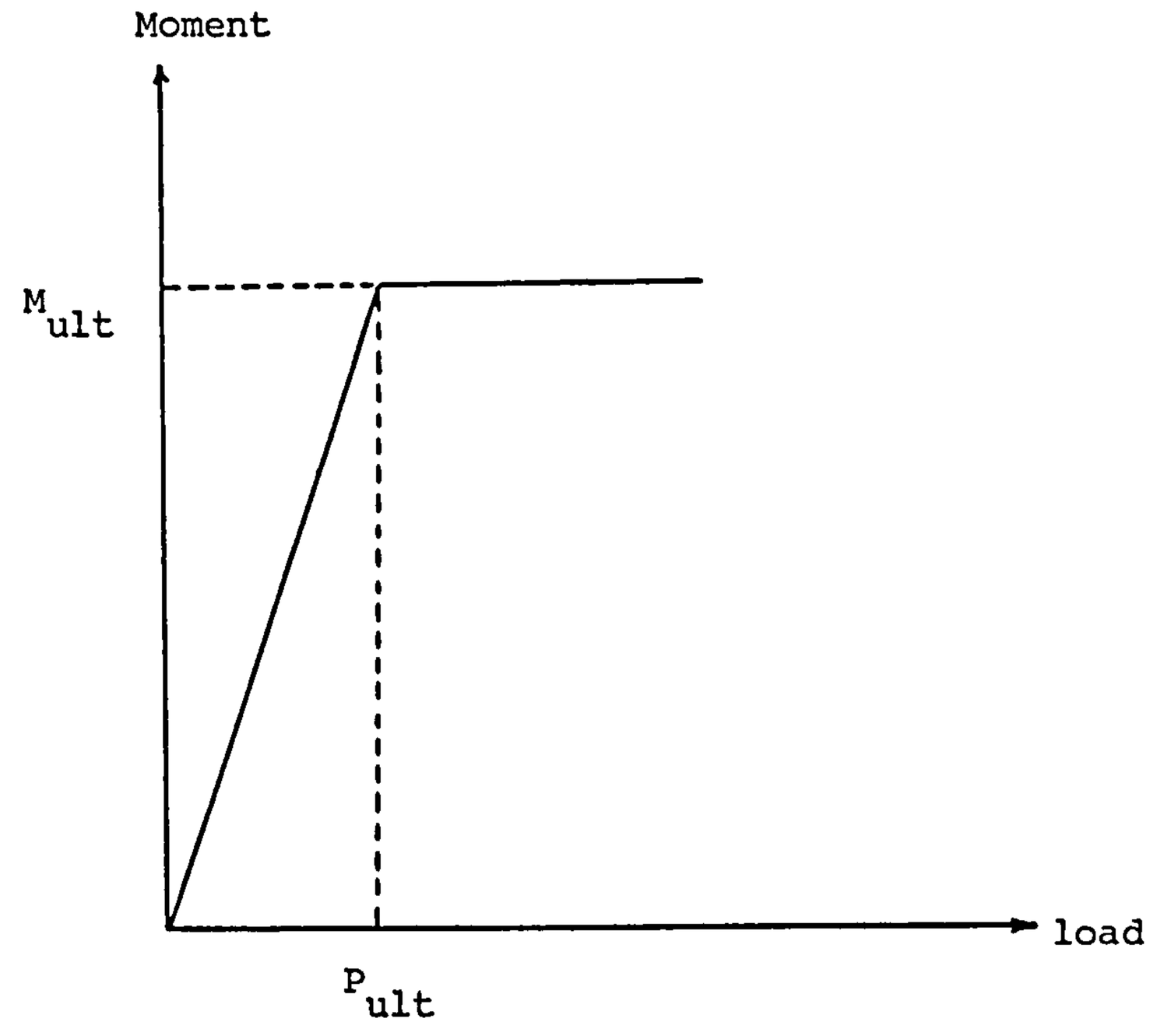

The assumed load-curvature relationship for the beam

Figure (4.2)

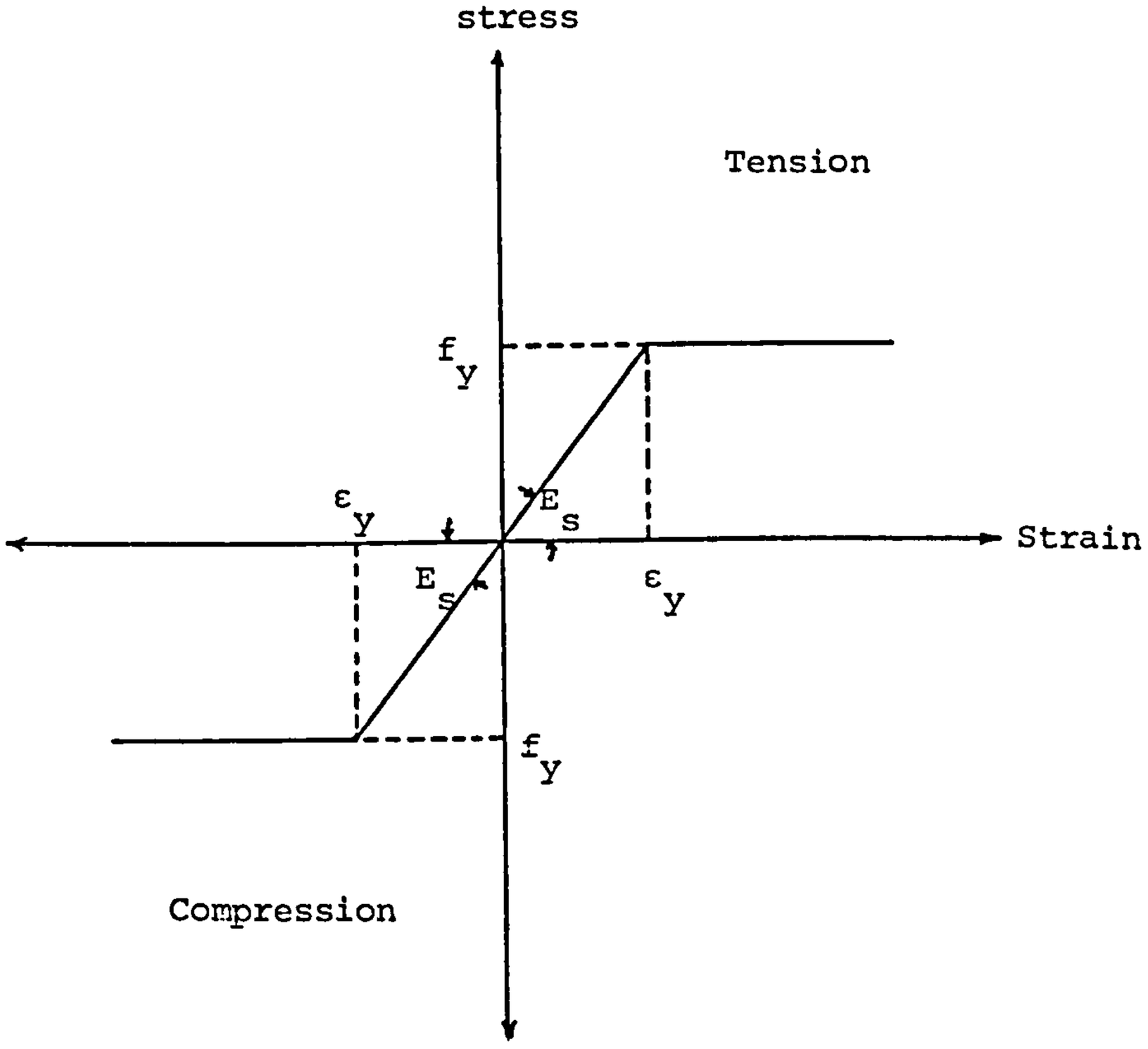

The assumed stress-strain relationship for the reinforcement

Figure (4.3)

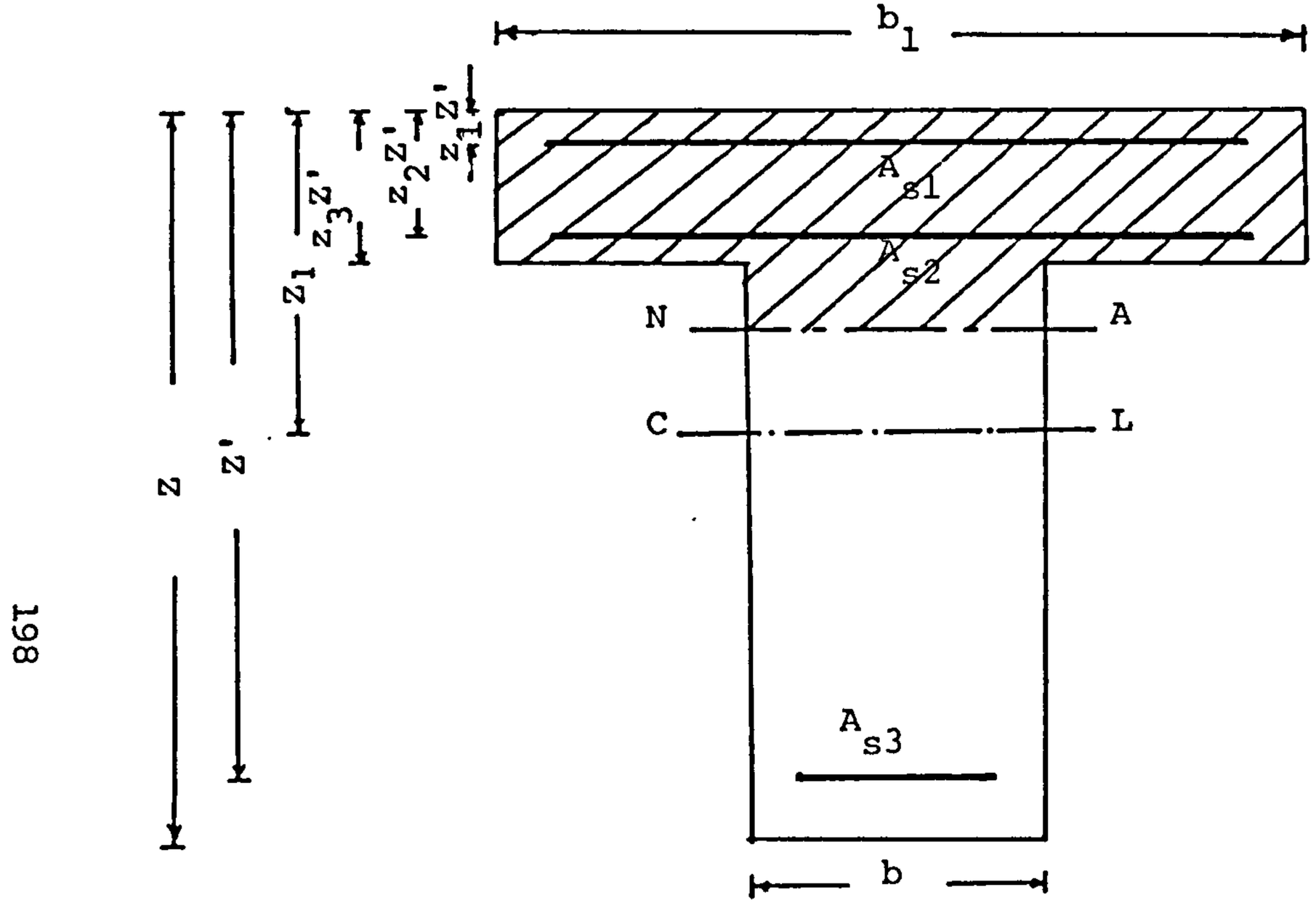

The cross section of the beam

(a)

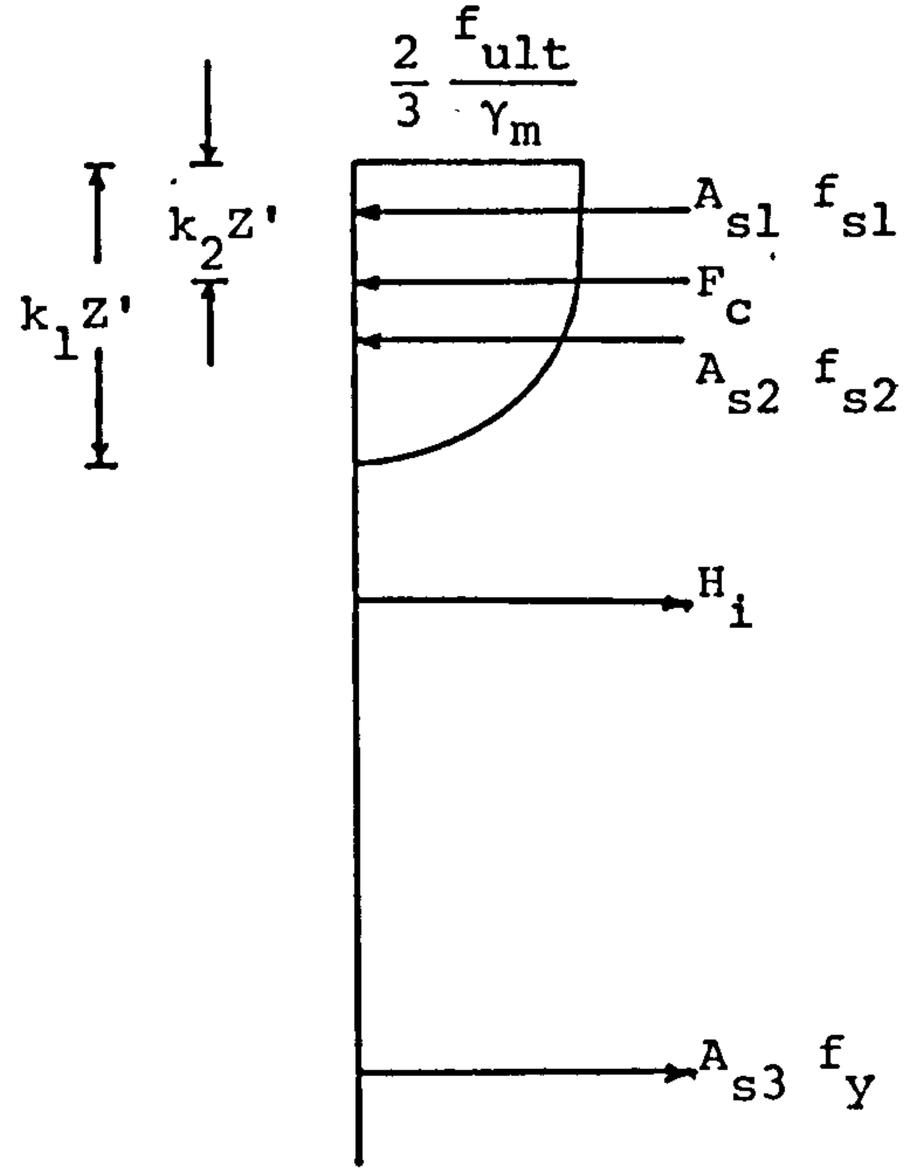

The stress diagram

(b)

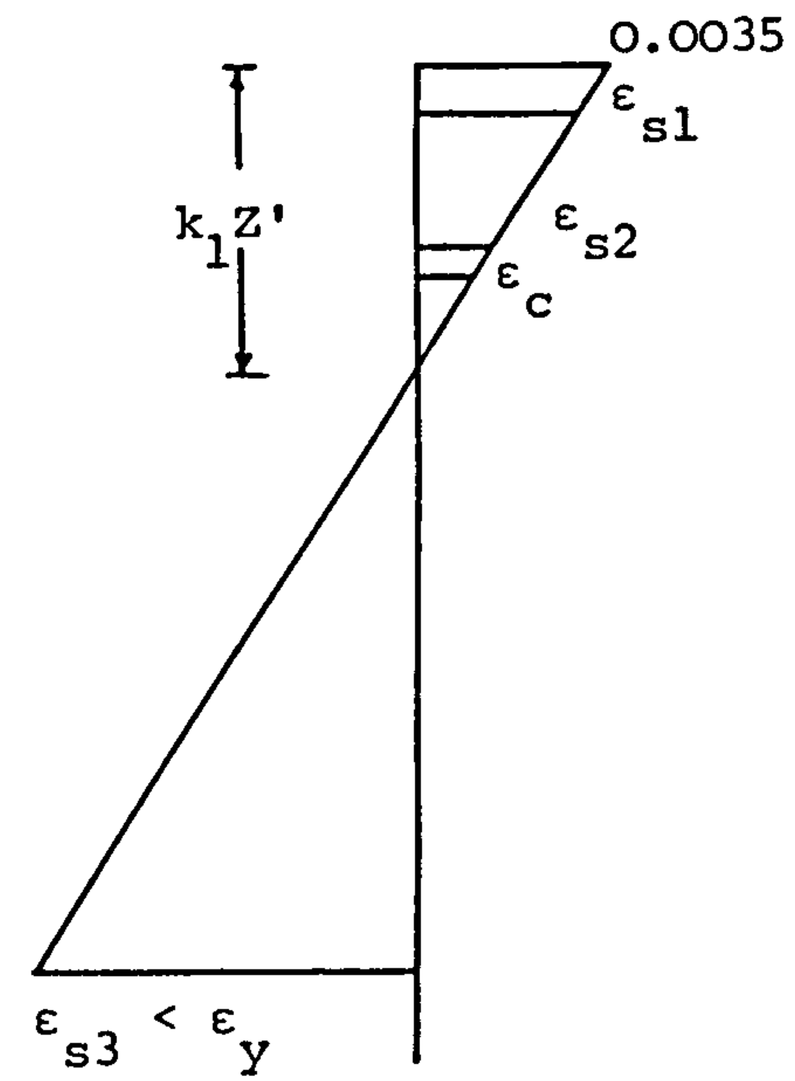

The strain diagram

(c)

Figure (4.4)

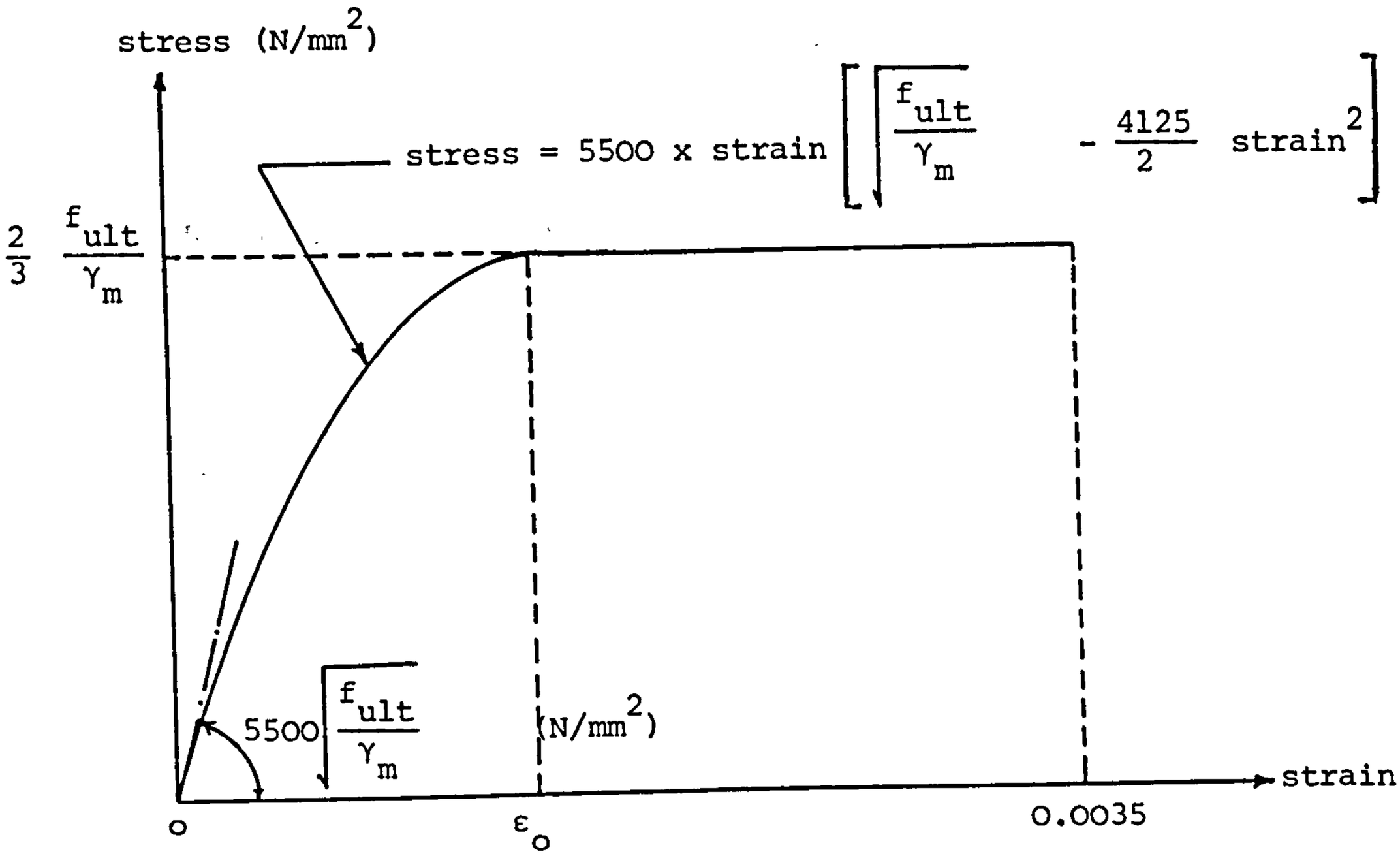

The stress-strain relationship of the concrete

Figure (4.5)

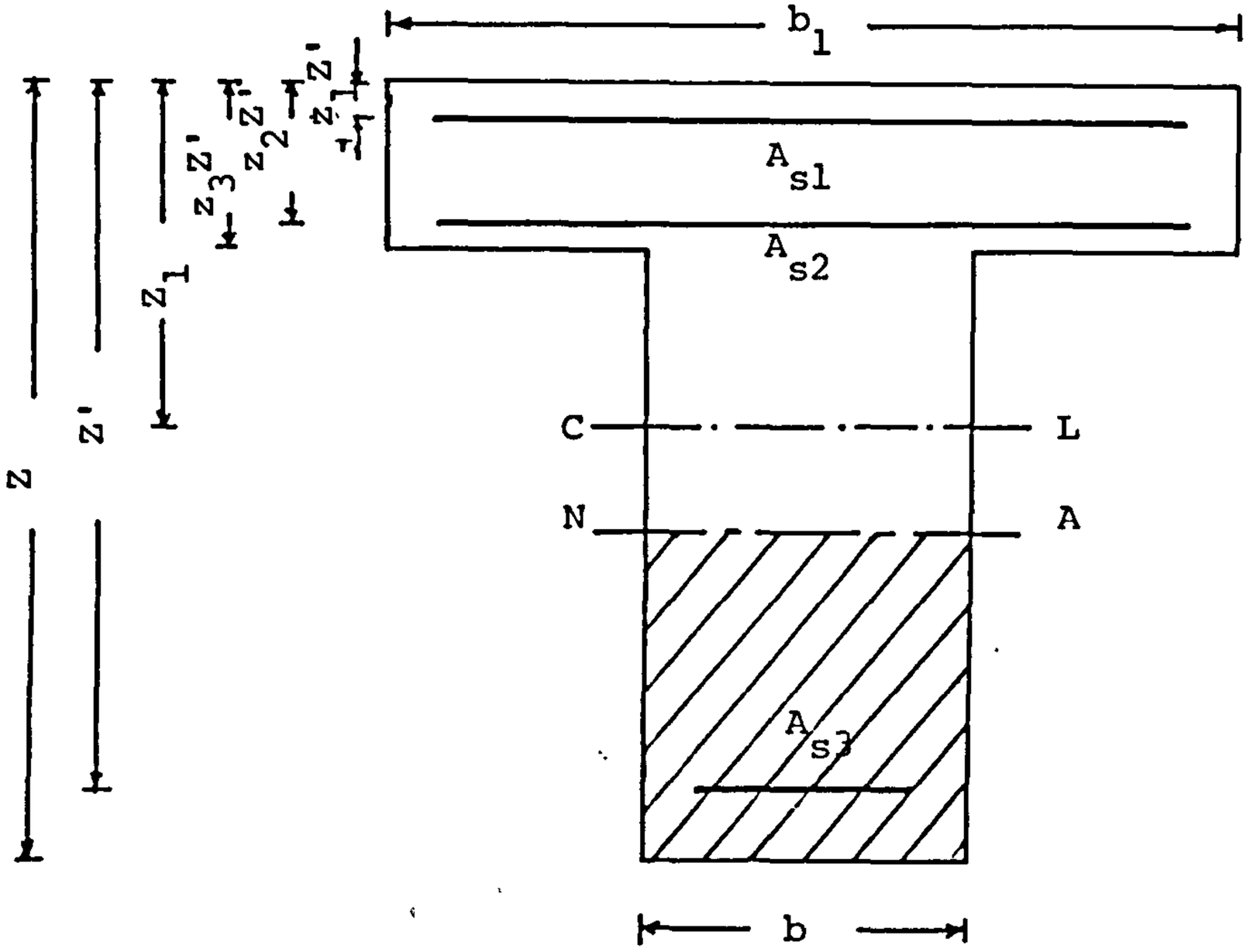

The cross section of the beam

(a)

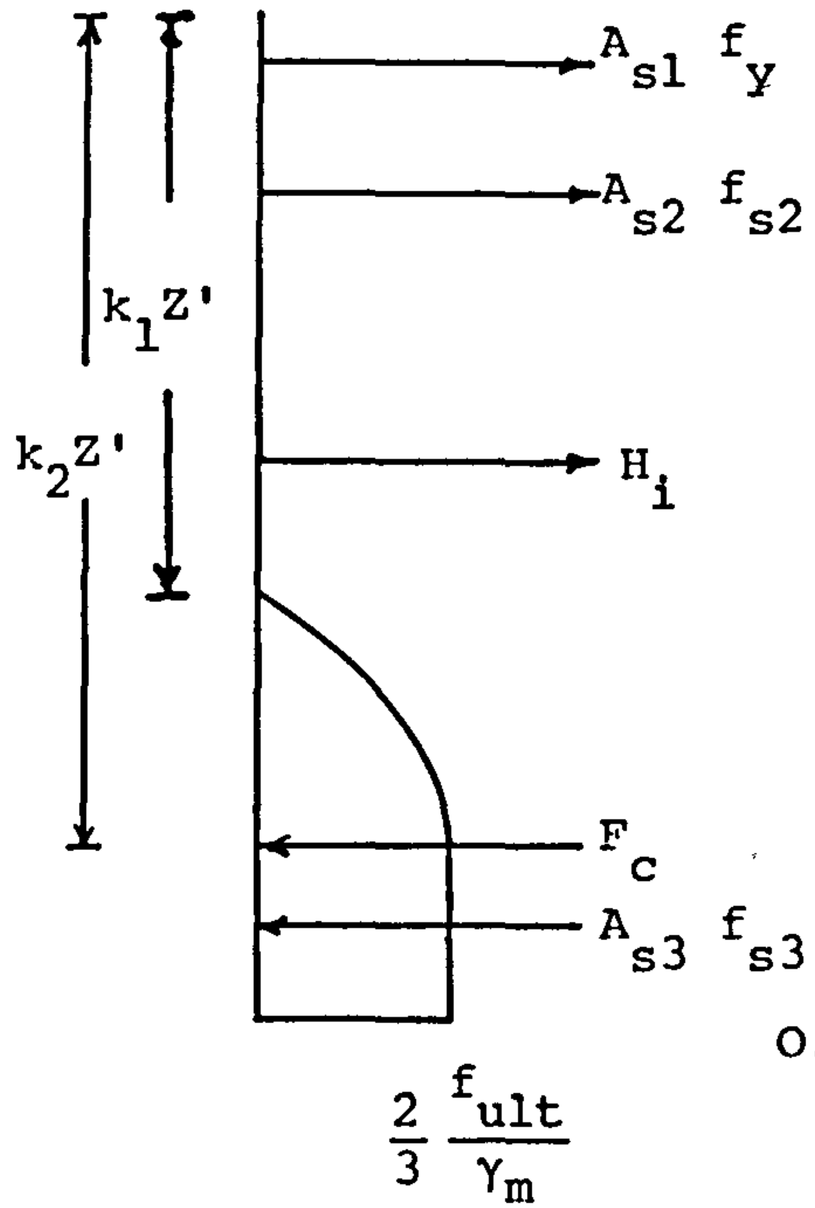

The stress diagram

(b)

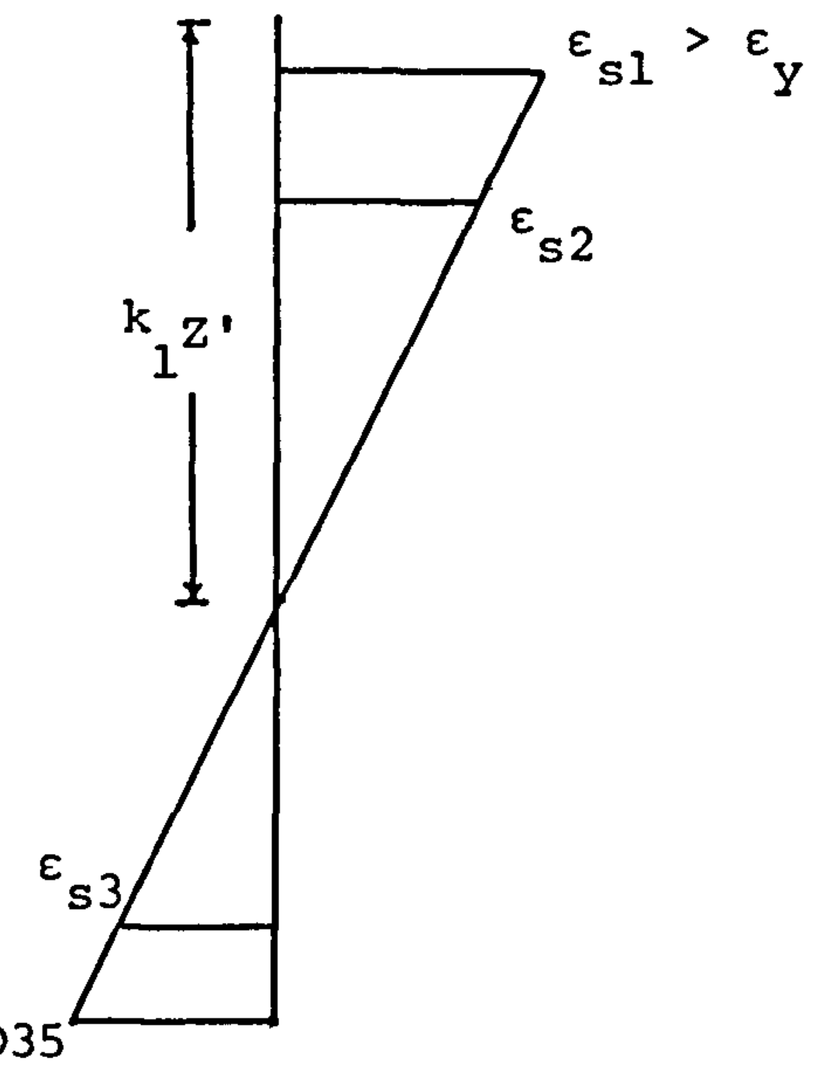

The strain diagram

(c)

Figure (4.6)

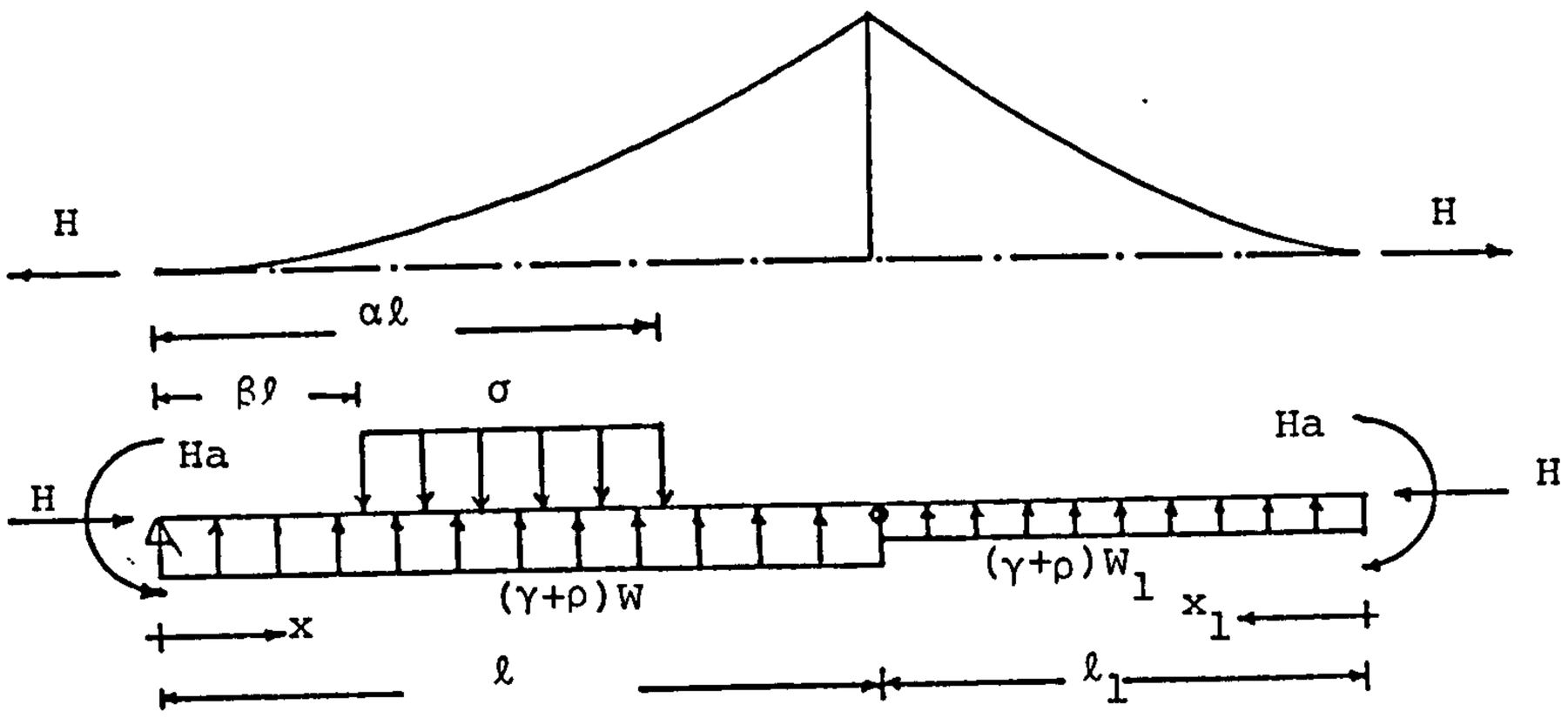

(a)

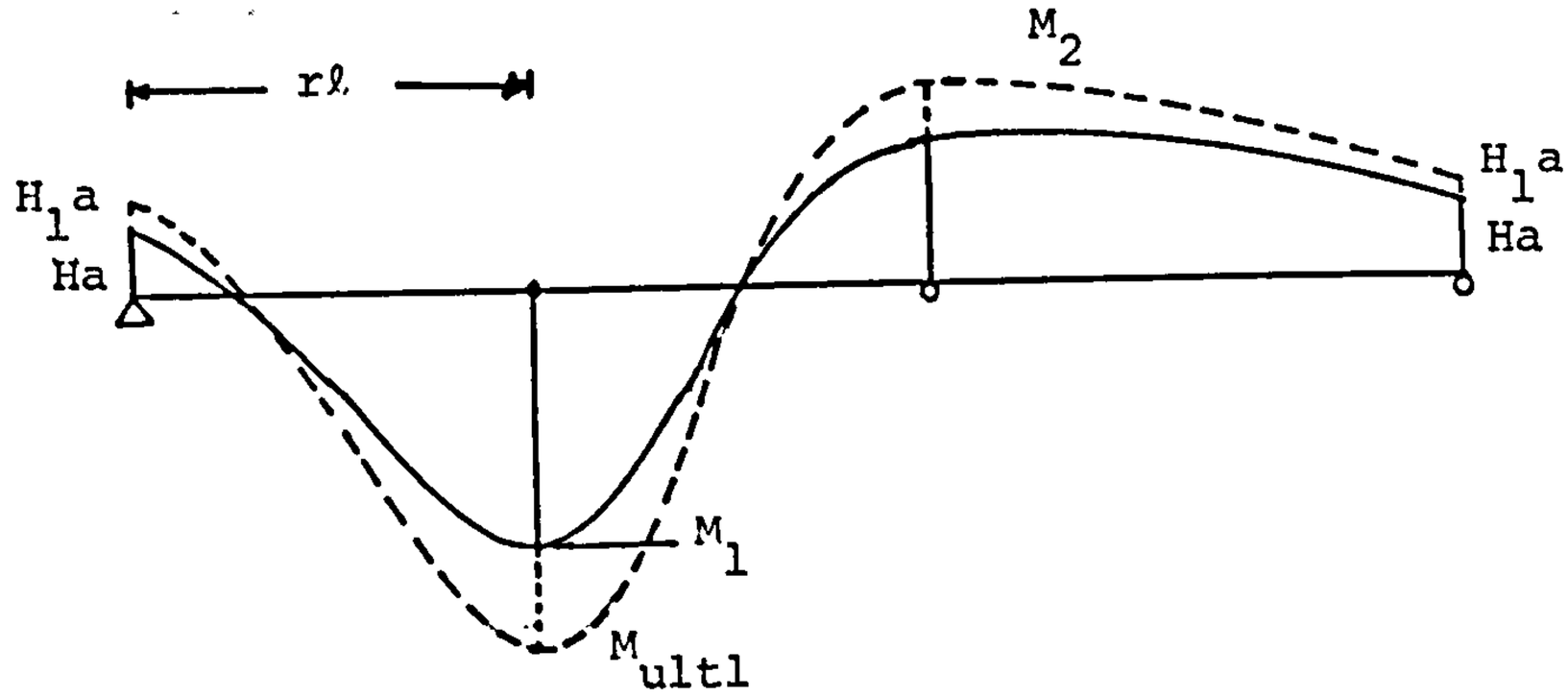

(b)

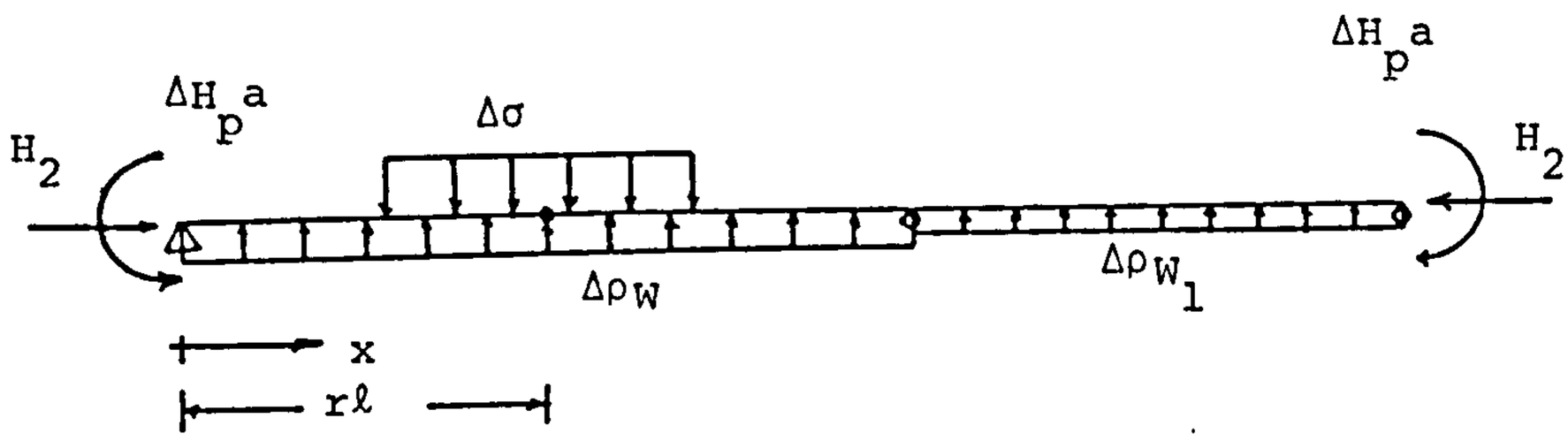

(c)

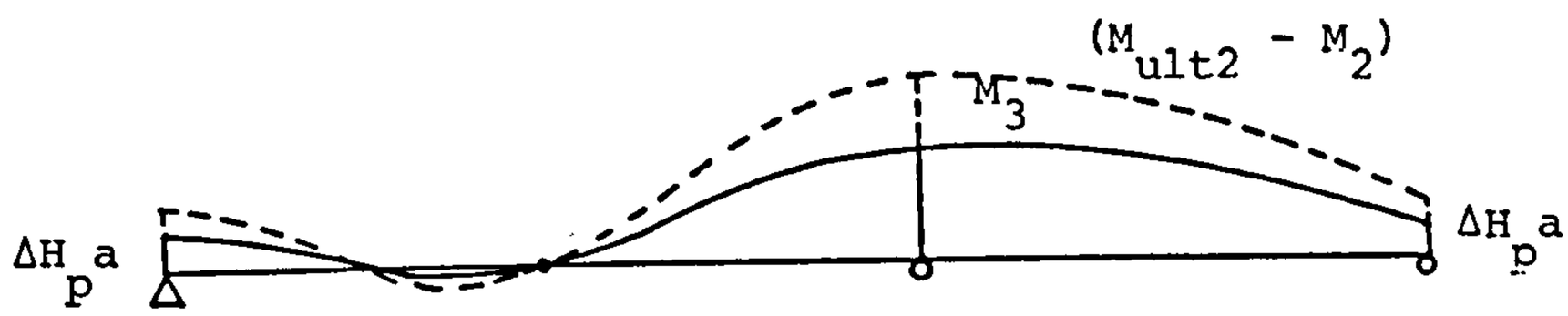

(d)

The failure stages of an ungrouted prestressed concrete suspended beam

Figure (4.7)

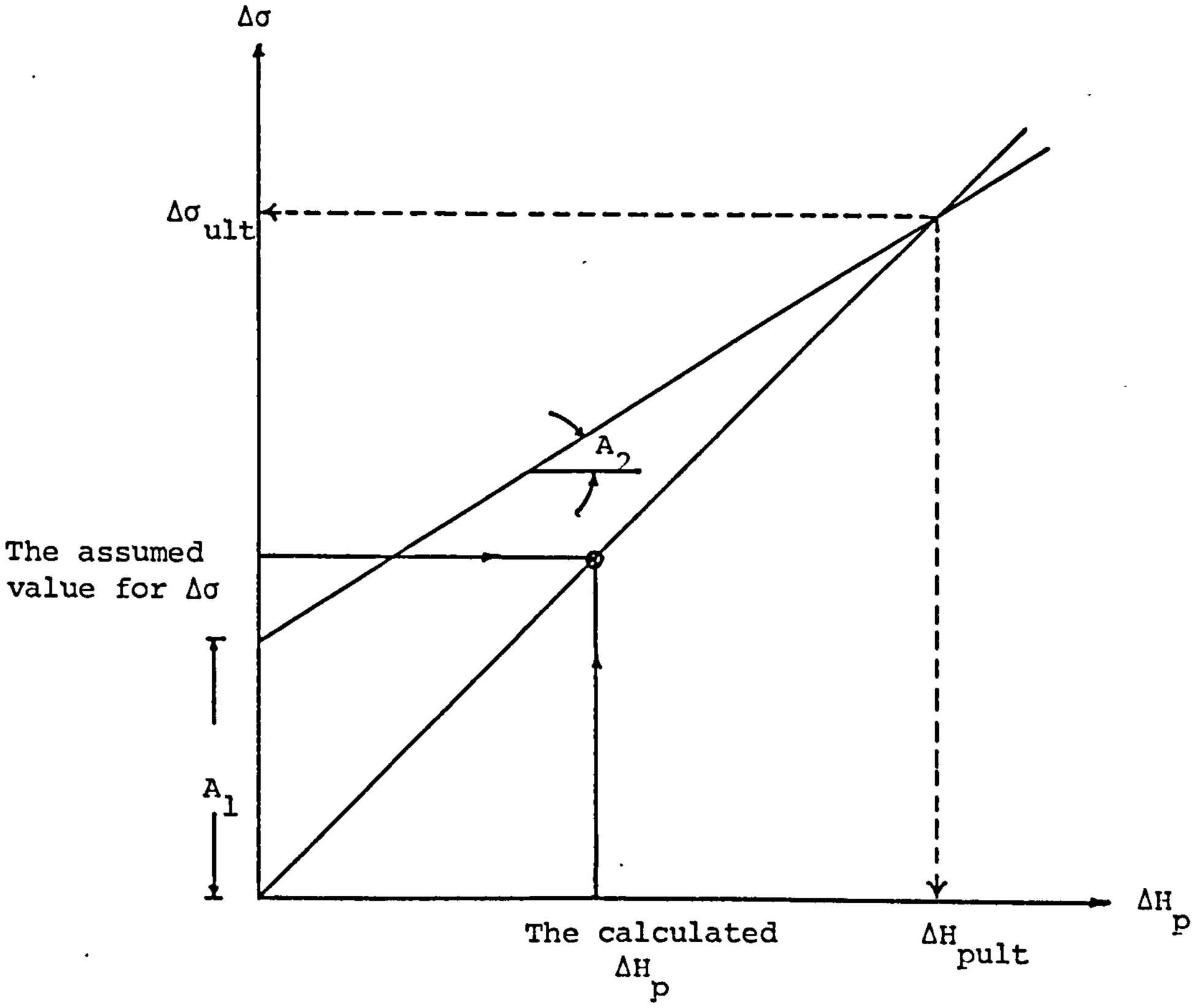

Approximate method for the determination of the load required to exceed the first plastic hinge load for the failure of the structure

Figure (4.8)

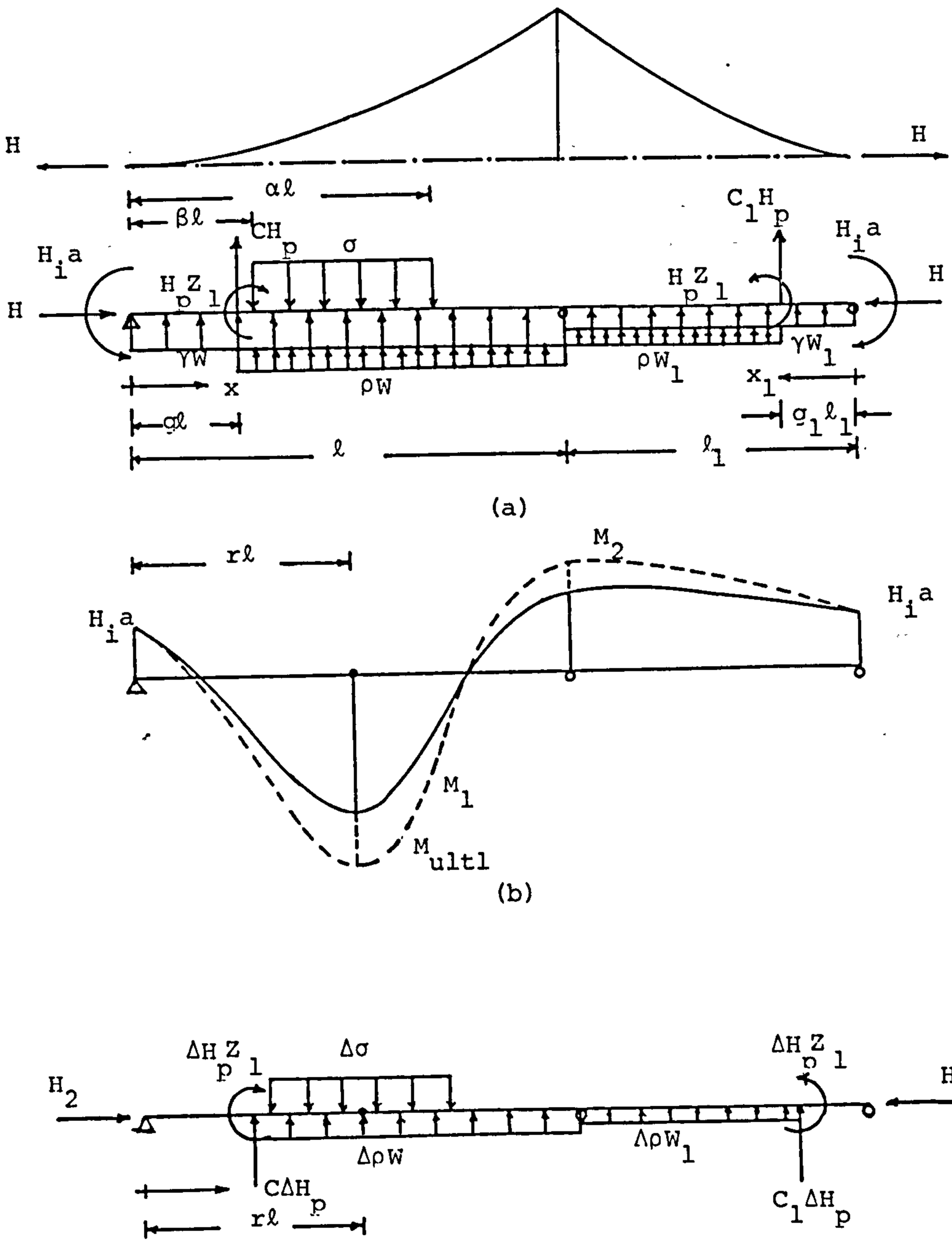

The failure stages of a grouted prestressed concrete suspended beam

Figure (4.9)

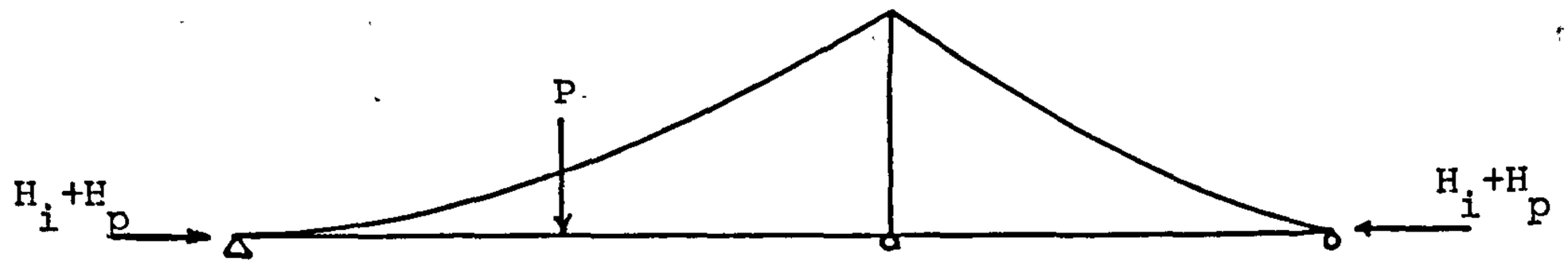

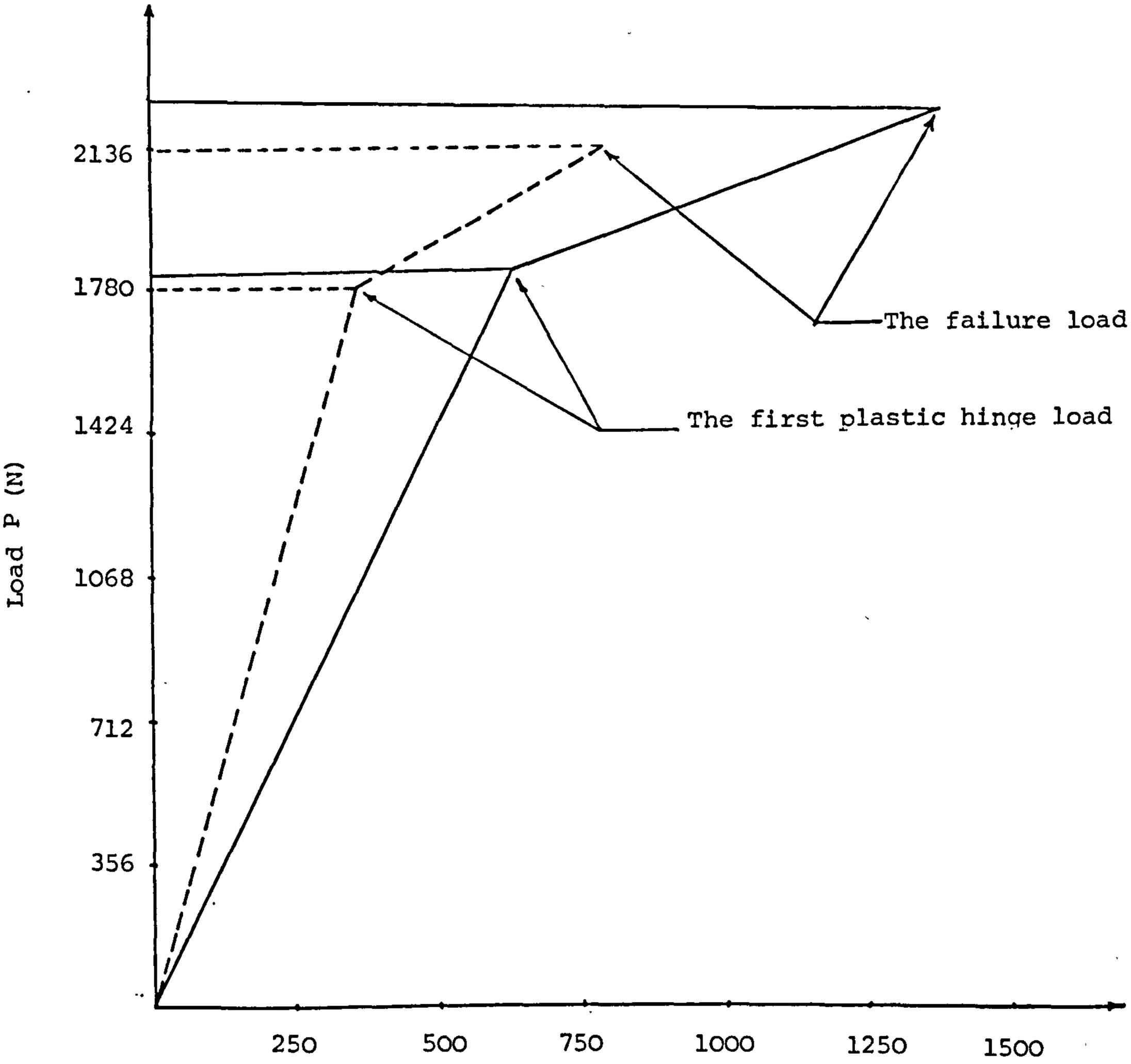

——— The grouted test beam

------- The ungrouted test beam

The effect of grout on the increase in the prestressing force at failure

Figure (4.10)

CHAPTER 5

5. The Influence of Time Effects on the Magnitude of the Prestressing Force

5.1 Introduction

Efficient design of prestressed concrete suspension bridges requires the prestressing force to be such that the upward forces exerted by the main cable on the suspended structure, via the suspenders, exceed on the whole the self weight of that structure. The reason for this can be deduced, as mentioned earlier, from the fact that a prestressing force equal to $H = \frac{Wl^2}{8f}$, will exert upwards forces W and W_1 in the left and right hand spans, Equations (2.12).

These forces are exactly in balance with the dead loads at those spans. After a period of time the magnitude of the prestressing force will most certainly diminish below the value of H_w due to time effects such as shrinkage, relaxation and creep of the various parts of the structure. Consequently, the upward forces will also decrease to a value less than W and W_1 for both spans and the suspended structure will deflect under its dead loads alone.

For the above reason, the magnitudes of the initial and final prestressing forces have been assumed to be H_i and H_f respectively, where from Equations (2.36) we have:

$$H_i = H_w\ (1+\gamma) \qquad (5.1a)$$

$$H_f = H_w\ (1+\tau) \qquad (5.1b)$$

$$\gamma > \tau \qquad (5.1c)$$

γ and τ are factors used to increase the value of the prestressing force to ensure that it remains higher than H_w after the time effects take place. These factors have also been used to adjust precisely the magnitude of the initial prestressing force in a way which cause the suspended beam to operate in the most economical and efficient

manner, see Section 2.4. The main purpose of this chapter is to establish a relationship between γ and τ to enable the designer to choose the correct value for the initial prestressing force.

It is essential to keep in mind that time effects on the magnitude of the prestressing force of prestressed concrete suspension bridges, differ significantly from the corresponding problem for conventional prestressed concrete structures. This is due to the contribution to the analysis of the cable upward forces on the suspended beam as well as the forces in the suspenders and the tower. Therefore, special considerations are required to evaluate the loss in the prestressing force due to time effects for our type of bridge. Subsequently, we will give a comparison between the losses in the prestressing force for conventional prestressed concrete structures and our type of structure.

Early research was undertaken in this field by the inventor of prestressed concrete suspensions bridges, Vandipette, (33) and (34). However, his theory was developed solely for three-span prestressed concrete suspension bridges and therefore, it was necessary to modify his work to suit two-span bridges. It is convenient to start this chapter by defining some of the quantities which will be used in the analysis as follows:

ε_s is the shrinkage strain of the concrete of the suspended beam occurring after prestressing is carried out. It can be evaluated experimentally but may be assumed to be 0.0001 if the concrete is several months old at the time of prestressing in a moderate climate, (34).

$\frac{E}{\Psi}$ is the final value of the modulus of elasticity of the concrete for loads of very long duration applied after the prestressing operation. In other words, the strain instanteously produced by a constant compressive stress f_c is $\frac{f_c}{E}$, but increases with time due to creep, and its final value is $\frac{\Psi f_c}{E}$, where Ψ is supposed to be independant of f_c. It may

be determined experimentally or assumed to be in the order of 2.25 to 2.75 for good quality concrete, depending on its age at prestressing time, (34).

ψ_c is the creep strain of the main cable under the average permanent working stress $\frac{H_i}{A_c}$ sustained in the structure. In other words, the magnitude of strain produced by this constant stress is $\frac{H_i}{A_c E_c}$, but it gradually increases slightly and its final value becomes $\frac{H_i}{A_c E_c}(1+\psi_c)$. ψ_c can be determined experimentally or assumed about 0.01 to 0.02 for cables made up of 0.01 to 0.02 for cables made up of parallel galvanized wires of good quality with a working stress equal to, or slightly exceeding, half of their ultimate strength, (34).

$\frac{E_{su}}{\psi_s}$ is the final value of the modulus of elasticity of the suspenders under the average permanent working stress as affected by creep. ψ_s may be obtained experimentally or assumed as 1.0 for suspenders made of solid steel bars or 1.30 for strands, (34).

L is the average loss in the prestressing force and, $L = \frac{y-\tau}{1+y}$

5.2 The Deformability of the Superstructure

Clearly, time effects only take place for loads of very long duration applied on the suspended beam after prestressing is carried out. Therefore, we will only consider the combination of the dead loads, W and W_1, and the forces produced by the initial prestressing force, H_i, in this analysis, Figure (5.1a). The resultant of these forces are yW, yW_1 and the end moment, $H_i a$ in the left and right hand spans as shown in Figure (5.1b).

Due to the fact that the suspended beam is a once indeterminate structure, the deformability of its different parts, due to the loads shown in Figure (5.1b), is evaluated by adopting a similar principle to that used in the determination of the increase of the cable tension by Steinman's approach, (20) and (21), (Section 2.5.2). We imagine the cable to be severed at a section close to one of its anchorages, Figure (5.1a). Due to the action of the applied loads, the two cut ends would be separated by some horizontal distance δ. This gap can be defined, according to Castigliano's first theorem (2), as the derivative, with respect to H_i, of the internal energy Ω stored in the superstructure. Hence, similarly to Equation (2.41), we have:

$$\delta = \delta_{bm} + \delta_{bn} + \delta_c + \delta_s + \delta_T$$

which can be rearranged as:

$$\delta = \frac{H_i \ell}{EI} \left[\Gamma_{bm} + \Gamma_{bn} + \Gamma_c + \Gamma_s + \Gamma_T\right] \qquad (5.2)$$

where Γ_{bm}, Γ_{bn}, Γ_c, Γ_s and Γ_T represent, in terms of $\frac{H_i \ell}{EI}$, the gaps generated by the bending moments of the beam, the direct forces in the beam, the main cable, the suspenders and the tower respectively. EI can be defined as the flexural rigidity of the suspended beam.

Hence, by making use of Formulae (2.43 - 47), the above quantities can be directly evaluated for the loads shown in Figure (5.1b). Thus, the gap δ_{bm}, produced by the bending moments of the beam can be obtained from Equation (2.43) which gives at $H = H_i$:

$$\delta_{bm} = \frac{H_i \ell}{EI} \Gamma_{bm}$$

$$\Gamma_{bm} = \frac{1}{3}(1+\lambda)\left[\frac{8}{5} f^2 \frac{(1+\omega^2\lambda^5)}{(1+\lambda)} - \left(fe - \frac{3}{2}a\right)\left(fe + \frac{1}{2}a\right)\right] \qquad (5.3)$$

in which:

f is the cable sag at the left hand span and equal to $\frac{W\ell^2}{8\ H_w}$,

a is the eccentricity at the ends of the main cable from the centre line of the beam,

$\lambda = \frac{\ell_1}{\ell}$,

$\omega = \frac{W_1}{W}$,

and $e = \frac{1+\omega\lambda^3}{1+\lambda}$.

The gap δ_{bn}, developed by the normal (prestressing) force in the suspended beam, can be directly evaluated from Equation (2.44) at $H = H_i$. which yields:

$$\delta_{bn} = \frac{H_i \ell}{EI} \Gamma_{bn}$$

$$\Gamma_{bn} = \frac{I}{A} \ (1+\lambda) \qquad (5.4)$$

The gap δ_c, generated by the tension of the main cable can be directly calculated from Equation (2.46), at $H = H_i$, for ungrouted cables, as follows:

$$\delta_c = \frac{H_i \ell}{EI} \Gamma_c$$

$$\Gamma_c = \frac{EI}{A_c E_c} \left[1 + \lambda + \frac{3}{8} \frac{(F+4n)^2}{\lambda^3} \left[4\lambda^2(1+\lambda) + 32\lambda^3 n^2 \ (1+\omega^2\lambda) + (F+4n)^2 \right.\right.$$

$$\left.\left. (1+\lambda^3)\right] + \frac{8}{5} n^2 \left[5(1+\omega^2\lambda^3) + 12n^2 \ (1+\omega^4\lambda^5)\right]\right] \qquad (5.5)$$

where A_c and E_c are the cross sectional area and Young's modulus of elasticity for the main cable respectively,

F is the slope of the main at its left hand end where

$F = \frac{h+a-4f}{\ell}$,

h is the height of the tower above the centre line of the beam,

and where $n = \frac{f}{\ell}$.

For grouted cables, the gap δ_{cf}, produced by the tension in the free ungrouted part of the cable can be determined by using Equation (3.20), at $H = H_i$, which gives:

$$\delta_{cf} = \frac{H_i \ell}{EI} \Gamma_{cf}$$

$$\Gamma_{cf} = \frac{EI}{16nA_cE_c} \left[(F+8n)[2+(F+8n)^2] - C\ (2+C^2) + \frac{1}{\omega}\ [(F_1+8n_1)\right.$$

$$\left.[2+(F_1+8n_1)^2] - C_1\ (2+C_1^2\ )]\right] \qquad (5.6)$$

where $(F+8n)$ and (F_1+8n_1) are the cable slopes at the top of the tower in the left and right hand spans respectively,

$$F_1 = \frac{h+a-4f_1}{\ell_1} ,$$

f_1 is the cable sag in the right hand span,

C and C_1 are the cable slopes at the ends of its free ungrouted part in the left and right hand span and can be evaluated from Equations (3.2).

The gap, δ_s, caused by the forces in the suspenders can be found from Equation (2.46a), at $H = H_i$, as follows:

$$\delta_s = \frac{H_i \ell}{EI} \Gamma_s$$

$$\Gamma_s = 64\ \frac{EI}{E_{su}}\ \frac{f^2}{\ell^5}\ \left[\frac{d}{A_{su}}\ \sum 1_s + \frac{\omega^2 d_1}{A_{su1}}\ \sum 1_{s1}\right] \qquad (5.7)$$

where E_{su} is Young's modulus of elasticity for the material of the suspenders,

d and d_1 are the spacings of the suspenders in the left and right hand spans, Figure (5.1a),

A_{su} and A_{sul} are the average cross sectional areas for the suspenders in the left and right hand spans,

and where $\sum l_s$ and $\sum l_{s1}$ are the sum of the lengths of the suspenders in the left and right hand spans and can be directly evaluated from Equations (2.46b and c).

Finally, the gap δ_T, produced by the force in the tower can be determined from Equation (2.47), at $H = H_i$, which gives:

$$\delta_T = \frac{H_i \ell}{EI} \Gamma_T$$

$$\Gamma_T = \frac{EI}{A_T E_T} \left[(F+8n) + (F_1+8n_1)\right]^2 \qquad (5.8)$$

where A_T and E_T are the average cross sectional area and Young's modulus of elasticity for the tower. The tower material is usually concrete.

It is worth mentioning that, for simplicity, the contribution of the secondary effect produced by the axial force, H_i, to the total value of the total gap δ, was ignored in this analysis.

5.3 Relative Displacements of the Ends of the Severed Cable due to Time Effects

5.3.1 Discussion

We now study the relative displacement of the imaginary cut ends of the cable which would gradually occur due to each time effect taken separately. The main reason for the development of these relative displacements is the gradual decrease of the initial prestressing force H_i, applied at the cut ends (Figure (5.1a)), until it reaches the final prestressing force H_f.

Hence, in this section, we will consider, separately, the shrinkage of the concrete of the suspended beam, the creep contraction of the axis of the beam and the tower due to the applied axial forces, the relaxation of the main cable and the suspenders due to creep and the creep flexure of the suspended beam.

5.3.2 Shrinkage

Shrinkage of the axis of the suspended beam alone produces an overlap Δ_1, at the cut ends of the severed cable, given by:

$$\Delta_1 = (1+\lambda)\ \ell\ \varepsilon_s \qquad (5.9)$$

where $\lambda = \frac{\ell_1}{\ell}$

5.3.3 Creep Contraction

The immediate contraction of the axis of the suspended beam generated by the prestressing operation is $\frac{H_i \ell}{EI}\ \Gamma_{bn}$. After a period of time, the beam finally shortens a total amount $\frac{H_f \ell}{EI}\ \psi\ \Gamma_{bn}$ (as the final value for the modulus of elasticity becomes $\frac{E}{\psi}$, section 5.1).

Consequently, the overlap Δ_2 due to creep contraction is:

$$\Delta_2 = \frac{H_f \ell}{EI} \psi \Gamma_{bn} - \frac{H_i \ell}{EI} \Gamma_{bn}$$

Substituting for H_i and H_f from Equations (5.1), we finally obtain:

$$\Delta_2 = \frac{H_w \ell}{EI} \Gamma_{bn} \left[(\psi-1) + \psi\tau - \gamma\right] \tag{5.10}$$

where Γ_{bn} can be evaluated from Equation (5.4).

Similarly, the immediate contraction of the tower axis generated by the prestressing operation is $\frac{H_i \ell}{EI} \Gamma_T$, Equation (5.8). After a period of time, the final value for this contraction becomes $\frac{H_f \ell}{EI} \psi \Gamma_T$ (providing that the tower material is concrete). Thus, the final overlap Δ_3 can be evaluated as:

$$\Delta_3 = \frac{H_w \ell}{EI} \Gamma_T \left[(\psi-1) + \psi\tau-\gamma\right] \tag{5.11}$$

where Γ_T can be computed from Equation (5.8).

5.3.4 Relaxation due to Creep

Since the elongation of the main cable under the initial prestressing force H_i instantaneously produces a total gap $\frac{H_i \ell}{EI} \Gamma_c$ for ungrouted cables and $\frac{H_i \ell}{EI} \Gamma_{cf}$ for grouted ones, the overlap Δ_4 studied here is:

$$\Delta_4 = \frac{H_f \ell}{EI} (1+\psi_c) \Gamma_c - \frac{H_i \ell}{EI} \Gamma_c$$

Substituting for H_i and H_f from Equations (5.1), we find for ungrouted cables:

$$\Delta_4 = \frac{H_w \ell}{EI} \Gamma_c \left[\psi_c + (1+\psi_c)\, \tau-\gamma\right] \tag{5.12}$$

where the final value of Young's modulus of elasticity of the main cable is $\frac{E_c}{(1+\psi_c)}$ (Section 5.1) and where Γ_c can be evaluated form Equation (5.5).

A similar expression can be written for grouted cables as we replace Γ_c in Expression (5.12) by Γ_{cf} to find the overlap produced by the relaxation of the free ungrouted part of the cable. The term Γ_{cf} can be determined from Equation (5.6).

For the suspenders, their elongation due to the initial prestressing force would produce a total gap $\frac{H_f \ell}{EI} \Gamma_s$ which becomes equal to $\frac{H_f \ell}{EI} \psi_s \Gamma_s$ after a while. Thus, the overlap Δ_5 produced by the relaxation of the suspenders due to creep is:

$$\Delta_5 = \frac{H_w \ell}{EI} \Gamma_s \left[(\psi_s - 1) + \psi_s \tau - \gamma\right] \qquad (5.13)$$

where the final value of Young's modulus of elasticity for the suspenders is $\frac{E_s}{\psi_s}$, Section 5.1, and where Γ_s can be evaluated from Equation (5.7).

Expression (5.13) slightly over estimates the overlap Δ_5, for we calculated Γ_s on the assumption that the full force in the cable induces tensile forces in the suspenders, Section 2.5.2.2. However, part of the actual tension of the cable, H_i or H_f, serves to carry its own weight and does not stress the suspenders. This error is almost negligible providing that the spans are not very long and the cable is not too heavy. Nevertheless, Expression (5.13) can be easily corrected by multiplying it by the correction factor $\left[1 - \frac{w_c}{W_{av}}\right]$ where w_c is the weight of the cable and W_{av} is the average dead load of the suspended beam, $W_{av} = \frac{W+W_1}{2}$.

5.3.5 Creep Flexure of the Suspended Beam

Similarly, to the aforementioned procedures, the gap immediately produced by the prestressing operation is $\frac{H_i \ell}{EI} \Gamma_{bm}$. After

a period of time, the final value of this gap becomes $\frac{H_f \ell}{EI} \psi \Gamma_{bm}$. Thus the overlap Δ_6 produced by creep flexure of the beam is the difference between those gaps which yields:

$$\Delta_6 = \frac{H_w \ell}{EI} \Gamma_{bm} \left[(\psi-1) + \psi\tau-\gamma\right] \qquad (5.14)$$

where Γ_{bm} can be calculated from Equation (5.3).

Having found the different overlaps produced by time effects, we can now find a relationship between τ and γ as shown in the following section.

5.4 The Relationship between τ and γ

To find this relationship, we have to consider the fact that there is no gap in the real structure, neither immediately after prestressing nor at any time afterwards. This is because the prestressing force varies in such a way that the imaginary cut ends permanently remain in contact. Therefore, the final value of the prestressing force H_f is precisely governed by that condition. Whence, we may write:

$$\sum_{n=1}^{6} \Delta_n = o$$

which yields, from Formulae (5.9 - 14):

$$(1+\lambda)\ \ell\ \varepsilon_s + \frac{H_w \ell}{EI} \left[\Gamma_{bm} + \Gamma_{bn} + \Gamma_T\right]\left[(\psi-1) + \psi\tau - \gamma\right] + \frac{H_w \ell}{EI} \Gamma_c \left[\psi_c + (1+\psi_c)\right.$$

$$\left.\tau - \gamma\ \right] + \frac{H_w \ell}{EI} \Gamma_s \left[(\psi_s-1) + \psi_s\ \tau-\gamma\right] = o$$

Rearranging this equation, we obtain the relationship between τ and γ for ungrouted cables as follows:

$$\tau = G\gamma - D \qquad (5.15a)$$

$$\text{where } G = \frac{(\Gamma_{bm} + \Gamma_{bn} + \Gamma_c + \Gamma_s + \Gamma_T)}{\left[\psi\ (\Gamma_{bm} + \Gamma_{bn} + \Gamma_T) + (1+\psi_c)\ \Gamma_c + \psi_s\ \Gamma_s\right]}, \quad < 1 \qquad (5.15b)$$

$$\text{and } D = \frac{\left[(\psi-1)(\Gamma_{bm} + \Gamma_{bn} + \Gamma_T) + \psi_c\Gamma_c + (\psi_s-1)\,\Gamma_s + \frac{EI}{H_w}\,\varepsilon_s\,(1+\lambda)\right]}{\left[\psi\,(\Gamma_{bm} + \Gamma_{bn} + \Gamma_T) + (1+\psi_c)\,\Gamma_c + \psi_s\,\Gamma_s\right]}\,, \quad > o$$

(5.15c)

For grouted cables, this relationship can be determined by simply replacing Γ_c by Γ_{cf} in Equations (5.15).

Expression (5.15a) gives an approximate linear relationship between τ and γ where G and D are constants as shown in Figure (5.2). These constants can easily be computed by using Formulae (5.3 - 8), provided, of course, that the properties of the materials, ε_s, ψ, ψ_c and ψ_s, are known or assumed. Thus, as mentioned in Section 2.4, we select a value for τ and find the corresponding γ, from Equations (5.15). Then, we check the value of γ to comply with the condition (2.38b) to ensure that the stresses of the beam, at the initial prestressing force, are adjusted for maximum efficiency. The average loss, L, in the prestressing force can then be evaluated as:

$$L = \frac{\gamma-\tau}{1+\gamma}$$

Figure (5.2), Expression (5.15), shows that at γ = o the value of τ becomes negative. This means that, as mentioned before, if the initial prestressing force is such that the forces acting upward on the suspended beam are exactly in balance with the dead loads, the beam will, after a while, deflect below its unstressed shape under the dead loads alone. For this reason, the minimum value of γ must not be less than γ_{min} where:

$$\gamma_{min} = \frac{D}{G} = \frac{\left[(\psi-1)(\Gamma_{bm} + \Gamma_{bn} + \Gamma_T) + \psi_c\Gamma_c + (\psi_s-1)\,\Gamma_s + \frac{EI}{H_w}\,\varepsilon_s\,(1+\lambda)\right]}{(\Gamma_{bm} + \Gamma_{bn} + \Gamma_c + \Gamma_s + \Gamma_T)} \qquad (5.16)$$

The average loss in the prestressing force for ungrouted suspended beams is found to be higher than for the grouted ones. The reason is that grouting restrains the main cable and makes it less

likely to lose its force due to time effects. This represents another advantage for grouting prestressed concrete suspension bridges.

Finally, it is worth mentioning that the average loss in the prestressing force decreases with the increase of the span length as can be deduced from Expression (5.15). This is due to the fact that for long spans, the flexibility of the suspended beam increases and consequently any loss taking place in the prestressing force would be lesser than for a more rigid form of structure.

5.5 Comparison between the Losses in the Initial Prestressing Force for Conventional Prestressed Beams and Prestressed Concrete Suspended Beams due to Time Effects

To achieve the benefit of the comparison, we consider a post-tensioned two-span conventional prestressed concrete beam with its tendon on the line of centroids. The initial prestressing force is denoted by H which, after a period of time, reduces to become H (1-L). Here L is the average loss of the prestressing force due to time effect.

If the tendon is imagined to be detached from one end of the concrete beam, the time effects, as before, will cause the following gaps between the end of the beam and the end of the cable:

1. due to shrinkage, we have:

$$\Delta_1 = (1+\lambda)\, \ell\, \varepsilon_s.$$

2. Due to creep, the relaxation of the tendon produces the following gap.

$$\Delta_2 = \frac{H\ell}{A_c E_c} (1-L)\ (1+\psi_c)\ (1+\lambda) - \frac{H\ell}{A_c E_c} (1+\lambda)$$

$$\Delta_2 = \frac{H\ell}{A_c E_c} (1+\lambda)\ \left[\psi_c - (1+\psi_c)\ L\right]$$

3. Due to creep contraction of the beam, we have:

$$\Delta_3 = \frac{H\ell}{AE} (1-L) \psi (1+\lambda) - \frac{H\ell}{AE} (1+\lambda)$$

$$\Delta_3 = \frac{H\ell}{AE} (1+\lambda) \left[(\psi-1) - \psi L\right]$$

and the flexure of the beam does not cause any gap in this case. Even if the tendon was assumed to have an eccentricity from the centre line, the value of the gap caused by flexure would be very small.

As there would be no gap in the real structure, we may write:

$$\sum_{n=1}^{3} \Delta_n = o$$

which yields;

$$L = \frac{\left[\frac{A_c E_c}{H} \left[\varepsilon_s + \frac{H}{AE} (\psi-1)\right] + \psi_c\right]}{\left[\frac{A_c E_c}{AE} + 1 + \psi_c\right]} \qquad (5.17)$$

This equation immediately gives the average loss L in the prestressing force due to time effects.

The working stress in the tendon of a conventional post-tensioned beam is normally much larger than half its ultimate strength. Consequently, the value of ψ_c would be higher than for a prestressed suspended beam, Section 5.1, when its main cable is made up of parallel wires. This means that the average loss in the prestressing force is always higher for conventional prestressed beams than for the suspended ones. Even when identical values of ε_s, ψ and ψ_c are introduced in Expression (5.15) and (5.17), the average loss, L, of prestress turns out to be smaller for a prestressed concrete suspended beam than for a conventional one. This is because the former system is less rigid than the latter. For this reason, the average loss of prestressing force L in a prestressed concrete suspension bridge decreases with an increase of the span length.

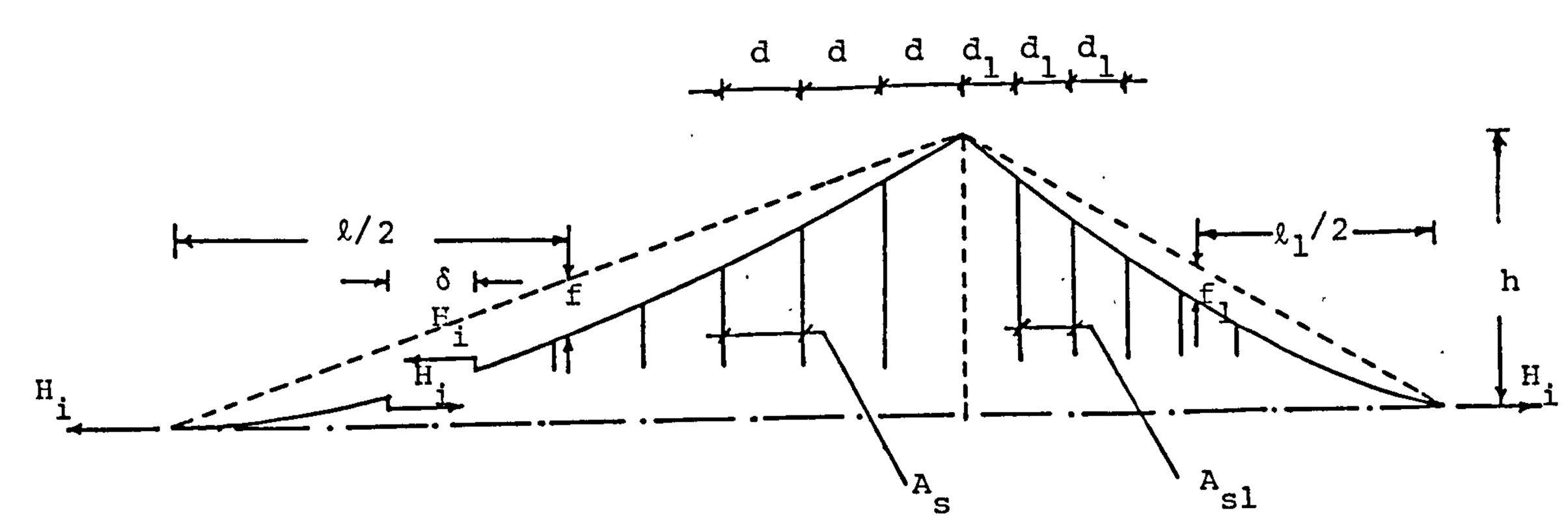

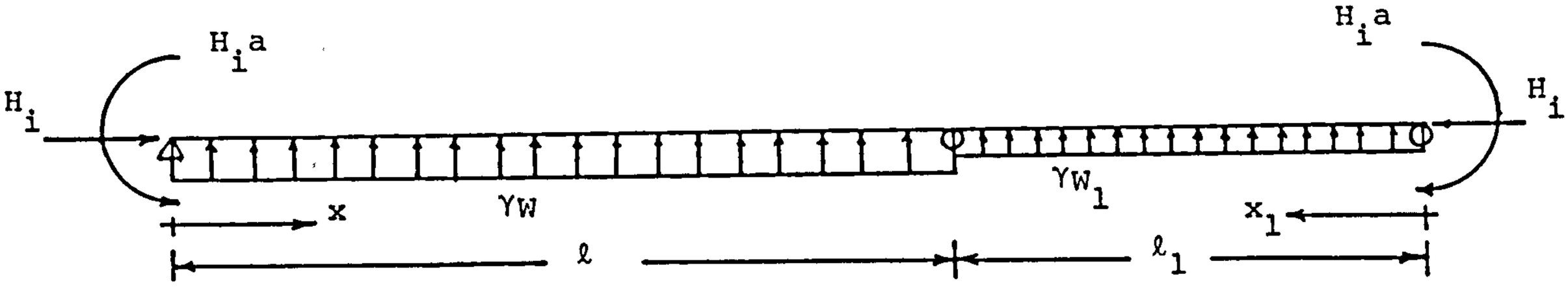

The very long duration loads

Figure (5.1)

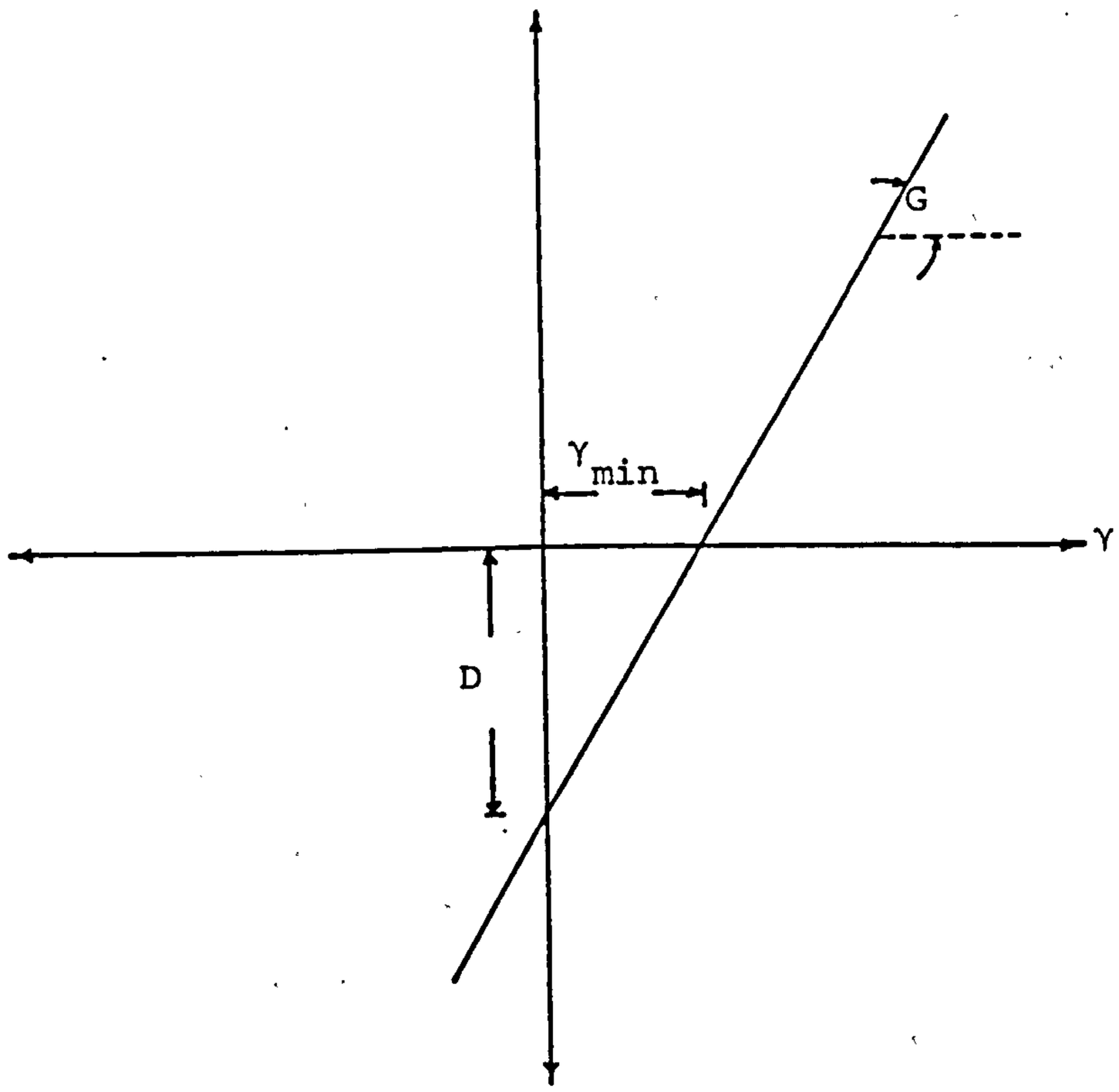

The relationship between the initial and final magnitude of the prestressing force

Figure (5.2)

CHAPTER 6

6. Construction of Prestressed Concrete Suspension Bridges

6.1 Introduction

The construction of this type of bridge shares many of the characteristic features of the construction of both ordinary steel suspension and conventional prestressed concrete bridges. For example, the suspender connections with both the main cable and the suspended beam are virtually identical to those used in conventional steel suspension bridges. Moreover, the type of anchorages installed at the ends of the prestressed cable suspended beam are the same as those used for conventional prestressed concrete beams. For this reason, we will concentrate, in this chapter, on the special features of the construction procedures of prestressed concrete suspension bridges.

As mentioned earlier,only four three-span prestressed concrete suspension bridges have been constructed, these in the vicinity of Gent, Belgium, which is the home of the inventor of this type of bridge, Vandepitte, (30) - (36). These bridges represent virtually all ranges of application as they have short, medium, long and fairly long spans. However, to the best of this writer's knowledge, no two-span prestressed concrete suspension bridge has yet been constructed anywhere in the world. Nevertheless, it is reasonable to believe that there is no significant difference between the construction techniques needed for two and three-span prestressed concrete suspension bridges.

Here, we give a brief description of the construction of two of the four already built three-span prestressed concrete suspension bridges, (32). These two bridges have been selected from the short and long span ranges, in order to demonstrate the construction procedure as well as to stress the advantages of using this type of bridge in each range of span length in a more practical manner.

Furthermore, we will also describe a new technique of prestressing two-span bridges by means of shortening the suspenders to develop the initial prestressing force.

6.2 The Methods of Construction for the Superstructure

The superstructure of prestressed concrete suspension bridges can be built in two different ways, by using scaffolding or by prefabrication. Scaffolding was successfully used for the construction of all the four bridges in the vicinity of Gent, Belgium, because they were all built across a canal which was not yet dug at the time of construction.

However, it is possible to construct prestressed concrete suspension bridges without the use of any scaffolding, (35), by dividing the suspended beam into a number of prefabricated segments. These segments can then be erected on a system of temporary trestles and stressed together by the main cable.

If the construction is such that intermediate temporary support is difficult or expensive (deep rivers or valleys), it would be possible to use the Cantilever method which has been successful in constructing many ordinary prestressed concrete bridges. As shown in Figure (6.1a), construction starts at the two ends of the suspended beam as well as the tower. At the tower, we begin by erecting equal number of segments on both sides in a balanced cantilever way and joining the new segments with the ones which precede them. At a later stage, the cantilevers may become too long to be self-supported and therefore, they are given temporary support by inclined cables, stays, Figure (6.1a). The tower is usually a portal frame structure, Figure (6.9), and is designed to the vertical forces developed by the cable at the point where it changes its slopes between the two spans.

The construction at both ends of the suspended beam begins by erecting the precast segments and supporting them by means of conventional auxiliary structures, (Figure (6.1a)). After establishing

the ends of the suspended beam, we lay down the main cable with the design eccentricities from the centre line of the suspended beam and start to install the suspenders in the designed positions (Figure 6.1b). Eventually, the construction of the suspended beam is completed when its three parts join and all the suspenders installed. Whence, all the segments of the beam become permanently joined after performing the prestressing operation. Consequently, all stays and auxiliary supports are to be removed, Figure (6.1c).

6.3 The Design and Construction of the Abutments

Figure (6.2) shows the left hand end of the suspended beam where the vertical and horizontal components of the cable tension are V_o and H, see Figure (2.4). This vertical component, V_o, acts as an upward force applied on that end of the beam and its maximum value is equal to F H_{max}, Equation (2.18a) where F is the cable slope at this end. In addition, more upward forces will be generated at that end as reactions, R, for the upward cable forces as well as the live loads applied in the right hand span and vice versa. Therefore, an extensive investigation must be carried out for all possible combinations of live loading which is likely to affect the bridge. As a result of this investigation and by making use of the shear forces equations given in Chapters (2) and (3), it will be possible to establish the values of the maximum upward forces applied at both ends of the bridge, Figure (6.2).

Obviously, as mentioned earlier in Chapter (1), these upward forces would lift the ends of the suspended beam unless some means of applying downward forces are affected at those ends. The cheapest and most effective solution for this problem is provided by means of the sheer weight of heavy concrete boxes filled with sand which act as abutments for the bridge, (32). The weights of these concrete boxes must exceed, on the whole, the values of those maximum upward forces at the ends of the beam.

The connections between the abutments and each end of the beam can then be installed as the type of support required at this particular end of the structure. We recommend that two of the three supports of the structure must be of the rollers, eye-bars, type with the third support a hinge of the Mesnager type. The reason for this arrangement is that the structure must be allowed to expand or contract freely due to temperature changes without any effect on its stresses. Furthermore, any small accidental horizontal reaction of the suspended structure would be transferred to one of the abutments through the hinged support.

6.4 The Prestressing Operation

6.4.1 The Methods of Prestressing

The suspended structure can be prestressed in many different ways. One of the methods is the conventional way of installing one of the anchorages at one end and applying a hydraulic jack at the other end. The cable is then pulled until its tension reaches the initial prestressing force value, H_i, and the second anchorage is installed. One of the disadvantages of using this method is that the suspenders will deviate from the vertical as a result of the prestressing operation. However, the connections between the suspenders and the main cable allow for the possibility of straightening them back to the vertical after the prestressing operation, Figure (6.7). It is possible to avoid the deviation of the suspenders by installing them deviated in the opposite direction of the jack pull prior to the prestressing operation. The amount of that deviation can be calculated for each suspender as a ratio of the total change in the cable length due to the initial prestressing force, Equation (2.35).

Another method to prestress the suspended beam is by raising the towers, or tower, Vandipette (32) and (35). This method has been successfully practiced in prestressing all of the four, already built, three-span bridges near Gent, Belgium. It has been proved to be the most efficient and economical method for prestressing three-span prestressed concrete suspension bridges. The basic idea

behind this technique is to take advantage of the increase in the cable length which results from raising the towers, or tower. This increase is always accompanied by an increase in the cable tension which can be calculated as mentioned in Section 2.3.4.4. Thus, a relationship between the tower rise and the cable tension can be established and used to precisely evaluate the amount of rise required to tension the main cable by the initial prestressing force.

The prestressing operation is carried out when the floor structure and the towers, or tower, are concreted, with the latter several centimetres below their, or its, design value depending on the span lengths. Hence, the main cables are strung without any tension and all their connections with the suspenders as well as their anchorages at the ends of the beam are installed. Then, the towers, or tower, are alternately jacked up in relation to the piers, or pier, by means of hydraulic jacks until they reach their design elevation, and steel hinges are subsequently inserted under the tower columns. The elevation of the road way above the piers remains unaltered by the prestressing operation as the towers, or tower, are entirely independent of both the road way and the piers, Figure (6.7). The suspenders are then straightened to the vertical as mentioned earlier.

Although this method is also applicable to prestress two-span bridges, it can hardly be recommended for this purpose. The reason for this is that changing the tower height has a smaller effect on the geometry of parabolic cables which their ends are at different levels than those with their ends at the same level. Consequently, the cable would gain lesser tension for the former than for the latter if the towers, or tower, were raised by the same distance for both types of parabolic cables. This is clearly illustrated when performing the calculation for the test beams by using Equations (2.27) and (2.35). It has been found that to tension the cable by 14.800 KN, the tower would have to be jacked up a distance of 51 mms. This is totally impractical when learning that the design height of the tower is 237.5 mms which means that it must be raised by more than 20% of its own height to produce the required cable tension. In other words, in full scale bridges we would need to jack up the tower

by perhaps several metres to tension the cable by the desired initial prestressing force. For this reason, this method is abandoned for the prestressing of our type of bridge.

An alternative method for prestressing two-span bridges is by shortening the suspenders. The principle behind this technique is, again, inspired by changing the geometry of the parabolic cable to produce the desired initial prestressing force. If we assume that each of the suspender lengths will be shortened by a ratio of Λ of its own design length, hence, the total change in the cable sags will be, from Equation (2.24):

$$\Delta f = + \Lambda \frac{\ell^2}{4} \sum_{m=1}^{i} \frac{l_{sm}}{x_m (\ell - x_m)}$$

$$\Delta f_1 = + \Lambda \frac{\ell_1^2}{4} \sum_{m=1}^{j} \frac{l_{s1m}}{x_{1m} (\ell - x_{1m})}$$

where positive signs in the equations indicate the increase in the original cable sags and where l_{sm} and l_{s1m} are the lengths of suspenders number m which are at distances x_m and x_{1m} from the left and right hand end supports respectively. i and j in the equations denote the total number of the suspenders in the left and right hand span, Figure (2.9).

These changes in the cable sags will subsequently change the cable lengths by amounts ΔS and ΔS_1 in the left and right spans which can be evaluated from Equations (2.25) or (2.26) for exact or approximate values. Consequently, the cable tension will also alter by an amount ΔH which can be calculated from Equation (2.35) when substituting by the values of ΔS and ΔS_1. Assuming no tension in the cable, thus, the ratio Λ by which the suspenders must be shortened to produce the initial prestressing force in the cable can be calculated as follows:

$$\left[\frac{\left[5\left[2-3\ (F+4n)^2\ \right] - 48n^2\right]}{\left[1+F\ (F+8n) + \frac{64}{3}\ n^2\ \right]} \sum_{m=1}^{i} \frac{l_{sm}}{x_m\ (\ell - x_m)} + \omega\lambda^2 \frac{\left[5\left[2-3\ (F_1+4n_1)^2\right] - 48n_1^2\right]}{\left[1+F_1\ (F_1+8n_1) + \frac{64}{3}\ n_1^2\right]} \right.$$

$$\sum_{m=1}^{j} \frac{l_{slm}}{x_{lm}\,(\ell_l - x_{lm})} \Bigg] \Lambda = \frac{15}{2} \frac{H_i}{A_c E_c f} \qquad (6.1)$$

in which $f = \frac{W\ell^2}{8\,H_w}$,

$n = \frac{f}{\ell}$,

$F = \frac{h+a\ -\ 4f}{\ell}$,

$F_l = \frac{h+a\ -\ 4f_l}{\ell_l}$,

$f_l = \omega\lambda^2 f$,

$n_l = \omega\lambda n$,

$\omega = \frac{W_l}{W}$,

and $\lambda = \frac{\ell_l}{\ell}$.

In practice, after laying down the cable, untensioned, the suspenders are installed with their lengths (1 + Λ) times their original design values. Hence, by shortening each suspender by a distance Λ times its design length, the main cable will be tensioned by the desired initial prestressing force and the final lengths of the suspenders will be equal to their design values. The suspenders can be shortened by means of any height adjustment device which is capable of sustaining the suspender load.

When applying Equation (6.1) to the test beams, it has been found that each suspender needed to be shortened by 12.3% of its own design length to produce a force 14.800 KN in the main cable. After shortening the suspenders by the above ratio, the force in the main cable has been measured to be 14.200 KN. This error may have been due to increasing strains in the suspenders which effectively reduced the shortening ratio Λ or due to some initial slipe on the main cable

anchorages. Consequently, the ratio Λ had to be increased to the value 12.8% to produce the desired initial prestressing force. It is reasonable to assume that for a full size bridge this error would not take place as the suspenders are much more rigid than those used for the test beam. However, if such error should take place, it can easily be corrected by shortening the suspenders by a further distance and monitor the prestressing force until the correct value is reached. The effect of the extra shortening below the design lengths on the behaviour of the structure can then be taken into account by making use of Equations (2.25 - 27) for ungrouted and grouted two-span prestressed concrete suspension bridges.

One advantage of using this procedure is that by keeping record of the initial prestressing force as time passes, any losses due to time effects in this force can easily be corrected by shortening each suspender a further distance LΛ times its design length, where L denotes the percentage loss in the prestressing force at this particular time. Moreover, as the bridge ages towards the end of its working life, all cracks can be eliminated by a further shortening of the suspenders to increase its prestressing force and consequently prolongs the bridge service life.

Another advantage of prestressing the suspended beam by shortening the suspenders is that unlike the other methods of prestressing, the suspenders remain straight after being shortened. Therefore, no extra time of labour is required to straighten the suspenders back to the vertical position.

6.4.2 The Methods of Checking the Value of the Prestressing Force

The prestressing force can be checked in many different ways. The most accurate method is by using strain gauges at a particular position of the main cable. Hence, knowing the strain at this position, the stress can be evaluated and consequently the cable tension can easily be obtained at this position. Then, from Equations (2.13), the prestressing force can be determined. The advantage of using this method is that the strain gauges will

permanently remain on the main cables to monitor the decline in the prestressing force due to time effects which enable the designer to check the performance of the bridge during its working life.

Another method of checking the prestressing force is to measure it directly by using a load cell at one of the ends of the suspended beam. However, the readings of this load cell will most certainly be affected by the changes in the temperature. Therefore, we only recommend the use of strain gauges to monitor the prestressing force as they can be fully protected against any weather changes.

6.4.3 The Procedure of Grouting (For Grouted Prestressed Concrete Suspension Bridges)

Figure (6.3) shows the grouting duct through which the cable passes at both ends of the suspended beam. The grouting duct is usually made of spirally wound corrugated steel and has an internal area which must be at least twice the area of the main cable, (37). The figure also shows one of the injecting vents which are required at distances 600 mm from the anchorages. These vents are highly recommended since the injection points at the cable anchorages are often found to be inadequate.

The grout is usually made of cement and water with the ratio 3:1 in weight. The use of sand is not recommended unless ducts of exceptionally large section (greater than 150 mm diameter) are to be grouted. If a fine aggregate is necessary, it should pass a 1.18 mm sieve and consist of finely ground limestone or quartz, (37). The weight of fine aggregate added should not exceed 30% of the weight of the cement.

Admixtures may be used to improve the fluidity of the grout. Usually these admixtures contain aluminium powder as their main active ingredient. The weight of this powder should never exceed 0.03% of the weight of cement to avoid any chemical reaction taking place with the cement, (37).

Grouting starts after 6 - 24 hours from the time of prestressing. The grout is injected by using pumps at a steady rate beginning from the anchorages. The grouting operation is completed when the grout starts to flow out of the other end of duct, at the surface of the beam. If the length of the duct is more than 15 m, an extra vent would be essential at its midpoint to check the fluidity of the grout. After 3 days, the grout will become hard and the beam will be ready to start its service life, (37).

6.5 Examples of already Constructed Three-Span Prestressed Concrete Suspension Bridges

6.5.1 The Bridge at Merelbeke

(a) Design and Construction

Figure (6.4) shows the elevation of the structure built at Merelbeke near Gent, Belguim, (32). It was built to span across a new canal that was not yet dug at the time of construction. Tenders were sought for this design and another one involving conventional continuous prestressed concrete beams. The prestressed suspension design was cheaper by about 8%.

Figure (6.4) also shows the bridge with the centre span alone is suspended. If the side spans were longer, they too would be suspended. The bridge comprises two prestressed concrete suspended beams which are continuous over their interior supports. The main cables are of parabolic geometry with their ends at the same level in the centre span. The cable sags are 4.04 ms as shown in the figure.

Figure (6.5) shows one half of the longitudual section. The superstructure always tends to lift up the abutments due to the steep slope of the main cables in the side spans (a feature of the transformed profile of the prestressing cable). For this reason, the abutments were designed in the form of heavy concrete boxes filled

with sand so that their weight exceed the upward reactions applied on them. The superstructure is pin-connected to the two piers and one of the abutments by means of eye-bars, roller supports, which allow it to shorten and lengthen freely. The other abutment is connected to the superstructure by a hinge of the Mesnager type, hinged support, which transfers any accidental horizontal reaction that the superstructure may experience to that abutment.

Figure (6.6) shows a cross section of the roadway where the depth of the suspended beams is constant throughout their length and is equal to 1.60 m. The roadway slab acts as the upper flange of the suspended beams. The lower flanges, the webs and the slab were cast separately with shear keys along the joints between them. The floor beams are simply reinforced solely designed to carry part of the roadway slab as well as provide the connections between the suspenders and the suspended beam.

The suspenders are bent rods bearing on the cable bands. Figure (6.7) shows one of the cable bands where it is almost identical to that used in ordinary steel suspension bridges. Each one comprises two semi-circular steel castings which are bolted together in order to clamp the cable tightly between them. The aggregate tension in the four bolts must develop sufficient friction between cable and band to prevent it from slipping towards the lowest point of the cable curve. As mentioned earlier, this type of connection between cable and suspender allows the latter to be straightened in case of any deviation from the vertical due to the prestressing operation.

Each cable is composed of 510 galvanized steel wires which are 5mm diameter each. Apart from the zinc coating, which protects it against the weather conditions, they hardly differ from those generally used in prestressed concrete structures. The wires were not twisted into strands, but are parallel forming a compact cylindrical cable of 125 mm diameter. In fact, the two main cables are parts of one endless strand which loops around the two end blocks of the bridge deck, Figure (6.8). At one point, the 510 - wire cable divides into three 170 - wire strands the lowest strand remains

parallel to the sloping plane defined by the cables in the side span. The other two strands are bent up in the manner showed in the figure. Each of the three strands is placed in a curved channel which is applied against the end block. Splicing of the individual wires was affected by wrapping their overlapping ends with fine wire.

Figure (6.9) shows a cross section of the roadway, its connections with one of the piers and one of the towers. The figure also shows the saddles on the top of the tower which are made of cast iron and solely designed in order to accommodate the cable. The concrete towers and their bracings were not cast in their design position as shown in the figure but were 37 cms lower. They were in the latter position while the main cable was placed untensioned and all its connections with the suspenders and the anchorages were installed. The figure shows the ties between the suspended beam and the foundation at the tower position which are designed in order to prevent the beam from lifting up due to the upward cable forces.

(b) <u>The Prestressing Operation</u>

Prestressing of the entire superstructure was affected by raising the towers, as mentioned earlier in this chapter, by using hydraulic jacks. Two jacks were needed under each column, i.e. total number of jacks required were eight. Since the cables were tied to the roadway at the end blocks and by the suspenders, the 37 cms rise of the towers forced the cable to elongate and thus produced in each cable the desired tension of 6984 KN.

When each tower had been jacked up 37 cms, a cast-steel hinge was inserted under each of its columns between the two jacks. The elevation of the roadway was not altered by the prestressing operation as each tower was constructed entirely independent of the roadway and its connections with the piers, Figure (6.9). Before the prestressing operation, the suspenders were installed with each one of them deviating 94 mms from the vertical starting of the towers and

reaching zero deviation at the midpoint of the centre span. As a result of the prestressing operation, all the suspenders became in plumb.

In order to check the prestressing force in the cable, two rings spaced 2440 mms were clamped on each cable close to the mid-point of the centre span before the prestressing operation. Thereafter, the increase in the spacing between the two rings was measured to be 9.10 mm. By performing this simple operation, the average strain in the cable was known and consequently, the cable tension was checked.

(c) Protection of the Wires

The steel wires were protected against corrosion by using zinc coating. Additional protection of the cables was provided by a layer of soft galvanised wires of 3.50 mm diameter wrapped around the cable, under tension, after the prestressing operation. This method of screening the cables was borrowed from American suspension bridge construction practice.

6.5.2 The Bridge at Mariakerke

(a) Design

Figure (6.10a) shows the elevation of the bridge at Mariakerke near Gent, Belguim, (32). It was built to span across the same canal as the Merelbeke bridge. Both bridges are designed on the same lines, but the one at Mariakerke is nearly twice as long and more than twice as wide as that at Merelbeke.

The three spans are suspended. The cable sag in the 100 m centre span is 9 m. The suspended beams are 1.90 ms deep throughout their length. The cables have a diameter of 200 mm where each is composed of 1780 galvanised 5 mms wires. Each suspender consists of two eye-bars that are pin-connected to the cable band and to the end

of the floor beams. The rest of the details of the structure are identical to those mentioned earlier for the Merelbeke bridge but, of course, at a much larger scale.

(b) The Prestressing Operation

Prestressing was affected by raising the towers a distance of 72 cms. This was achieved by the aid of eight 300 ton jacks, two placed under each column of the two towers. The prestressing force for the entire cross section of the bridge was 54713 KN. Most suspenders were out of plumb before the prestressing by a maximum deviation 200 mms at the towers and diminishing to zero deviation at mid-point of the centre span.

The methods for checking the prestressing force and protecting the main cables against the weather conditions were identical to those used for the Merelbeke bridge.

6.5.3 Comments

Clearly, the choice of the aforementioned two examples with their main span lengths 56m and 100m demonstrates some of the advantages of this type of bridges. The interaction between the main cable and the suspended beam was found to decrease the live load moments by 10% for the Merelbeke bridge. On the other hand, the decrease was found to be as much as 25% for the Mariakerke bridge, (32). This clearly demonstrates that the bridge at Merelbeke is not a very representative specimen of this type of bridge. The reason for this is that the length of its spans is quite close to the lower limit of the range of span lengths defining the natural field of application of the system.

A two-span grouted prestressed concrete suspension bridge might have provided a better solution for the bridge at Merelbeke. The left hand span could have been 60 ms with the right hand span 32 ms, the depth of the suspended beam 1.30 m and remaining constant

throughout its length, Figure (6.11). The eccentricities at the ends of the main cable could have been 0.22 m from the centre line of the suspended beam. The shape of the cross section of the bridge would have been similar to that shown in Figure (6.6). The total prestressing force would have been in the order of 11390 KN., if using tower height equal to 8 m. The prestressing operation could have been carried out by shortening each suspender by a distance about 14% of its own design value. The interaction between the main and the suspended beam could have decreased the live load moments by as much as 38%. The cost of such design should have been cheaper than the Merelbeke bridge as only one tower and one pier are required as well as a lesser prestressing force.

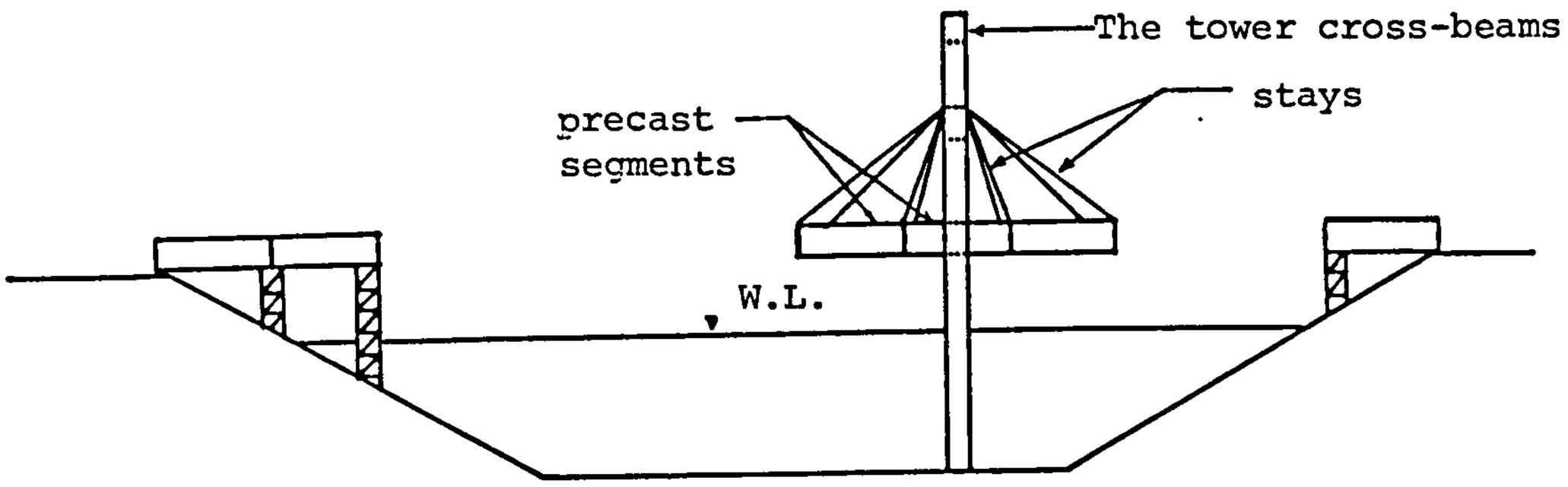

(a)

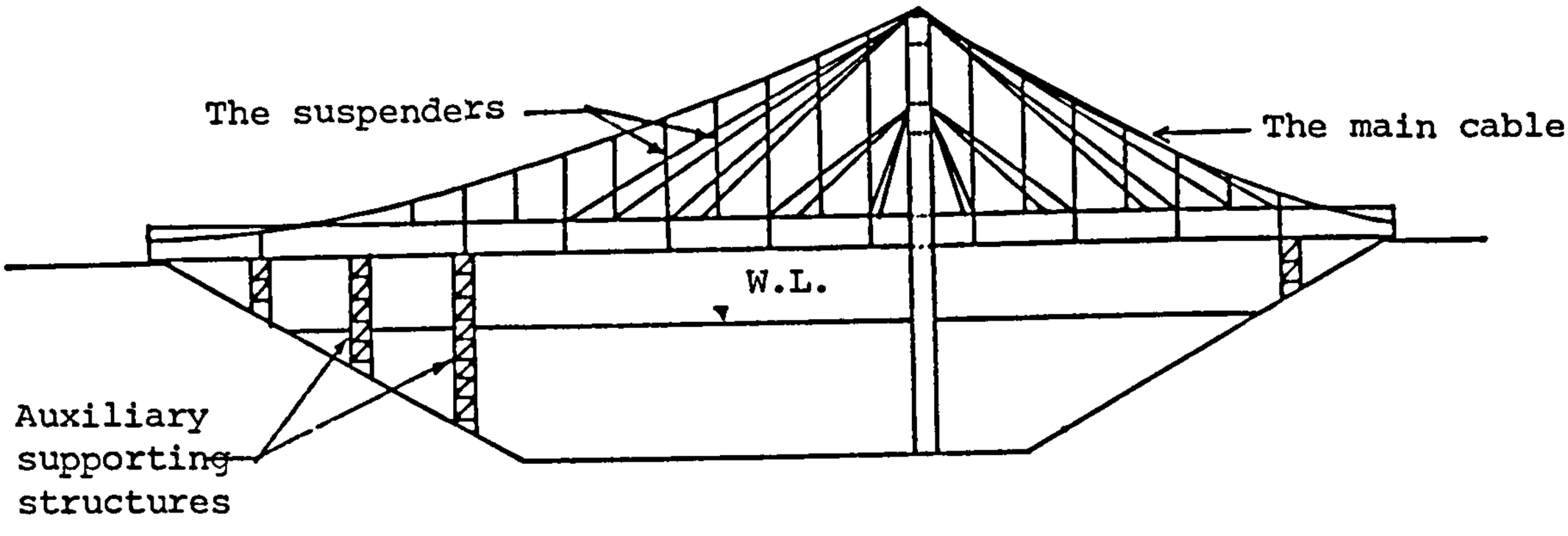

(b)

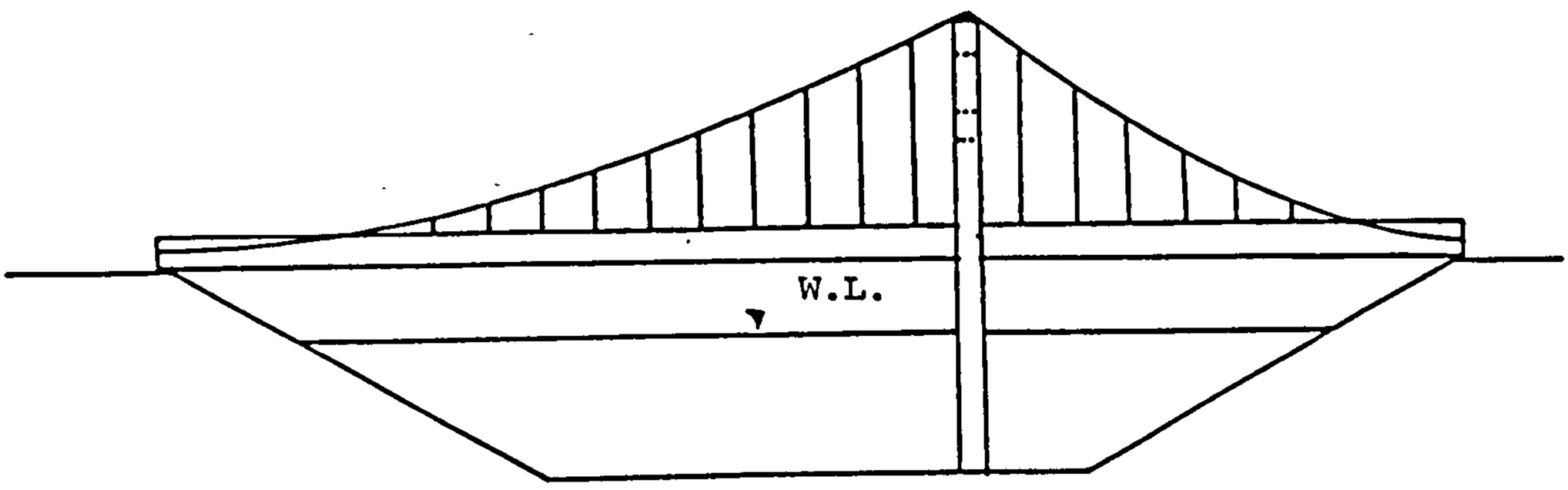

(c)

An impression of the construction of a two-span prestressed concrete suspended beam without scaffolding

Figure (6.1)

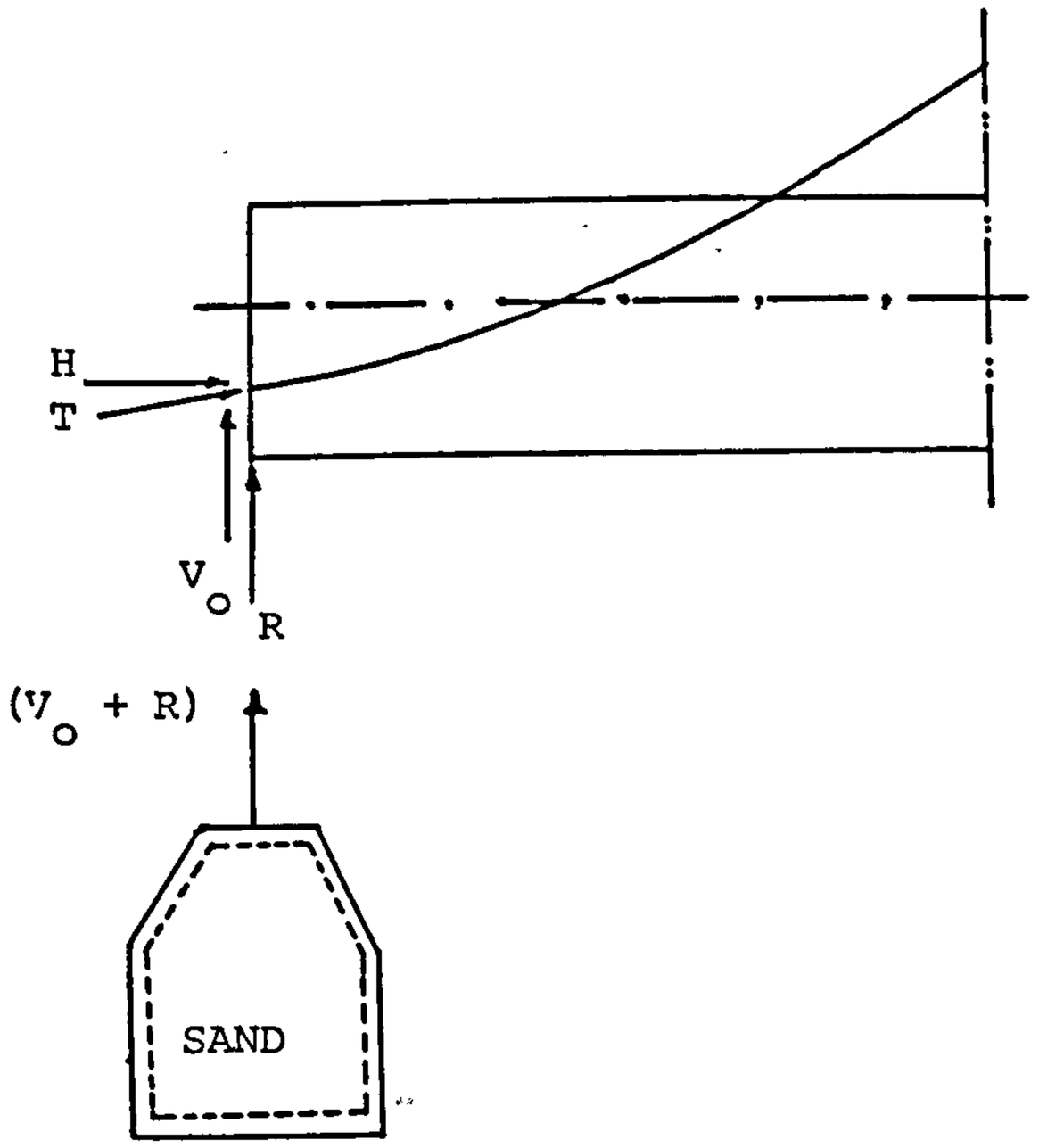

The upward forces applied at the ends of the suspended beam

Figure (6.2)

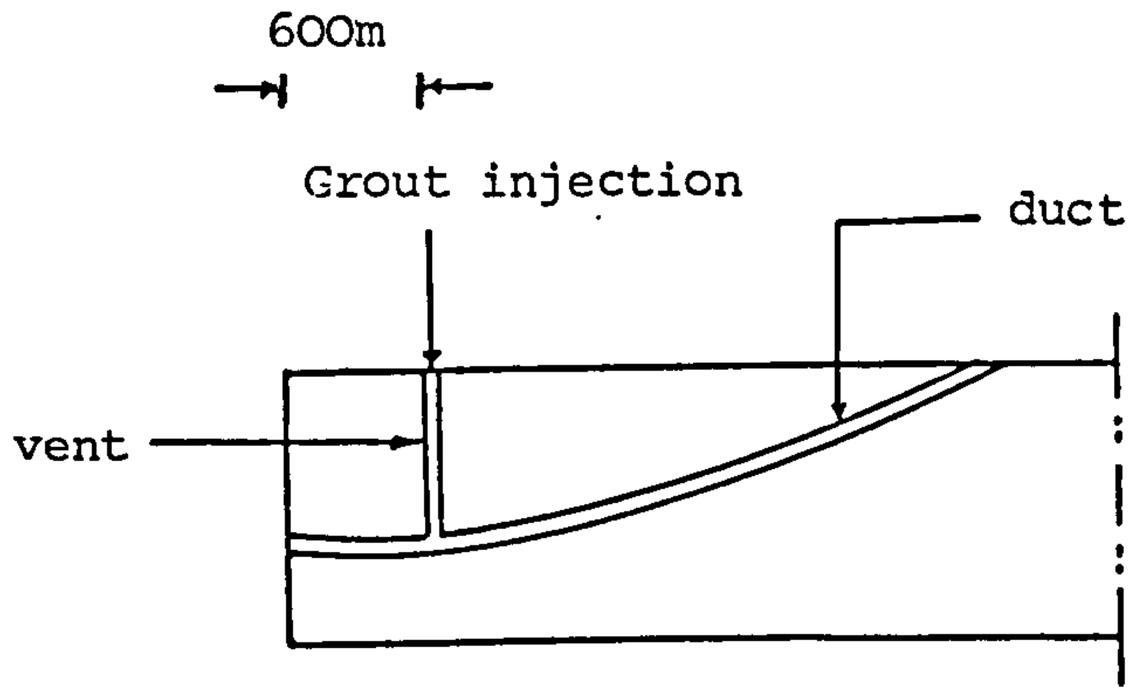

The grouting procedure

Figure (6.3)

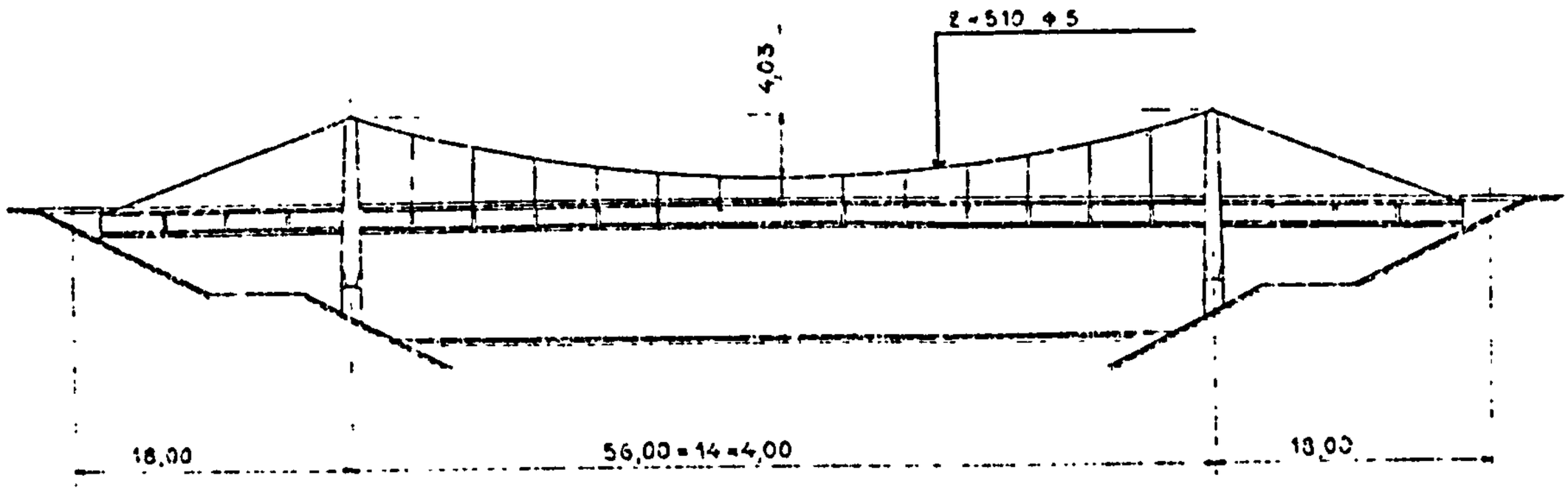

The Merelbeke bridge at Gent (Belgium)

Figure (6.4)

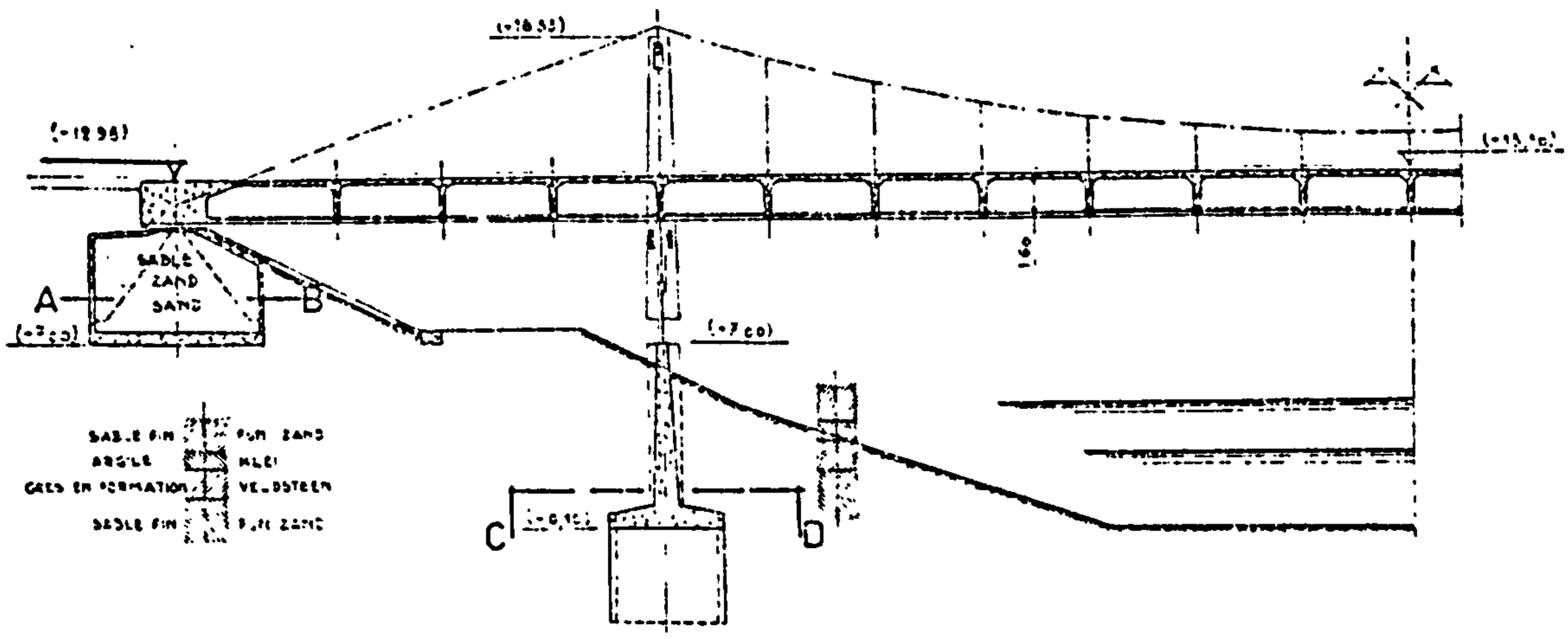

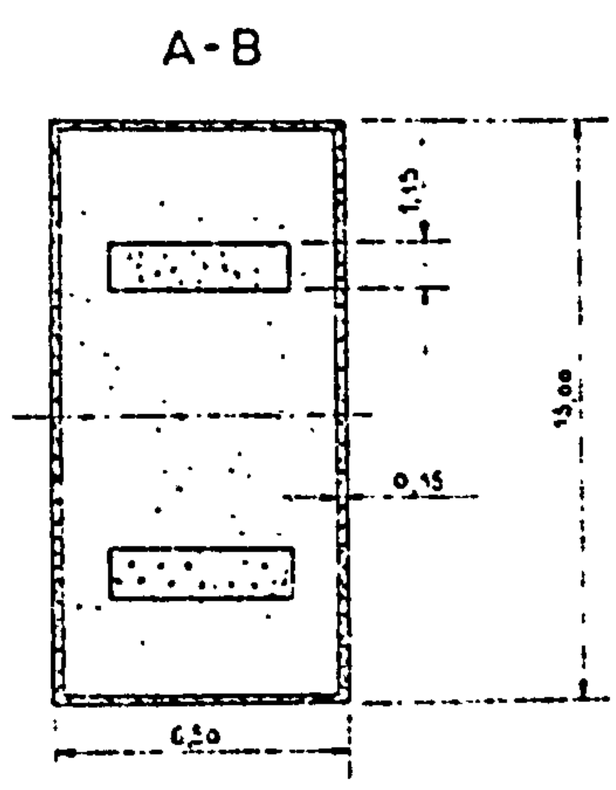

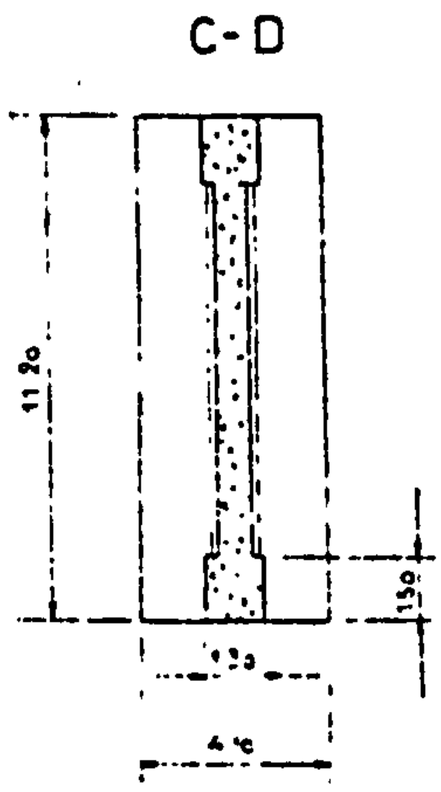

Half longitudual section of the Merelbeke bridge

Figure (6.5)

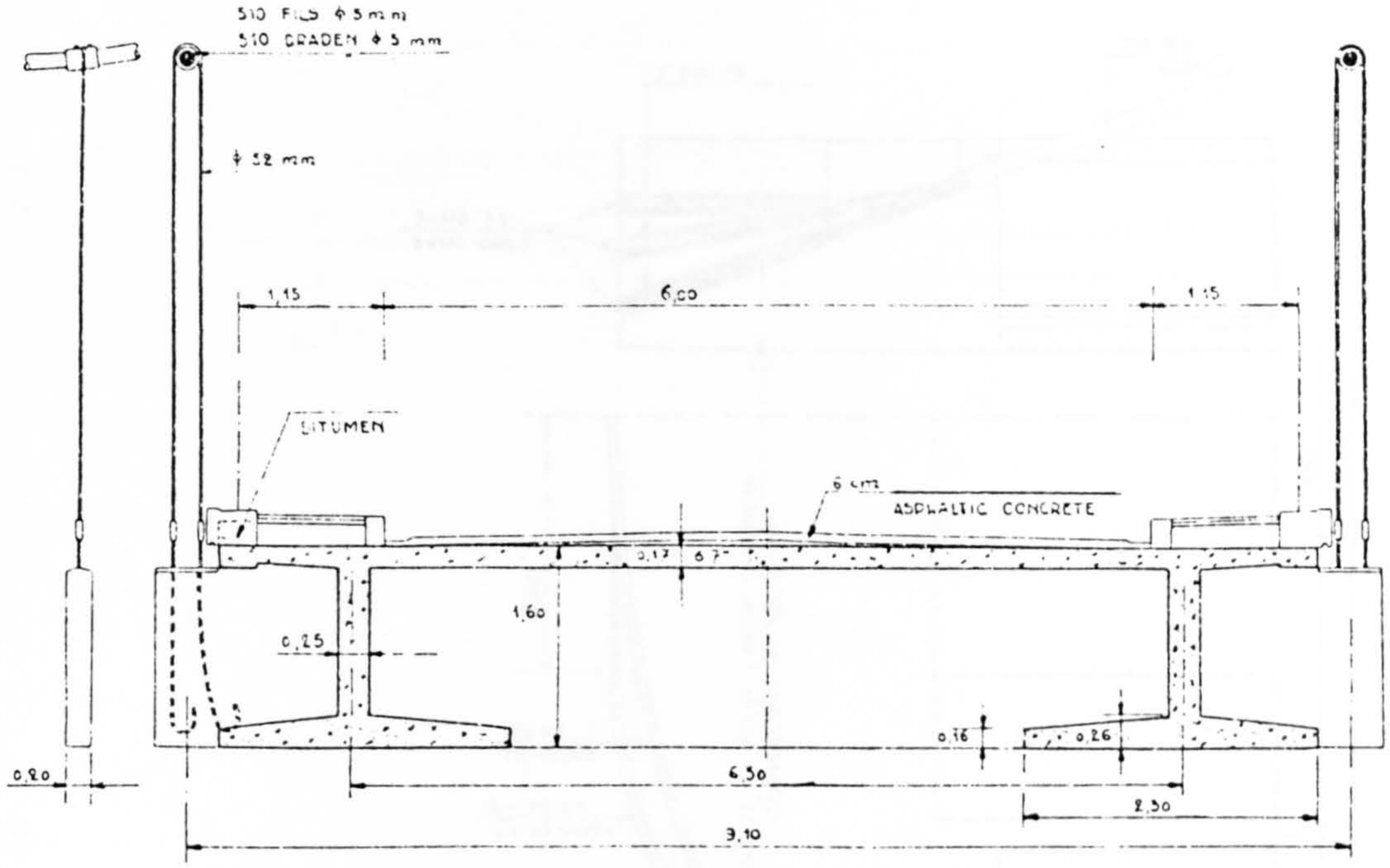

Cross-section of the roadway

Figure (6.6)

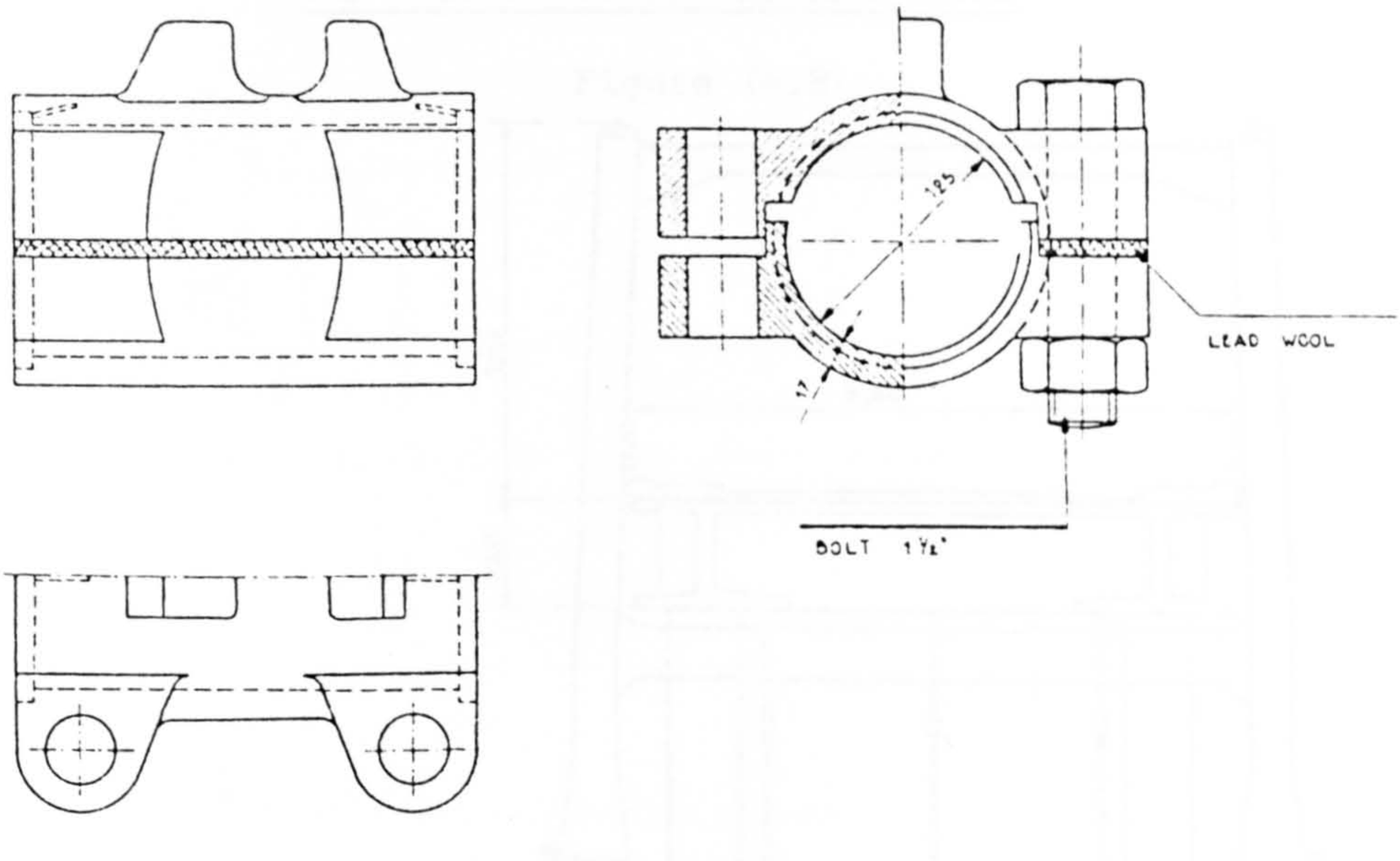

The cable band

Figure (6.7)

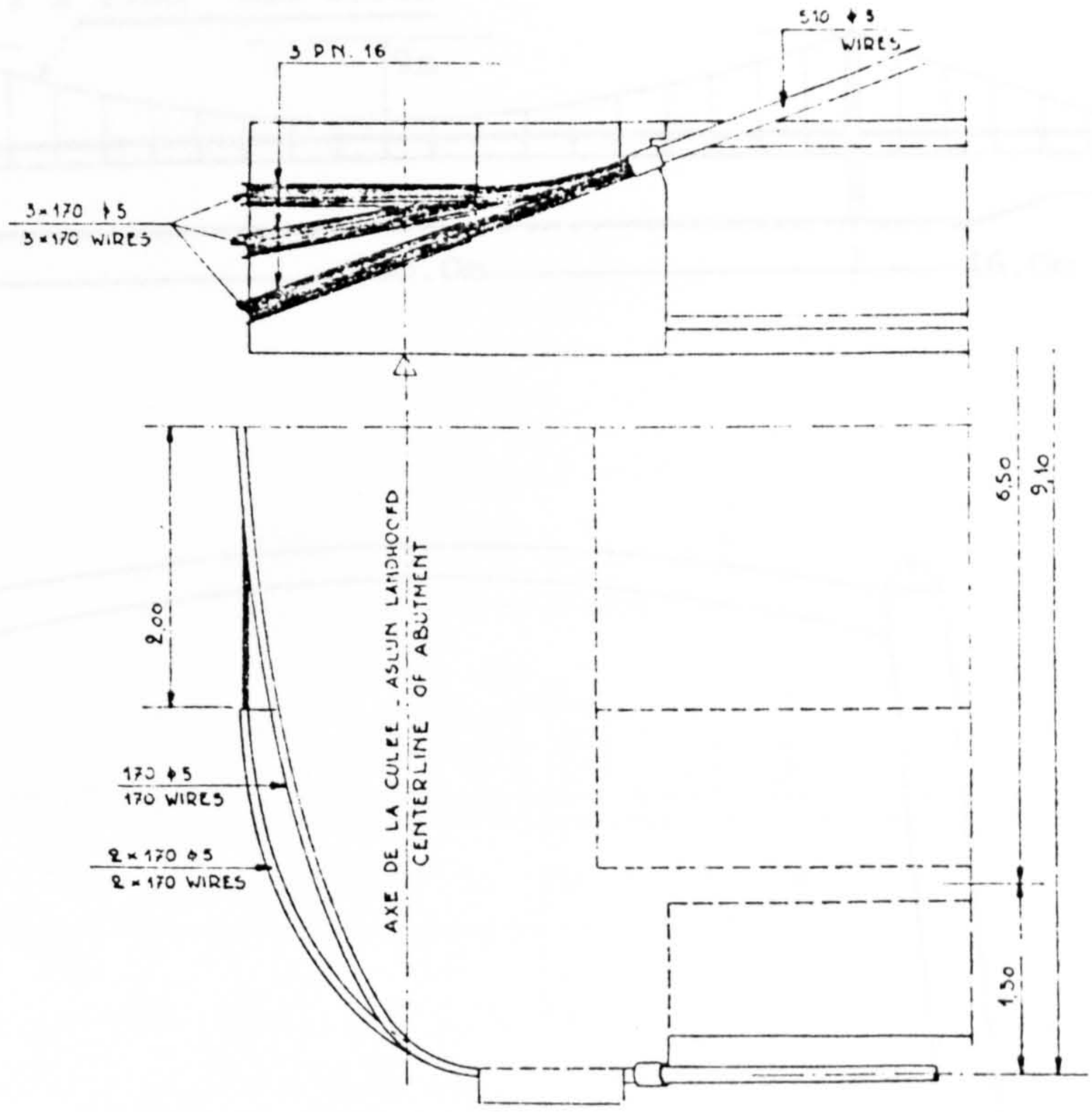

The main cable at the end block

Figure (6.8)

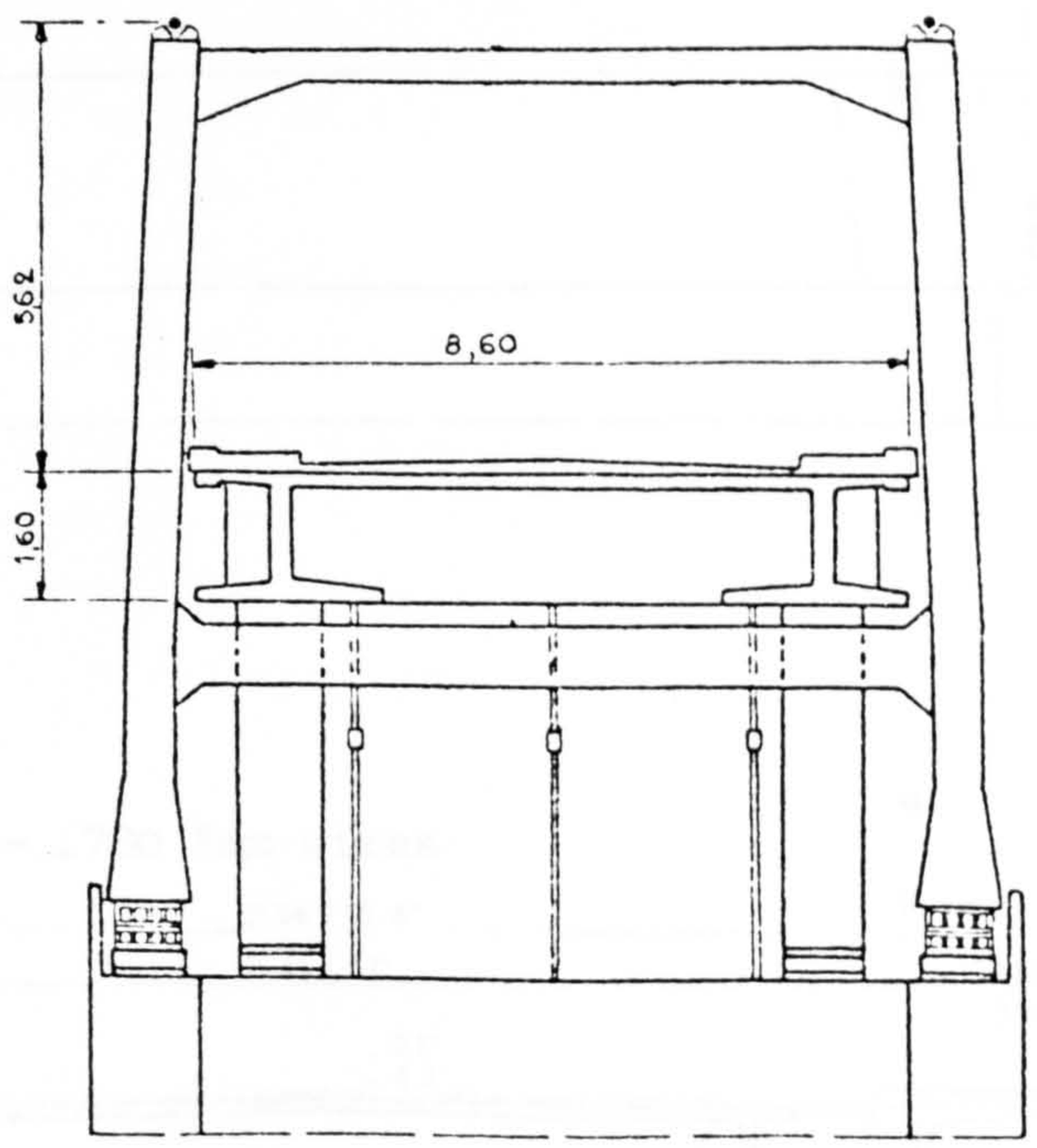

Simplified cross-section

Figure (6.9)

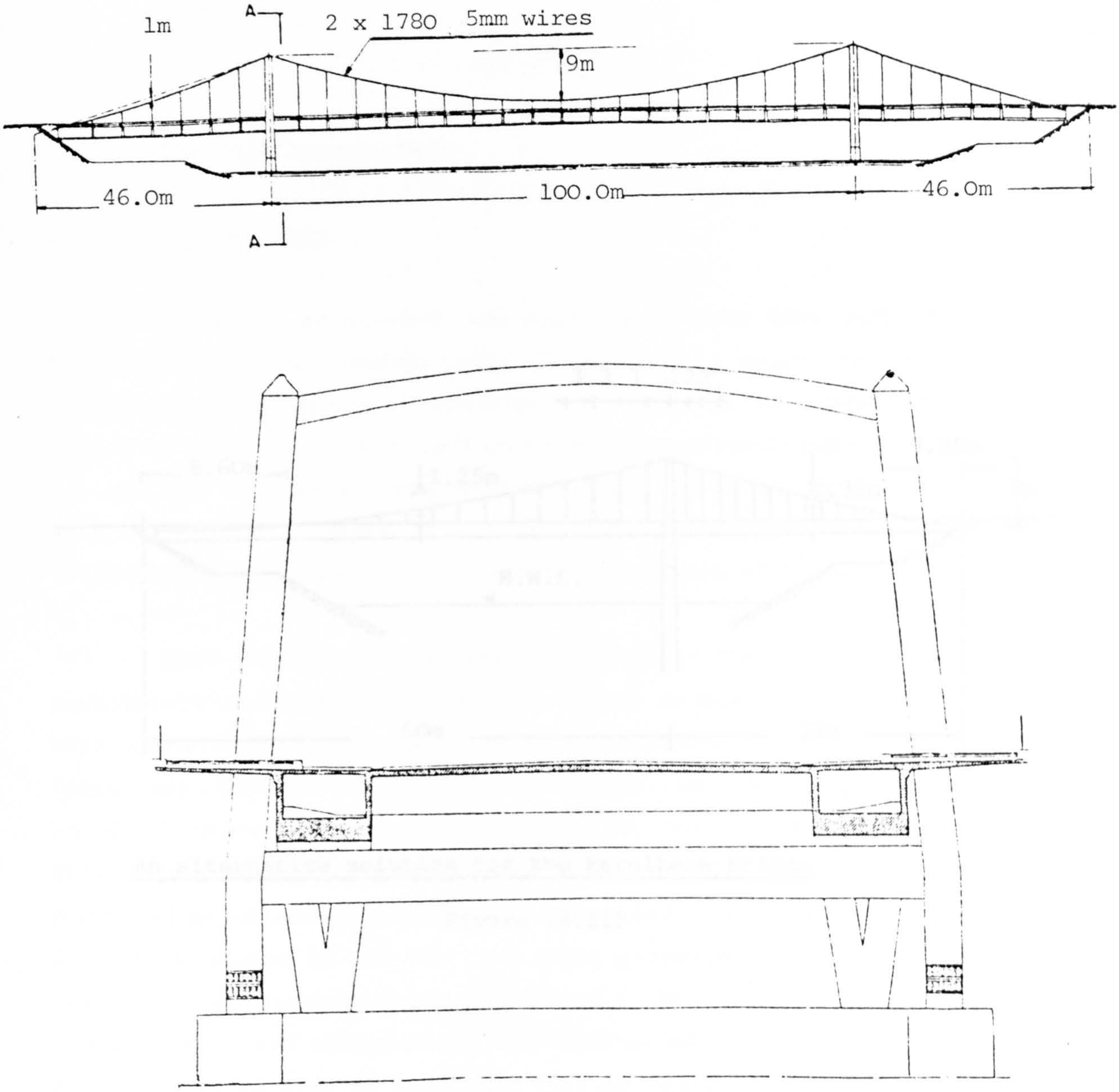

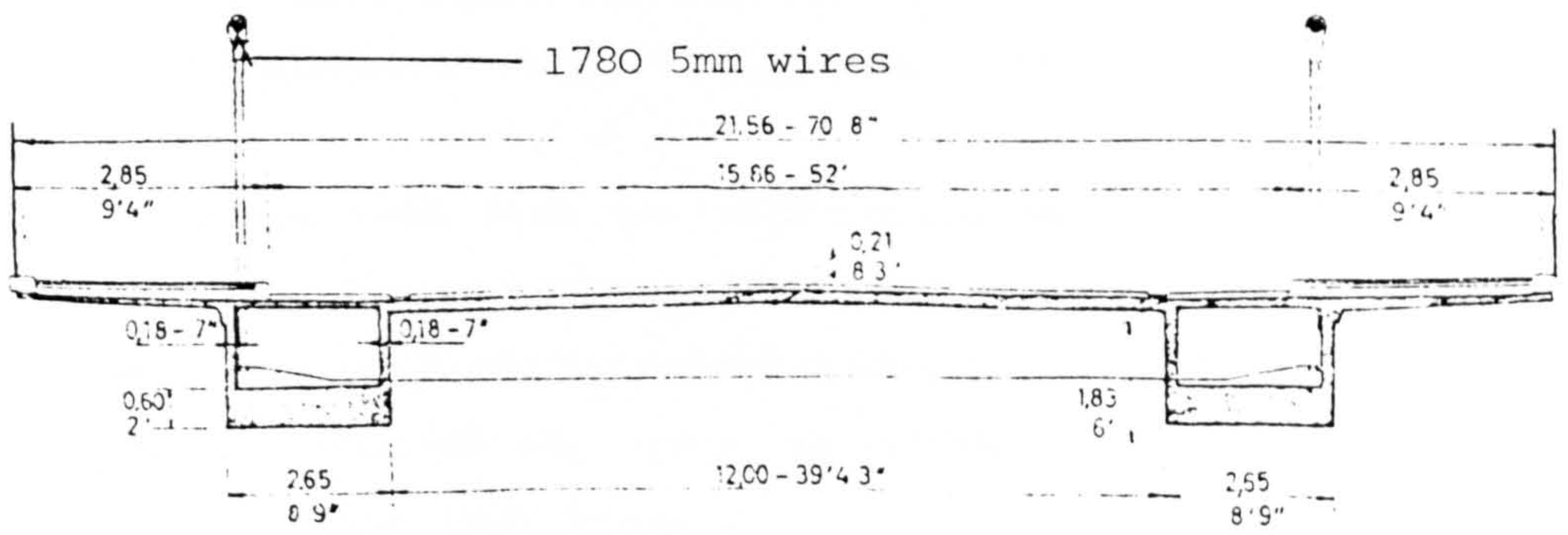

The Mariakerke bridge

Figure (6.10)

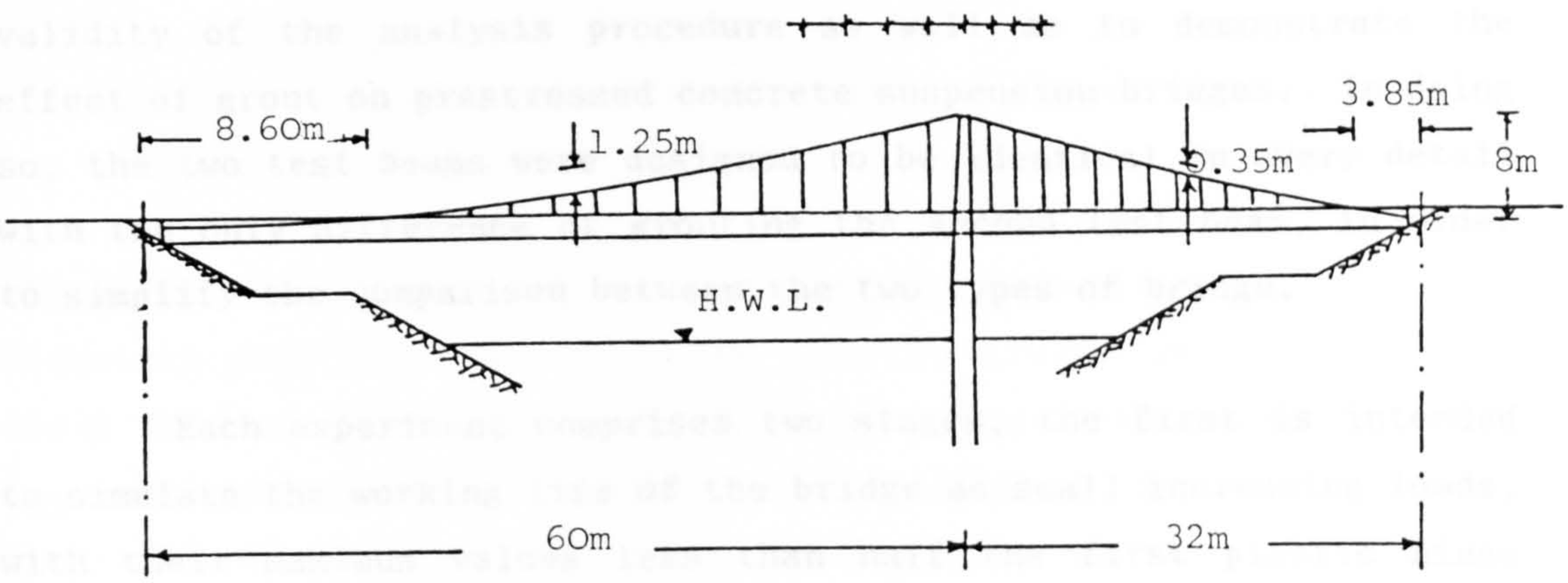

An alternative solution for the Merelbeke bridge

Figure (6.11)

CHAPTER 7

7. The Experimental Work

7.1 Introduction

As mentioned earlier, two experiments have been performed for the ungrouted and grouted types of bridge in order to check the validity of the analysis procedure as well as to demonstrate the effect of grout on prestressed concrete suspension bridges. In doing so, the two test beams were designed to be identical in every detail with the only difference of grouting the second test beam, in order to simplify the comparison between the two types of bridge.

Each experiment comprises two stages, the first is intended to simulate the working life of the bridge as small increasing loads, with their maximum values less than half the first plastic hinge loads, were applied at different positions, and the resulting changes in the prestressing force as well as the bending moments and deflections were measured. The second stage of the experiments is concerned with the behaviour of the test beams at failure. To do so, a load was placed in the position which generated the maximum moments for the first stage and increased until the formation of the first plastic hinge and subsequently the failure of the structure. During this, the first plastic hinge and failure loads were recorded as well as the corresponding changes in the prestressing force, bending moments and deflections. For the two stages of each experiment, the results obtained and those found from the analysis, computer program in Appendix 28, were tabulated and plotted side by side in order to illustrate the accuracy of the theory behind the analysis.

The first test beam was prestressed by means of a hydraulic jack and for the second, the prestressing operation was carried out by shortening the suspenders, as mentioned in Section 6.4.1. The two methods were performed in order to produce the same amount of prestress for the two test beams.

It is convenient to start this chapter by a description of the properties of materials used for the test beams.

7.2 The Properties of the Materials Used for the Two Test Beams

Every precaution was taken to construct the two test beams to be identical in every respect. Therefore, they were both made of concrete with the following mix design:

Cement	:	Water	:	Fine Aggregate	:	Coarse Aggregate	
306	:	205	:	699	:	1140	kg/m^3

where the cement was of ordinary portland type and the maximum diameters for the sand particles and the gravel were found, by a sieve analysis test, to be 2360 μm and 10mm. the cube strength, f_{ult}, for the concrete was found to be 48.53 N/mm^2 for the first test beam and 50.12 N/mm^2 for the second one, at the time of the experiments. Their Young's moduli of elasticity, E, were determined from a bending test as three small beams, 1500 mms long, were cast with each test beam with identical cross section and reinforcement in order to eliminate any cause for errors. Whence, they were tested, as shown in Figure (7.1), and the values of Young's moduli of elasticity were computed from their load-deflection relationships to be 33.417 KN/mm^2 and 35.162 KN/mm^2 for the first and second test beams.

This bending test was also used to check the validity of the theory developed in Chapter (4) for the determination of the ultimate moment of resistance of the cross section of the small beams, with the axial force taken zero. The failure loads of these beams were all in close agreement with the predicted ones. To minimize the errors in the experiments, the conventional value of the reinforced concrete density, $\gamma_c = 25\ KN/m^3$, was not used as the weight of those small reinforced beams provided its exact value to average 24.73 KN/m^3 for both test beams.

The reinforcement used was made of mild steel with a 6mm diameter. Several specimens were pulled to determine its yield stress, f_y, and Young's modulus of elasticity, E_s, as they were found to average 379.85 N/mm^2 and 203.40 KN/mm^2 respectively. The stress-strain relationship of the reinforcement, as automatically plotted by the testing machine, was distinct in the manner shown in Figure (4.3), B.S. (5) and (18), as its stress ceased to increase for loads higher than the yield load while its strains increased excessively (until the strain reached about triple the value of the yield strain).

The main cable was made of a single wire indented high tensile steel of a 5mm diameter. Several specimens were tensioned and their Young's moduli of elasticity, E_c, and failure stresses were found to average 208.1 KN/mm^2 and 1768.0 N/mm^2. The theoretical yield stress, at 0.2% strain, was found to be 1682 N/mm^2. The suspenders were made of stainless steel wires of diameters 0.90 mm. Young's modulus of elasticity, E_{su}, was found as a result of several tension tests to be 236.6 KN/mm^2 and the failure stress averaged 2326 N/mm^2.

The tower was made of welded hollow tubes with the dimensions shown in Figure (7.6). Its material was an alloy of aluminium and steel which its Young's modulus of elasticity, E_T, was found by compressing several specimens, in order to simulate the stresses to which the tower will be subjected, to average 117.50 KN/mm^2.

7.3 The Design and Construction of the Different Parts of the Test Structures

7.3.1 The Test Beam

The suspended test beams were chosen to span for a total length of 5600 mm, with the left and right hand spans 3500 mm and 2100 mm respectively. Their cross sections were of rectangular shape with the dimensions and reinforcement shown in Figure (7.2). The dead load of the suspended beams was calculated to be 185.50 N/m^2 in

both spans. However, this value was regarded to be too small in comparison with reality, as the bending moments produced by the dead loads in full size bridges are usually of considerable values (more than the live load bending moments in most cases). Therefore, the dead loads were increased by means of hanging weights of 20 kgs to the bottom of the beam during prestressing in the manner shown in Figure (7.2) and Plate (1). The total value of the dead loads, W and W_1, became equal to 470.0 N/m' is both left and right hand spans where this value includes the average weight of the main cable, suspenders and hangers.

The value of the prestressing force was calculated with some allowance for small tension stresses to develop during the first stage of the experiments. The values of these tension stresses did not exceed 3 N/mm^2 for the case when the test beams experienced the development of the greatest values for the bending moments, for the load applied in the mid-point of the left hand span, as confirmed by the strain gauges at this position. The reason for allowing these tension stresses to develop was to simplify the task for the second stage of the experiment by bringing about failure sooner, as well as to minimise the prestressing force. Therefore, the most convenient preliminary value of the prestressing force, H_w, was found to be 14.800 KN as the stress in the main cable was about half its theoretical yield stress, 754 N/mm^2. It is worth mentioning that if the prestressing force was designed so that no tension stresses would develop, its value would have been 41.500 KN.

As the experiments were performed in a short period of time, the factor γ, which is used to increase the prestressing force to overcome the time effects, was not included in our design and consequently the initial prestressing force was also equal to 14.800 KN, $H_i = H_w$. Hence, the cable sags were calculated to be 49 mm and 17.50 mm in the left and right hand spans.

For simplicity, the main cable was chosen not to have any eccentricities at its ends for both test beams. The initial cable eccentricities, Figure (7.3b), were evaluated when the dead load bending moment diagram, Figure (7.3a), was divided by the preliminary

prestressing force. Then, as mentioned earlier, these initial cable eccentricities were transformed above the centre line of the beam by means of applying the linear transformation system shown in Figure (7.3c). It is worth noting that the system shown in this figure was chosen in order to produce the convenient tower height 237.50 mm above the centre line of the test beams. Consequently, the final cable eccentricities were obtained as shown in Figure (7.3d), where the suspender lengths can be calculated when subtracting half the thickness of the beam from the shown values. The figure also shows the lengths, $g\ell$ and $g_1\ell_1$, through which the cable passes the ends of the test beams by means of two ducts with the lengths shown. These ducts were made of corrugated steel with a diameter 8.0 mm and they were used to grout the cable in the second experiment.

The cable, at its final position, exerted upward forces exactly in balance with the dead loads, when tensioned by 14.800 KN (Equations (2.12)), for both spans of the test beams. This means that the test beams, at this stage, did not experience any internal bending stresses as they had straight centre lines, see Table 7.1. However, the ends of the beam had the tendency to rise above their supports due to the vertical component of the cable tension. For this reason, two clamps, which simulate the abutments, were provided at these ends in order to stop this effect in the manner shown in Figure (7.2) and Plate (2). Each of these clamps was fitted with a small lubricated ball at its tip in order to allow for rotations at the ends of the beam.

The maximum shear stresses in the two test beams were checked in order to make sure that only flexure failure takes place in the experiments. From the computer program, Appendix 28, the maximum shear force was found at the left of the intermediate support, for the ungrouted test beam, to be about 1750 N. Thus, according to B.S., (5), the maximum shear stress was found to be 0.27 N/mm^2 which is very safe when considering that the allowable shear stress, without the need for shear reinforcement, is 1.11 N/mm^2.

The test beams were supported by three bearings, as shown in Figure (7.2), two of which were rollers with the third hinged so that any horizontal movements would not affect the stresses of the structure. They were made of good quality hardened steel plates and cylinders with the dimensions shown in the figure. Moreover, due to the delicacy of the test beams, two auxiliary props were used for each one, one at the mid-point of each span, in order to decrease the dead loads stresses prior to prestressing. These were removed afterwards.

Finally, it is worth noting that the test beams were cured by means of a chemical product, sealocure, which was regularly sprayed up to the time of the experiments, about 30 days after casting. The cubes and the aforementioned small beams were also cured in the same manner.

7.3.2 The Design of the Suspenders

The suspenders for the two test beams were designed to sustain the cable forces which developed as a result of the failure loads, in order to ensure that they will not fail before the flexural failure of the test beams, assumption (2) Section 4.1. For full size bridges, the suspenders would be designed to sustain the maximum cable forces which result from an investigation in all cases of live loading likely to affect the bridge, Sections 2.6.2. and 3.5.2. Thus, from the computer program, Appendix 28, the total change in the prestressing force at failure was found to be 927 N and 1420.0 for the first and second test beams respectively. The corresponding maximum suspenders loads were calculated from Equations (2.86) and (3.60) to average 533 N/m' and 559 N/m' for the test beams. Consequently, the suspenders forces were evaluated as the reactions for the fictitious structure shown in Figure (7.4) and the maximum suspender force was found to be 462.0 N at suspender number (1).

As mentioned before, the suspenders were made of stainless steel wires of 0.9 mm diameter and their connections with the main cable and the test beams were installed in the manner shown in Figure

(7.5) and Plate (3). The figure and plate show that the suspenders were bent around wheels, through which the cable passes, and a collar was provided for each wheel to prevent them from slipping towards the lower point of the cable curve. On the other end, the suspenders were joined to the top fibre of the test beams by means of two hollow bolts, Figure (7.5), which were screwed into two small tubes of steel. These tubes were attached to the stirrups, of the test beam, and embeded in the concrete.

As two branches were used for each suspender, this resulted in a much stronger link between the main cable and the test beam as the maximum stress in the suspenders was calculated for suspender number (1), Figure (7.4), to be only 365.0 N/mm^2. Furthermore, as the suspenders extensions could reduce the upward forces exerted by the main cable on the structure, assumption (3) Section 2.1, they were calculated and their maximum value was found to be about 0.01 mm in suspender number (6), see Figure (7.4). Whence, by making use of Equations (2.24, 25 and 35), their effect on the prestressing force was evaluated to be insignificant. In addition, the task of shortening the suspenders, to prestress the second test beam, was simplified as each of the aforementioned two bolts was screwed into the small steel tubes by half the required distances, as will be discussed later.

In fact, the above procedure may suggest an economical alternative for the suspender connections with the main cable in full size bridges, as the use of wheels and collars requires less labour and materials than the other method described in Section 6.5.1, Figure (6.7). Consequently, the use of undivided suspenders will most certainly result in a more efficient link between cable and beam than having to use two lengths in the manner shown in Figure (6.6). Furthermore, if the suspenders became out of plumb, due to the prestressing operation, they can easily be adjusted by making use of the collars, Figure (7.5) and Plate (3).

7.3.3 The Design of the Tower

As mentioned earlier, the tower was made of a number of hollow tubes which their material was an alloy of aluminium and steel. These tubes were welded together with the configuration and dimensions shown in Figure (7.6) and Plate (4). The figure also shows that the tower was provided with an adjustable screw at its top in order to correct the tower height to its designed value which is 200 mm above the top fibre of the test beams. This adjustable screw head was also used for the purpose of checking the validity of the method of prestressing the test beams by raising the tower as the rise required to produce 14.800 KN in the cable was about 51 mm. Although the calculations proved accurate, it is not recommended to be used for full size bridges for the reasons mentioned in Section 6.4.1.

The tower was designed to sustain the forces produced by the main cable at failure, similarly to the suspenders. These forces were calculated by using Equations (2.89) and (3.61) to be 4.243 KN and 4.376 KN for the first and second test beams respectively. The maximum compression stress was calculated to be 16 N/mm^2 for the tower with a corresponding change in its height about 0.03 mm. Clearly, the latter is very small and did not affect the cable tension.

7.4 The Arrangement of the Measuring Devices and The Loading Stations

Figure (7.7) and Plate (1) show positions (A - H) which were used, by means of hangers, to provide the extra dead loads as mentioned earlier. They were also used as loading stations for the first stage of the experiments as the live loads were hung to the bottom of the dead loads in the manner shown in plate (5). Displacement transducers were placed in positions (1 - 6) to measure the deflections as they were calibrated, prior to the experiments, and connected to a data logger, Figure (7.7) and Plate (6).

Strain gauges, 120 ohms, were also used in order to measure the stresses and bending moments at positions C, Tower and G, Plates (4) and (6). They were placed, two at each side, at distances 10 mm from the top and bottom fibres of the beam. Each of the top and bottom pairs were connected together in parallel in order to produce two strain gauges of resistance 240 ohms each which effectively average the strains on the two sides of the beam at the specified distances. Thus, they were all connected to the same data logger, used for the transducers, in order to calculate the average differences of voltage for each one due to the applied loads. Subsequently, those voltages were translated into strains by means of a factor which was supplied with the strain gauges by the manufacturer.

The prestressing forces for the two experiments, were measured by two methods, the first was carried out by placing four strain gauges, in a full bridge arrangement, on the cable at a distance 175 mm from the tower in the right hand span, Figure (7.7) and Plate (4), these gauges were connected to a strain indicator in order to directly measure the strains in the cable at this position. From Equation (2.13b), the cable tension at this position was found to be equal to 1.01 the prestressing force. It is worth noting that both the cable gauges and the strain indicator were calibrated in relation to each other as a specimen of the cable, with the gauges placed in the same arrangement, was tested against an accurate recently calibrated loading machine prior to the experiments.

The second method uses a load cell to measure the prestressing force directly at the right hand end of the test beams. It was made of a thin walled aluminium tube, in order to increase its sensitivity to small loads, with four strain gauges, two vertical and two horizontal, in a full bridge arrangement. The load cell was connected to the aforementioned strain indicator, by a switch box, as they were both calibrated in relation to each other against an accurate recently calibrated loading machine prior to the experiments. Then, the load cell was placed between the right hand cable anchorage and the end of the beam which was protected by a steel plate as shown in Figure (7.7) and Plate (2).

Finally, the load cell had a limited use for the second experiment as it did not register any changes in the initial prestressing force in both stages of the experiment due to the effect of grouting. Therefore, the cable gauges provided the only method used to determine the effect of the interaction between the cable and the grouted test beam on its prestressing force.

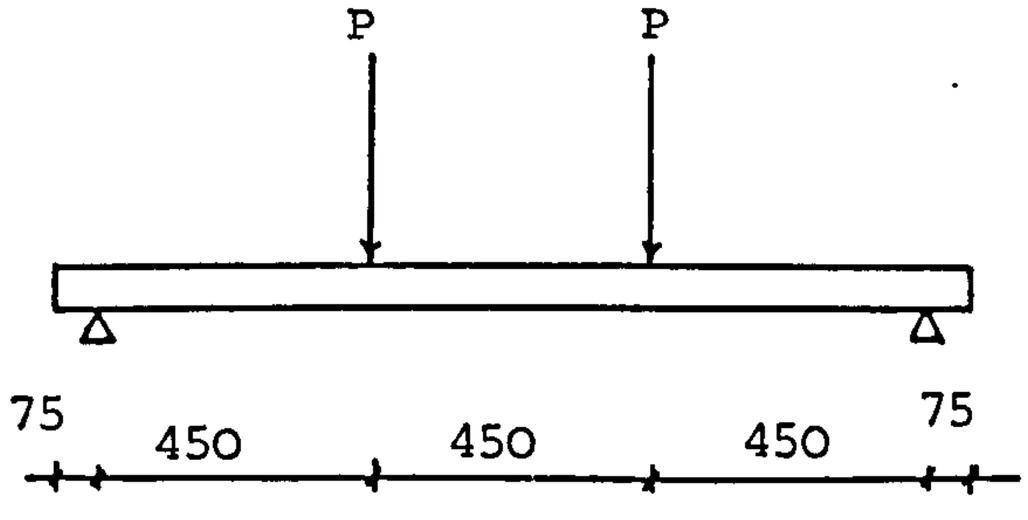

The bending test

Figure (7.1)

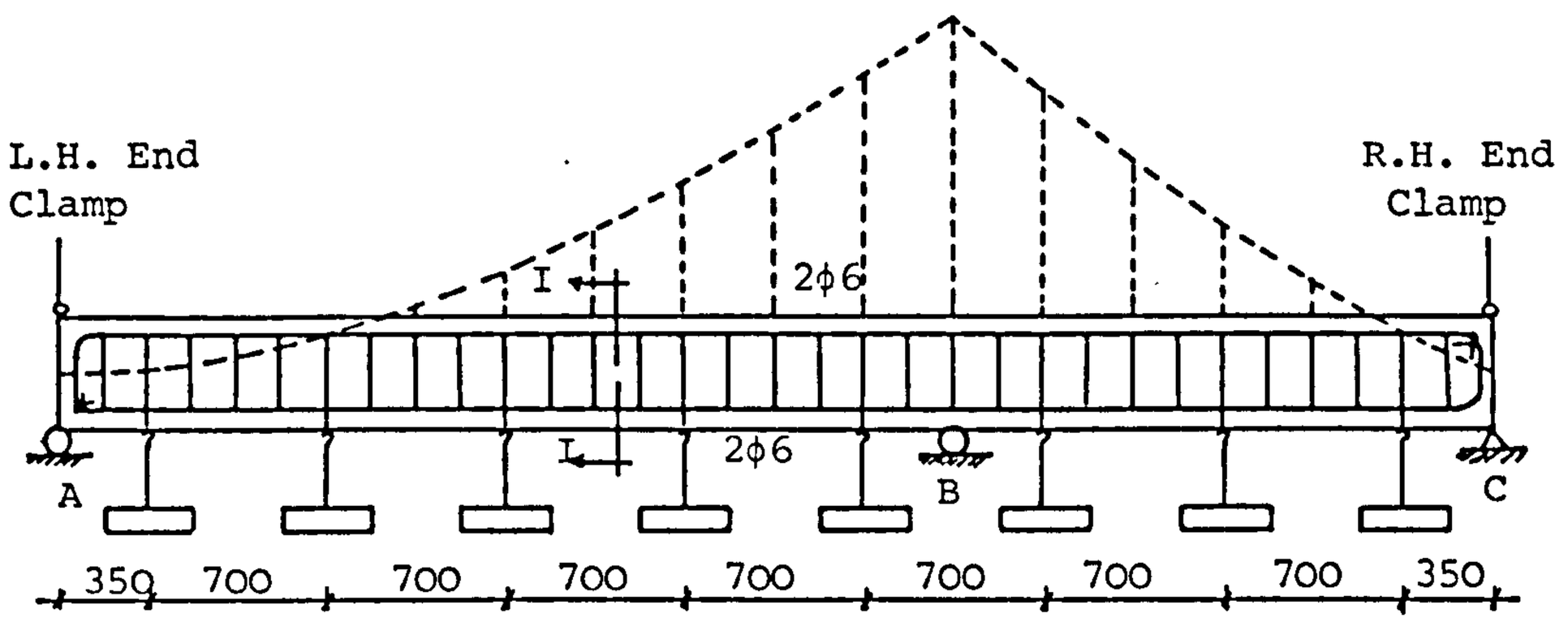

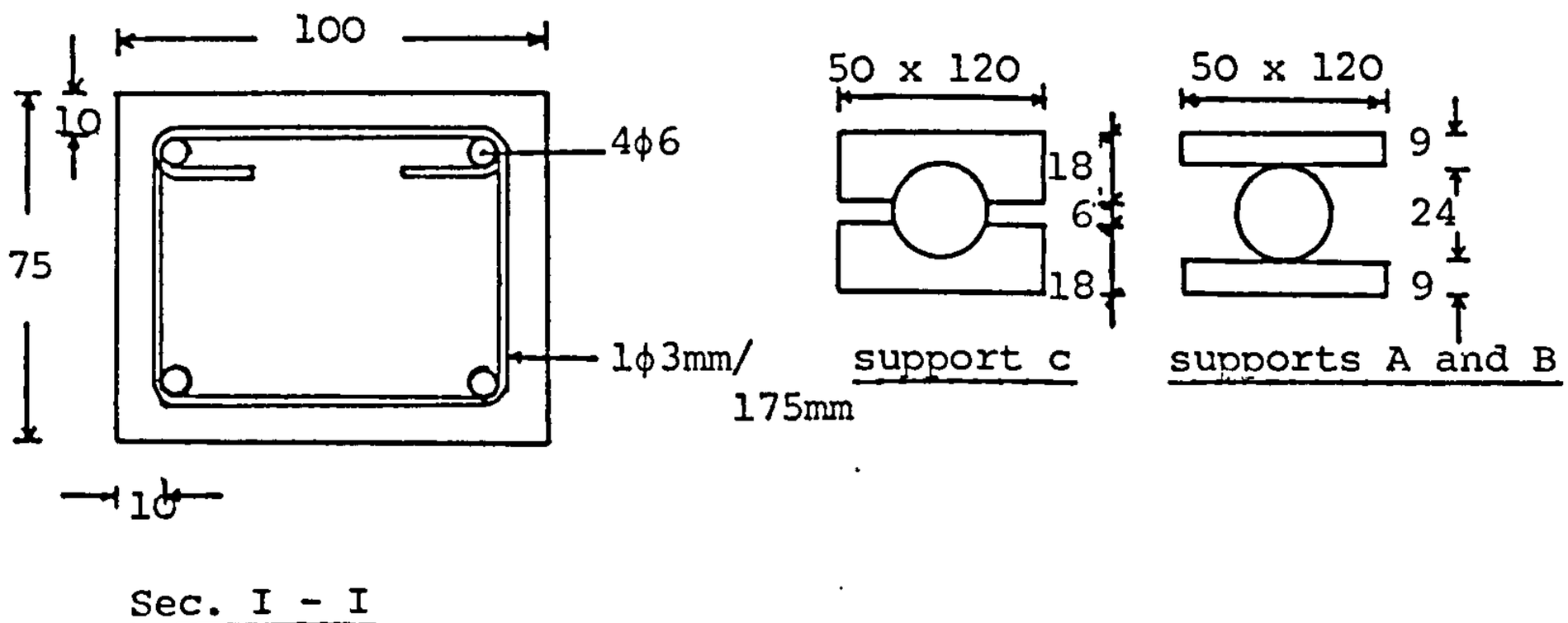

support c

supports A and B

Sec. I - I

The prestressed concrete test beam

Figure (7.2)

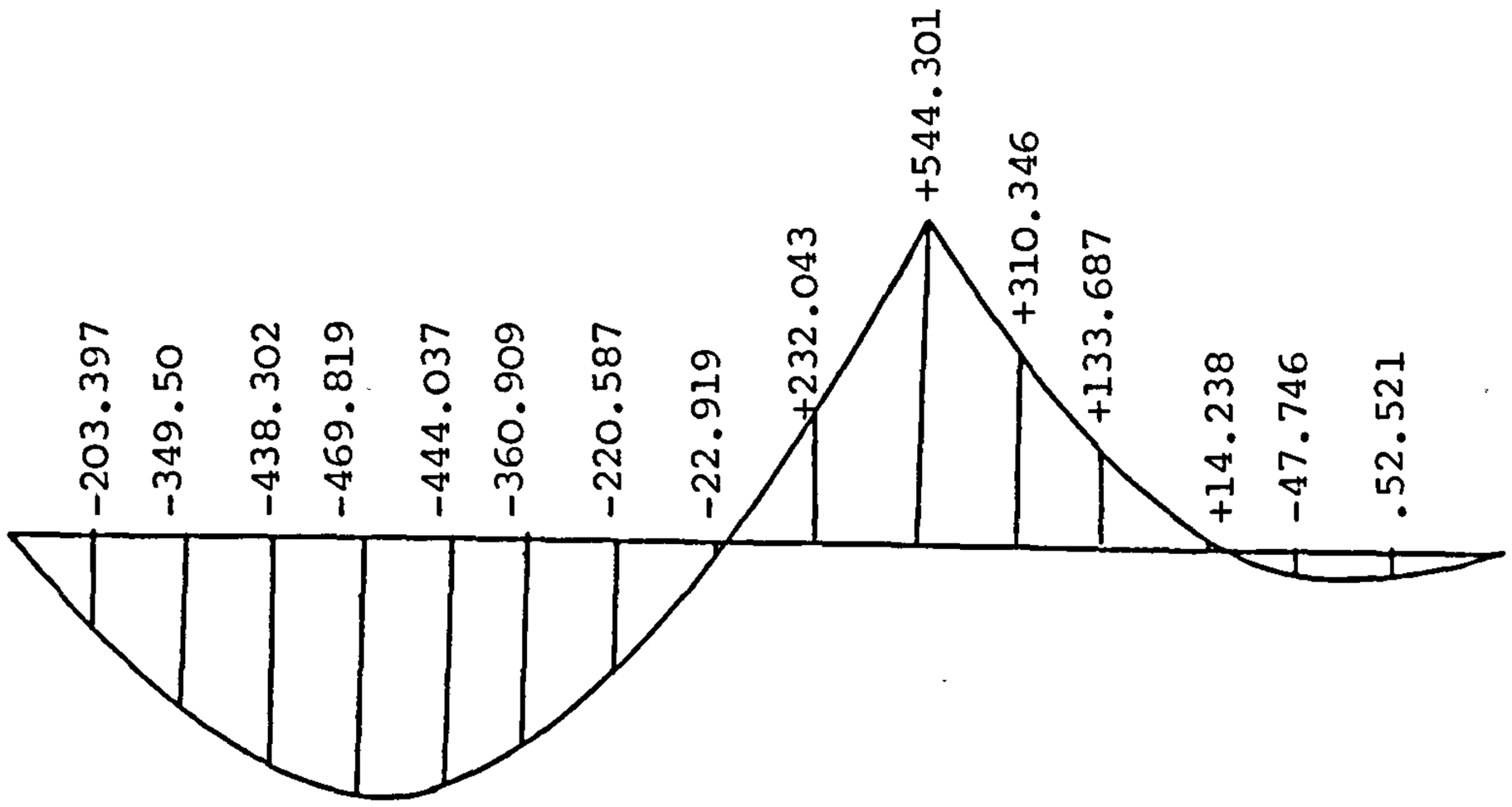

The dead load bending moment diagram (N.m)

(a)

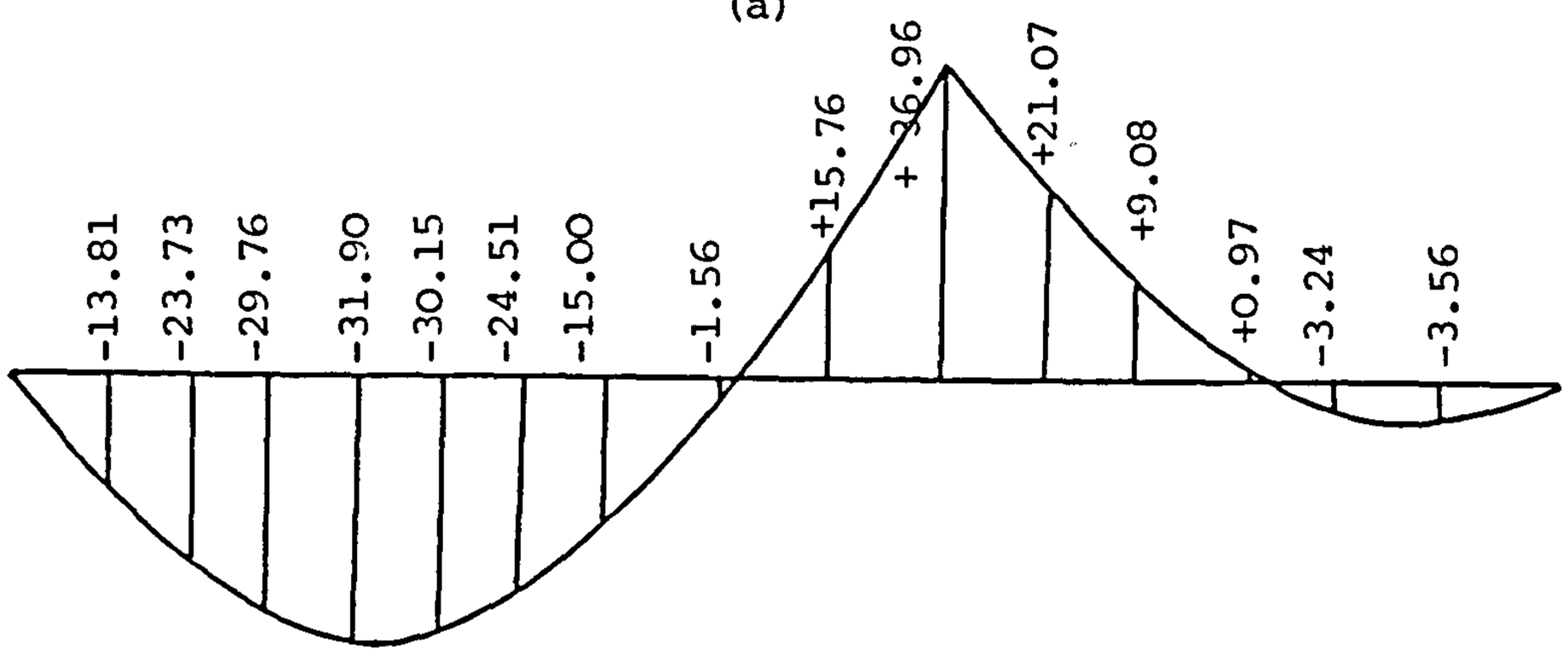

The initial cable eccentricities (mm)

(b)

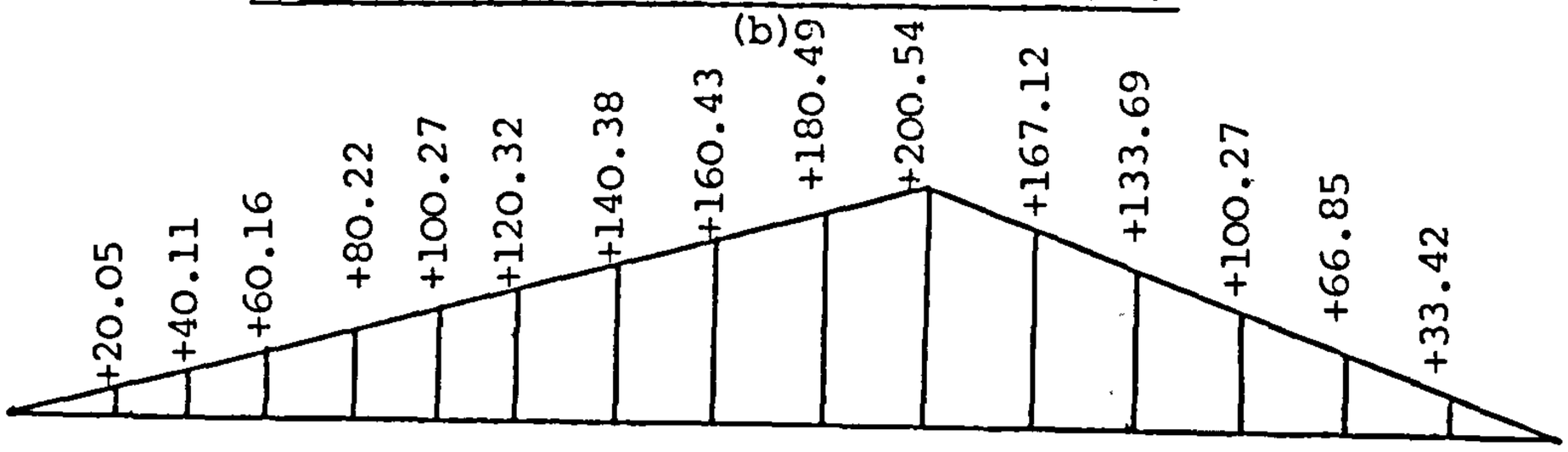

The linear transformation system (mm)

(c)

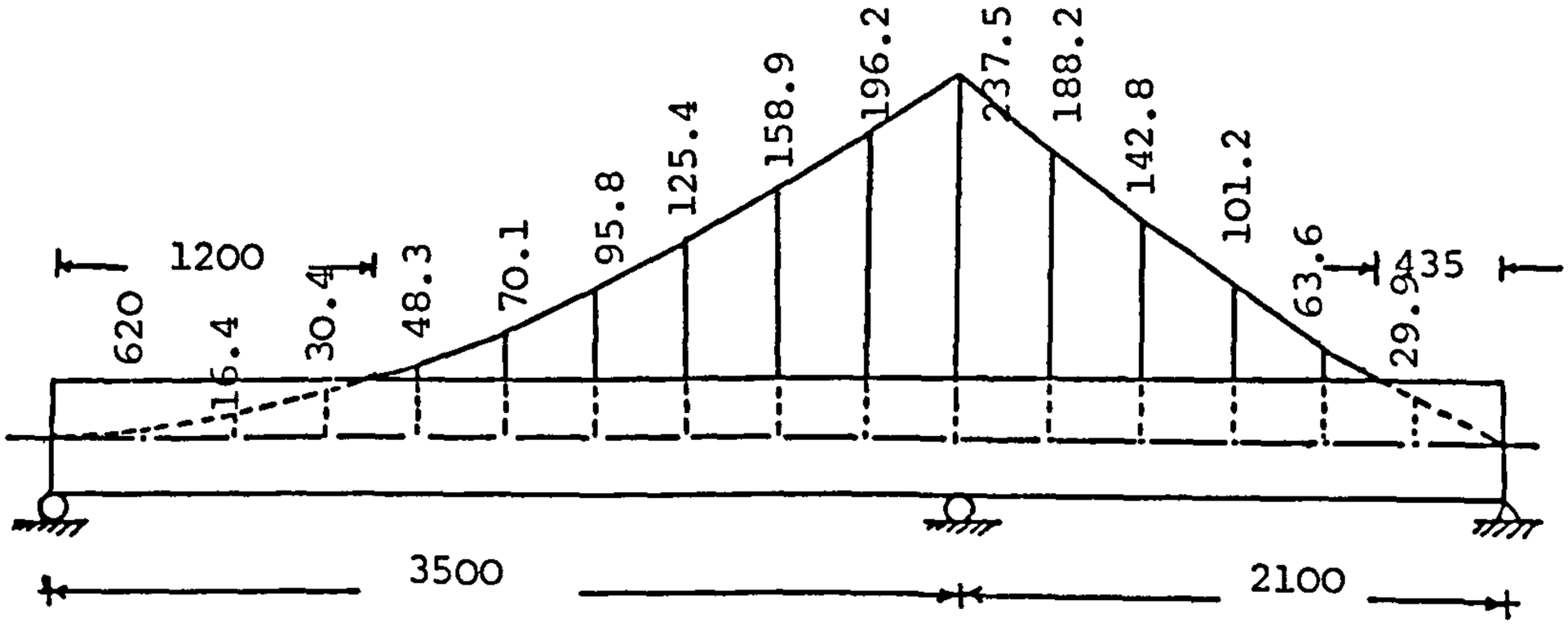

The final cable eccentricities (mm)

(d)

Figure (7.3)

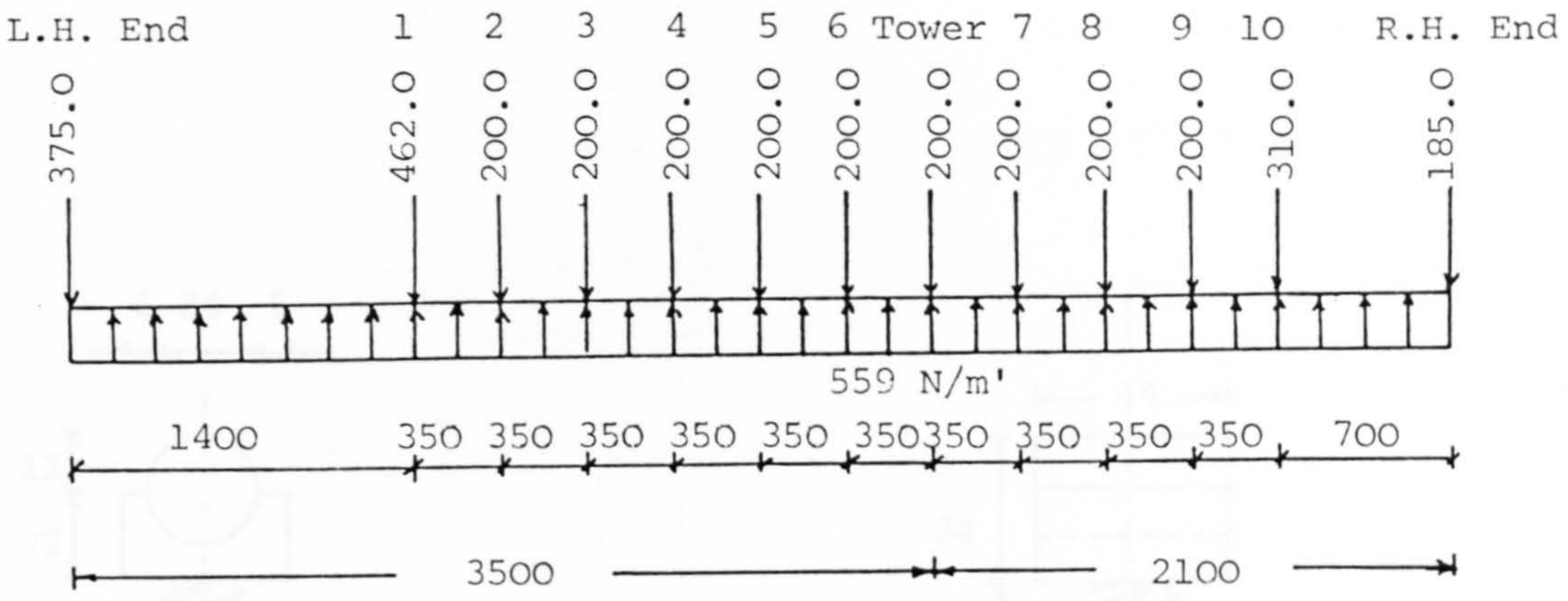

The forces in the suspenders

Figure (7.4)

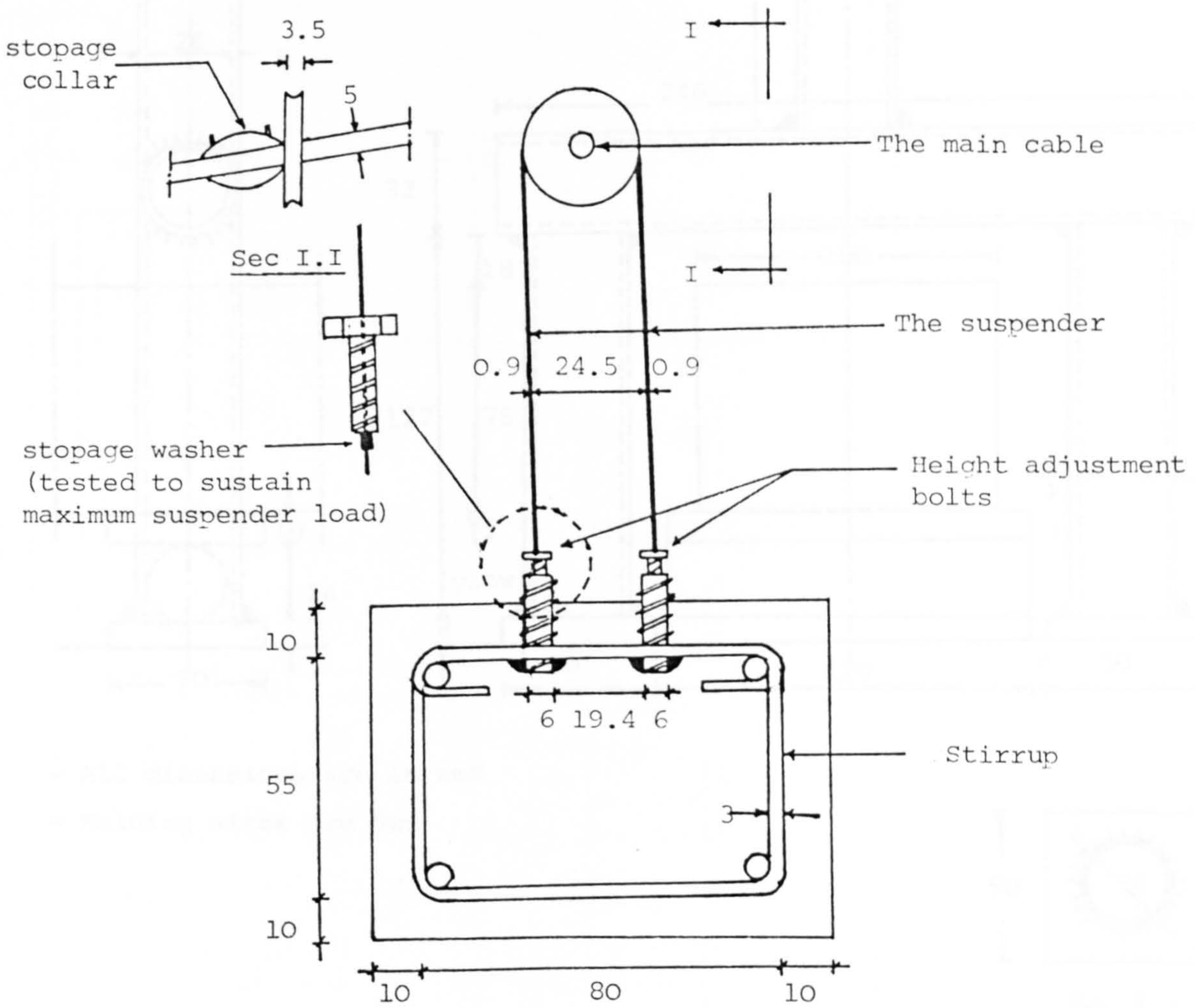

The suspender connections with the main cable and suspended beams

Figure (7.5)

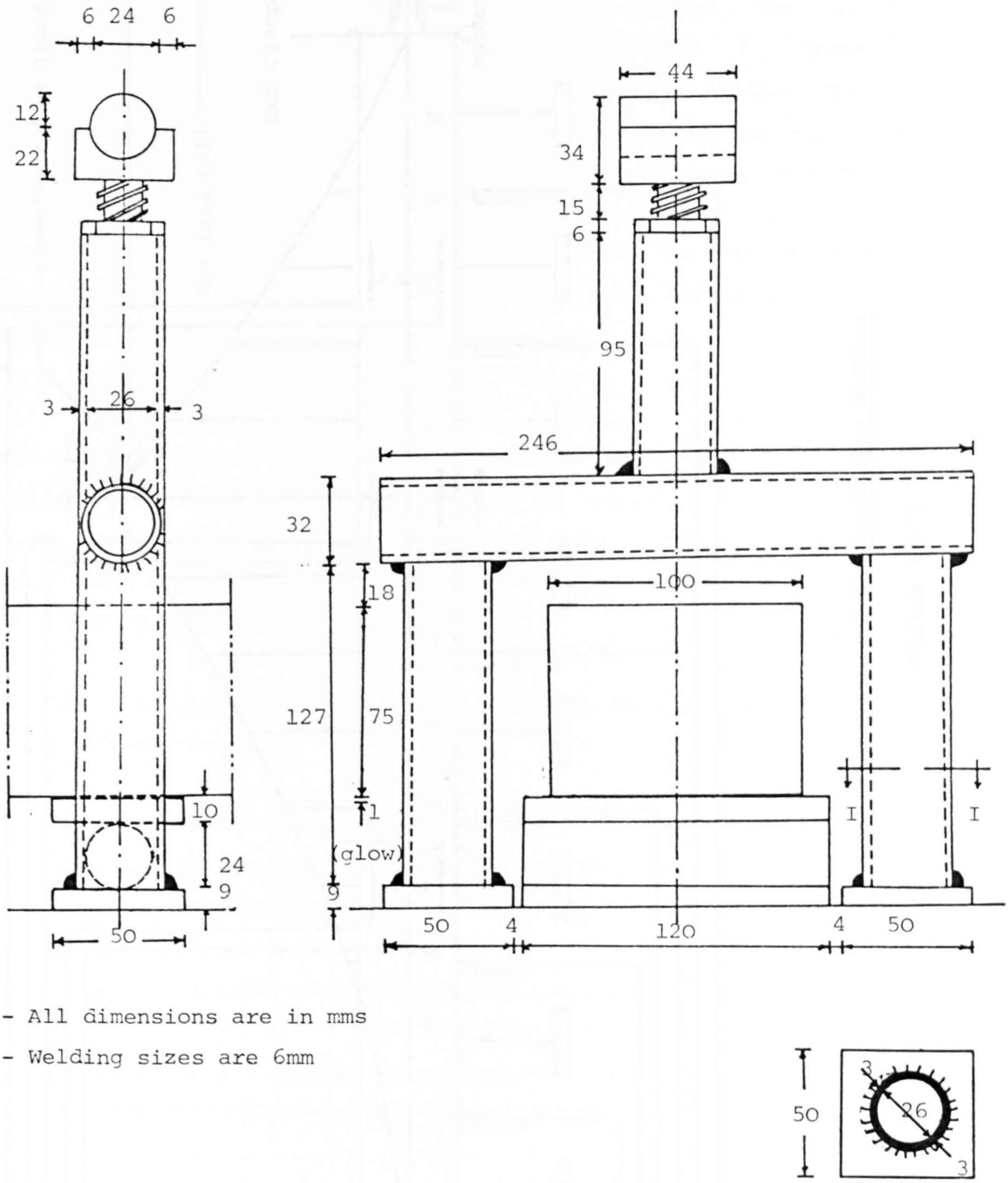

- All dimensions are in mms
- Welding sizes are 6mm

The Tower

Figure (7.6)

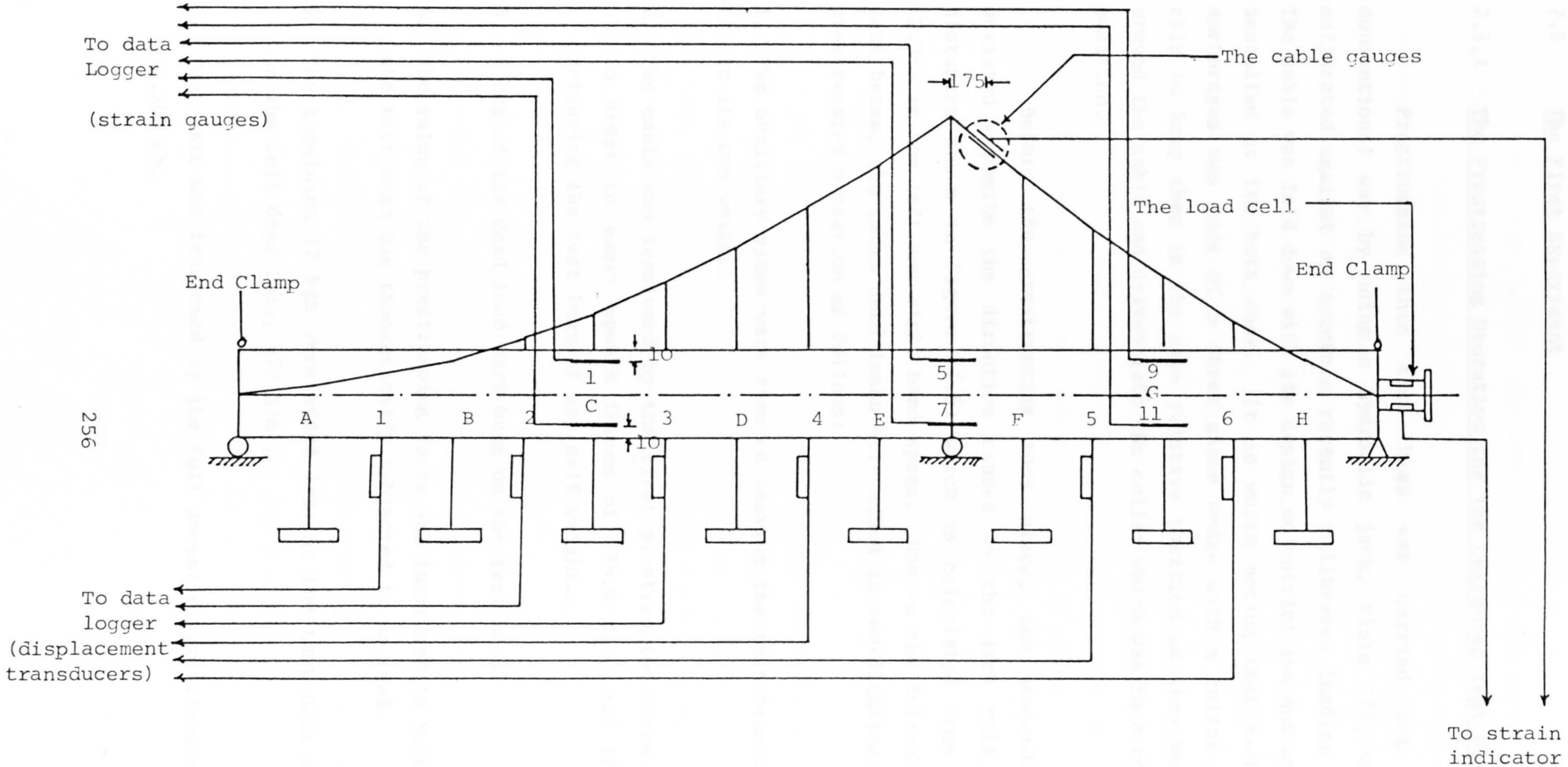

The arrangement of the measuring devices

Figure (7.7)

7.5 The First Experiment

7.5.1 The Prestressing Operation for the Ungrouted Test Beam

Prestressing this test beam was carried out in the conventional way by using a hydraulic jack, Plate (7), which was calibrated against an accurate recently calibrated loading machine. The cable was laid down with its design eccentricities and anchorages installed at its both ends. It is worth noting that each of the anchorages was made of a three piece wedge with a collar and wire clip to keep them in the same relative position as they were fixed around the cable and driven into the collar which was in a concentric position.

Before the prestressing took place, the suspenders were deviated opposite the direction caused by the jack pull, by the distances shown in Figure (7.8) which is calculated from Equation (2.35) in the left and right hand spans. Due to the delicacy of the test beams, the extra dead loads were added in coordination with the prestressing operation as follows:

1. The auxiliary props were removed leaving the test beam subjected to its own weight.

2. The cable was tensioned by the first prestressing force 5.750 KN in order to exert upward forces of 186.0 N/m' and therefore, relieving the test beam of its self weight.

3. 8 kgs of the dead load were hung on the test beam.

4. The value of the prestressing force was increased to 9.500 KN and the test beam was theoretically subjected to no load.

5. The remaining 12 kgs were added leaving the test beam subjected to the full dead load, 470 N/m'.

6. The cable was tensioned by the full amount of prestressing force, 14.800 KN.

Table (7.1) shows all the readings obtained from the displacement transducers, strain gauges, cable gauges and load cell as well as the calculated ones, computer program Appendix 28. Although the test beam was theoretically relieved from any stresses at steps 2, 4 and 6, the measuring devices registered small values of bending moments and deflections in the opposite of its loading direction, Table (7.1). This suggests that the prestressing force was slightly larger than the intended value. Moreover, the table shows that the cable responded to the increments of dead loads added on the hangers by changing its tension by small values as shown in steps (3) and (5). Clearly, this signifies the accuracy of both the load cell and the cable gauges as they were capable of detecting these small changes in the cable tension. Finally, it is worth noting that all the suspenders were exactly in plumb after the prestressing operation.

7.5.2 Testing of the Working Life of the Ungrouted Test Beam

The suspended test beam was subjected to concentrated loads applied one at a time at positions (A - H) by hanging weights in the manner shown in Plate (5). Each of these loads comprised eight increments of 89.0 N, 20lb, as the maximum loading in each position was 712 N which is less than half the first plastic hinge load. Obviously, this value was chosen in order to ensure that no cracks will develop during this stage of the experiment.

The test at each loading position was repeated several times and the final experimental values of the deflections, bending moments and changes in the prestressing force are shown in Tables (7.2 - 9) as well as the calculated ones obtained from the analysis, computer program in Appendix 28. The results were also plotted, Figure (7.9 - 16), as each figure comprises the calculated plot as well as the best fitting line for the experimental one which was obtained by means of a least square analysis.

When removing the loads at each position, the suspended test beam immediately recovered by almost 90% to its initial position prior to loading. Whence, as time passed, the beam slowly returned to its exact initial position. From the results, we also notice that the cable tension decreased due to loads applied in the right hand span. This can be explained when examining the general formula, (2.57), for the determination of the change in the cable tension due to the applied live loading, Timoshenko (23), (25) and (26). As the formula is based on the energy produced by the live loads in calculating the sum of the areas under the deflection curves in both spans, a decrease in the cable tension is bound to occur as a result of a negative deflection in the larger span depending on the difference in the span lengths.

Tables (7.2 - 9) and Figures (7.9 - 16) show that all the experimental results were within an acceptable margin of error from the values calculated by the computer program, Appendix 28. Finally, we note that no sign of cracks were detected anywhere in the test beam at this stage of the experiment.

7.5.3 Testing to Failure of the Ungrouted Test Beam

From Table (7.4), it was clear that maximum deflections and bending moments were obtained when the load was applied at the mid-point of the left hand span, position C. For this reason, this position was chosen for increasing loading to cause the failure of the structure. From Sections 4.2 and 4.3, computer program Appendix 28, the ultimate moment of resistance of the cross section of the test beam was calculated to be 1479.0 N.m for hogging and sagging moments. Furthermore, the first plastic hinge was expected to form under the applied load, position C, at a load 2081.0 N and the failure load was evaluated to be 2472.0 N with the second plastic hinge forming at the intermediate support. Therefore, the loading increments were chosen to be 178.0 N until the load reaches the value 1780.0 N, and decreasing afterwards to 89.0 N in order to allow for an accurate assessment of the failure loads.

The experimental and calculated results are tabulated and plotted in Table (7.10) and Figures (7.17) in the manner described in the preceeding section. We observed that the first crack appeared at position C corresponding to the load 1246 N. Thereafter, cracks developed rapidly around this position and at the load 1780 N they became very wide and the rate of increase for the deflections and cable tension became much greater, Figures (7.17), which left little doubt that the beam had reached the ultimate moment of resistance at this section. When increasing the load to 1869 N, the section of the beam adjacent to the tower developed its first crack. As the load was increased further, more cracks appeared and became wider with the deflections also increasing rapidly until the load reached the value 2047 N. Afterwards, the deflections increased out of control and the test beam collapsed, Plate (8).

All the experimental results were close to the calculated ones found from the analysis, computer program in Appendix 28, until the formation of the first plastic hinge. Thereafter, the measured values were greater than the calculated ones especially when the beam was close to failure. Nevertheless, as shown in Table (7.10) and Figures (7.17), the experimental results were always within an acceptable margin of error when compared with the computed ones. Finally, it is worth noting that the suspenders carried the applied loads successfully up to failure as did the cable where its maximum recorded stress was about 800 N/mm^2. Plate (9) shows position C as failed after the collapse of the beam.

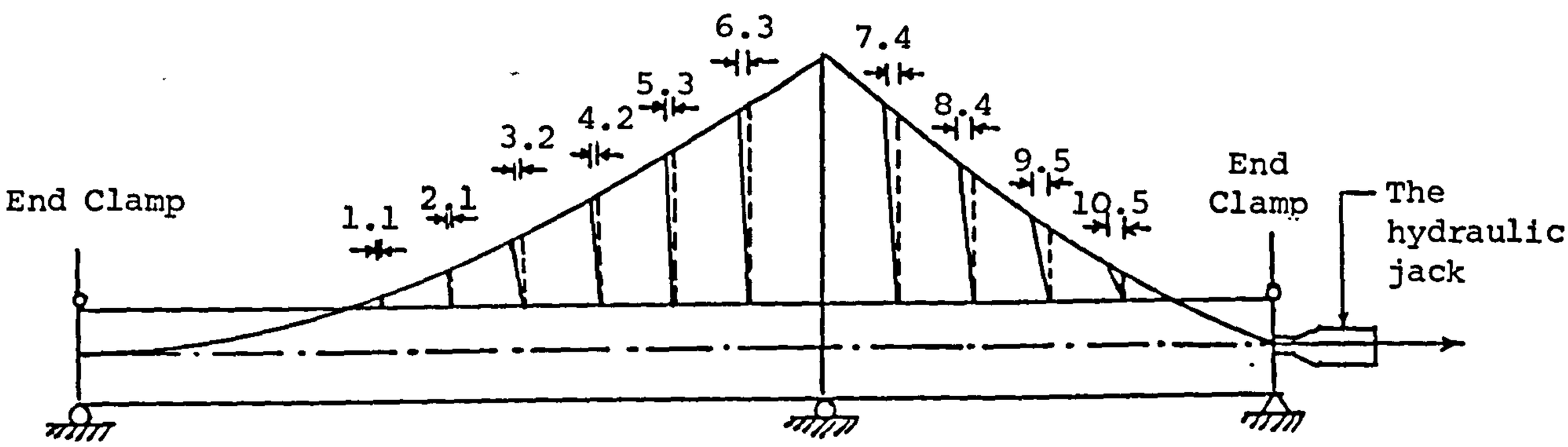

The suspenders out of plumb

Figure (7.8)

Table 7.1

Stage No.	Jack Load (N)	Reading of Load Cell (N)	Reading of Cable Gauges (N)	DEFLECTIONS (mms)											
				Station (1)		Station (2)		Station (3)		Station (4)		Station (5)		Station (6)	
				Cal.	Exp.	Cal.	Exp.	Cal.	Exp.	Cal.	Exp.	Cal.	Exp.	Cal.	Exp.
Stage (1)	0.00	0.00	0.00	1.3290	1.2980	2.0050	2.1250	1.7910	1.6910	0.8990	0.9540	-0.1830	-0.1690	-0.0630	-0.0730
Stage (2)	5727.00	5700.00	5793.00	0.0000	0.0007	0.0000	0.0012	0.0000	0.0009	0.0000	0.0002	0.0000	0.0001	0.0000	0.0000
Stage (3)	5733.00	5712.00	5805.00	0.8650	0.9030	1.3050	1.4110	1.1650	1.2910	0.5850	0.4150	-0.1190	-0.1470	-0.0410	-0.0320
Stage (4)	9445.00	9419.00	9530.00	0.0000	-0.0060	0.0000	-0.0080	0.0000	0.0070	0.0000	-0.0030	0.0000	0.0080	0.0000	0.0030
Stage (5)	9459.00	9447.00	9552.00	1.2300	1.1430	1.8570	1.7660	1.6580	1.5370	0.8330	0.7110	-0.1690	-0.1480	-0.0580	-0.0650
Stage (6)	14726.00	14730.00	14912.00	0.0000	-0.0070	0.0000	-0.0100	0.0000	0.0089	0.0000	-0.0050	0.0000	0.0010	0.0000	0.0004

BENDING MOMENTS (N.m.)					
Position C		Tower		Position G	
Cal.	Exp.	Cal.	Exp.	Cal.	Exp.
172.312	-153.701	211.221	189.996	5.6265	4.914
0.000	0.741	0.000	-1.129	0.0000	-0.082
112.121	-129.338	137.439	143.967	3.6610	2.159
0.000	2.950	0.000	-3.174	0.0000	-0.011
170.647	-183.614	202.863	216.394	10.1490	8.627
0.000	3.441	0.000	-4.987	0.0000	-0.215

The calculated and experimental results during the prestressing operation of the ungrouted test beam

Table 7.2

Applied Load (N)	DEFLECTIONS (mm)											
	Station (1)		Station (2)		Station (3)		Station (4)		Station (5)		Station (6)	
	Cal.	Exp.	Cal.	Exp.	Cal.	Exp.	Cal.	Exp.	Cal.	Exp.	Cal.	Exp.
89.00	0.130	0.111	0.164	0.141	0.129	0.111	0.062	0.056	- 0.026	- 0.029	-0.021	- 0.020
178.00	0.261	0.236	0.329	0.275	0.258	0.215	0.123	0.119	- 0.052	- 0.064	-0.042	- 0.038
267.00	0.391	0.298	0.493	0.494	0.388	0.312	0.185	0.169	- 0.078	- 0.089	-0.063	- 0.058
356.00	0.522	0.487	0.657	0.657	0.517	0.450	0.246	0.209	- 0.104	- 0.121	-0.084	- 0.086
445.00	0.652	0.531	0.822	0.919	0.646	0.566	0.308	0.273	- 0.130	- 0.154	-0.106	- 0.112
534.00	0.783	0.659	0.986	1.085	0.775	0.638	0.370	0.301	- 0.156	- 0.173	-0.127	- 0.128
623.00	0.913	0.771	1.151	1.346	0.904	0.799	0.431	0.383	- 0.182	- 0.204	-0.148	- 0.153
712.00	1.044	0.873	1.315	1.458	1.034	0.865	0.493	0.406	- 0.209	- 0.262	-0.169	- 0.175

Applied Load (N)	BENDING MOMENTS (N.m.)						INCREASE IN TENSION (N)		
	Position C		Tower		Position 6		Cal.	Load Cell	Cable Gauges
	Cal.	Exp.	Cal.	Exp.	Cal.	Exp.			
89.00	-12.297	- 11.558	10.479	8.935	5.752	4.623	6.368	5.742	6.068
178.00	-24.597	- 20.805	20.595	18.870	11.506	9.246	12.736	14.354	12.136
267.00	-36.898	- 32.363	31.440	29.805	17.260	15.111	19.104	21.531	20.228
356.00	-49.200	- 46.233	41.923	37.741	23.016	20.805	25.472	28.708	28.319
445.00	-61.505	- 56.879	52.406	47.610	28.772	26.013	31.839	34.450	34.387
534.00	-73.811	- 67.039	62.891	59.922	34.533	30.225	38.207	41.627	42.479
623.00	-86.119	- 82.908	73.376	68.363	40.288	37.004	44.575	48.804	46.524
712.00	-98.429	- 94.778	83.863	89.856	46.048	44.555	50.943	54.545	52.593

The calculated and experimental results when the load is applied at loading station A

Table 7.3

Applied Load (N)	DEFLECTIONS (mms)											
	Station (1)		Station (2)		Station (3)		Station (4)		Station (5)		Station (6)	
	Cal.	Exp.	Cal.	Exp.	Cal.	Exp.	Cal.	Exp.	Cal.	Exp.	Cal.	Exp.
89.00	0.294	0.264	0.421	0.498	0.345	0.299	0.168	0.147	−0.071	− 0.084	−0.058	−0.058
178.00	0.588	0.487	0.841	0.963	0.690	0.589	0.335	0.275	−0.143	− 0.164	−0.116	−0.115
267.00	0.883	0.712	1.262	1.436	1.035	0.859	0.503	0.426	−0.214	− 0.231	−0.174	−0.184
356.00	1.177	0.999	1.684	1.903	1.381	1.173	0.671	0.560	−0.286	− 0.311	−0.232	−0.257
445.00	1.472	1.333	2.105	2.431	1.726	1.482	0.839	0.709	−0.357	− 0.412	−0.290	−0.310
534.00	1.766	1.567	2.526	2.811	2.071	1.805	1.007	0.857	−0.429	− 0.474	−0.348	−0.371
623.00	2.061	1.867	2.948	3.236	2.417	2.133	1.175	1.010	−0.500	− 0.591	−0.406	−0.421
712.00	2.356	1.995	3.369	3.783	2.763	2.476	1.343	1.172	−0.572	− 0.631	−0.464	−0.479

Applied Load (N)	BENDING MOMENTS (N.m.)						INCREASE IN TENSION (N)		
	Position C		Tower		Position G		Cal.	Load Cell	Cable Gauges
	Cal.	Exp.	Cal.	Exp.	Cal.	Exp.			
89.00	−37.494	− 32.363	28.715	22.181	15.763	13.558	15.831	17.225	16.182
178.00	−75.001	− 71.661	57.439	49.986	31.533	26.117	31.663	34.450	34.387
267.00	−112.521	−113.271	86.170	80.168	47.310	38.363	47.494	48.804	48.547
356.00	−150.053	−161.816	114.910	107.662	63.094	56.610	63.325	68.900	62.707
445.00	−187.599	−211.919	143.655	131.843	78.885	73.414	79.156	83.253	80.912
534.00	−225.257	−239.528	172.410	152.336	94.683	89.972	94.988	101.914	105.185
623.00	−262.728	−291.004	201.172	184.547	110.488	104.699	110.819	114.832	117.322
712.00	−300.311	−320.202	229.941	209.325	126.300	119.908	126.650	133.493	133.504

The calculated and experimental results when the load is applied at loading station B

Table 7.4

Applied Load (N)	DEFLECTIONS (mm)											
	Station (1)		Station (2)		Station (3)		Station (4)		Station (5)		Station (6)	
	Cal.	Exp.	Cal.	Exp.	Cal.	Exp.	Cal.	Exp.	Cal.	Exp.	Cal.	Exp.
89.00	0.291	0.252	0.470	0.399	0.436	0.367	0.224	0.203	-0.097	-0.110	-0.078	-0.081
178.00	0.583	0.497	0.941	1.115	0.873	0.753	0.447	0.375	-0.194	-0.222	-0.157	-0.171
267.00	0.874	0.786	1.412	1.584	1.310	1.178	0.671	0.585	-0.291	-0.335	-0.236	-0.268
356.00	1.166	0.991	1.883	2.147	1.747	1.585	0.895	0.788	-0.388	-0.412	-0.314	-0.329
445.00	1.458	1.290	2.354	2.963	2.184	2.027	1.119	1.019	-0.485	-0.546	-0.393	-0.429
534.00	1.750	1.613	2.826	3.282	2.621	2.481	1.343	1.241	-0.582	-0.694	-0.472	-0.540
623.00	2.042	1.739	3.297	3.991	3.058	2.954	1.567	1.478	-0.679	-0.782	-0.550	-0.542
712.00	2.334	2.003	3.769	4.301	3.497	3.393	1.791	1.700	-0.776	-0.911	-0.629	-0.605

Applied Load (N)	BENDING MOMENTS (N.m.)						INCREASE IN TENSION (N)		
	Position C		Tower		Position G		Cal.	Load Cell	Cable Gauges
	Cal.	Exp.	Cal.	Exp.	Cal.	Exp.			
89.00	-64.503	- 62.414	39.014	31.428	21.379	17.869	17.899	20.096	18.205
178.00	-129.026	-136.388	78.039	67.168	42.769	37.740	35.798	37.321	40.459
267.00	-193.567	-216.542	117.075	99.908	64.170	55.152	53.697	57.416	56.638
356.00	-258.127	-281.762	156.123	138.336	85.582	73.349	71.597	80.383	74.843
445.00	-322.707	-340.982	195.183	176.453	107.005	96.999	89.496	101.914	93.048
534.00	-387.306	-406.824	234.254	215.034	128.439	116.089	107.395	114.832	111.254
623.00	-451.924	-478.333	273.336	252.103	149.884	140.001	125.294	132.057	127.436
712.00	-516.562	-543.445	312.430	287.123	171.340	163.959	143.193	146.411	149.687

The calculated and experimental results when the load is applied at loading station C

Table 7.5

Applied Load (N)	DEFLECTIONS (mm)											
	Station (1)		Station (2)		Station (3)		Station (4)		Station (5)		Station (6)	
	Cal.	Exp.	Cal.	Exp.	Cal.	Exp.	Cal.	Exp.	Cal.	Exp.	Cal.	Exp.
89.00	0.186	0.162	0.315	0.345	0.334	0.300	0.199	0.176	−0.091	−0.118	−0.073	−0.085
178.00	0.372	0.333	0.630	0.781	0.668	0.628	0.398	0.380	−0.181	−0.226	−0.147	−0.157
267.00	0.558	0.514	0.946	1.165	1.002	0.961	0.574	0.574	−0.272	−0.308	−0.220	−0.253
356.00	0.744	0.691	1.261	1.470	1.336	1.304	0.797	0.787	−0.362	−0.412	−0.294	−0.347
445.00	0.930	0.876	1.577	1.961	1.670	1.665	0.996	1.010	−0.453	−0.518	−0.367	−0.412
534.00	1.116	0.949	1.892	2.197	2.005	2.037	1.196	1.236	−0.544	−0.700	−0.440	−0.499
623.00	1.302	1.130	2.208	2.784	2.339	2.428	1.395	1.465	−0.634	−0.718	−0.514	−0.567
712.00	1.488	1.317	2.524	3.119	2.674	2.804	1.594	1.700	−0.725	−0.813	−0.588	−0.614

Applied Load (N)	BENDING MOMENTS (N.m.)						INCREASE IN TENSION (N)		
	Position C		Tower		Position G		Cal.	Load Cell	Cable Gauges
	Cal.	Exp.	Cal.	Exp.	Cal.	Exp.			
89.00	−32.674	− 34.674	36.540	29.805	19.966	16.870	12.470	14.354	14.159
178.00	−65.358	− 76.284	73.087	64.544	39.940	33.051	24.941	28.708	30.342
267.00	−98.054	−107.894	109.640	88.349	59.921	53.545	37.411	43.062	40.459
356.00	−130.760	−142.946	146.201	129.024	79.908	73.973	49.882	54.545	56.638
445.00	−163.476	−176.867	182.768	167.880	99.904	92.467	62.352	63.158	72.821
534.00	−196.204	−211.081	219.341	203.621	119.906	108.647	74.823	84.957	84.957
623.00	−228.942	−246.708	255.922	233.031	139.916	122.517	87.293	91.866	97.094
712.00	−261.691	−283.943	292.509	271.914	159.933	150.322	99.764	104.785	109.231

The calculated and experimental results when the load is applied at loading station D

Table 7.6

Applied Load (N)	DEFLECTIONS (mm)											
	Station (1)		Station (2)		Station (3)		Station (4)		Station (5)		Station (6)	
	Cal.	Exp.	Cal.	Exp.	Cal.	Exp.	Cal.	Exp.	Cal.	Exp.	Cal.	Exp.
89.00	0.053	0.048	0.092	0.079	0.103	0.082	0.074	0.060	−0.042	− 0.051	− 0.034	−0.038
178.00	0.106	0.089	0.183	0.164	0.206	0.174	0.148	0.130	−0.085	− 0.106	− 0.068	−0.073
267.00	0.159	0.137	0.275	0.240	0.308	0.265	0.221	0.199	−0.127	− 0.164	− 0.103	−0.122
356.00	0.212	0.184	0.367	0.412	0.411	0.357	0.295	0.269	−0.169	− 0.210	− 0.137	−0.169
445.00	0.264	0.236	0.459	0.515	0.514	0.449	0.369	0.343	−0.212	− 0.273	− 0.171	−0.202
534.00	0.317	0.291	0.550	0.543	0.617	0.550	0.443	0.421	−0.254	− 0.305	− 0.206	−0.225
623.00	0.370	0.348	0.642	0.692	0.720	0.647	0.517	0.495	−0.296	− 0.377	− 0.240	−0.261
712.00	0.423	0.385	0.734	0.816	0.823	0.782	0.591	0.570	−0.339	− 0.411	− 0.274	−0.284

Applied Load (N)	BENDING MOMENTS (N.m.)						INCREASE IN TENSION (N)		
	Position C		Tower		Position G		Cal.	Load Cell	Cable Gauges
	Cal.	Exp.	Cal.	Exp.	Cal.	Exp.			
89.00	−8.205	−6.987	17.123	18.666	9.321	6.913	3.487	2.871	4.046
178.00	−16.411	−13.152	34.247	37.189	18.644	14.014	6.974	7.177	8.091
267.00	−24.618	−20.012	51.371	53.795	27.968	23.363	10.462	11.483	10.113
356.00	−32.827	−27.334	68.497	71.796	37.292	33.000	13.949	15.789	14.159
445.00	−41.037	−36.225	85.622	91.232	46.618	40.882	17.436	18.660	20.228
534.00	−49.247	−44.001	102.749	111.419	55.944	49.111	20.923	21.531	24.273
623.00	−57.459	−51.873	119.877	130.018	65.272	58.762	24.410	25.837	26.296
712.00	−65.673	−59.431	137.005	151.355	74.600	67.515	27.897	31.579	30.342

The calculated and experimental results when the load is applied at loading station E

Table 7.7

Applied Load (N)	DEFLECTIONS (mm)											
	Station (1)		Station (2)		Station (3)		Station (4)		Station (5)		Station (6)	
	Cal.	Exp.	Cal.	Exp.	Cal.	Exp.	Cal.	Exp.	Cal.	Exp.	Cal.	Exp.
89.00	-0.034	-0.034	-0.060	-0.070	-0.068	-0.072	-0.050	-0.046	0.052	0.063	0.043	0.051
178.00	-0.070	-0.068	-0.121	-0.136	-0.136	-0.129	-0.099	-0.102	0.103	0.117	0.085	0.091
267.00	-0.104	-0.099	-0.181	-0.172	-0.203	-0.188	-0.149	-0.144	0.154	0.175	0.128	0.146
356.00	-0.139	-0.126	-0.241	-0.269	-0.271	-0.266	-0.199	-0.203	0.206	0.237	0.171	0.213
445.00	-0.174	-0.154	-0.302	-0.289	-0.339	-0.323	-0.248	-0.250	0.257	0.308	0.213	0.255
534.00	-0.209	-0.183	-0.362	-0.321	-0.407	-0.386	-0.298	-0.301	0.309	0.364	0.256	0.300
623.00	-0.244	-0.222	-0.422	-0.475	-0.474	-0.459	-0.348	-0.352	0.360	0.411	0.299	0.361
712.00	-0.279	-0.263	-0.483	-0.536	-0.542	-0.517	-0.397	-0.403	0.412	0.477	0.341	0.409

Applied Load (N)	BENDING MOMENTS (N.m.)						INCREASE IN TENSION (N)		
	Position C		Tower		Position G		Cal.	Load Cell	Cable Gauges
	Cal.	Exp.	Cal.	Exp.	Cal.	Exp.			
89.00	5.330	4.623	8.520	7.623	-12.086	-10.846	-0.838	-1.435	-0.000
178.00	10.660	11.869	17.040	14.558	-24.172	-21.393	-1.676	-2.871	-2.022
267.00	15.990	18.805	25.560	21.182	-36.259	-33.005	-2.514	-2.871	-2.022
356.00	21.321	24.739	34.080	29.739	-48.346	-42.986	-3.352	-4.306	-4.046
445.00	26.651	30.363	42.599	38.363	-60.433	-55.480	-4.191	-4.306	-4.046
534.00	31.982	34.675	51.119	46.234	-72.520	-69.350	-5.029	-5.741	-6.068
623.00	37.313	36.986	59.639	54.019	-84.607	-78.596	-5.867	-5.741	-6.068
712.00	42.644	46.233	68.158	62.314	-96.694	-89.623	-6.705	-7.177	-8.091

The calculated and experimental results when the load is applied at loading station F

Table 7.8

Applied Load (N)	DEFLECTIONS (mms)											
	Station (1)		Station (2)		Station (3)		Station (4)		Station (5)		Station (6)	
	Cal.	Exp.	Cal.	Exp.	Cal.	Exp.	Cal.	Exp.	Cal.	Exp.	Cal.	Exp.
89.00	-0.052	- 0.047	- 0.090	-0.099	- 0.101	- 0.089	- 0.074	- 0.068	0.101	0.114	0.107	0.117
178.00	-0.104	- 0.095	- 0.180	-0.205	- 0.202	- 0.186	- 0.148	- 0.130	0.202	.0.228	0.214	0.244
267.00	-0.156	- 0.137	- 0.270	-0.251	- 0.303	- 0.270	- 0.222	- 0.195	0.302	0.333	0.320	0.362
356.00	-0.207	- 0.189	- 0.359	-0.349	- 0.404	- 0.381	- 0.296	- 0.287	0.403	0.446	0.427	0.478
445.00	-0.259	- 0.213	- 0.449	-0.432	- 0.505	- 0.467	- 0.370	- 0.352	0.504	0.537	0.534	0.594
534.00	-0.311	- 0.276	- 0.539	-0.528	- 0.606	- 0.555	- 0.444	- 0.418	0.604	0.677	0.640	0.711
623.00	-0.363	- 0.312	- 0.629	-0.615	- 0.707	- 0.626	- 0.518	- 0.487	0.705	0.784	0.747	0.833
712.00	-0.415	- 0.385	- 0.719	-0.815	- 0.808	- 0.719	- 0.592	- 0.551	0.806	0.906	0.854	0.924

Applied Load (N)	BENDING MOMENTS (N.m.)						INCREASE IN TENSION (N)		
	Position C		Tower		Position G		Cal.	Load Cell	Cable Gauges
	Cal.	Exp.	Cal.	Exp.	Cal.	Exp.			
89.00	7.977	8.493	12.675	13.870	- 42.172	-38.363	-2.320	- 2.871	-2.023
178.00	15.954	17.116	25.350	23.117	- 84.344	-79.715	-4.639	- 5.742	-4.045
267.00	23.932	27.051	38.025	35.363	-126.517	-109.356	-6.959	- 8.612	-6.068
356.00	31.911	34.167	50.700	50.856	-168.692	-145.764	-9.279	-11.483	-8.091
445.00	38.890	43.921	63.374	60.103	-210.867	-187.439	-11.599	-12.919	- 10.110
534.00	47.870	50.883	76.048	76.284	-253.043	-228.802	-13.918	-18.660	- 12.137
623.00	55.851	55.478	88.723	87.038	-295.220	-265.840	-16.238	-20.095	- 16.182
712.00	63.832	62.415	101.397	99.001	-337.397	-299.477	-18.558	-21.531	- 18.205

The calculated and experimental results when the load is applied at loading station G

Table 7.9

Applied Load (N)	DEFLECTIONS (mm)											
	Station (1)		Station (2)		Station (3)		Station (4)		Station (5)		Station (6)	
	Cal.	Exp.	Cal.	Exp.	Cal.	Exp.	Cal.	Exp.	Cal.	Exp.	Cal.	Exp.
89.00	-0.022	- 0.017	- 0.039	-0.046	- 0.044	- 0.040	- 0.032	- 0.039	0.046	0.051	0.061	0.060
178.00	-0.045	- 0.038	- 0.078	-0.081	- 0.088	- 0.082	- 0.064	- 0.073	0.092	0.100	0.123	0.119
267.00	-0.067	- 0.074	- 0.117	-0.125	- 0.132	- 0.126	- 0.097	- 0.104	0.138	0.150	0.184	0.177
356.00	-0.090	- 0.092	- 0.156	-0.161	- 0.175	- 0.188	- 0.129	- 0.140	0.184	0.203	0.246	0.239
445.00	-0.113	- 0.104	- 0.195	-0.216	- 0.219	- 0.245	- 0.161	- 0.177	0.230	0.255	0.307	0.289
534.00	-0.135	- 0.118	- Q.234	-0.271	- 0.263	- 0.286	- 0.193	- 0.213	0.276	0.304	0.369	0.355
623.00	-0.158	- 0.133	- 0.273	-0.302	- 0.307	- 0.322	- 0.225	- 0.257	0.322	0.358	0.430	0.421
712.00	-0.180	- 0.151	- 0.312	-0.370	- 0.351	- 0.373	- 0.257	- 0.307	0.368	0.409	0.491	0.480

Applied Load (N)	BENDING MOMENTS (N.m.)						INCREASE IN TENSION (N)		
	Position C		Tower		Position G		Cal.	Load Cell	Cable Gauges
	Cal.	Exp.	Cal.	Exp.	Cal.	Exp.			
89.00	3.473	4.623	5.506	6.935	- 13.705	- 12.313	- 1.318	- 1.435	- 2.022
178.00	6.947	8.146	11.012	13.869	- 27.411	- 24.907	- 2.636	- 2.871	- 2.022
267.00	10.421	12.493	16.518	18.493	- 41.116	- 38.015	- 3.955	- 5.740	- 4.045
356.00	13.895	16.234	22.023	25.428	- 54.822	- 52.701	- 5.273	- 7.177	- 4.045
445.00	17.369	20.805	27.529	30.363	- 68.528	- 65.334	- 6.591	- 7.177	- 6.068
534.00	20.843	23.563	33.035	36.986	- 82.234	- 78.871	- 7.909	- 8.612	- 6.068
623.00	24.317	27.739	38.541	39.298	- 95.940	- 92.001	- 9.228	- 11.483	- 8.091
712.00	27.791	32.367	44.046	43.921	-109.647	-105.662	-10.546	- 14.354	- 10.114

The calculated and experimental results when the load is applied at loading station H

Table 7.10

Applied Load (N)	DEFLECTIONS (mms)											
	Station (1)		Station (2)		Station (3)		Station (4)		Station (5)		Station (6)	
	Cal.	Exp.	Cal.	Exp.	Cal.	Exp.	Cal.	Exp.	Cal.	Exp.	Cal.	Exp.
178.00	0.585	0.518	0.944	1.111	0.876	0.811	0.449	0.412	−0.194	− 0.214	− 0.157	− 0.170
356.00	1.170	0.992	1.889	2.034	1.752	1.665	0.898	0.838	−0.388	− 0.425	− 0.315	− 0.359
534.00	1.755	1.516	2.834	3.282	2.629	2.534	1.347	1.269	−0.583	− 0.628	− 0.472	− 0.502
712.00	2.341	2.128	3.780	4.285	3.506	3.533	1.796	1.769	−0.777	− 0.854	− 0.630	− 0.653
890.00	2.928	2.700	4.727	5.116	4.384	4.470	2.246	2.238	−0.972	− 1.150	− 0.787	− 0.795
1068.00	3.514	3.606	5.674	6.861	5.262	5.956	2.696	2.908	−1.167	− 1.341	− 0.945	− 1.030
1246.00	4.101	4.575	6.621	7.121	6.141	7.070	3.147	3.626	−1.362	− 1.562	− 1.103	− 1.248
1424.00	4.688	5.173	7.570	8.064	7.021	7.937	3.597	3.999	−1.557	− 1.718	− 1.261	− 1.410
1602.00	5.276	5.683	8.518	9.682	7.900	8.415	4.048	4.427	−1.752	− 2.171	− 1.419	− 1.625
1780.00	5.864	6.023	9.468	11.371	8.781	9.674	4.499	4.989	−1.948	− 2.696	− 1.578	− 2.413
1869.00	6.685	7.211	11.136	12.317	10.379	11.004	5.162	5.678	−2.207	− 2.813	− 1.780	− 2.633
1958.00	7.842	8.456	13.485	14.679	12.631	13.109	6.097	7.212	−2.572	− 3.016	− 2.065	− 2.825
2047.00	9.000	9.734	15.835	16.883	14.883	15.311	7.031	8.111	−2.937	− 3.362	− 2.350	− 3.080
2136.00	10.157	13.613	18.185	22.851	17.134	20.913	7.966	10.041	−3.302	− 4.215	− 2.635	− 3.989

Applied Load (N)	BENDING MOMENTS (N.m.)						INCREASE IN TENSION (N)		
	Position C		Tower		Position 6		Cal.	Load Cell	Cable Gauges
	Cal.	Exp.	Cal.	Exp.	Cal.	Exp.			
178.00	−129.350	−143.323	78.423	68.856	42.790	39.051	35.798	30.144	32.365
356.00	−258.761	−288.960	156.881	140.367	85.614	79.480	71.597	63.158	68.775
534.00	−388.231	−406.790	235.376	203.987	128.472	117.154	107.395	94.737	101.140
712.00	−517.762	−561.034	313.907	281.316	171.365	162.894	143.193	129.187	129.459
890.00	−647.353	−701.366	392.474	352.716	214.293	202.568	178.991	163.636	161.823
1068.00	−777.004	−819.315	471.076	431.449	257.255	241.570	214.790	203.828	202.279
1246.00	−906.715	−952.463	549.716	507.882	300.251	283.661	250.588	244.019	230.600
1424.00	−1036.487	− 1092.764	628.391	569.368	343.282	317.632	286.386	275.598	262.963
1602.00	−1166.319	− 1275.924	707.103	743.811	386.348	378.526	322.185	301.435	295.328
1780.00	−1296.215		785.850	836.720	429.449	433.436	357.891	373.906	364.103
1869.00			906.582	987.361	490.555	523.655	428.600	410.815	404.559
1958.00			1060.641	1251.760	567.896	641.486	528.005	501.621	495.121
2047.00			1214.700		615.237	923.615	627.487	702.124	685.470
2136.00					722.578	1105.221	727.000	815.351	789.130

The calculated and experimental results when the load to failure is applied at loading station C

Text cut off in original

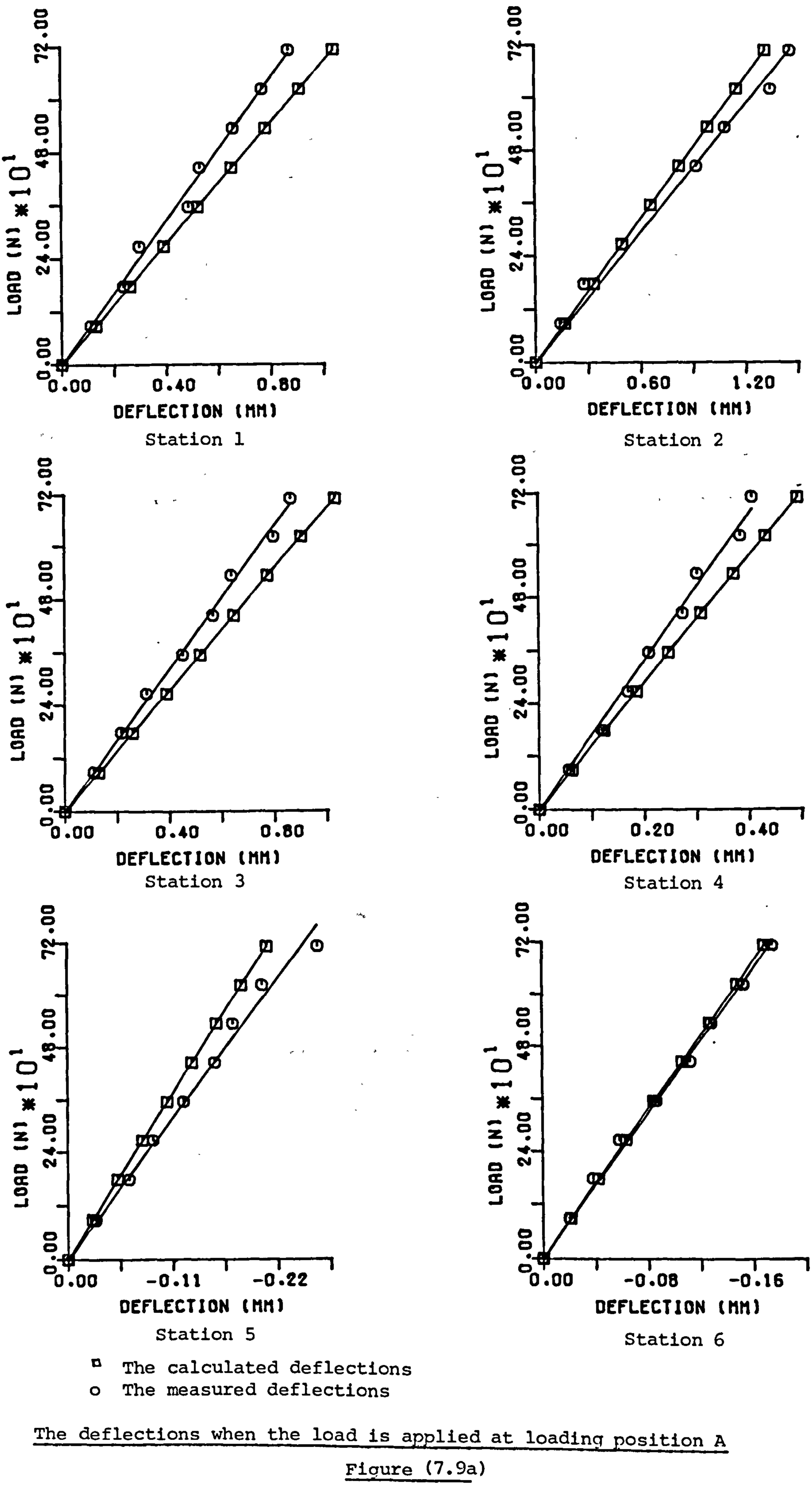

□ The calculated deflections
o The measured deflections

The deflections when the load is applied at loading position A

Figure (7.9a)

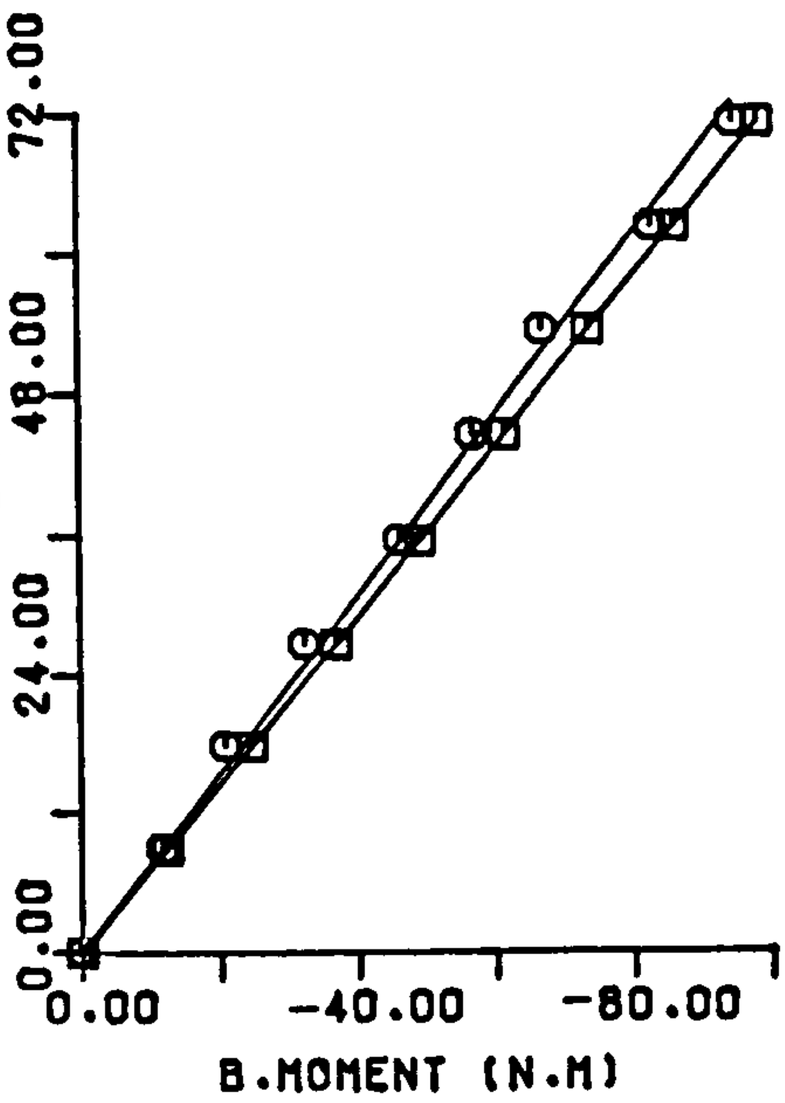

Position C

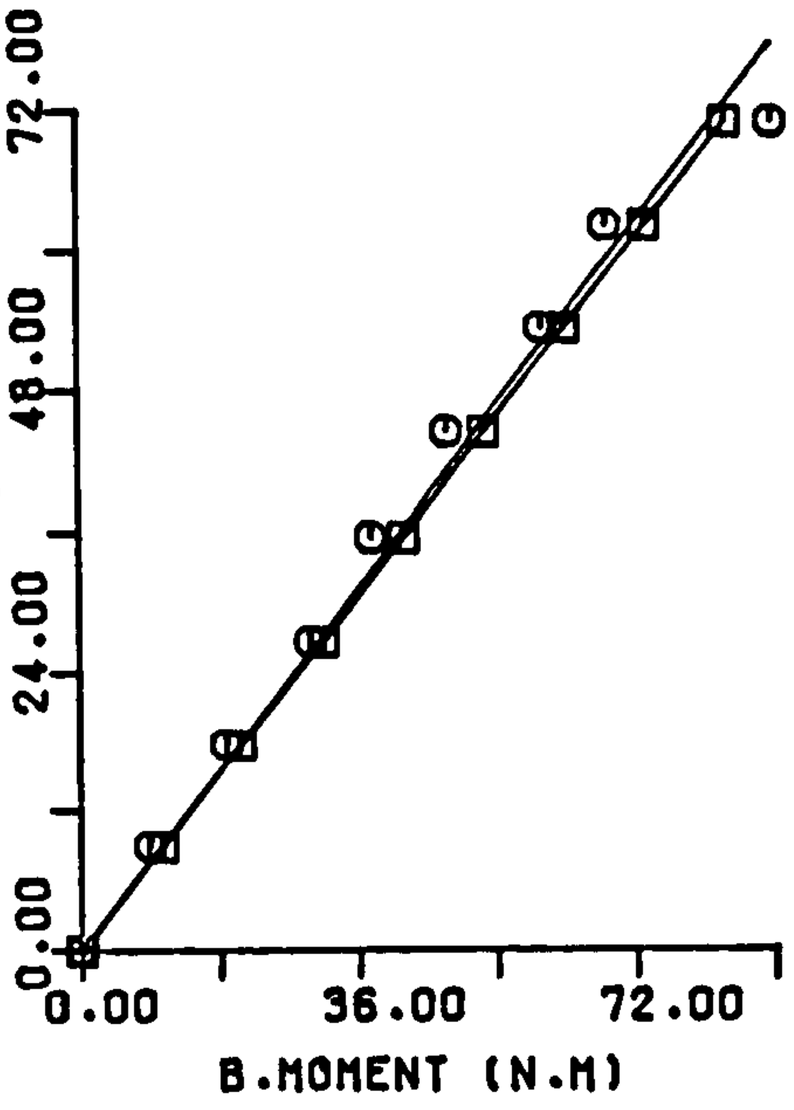

Tower Position

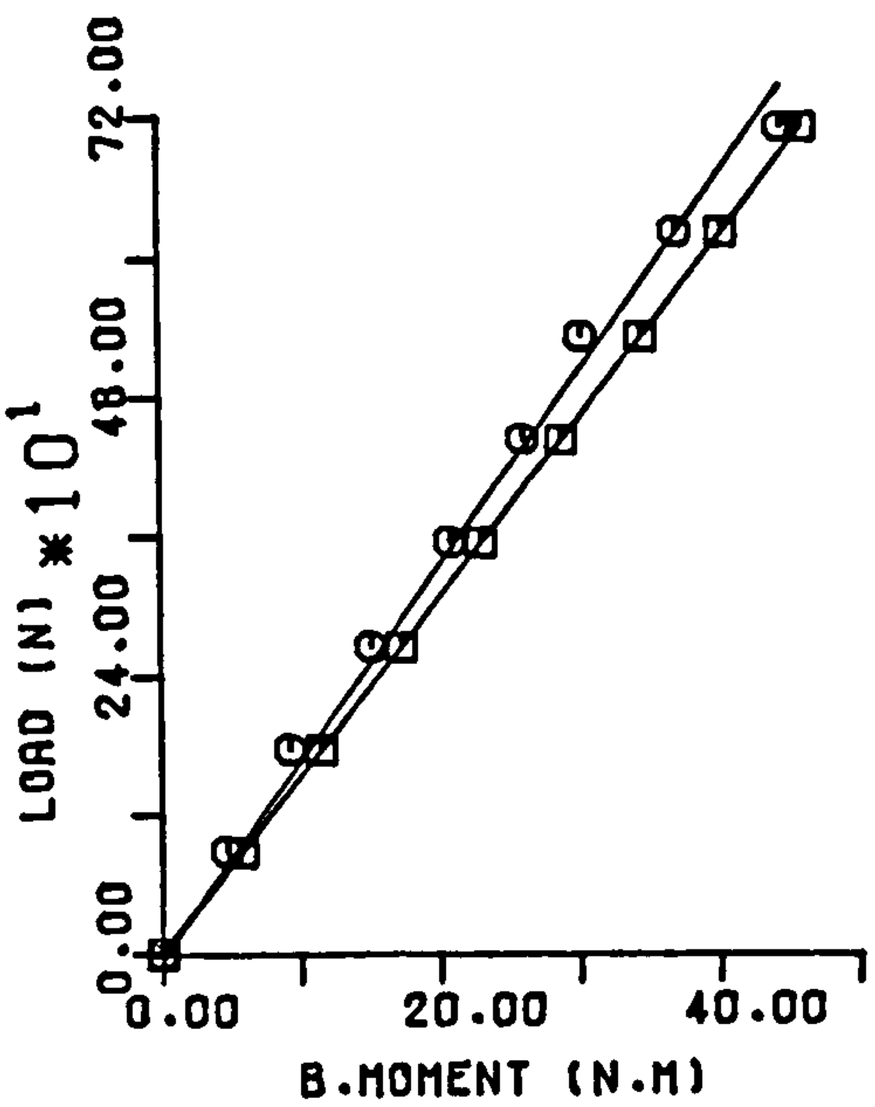

Position G

- ▫ The calculated bending moments
- o The actual bending moments

The bending moments when the load is applied at loading station A

Figure (7.9b)

Text cut off in original

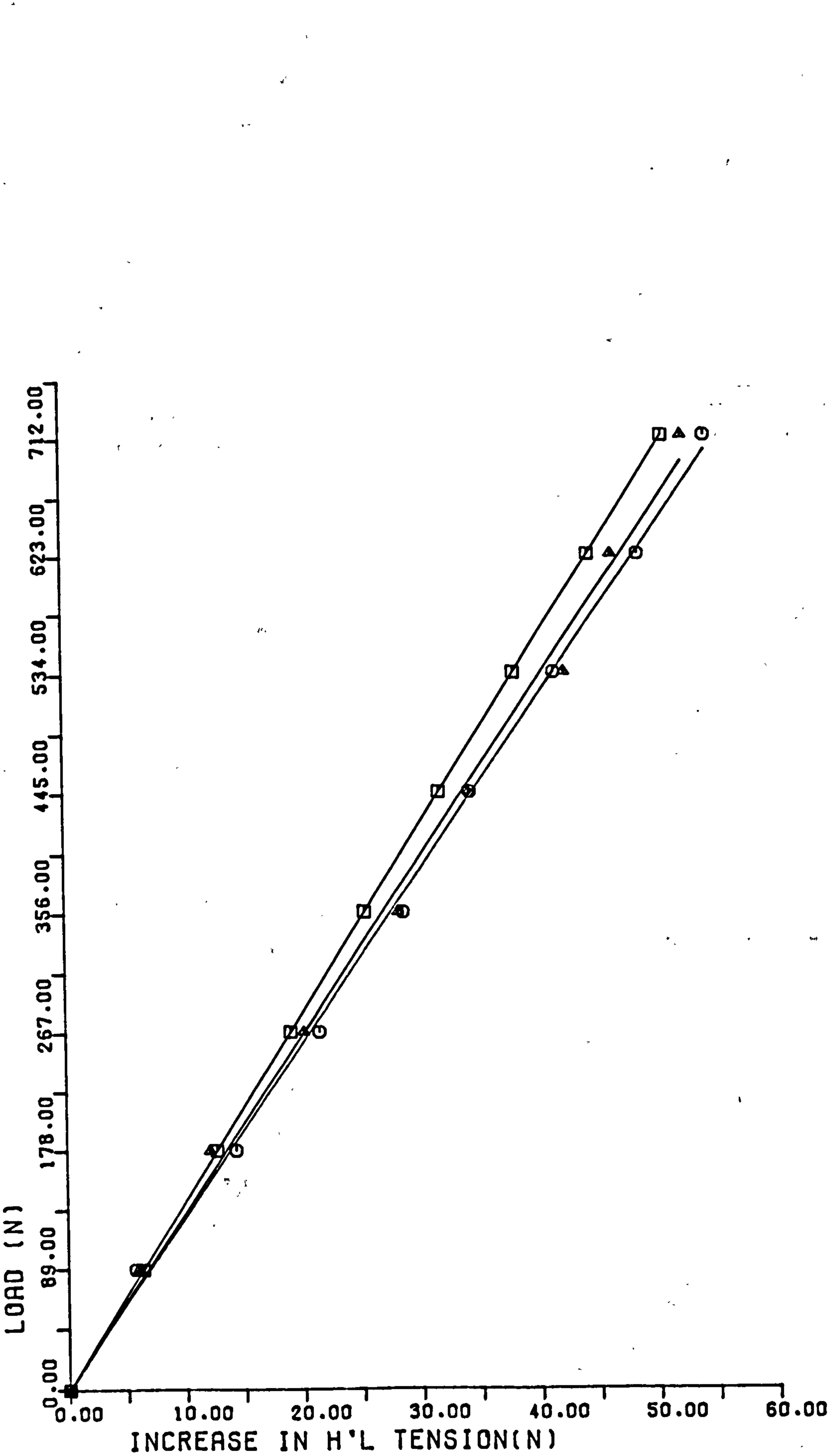

▫ The calculated values
o Load cell readings
Δ Cable gauges readings

The change in the prestressing force when the load is applied at loading station A

Figure (7.9c)

Text cut off in original

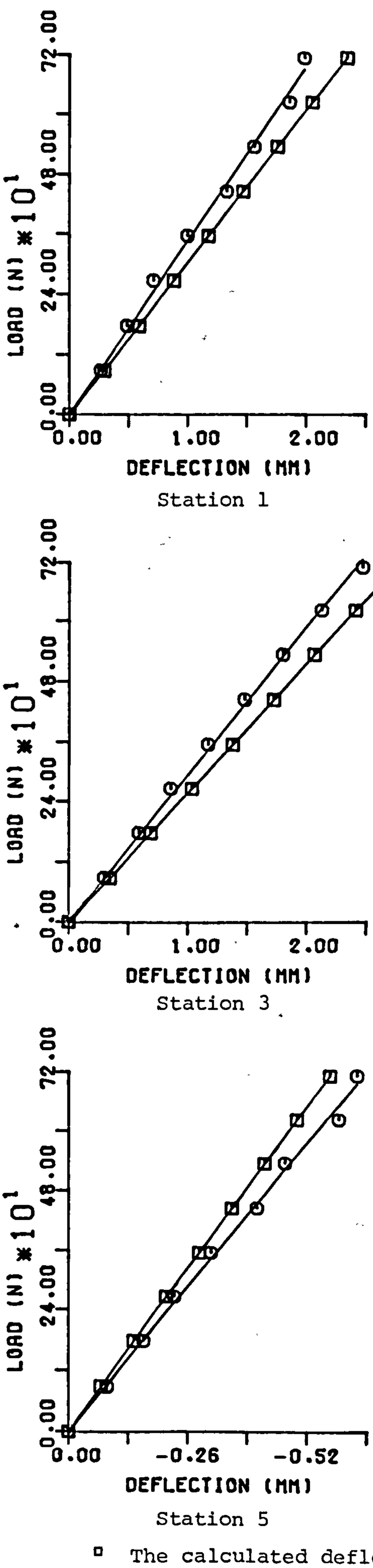

□ The calculated deflections
o The measured deflections

The deflections when the load is applied at loading position B

Figure(7.10a)

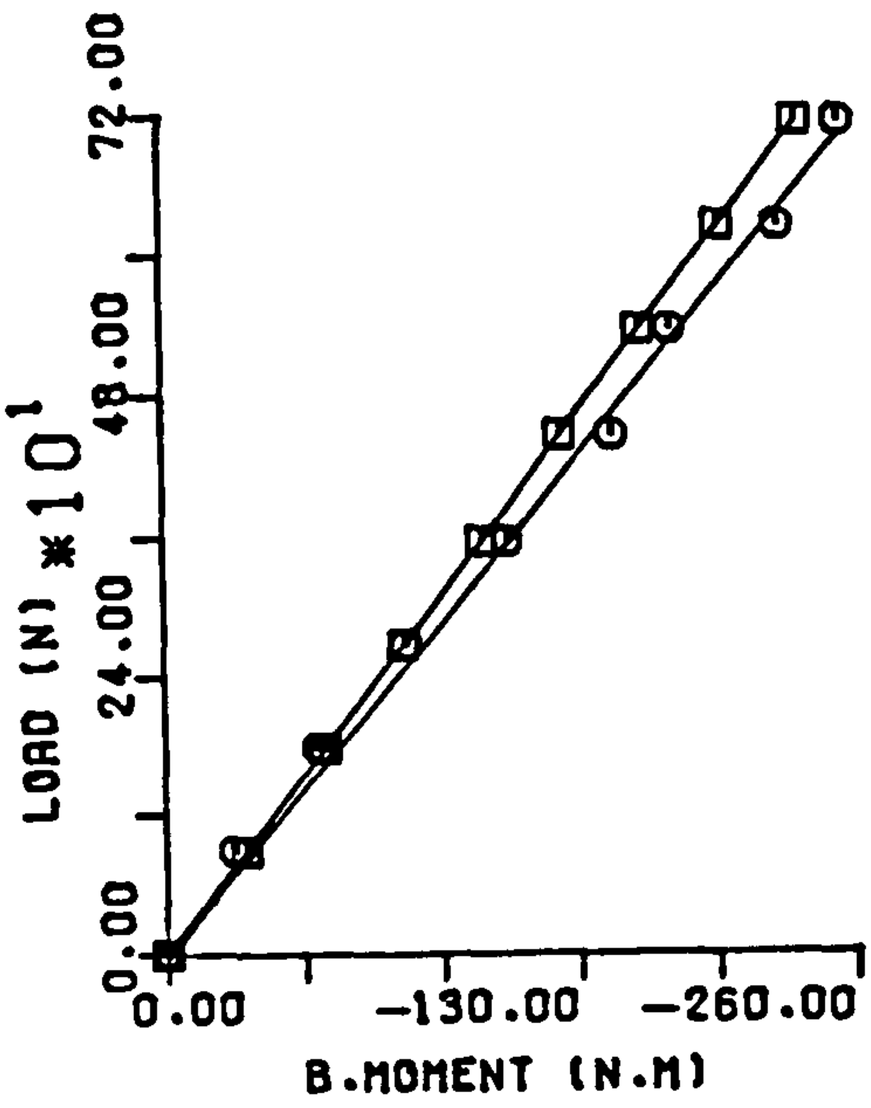

Position C

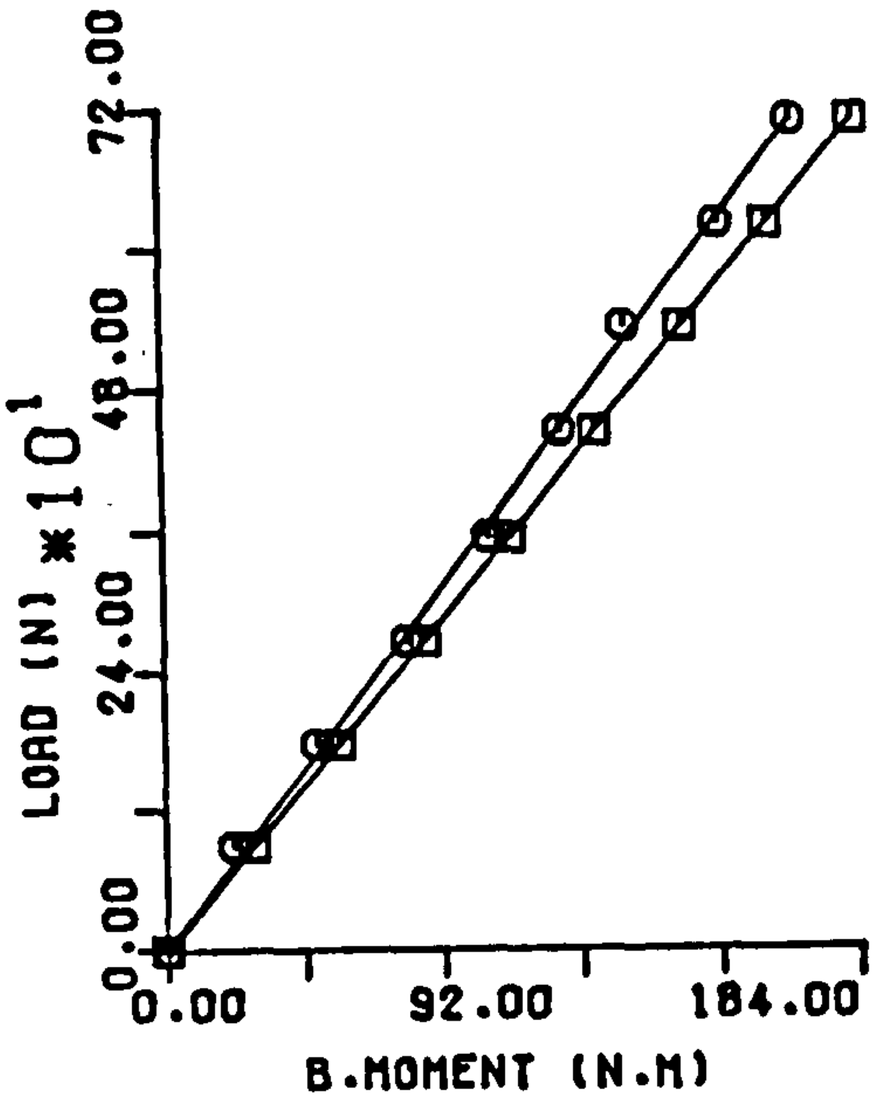

Tower Position

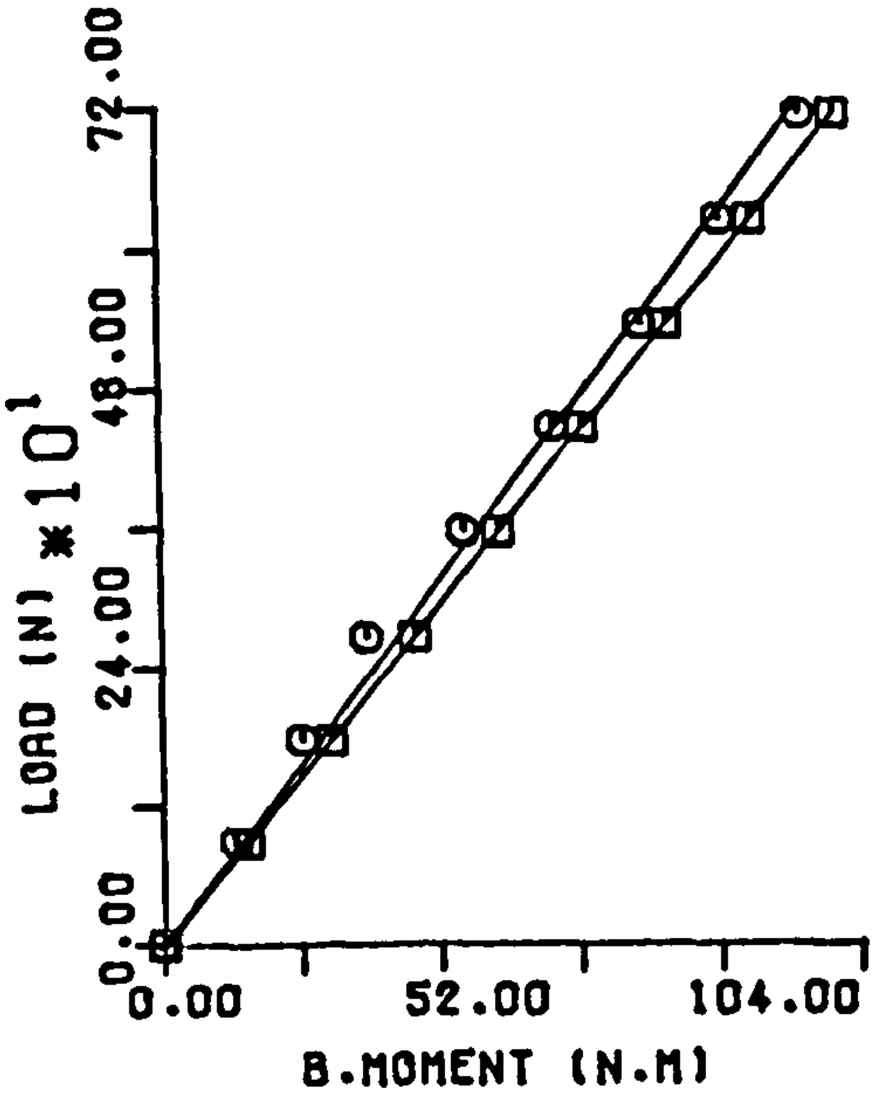

Position G

- ▫ The calculated bending moments
- o The actual bending moments

The bending moments when the load is applied at loading station B

Figure (7.10b)

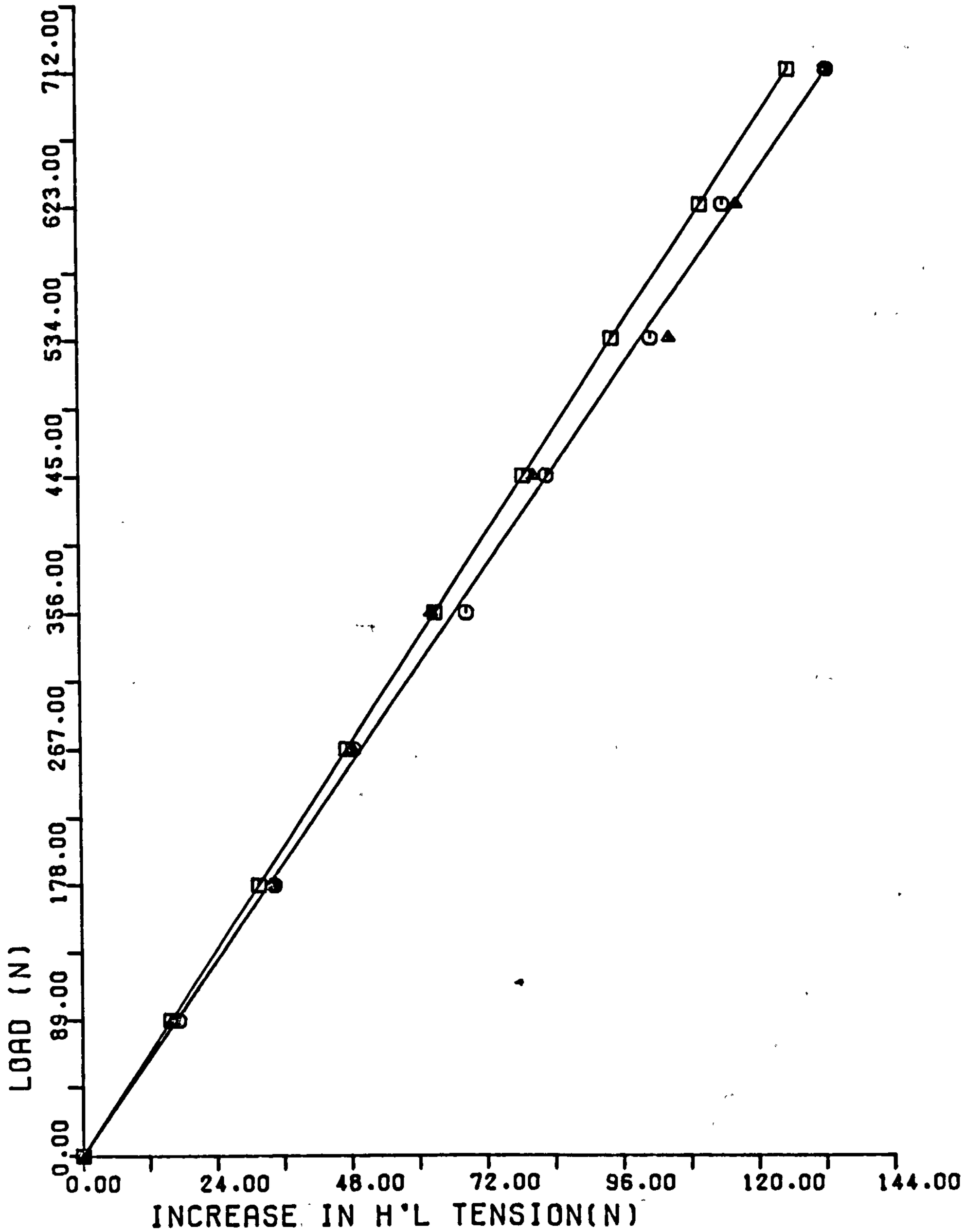

□ The calculated values
o Load cell readings
Δ Cable gauges readings

The change in the prestressing force when the load is applied at loading station B

Figure (7.10c)

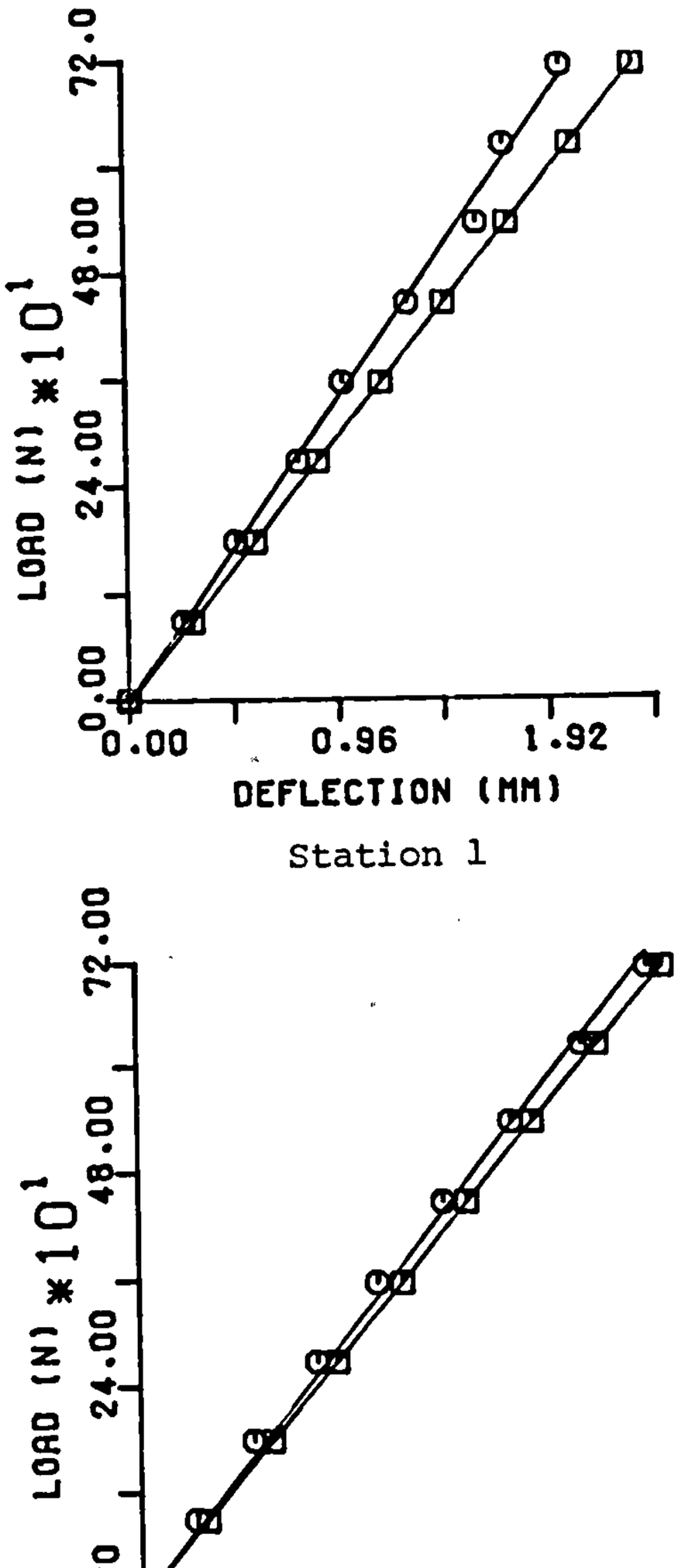

Station 1

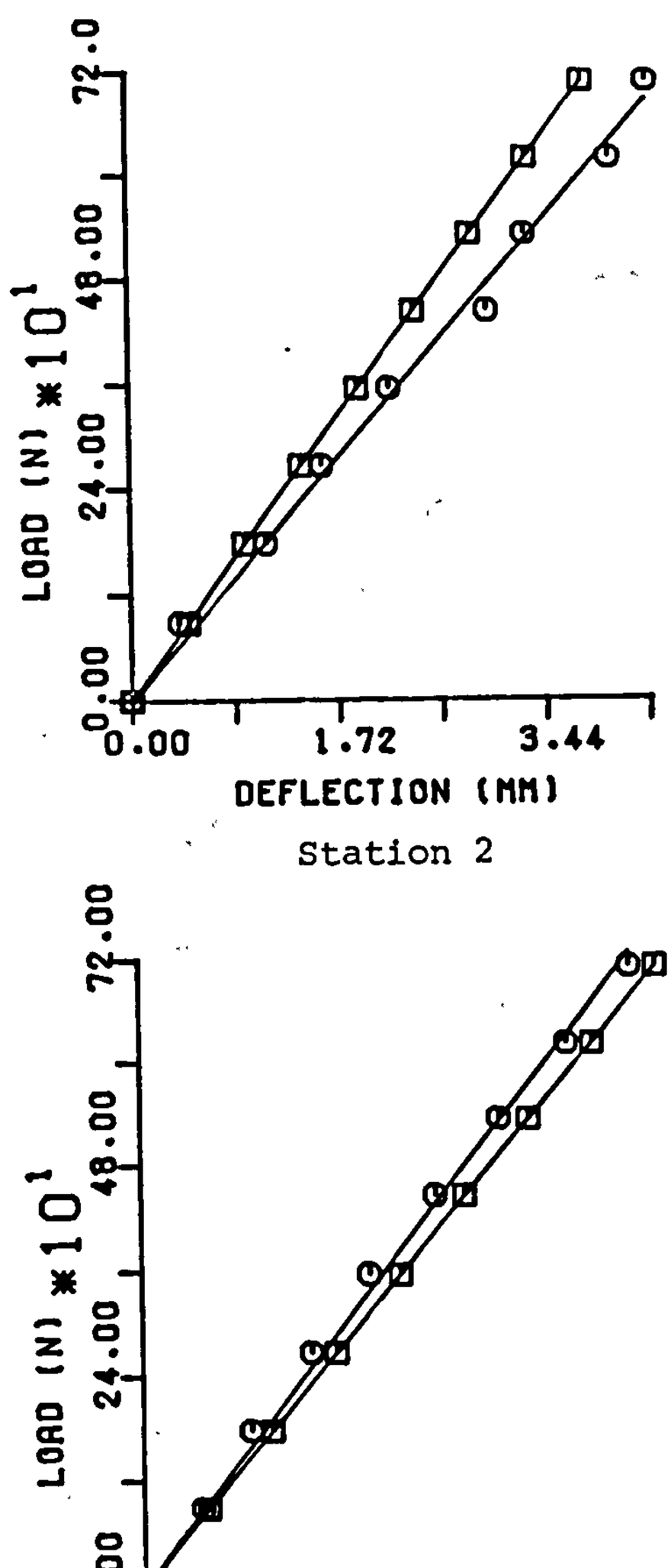

Station 2

Station 3

Station 4

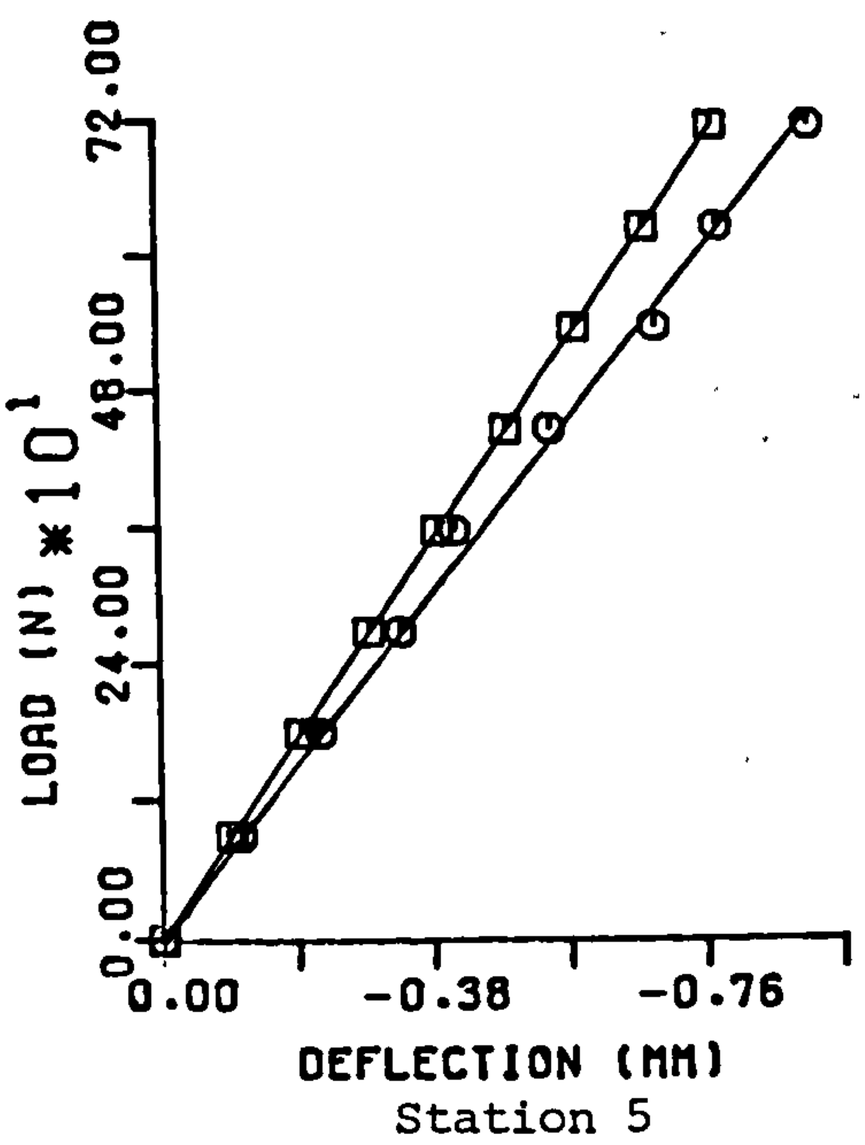

Station 5

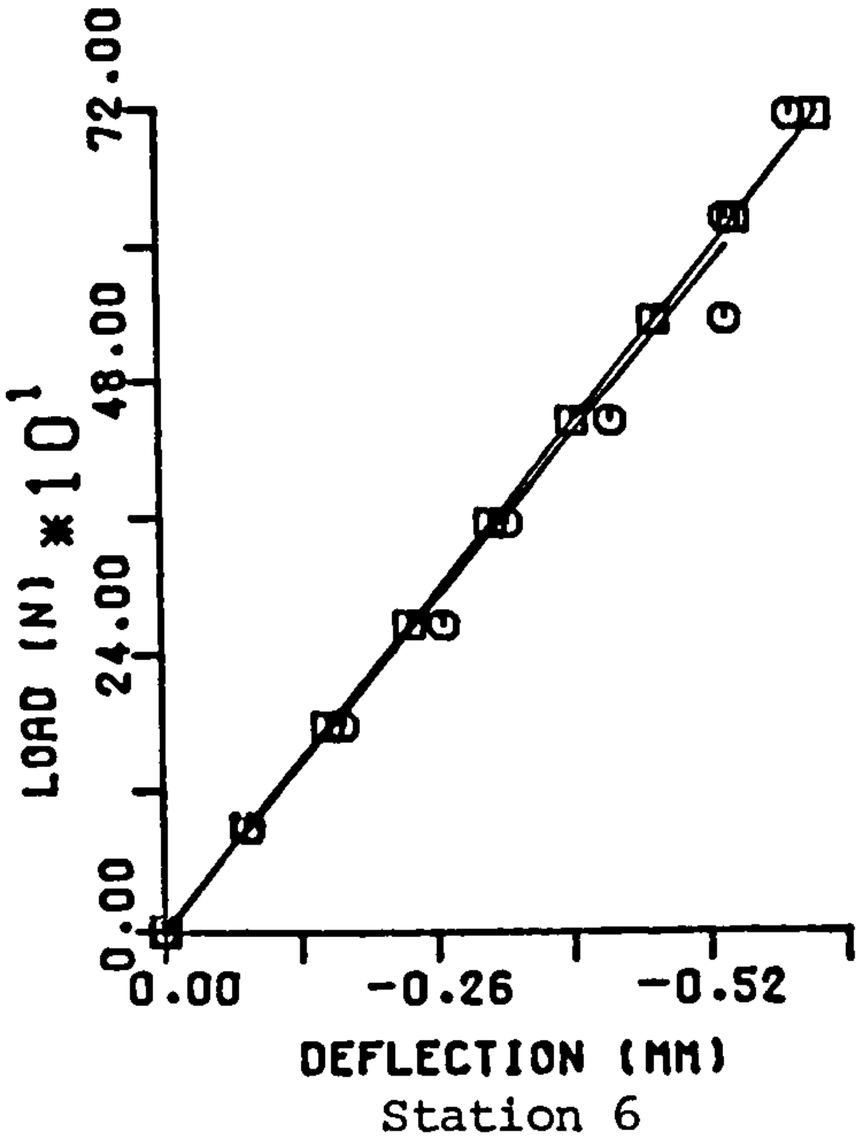

Station 6

▫ The calculated deflections
o The measured deflections

The deflections when the load is applied at loading position C

Figure (7.11a)

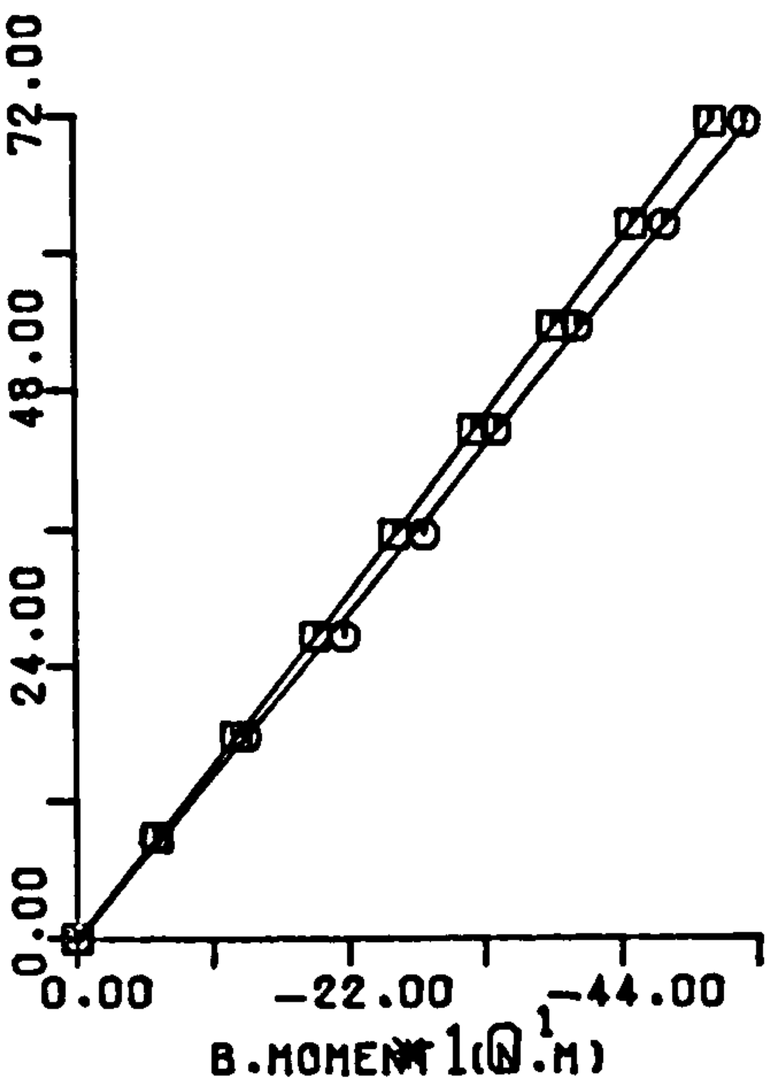

Position C

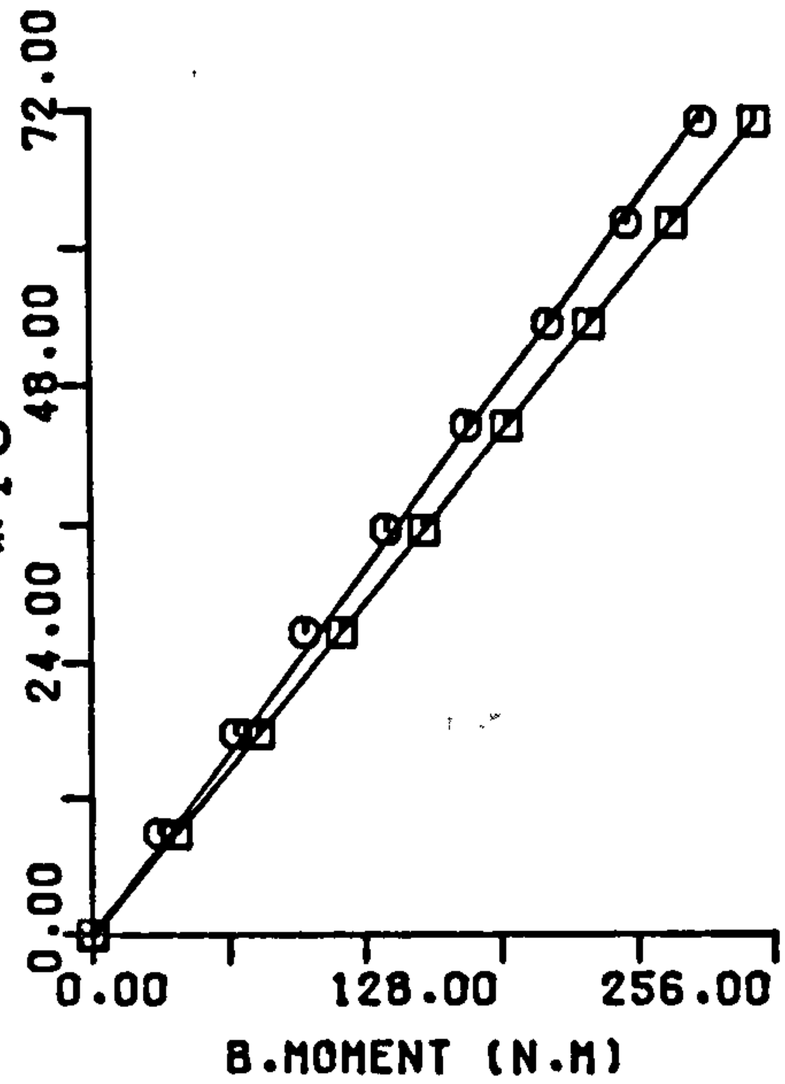

Tower Position

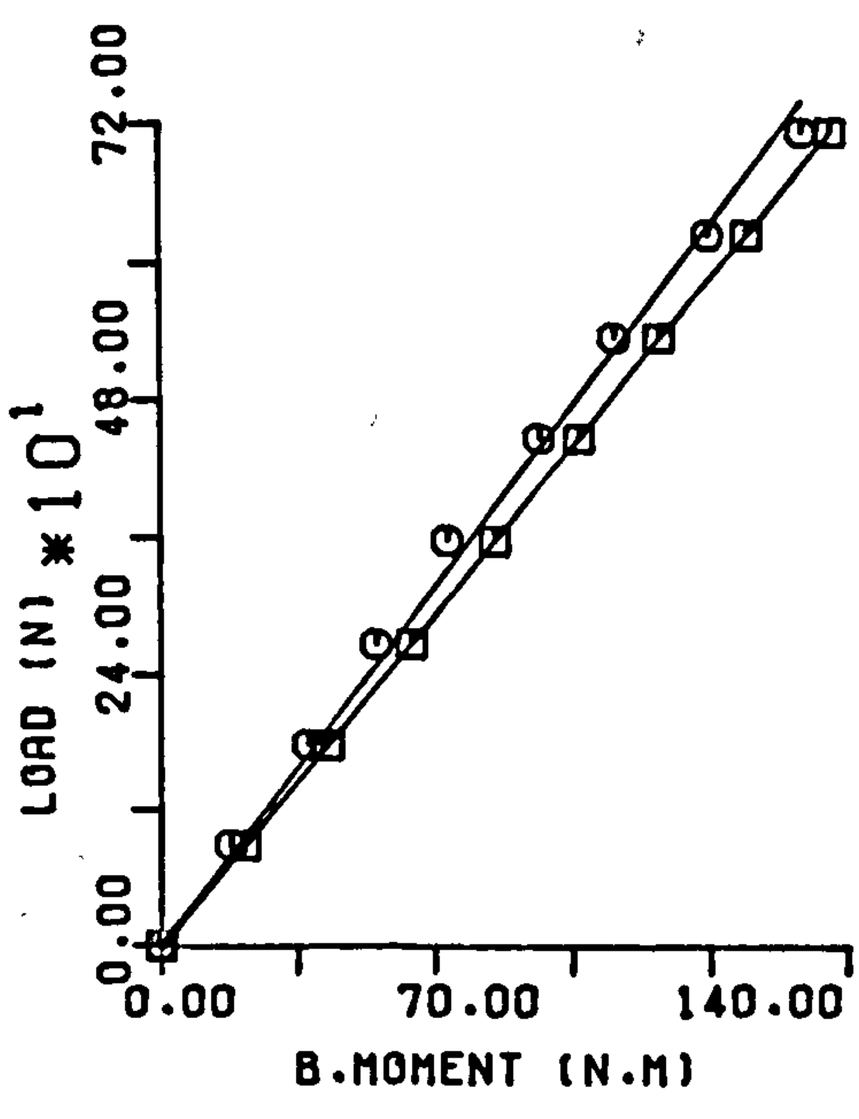

Position G

- ▫ The calculated bending moments
- o The actual bending moments

The bending moments when the load is applied at loading station C

Figure (7.11b)

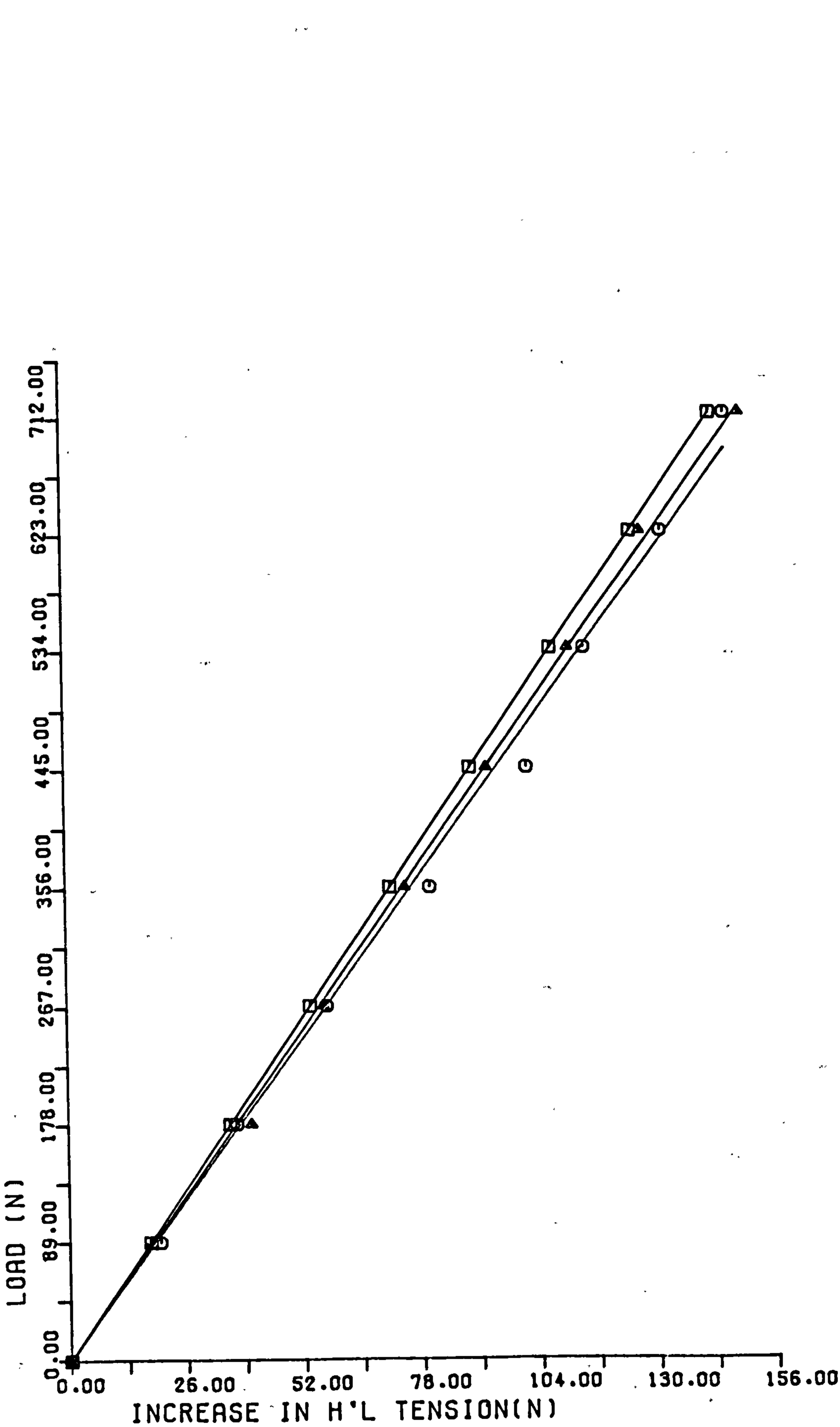

□ The calculated values
o Load cell readings
Δ Cable gauges readings

The change in the prestressing force when the load is applied at loading station C

Figure (7.11c)

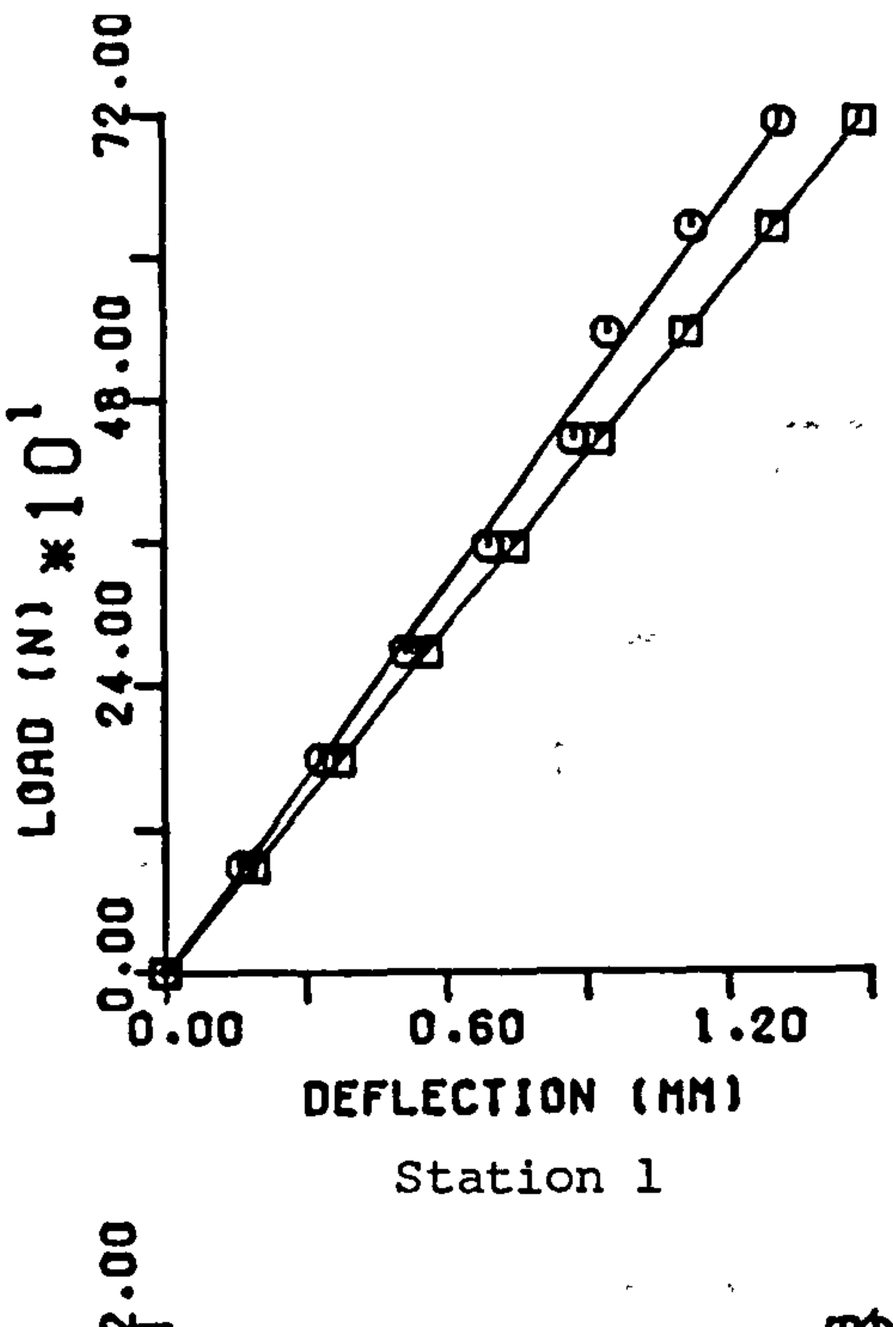

Station 1

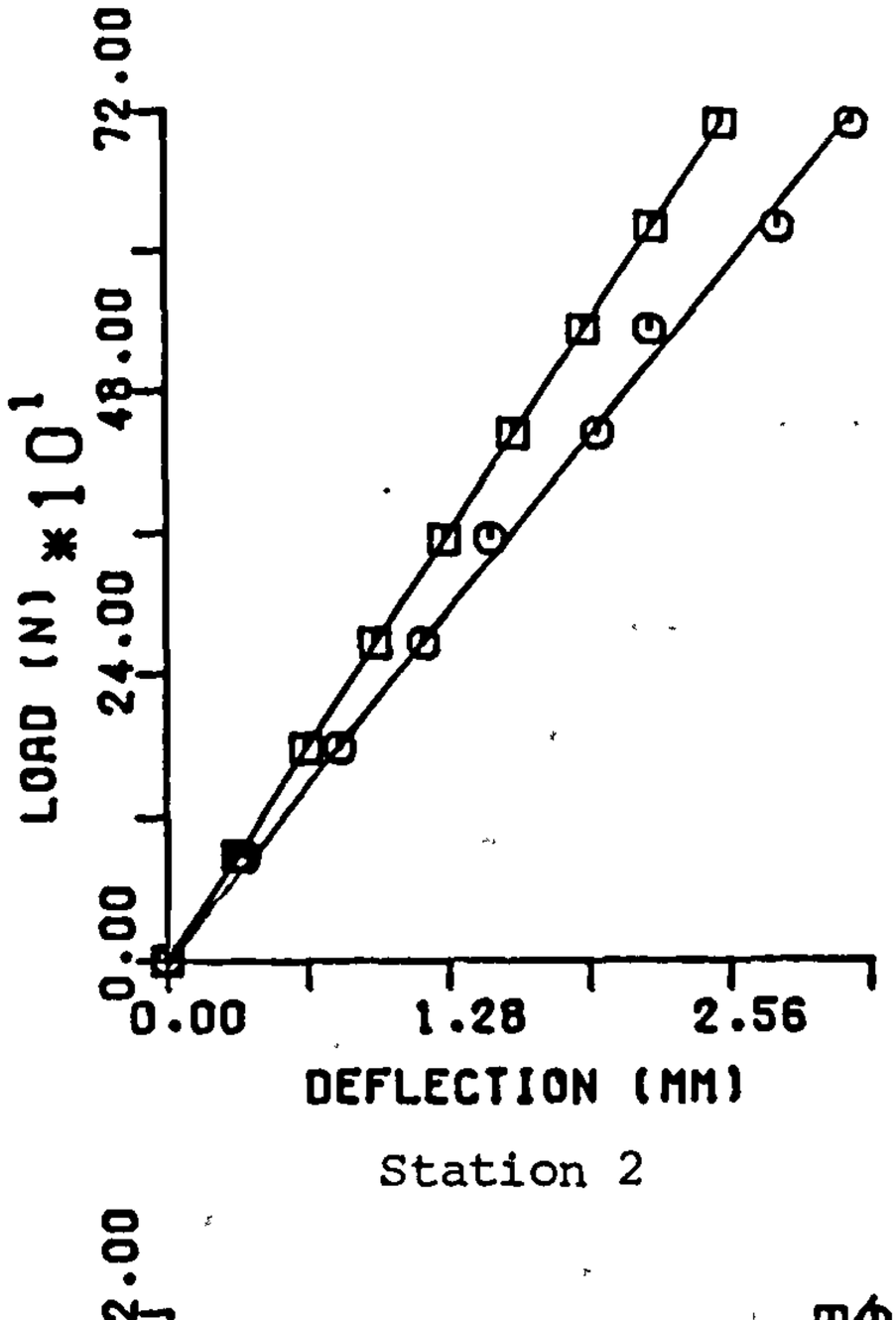

Station 2

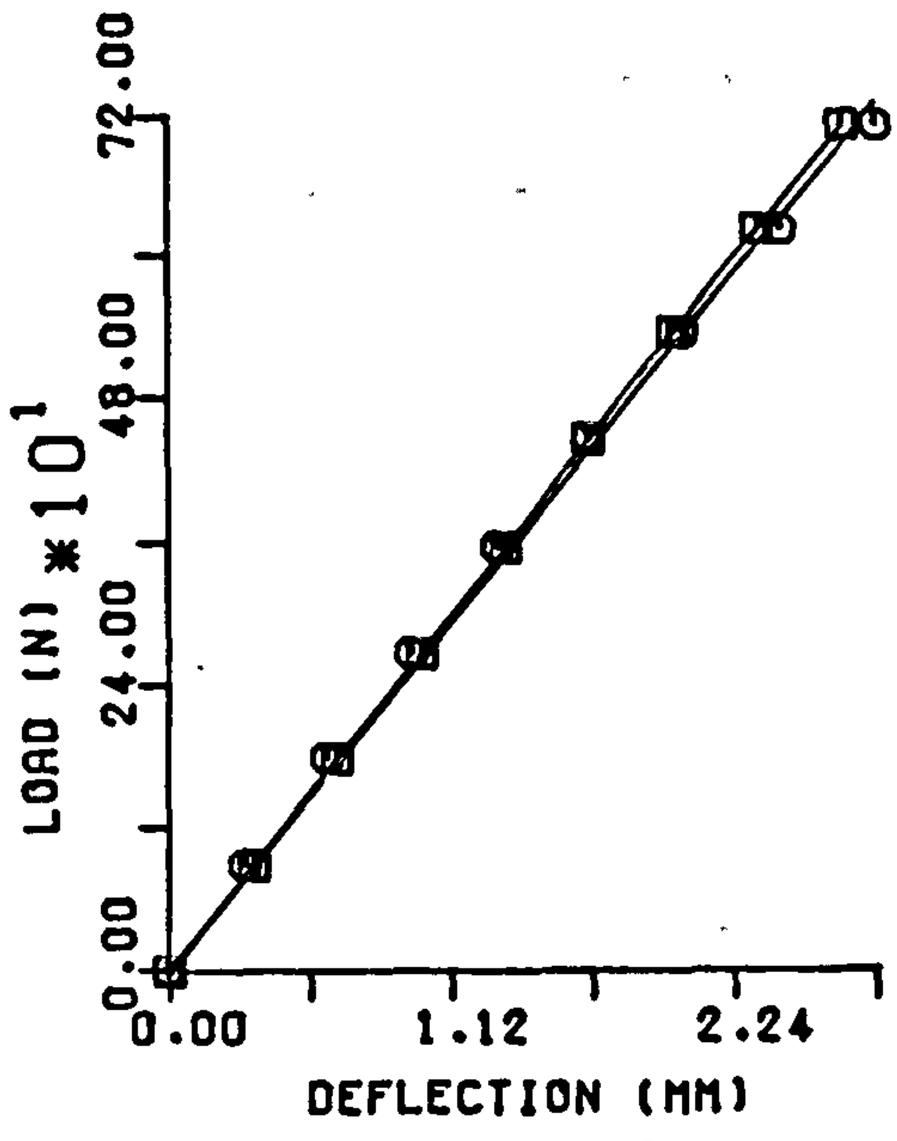

Station 3

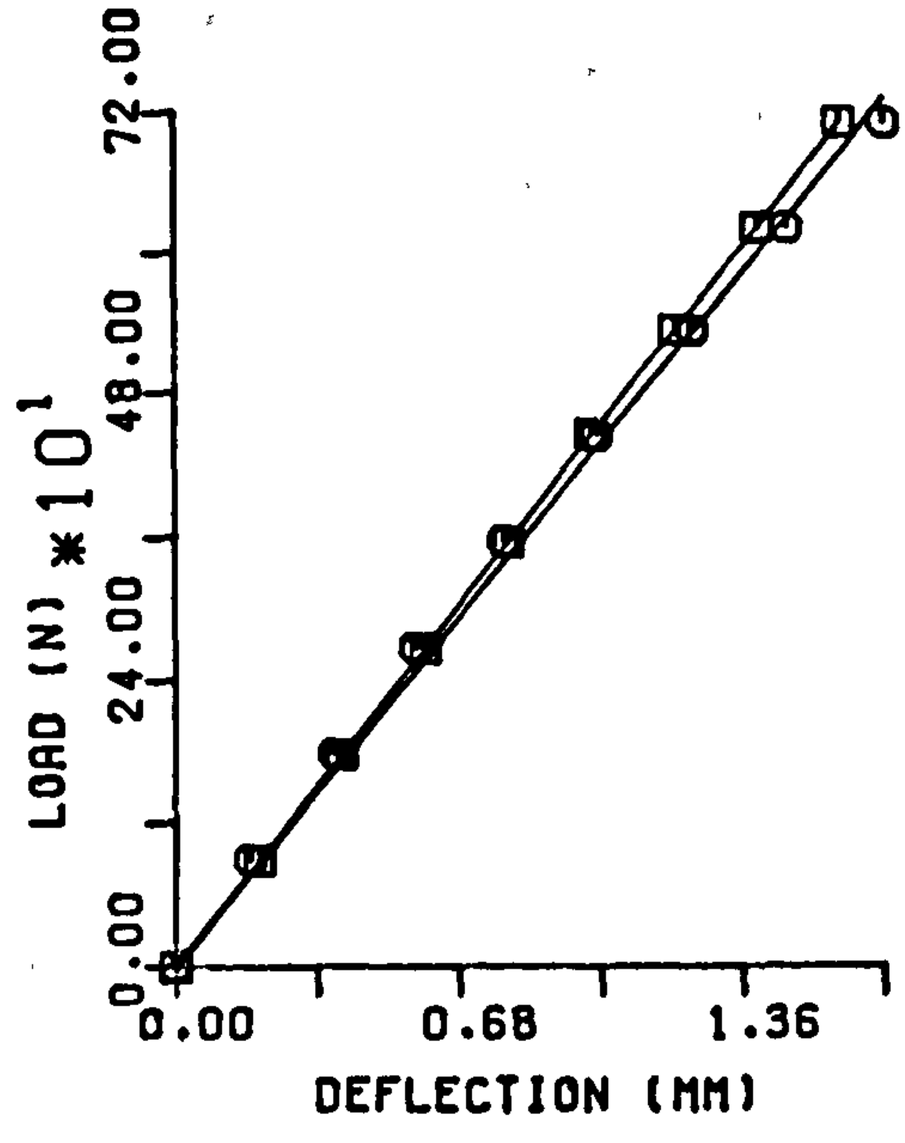

Station 4

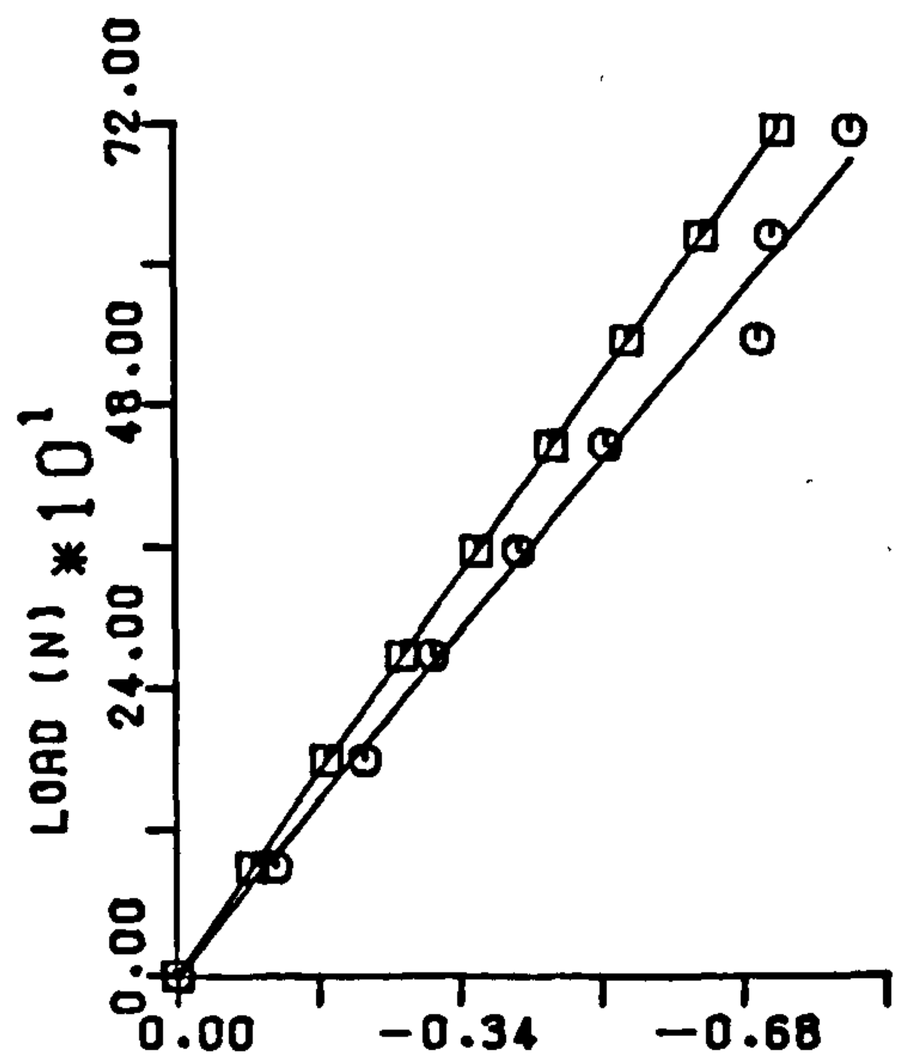

Station 5

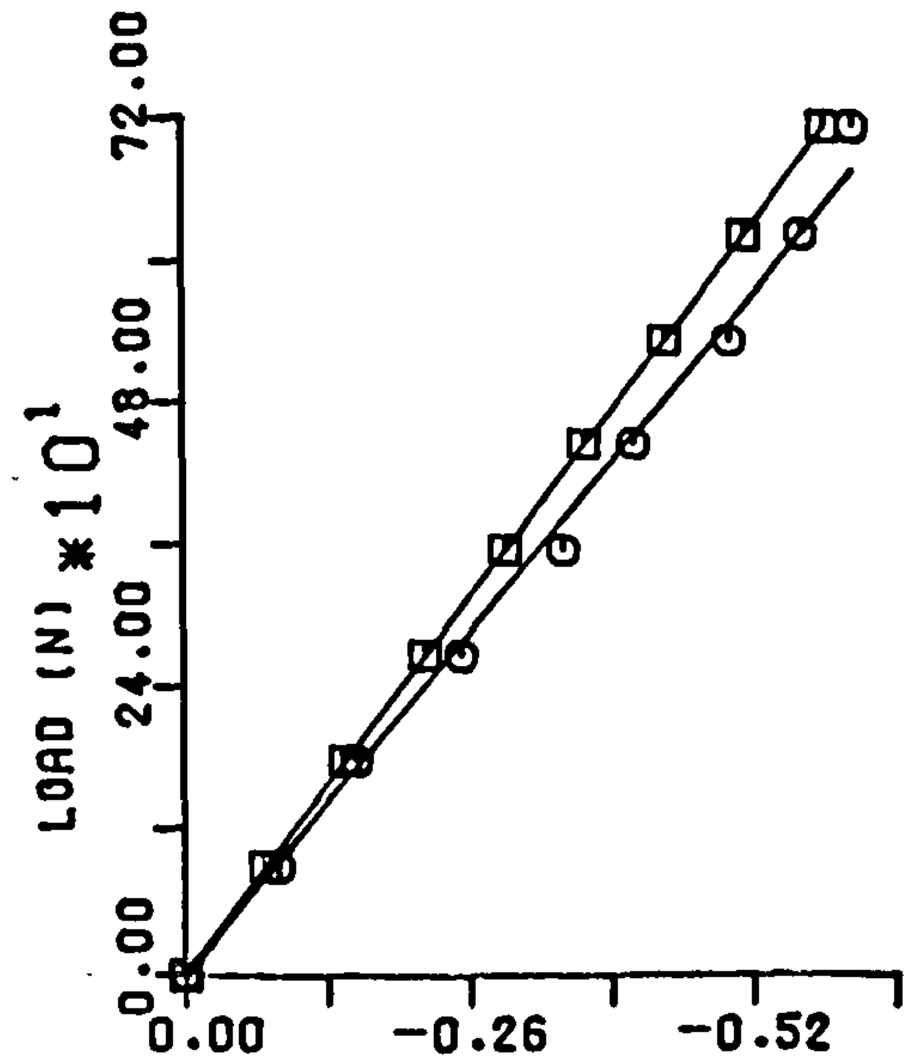

Station 6

▫ The calculated deflections
o The measured deflections

The deflections when the load is applied at loading position D

Figure(7.12a)

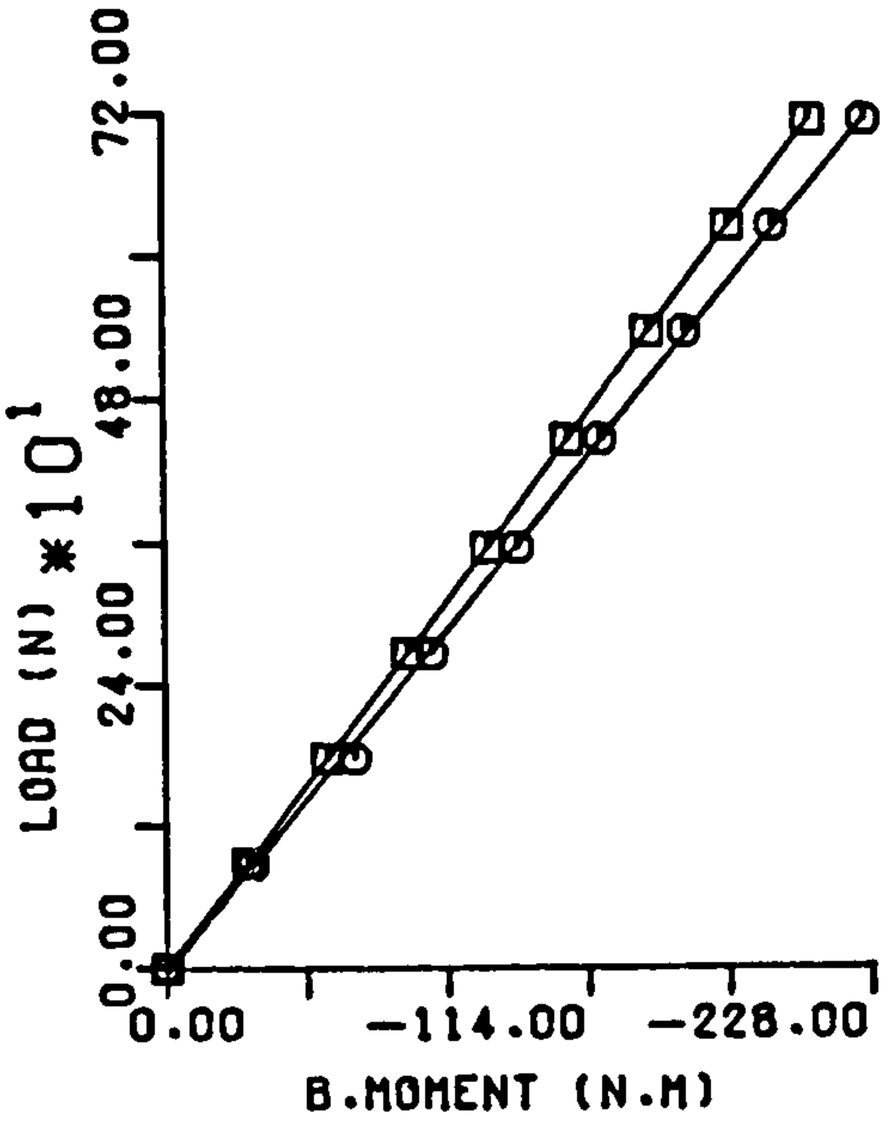

Position C

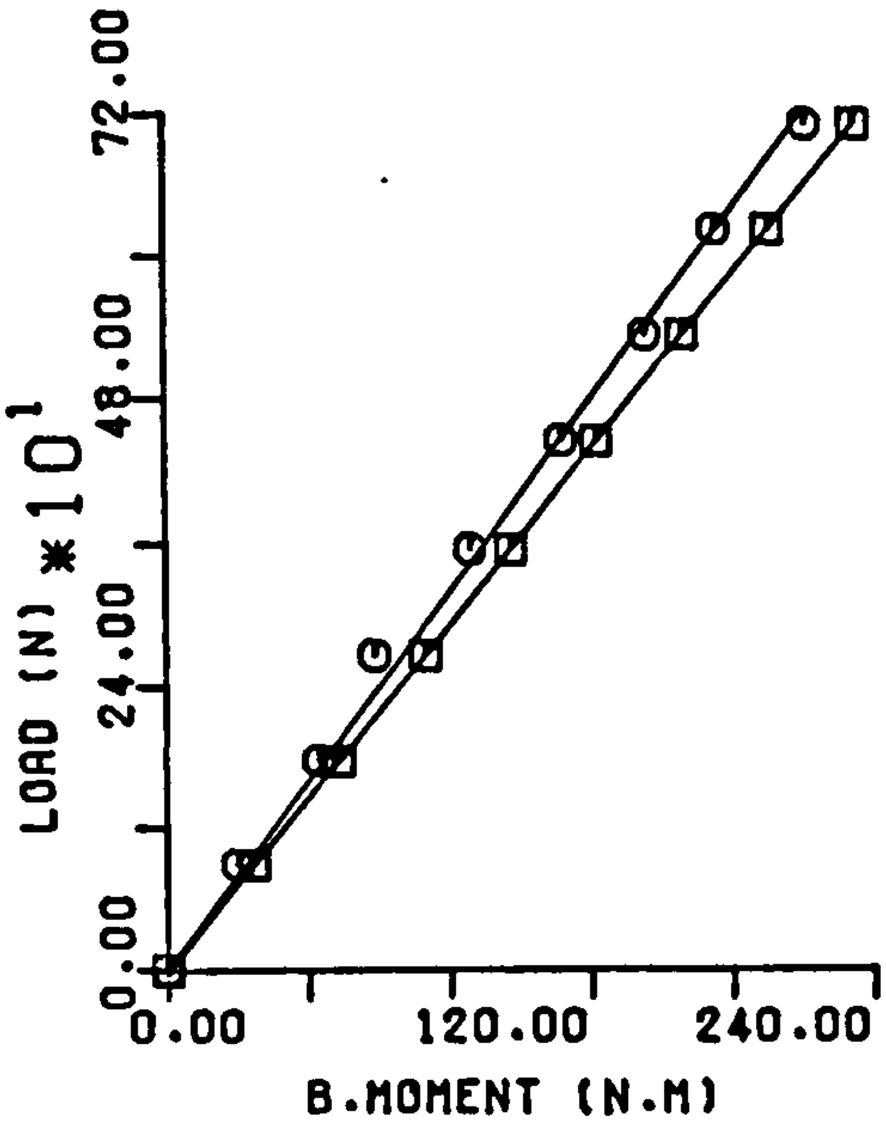

Tower Position

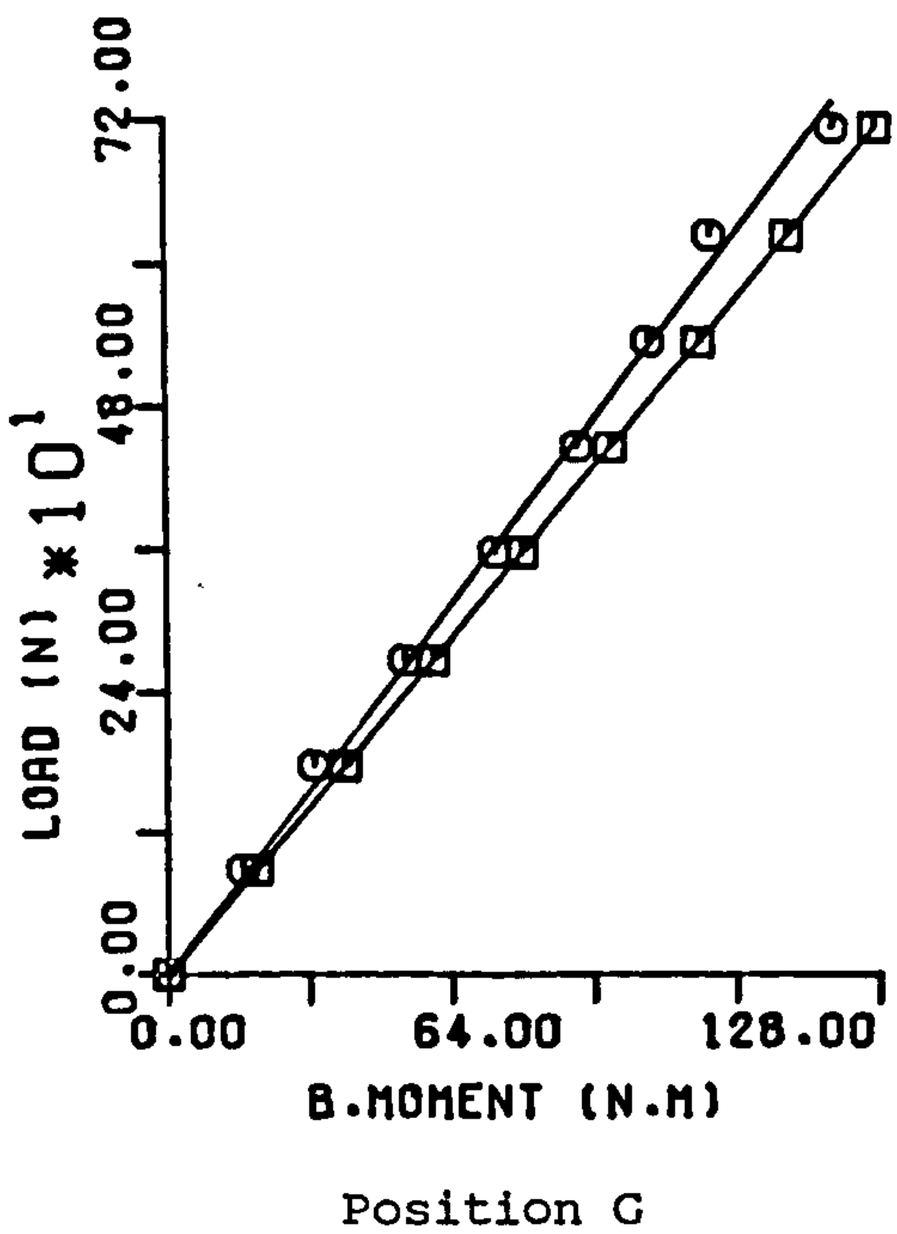

Position G

- ▫ The calculated bending moments
- o The actual bending moments

The bending moments when the load is applied at loading station D

Figure (7.12b)

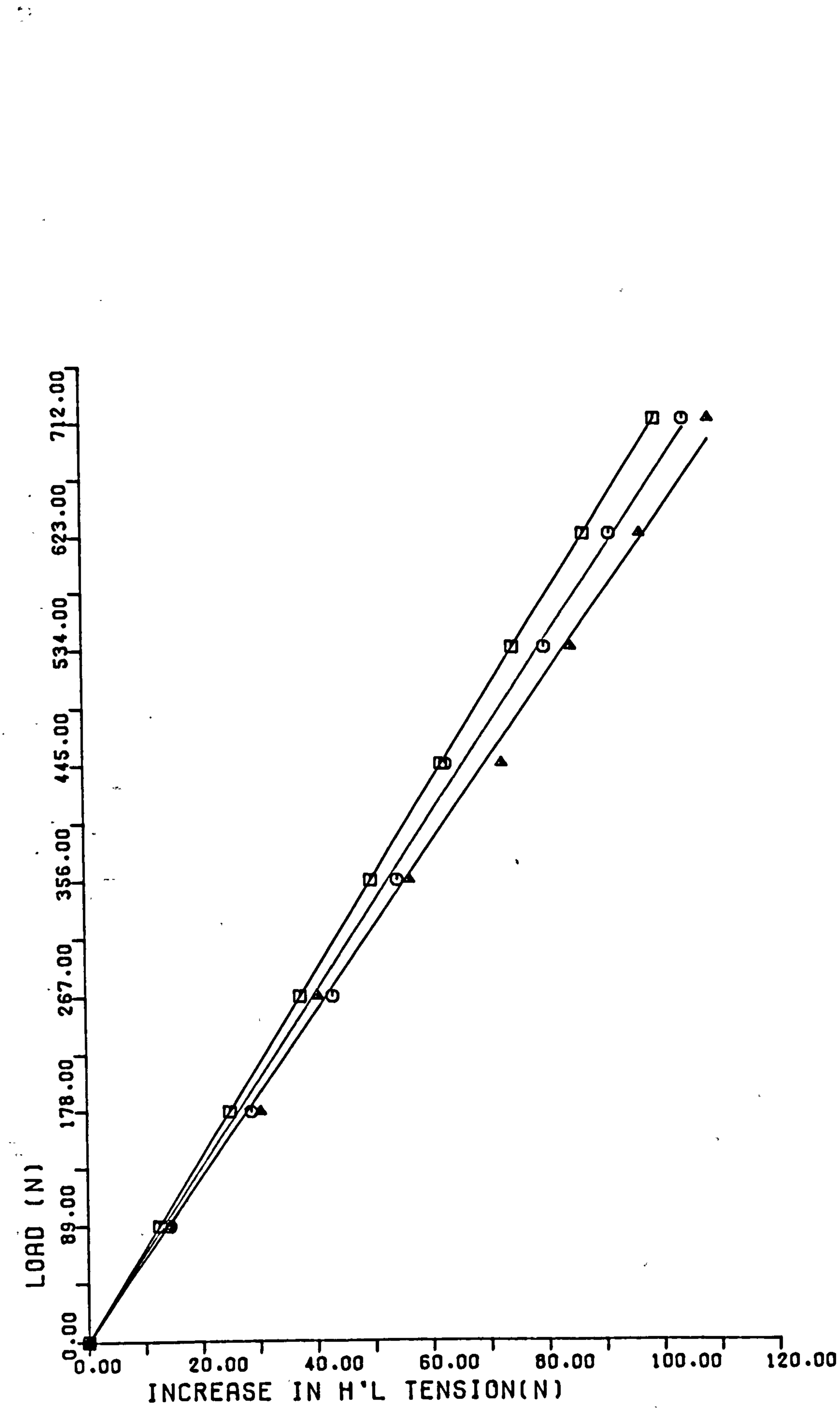

▫ The calculated values
o Load cell readings
Δ Cable gauges readings

The change in the prestressing force when the load is applied at loading station D

Figure (7.12c)

Station 1

Station 2

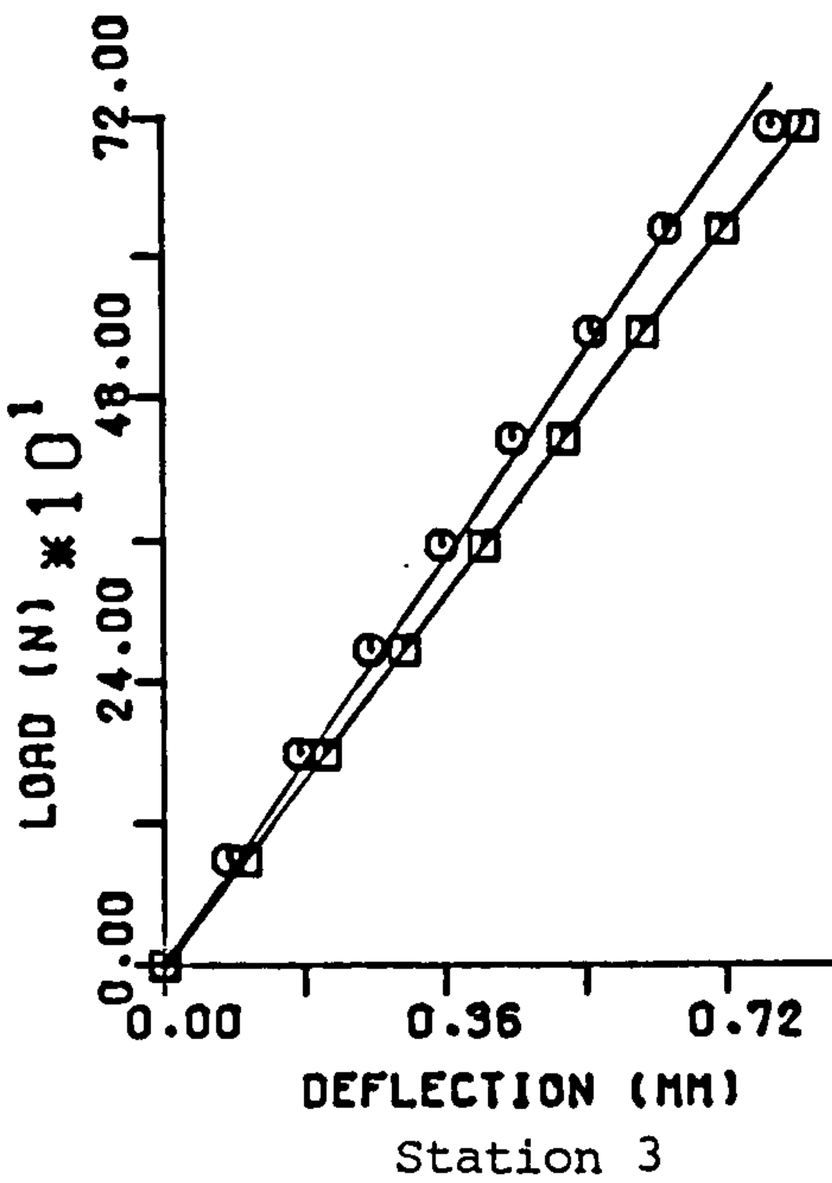

Station 3

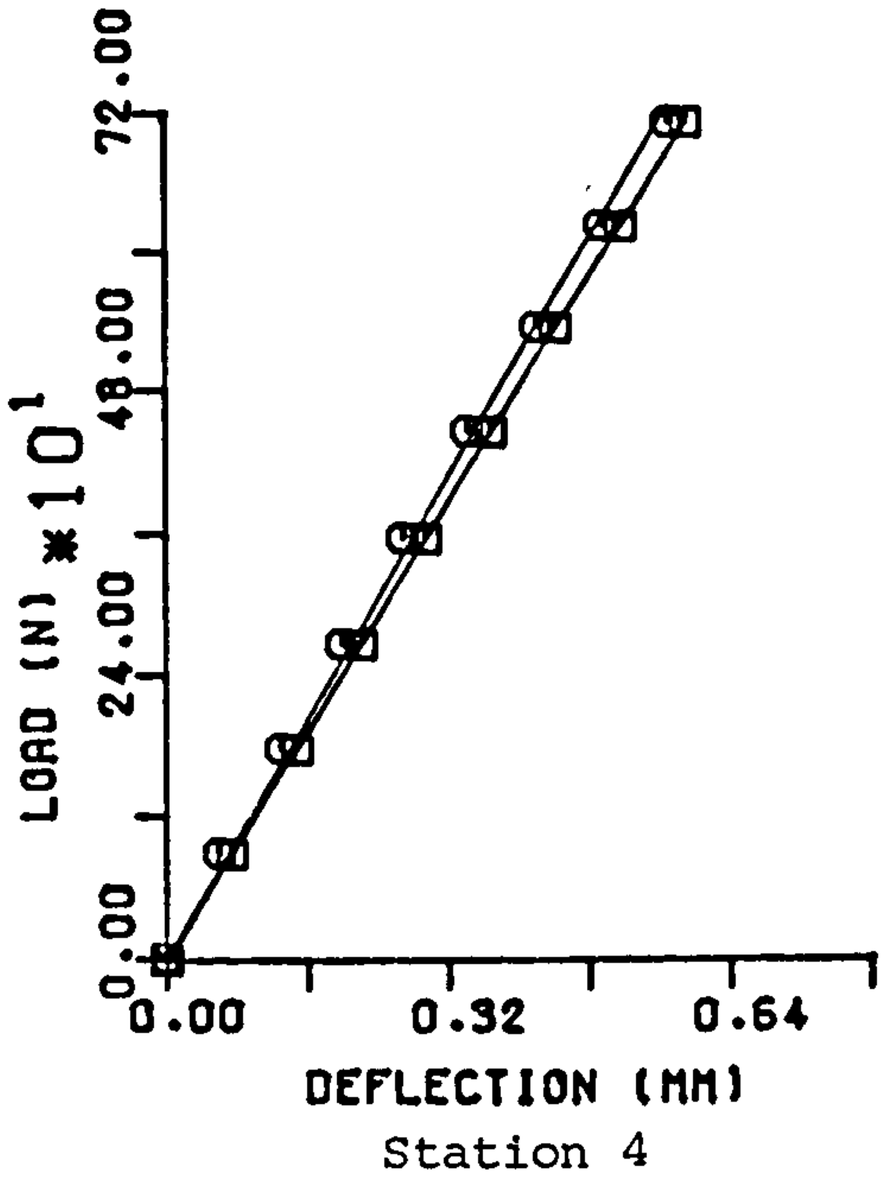

Station 4

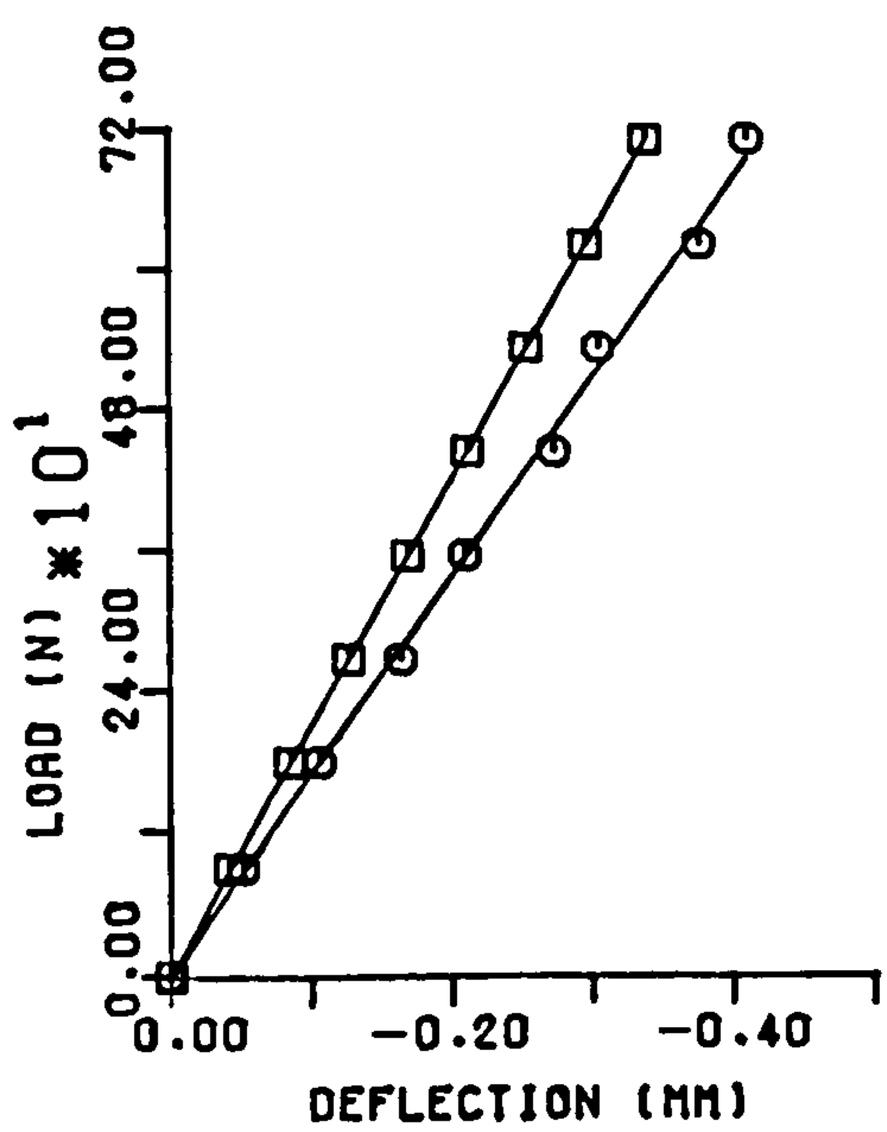

Station 5

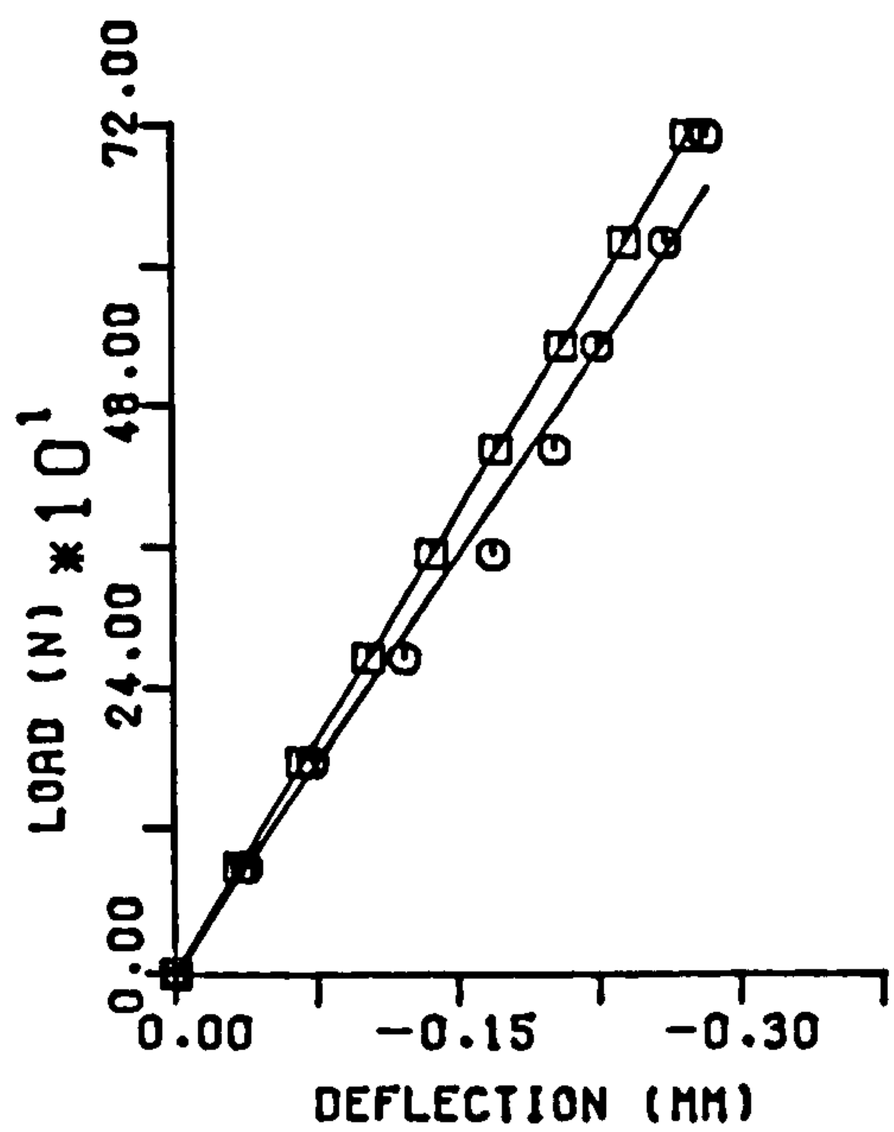

Station 6

▫ The calculated deflections
o The measured deflections

The deflections when the load is applied at loading position E

Figure (7.13a)

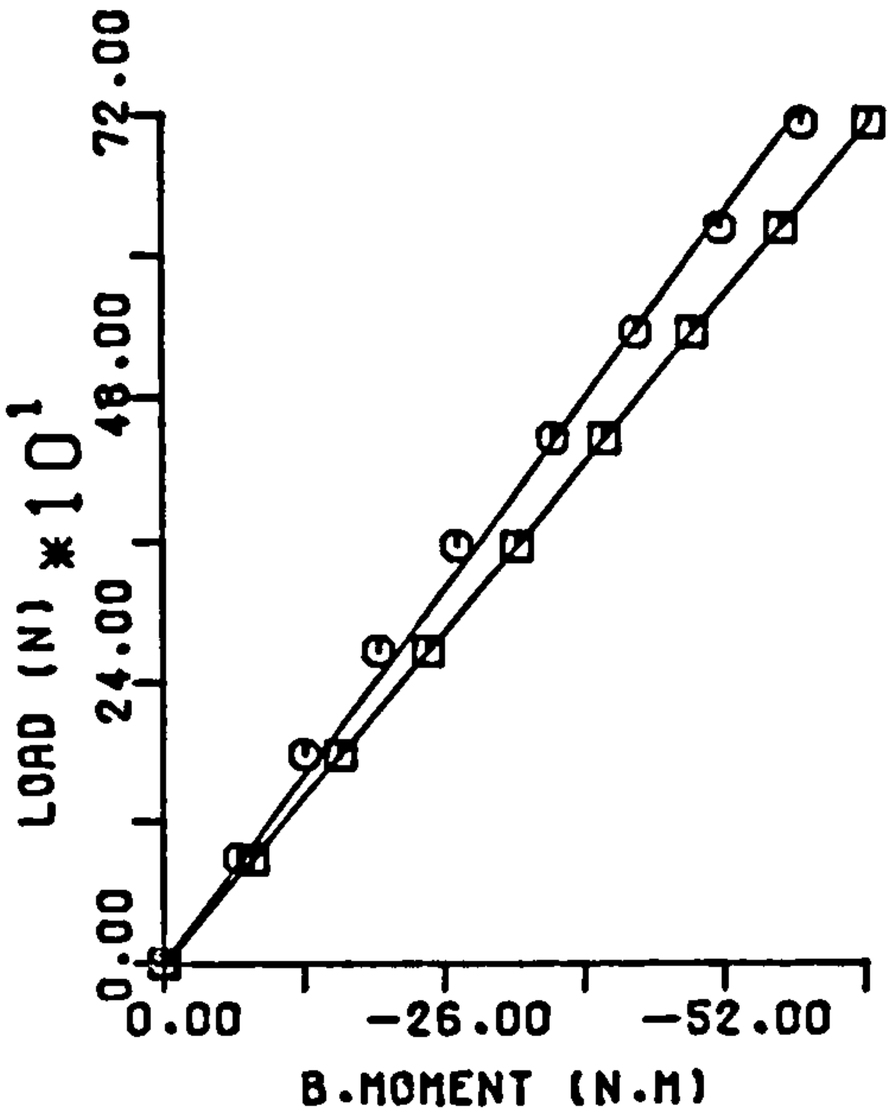

Position C

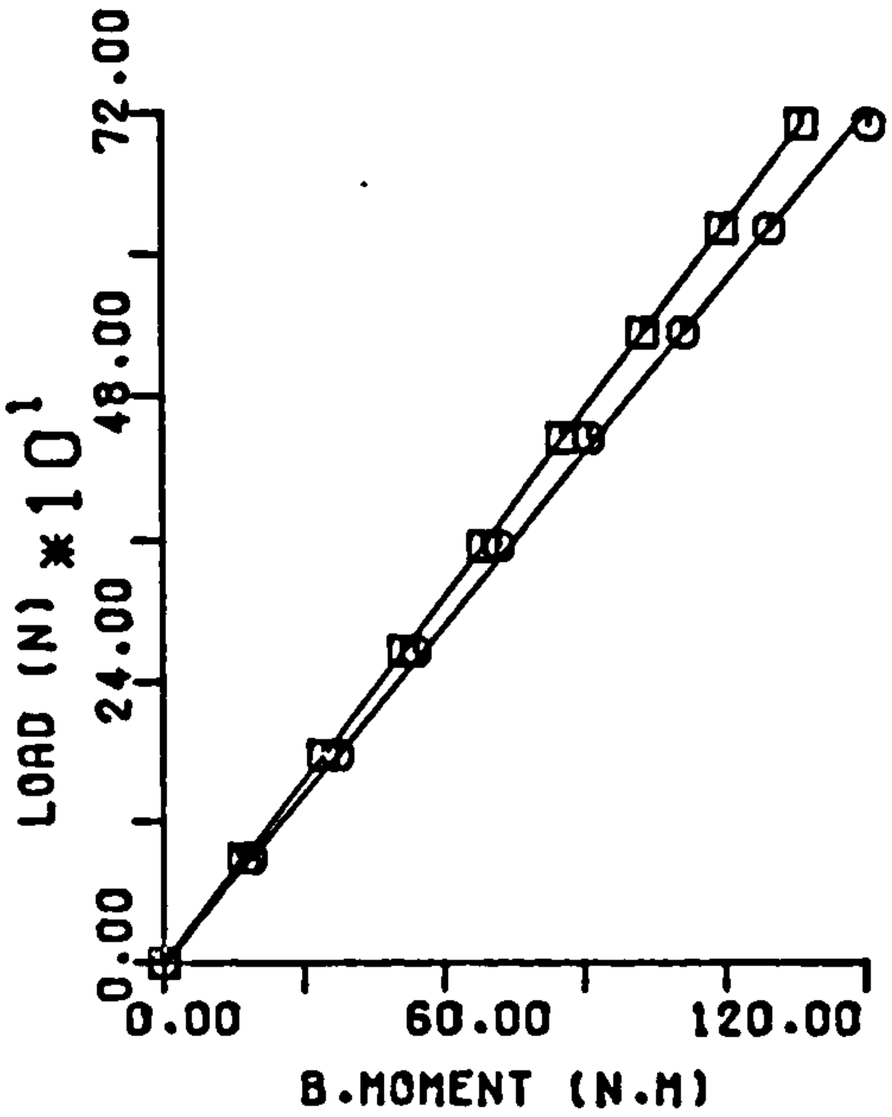

Tower Position

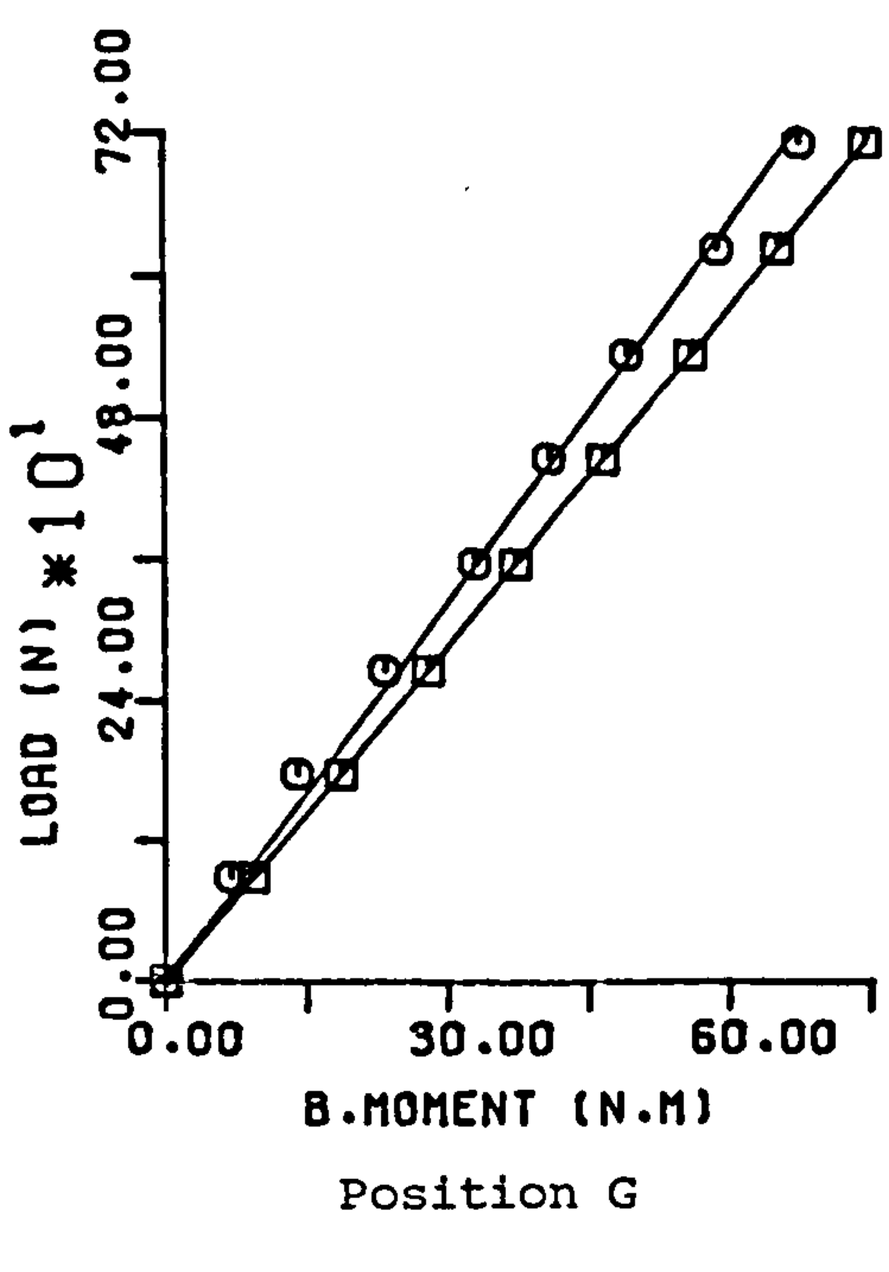

Position G

- ▫ The calculated bending moments
- o The actual bending moments

The bending moments when the load is applied at loading station E

Figure (7.13b)

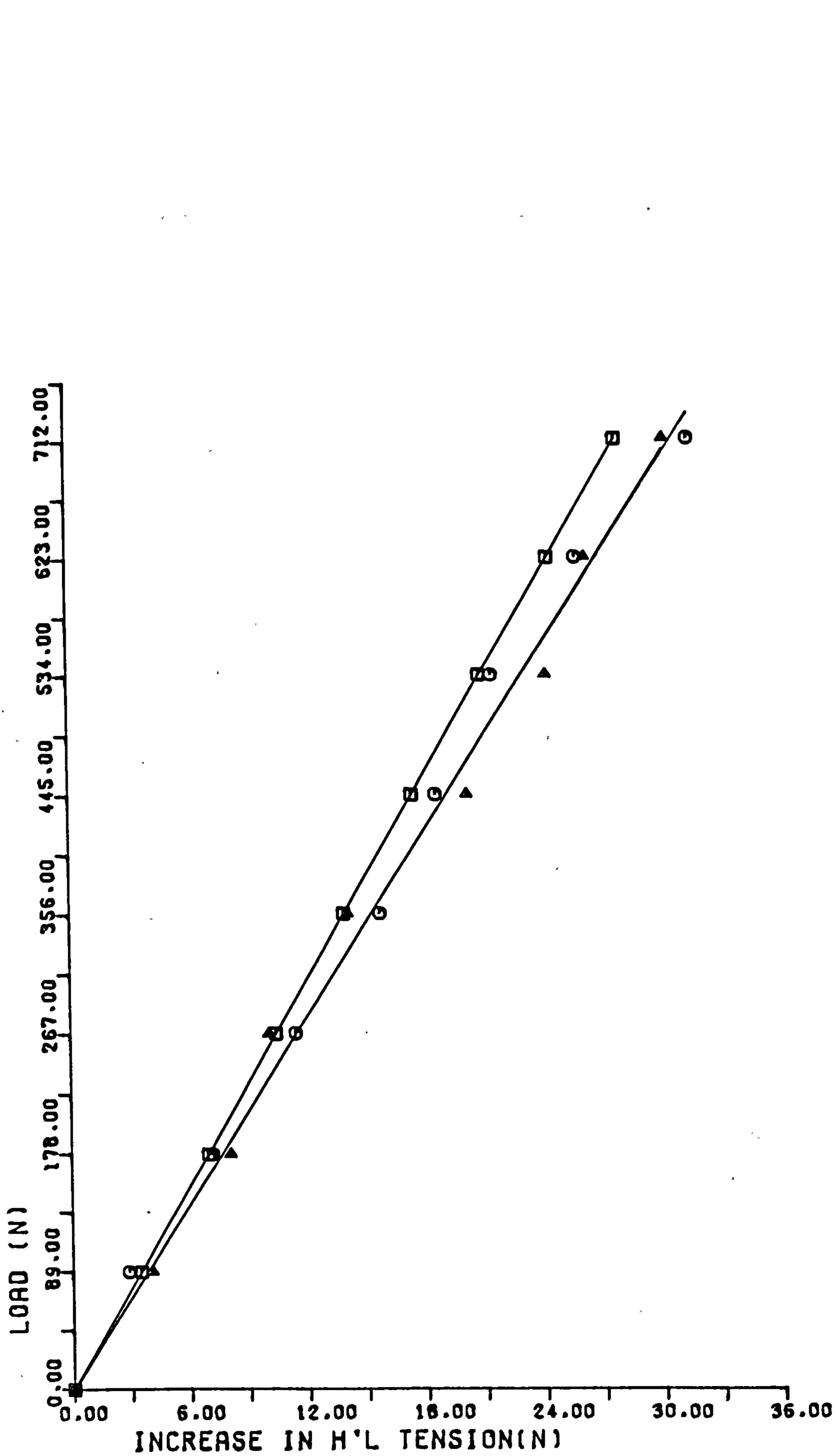

□ The calculated values
o Load cell readings
Δ Cable gauges readings

The change in the prestressing force when the load is applied at loading station E

Figure (7.13c)

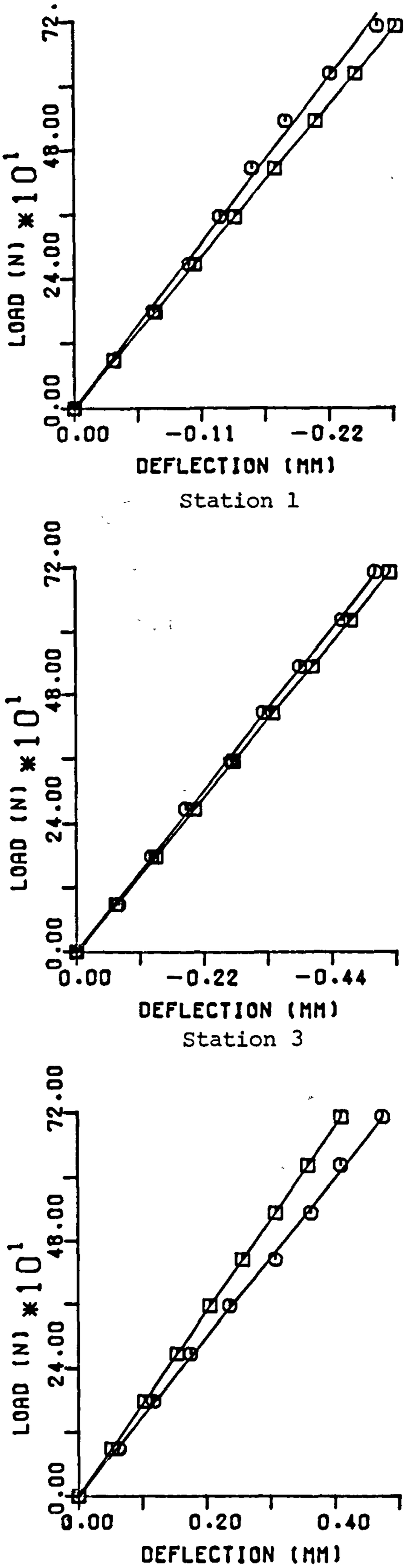

- ▫ The calculated deflections
- o The measured deflections

The deflections when the load is applied at loading position F

Figure (7.14a)

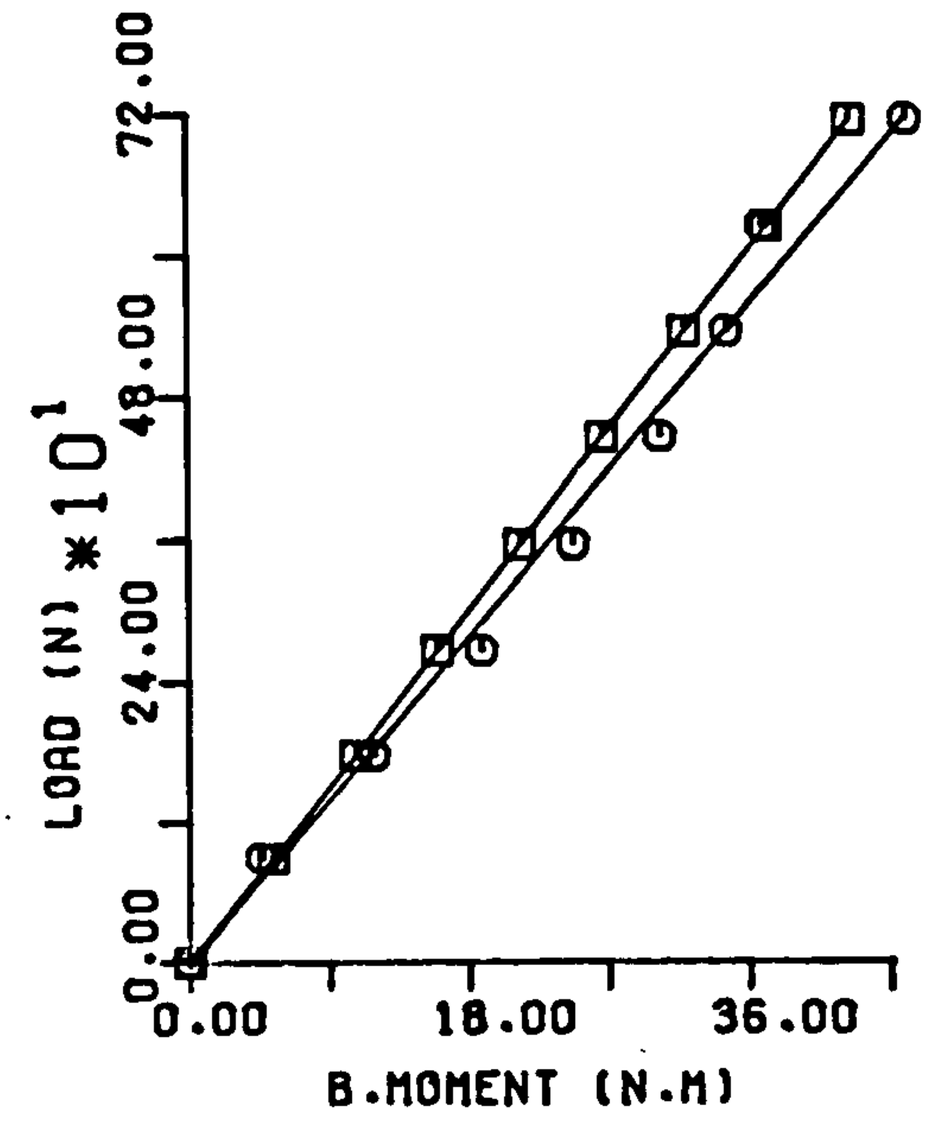

Position C

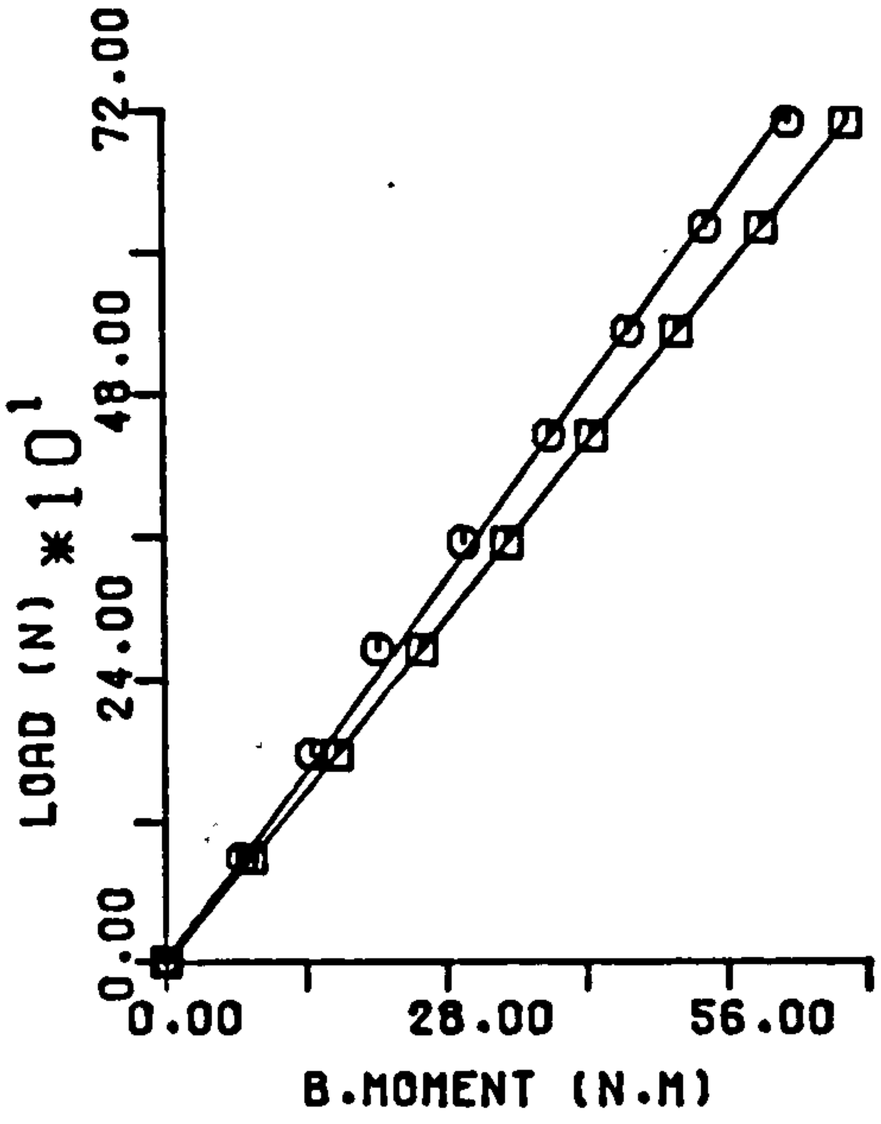

Tower Position

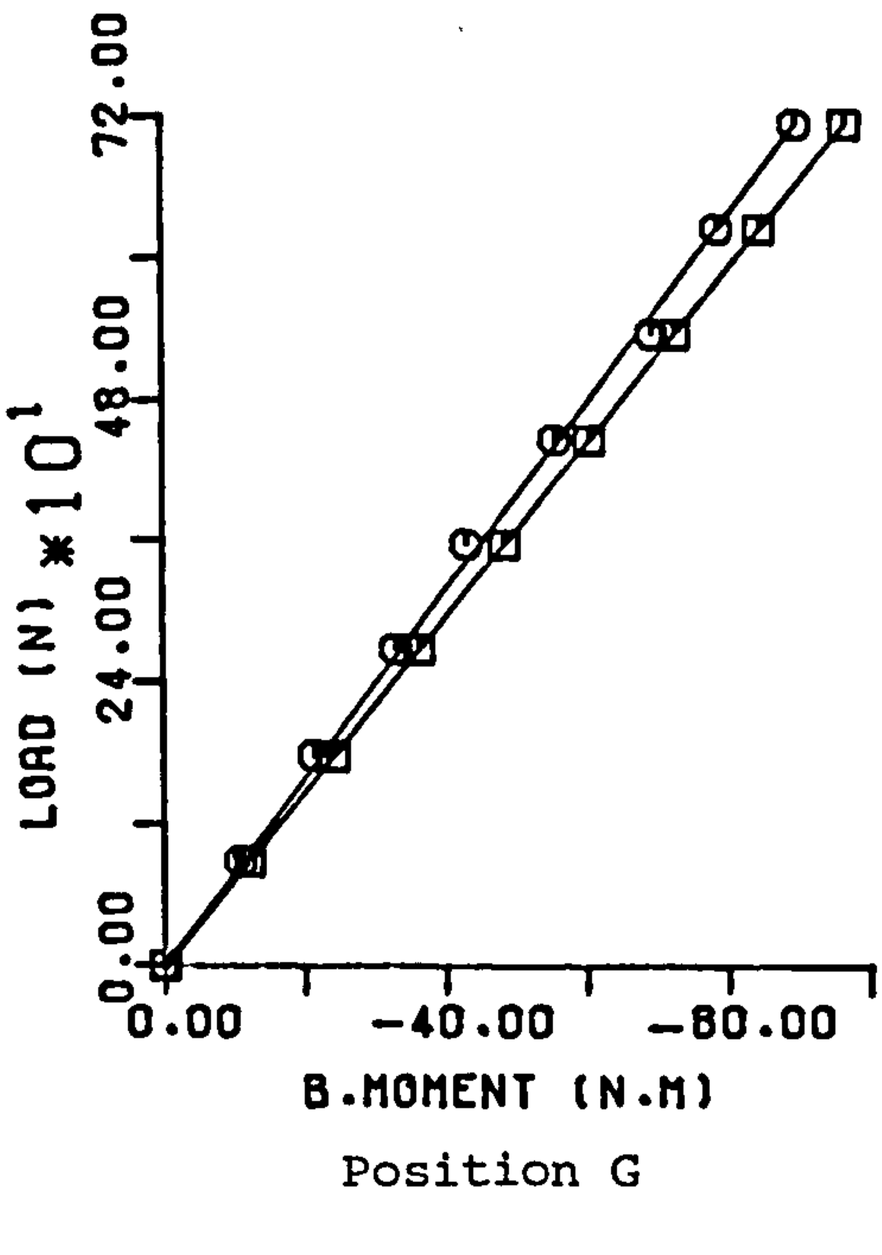

Position G

- ◘ The calculated bending moments
- o The actual bending moments

The bending moments when the load is applied at loading station F

Figure (7.14b)

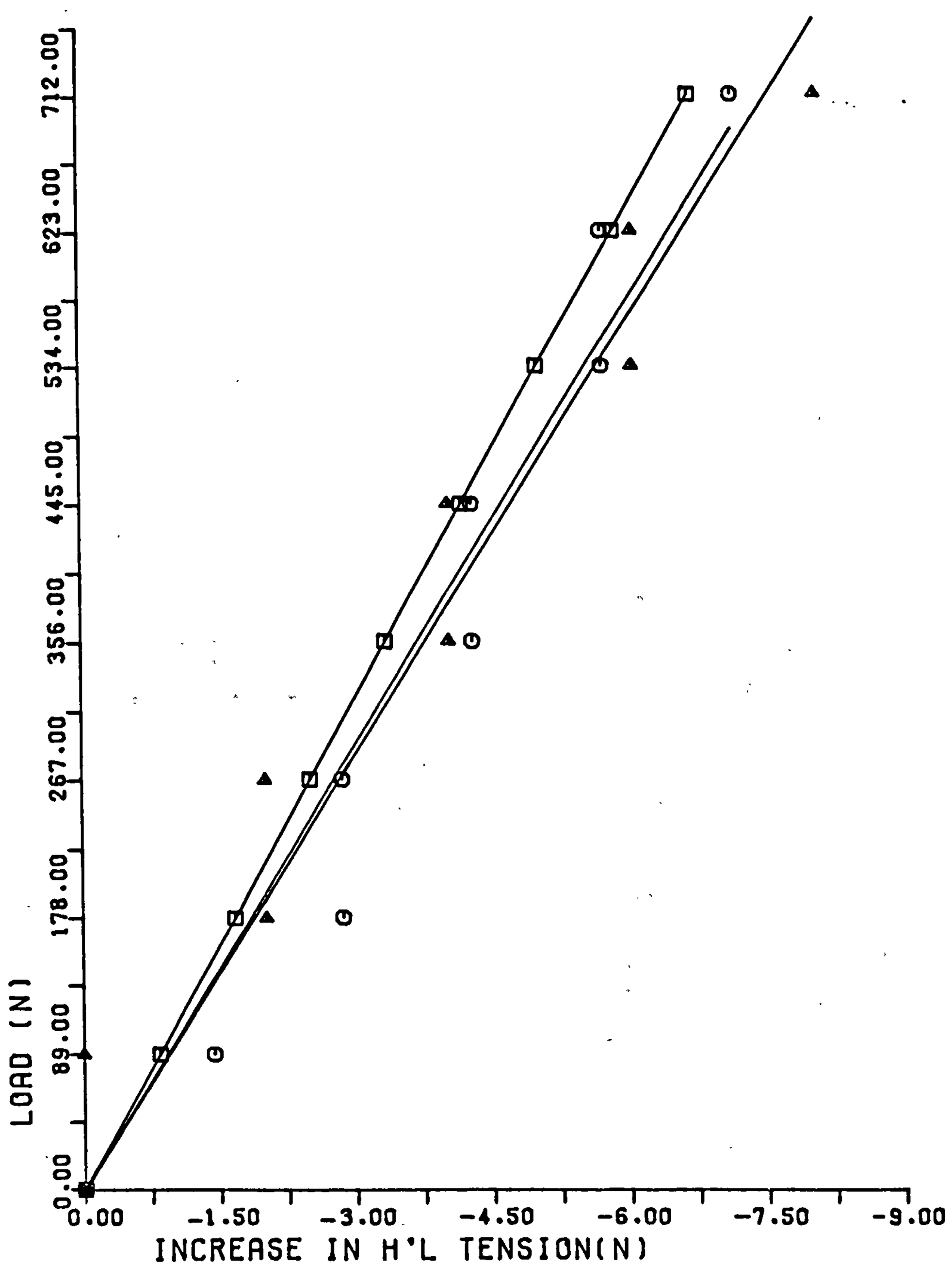

□ The calculated values
o Load cell readings
Δ Cable gauges readings

The change in the prestressing force when the load is applied at loading station F

Figure (7.14c)

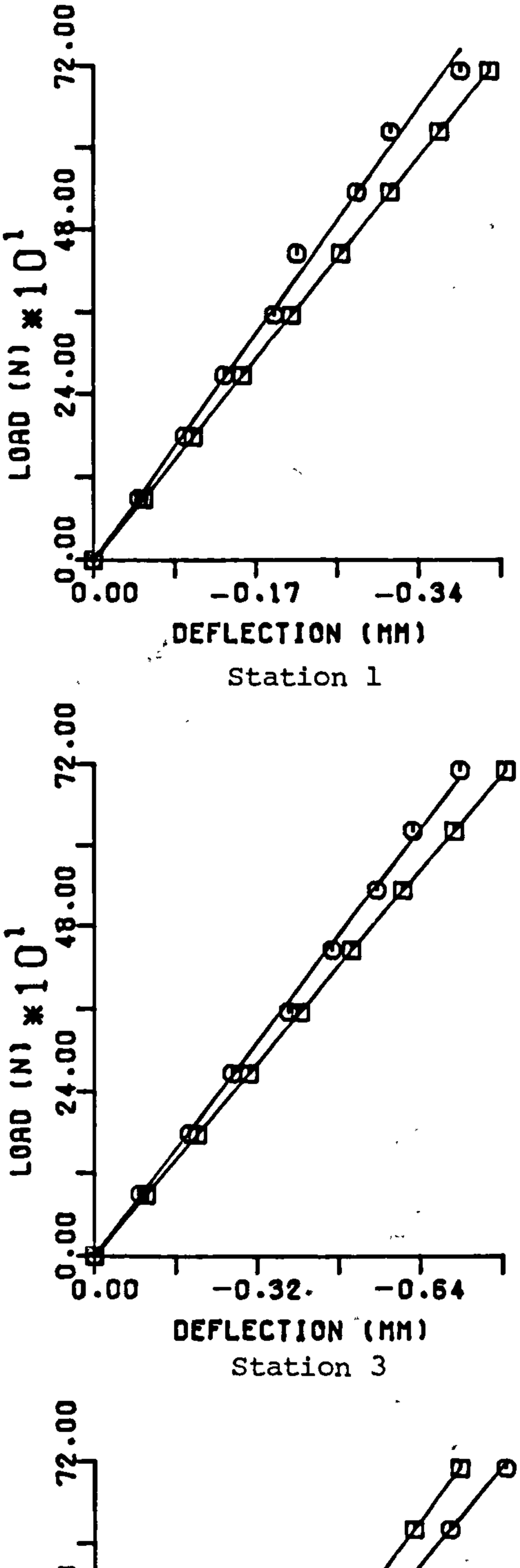

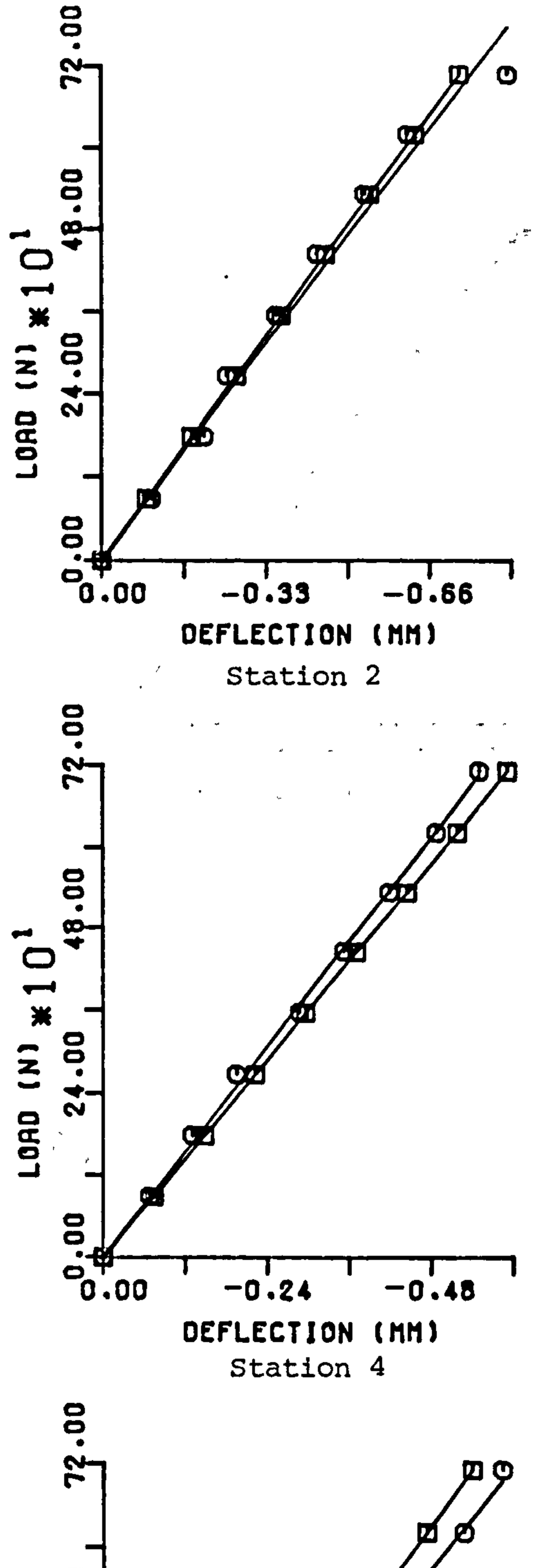

▫ The calculated deflections
o The measured deflections

The deflections when the load is applied at loading position G

Figure (7.15a)

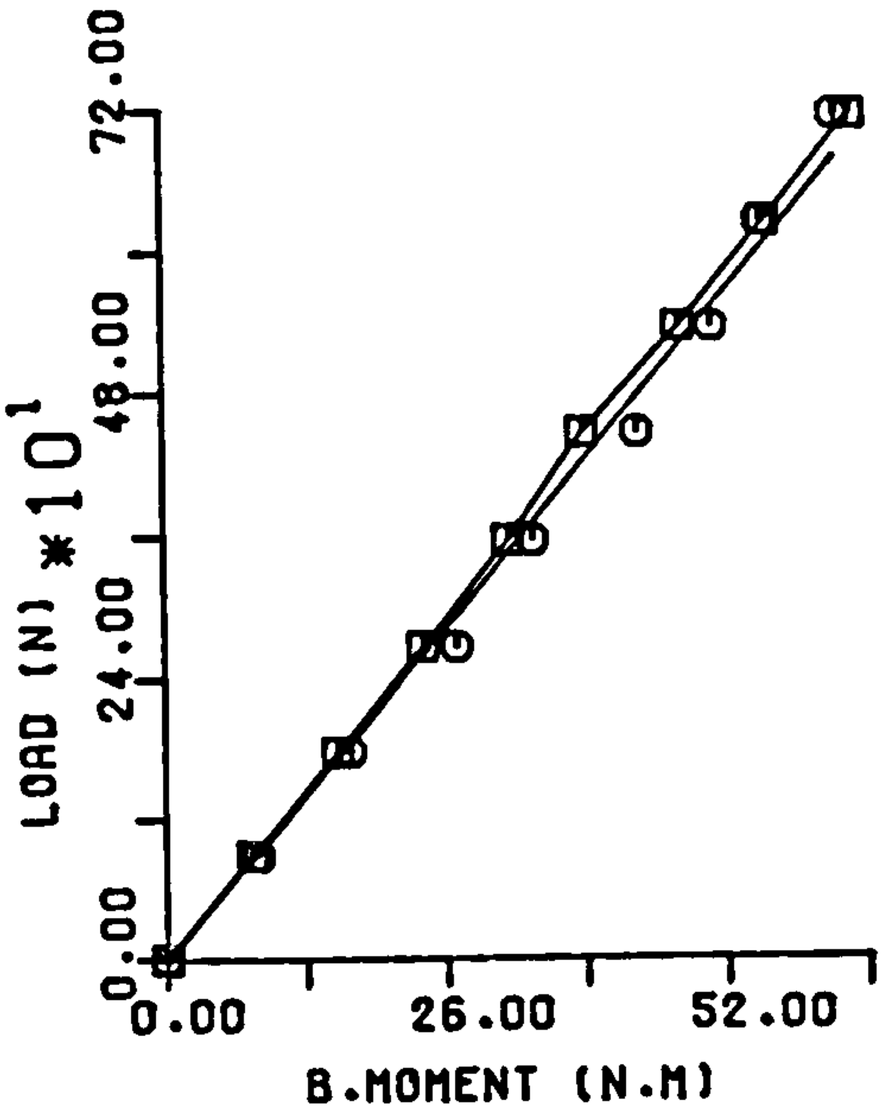

Position C

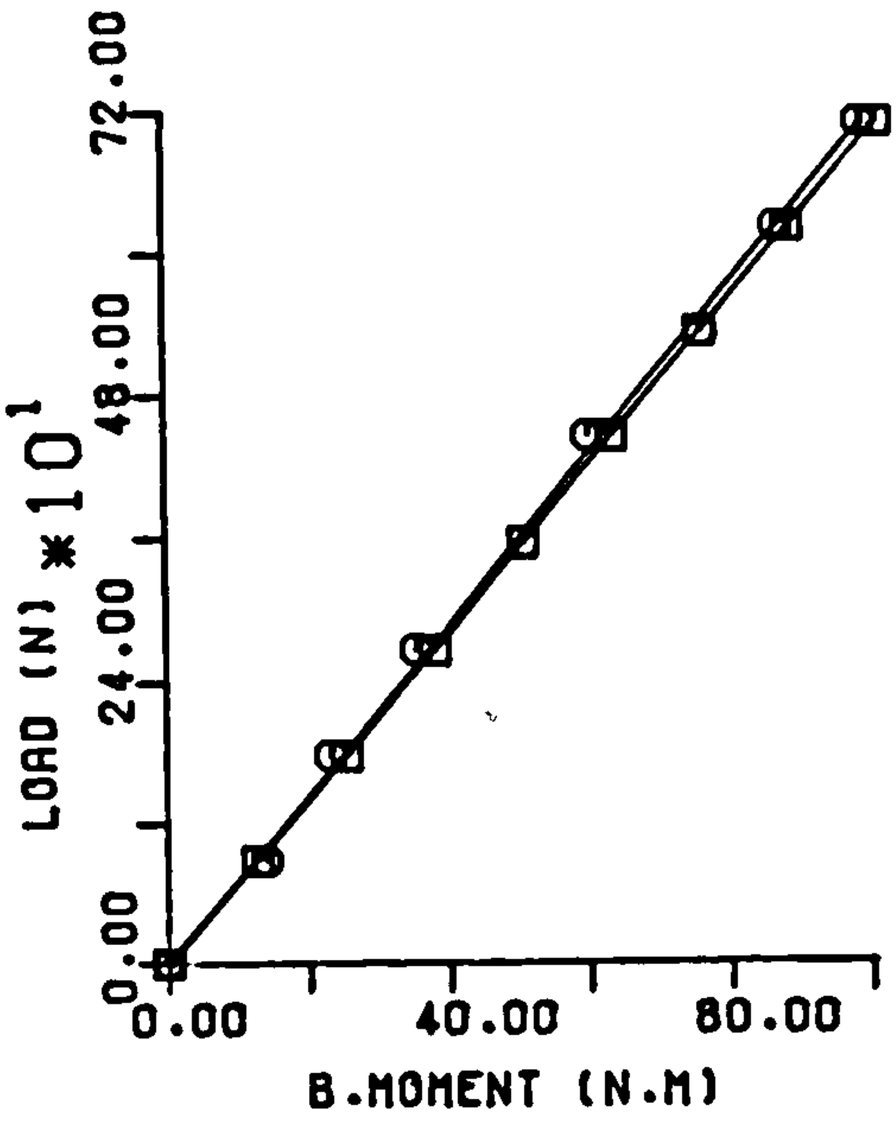

Tower Position

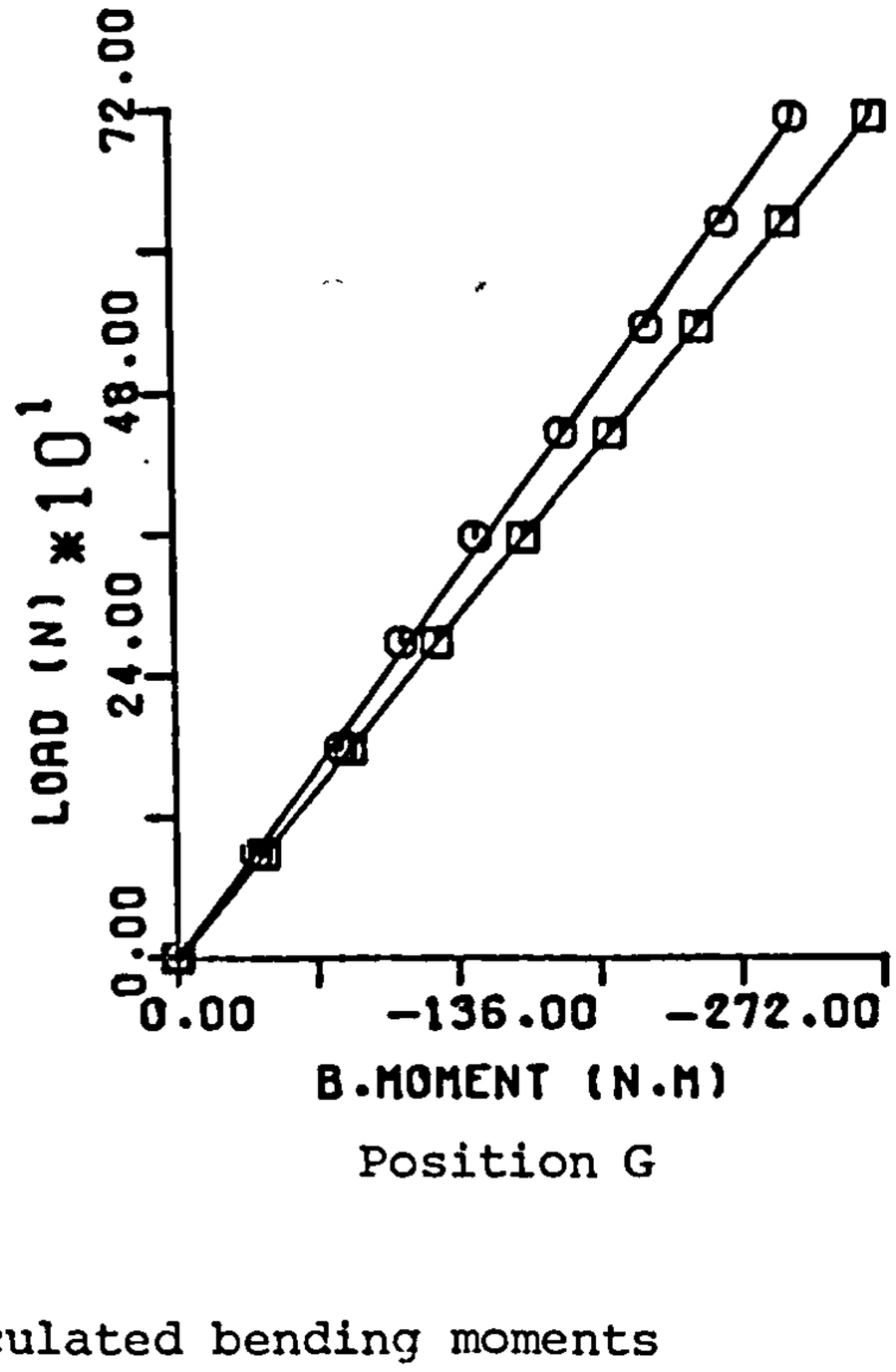

Position G

- ▫ The calculated bending moments
- o The actual bending moments

The bending moments when the load is applied at loading station G

Figure (7.15b)

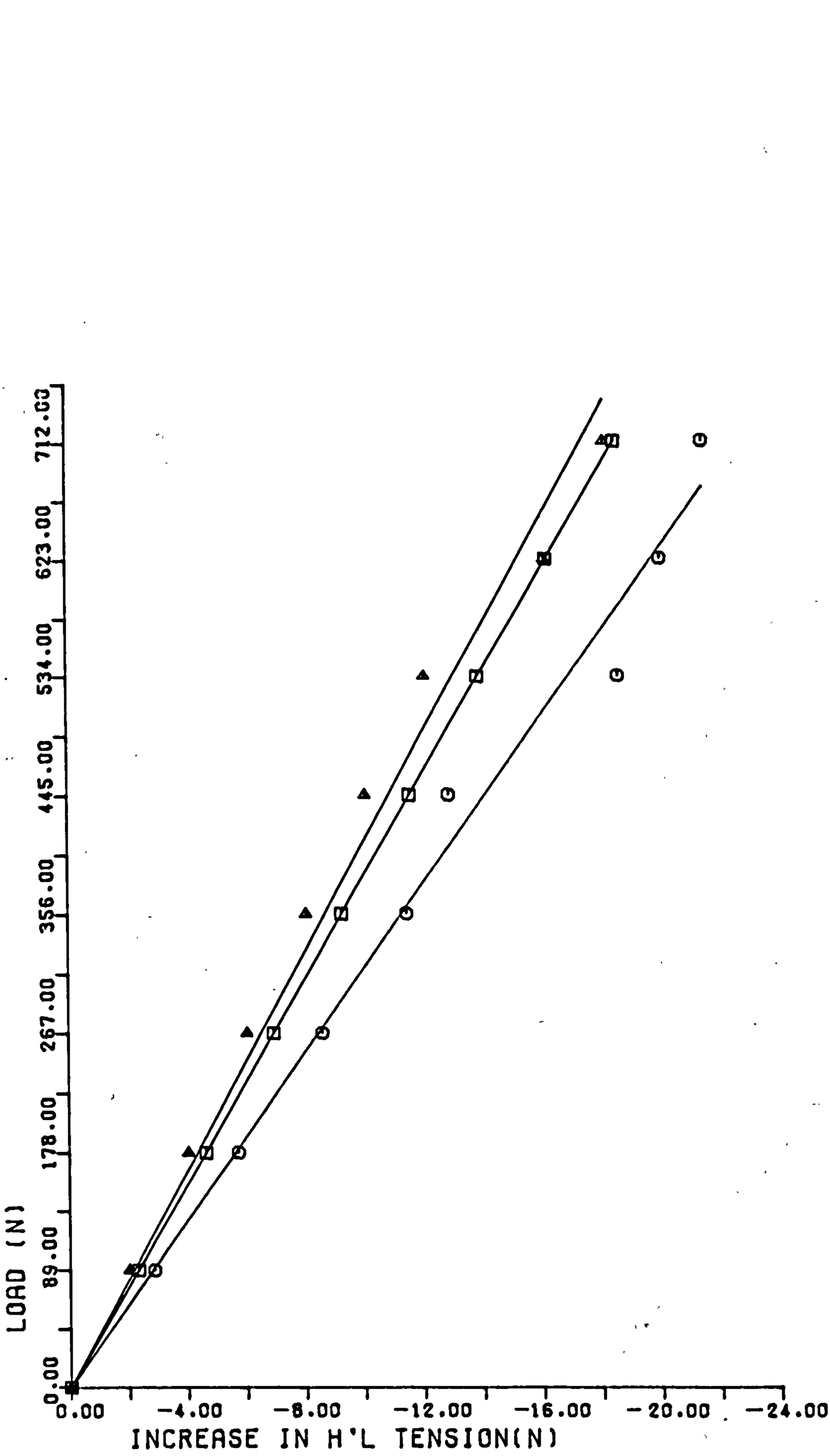

□ The calculated values
o Load cell readings
Δ Cable gauges readings

The change in the prestressing force when the load is applied at loading station G

Figure (7.15c)

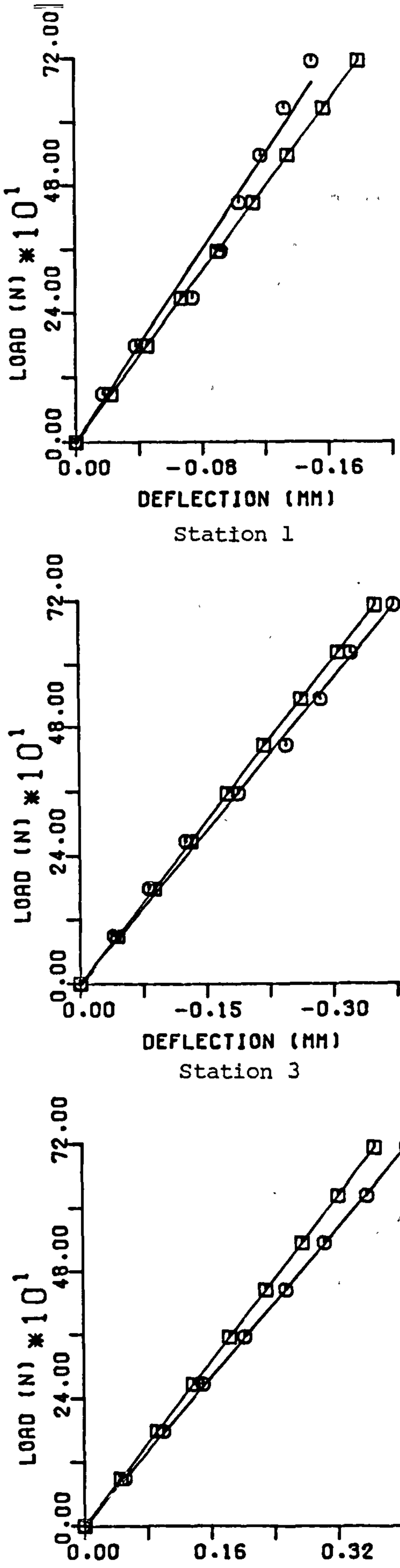

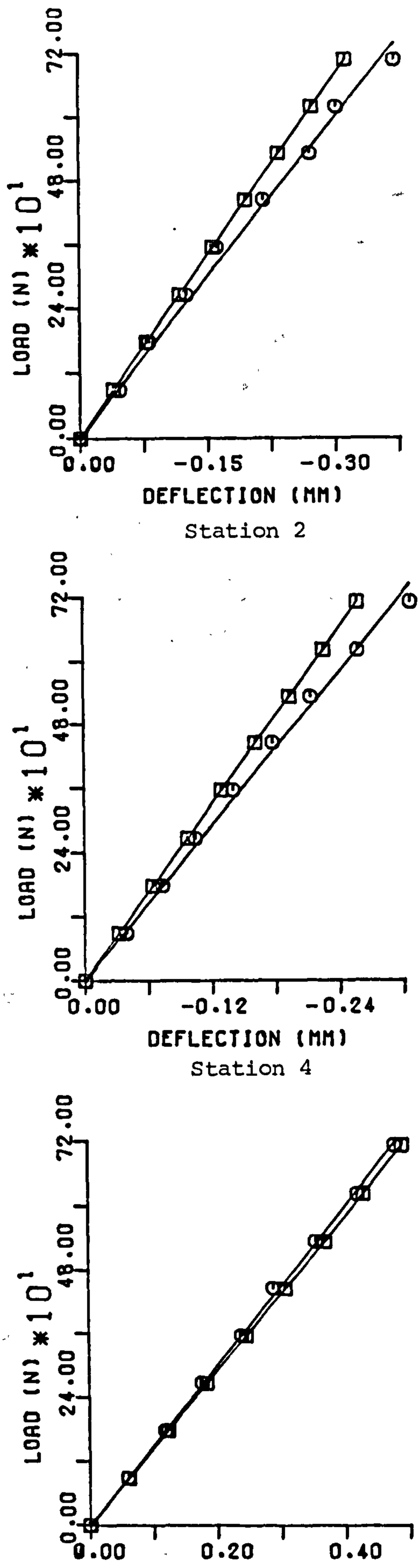

- ▫ The calculated deflections
- o The measured deflections

The deflections when the load is applied at loading position H

Figure (7.16a)

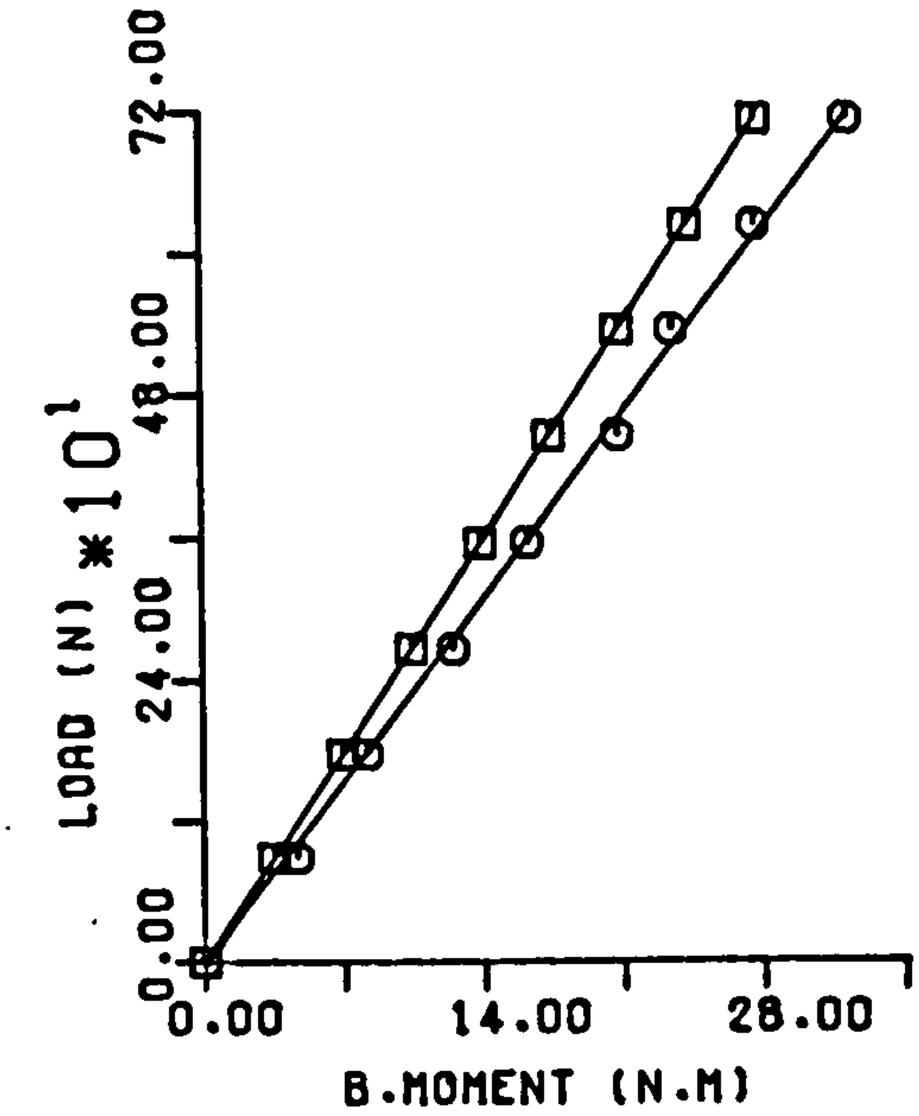

Position C

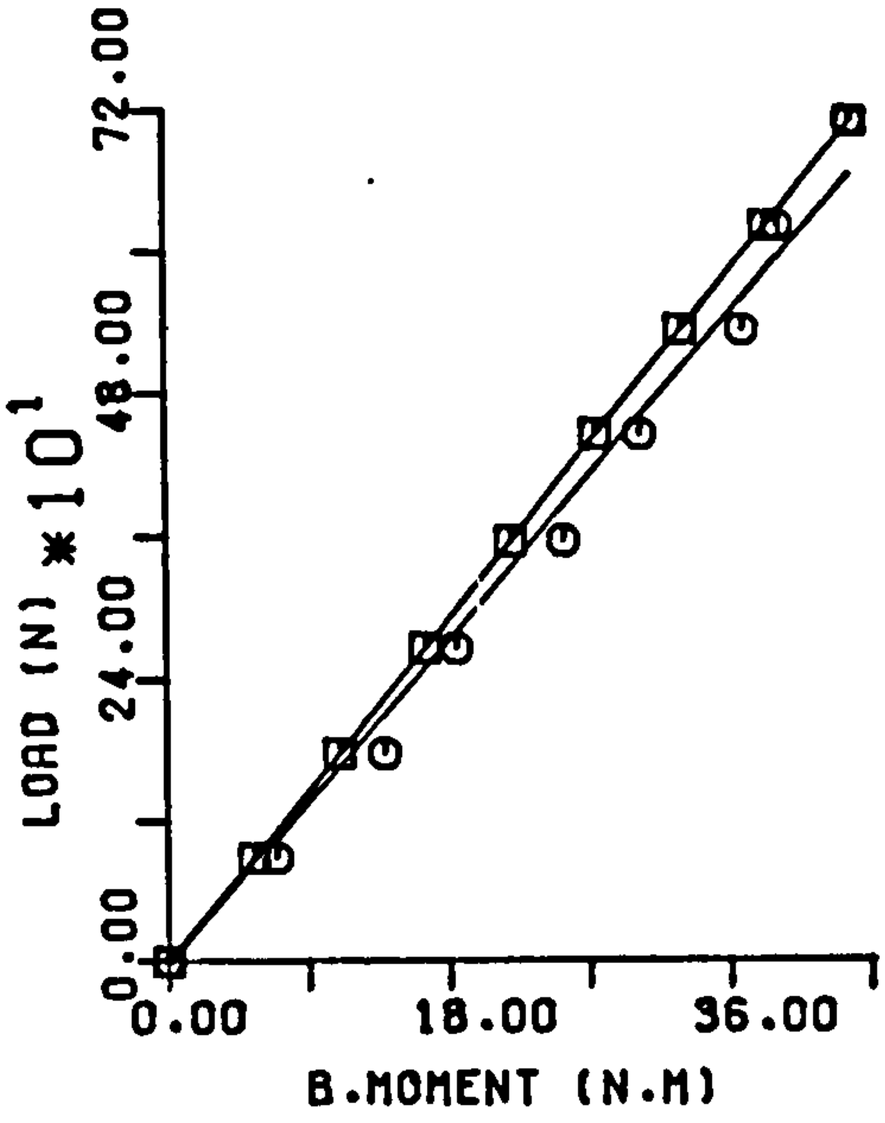

Tower Position

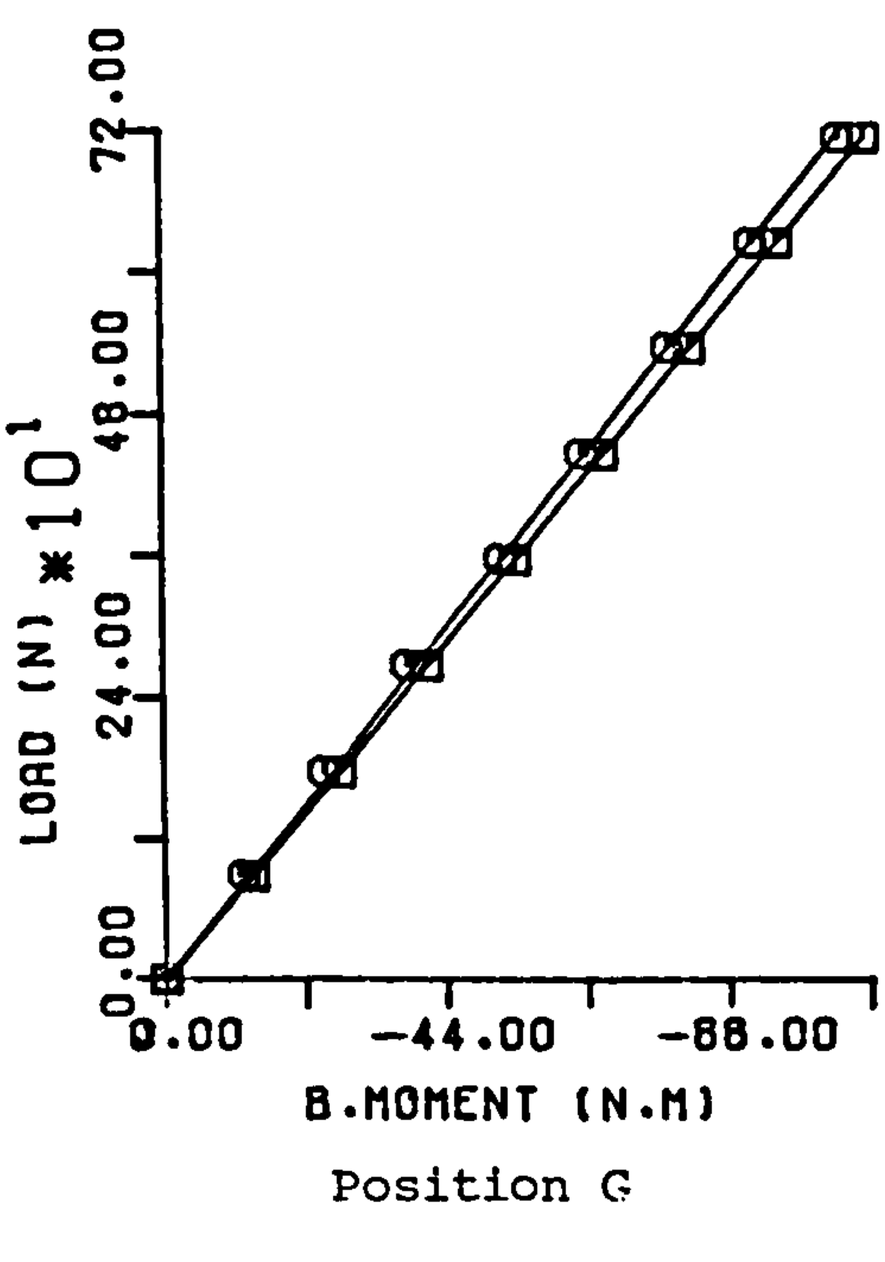

Position G

- ▫ The calculated bending moments
- o The actual bending moments

The bending moments when the load is applied at loading station H

Figure (7.16b)

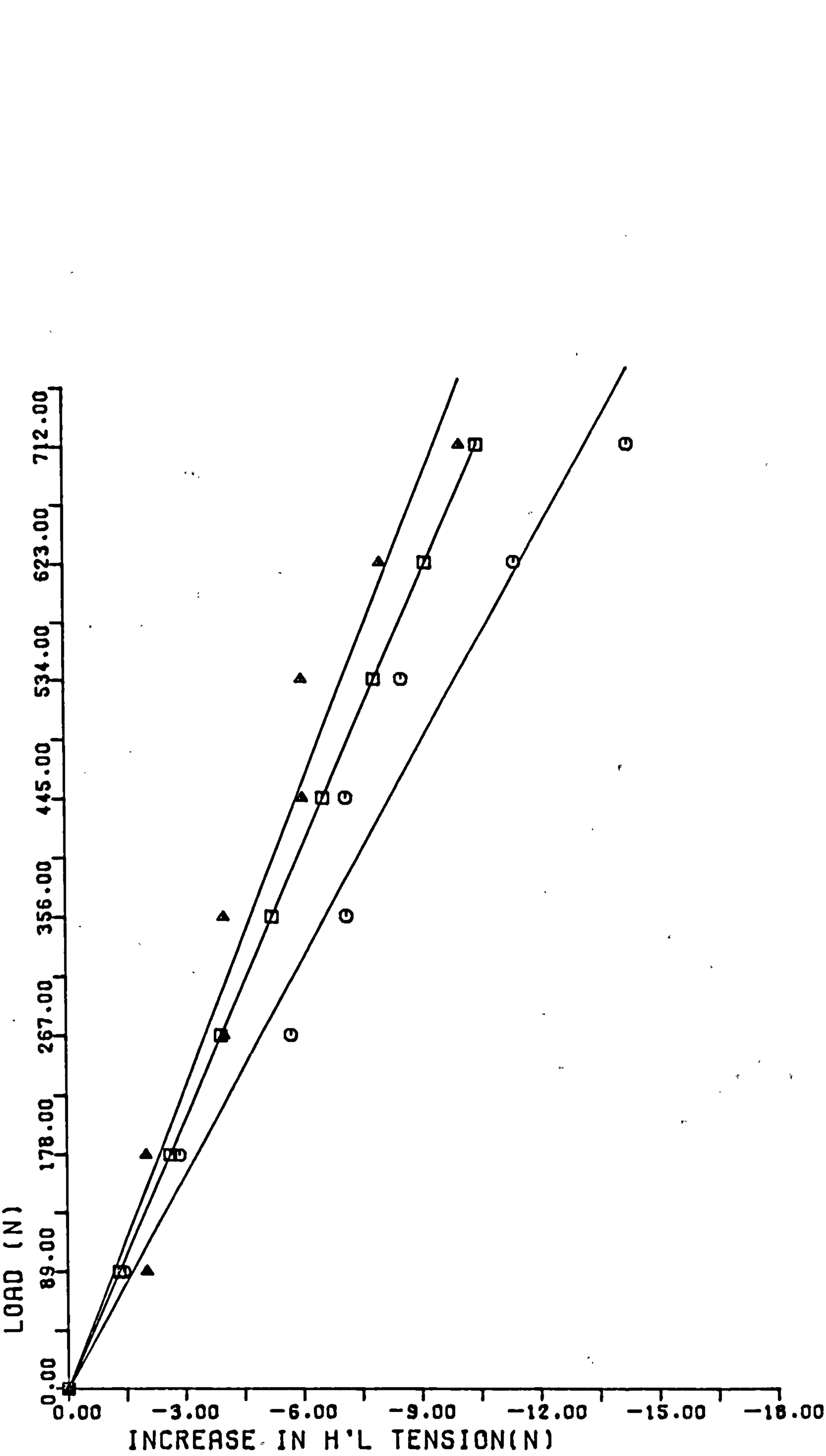

▫ The calculated values
o Load cell readings
Δ Cable gauges readings

The change in the prestressing force when the load is applied at loading station H

Figure(7.16c)

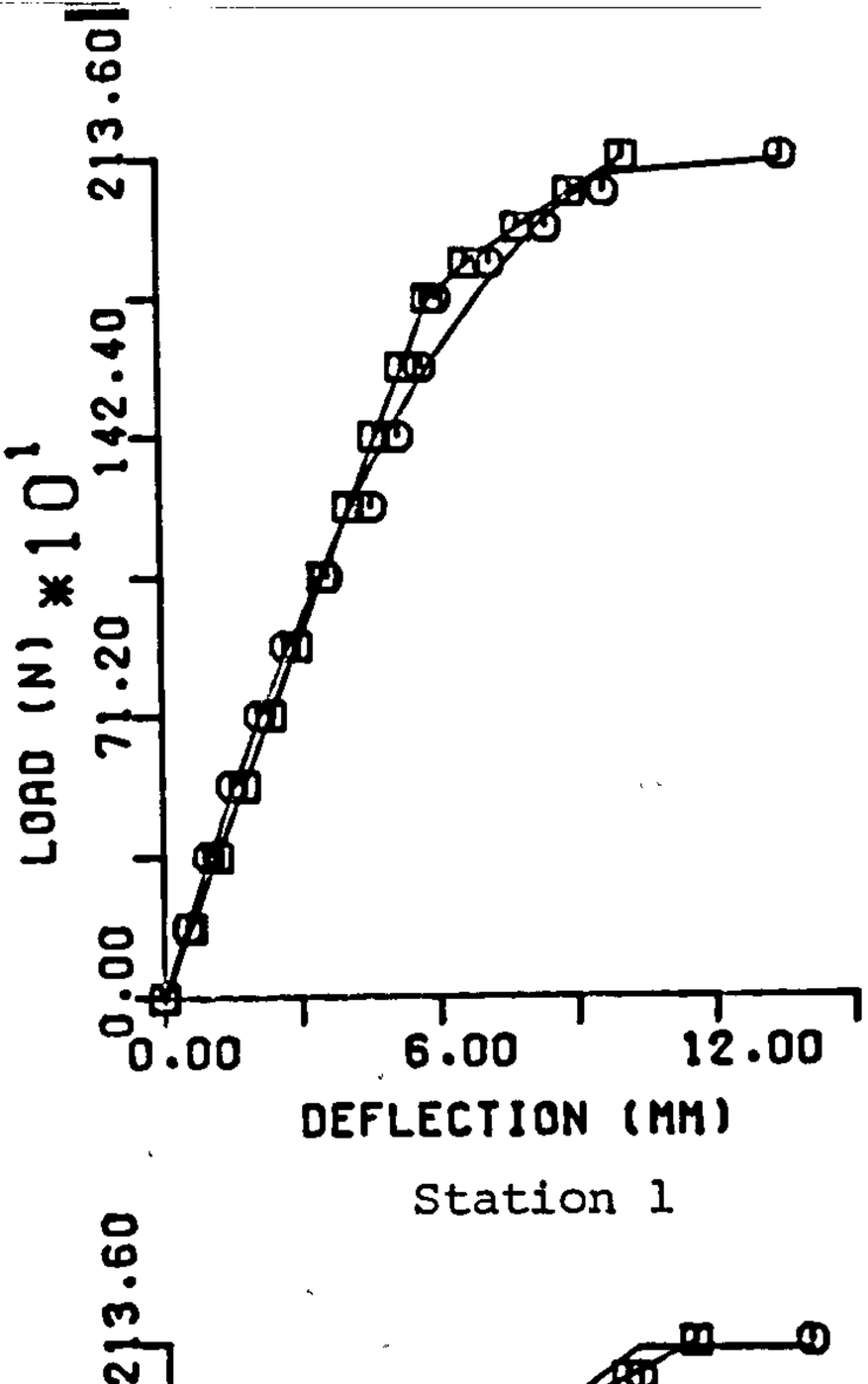

Station 1

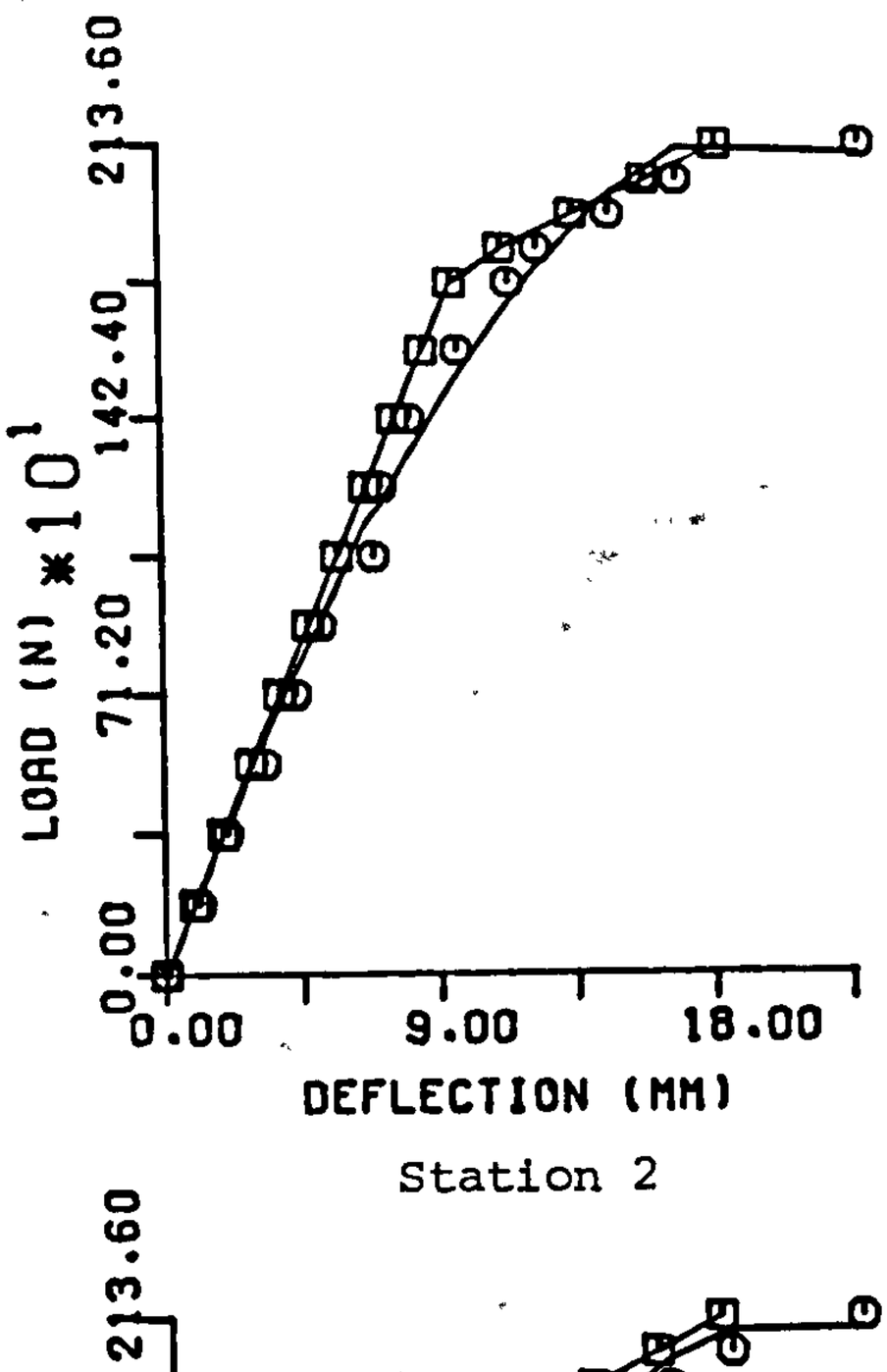

Station 2

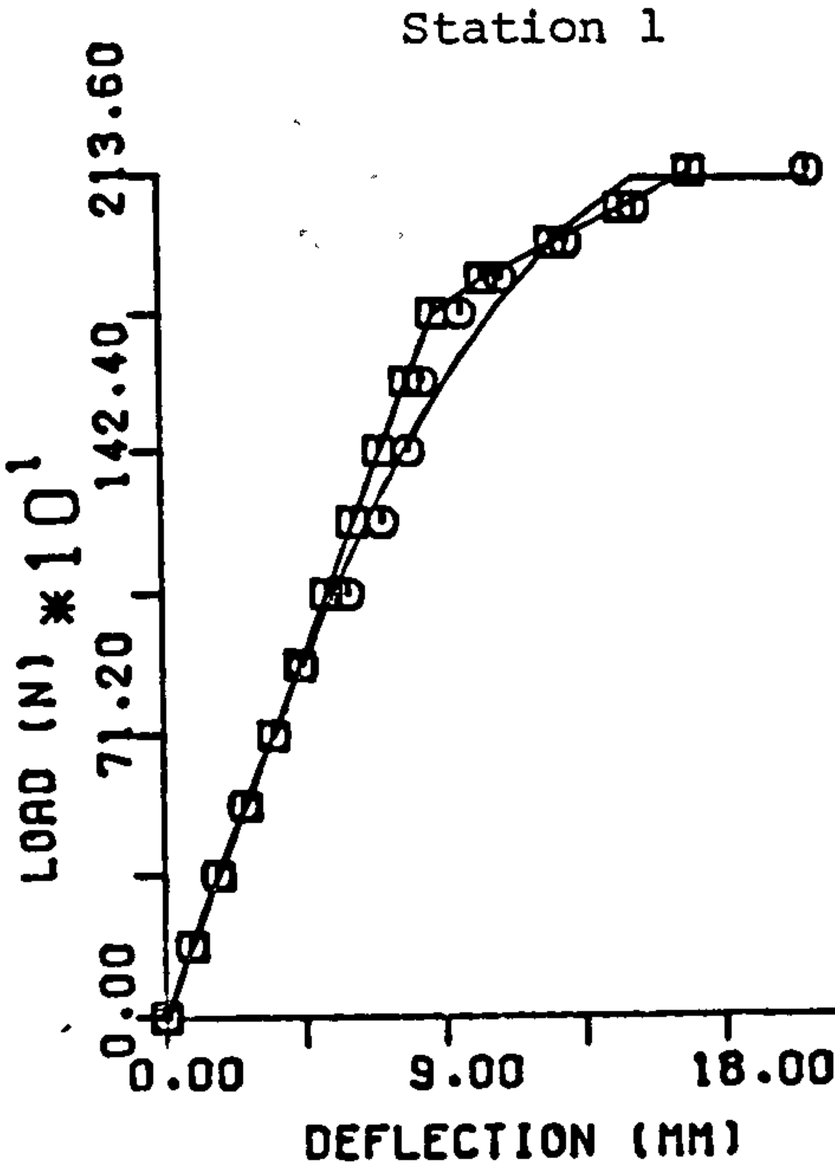

Station 3

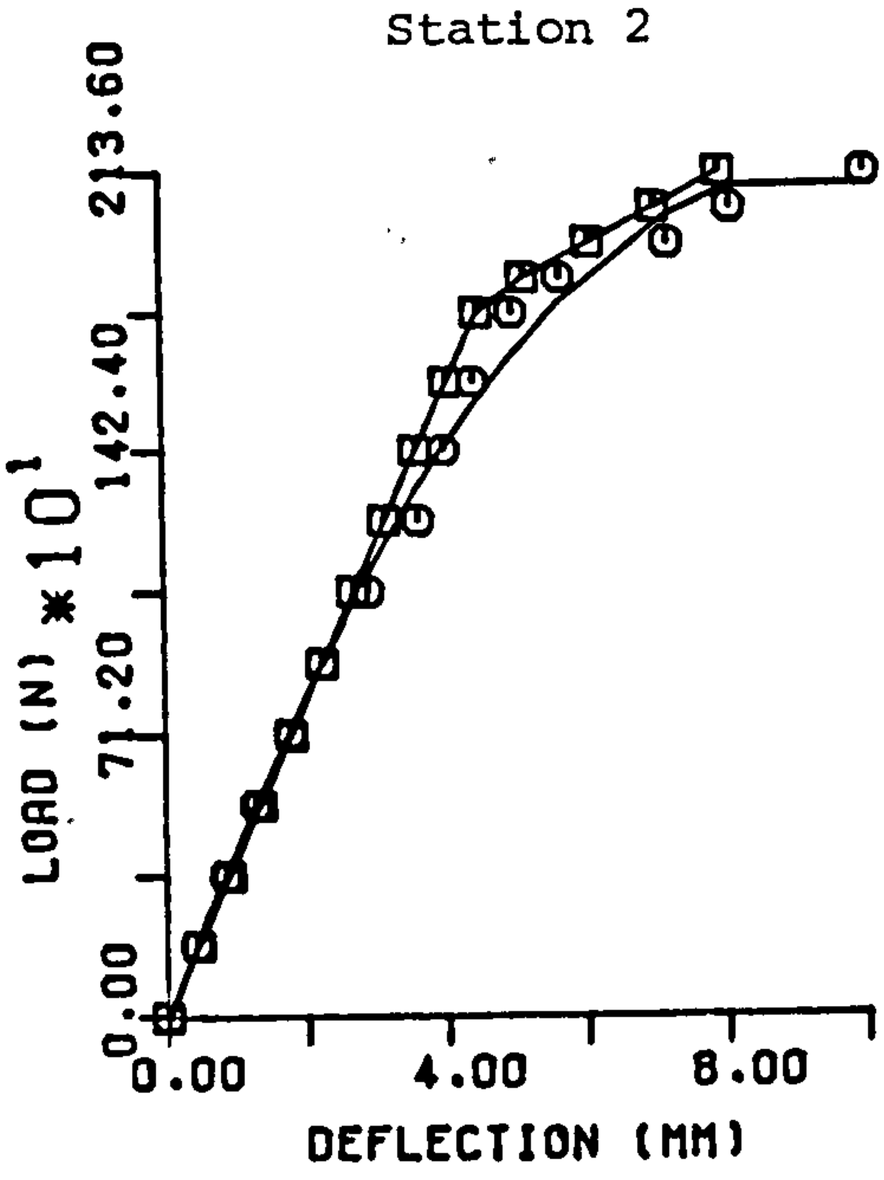

Station 4

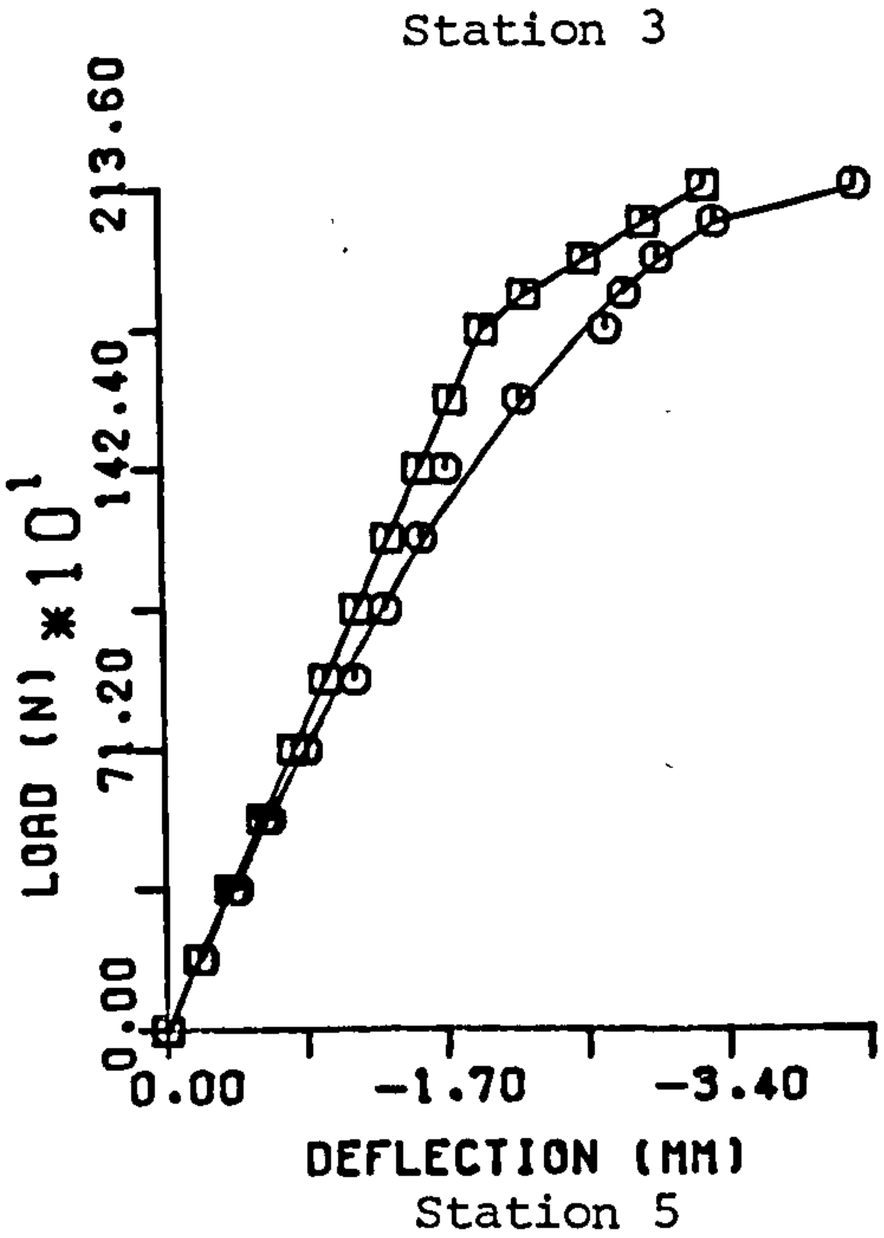

Station 5

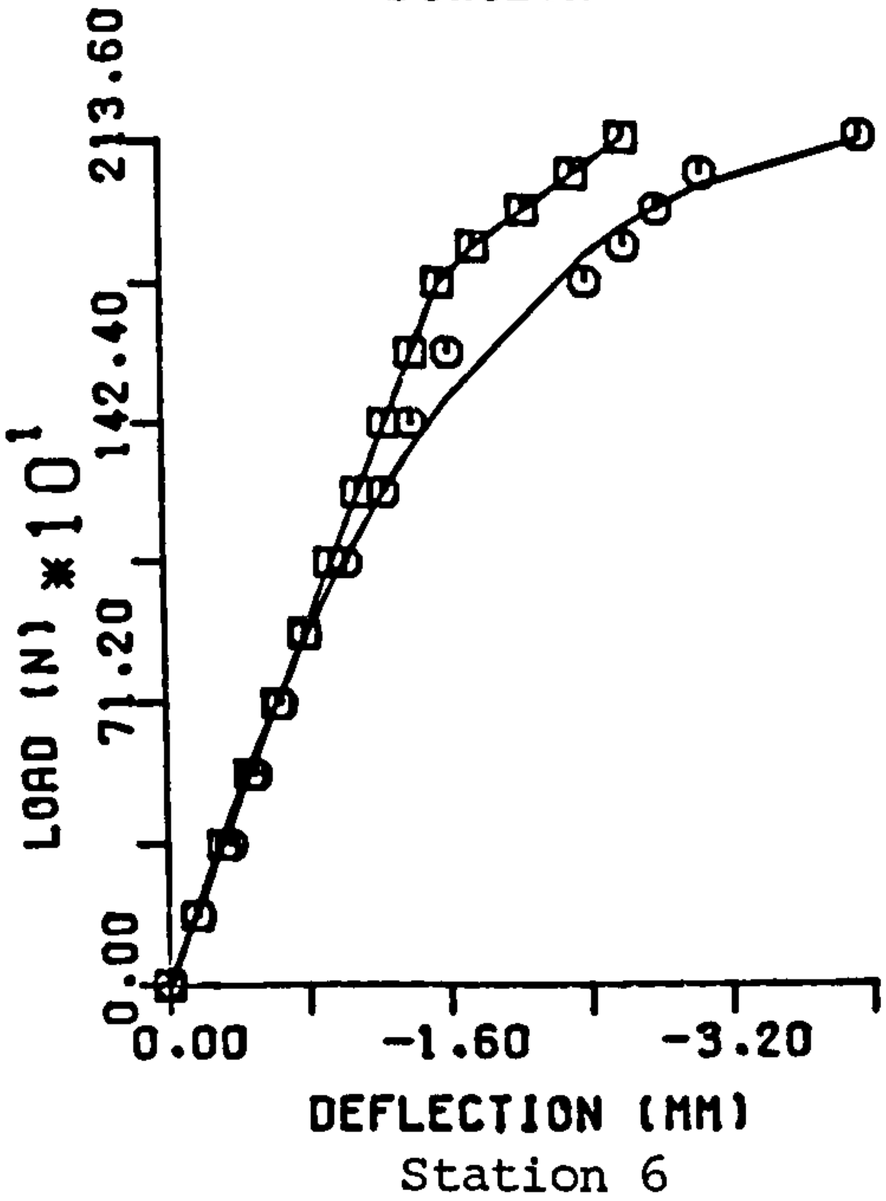

Station 6

□ The calculated deflections
o The measured deflections

The deflections when a load to failure is applied at loading position C

Figure (7.17a)

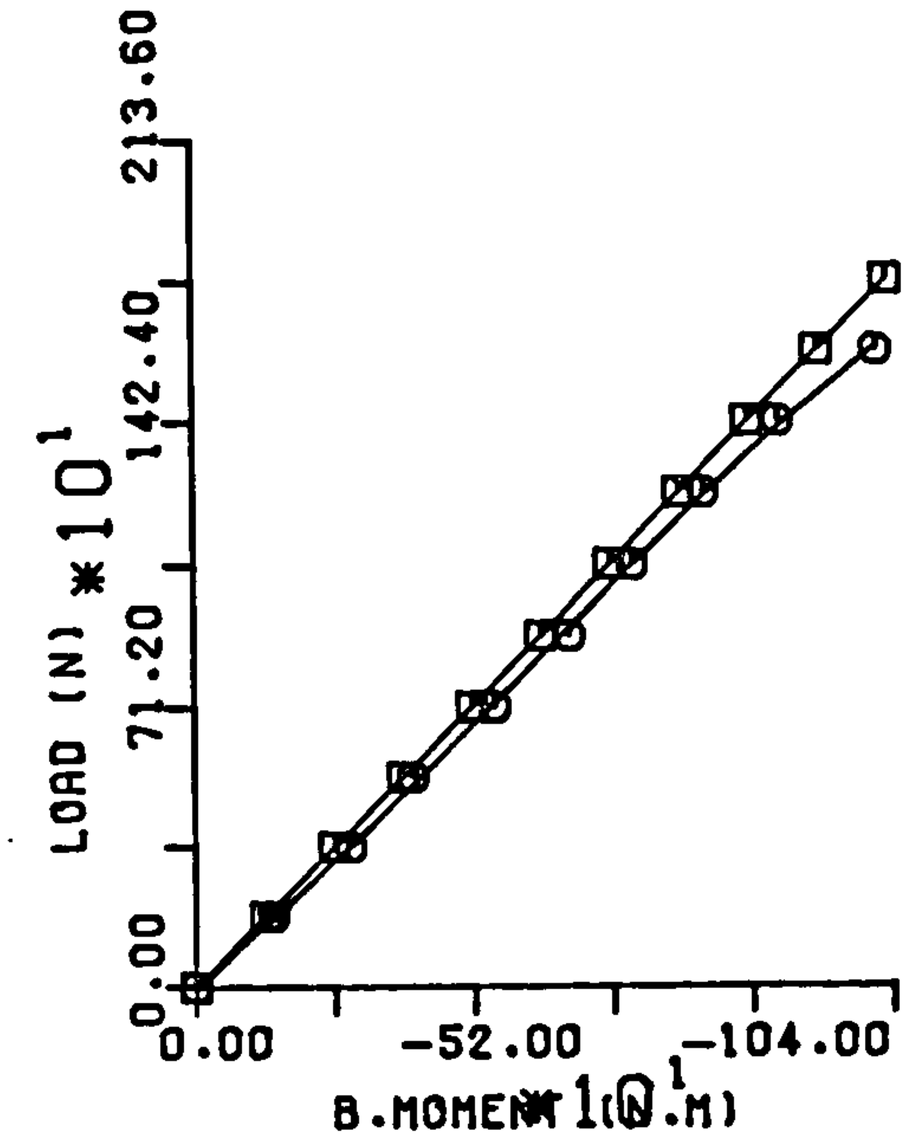

Position C

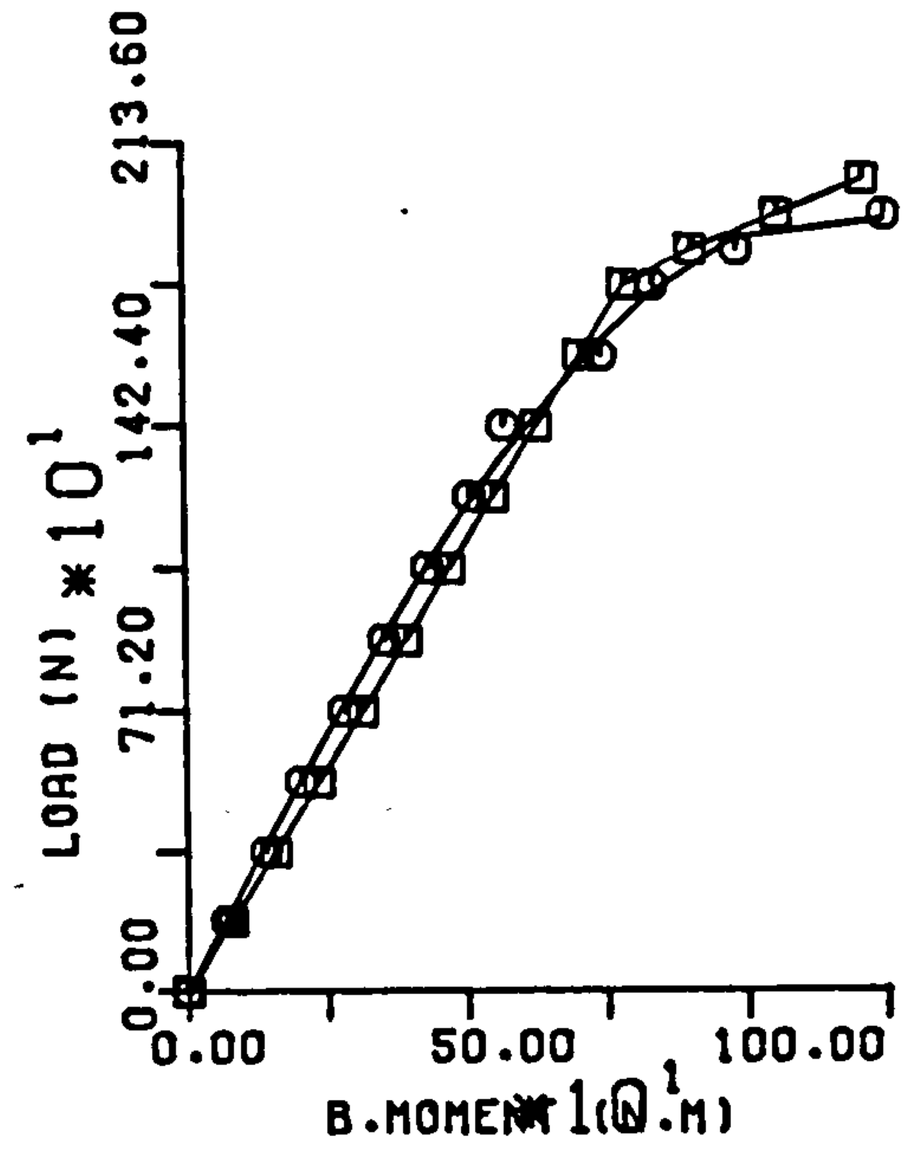

Tower Position

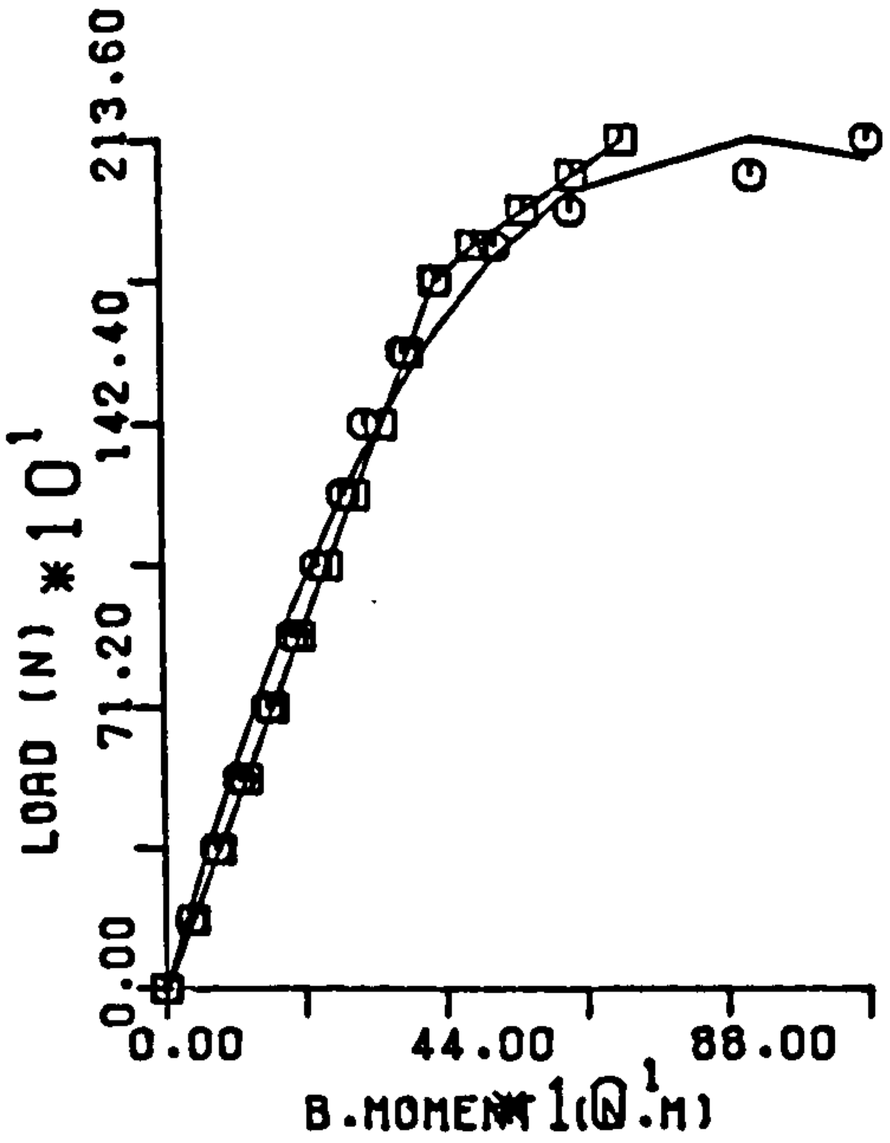

Position G

□ The calculated bending moments
o The actual bending moment

The bending moments when a load to failure is applied at loading station C

Figure (7.17b)

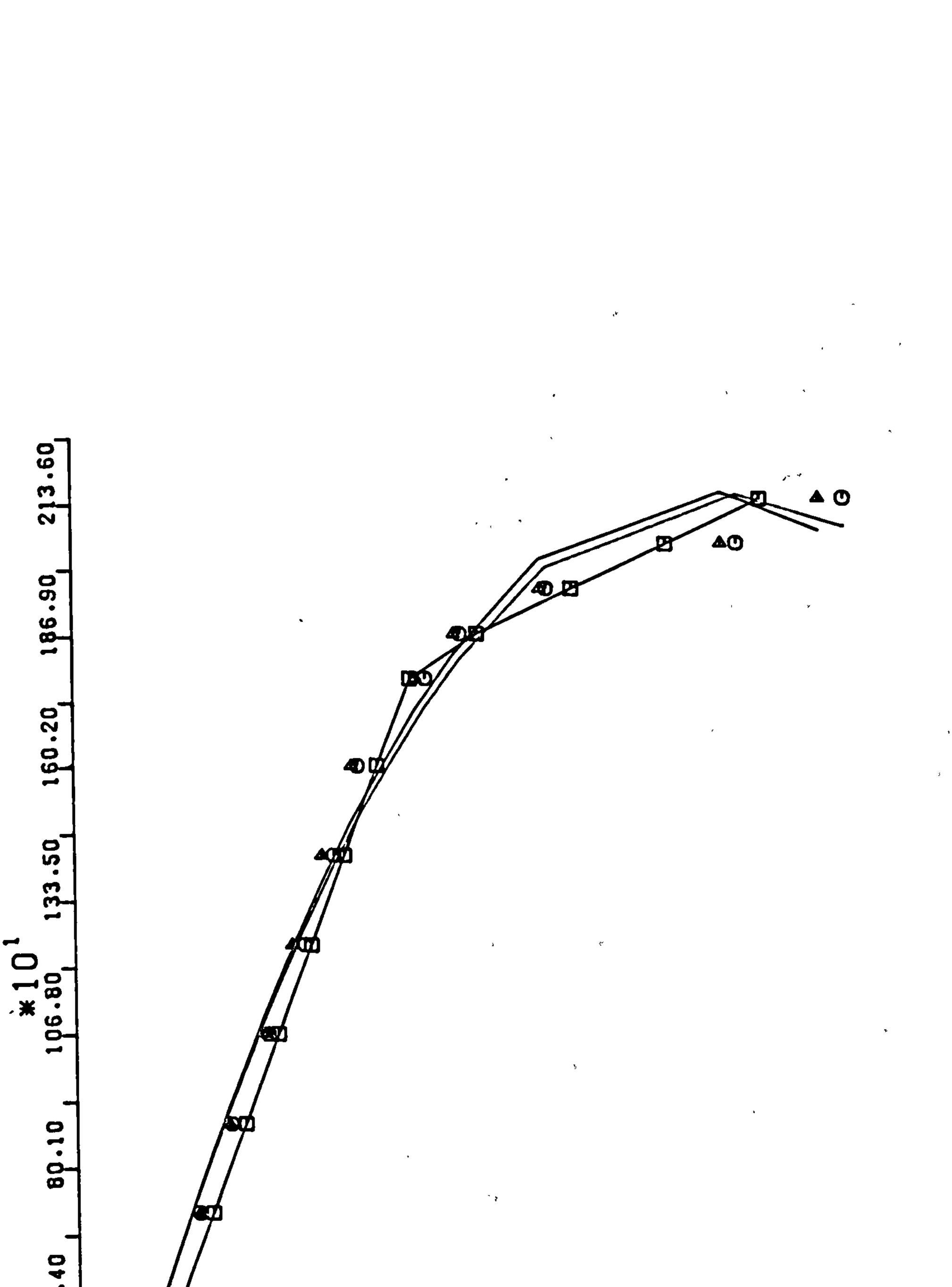

- ▫ The calculated values
- o Load cell readings
- Δ Cable gauges readings

The change in the prestressing force when a load to failure is applied at loading station C

Figure (7.17c)

7.6 The Second Experiment

7.6.1 The Prestressing Operation for the Grouted Test Beam

As mentioned earlier, prestressing was carried out for the second test beam by means of shortening the suspenders. From Equation (6.1) and Table (7.11), the shortening ratio, Λ, required in each suspender in order to produce the desired prestressing force 14.800 KN in the cable was found to be 12.3%. Therefore, every suspender was installed with its length 1.123 times its design value as indicated in Table (7.11) and the cable was laid down without any tension with its anchorages installed. Whence, prestressing was carried out as half the required extra dead loads, 10 kg, were placed in position (A - H) with the auxiliary props supporting the structure in the mid-points of both spans. Then, the suspenders were shortened with the full distances, specified in Table (7.11), and the auxiliary props were removed. The rest of the extra dead loads were added and the prestressing operation was completed.

Shortening the suspenders was carried out, as mentioned in Section 7.3.2, by screwing each of the two bolts, Figure (7.5) and Plate (3), by half the required distance into the small tubes. The prestressing force corresponding to 12.3% strain in the suspenders was measured by both the cable gauges and load cell to average 14.200 KN. Therefore, the shortening ratio, Λ, needed to be increased to 12.8% in order to produce the desired cable tension 14.800 KN. Thus, the suspenders were shortened further by the distances calculated in Table (7.11). It can be shown that these distances do not have any significant effect on the value of the cable sags in both left and right hand spans, Equations (2.24). The reason for this error, about 4%, could be due to the strains which develop in the suspenders as a result of the applied forces and consequently, reduce the shortening ratio Λ, as mentioned in Section 6.4.1, or due to some initial slip in the main cable anchorages. It is worth noting that all the suspenders remained in plumb after the prestressing operation.

After 24 hours, the test beam was grouted using a cement and water mortar with the ratio 3:1 in weight. As two steel plates were provided at the ends of the test beam to protect them from corrosion due to the cable anchorages, they were also used to inject the grout through channels which were engraved through them connecting the ducts, at their centre, with holes on their tops, Figure (7.18) and Plate (2). A manual pump was used for this purpose in order to assist the flow of the grout from each of the ends of the beam to its top fibre. After three days, the grout became sufficiently hard and the test beam was ready for the first stage of the experiment.

7.6.2 Testing of the Working Life of the Grouted Test Beam

The grouted test beam was subjected to increments of concentrated loading which were applied once at a time at positions (A - H) with the magnitudes and manner described in Section 7.5.2, Plate (5). Each test was repeated several times at each loading position and the final experimental and calculated deflections, bending moments and changes in the prestressing force are tabulated side by side as shown in Tables (7.12 -7.19). The results are also represented in graph form as illustrated in Figures (7.19 - 26) with the same arrangement described in Section 7.5.2, Figures (7.9 - 16).

When the loads were removed from each position, the grouted test beam seemed to recover to its exact position prior to loading. As the load cell did not register any changes in the initial prestressing force, due to grouting, the results obtained from the cable gauges came in close agreement with the calculated ones. Furthermore, the results obtained for the deflections and bending moments were generally about 8% less than those obtained for the first ungrouted test beam as the second one was more rigid due to grouting. However, the changes in the prestressing force were greater than those found for the first test beam by about 30% due to the same reason. This perhaps explains the cause for the immediate recovery of the grouted test beam when the loads were removed, as the cable became more responsive to the loading or unloading of the beam.

Tables (7.12 - 19) and Figures (7.19 - 26) show that the experimental results were within an acceptable difference from the calculated ones. Finally, no sign of cracks was found anywhere along the beam length at this stage of the experiment.

7.6.3 Testing to Failure of the Grouted Test Beam

As mentioned in Section 7.5.3, the load for this stage of the experiment was applied in position C to bring about earliest failure. From the computer program, Appendix 28, the theoretical value of the ultimate moment of resistance for the rectangular cross section was calculated to be 1502.0 N.m for hogging and sagging moments. Moreover, the first plastic hinge was expected to form at position C, under the applied load, at a load 2165.0 N and the failure load was computed to be 2601.0 N with the second plastic hinge forming at the tower position. For this reason, similar increments of loading to that described in Section 6.5.3 were used in this stage of the second experiment.

The load was increased and the first crack developed at a load 1246.0 N at position C. The cracks spread as a result of increasing the load and the first plastic hinge formed at the load 1869 N. This was confirmed by the sudden increase in the deflections and cable tension as can be seen from Table (7.20) and Figure (7.27). Cracks started to appear at the tower section of the beam when the load reached the value 1958.0 N. Afterwards, the increase in the deflections became out of control and at a load of 2136 N the beam completely collapsed as shown in Plate (8).

Similarly to the first experiment, all the experimental results seemed to agree closely with the calculated ones up to the formation of the first plastic hinge. Thereafter, they increased in a rate greater than the calculated one, but with an acceptable margin of error. As before, the deflections and bending moments were clearly less than those obtained for the first experiment, by about 8%, especially after the formation of the first plastic hinge. As

expected, the change in the prestressing force, measured by the cable gauges, was much larger than the corresponding one in the first experiment before and after the formation of the first plastic hinge. Moreover, none of the suspenders failed before the failure of the beam as did the cable whose maximum recorded stress was 860 N/mm^2.

Finally, when the failure loads were removed off both the collapsed test beams, they recovered, to our astonishment, by about 60% for the ungrouted beam and about 70% for the grouted one as shown in Plate (10).

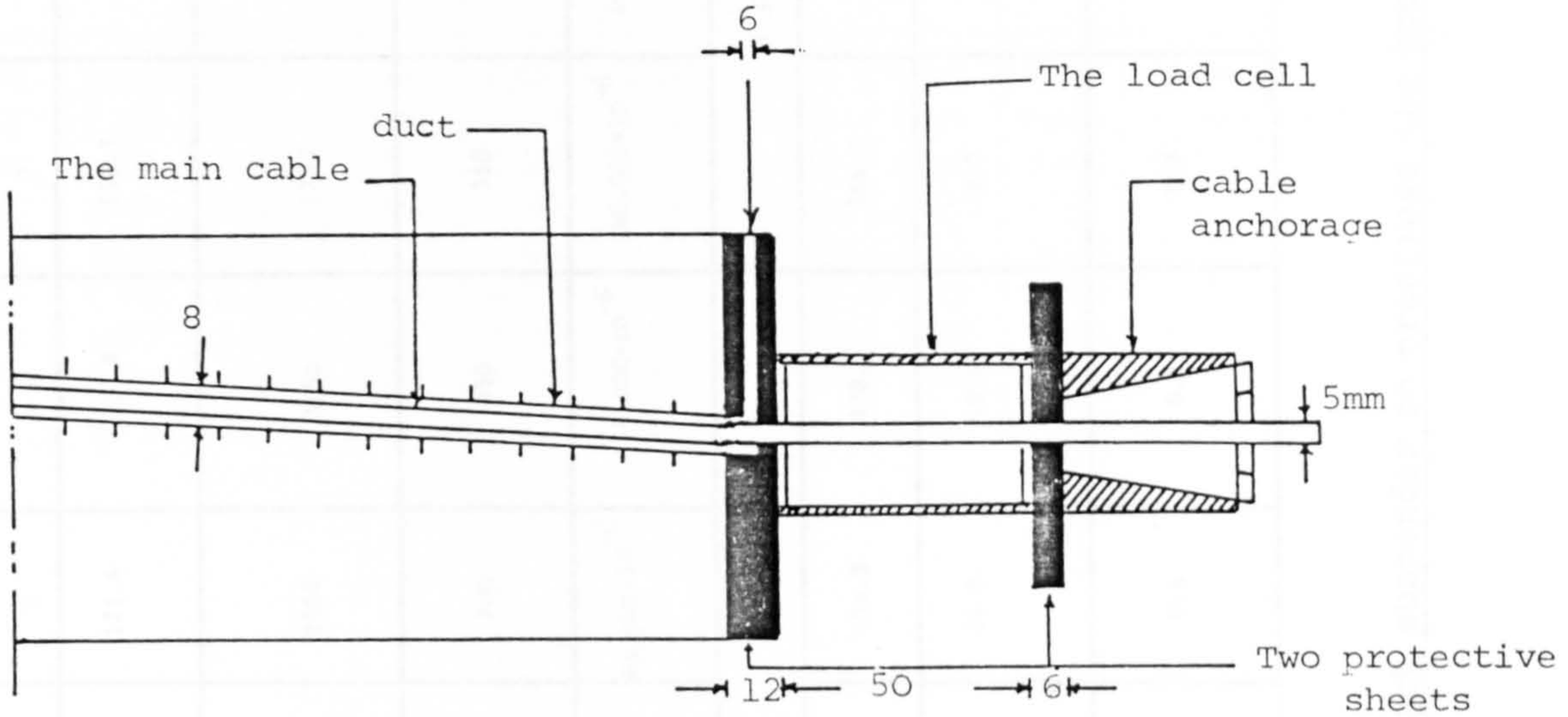

The grouting of the second test beam

Figure (7.18)

Table 7.11

	Suspenders in the Left Hand Span						Suspenders in the Right Hand Span			
Suspender Number	1	2	3	4	5	6	7	8	9	10
Suspenders Design Lengths l_{sm} (mm)	10.8	32.6	58.3	87.9	121.4	158.8	150.7	105.3	63.7	26.1
Distance from left or right end of supports x_m (mm)	1400	1750	2100	2450	2800	3150	1750	1400	1050	700
Distance from the tower $(\ell - x_m)$ (mm)	2100	1750	1400	1050	700	350	350	700	1050	1400
$\frac{l_{sm}}{x_m(\ell - x_m)}$	3.673×10^{-6}	10.645×10^{-6}	19.830×10^{-6}	34.169×10^{-6}	61.940×10^{-6}	144.000×10^{-6}	246.000×10^{-6}	107.450×10^{-6}	57.778×10^{-6}	26.633×10^{-6}
Total Sum	2.743×10^{-4}						4.379×10^{-4}			
Suspender Construction Lengths (mm)	12.10	36.6	65.5	98.7	136.3	178.3	169.2	118.3	71.5	29.30
The required shortening (mm)	1.3	4.0	7.2	10.8	14.9	19.5	18.5	13.0	7.8	3.2
Further Shortening for the Suspenders (mm)	0.0	0.2	0.3	0.4	0.6	0.8	0.8	0.5	0.3	0.2

The shortening distances required for each suspender to prestress the grouted test beam

Table 7.12

Applied Load (N)	DEFLECTIONS (mms)											
	Station (1)		Station (2)		Station (3)		Station (4)		Station (5)		Station (6)	
	Cal.	Exp.	Cal.	Exp.	Cal.	Exp.	Cal.	Exp.	Cal.	Exp.	Cal.	Exp.
89.00	0.120	0.110	0.150	0.170	0.120	0.120	0.060	0.060	-0.030	-0.020	-0.020	-0.010
178.00	0.230	0.230	0.310	0.270	0.240	0.240	0.120	0.110	-0.050	-0.040	-0.040	-0.030
267.00	0.360	0.360	0.460	0.570	0.360	0.365	0.170	0.165	-0.080	-0.070	-0.060	-0.040
356.00	0.480	0.480	0.620	0.600	0.480	0.510	0.230	0.230	-0.100	-0.090	-0.090	-0.060
445.00	0.600	0.610	0.770	0.940	0.600	0.640	0.290	0.310	-0.130	-0.110	0.110	-0.085
534.00	0.720	0.740	0.920	0.990	0.730	0.770	0.350	0.360	-0.150	-0.135	-0.130	-0.100
623.00	0.840	0.860	1.080	1.020	0.850	0.890	0.400	0.420	-0.180	-0.165	-0.150	-0.120
712.00	0.950	1.005	1.230	1.270	0.970	1.020	0.460	0.470	-0.210	-0.195	-0.170	-0.140

Applied Load (N)	BENDING MOMENTS (N.m)						INCREASE IN PRESTRESSING FORCE (N)	
	Position C		Tower		Position G			
	Cal.	Exp.	Cal.	Exp.	Cal.	Exp.	Cal.	Exp.
89.00	-12.114	-10.697	10.292	8.011	5.667	3.321	8.777	7.125
178.00	-24.230	-23.106	20.585	17.635	11.336	7.567	17.557	14.250
267.00	-36.348	-34.213	30.879	27.090	17.006	11.873	26.339	23.451
356.00	-48.469	-51.347	41.174	36.538	22.676	17.527	35.122	31.002
445.00	-60.591	-63.794	51.471	47.466	28.349	22.013	43.908	39.511
534.00	-72.716	-78.655	61.769	55.246	34.022	29.672	52.697	46.170
623.00	-84.842	-91.318	72.068	74.318	39.696	35.700	61.487	54.200
712.00	-96.971	-102.429	82.368	83.087	45.372	41.819	70.280	64.316

The calculated and experimental results when the load is applied at loading station A

Table 7.13

Applied Load (N)	DEFLECTIONS (mms)											
	Station (1)		Station (2)		Station (3)		Station (4)		Station (5)		Station (6)	
	Cal.	Exp.	Cal.	Exp.	Cal.	Exp.	Cal.	Exp.	Cal.	Exp.	Cal.	Exp.
89.00	0.280	0.210	0.390	0.290	0.320	0.240	0.160	0.120	-0.070	-0.050	-0.060	-0.040
178.00	0.550	0.520	0.790	0.710	0.650	0.570	0.310	0.270	-0.140	-0.110	-0.120	-0.100
267.00	0.830	0.760	1.180	1.200	0.970	0.820	0.470	0.420	-0.210	-0.180	-0.180	-0.150
356.00	1.100	1.170	1.580	1.750	1.290	1.130	0.630	0.590	-0.280	-0.260	-0.230	-0.210
445.00	1.380	1.440	1.970	1.930	1.620	1.430	0.790	0.730	-0.350	-0.350	-0.290	-0.260
534.00	1.650	1.730	2.370	2.810	1.940	1.790	0.940	0.890	-0.420	-0.430	-0.350	-0.320
623.00	1.930	1.900	2.760	3.040	2.270	2.150	1.100	1.000	-0.490	-0.510	-0.410	-0.380
712.00	2.210	2.130	3.160	3.530	2.590	2.395	1.260	1.110	-0.560	-0.600	-0.470	-0.450

Applied Load (N)	BENDING MOMENTS (N.m)						INCREASE IN PRESTRESSING FORCE (N)	
	Position C		Tower		Position G			
	Cal.	Exp.	Cal.	Exp.	Cal.	Exp.	Cal.	Exp.
89.00	-37.074	-33.336	28.305	29.938	15.545	19.178	21.850	23.236
178.00	-74.162	-67.419	56.618	60.013	31.098	36.230	43.714	47.018
267.00	-111.263	-103.568	84.938	93.693	46.658	54.700	65.591	70.444
356.00	-148.378	-143.069	113.267	128.555	62.226	71.366	87.482	92.944
445.00	-185.507	-169.285	141.604	156.737	77.802	88.263	109.386	117.871
534.00	-222.650	-206.080	161.949	184.706	93.386	106.789	131.304	139.416
623.00	-259.806	-248.652	198.302	219.641	108.977	123.561	153.236	166.213
712.00	-296.977	-273.593	226.663	243.104	124.576	141.012	175.181	197.462

The calculated and experimental results when the load is applied at loading station B

Table 7.14

Applied Load (N)	DEFLECTIONS (mms)											
	Station (1)		Station (2)		Station (3)		Station (4)		Station (5)		Station (6)	
	Cal.	Exp.	Cal.	Exp.	Cal.	Exp.	Cal.	Exp.	Cal.	Exp.	Cal.	Exp.
89.00	0.270	0.270	0.440	0.350	0.410	0.420	0.210	0.200	-0.090	-0.080	-0.080	-0.060
178.00	0.550	0.610	0.880	0.730	0.820	0.850	0.420	0.460	-0.190	-0.190	-0.160	-0.140
267.00	0.820	0.930	1.330	1.340	1.230	1.170	0.630	0.700	-0.280	-0.310	-0.230	-0.220
356.00	1.090	1.260	1.770	1.880	1.640	1.505	0.840	0.980	-0.380	-0.430	-0.310	-0.300
445.00	1.360	1.570	2.210	2.370	2.050	1.930	1.050	1.260	-0.470	-0.550	-0.390	-0.400
534.00	1.640	1.810	2.650	2.820	2.460	2.310	1.260	1.490	-0.570	-0.630	-0.470	-0.490
623.00	1.910	2.240	3.100	3.510	2.870	2.650	1.470	1.760	-0.660	0.720	-0.550	-0.580
712.00	2.180	2.560	3.540	3.980	3.290	3.090	1.680	1.930	-0.760	-0.810	-0.630	-0.660

Applied Load (N)	BENDING MOMENTS (N.m)						INCREASE IN PRESTRESSING FORCE (N)	
	Position C		Tower		Position G			
	Cal.	Exp.	Cal.	Exp.	Cal.	Exp.	Cal.	Exp.
89.00	-62.428	-51.715	38.621	38.418	21.116	18.232	24.718	27.752
178.00	-124.873	-108.312	77.252	74.569	42.242	39.993	49.453	52.392
267.00	-187.335	-175.796	115.895	109.248	63.380	58.218	74.206	78.215
356.00	-249.813	-263.198	154.548	149.139	84.528	79.450	98.976	111.906
445.00	-312.309	-328.514	193.212	187.557	105.688	100.074	123.763	140.740
534.00	-374.822	-375.565	231.887	239.527	126.859	137.972	148.568	158.580
623.00	-437.353	-447.294	270.573	280.206	148.040	171.958	173.391	182.367
712.00	-499.898	-518.214	309.270	323.136	169.233	192.190	198.230	206.713

The calculated and experimental results when the load is applied at loading station C

Table 7.15

Applied Load (N)	DEFLECTIONS (mm)											
	Station (1)		Station (2)		Station (3)		Station (4)		Station (5)		Station (6)	
	Cal.	Exp.	Cal.	Exp.	Cal.	Exp.	Cal.	Exp.	Cal.	Exp.	Cal.	Exp.
89.00	0.170	0.180	0.300	0.260	0.320	0.360	0.190	0.210	-0.090	-0.080	-0.070	-0.060
178.00	0.350	0.390	0.590	0.680	0.640	0.740	0.380	0.430	-0.180	-0.180	-0.140	-0.130
267.00	0.520	0.500	0.890	0.960	0.950	1.030	0.560	0.670	-0.260	-0.300	-0.220	-0.215
356.00	0.700	0.620	1.190	1.240	1.270	1.400	0.750	0.890	-0.350	-0.410	-0.290	-0.300
445.00	0.870	0.740	1.480	1.750	1.590	1.760	0.940	1.030	-0.440	-0.500	-0.360	-0.400
534.00	1.050	0.890	1.780	2.030	1.910	2.170	1.130	1.260	-0.530	-0.590	-0.430	-0.490
623.00	1.220	1.070	2.080	2.420	2.230	2.530	1.320	1.440	-0.610	-0.670	-0.500	-0.560
712.00	1.390	1.280	2.370	2.740	2.540	2.860	1.500	1.680	-0.700	-0.790	-0.580	-0.660

Applied Load (N)	BENDING MOMENTS (N.m)						INCREASE IN PRESTRESSING FORCE (N)	
	Position C		Tower		Position G			
	Cal.	Exp.	Cal.	Exp.	Cal.	Exp.	Cal.	Exp.
89.00	-31.305	-24.769	36.350	33.152	19.761	19.191	17.231	14.203
178.00	-62.618	-58.820	72.706	75.768	39.528	35.983	34.471	36.925
267.00	-93.940	-86.685	109.067	116.025	59.301	55.166	51.719	49.237
356.00	-125.270	-123.833	145.433	161.009	79.081	76.756	68.976	68.926
445.00	-156.608	-144.188	181.806	201.265	98.867	93.548	86.241	94.619
534.00	-187.954	-175.706	218.183	246.250	118.660	117.537	103.515	119.389
623.00	-219.309	-200.907	254.567	281.770	138.458	136.728	120.797	141.160
712.00	-250.672	-233.292	290.956	322.018	158.263	163.108	138.088	162.363

The calculated and experimental results when the load is applied at loading station D

Table 7.16

Applied Load (N)	DEFLECTIONS (mms)											
	Station (1)		Station (2)		Station (3)		Station (4)		Station (5)		Station (6)	
	Cal.	Exp.	Cal.	Exp.	Cal.	Exp.	Cal.	Exp.	Cal.	Exp.	Cal.	Exp.
89.00	0.050	0.040	0.090	0.060	0.100	0.100	0.070	0.065	-0.040	-0.030	-0.030	-0.020
178.00	0.100	0.095	0.170	0.130	0.200	0.210	0.150	0.130	-0.080	-0.070	-0.070	-0.050
267.00	0.150	0.150	0.260	0.200	0.290	0.320	0.220	0.200	-0.120	-0.120	-0.100	-0.090
356.00	0.200	0.210	0.350	0.300	0.390	0.450	0.290	0.260	-0.160	-0.170	-0.130	-0.120
445.00	0.250	0.260	0.430	0.340	0.490	0.550	0.370	0.330	-0.200	-0.220	-0.170	-0.160
534.00	0.300	0.320	0.520	0.410	0.590	0.670	0.440	0.400	-0.240	0.270	-0.200	-0.200
623.00	0.350	0.360	0.610	0.520	0.690	0.780	0.510	0.480	-0.280	-0.330	-0.230	-0.240
712.00	0.400	0.440	0.690	0.600	0.790	0.900	0.590	0.550	-0.330	-0.380	-0.270	-0.280

Applied Load (N)	BENDING MOMENTS (N.m)						INCREASE IN PRESTRESSING FORCE (N)	
	Position C		Tower		Position G			
	Cal.	Exp.	Cal.	Exp.	Cal.	Exp.	Cal.	Exp.
89.00	-7.866	-6.440	17.127	15.501	9.249	6.306	4.855	3.056
178.00	-15.733	-13.015	34.255	30.013	18.500	14.067	9.710	7.216
267.00	-23.600	-21.700	51.384	44.506	27.750	24.112	14.566	12.619
356.00	-31.469	-26.006	68.513	61.689	37.002	33.900	19.422	17.414
445.00	-39.337	-32.653	85.642	79.233	46.254	39.720	24.280	22.314
534.00	-47.207	-40.832	102.772	107.615	55.507	47.313	29.138	26.555
623.00	-55.077	-47.549	119.902	130.087	64.761	53.679	33.997	30.950
712.00	-62.949	-53.616	137.033	143.764	74.015	60.454	38.856	35.345

The calculated and experimental results when the load is applied at loading station E

Table 7.17

Applied Load (N)	DEFLECTIONS (mms)											
	Station (1)		Station (2)		Station (3)		Station (4)		Station (5)		Station (6)	
	Cal.	Exp.	Cal.	Exp.	Cal.	Exp.	Cal.	Exp.	Cal.	Exp.	Cal.	Exp.
89.00	-0.020	-0.010	-0.030	-0.020	-0.040	-0.030	-0.030	-0.020	0.040	0.035	0.060	0.045
178.00	-0.040	-0.030	-0.070	-0.050	-0.080	-0.070	-0.050	-0.040	0.090	0.080	0.120	0.100
267.00	-0.060	-0.060	-0.100	-0.080	-0.120	-0.120	-0.080	-0.060	0.130	0.125	0.170	0.150
356.00	-0.080	-0.090	-0.140	-0.110	-0.160	-0.175	-0.110	-0.095	0.170	0.190	0.230	0.200
445.00	-0.100	-0.110	-0.170	-0.135	-0.200	-0.230	-0.140	-0.120	0.220	0.250	0.290	0.240
534.00	-0.120	-0.130	-0.210	-0.180	-0.240	-0.270	-0.160	-0.140	0.260	0.300	0.350	0.290
623.00	-0.140	-0.155	-0.250	-0.220	-0.280	-0.310	-0.190	-0.170	0.300	0.345	0.410	0.370
712.00	-0.160	-0.180	-0.280	-0.250	-0.320	-0.360	-0.220	-0.195	0.350	0.390	0.460	0.410

Applied Load (N)	BENDING MOMENTS (N.m)						INCREASE IN PRESTRESSING FORCE (N)	
	Position C		Tower		Position G			
	Cal.	Exp.	Cal.	Exp.	Cal.	Exp.	Cal.	Exp.
89.00	3.126	2.729	5.231	3.980	-12.335	-15.607	-1.853	0.000
178.00	6.251	4.774	10.461	8.135	-24.669	-32.214	-3.706	-4.534
267.00	9.377	8.184	15.692	11.083	-37.003	-44.821	-5.559	-4.534
356.00	12.503	11.378	20.923	16.764	-49.338	-55.017	-7.412	-7.894
445.00	15.628	13.013	26.153	21.380	-61.672	-72.220	-9.265	-7.894
534.00	18.754	16.895	31.384	25.227	-74.007	-88.515	-11.119	-15.316
623.00	21.880	19.093	36.615	30.002	-86.341	-102.251	-12.972	-15.316
712.00	25.006	22.014	41.846	35.181	-98.676	-116.856	-14.825	-20.365

The calculated and experimental results when the load is applied at loading station F

Table 7.18

Applied Load (N)	DEFLECTIONS (mm)											
	Station (1)		Station (2)		Station (3)		Station (4)		Station (5)		Station (6)	
	Cal.	Exp.	Cal.	Exp.	Cal.	Exp.	Cal.	Exp.	Cal.	Exp.	Cal.	Exp.
89.00	-0.050	-0.040	-0.080	-0.070	-0.090	-0.060	-0.070	-0.045	0.100	0.075	0.100	0.070
178.00	-0.100	-0.090	-0.170	-0.140	-0.180	-0.150	-0.140	-0.120	0.190	0.175	0.200	0.170
267.00	-0.150	-0.130	-0.250	-0.200	-0.270	-0.250	-0.220	-0.200	0.290	0.280	0.300	0.270
356.00	-0.200	-0.170	-0.330	-0.280	-0.360	-0.350	-0.290	-0.270	0.380	0.390	0.410	0.320
445.00	-0.250	-0.210	-0.410	-0.350	-0.450	-0.460	-0.360	-0.340	0.480	0.490	0.510	0.490
534.00	-0.300	-0.270	-0.500	-0.420	-0.540	-0.560	-0.430	-0.420	0.580	0.600	0.610	0.590
623.00	-0.350	-0.310	-0.580	-0.500	-0.630	-0.670	-0.510	0.500	0.670	0.720	0.710	0.700
712.00	0.390	-0.360	-0.660	-0.570	-0.720	-0.770	-0.580	-0.560	0.770	0.830	0.810	0.810

Applied Load (N)	BENDING MOMENTS (N.m)						INCREASE IN PRESTRESSING FORCE (N)	
	Position C		Tower		Position G			
	Cal.	Exp.	Cal.	Exp.	Cal.	Exp.	Cal.	Exp.
89.00	7.658	5.934	12.295	9.648	-37.212	-32.156	-3.262	-1.986
178.00	15.316	11.868	24.589	19.296	-74.424	-70.736	-6.524	-5.013
267.00	22.974	15.839	36.884	31.356	-111.636	-113.611	-9.786	-6.761
356.00	30.632	23.012	49.179	48.232	-148.848	-158.622	-13.048	-9.642
445.00	38.290	29.300	61.474	60.292	-186.060	-197.210	-16.309	-14.586
534.00	45.947	37.212	73.768	69.940	-223.273	-242.221	-19.571	-16.333
623.00	53.605	42.619	86.063	80.412	-260.485	-287.239	-22.833	-18.316
712.00	61.262	51.708	98.358	87.884	-297.697	-334.395	-26.095	-21.431

The calculated and experimental results when the load is applied at loading station G

Table 7.19

Applied Load (N)	DEFLECTIONS (mms)											
	Station (1)		Station (2)		Station (3)		Station (4)		Station (5)		Station (6)	
	Cal.	Exp.	Cal.	Exp.	Cal.	Exp.	Cal.	Exp.	Cal.	Exp.	Cal.	Exp.
89.00	-0.030	-0.010	-0.060	-0.040	-0.060	-0.030	-0.040	-0.030	0.050	0.050	0.040	0.050
178.00	-0.060	-0.030	-0.110	-0.080	-0.130	-0.070	-0.090	-0.070	0.100	0.090	0.080	0.100
267.00	-0.090	-0.070	-0.170	-0.120	-0.190	-0.120	-0.130	-0.100	0.150	0.140	0.120	0.160
356.00	-0.120	-0.100	-0.230	-0.170	-0.260	-0.190	-0.170	-0.130	0.200	0.180	0.170	0.210
445.00	-0.150	-0.120	-0.280	-0.230	-0.320	-0.270	-0.210	-0.170	0.250	0.220	0.200	0.260
534.00	-0.180	-0.150	-0.340	-0.280	-0.380	-0.320	-0.260	-0.200	0.310	0.280	0.250	0.320
623.00	-0.210	-0.180	-0.400	-0.360	-0.450	-0.390	-0.300	-0.240	0.360	0.320	0.290	0.370
712.00	-0.240	-0.210	-0.460	-0.420	-0.510	-0.450	-0.340	-0.290	0.410	0.360	0.330	0.410

Applied Load (N)	BENDING MOMENTS (N.m)						INCREASE IN PRESTRESSING FORCE (N)	
	Position C		Tower		Position G			
	Cal.	Exp.	Cal.	Exp.	Cal.	Exp.	Cal.	Exp.
89.00	4.930	2.630	7.470	5.853	-11.723	-9.865	-1.108	0.000
178.00	9.861	6.216	14.941	12.601	-23.447	-22.129	-2.216	-2.863
267.00	14.791	11.001	22.412	19.877	-35.170	-36.656	-3.325	-2.863
356.00	19.721	15.516	29.882	28.512	-46.894	-49.587	-4.433	-5.726
445.00	24.651	19.996	37.353	38.018	-58.617	-60.368	-5.541	-5.726
534.00	29.581	23.432	44.823	49.010	-70.340	-75.462	-6.649	-8.589
623.00	34.512	28.900	52.294	58.216	-82.064	-81.930	-7.758	-8.589
712.00	39.442	31.227	59.764	67.476	-93.787	-99.181	-8.866	-11.452

The calculated and experimental results when the load is applied at loading station H

Table 7.20

Applied Load (N)	DEFLECTIONS (mms)											
	Station (1)		Station (2)		Station (3)		Station (4)		Station (5)		Station (6)	
	Cal.	Exp.	Cal.	Exp.	Cal.	Exp.	Cal.	Exp.	Cal.	Exp.	Cal.	Exp.
178.00	0.550	0.640	0.880	0.700	0.820	0.870	0.420	0.470	-0.190	-0.210	-0.160	-0.140
356.00	1.090	1.210	1.770	1.830	1.650	1.460	0.840	0.950	-0.380	-0.430	-0.320	-0.290
534.00	1.640	1.880	2.660	2.800	2.470	2.310	1.260	1.460	-0.570	-0.620	-0.470	-0.460
712.00	2.180	2.570	3.540	3.930	3.290	2.990	1.680	1.900	-0.760	-0.810	-0.630	-0.650
890.00	2.730	3.090	4.430	4.960	4.110	3.880	2.100	2.380	-0.950	-1.060	-0.790	-0.760
1068.00	3.270	3.680	5.310	6.030	4.940	4.600	2.520	2.760	-1.140	-1.290	-0.950	-0.930
1246.00	3.820	4.370	6.200	6.990	5.760	5.850	2.940	3.200	-1.330	-1.540	-1.100	-1.060
1424.00	4.360	5.080	7.080	7.810	6.580	6.840	3.360	3.640	-1.520	-1.800	-1.260	-1.290
1602.00	4.910	5.630	7.970	8.890	7.400	7.800	3.780	4.030	-1.710	-2.150	-1.420	-1.560
1780.00	5.450	6.210	8.850	10.130	8.230	8.610	4.200	4.810	-1.900	-2.520	-1.570	-1.840
1869.00	6.090	7.000	10.280	11.650	9.670	9.810	4.800	5.360	-2.130	-2.970	-1.740	-2.680
1958.00	6.720	7.890	11.720	13.130	11.110	12.600	5.400	6.740	-2.370	-3.440	-1.910	-3.050
2047.00	7.350	9.070	13.150	15.910	12.540	14.520	6.000	7.550	-2.600	-4.280	-2.080	-3.730
2136.00	7.980	11.980	14.590	19.010	13.980	17.470	6.600	9.440	-2.830	-5.030	-2.260	-4.680
2225.00	8.610	14.440	16.020	26.380	15.420	23.780	7.200	11.680	-3.060	-6.210	-2.430	-5.720

Applied Load (N)	BENDING MOMENTS (N.m)						INCREASE IN PRESTRESSING FORCE (N)	
	Position C		Tower		Position G			
	Cal.	Exp.	Cal.	Exp.	Cal.	Exp.	Cal.	Exp.
178.00	-124.873	-100.987	77.252	70.326	42.242	36.013	49.453	50.680
356.00	-249.813	-249.155	154.548	153.894	84.528	74.482	98.976	117.333
534.00	-374.822	-390.310	231.887	248.650	126.859	146.575	149.568	163.232
712.00	-499.898	-538.229	309.270	347.498	169.233	193.990	198.230	212.896
890.00	-624.906	-683.948	386.260	419.758	211.533	239.617	247.788	268.117
1068.00	-749.915	-793.641	463.512	496.894	253.806	271.215	300.338	336.362
1246.00	-874.923	-913.474	540.764	585.629	296.120	304.312	352.890	410.716
1424.00	-999.931	-1023.745	618.016	652.542	338.431	345.591	405.441	475.668
1602.00	-1124.940	-1188.445	695.268	743.871	380.799	396.526	457.992	530.310
1780.00	-1249.948	-1333.855	773.520	816.540	423.038	451.066	510.543	612.881
1869.00	-1374.821		888.215	986.724	475.584	517.307	639.797	726.705
1958.00	-1499.694		1002.910	1236.586	528.135	597.411	769.051	847.458
2047.00			1117.605	1492.012	580.686	720.000	898.305	942.775
2136.00			1232.300		633.238	876.199	1027.559	1158.342
2225.00					685.788	1140.450	1156.813	1403.316

The calculated and experimental results when the load to failure is applied at loading station C

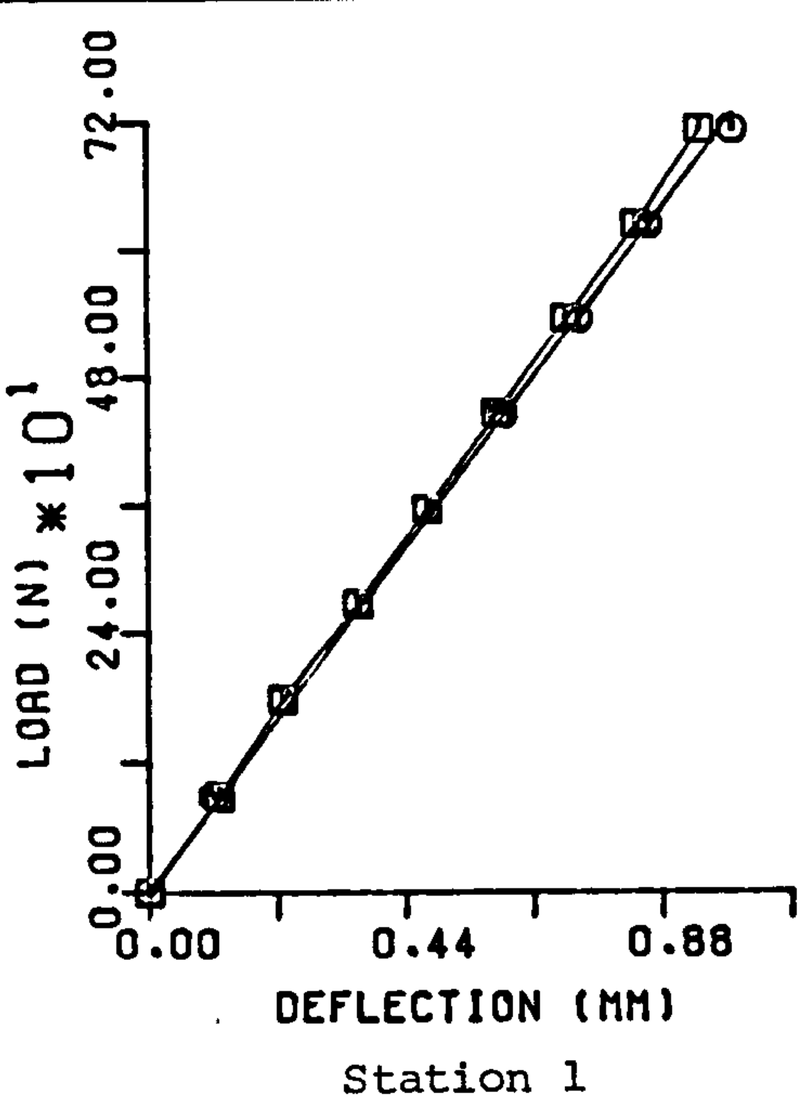

Station 1

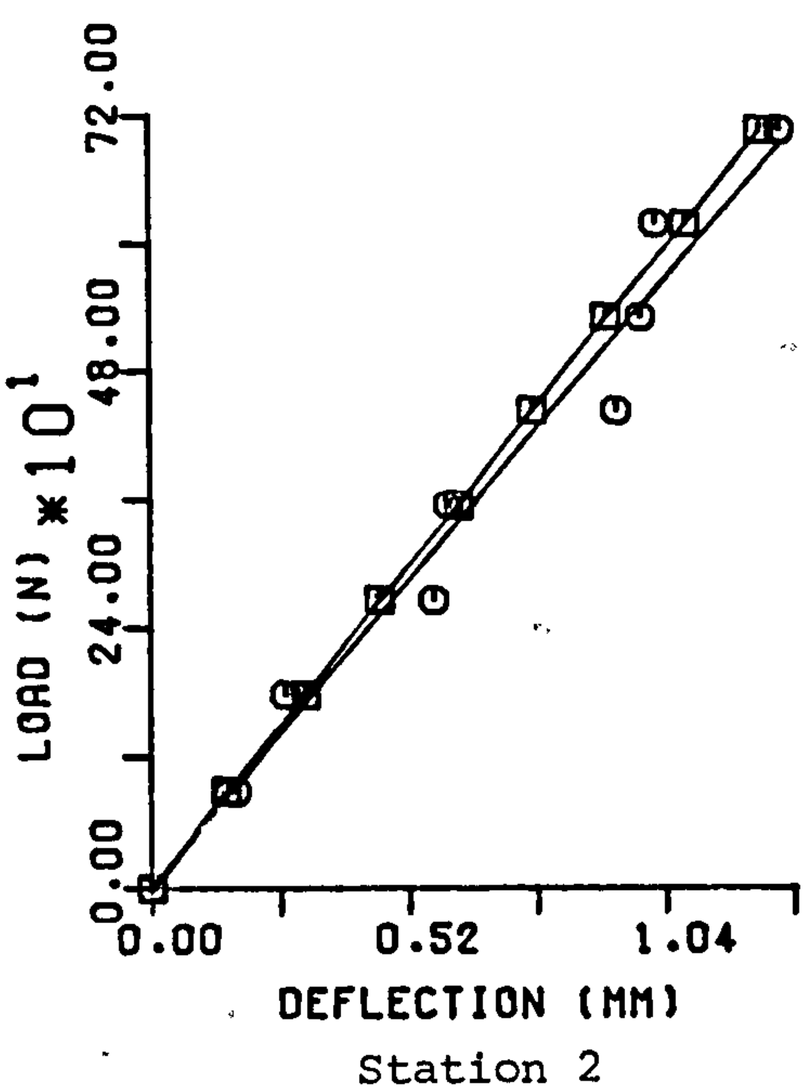

Station 2

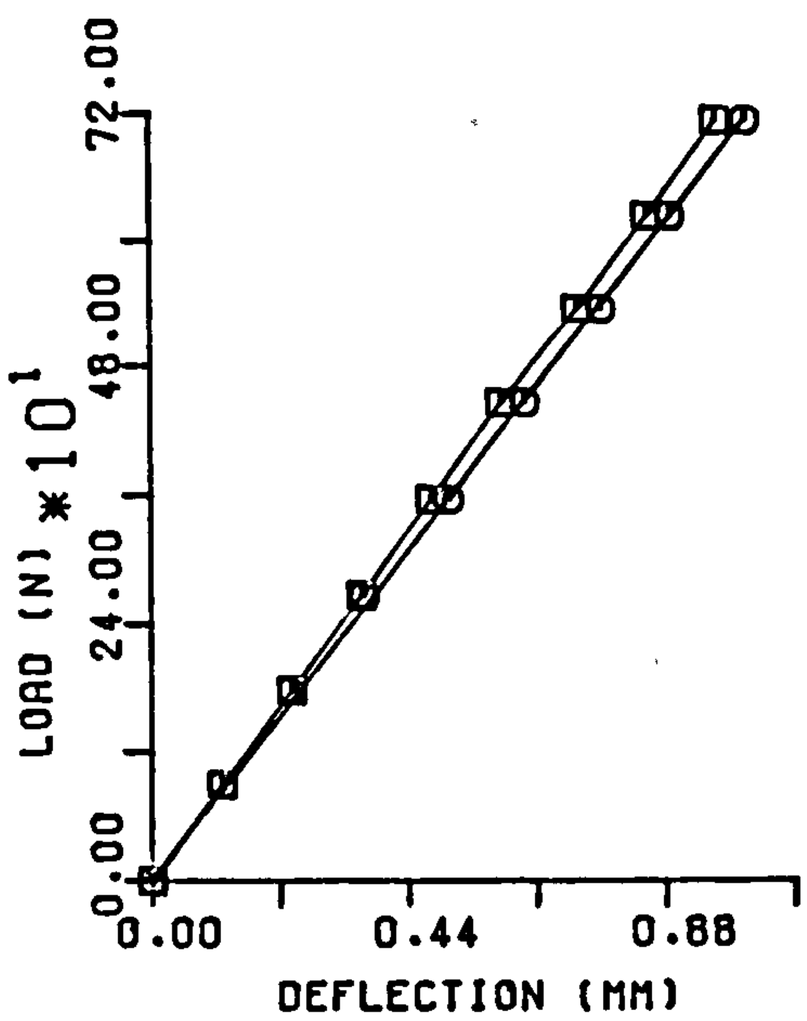

Station 3

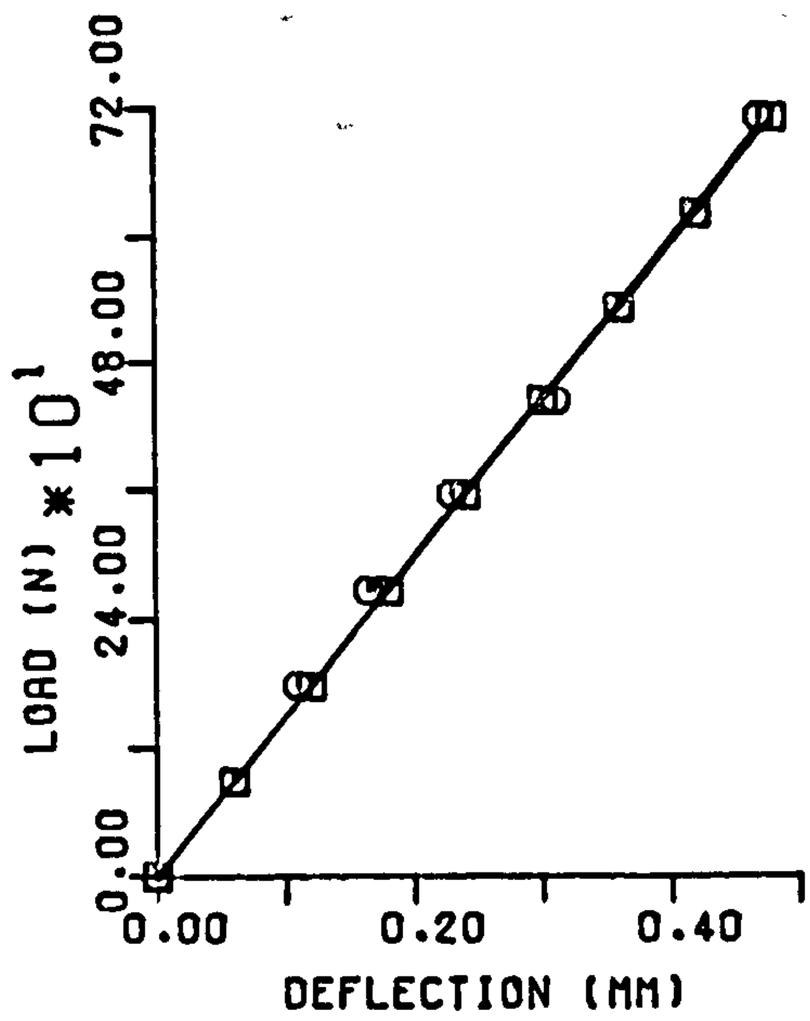

Station 4

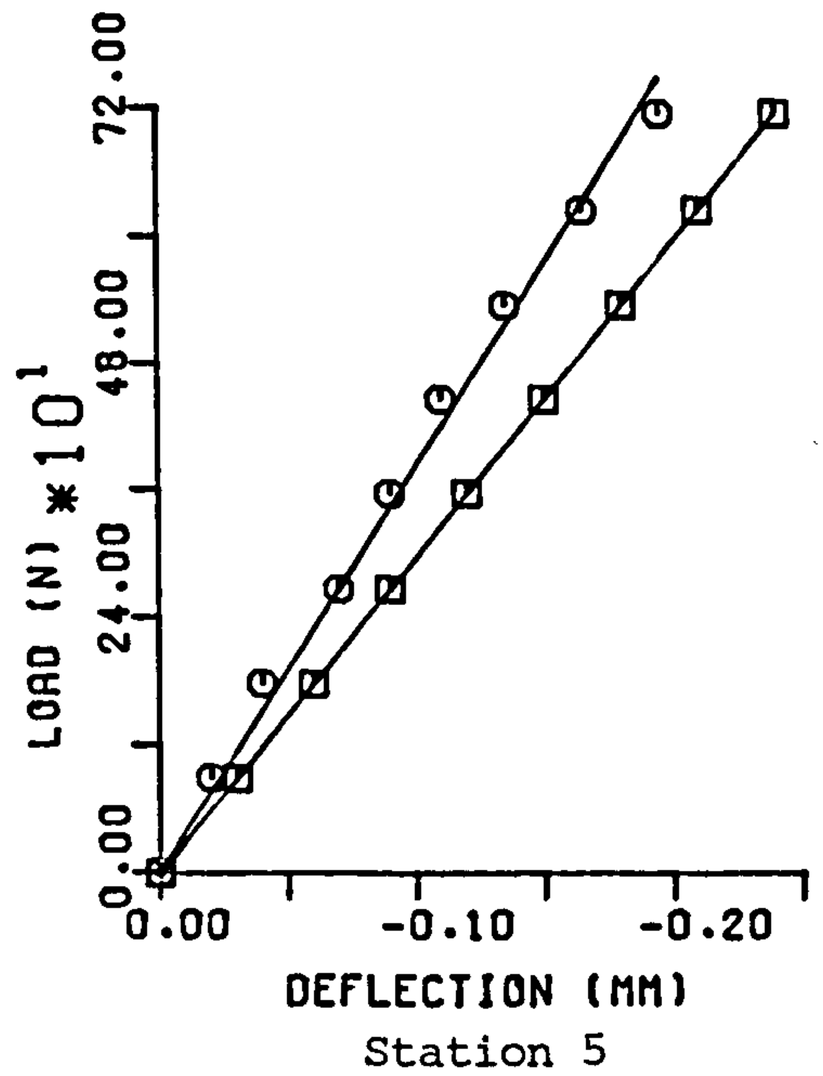

Station 5

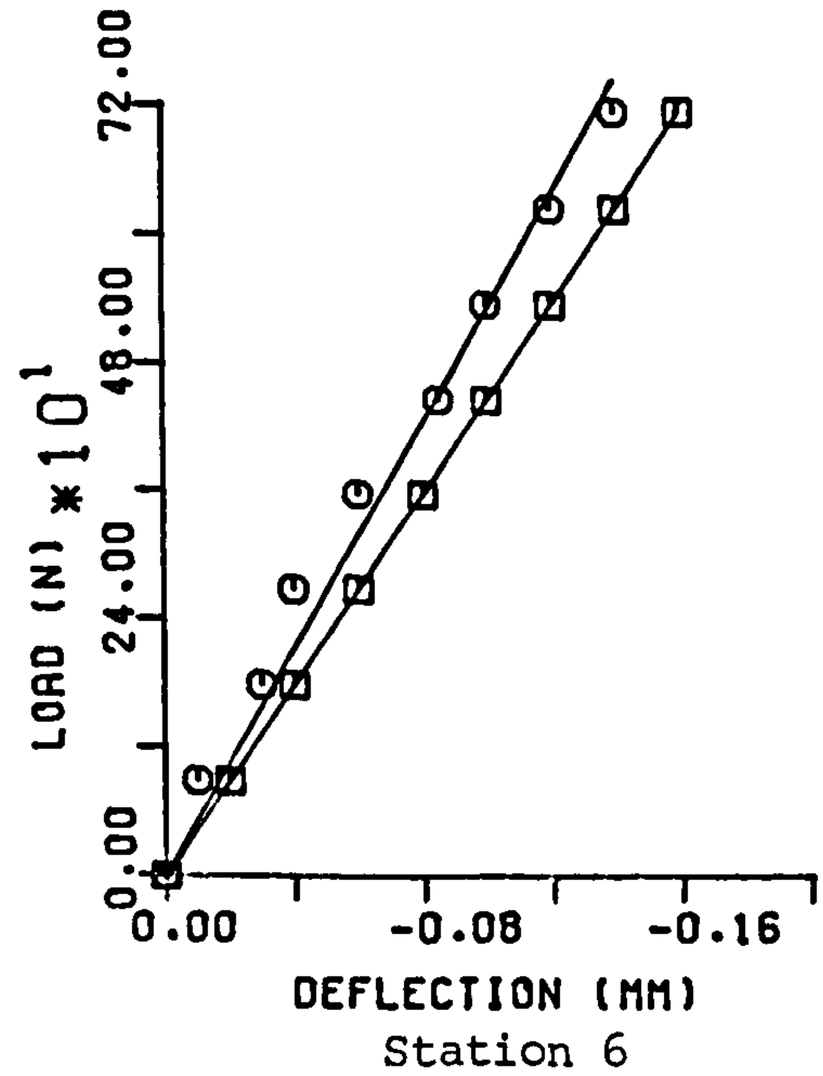

Station 6

□ The calculated deflections
o The measured deflections

The deflections when the load is applied at loading position A

Figure(7.19a)

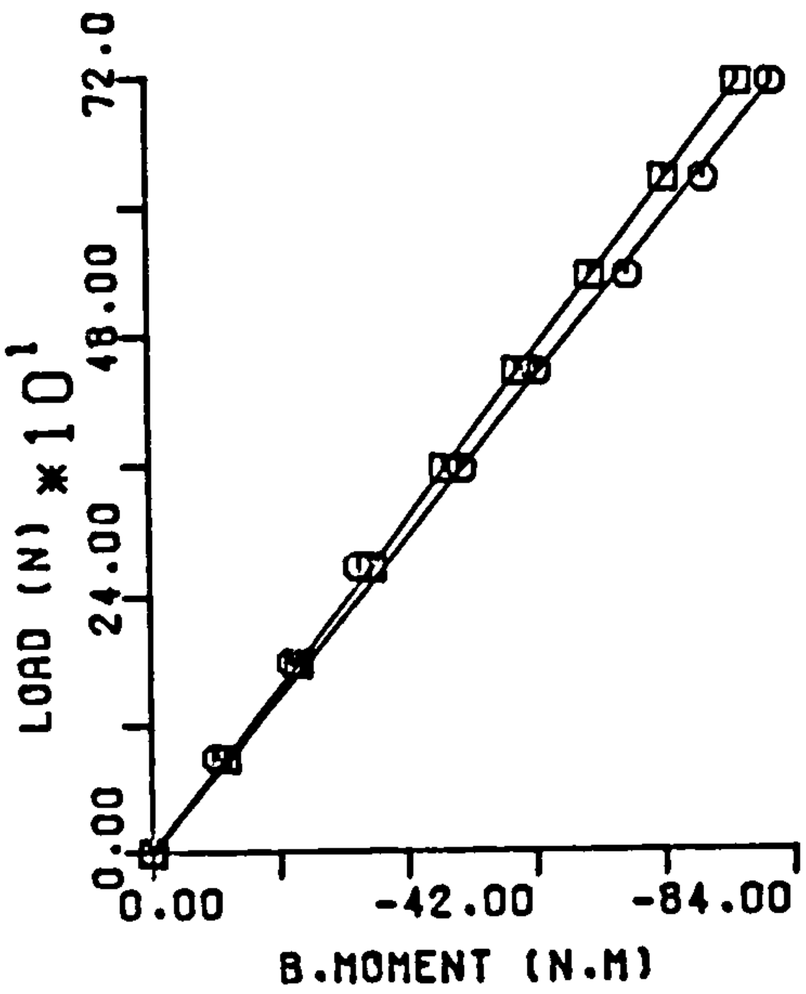

Position C

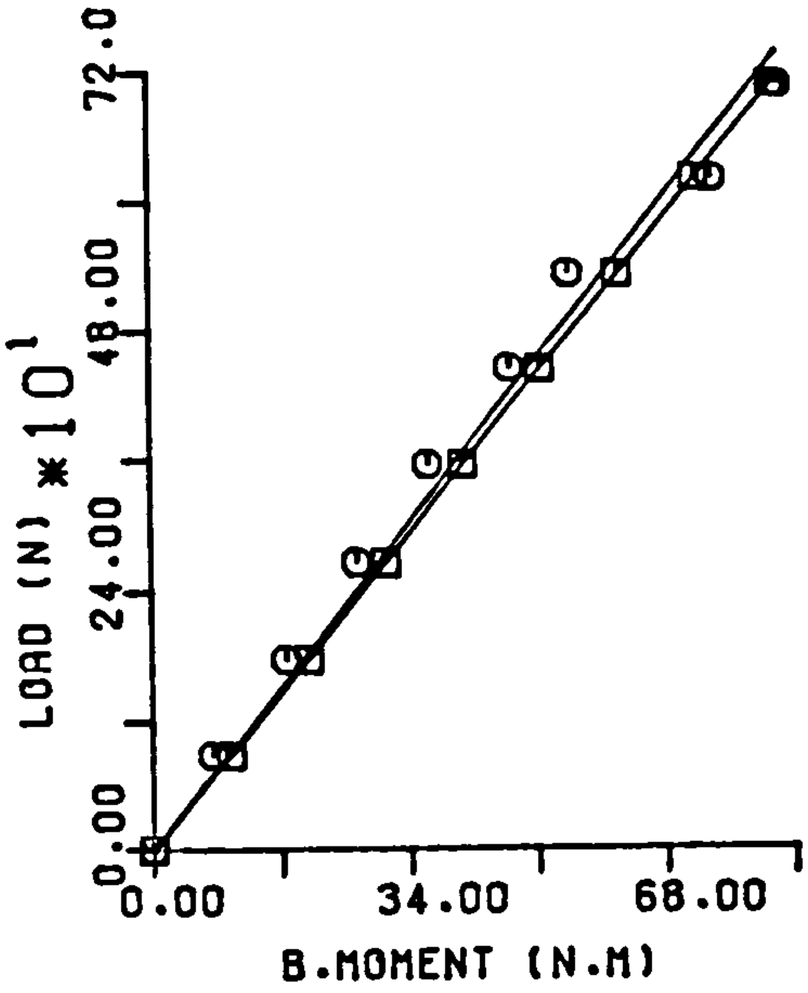

Tower Position

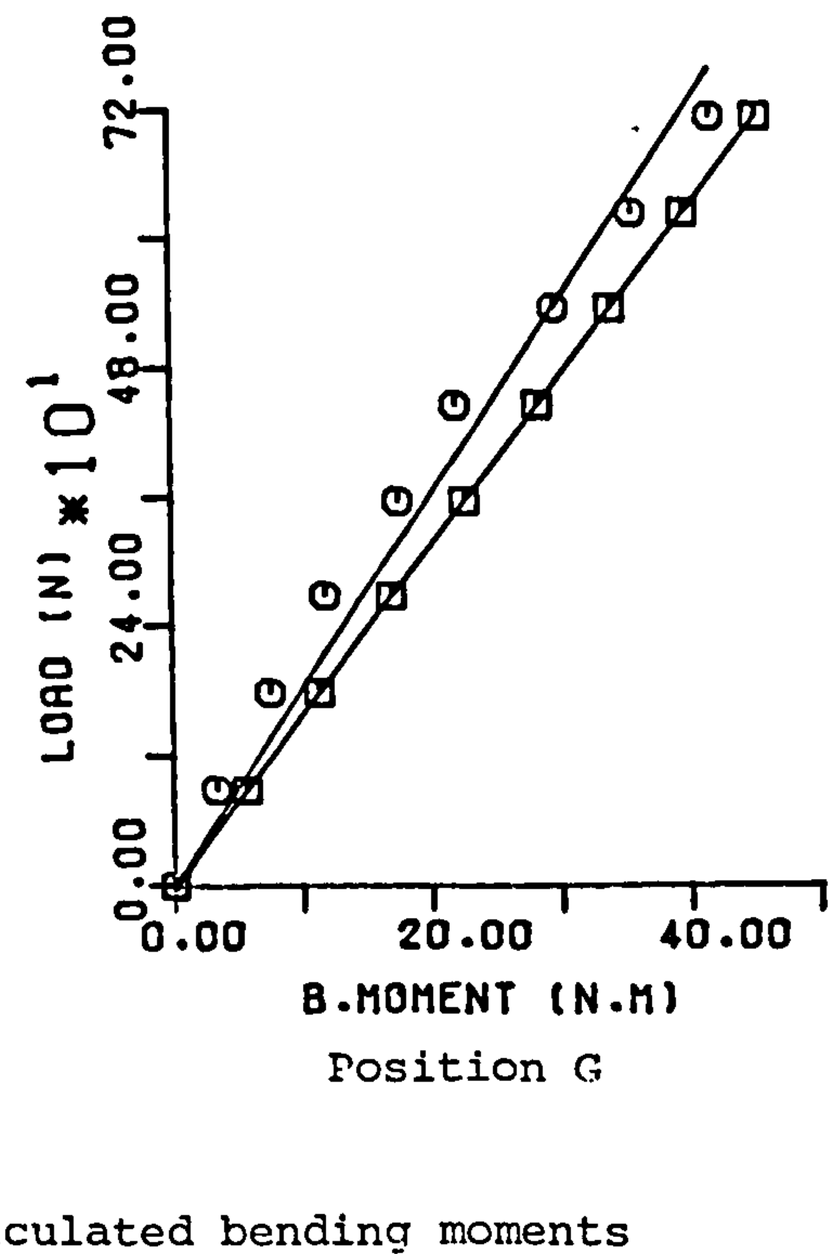

Position G

- ▫ The calculated bending moments
- o The actual bending moments

The bending moments when the load is applied at loading station A

Figure (7.19b)

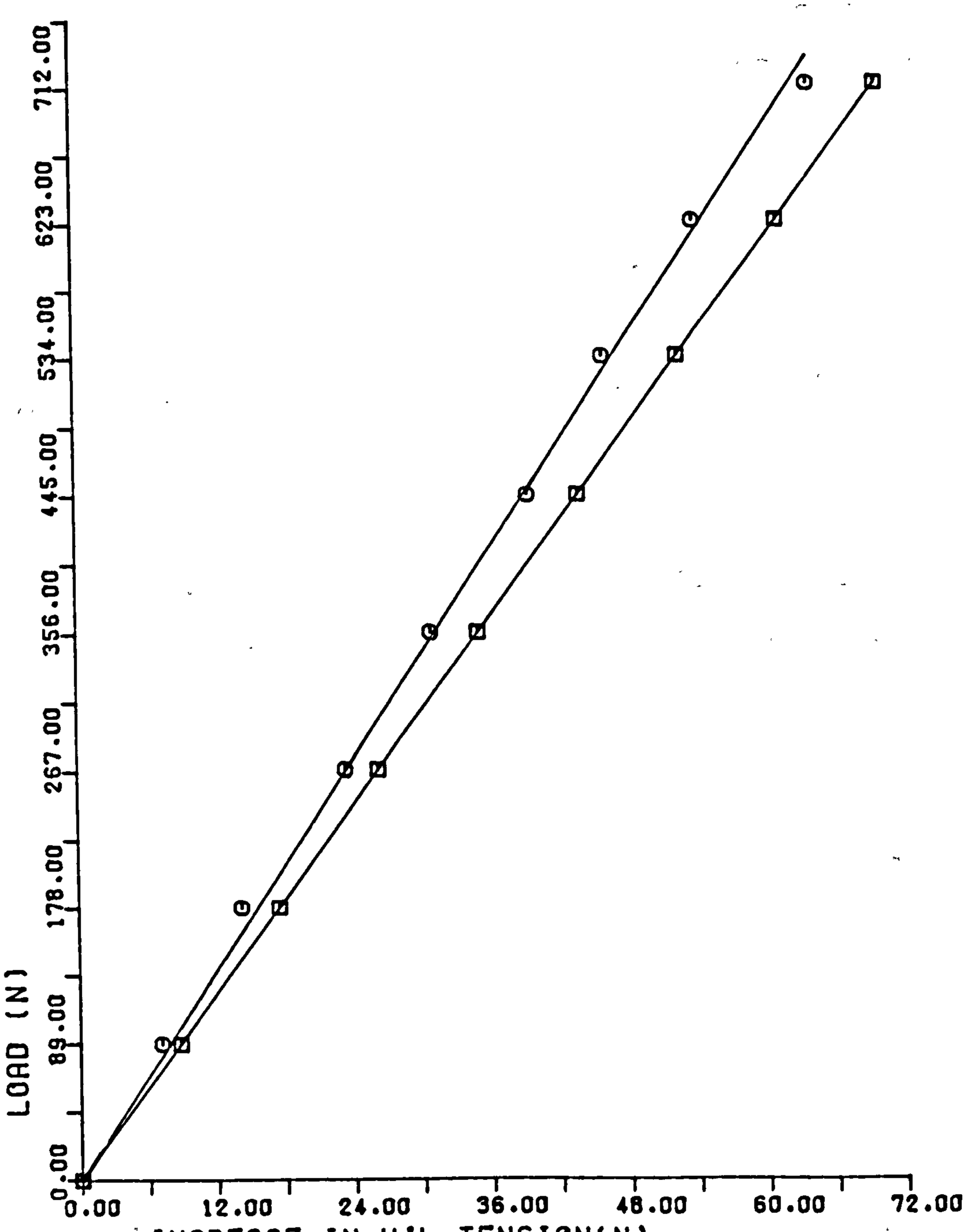

□ The calculated values
O Cable gauges readings

The change in the prestressing force when the load is applied at loading station A

Figure (7.19c)

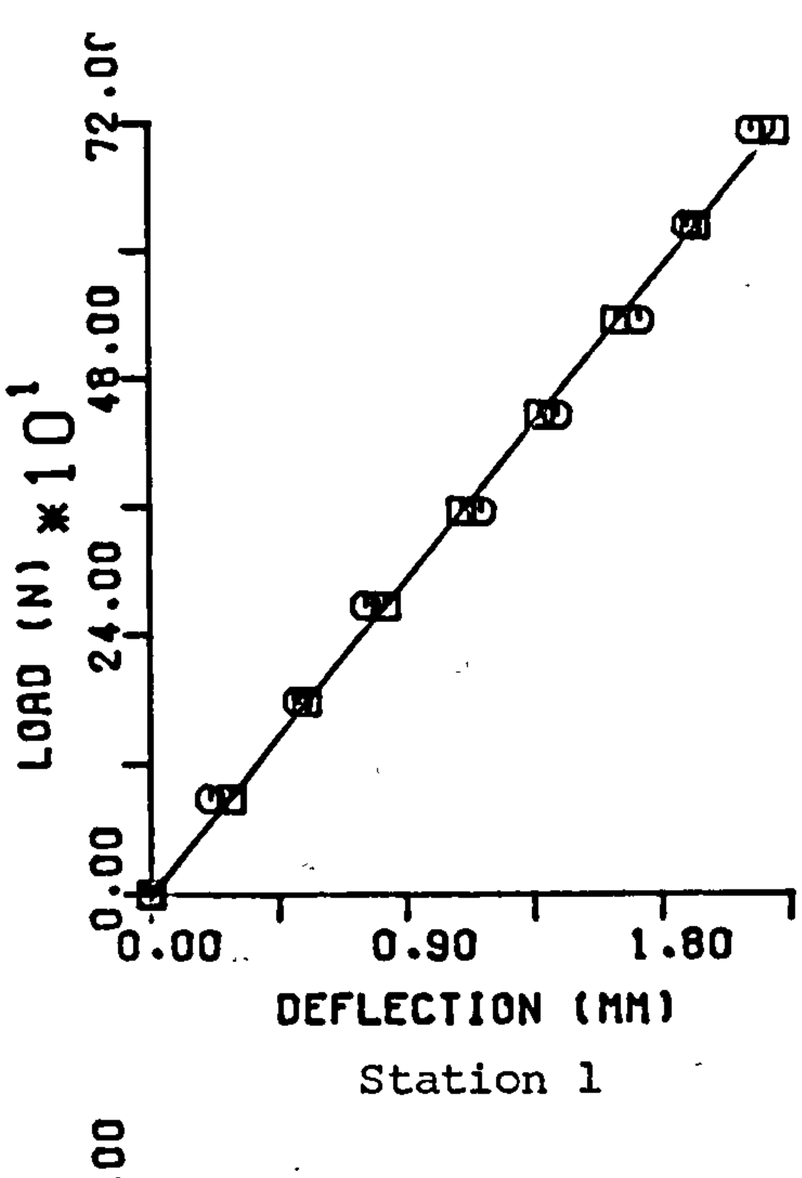

Station 1

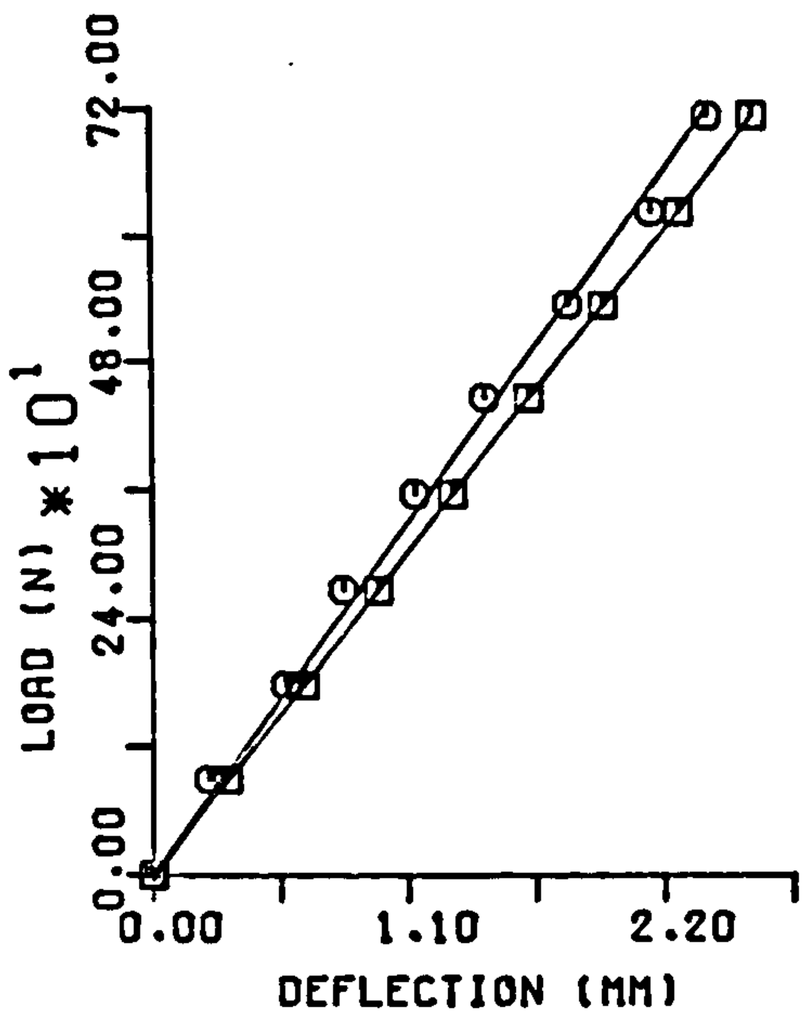

Station 2

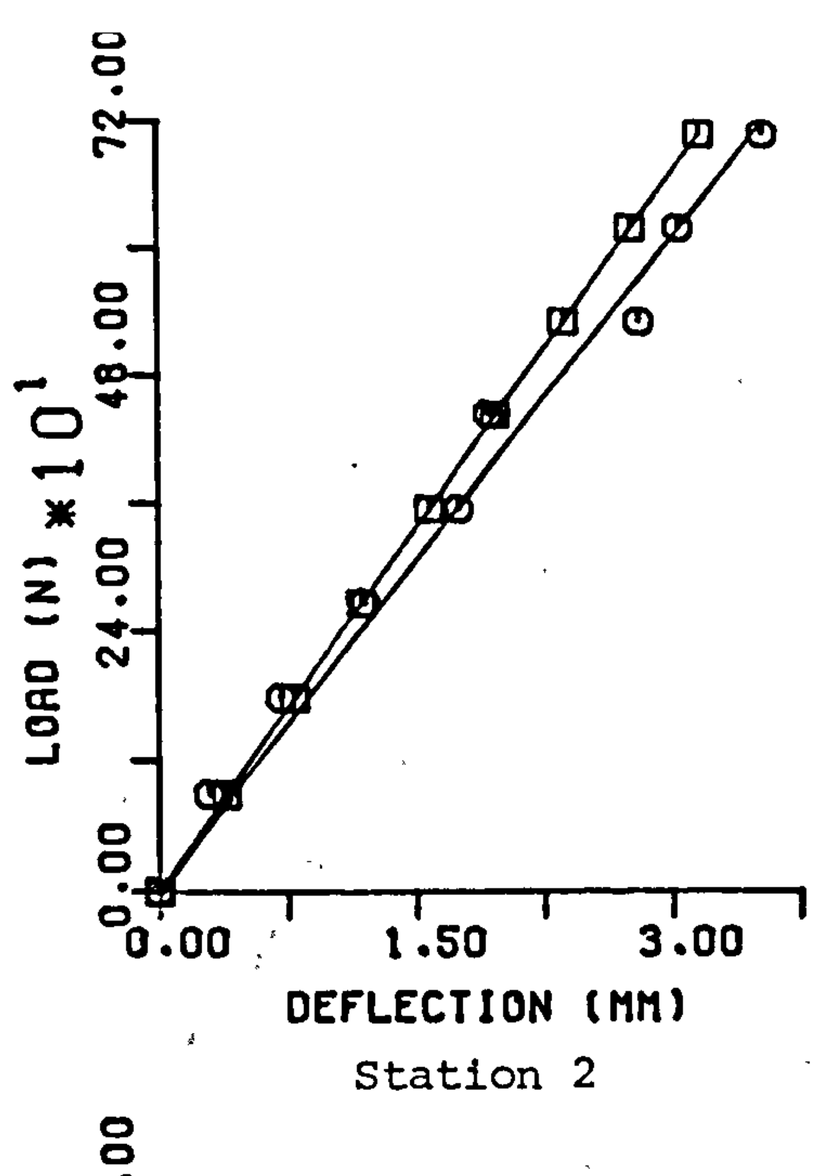

Station 3

Station 4

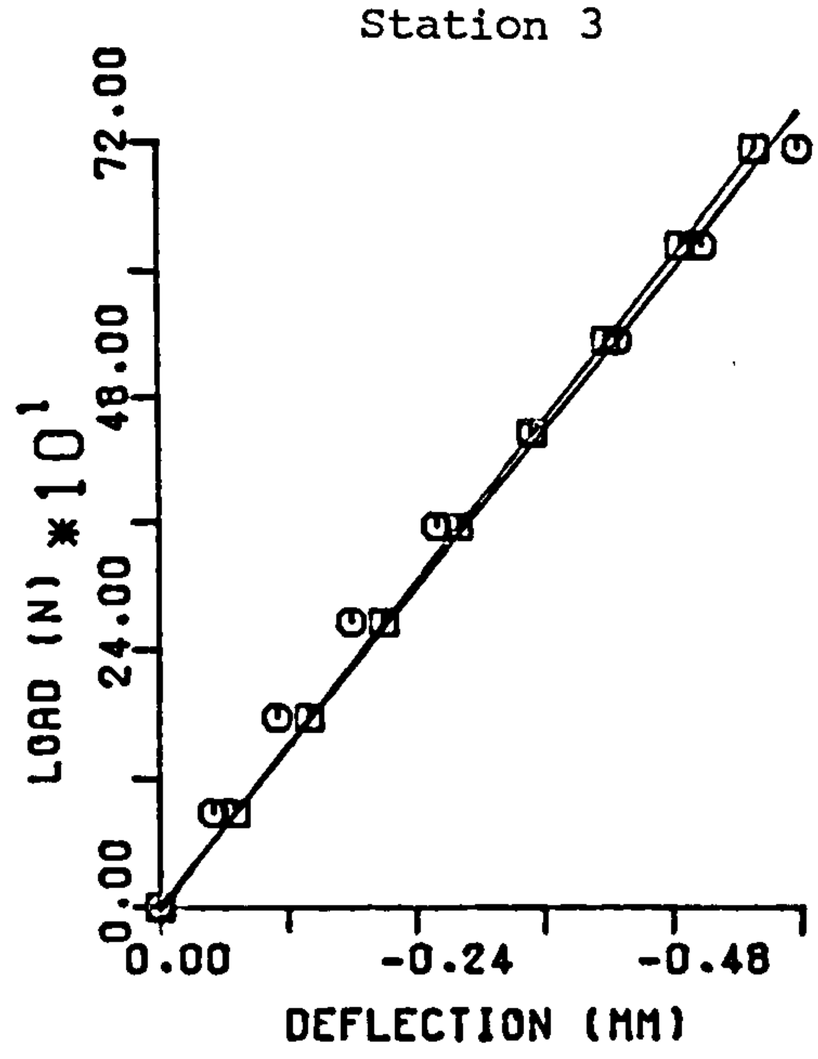

Station 5

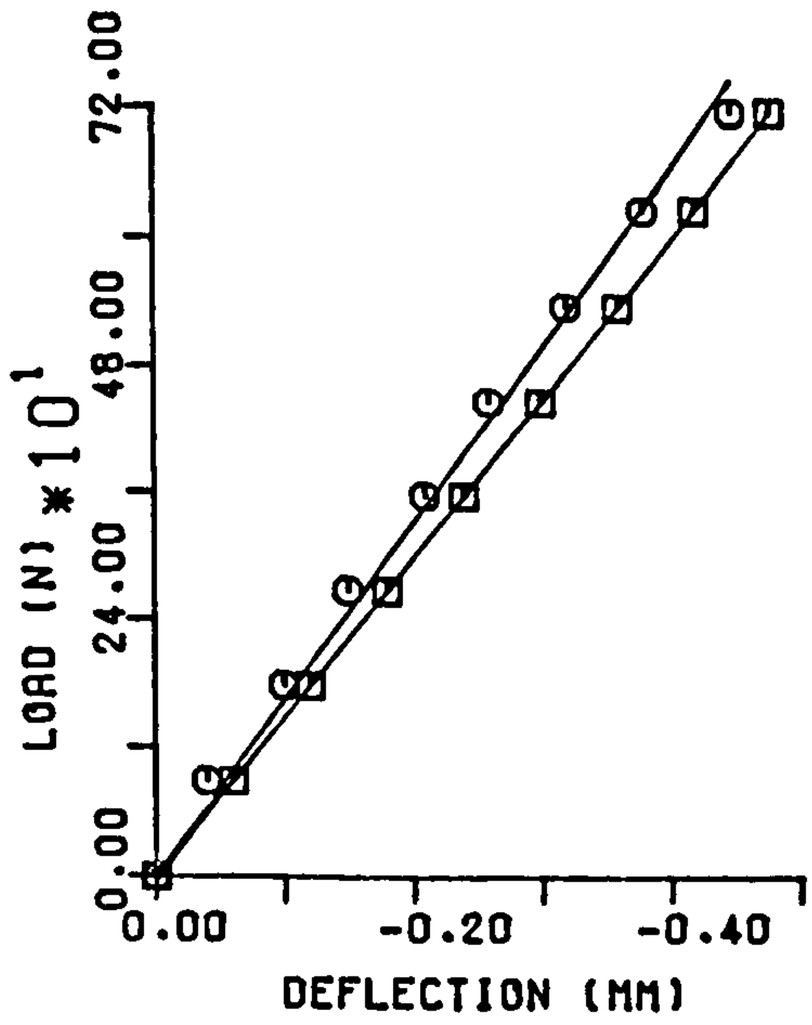

Station 6

▫ The calculated deflections
o The measured deflections

The deflections when the load is applied at loading position B

Figure (7.20a)

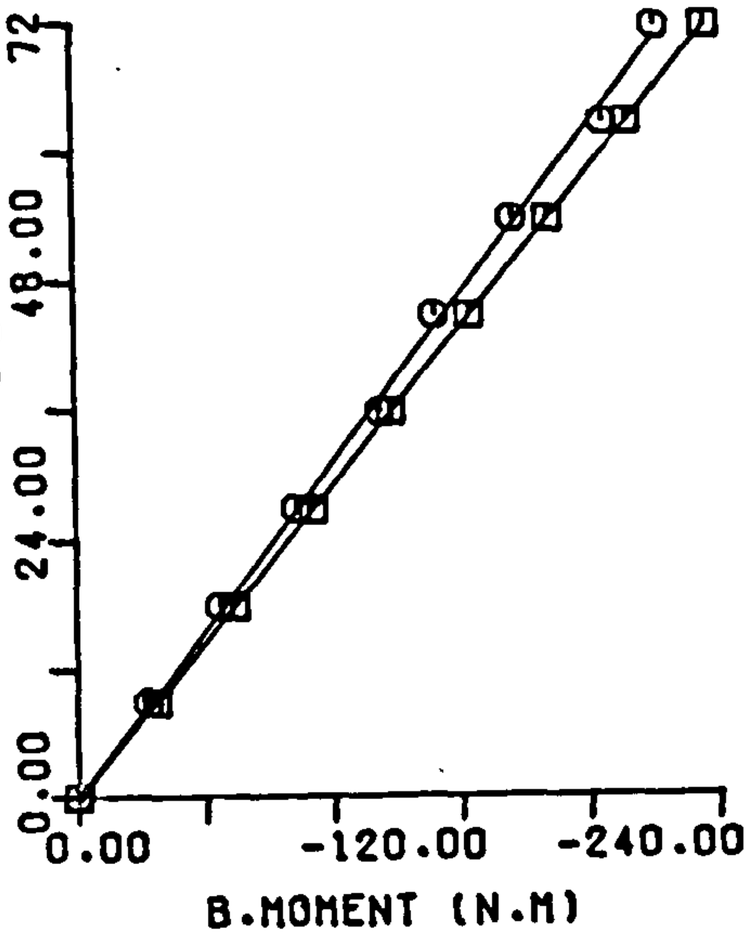

Position C

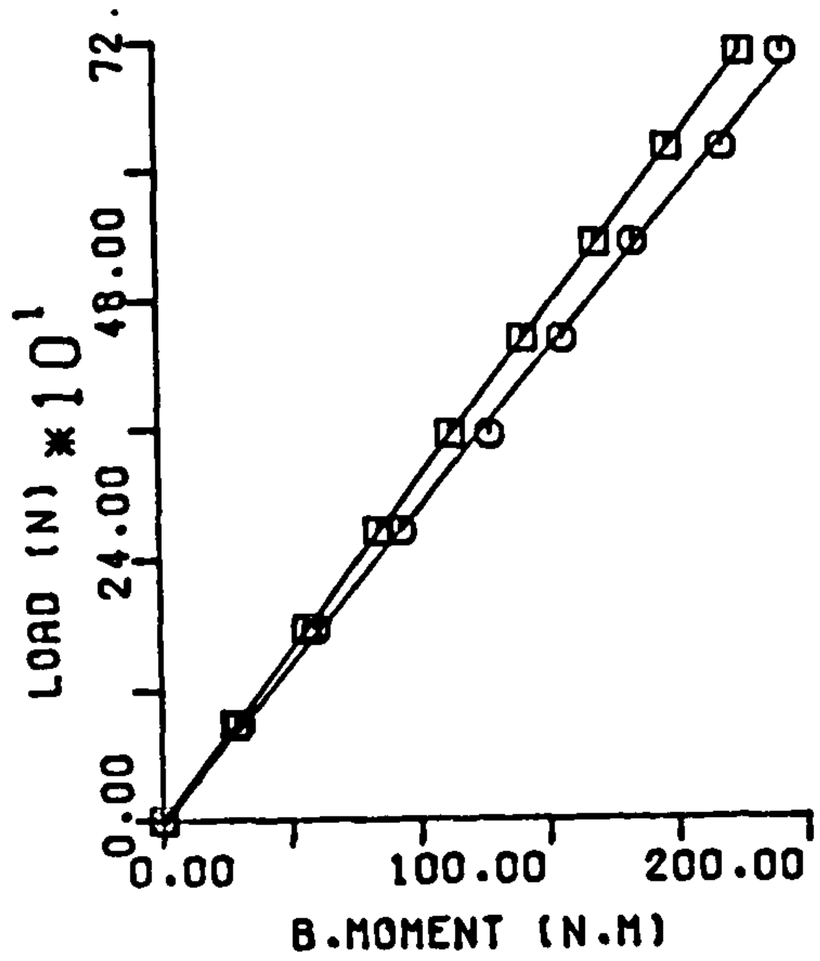

Tower Position

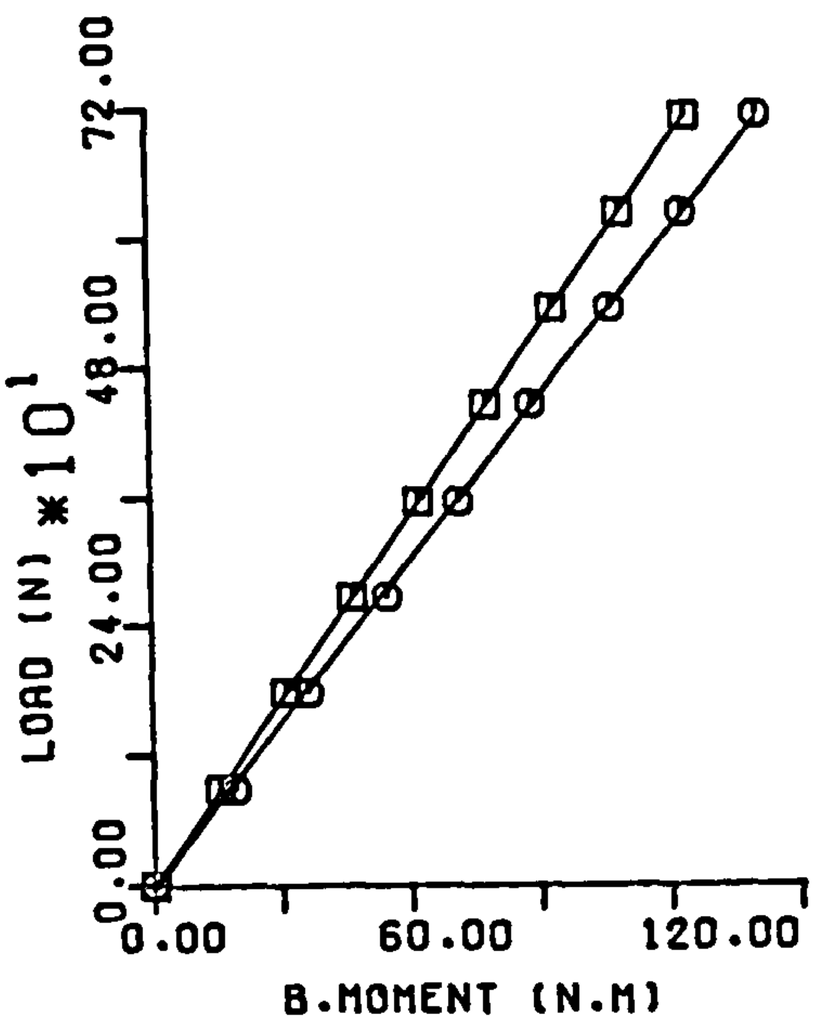

Position G

- The calculated bending moments
- The actual bending moments

The bending moments when the load is applied at loading station B

Figure(7.20b)

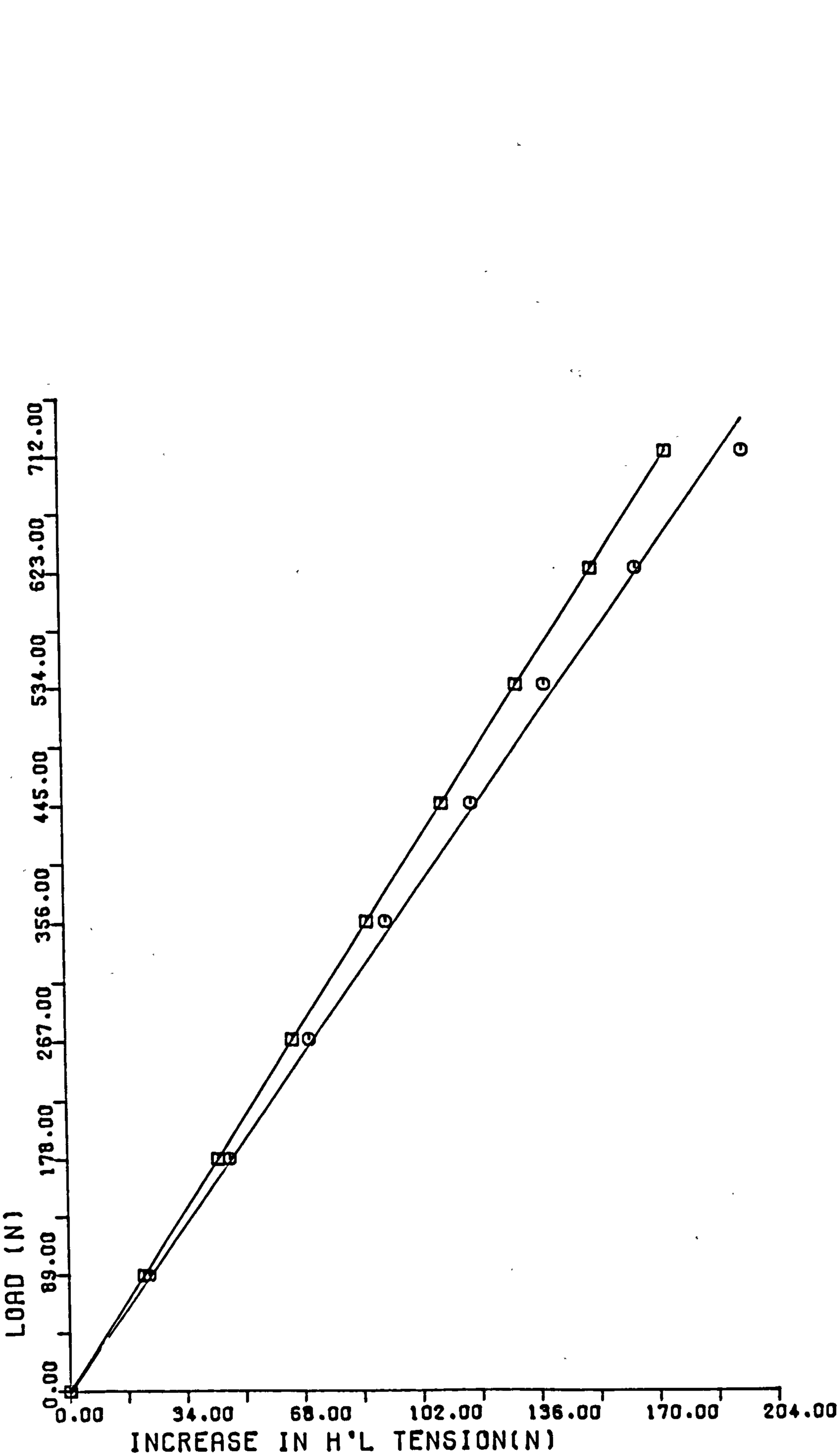

□ The calculated values
o Cable gauges readings

The change in the prestressing force when the load is applied at loading station B

Figure (7.20c)

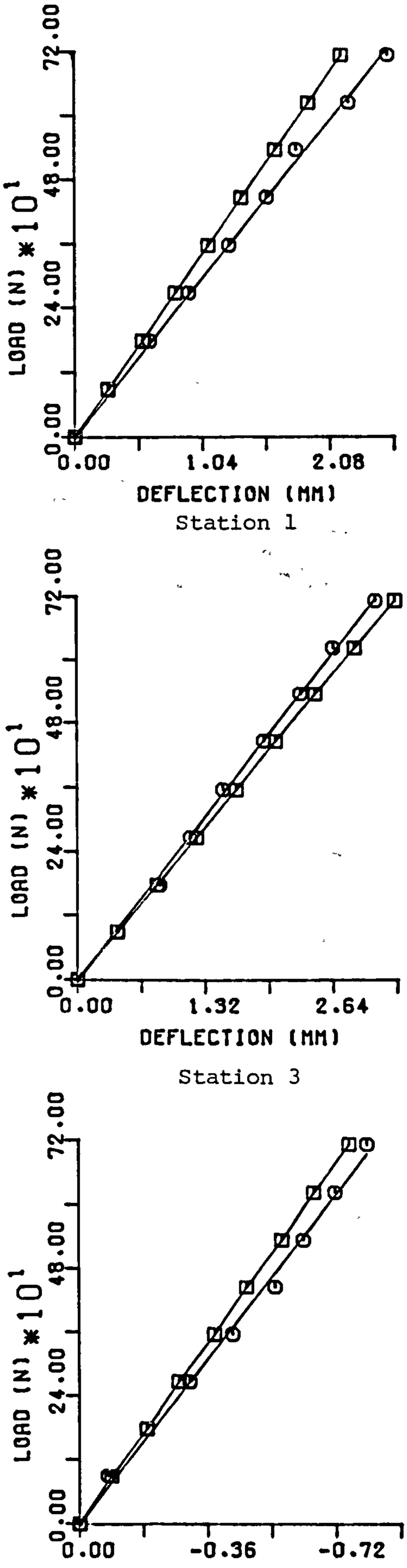

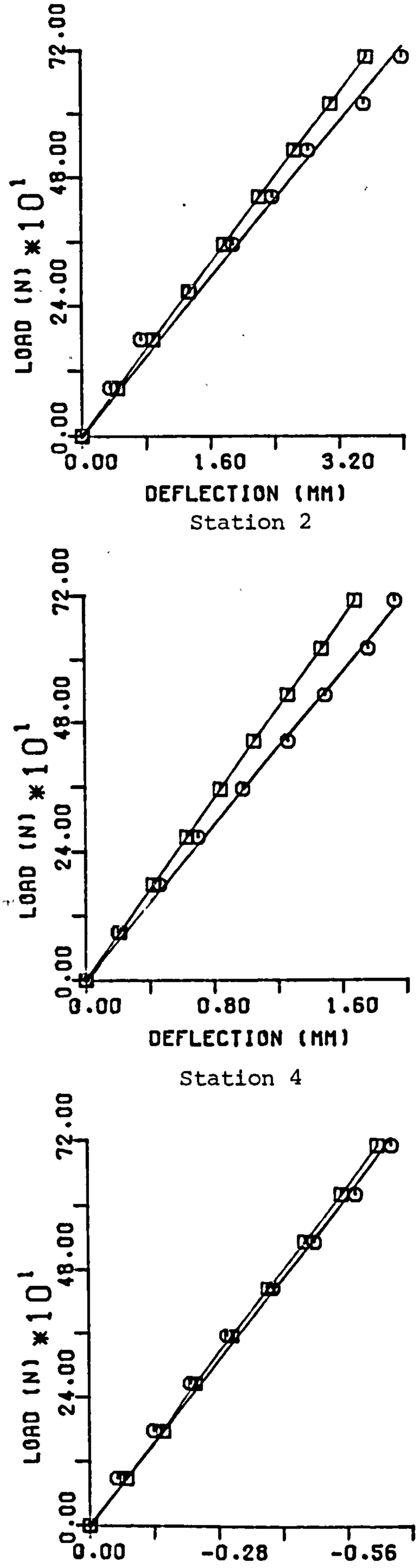

▫ The calculated deflections
o The measured deflections

The deflections when the load is applied at loading position C

Figure(7.21a)

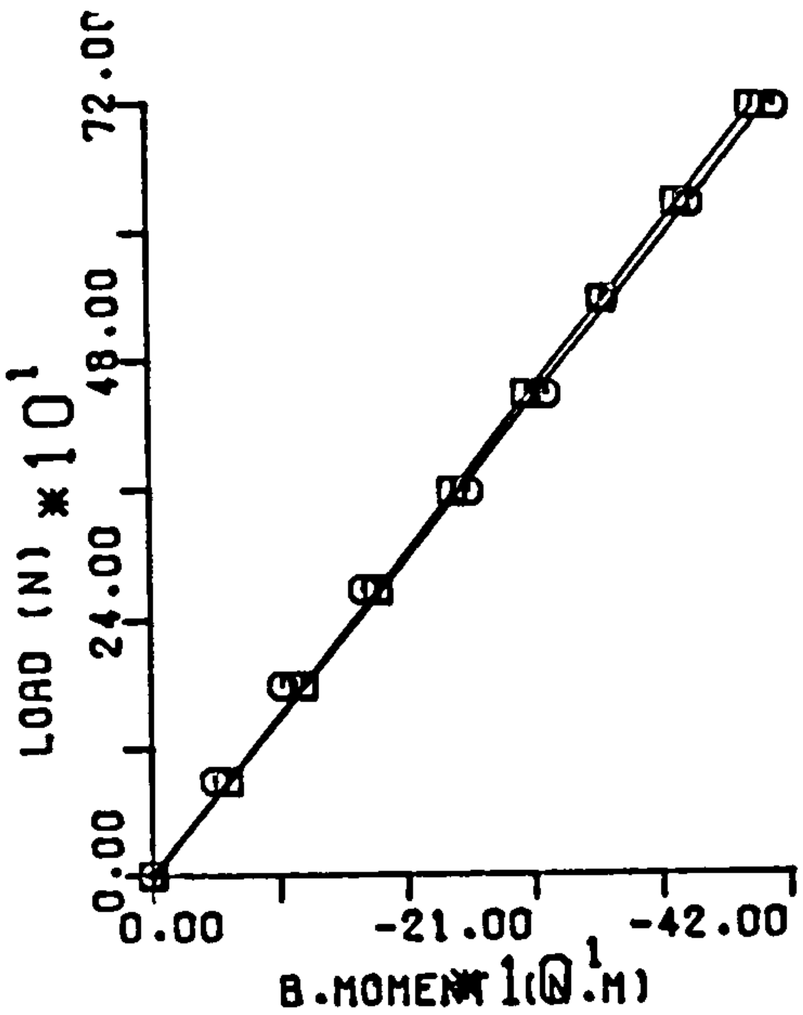

Position C

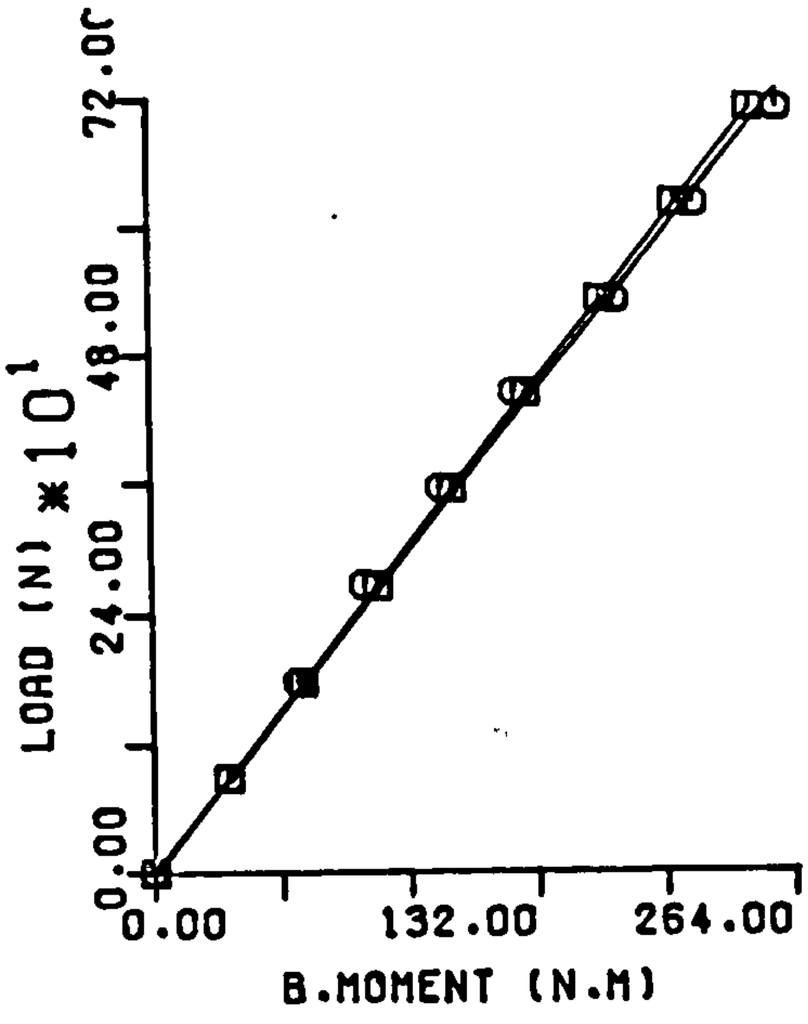

Tower Position

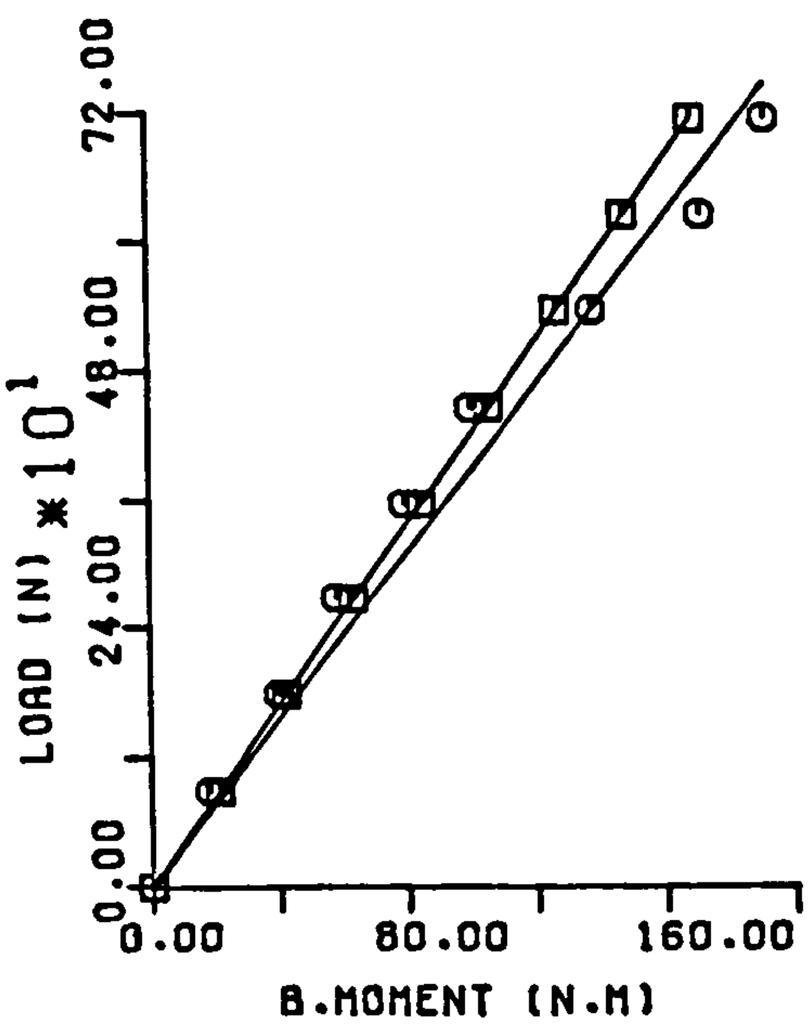

Position G

- ▫ The calculated bending moments
- o The actual bending moments

The bending moments when the load is applied at loading station C

Figure (7.21b)

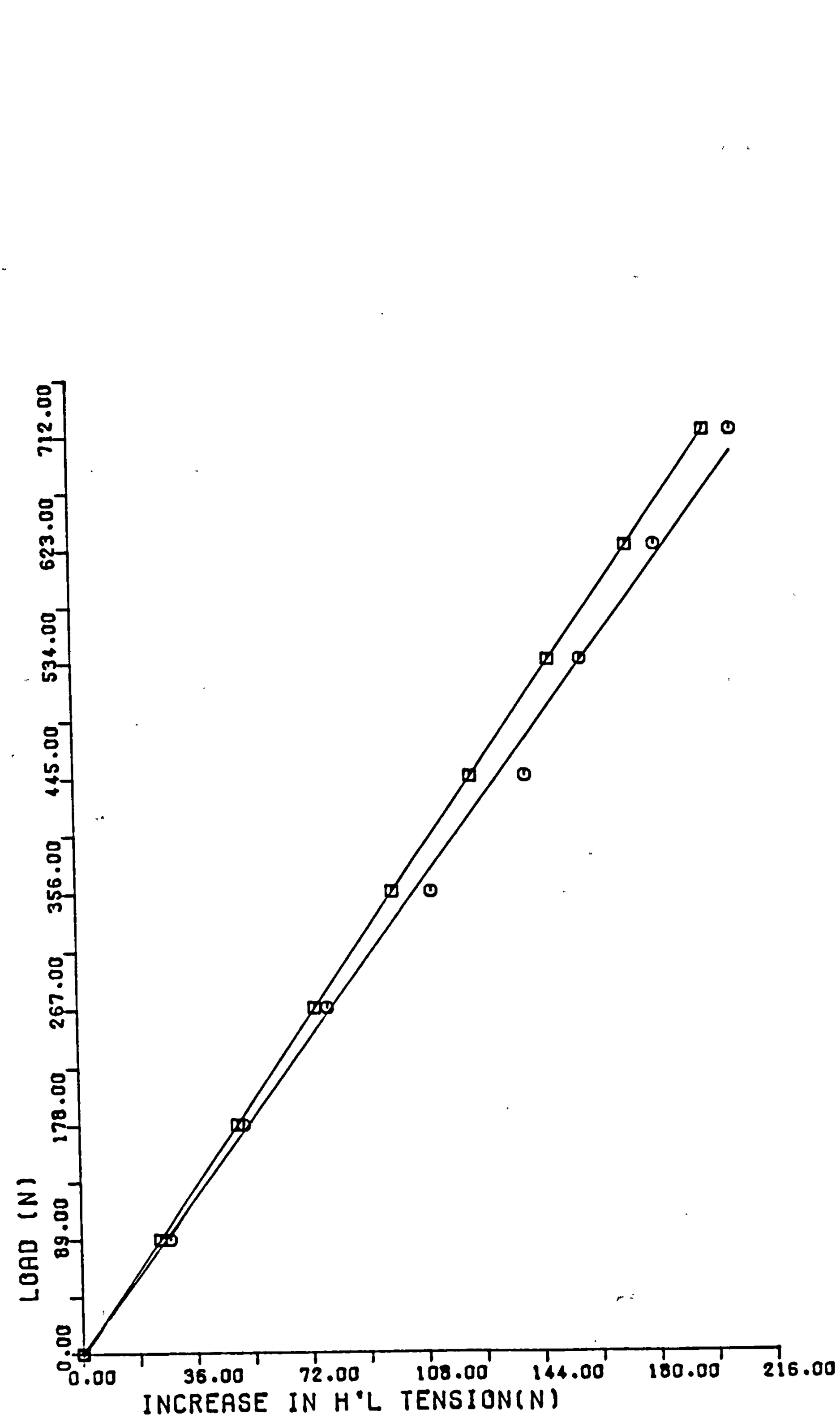

□ The calculated values
o Cable gauges readings

The change in the prestressing force when the load is applied at loading station C

Figure (7.21c)

Station 1

Station 2

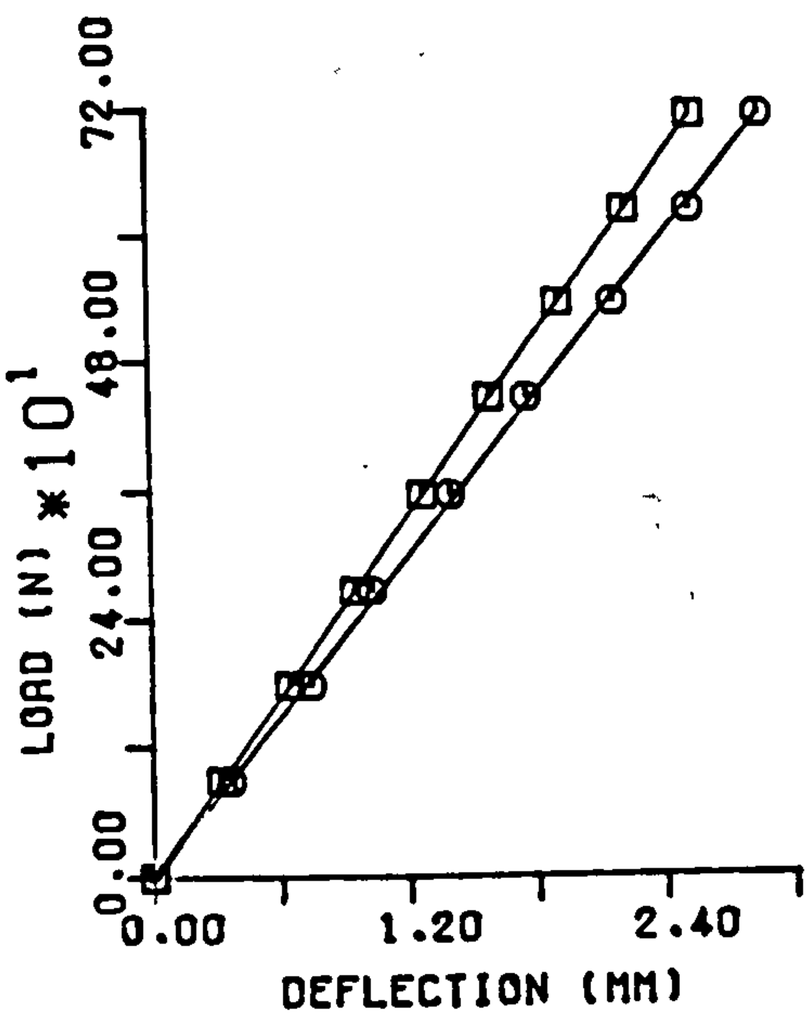

Station 3

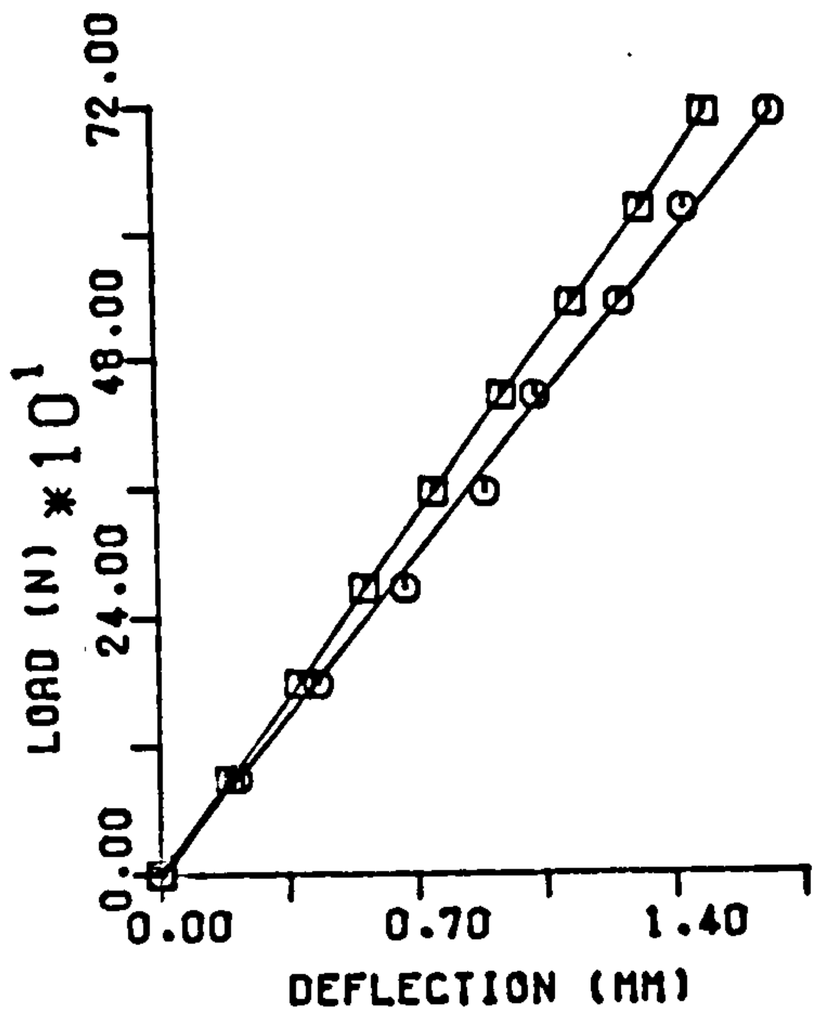

Station 4

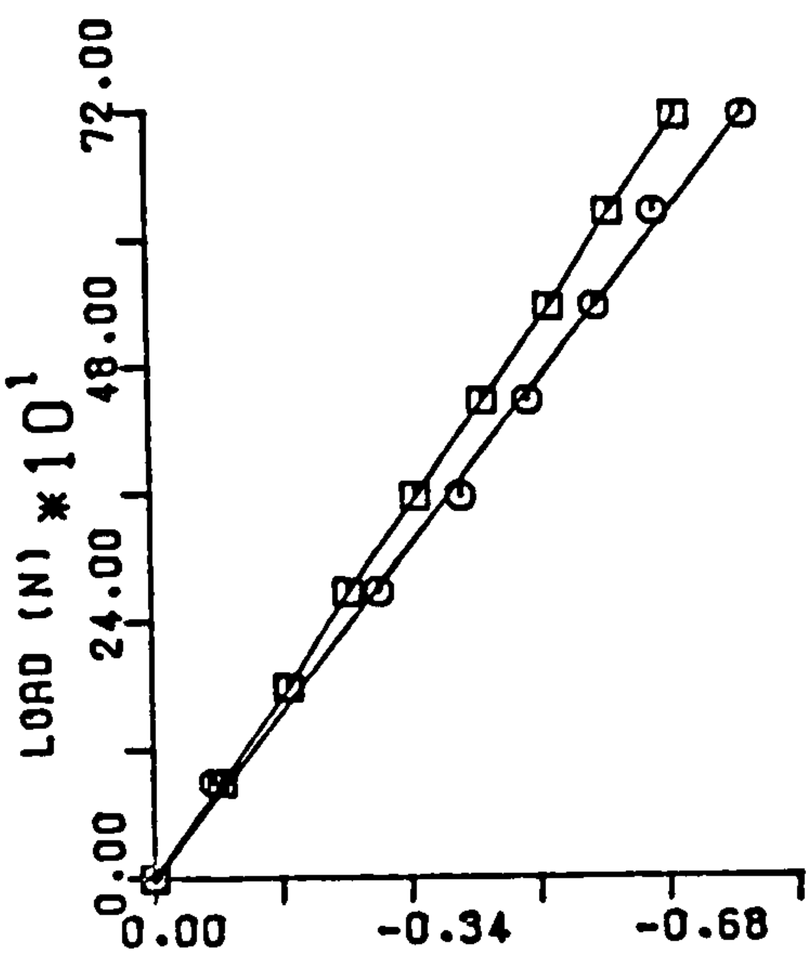

Station 5

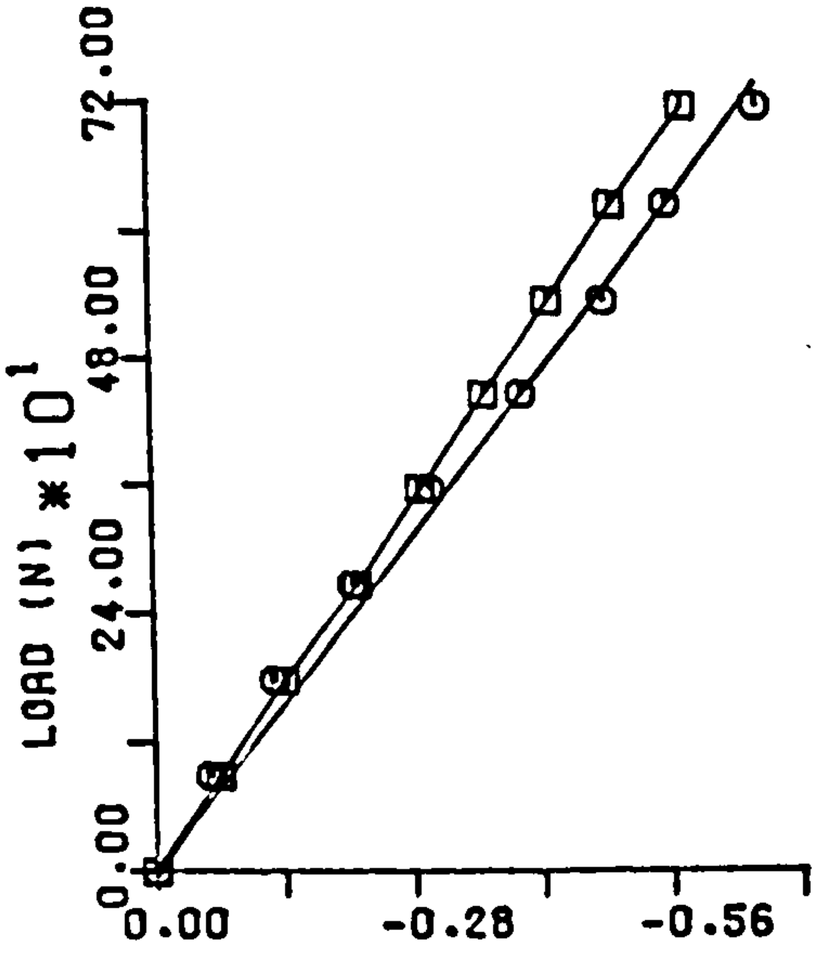

Station 6

□ The calculated deflections
o The measured deflections

The deflections when the load is applied at loading position D

Figure (7.22a)

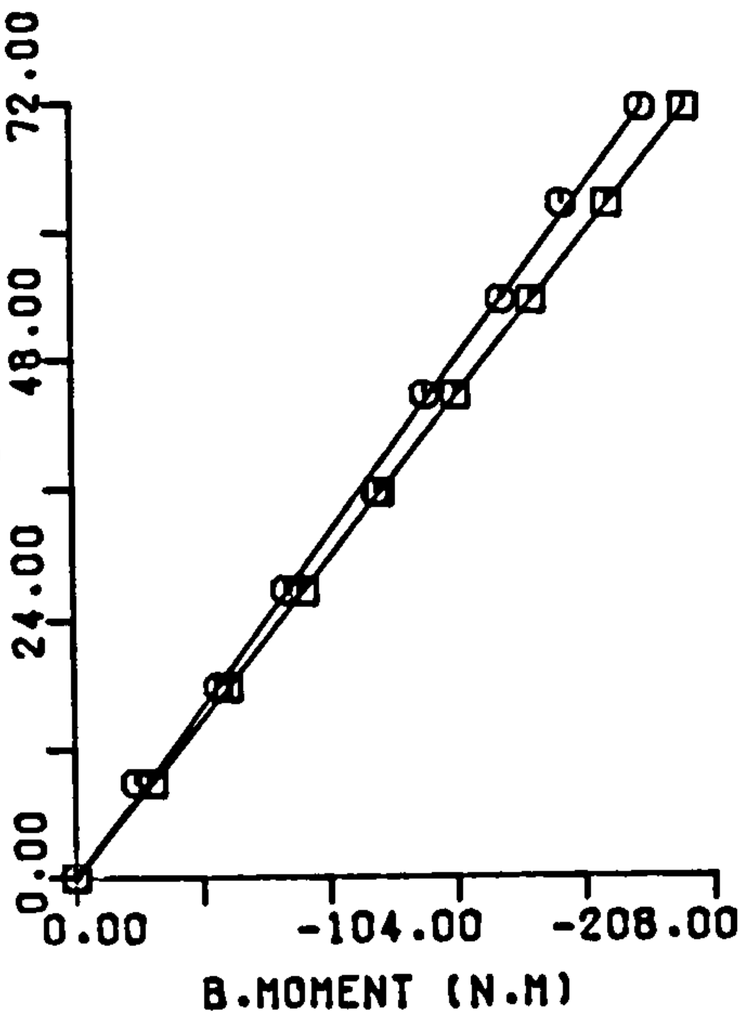

Position C

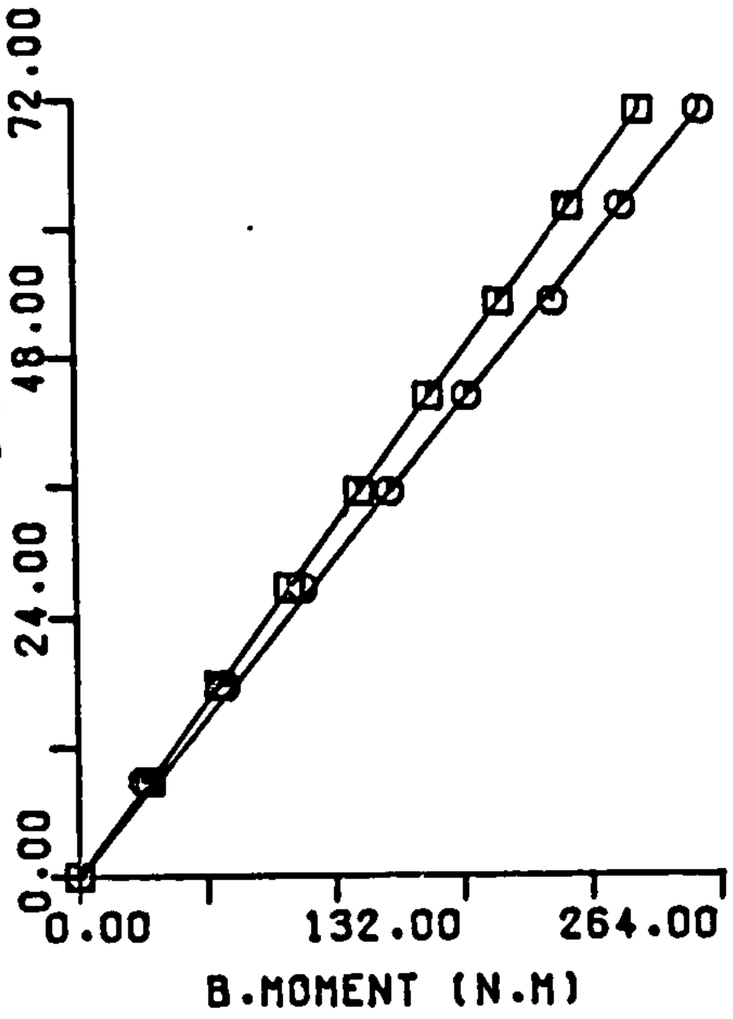

Tower Position

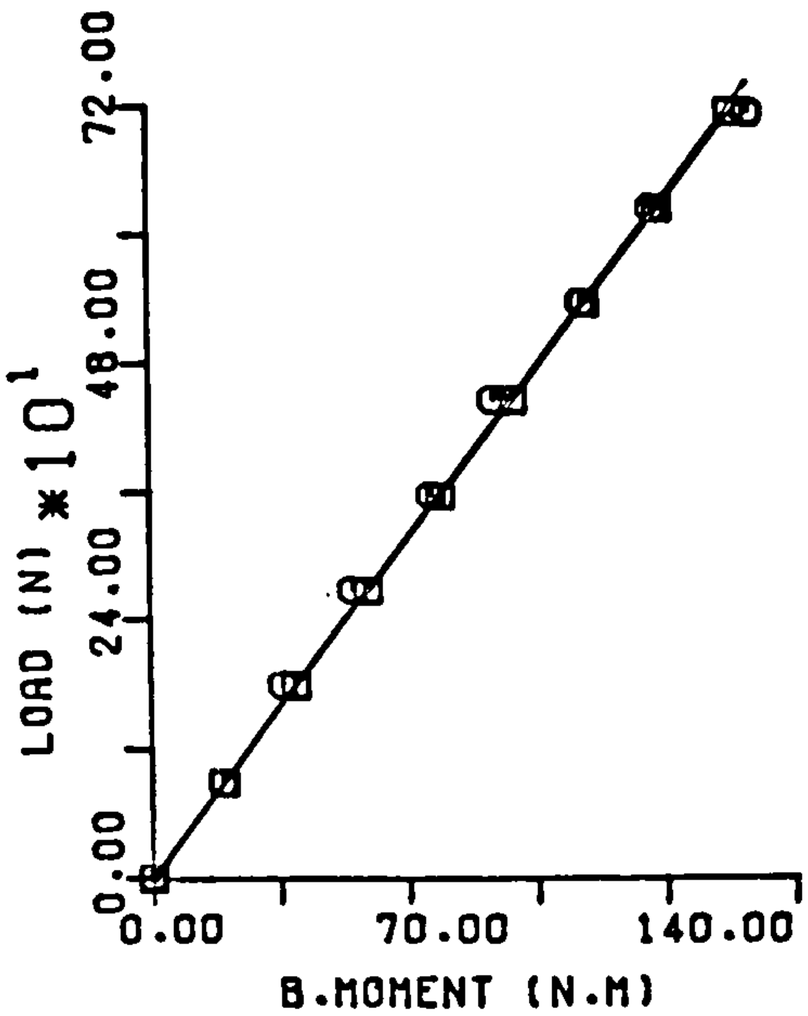

Position G

- The calculated bending moments
- The actual bending moments

The bending moments when the load is applied at loading station D

Figure(7.22b)

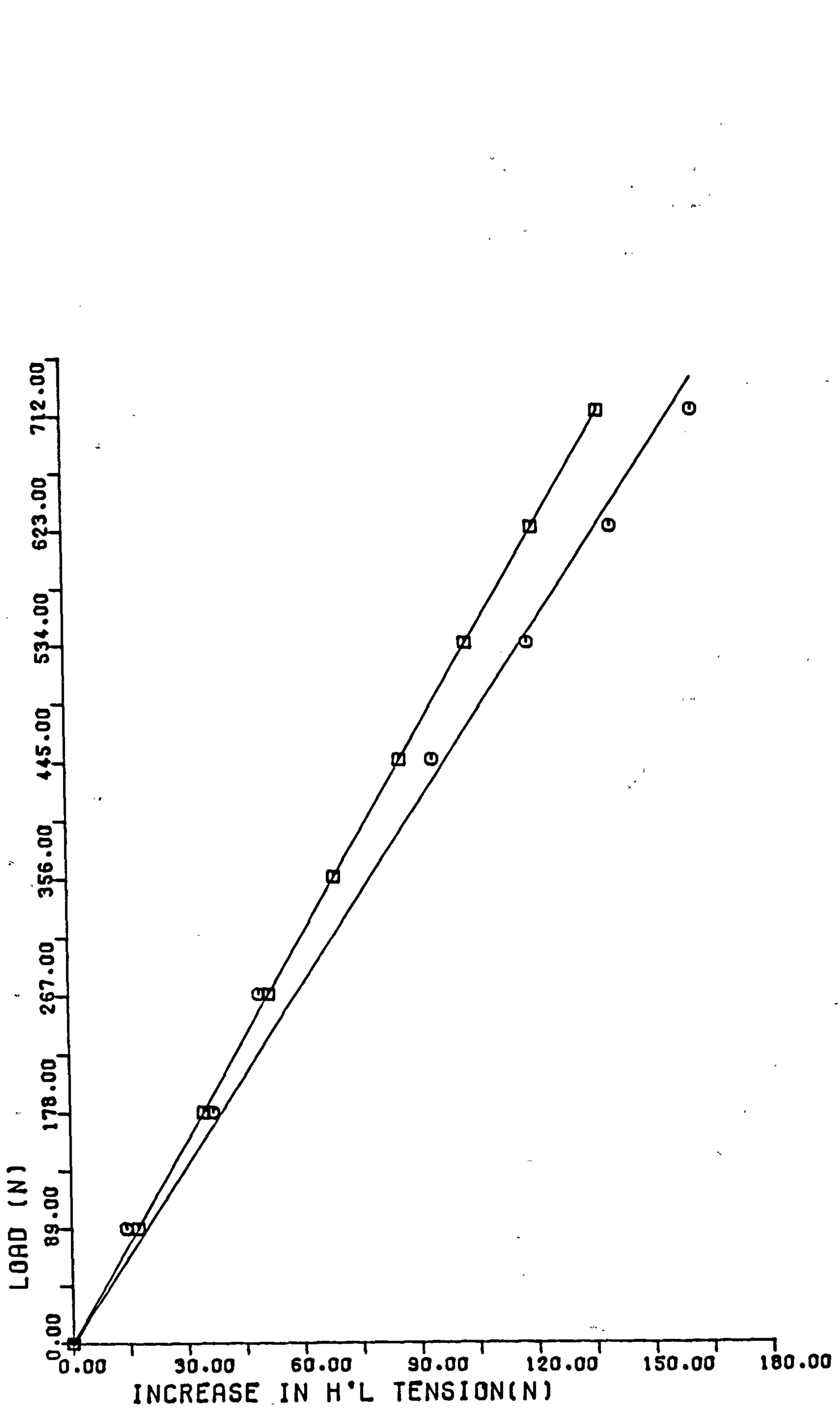

▫ The calculated values
o Cable gauges readings

The change in the prestressing force when the load is applied at loading station D

Figure (7.22c)

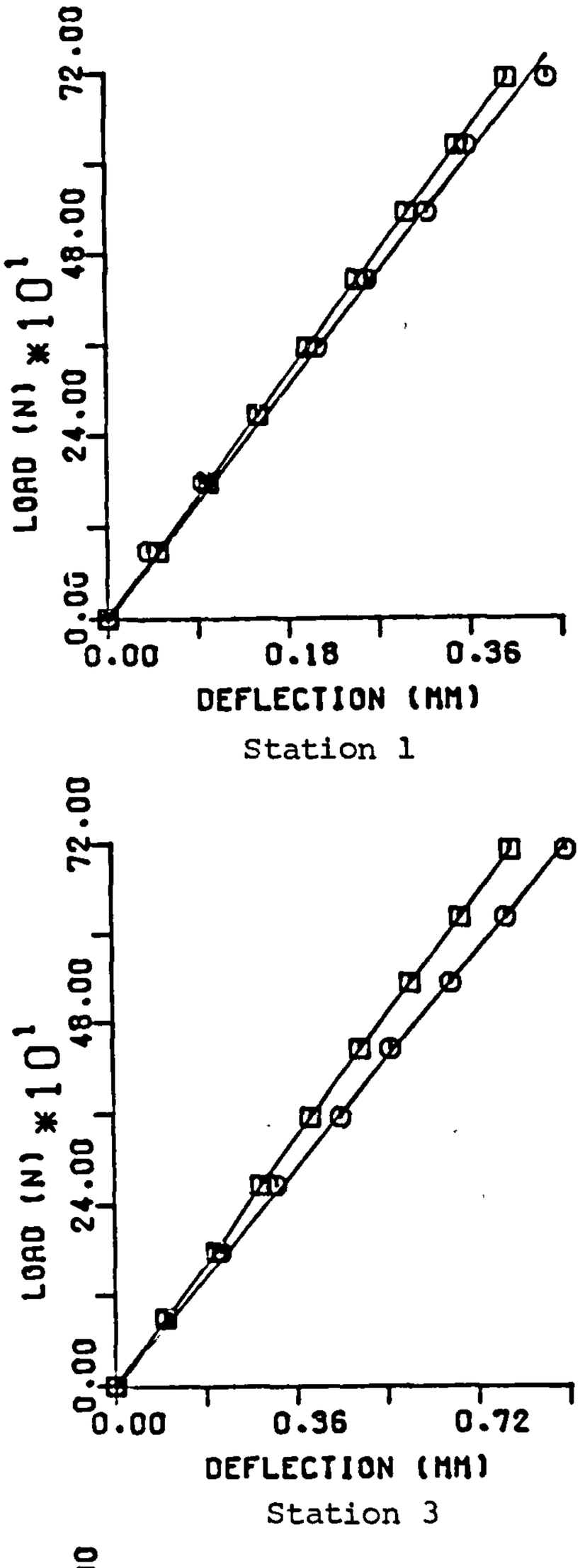

Station 1

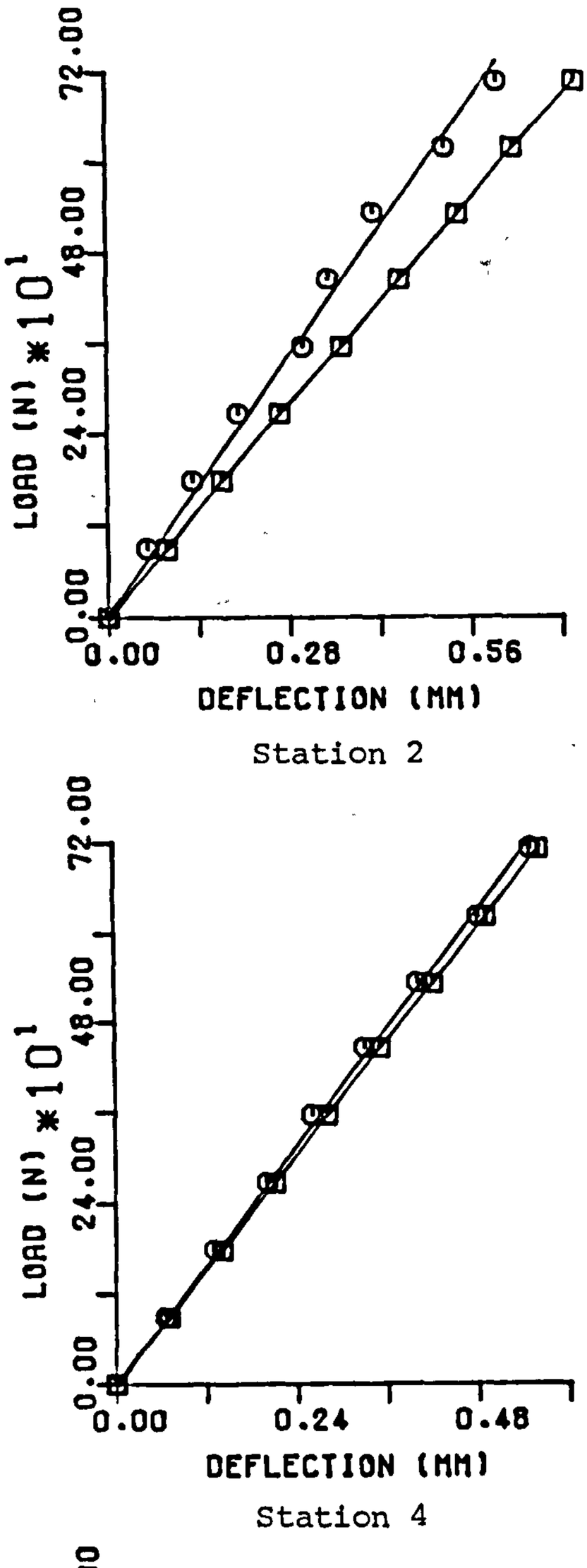

Station 2

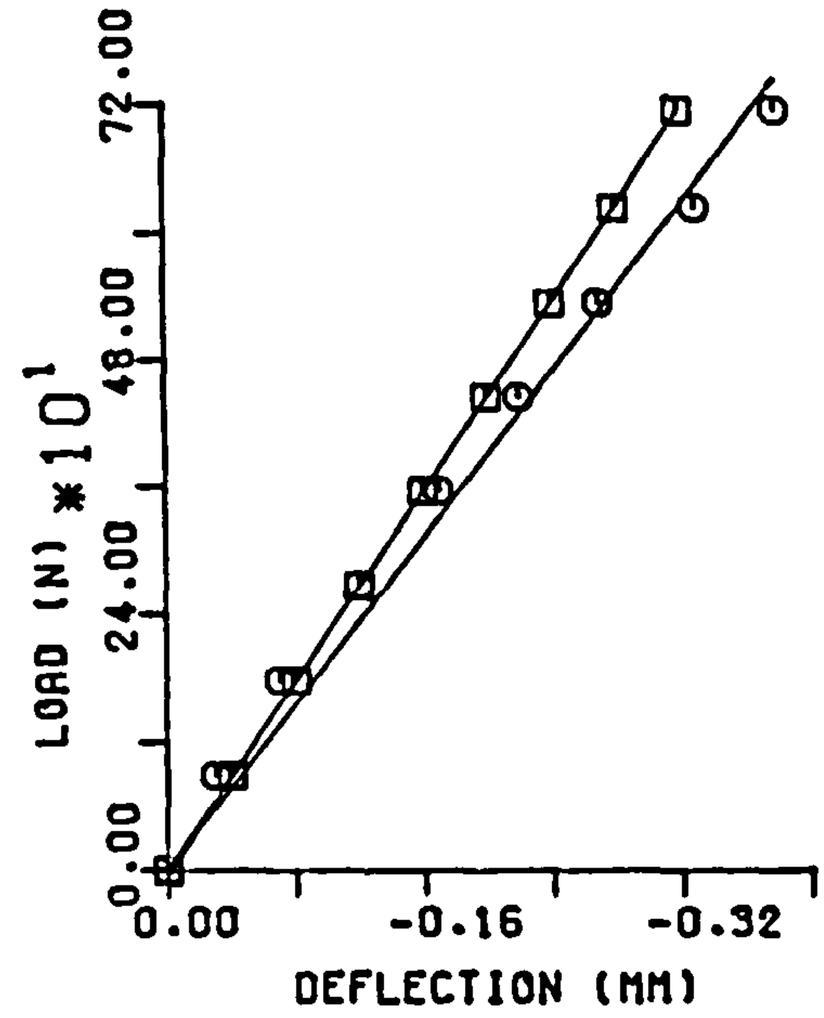

Station 3

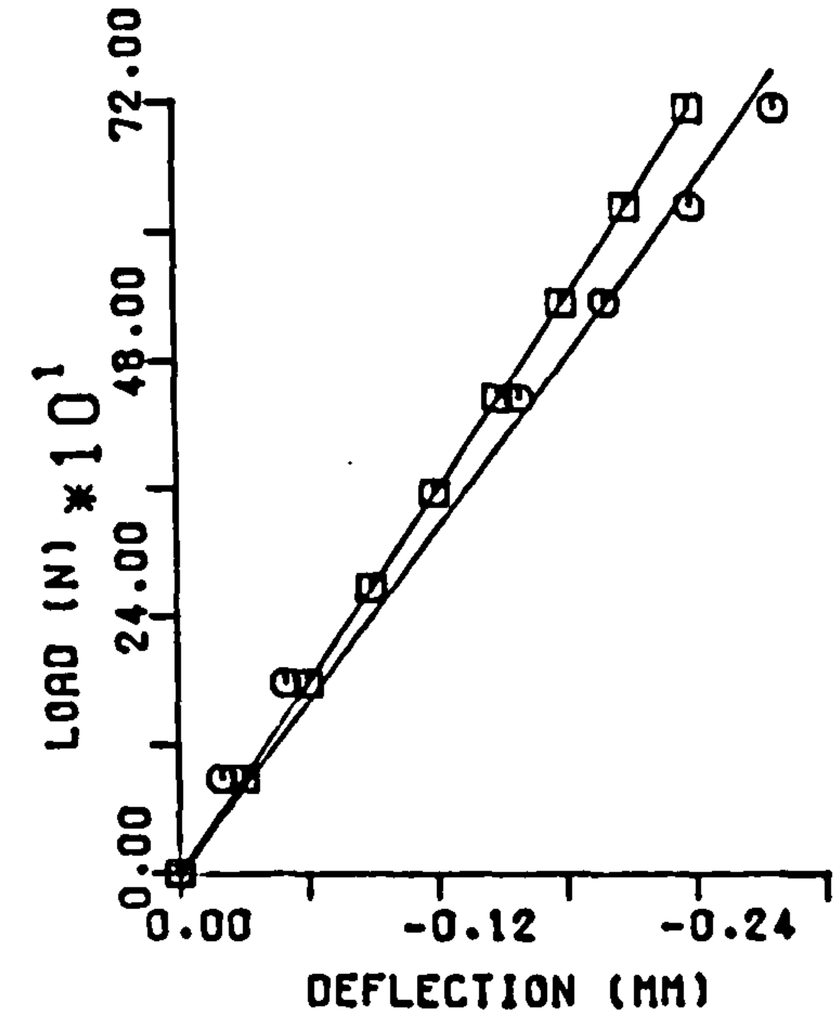

Station 4

Station 5

Station 6

□ The calculated deflections
o The measured deflections

The deflections when the load is applied at loading position E

Figure(7.23a)

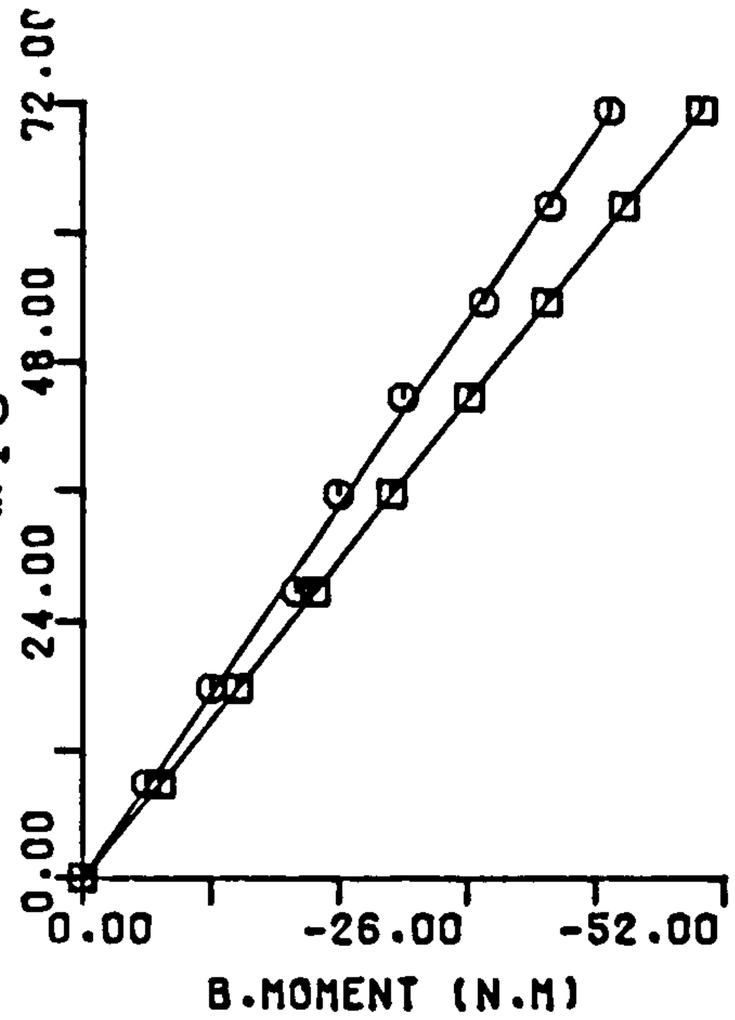

Position C

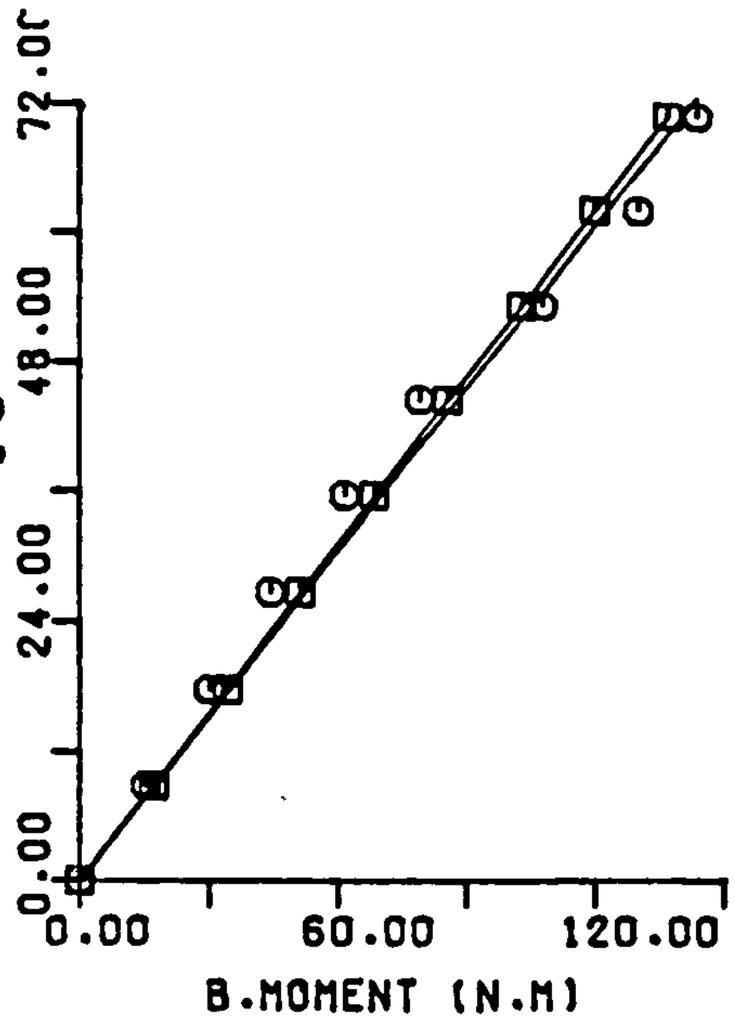

Tower Position

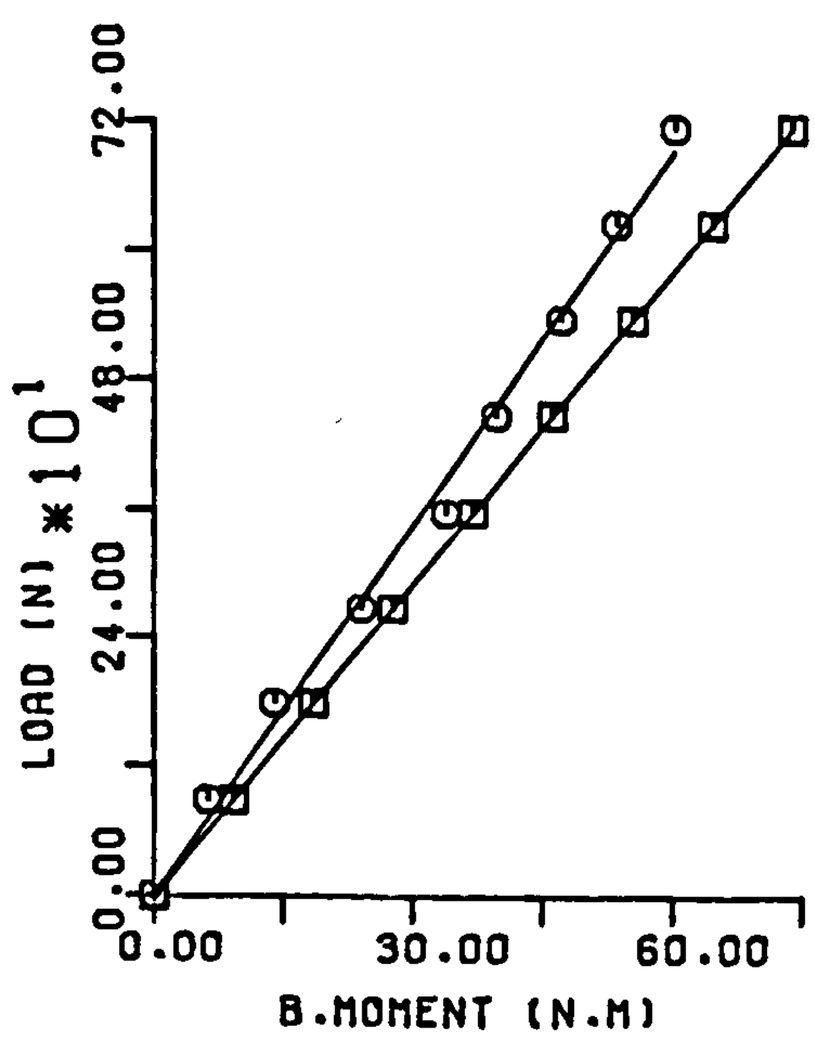

Position G

□ The calculated bending moments
o The actual bending moments

The bending moments when the load is applied at loading station E

Figure (7.23b)

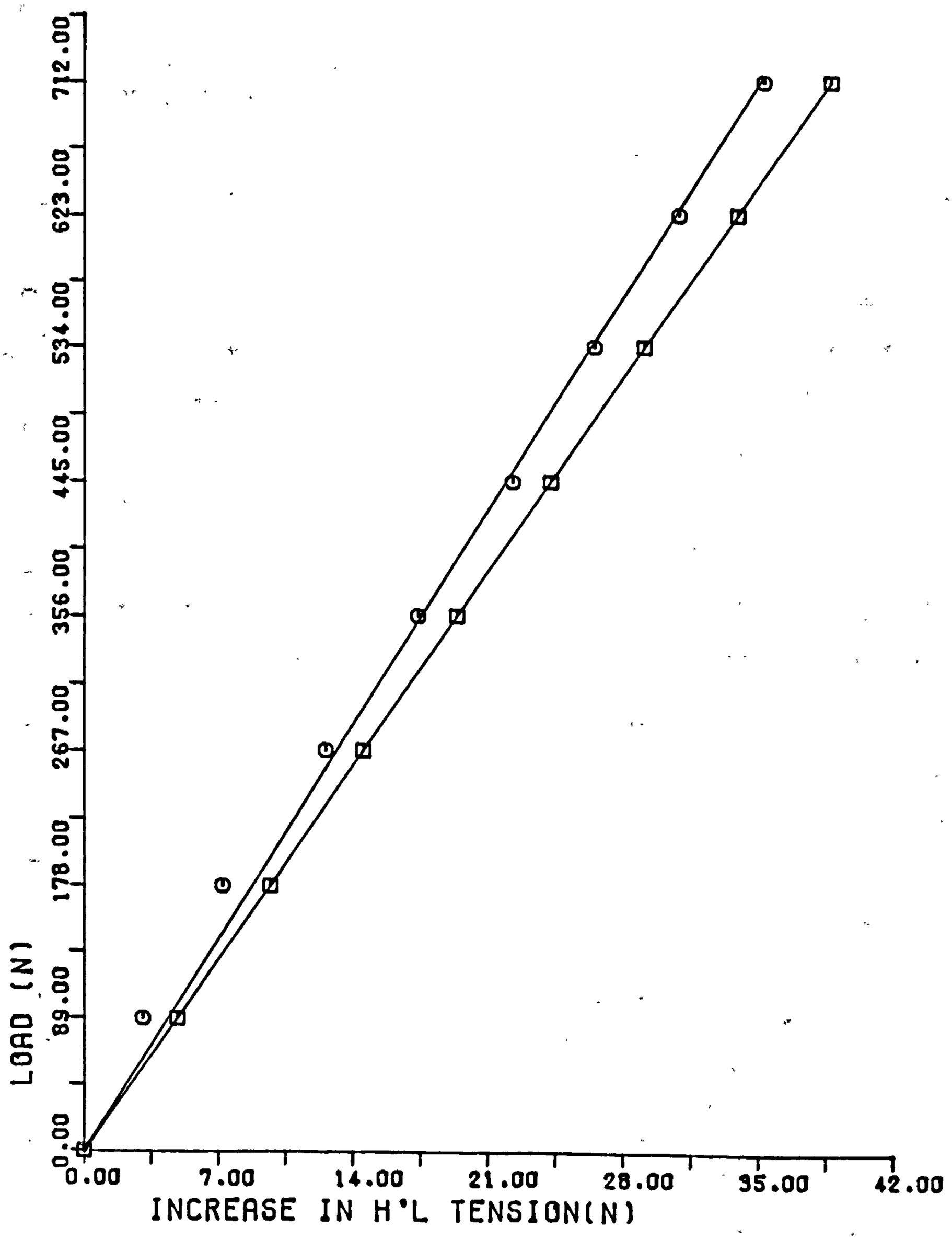

□ The calculated values
o Cable gauges readings

The change in the prestressing force when the load is applied at loading station E

Figure (7.23c)

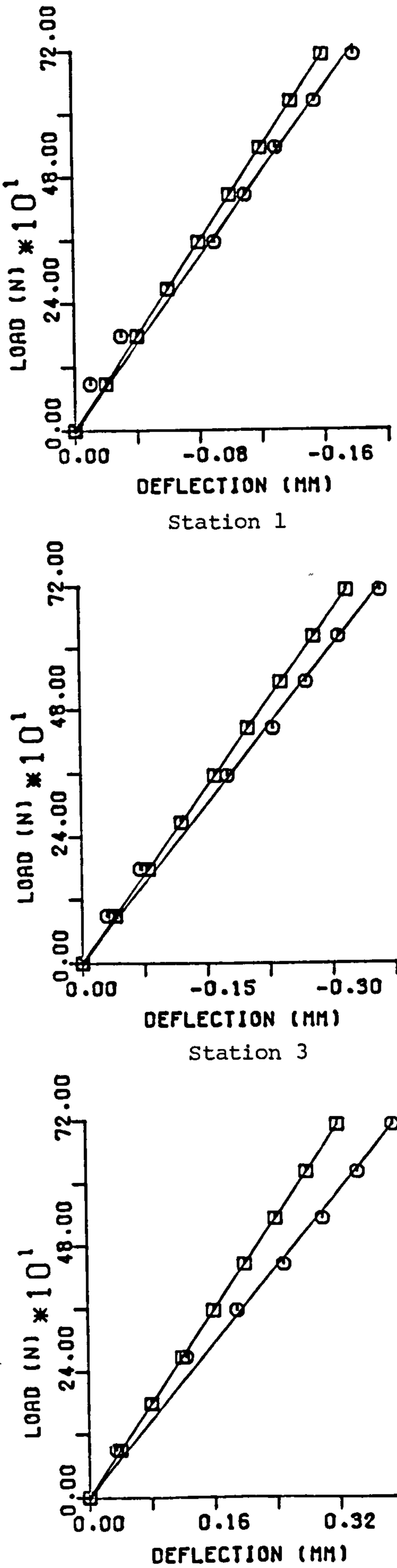

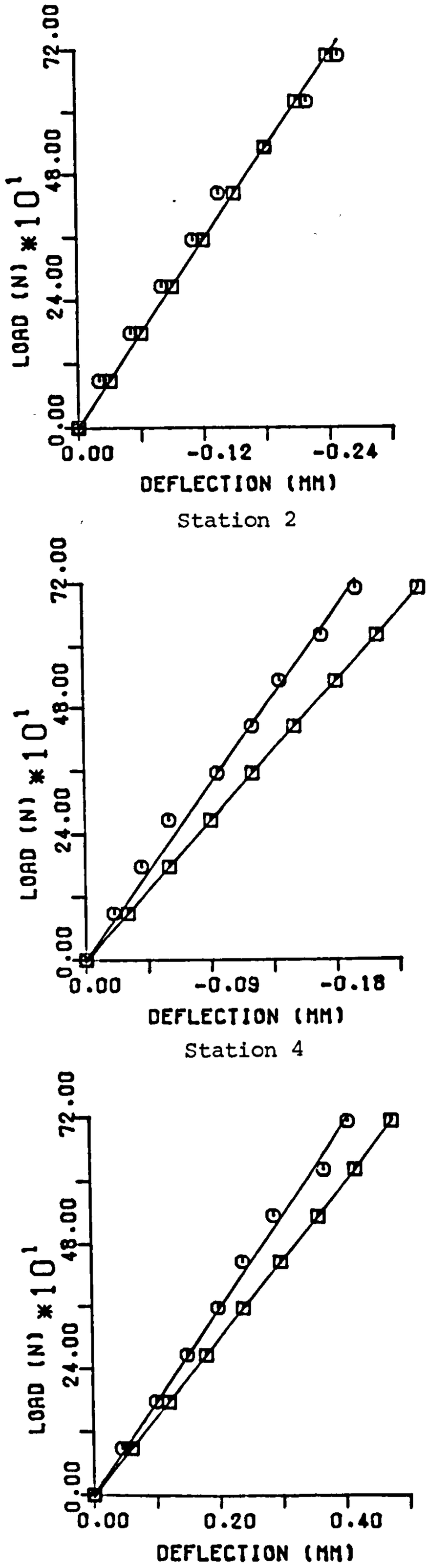

▫ The calculated deflections
o The measured deflections

The deflections when the load is applied at loading position F

Figure (7.24a)

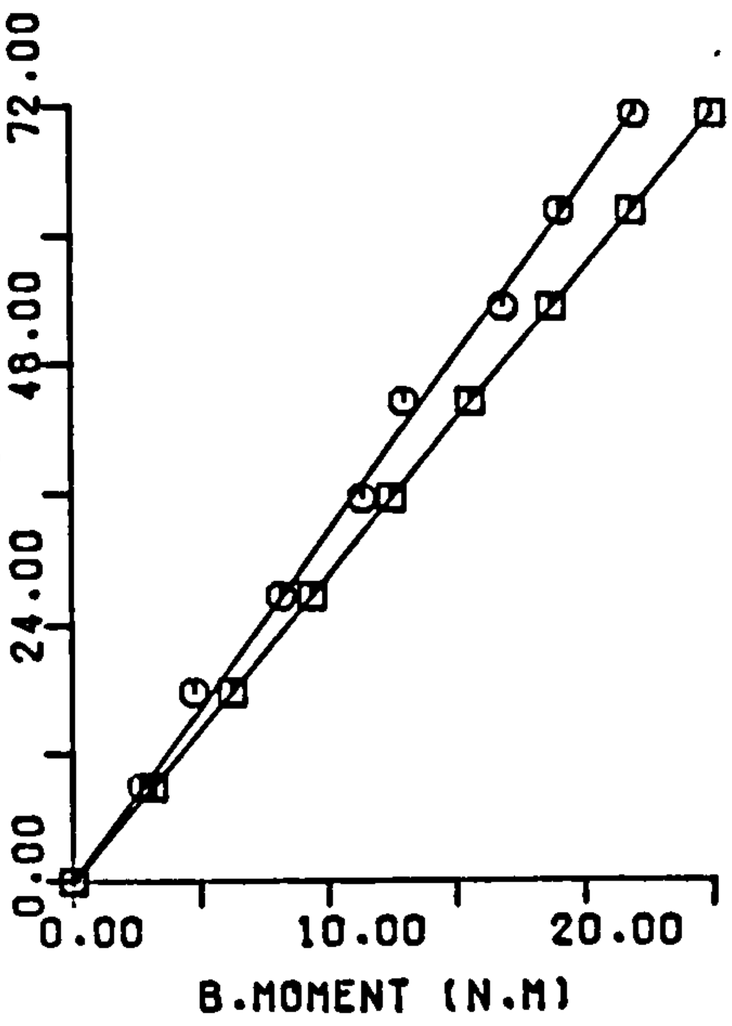

Position C

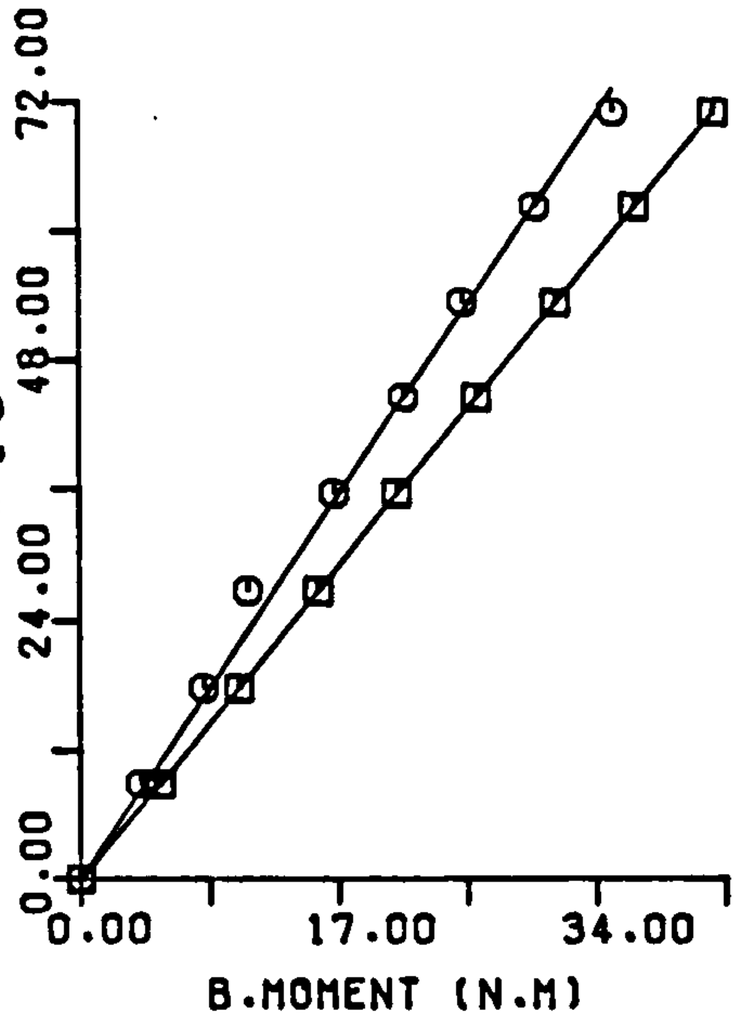

Tower Position

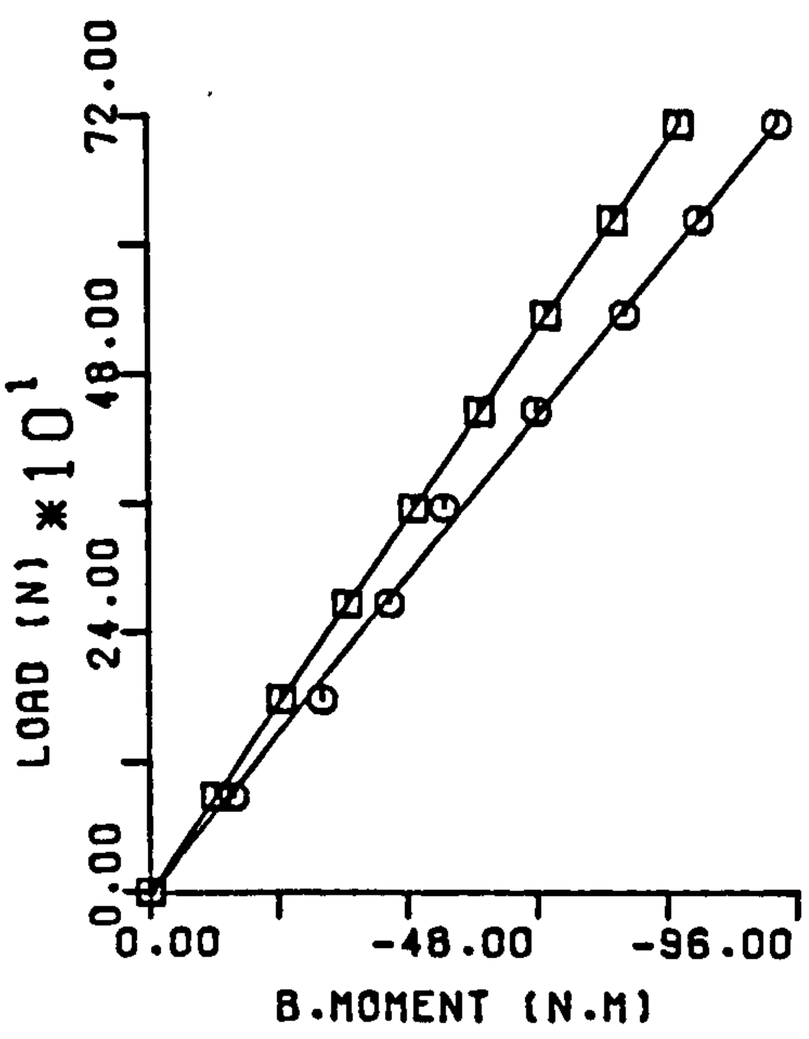

Position G

- ▫ The calculated bending moments
- o The actual bending moments

The bending moments when the load is applied at loading station F

Figure (7.24b)

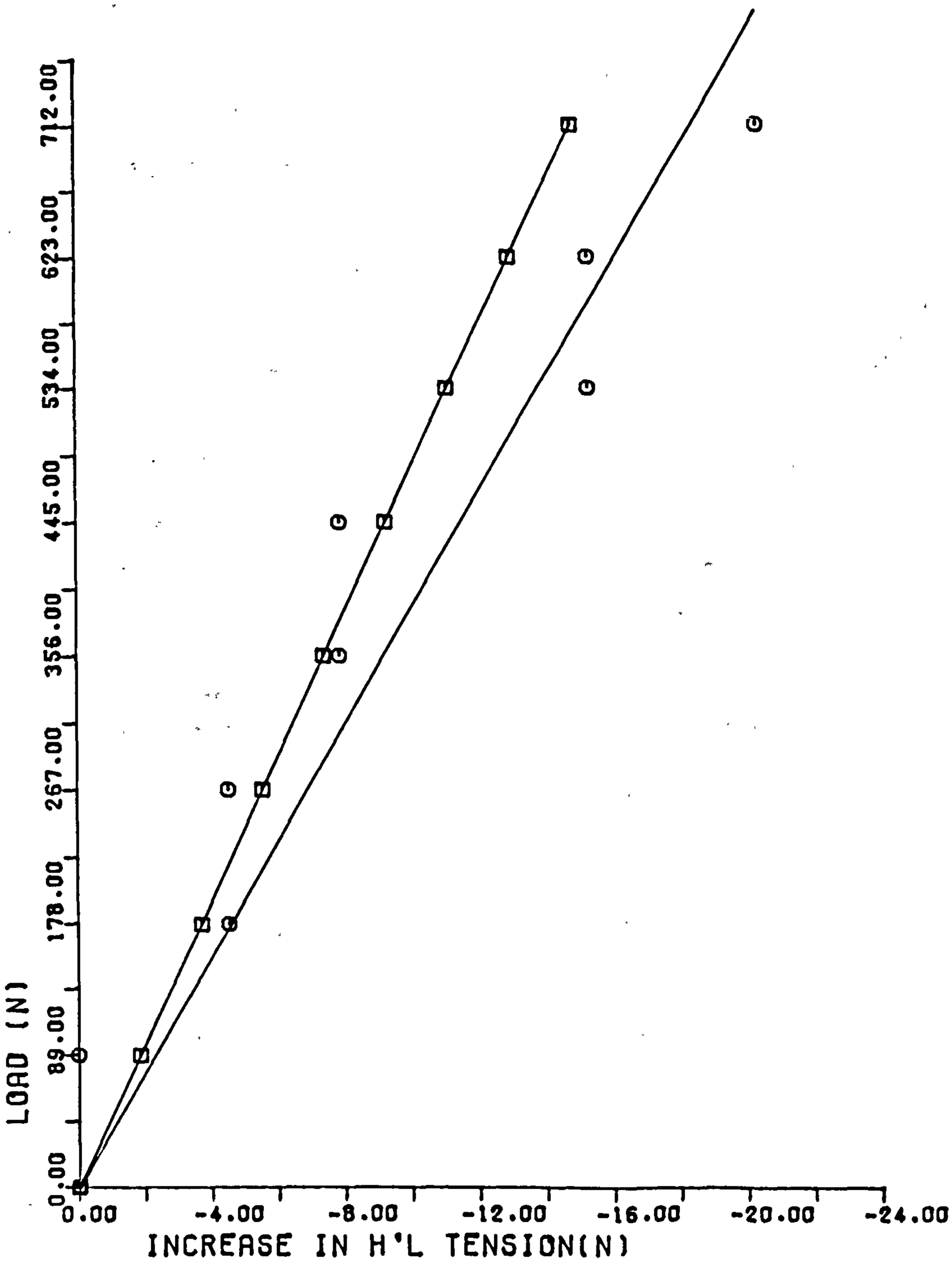

▫ The calculated values
o Cable gauges readings

The change in the prestressing force when the load is applied at loading station F

Figure (7.24c)

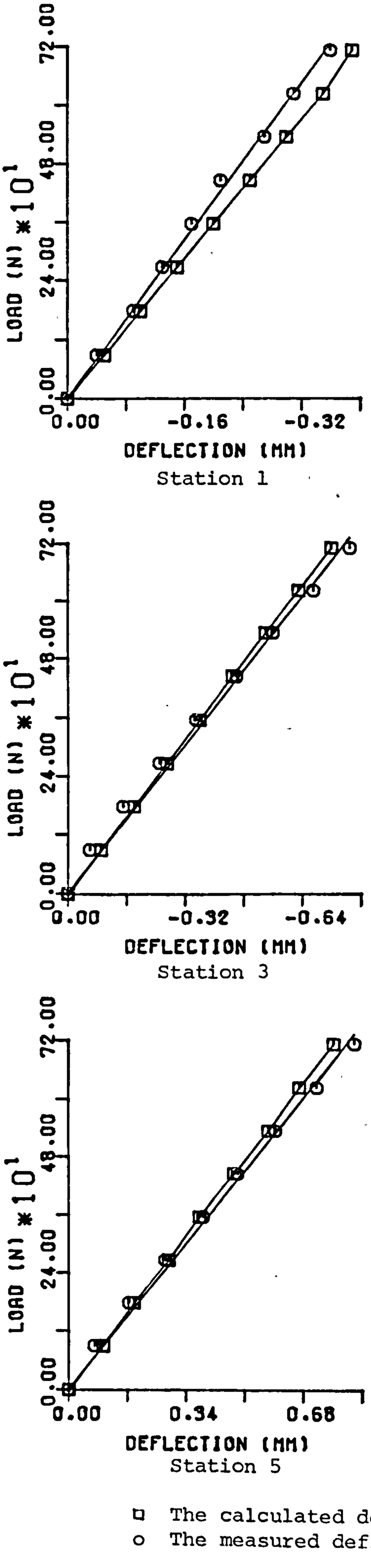

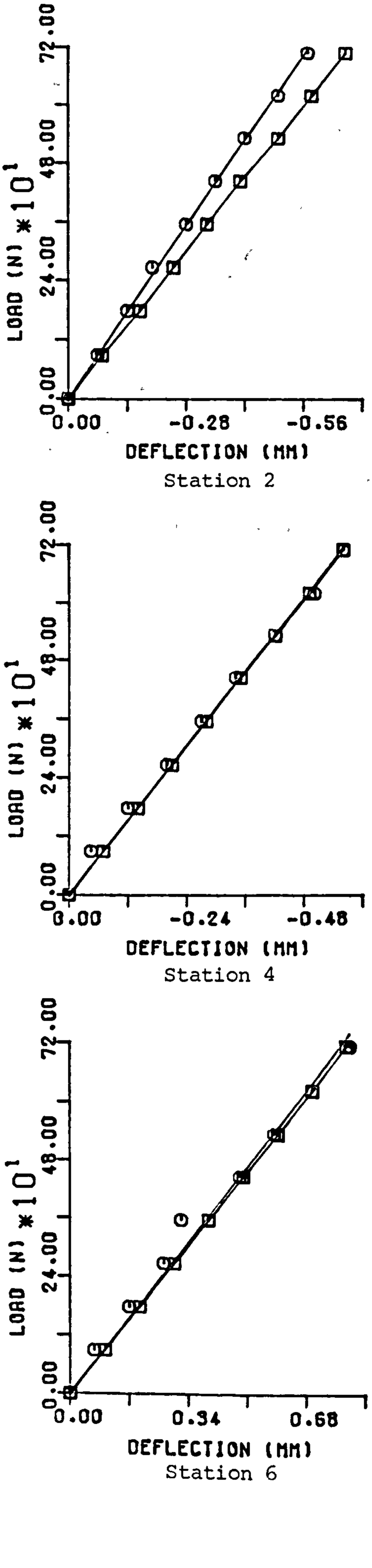

□ The calculated deflections
○ The measured deflections

The deflections when the load is applied at loading position G

Figure (7.25a)

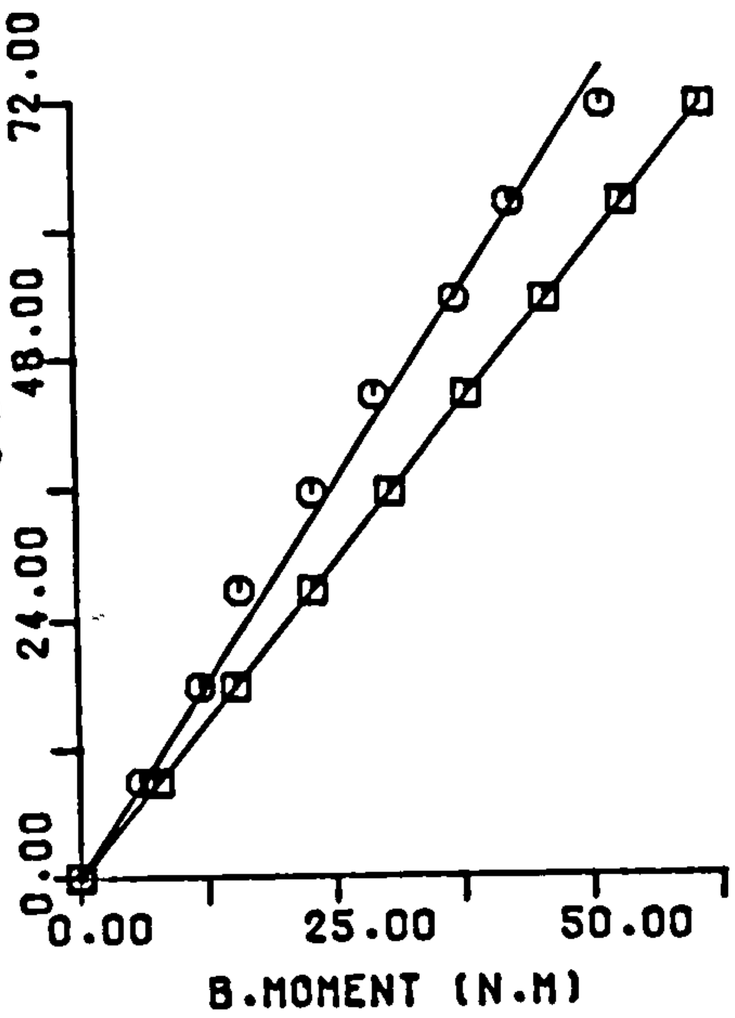

Position C

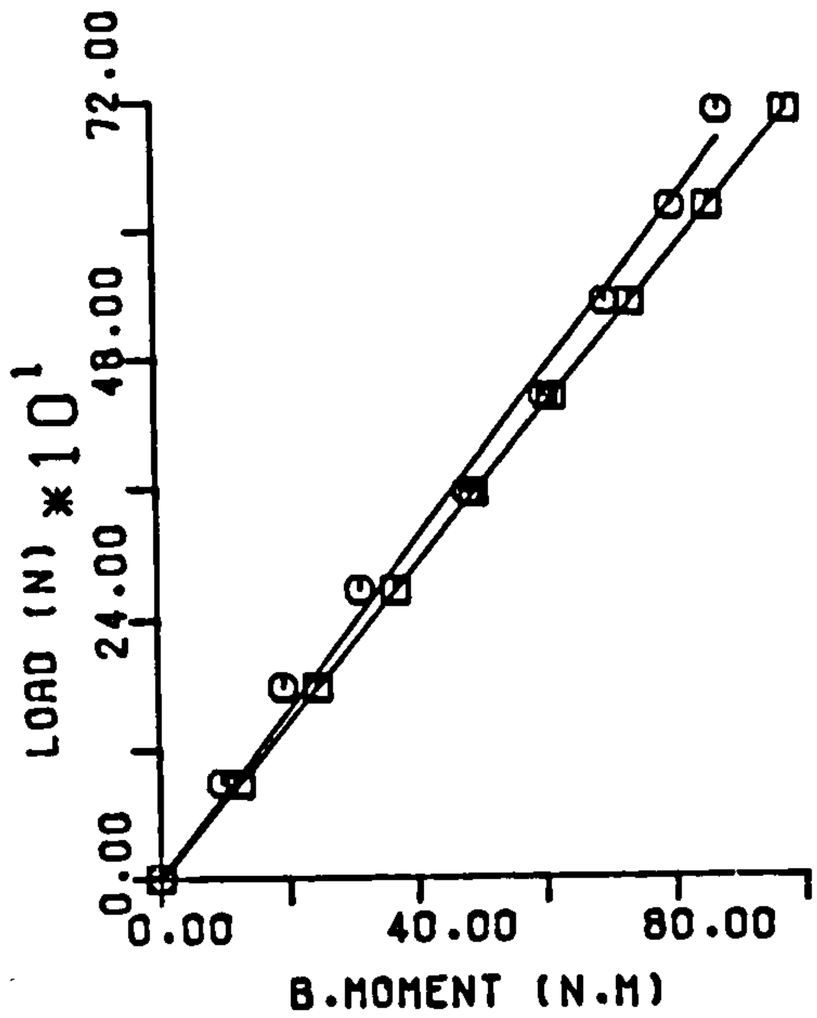

Tower Position

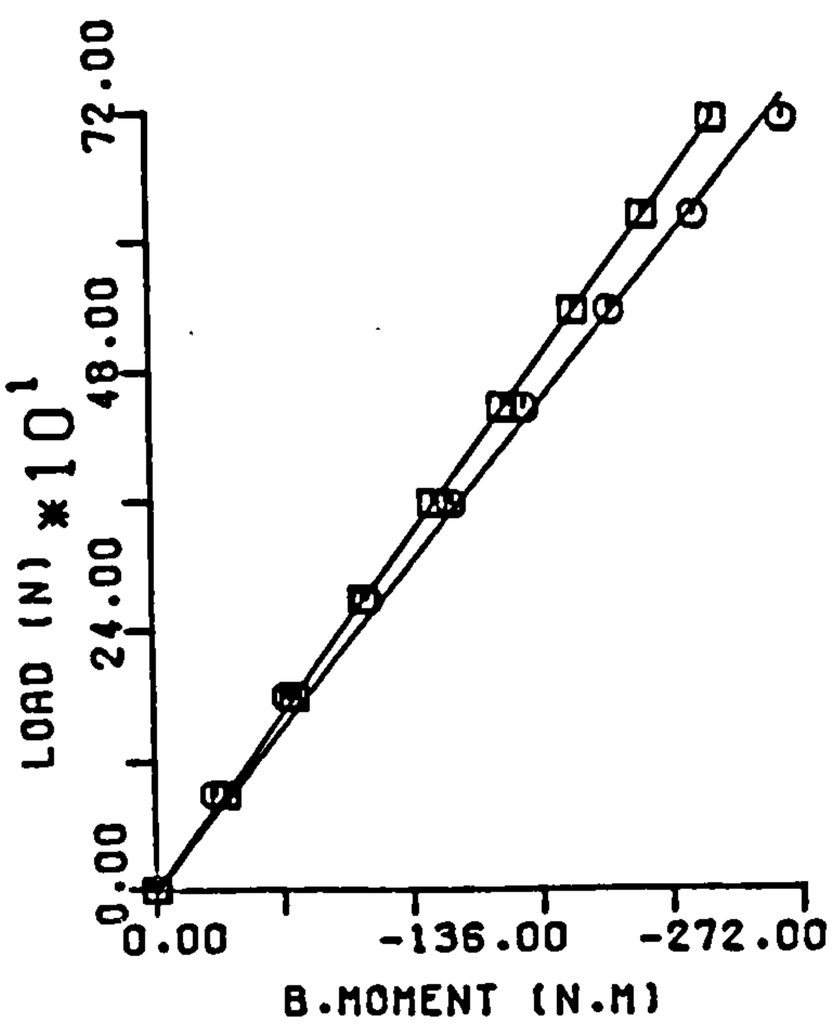

Position G

□ The calculated bending moments
o The actual bending moments

The bending moments when the load is applied at loading station G

Figure(7.25b)

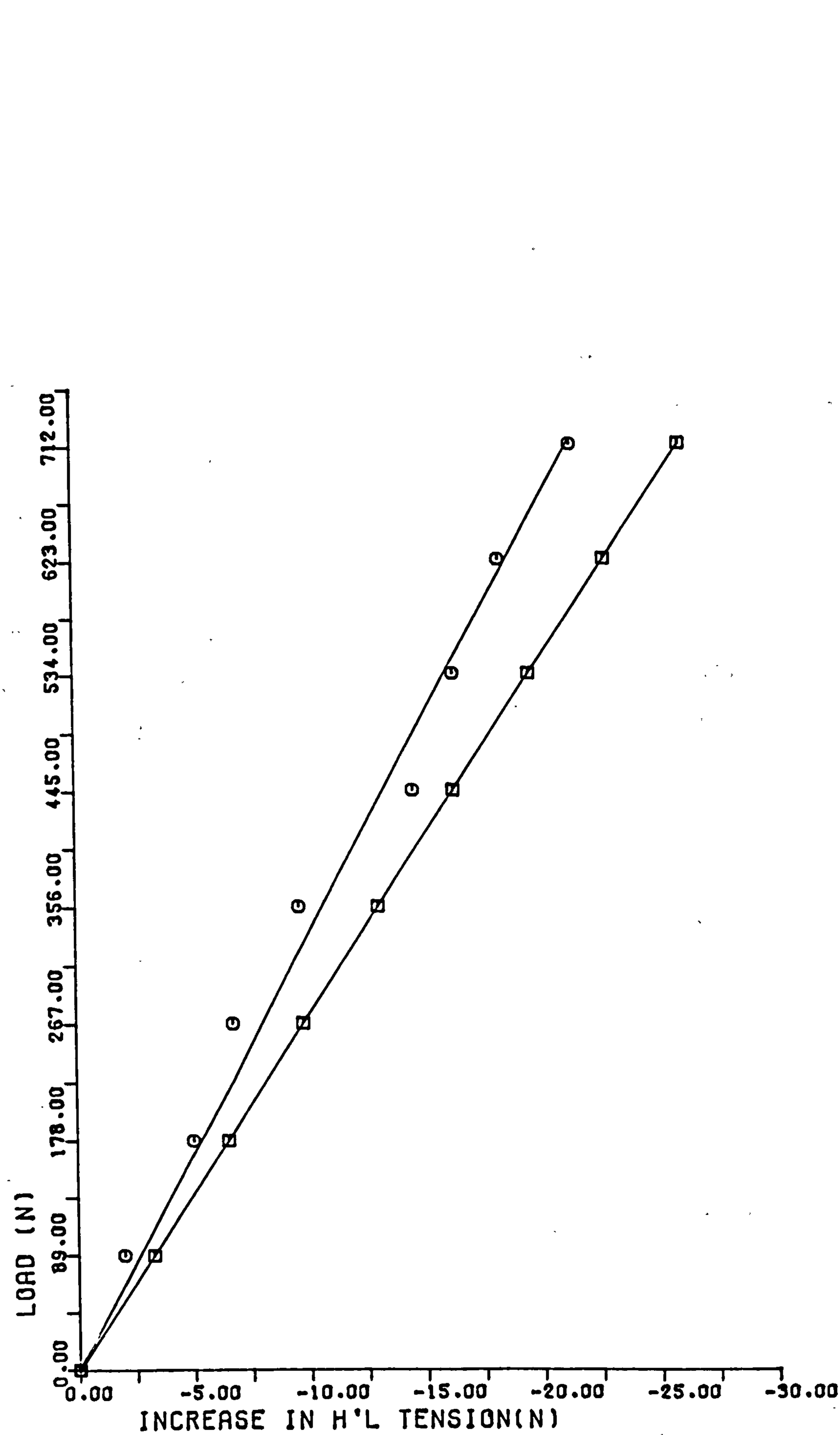

□ The calculated values
o Cable gauges readings

The change in the prestressing force when the load is applied at loading station G

Figure (7.25c)

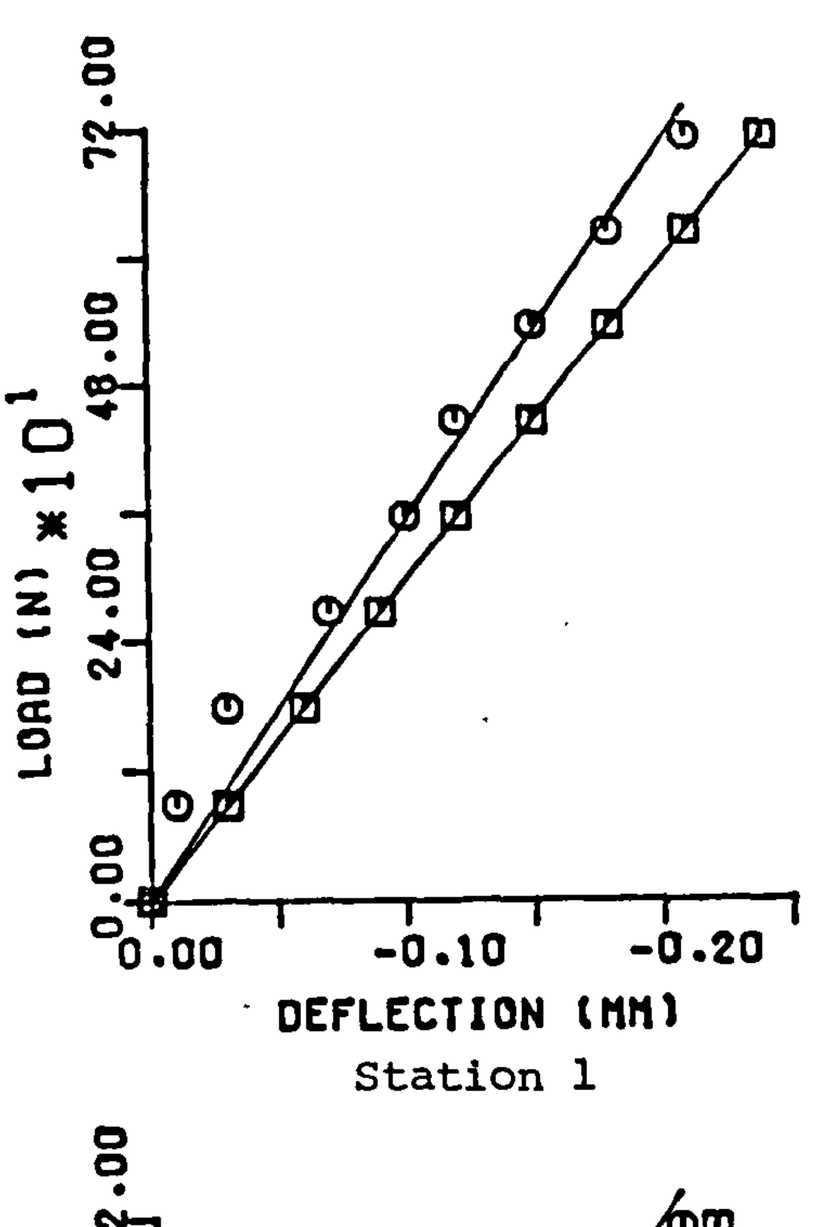

Station 1

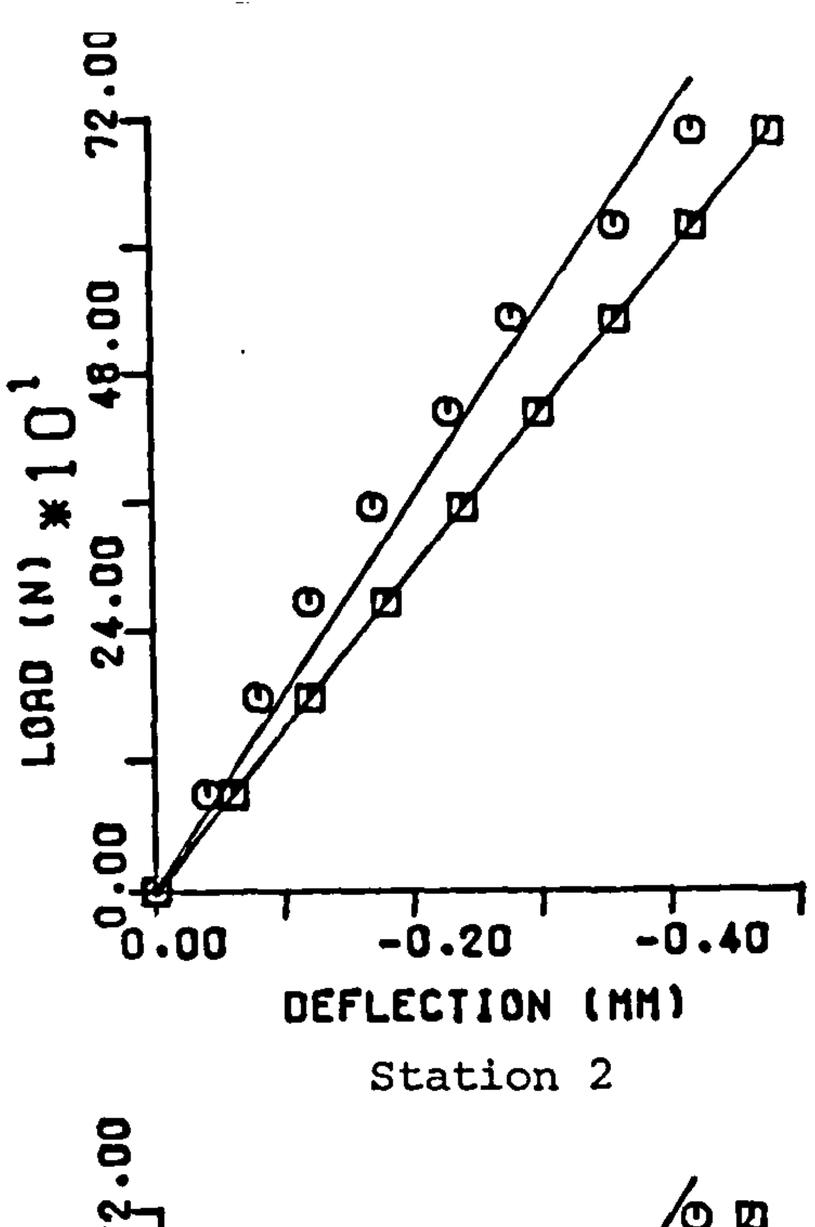

Station 2

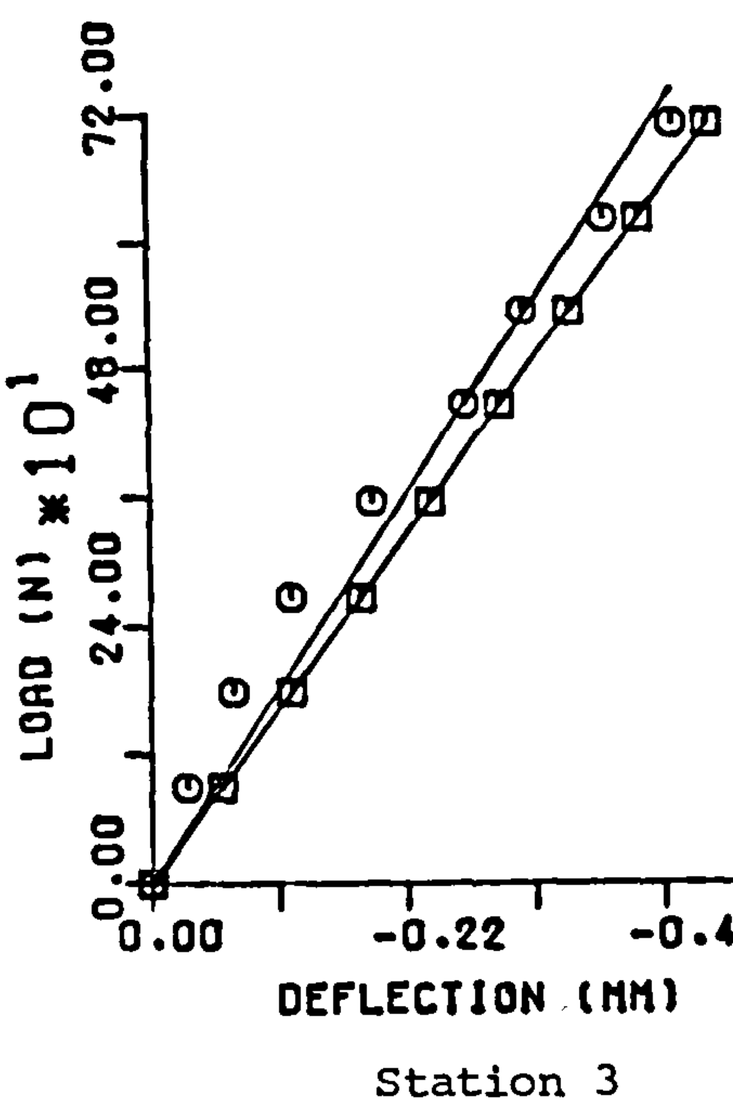

Station 3

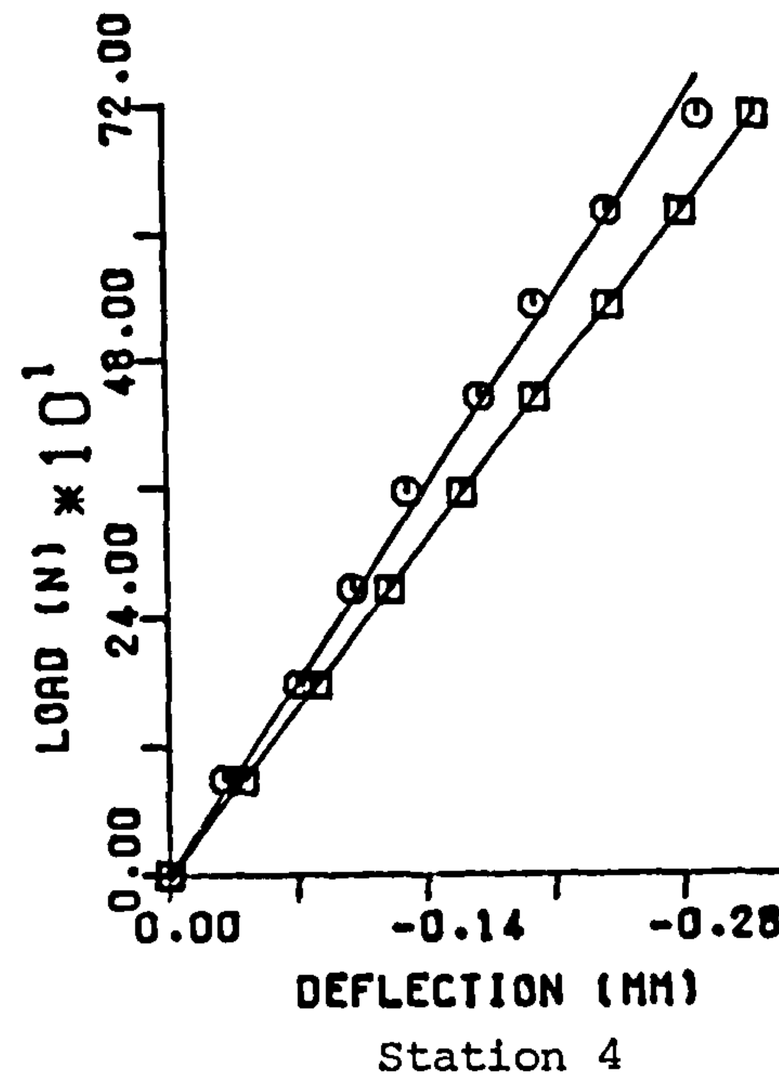

Station 4

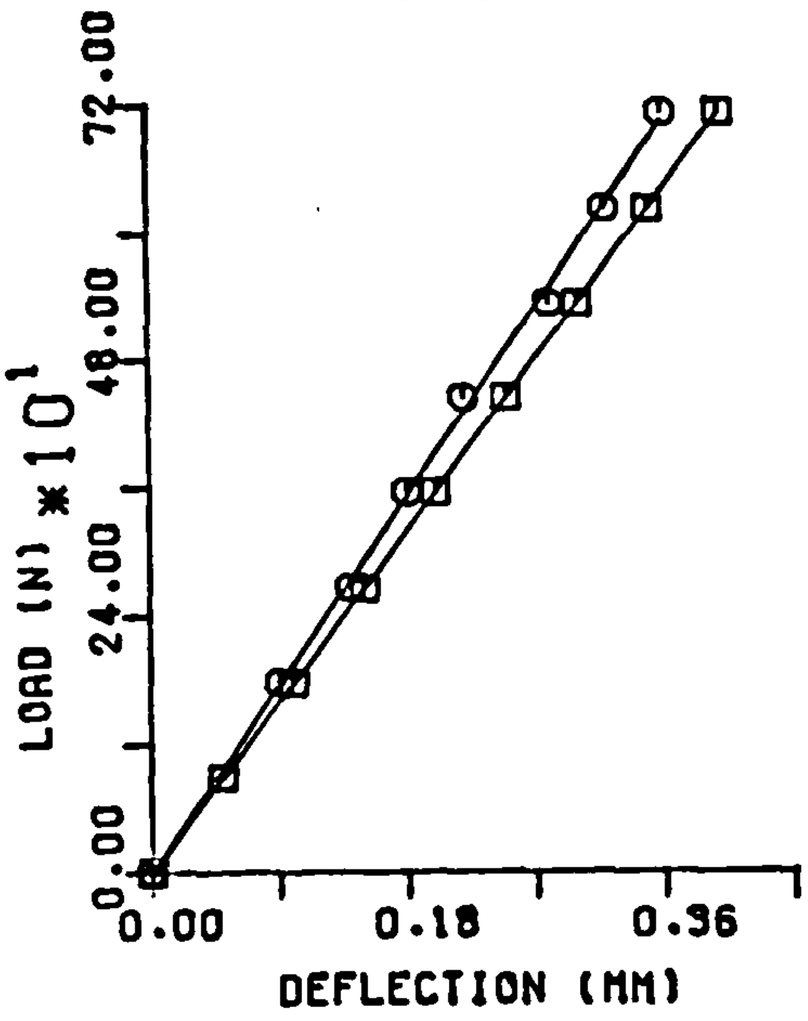

Station 5

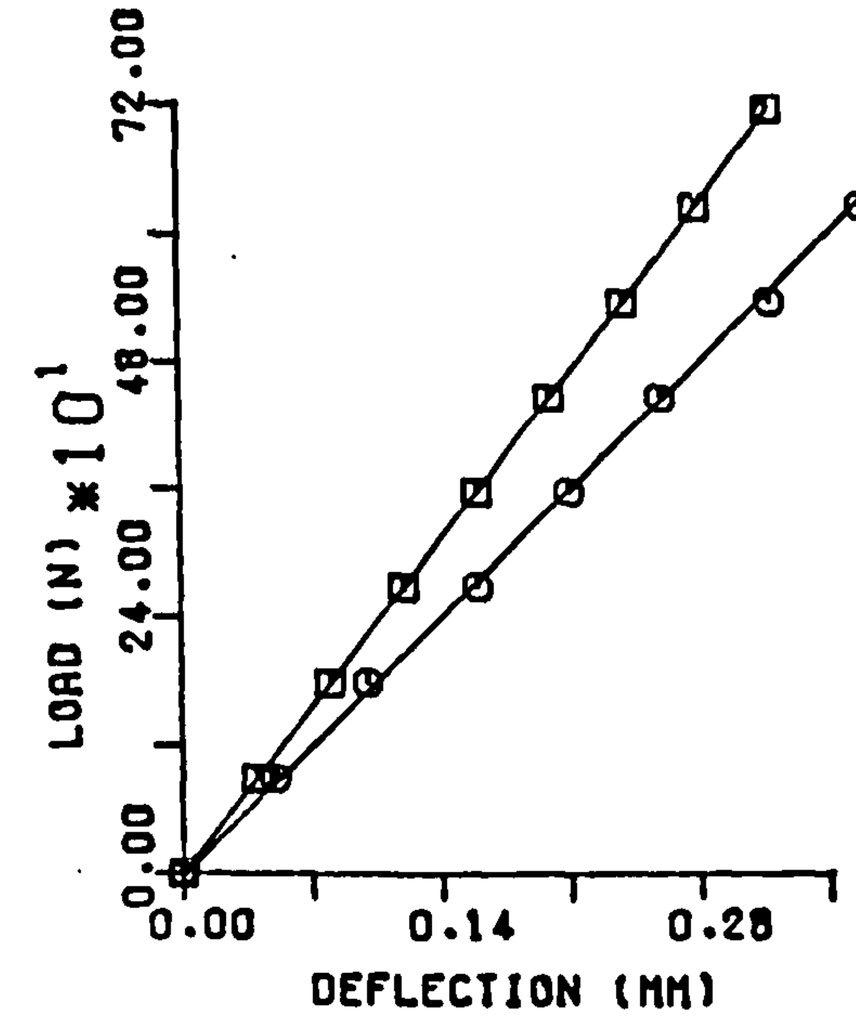

Station 6

□ The calculated deflections
o The measured deflections

The deflections when the load is applied at loading position H

Figure(7.26a)

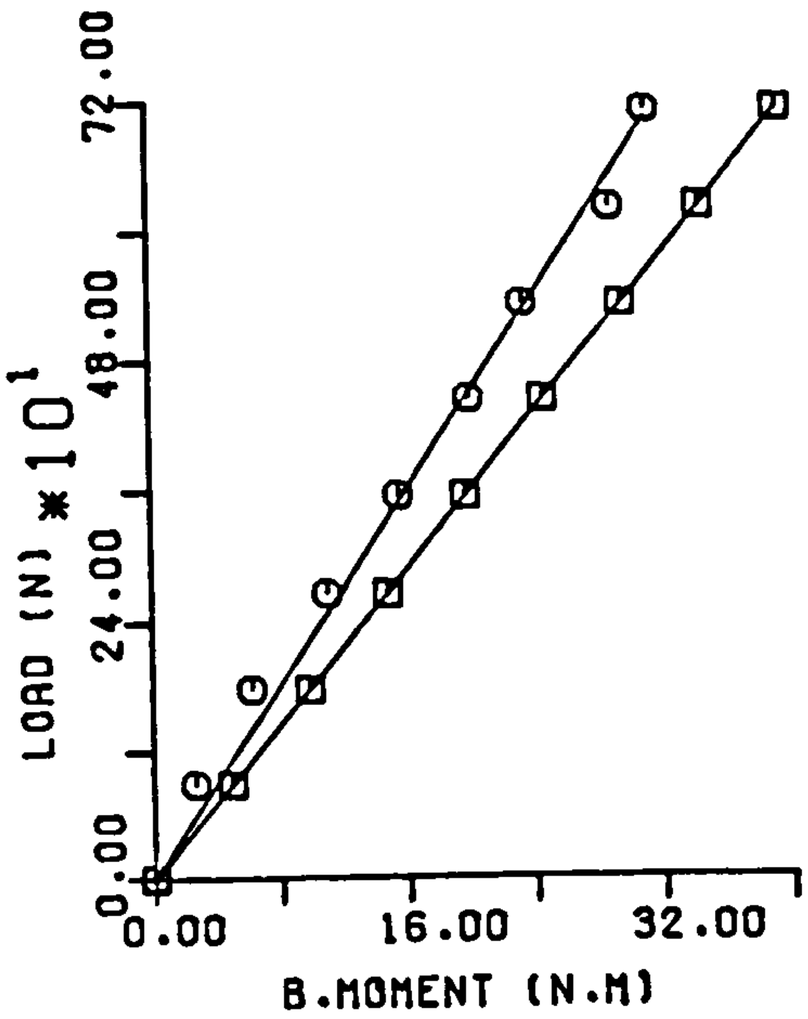

Position C

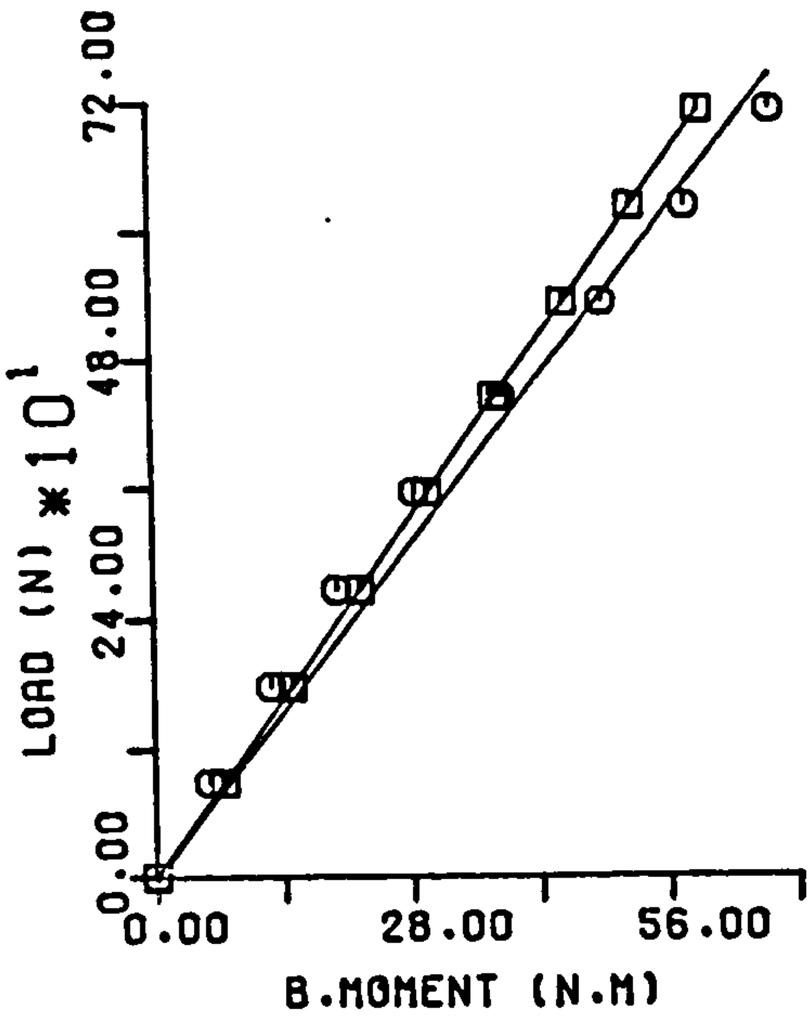

Tower Position

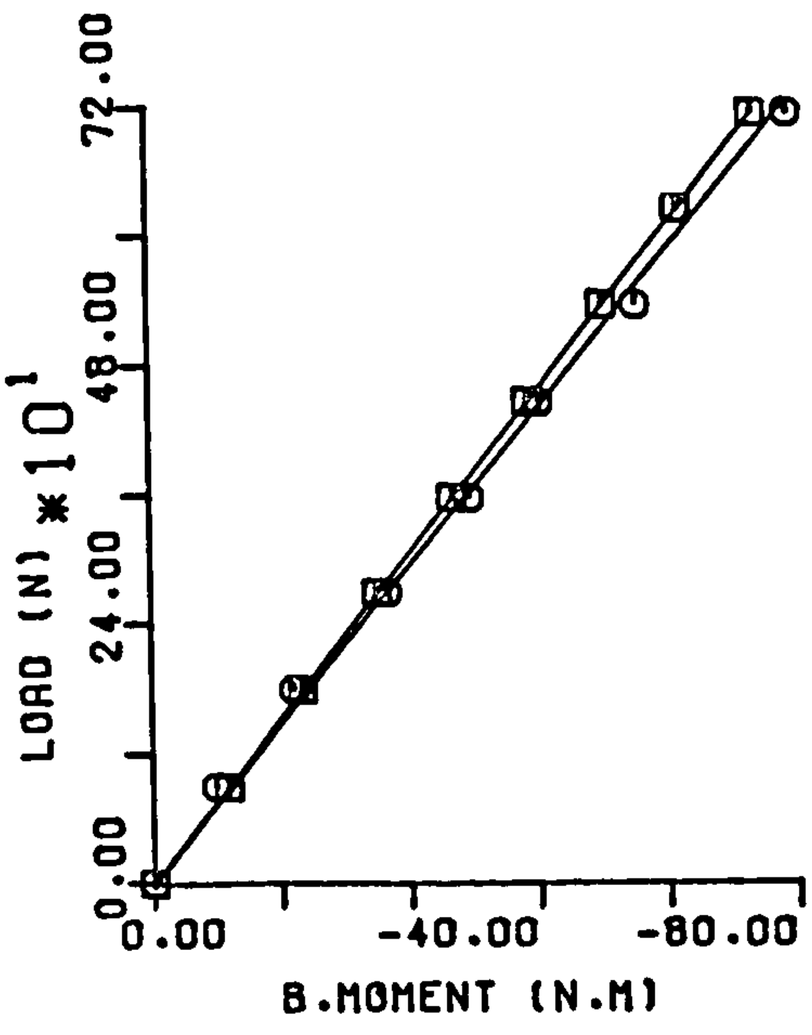

Position G

□ The calculated bending moments
o The actual bending moments

The bending moment when the load is applied at loading station H

Figure (7.26b)

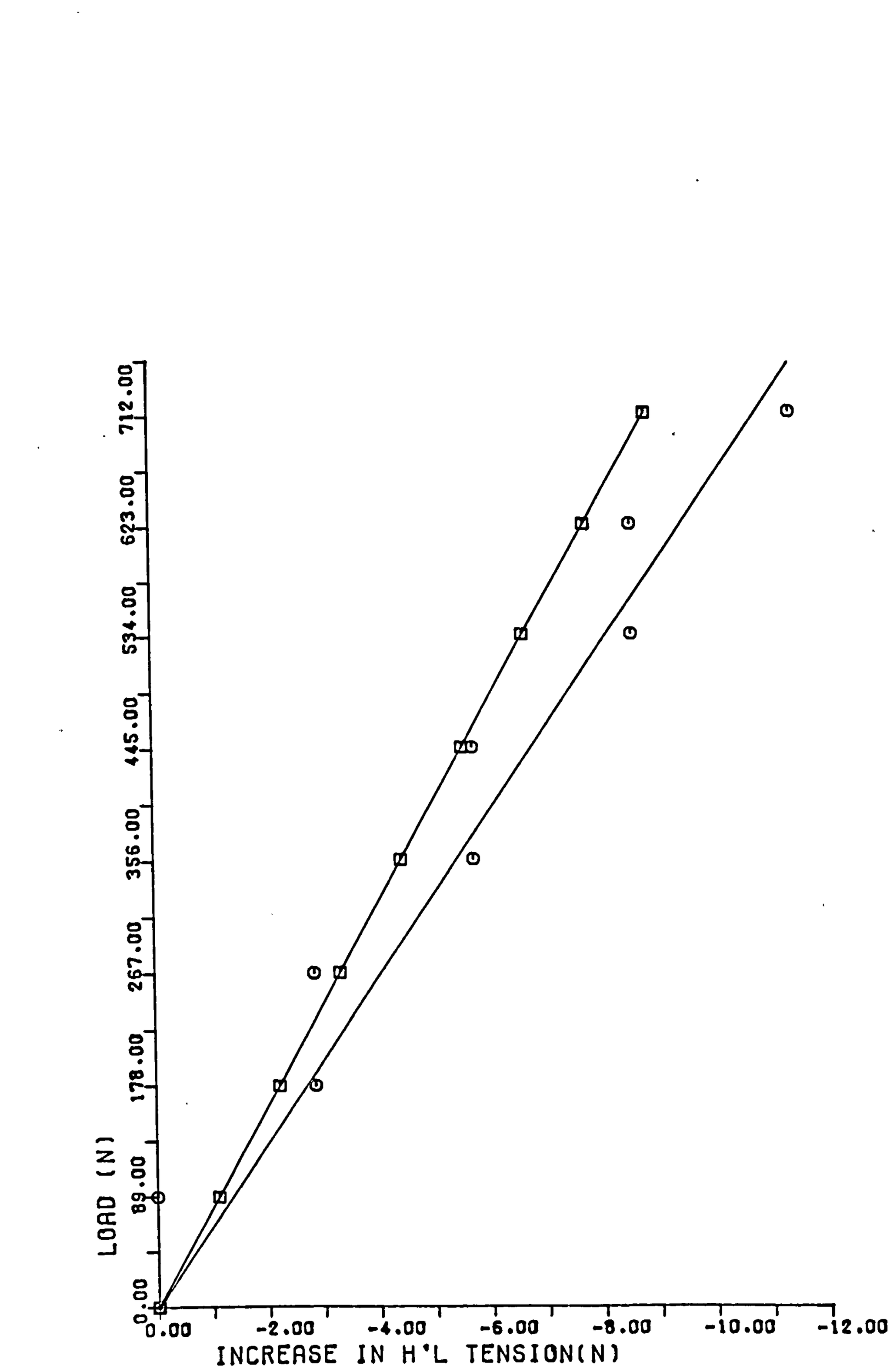

▫ The calculated values
o Cable gauges readings

The change in the prestressing force when the load is applied at loading station H

Figure (7.26c)

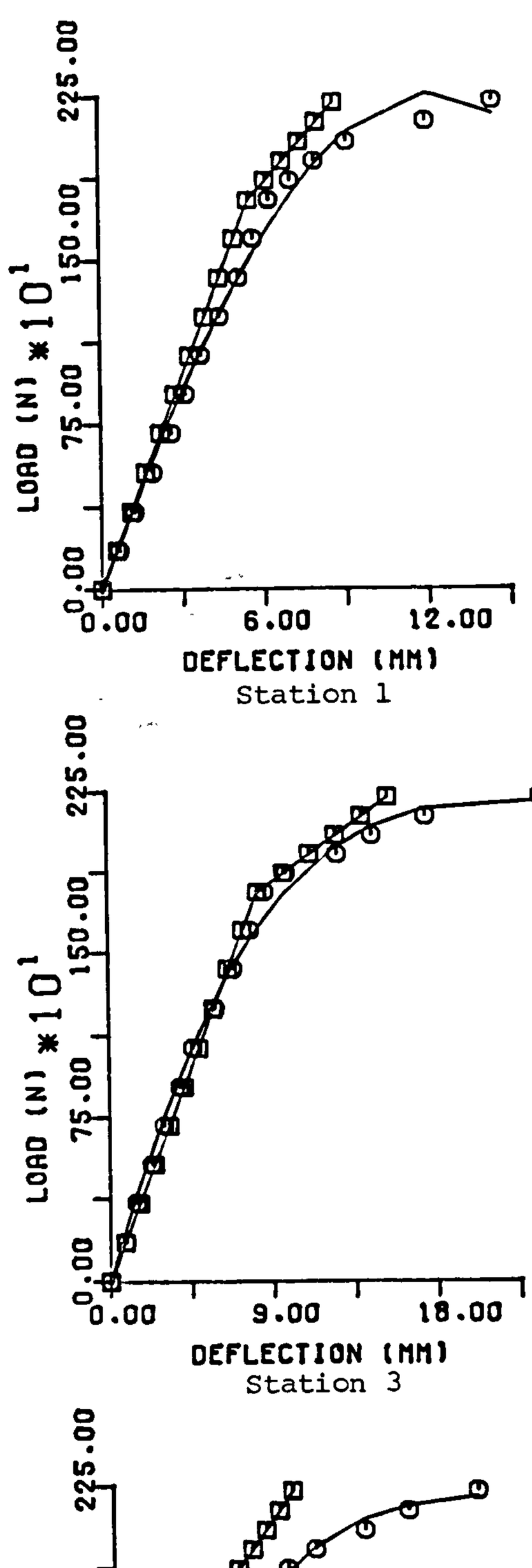

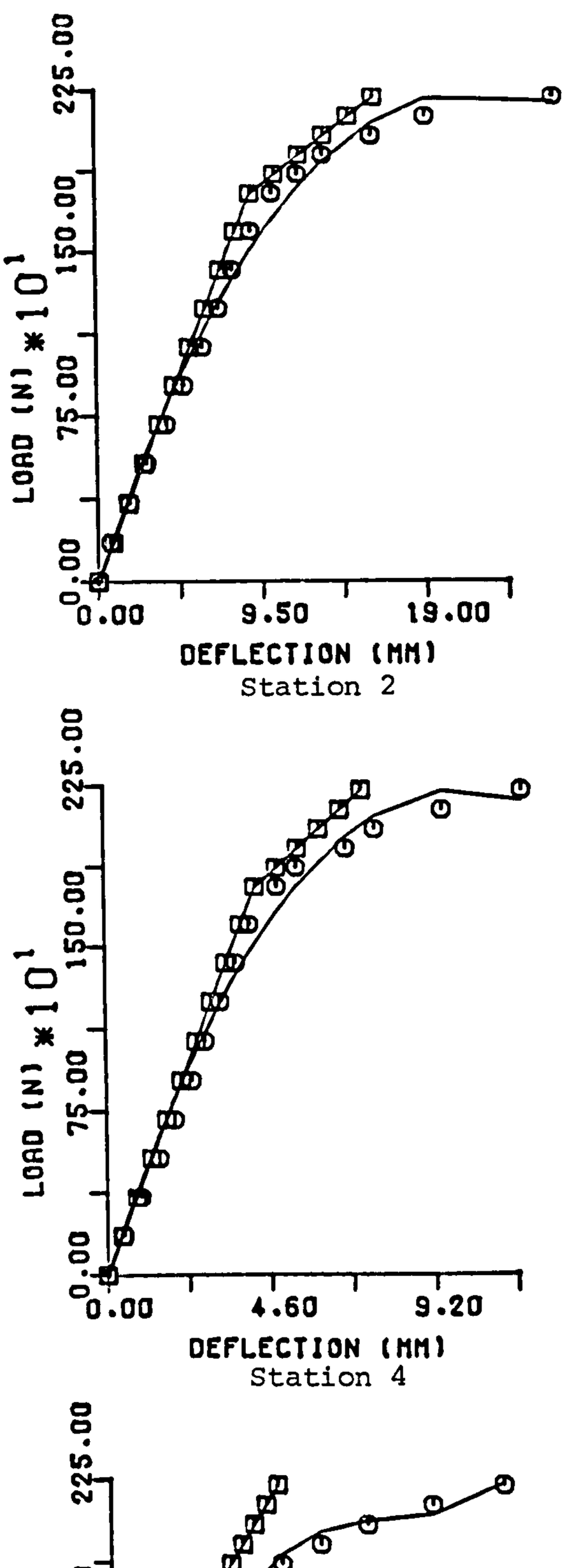

□ The calculated deflections
○ The measured deflections

The deflections when a load to failure is applied at loading position C

Figure (7.27a)

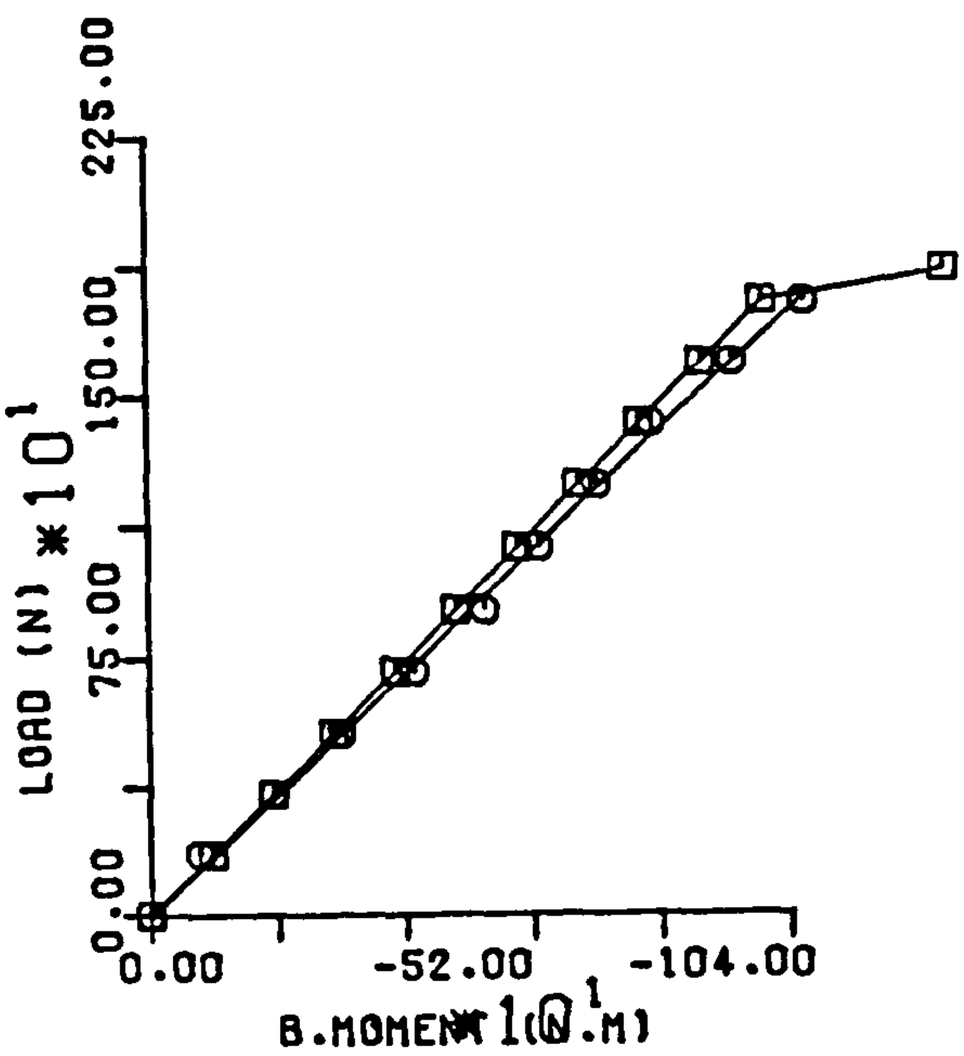

Position C

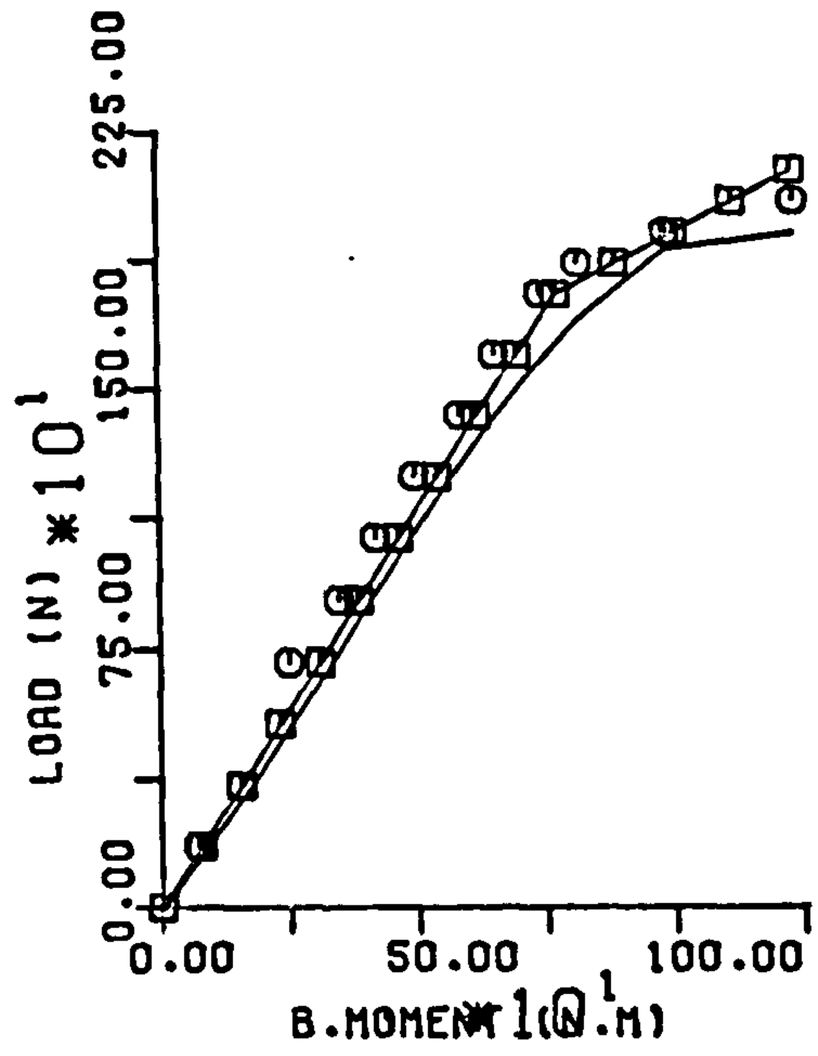

Tower Position

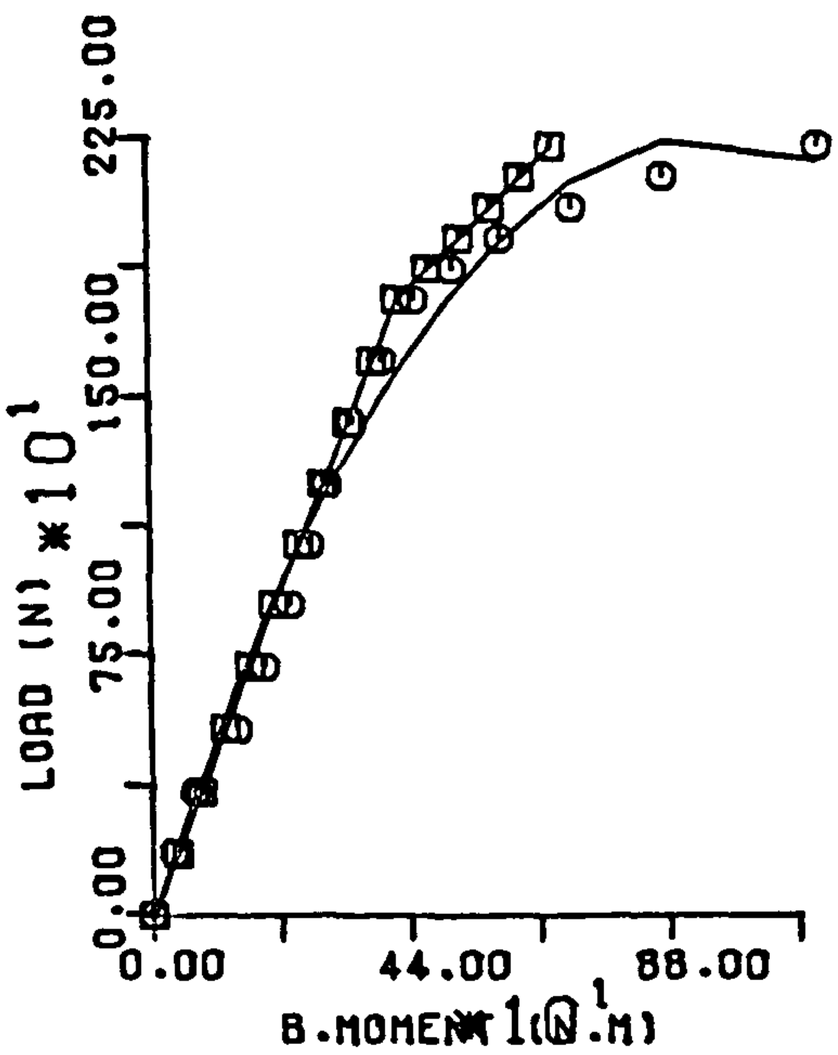

Position G

□ The calculated bending moments
o The actual bending moments

The bending moments when a load to failure is applied at loading station C

Figure(7.27b)

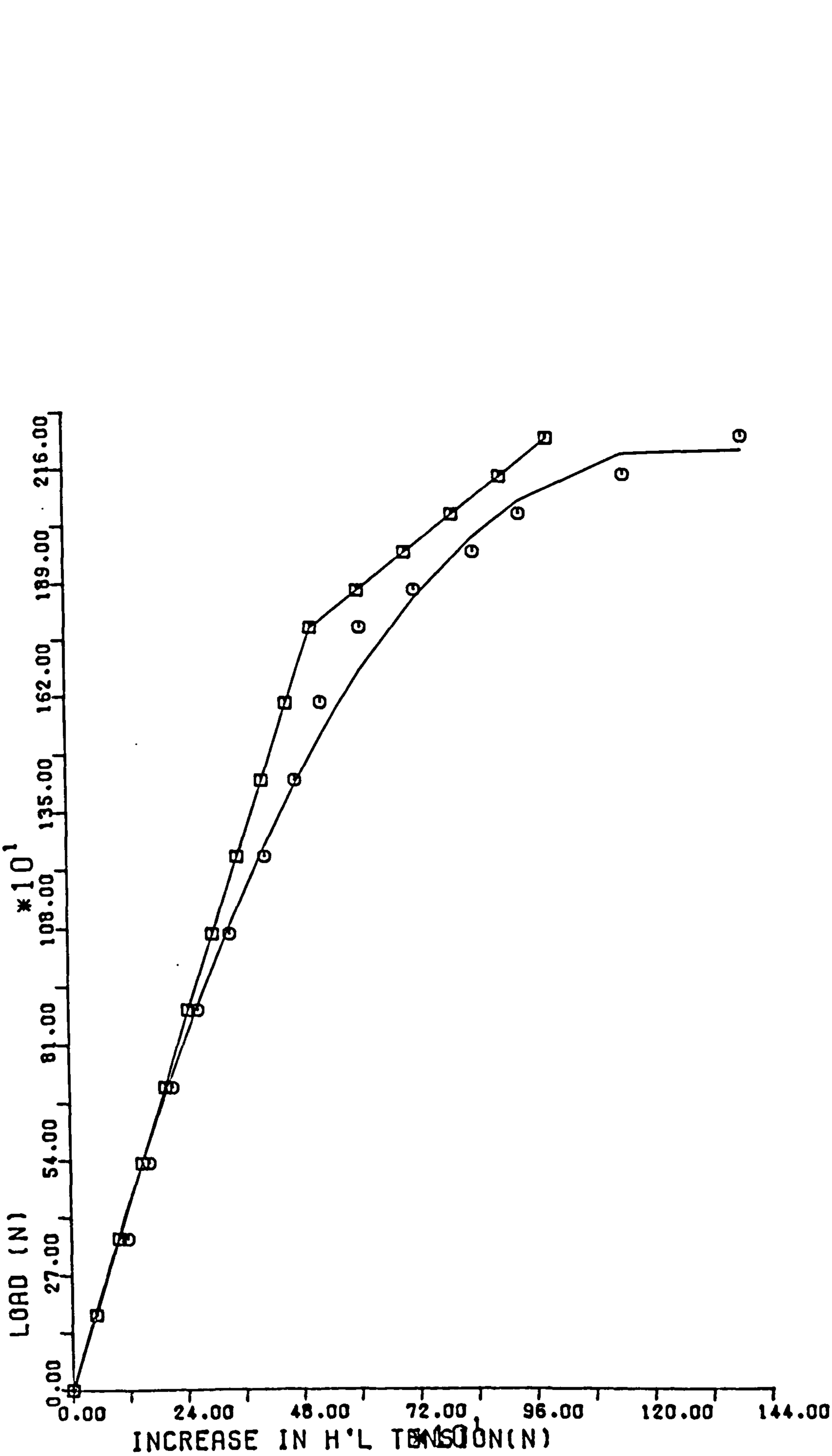

□ The calculated values
o Cable gauges readings

The change in the prestressing force when a load to failure is applied at loading station C

Figure (7.27c)

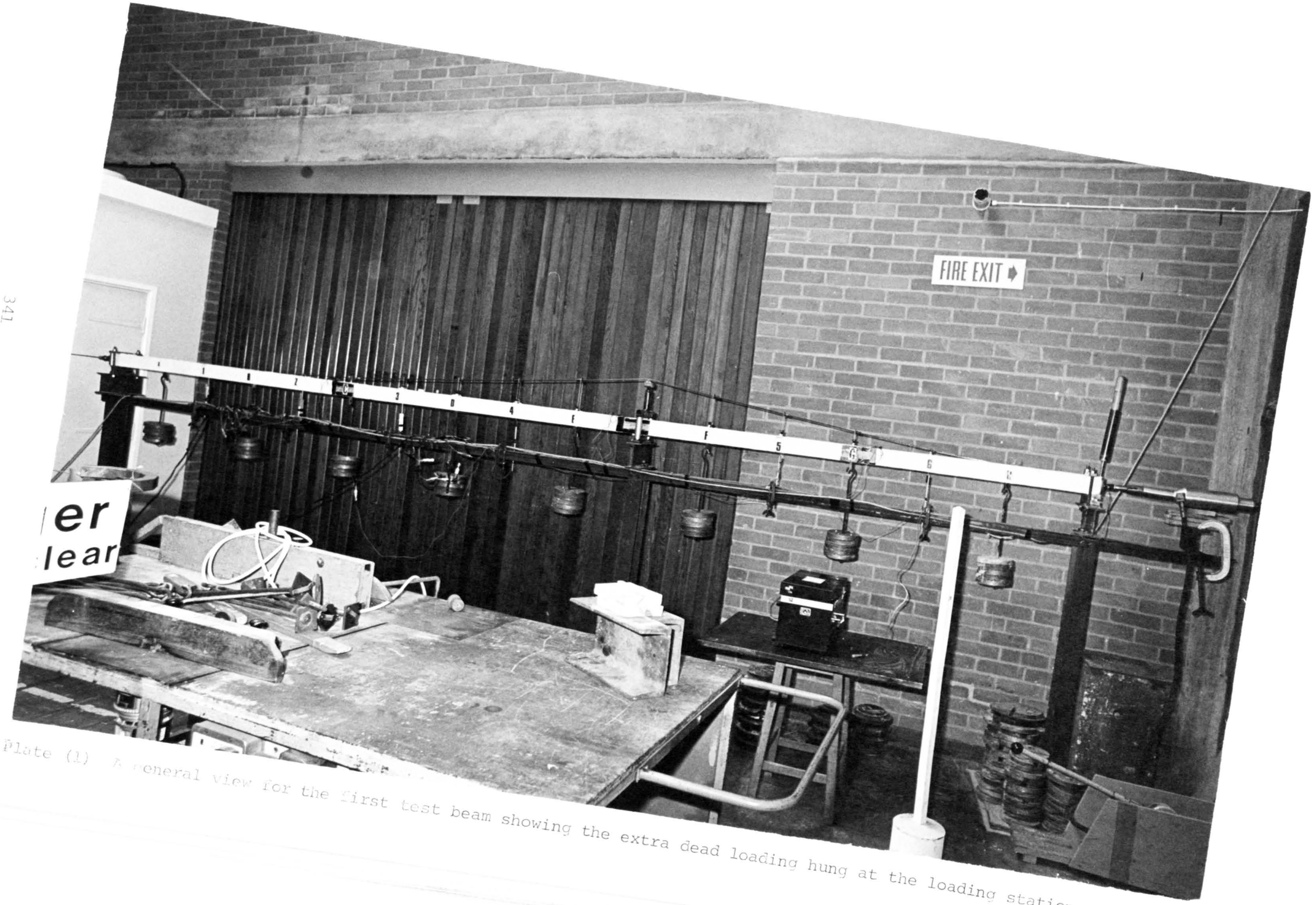

Plate (1) A general view for the first test beam showing the extra dead loading hung at the loading station

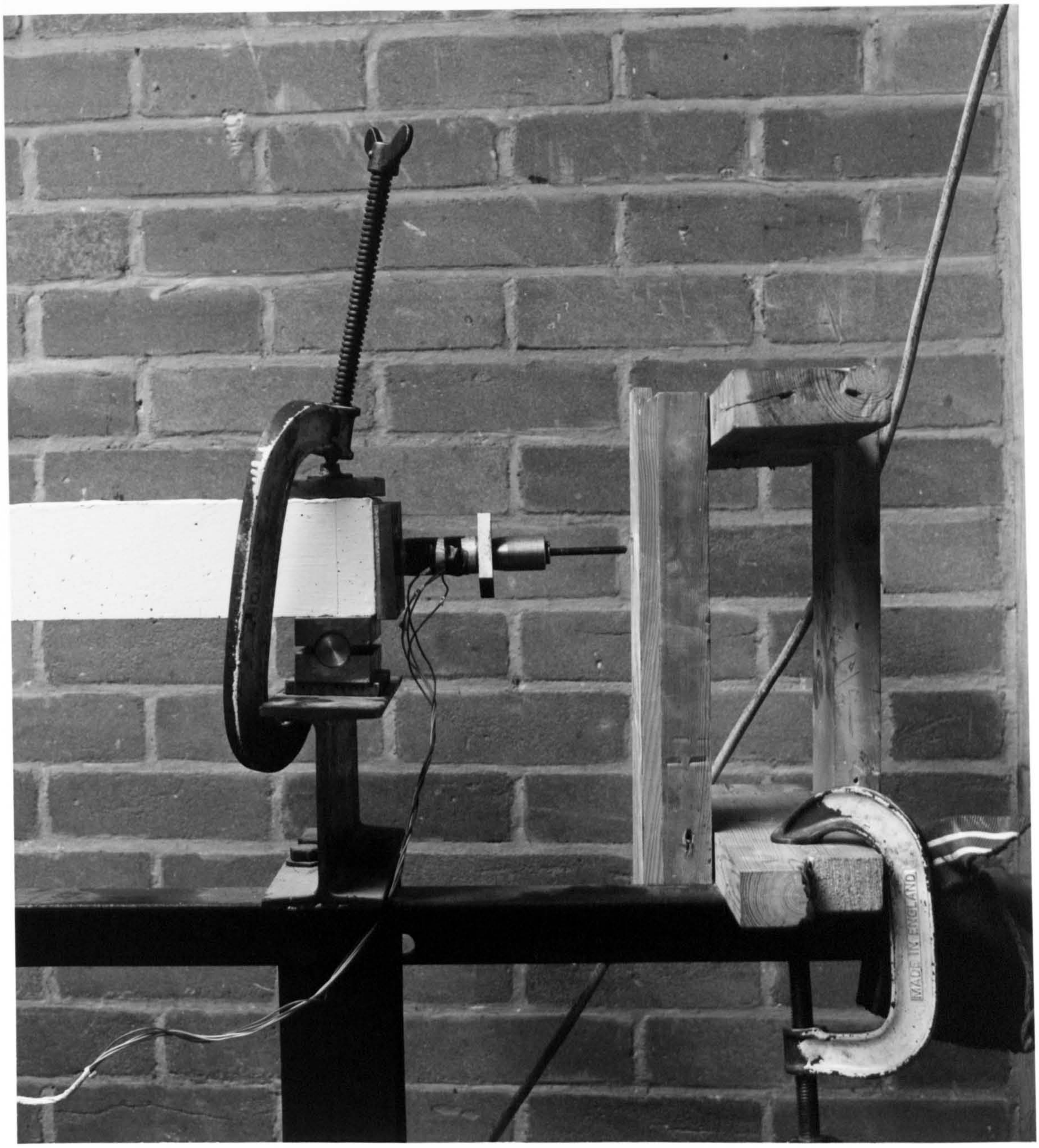

Plate (2) One of the end clamps and the load cell at the right hand end

Plate (3) The suspenders connections with the main cable and the test beam (note the device for height adjustment)

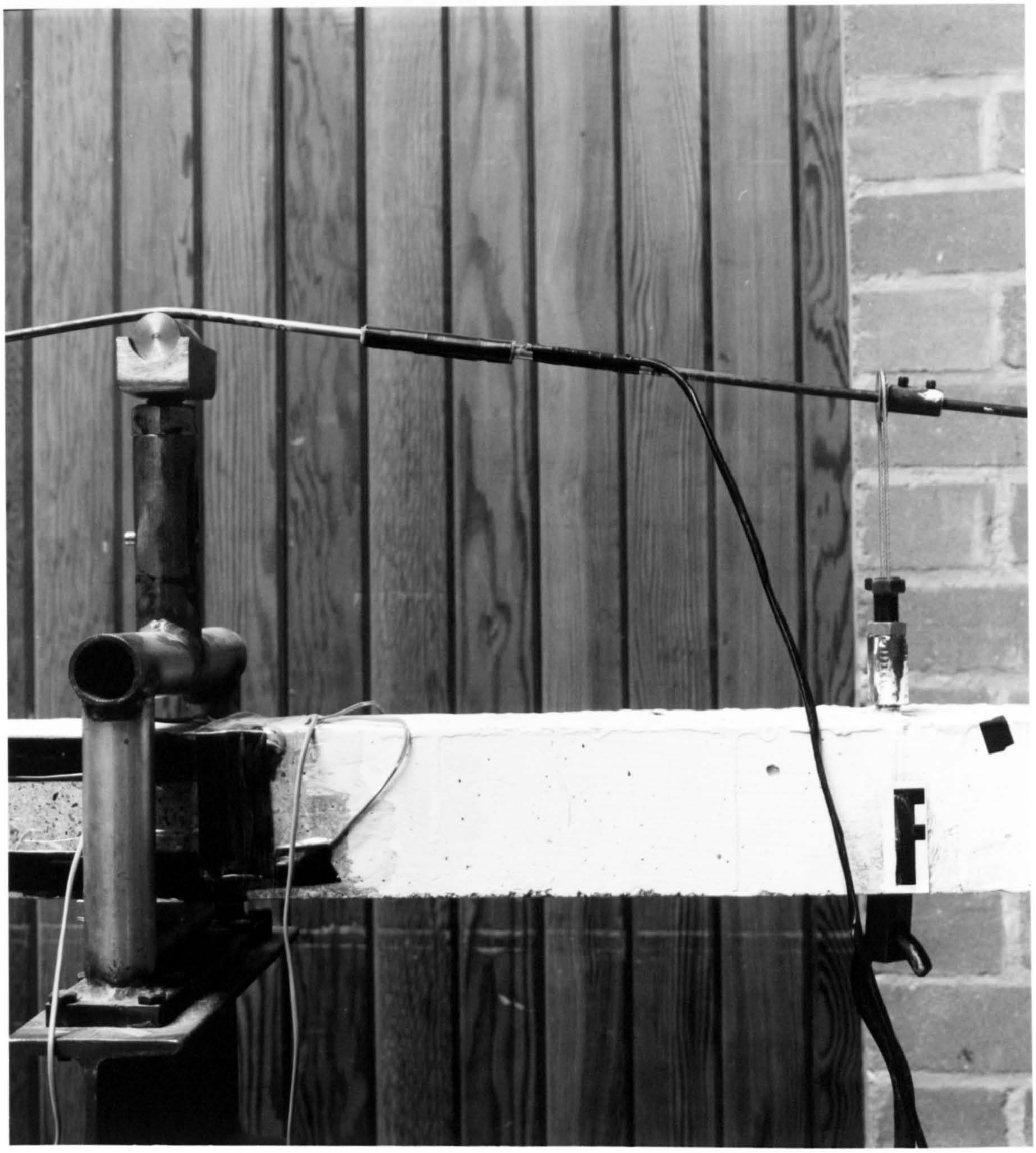

Plate (4) The tower, the cable gauges and the strain gauges at the tower position

Plate (5) The method of applying the live loads

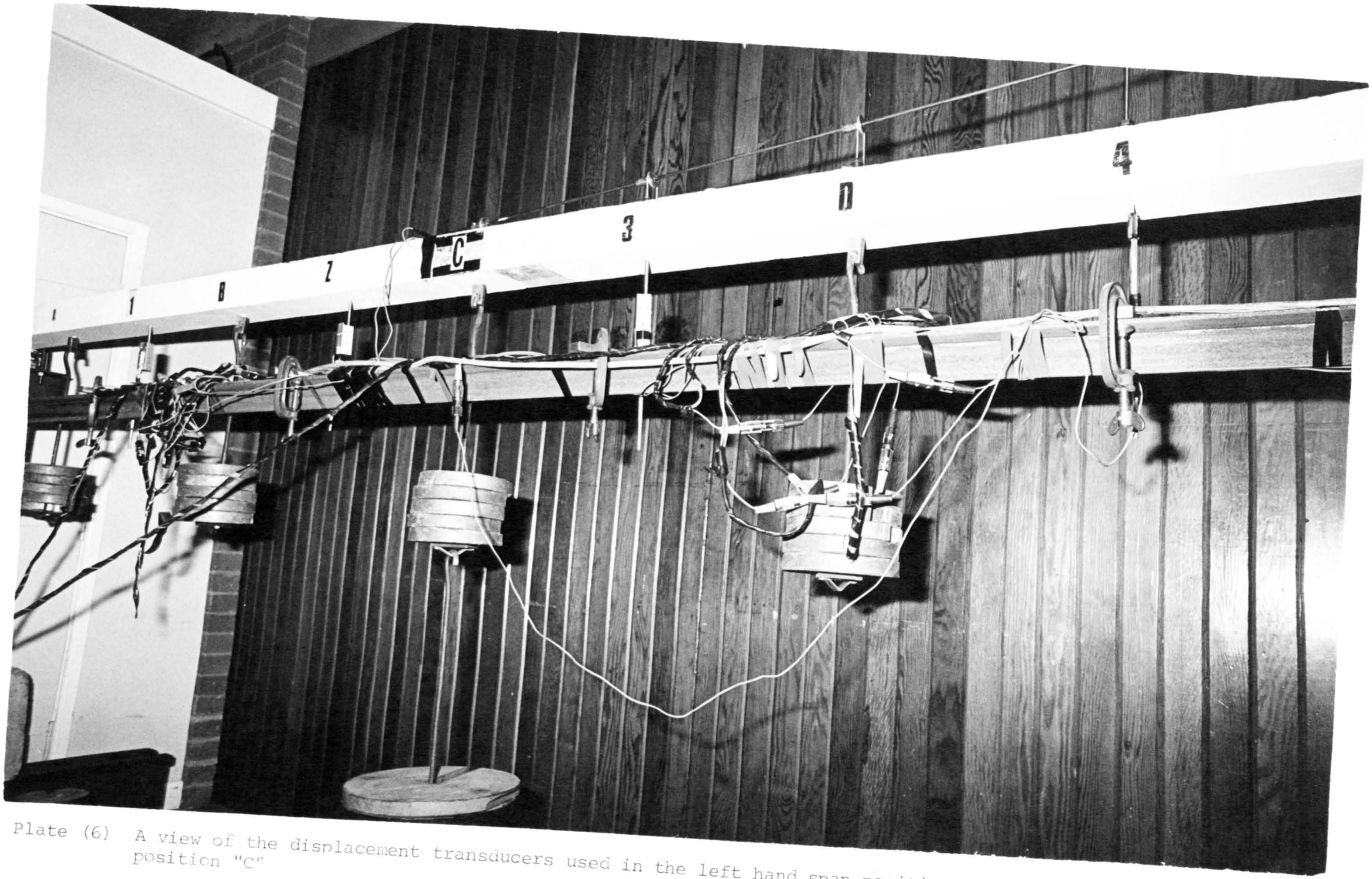

Plate (6) A view of the displacement transducers used in the left hand span position (1-4) and the strain gauges at position "C"

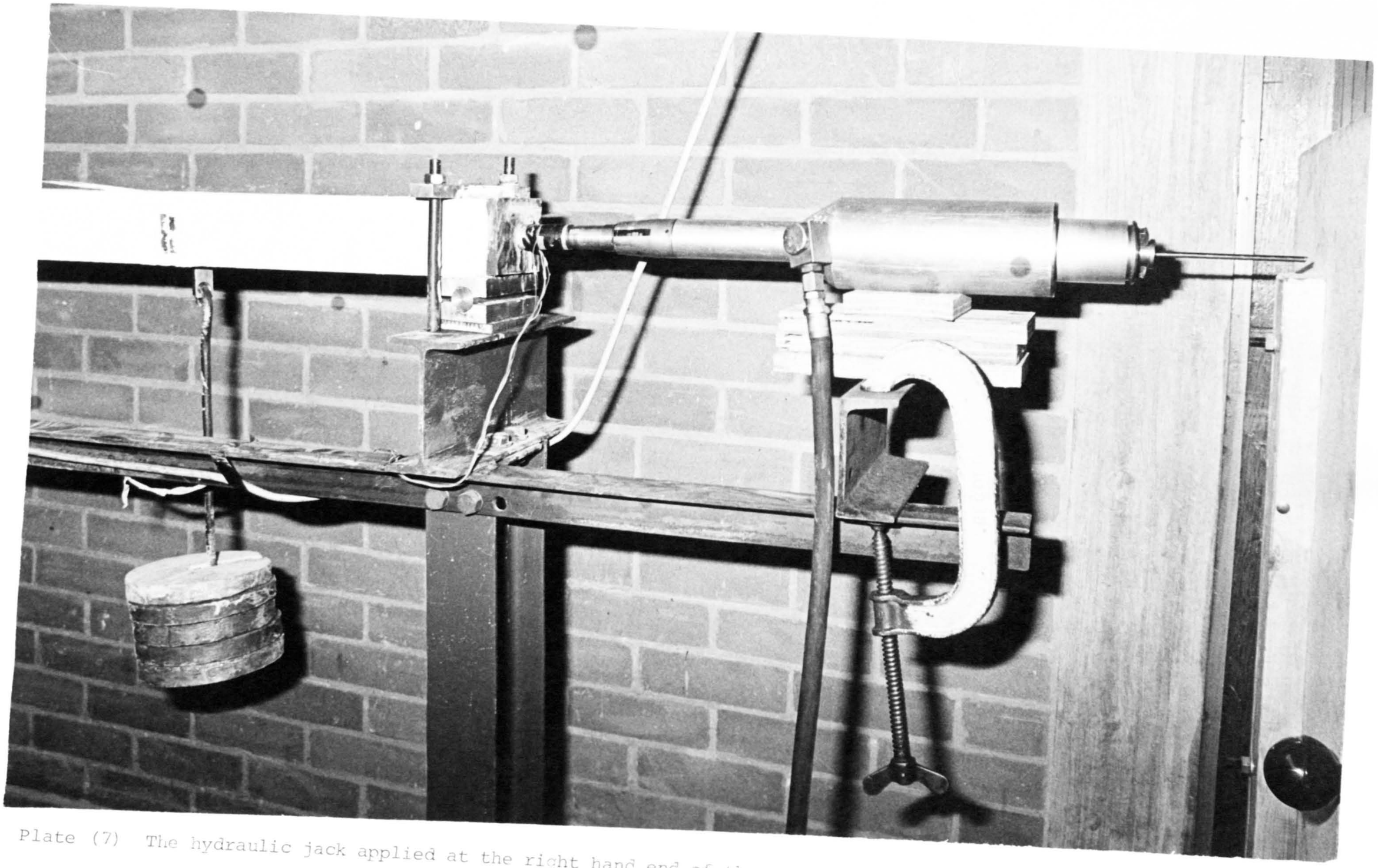

Plate (7) The hydraulic jack applied at the right hand end of the cable

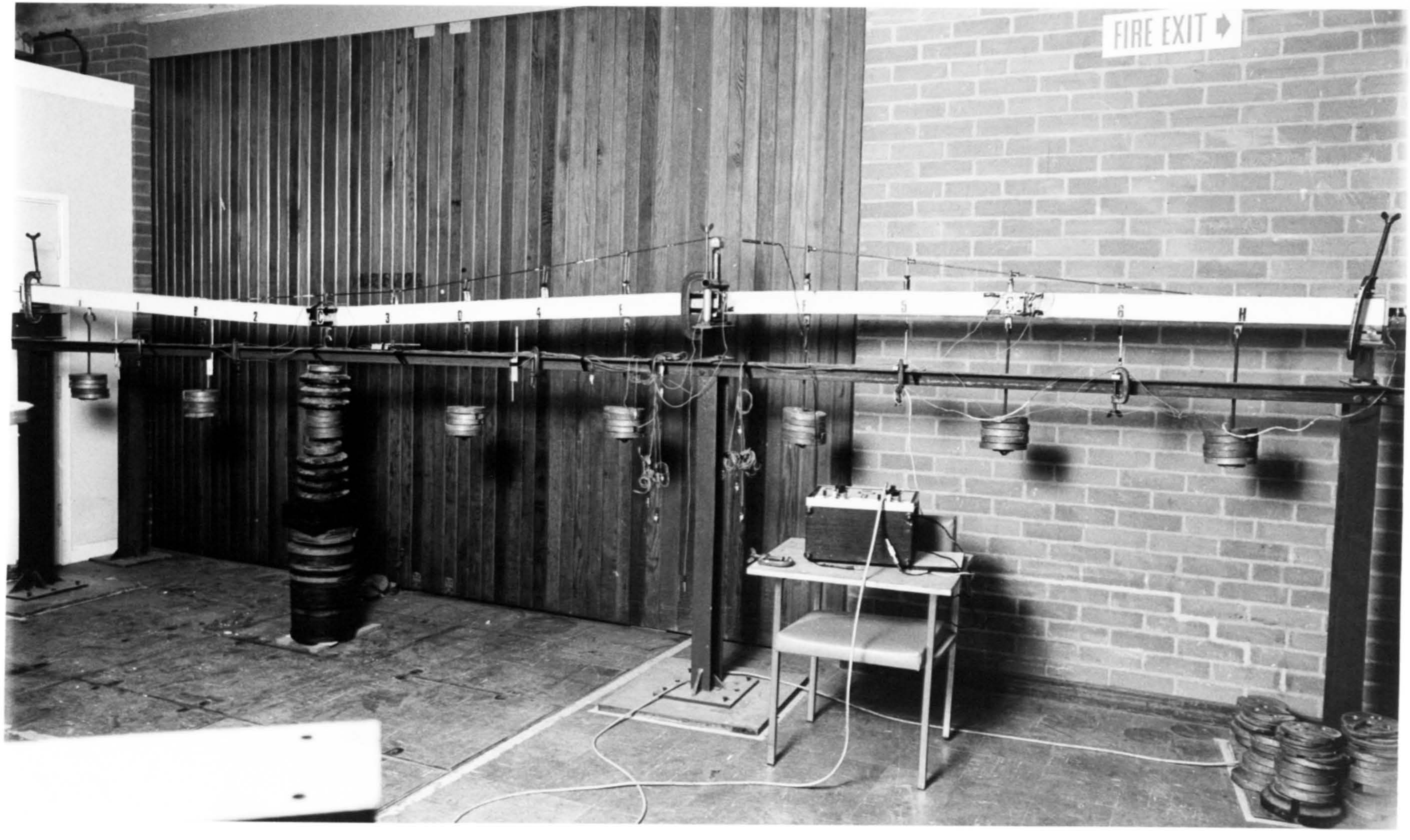

Plate (8) The collapsed test beam

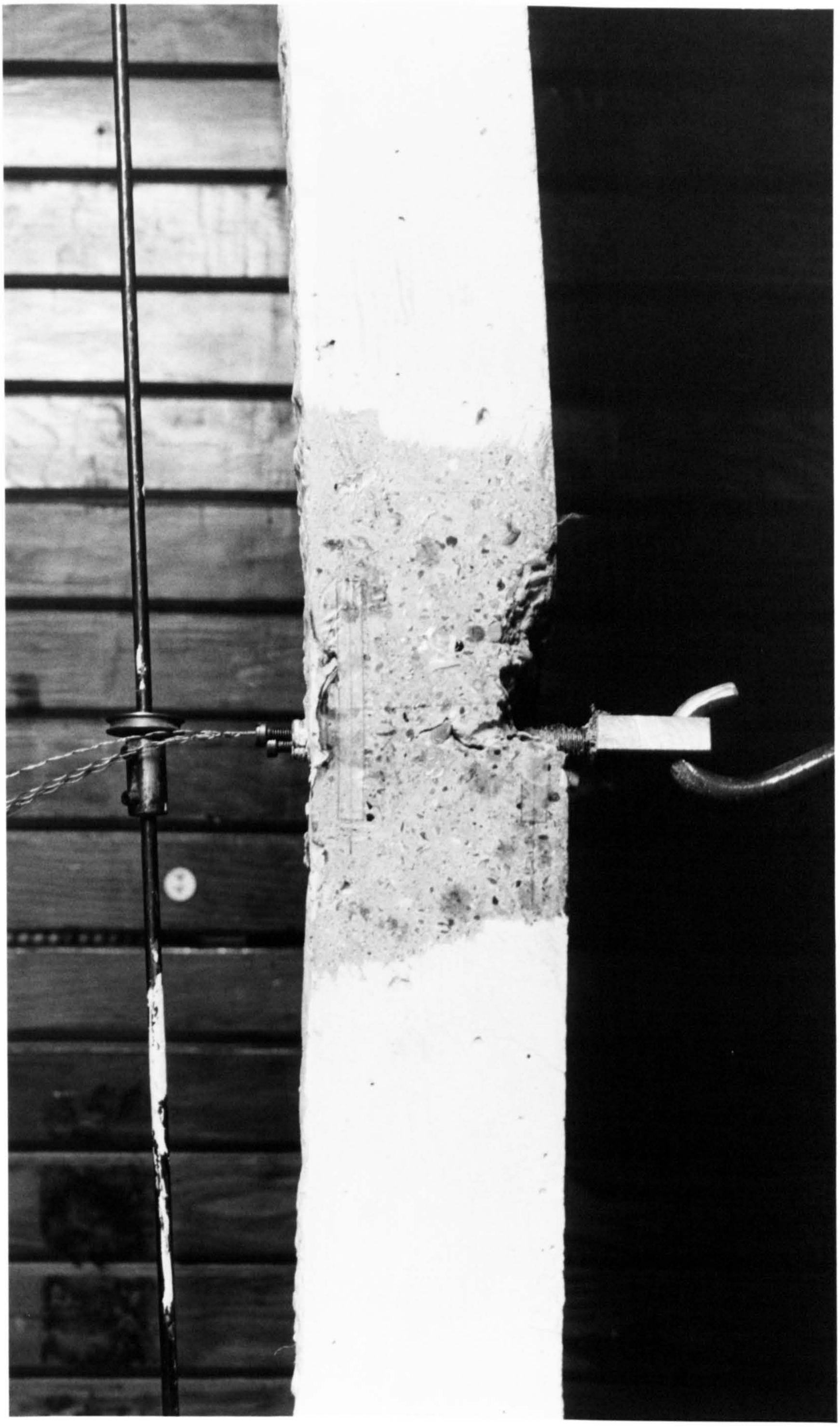

Plate (9) The mid-point of the left hand span after failure

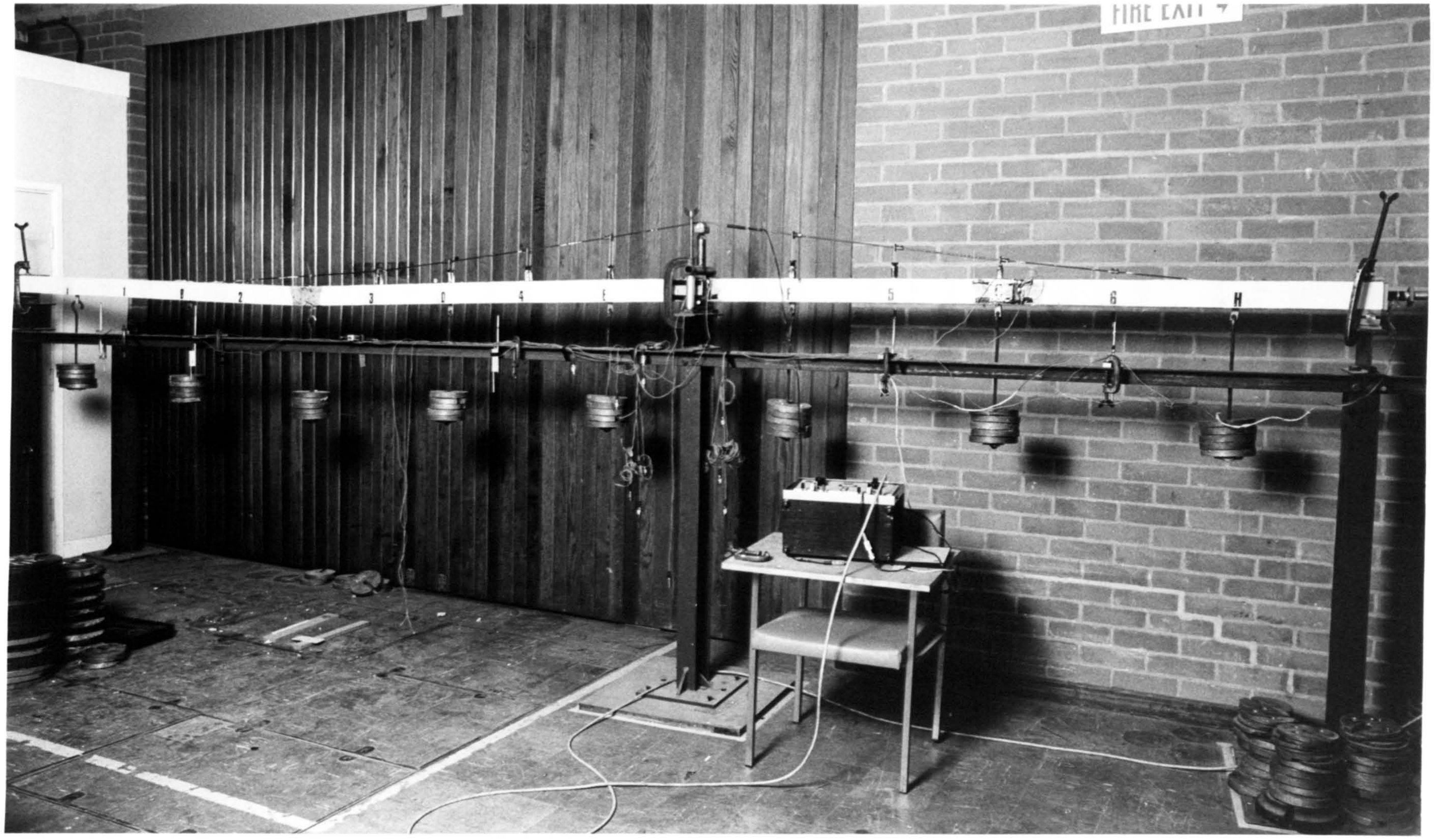

Plate (10) The collapsed test beam after recovery

CHAPTER 8

8. Conclusions and Suggestions for Future Research

The thesis has shown the development of a theoretical approach to the problem of the analysis of the elastic and ultimate behaviours of an unusual form of prestressed concrete structure, namely the two-span prestressed suspension bridge. Small scale experiments have shown that the theory is able to predict the behaviour in both regimes with acceptable accuracy for normal structural engineering design purposes. The analysis necessarily involves long and complex expressions which is partly developed from the original work of Steinman and Timoshenko, (20 - 28), after being modified to include the effect of the axial, prestressing, force. For practical calculation purposes, it has been desirable to produce a general computer program, Appendix 28, to evaluate numerical data.

The experimental results confirmed the suitability of Timoshenko's approach, (23 - 26), to calculate the interaction between the main cable and the suspended beam due to applied live loading. Not only is the approach capable of analysing both ungrouted and grouted types of bridge, but it is also applicable to both elastic and plastic stages of the structure. Furthermore, the approach can be used for all ranges of span lengths. Although the interaction between cable and beam was not very obvious in the first stage of the experiments, as the maximum reduction in the live load moments was about 7%, it did contribute considerably to the values of the failure loads as the live load moments reduction amounted to about 12% for the grouted test beam.

Although the theory suggested for the determination of the failure loads is approximate, it proved sufficiently accurate as the failure loads, obtained experimentally, were within an acceptable margin of error form the calculated ones. The formulae derived for the calculation of the ultimate moment of resistance were able to be used for any concrete section with any number of layers of reinforcement whether or not subjected to external axial force.

The experiments also showed that grouting the main cable ameliorates the performance of the prestressed concrete suspended beam in many different ways. It certainly improves the interaction between cable and beam and hence, the cable directly carries more live load. Consequently, less deflections, bending moments and shear forces would be generated in the case of grouted suspended beams as confirmed by the experimental results. This also results in an overall increase in the rigidity and strength of prestressed concrete suspended beams. Grouting appears to have another advantage which has not been able to be shown experimentally. This is that due to the partial restraint of the main cable, time effects on the magnitude of its tension are less. Consequently, a smaller initial prestressing force can be used resulting in a cheaper cable.

The experiments also showed the success of the technique of allowing for small tensile stresses to develop in the concrete which can be sustained by the main reinforcement of the beam and do not cause any cracks during the service life of the structure. This results in a considerably smaller prestressing force, Section 7.3.1., and hence, a further reduction in the cable cost. However, such approach must be supported by sufficient investigation in all possible cases of live loading likely to affect the structure in order to determine its maximum tensile stresses.

The second experiment showed the feasibility of prestressing suspended beams by shortening their suspenders. This innovative technique can be used for practical purposes but will require the development of a height adjustment device which is capable of sustaining maximum suspender load in full sized bridges. Consequently, as the bridge ages towards the end of its service life, all of its cracks can be eliminated and its life prolonged when increasing its prestressing force by further shortening its suspenders. The development of this height adjustment device represents a good subject for future research.

As noted in the body of the thesis, whilst very few bridges have been built, notably by Professor Vandepitte in Belgium (29 -36), there has been very little experimental research carried out previously to validate the theoretical approach to their design. It would seem therefore that if the very considerable economies which these bridges are capable of giving are to be made, further studies should be carried out. Clearly, one of the most useful directions for future research would be to instrument larger scale, or hopefully, full sized bridges. Even so, laboratory work to study modes of failure under different loading conditions, the time effects on the magnitude of the prestressing force (based upon the theory given in Chapter 5) and the dynamic behaviour should yield valuable additional information.

One of the most attractive subjects for future research is to investigate the use of prestressed concrete suspension bridges for very long crossings, over 1 km, in the form of a multi-span bridge. This form of structure would certainly improve the applicability of our type of bridge in the span range where a three-span bridge become uneconomical due to foundation cost. However, a problem needing study is the development of deflections increasing with the number of spans and due partly to the horizontal movements of the tower tops. One way of decreasing these deflections would be to link the main cables horizontally with the suspended girders at the centre of each span. Another way to control the deflections could be to connect the tops of the towers with the abutments and with each other by means of bracing systems. The effect of such systems could influence the structural analysis considerably and must be included in the calculations.

REFERENCES

1. ALLEN, H.G. and BULSON, P.S. "Back Ground to Buckling". McGraw-Hill. London, 1980.

2. ANDREWS, E.S. "Elastic Stresses In Structures". Translated from CASTIGLIANO'S "Theorm De L'Equilbre Des Systemes Elastiques Et Ses Applications". Scott, Greenwood and Son. London, 1919.

3. ASPLUND, S.O. "On The Deflection Theory of Suspension Bridges". Upsala. Stockholm, 1945.

4. ATKINSON, R.I. and SOUTHWELL, R.V. "On The Problem of Stiffened Suspension Bridges and its Treatment by Relaxation Methods". Journal of the Institute of Civil Engineering. 1939, No 5.

5. B.S. 8110. Part 1 and 2. 1985. "Structural Use of Concrete".

6. JAKKULA, A.A. "The Theory of the Suspension Bridge". Publication of the International Association for Bridge and Structural Engineering. Volume 4, 1936.

7. JOHNSON, B., BRYAN, C.W. and TURNEASURE, F.E . "The Theory and Practice of Modern Framed Structures", Part II. 9th Edition, John Wiley and Sons Inc. New York, 1911.

8. KONG, E.K. and EVANS, R.H. "Reinforced and Prestressed Concrete". 2nd Edition, Nelson. London, 1980.

9. MAGNEL, GUSTAVE. "Prestressed Concrete". 3rd Edition, Butler and Tanner Limited. London, 1954.

10. MORICE, P.B. and LEWIS, H.E. "The Ultimate Strength of Two-Span Continuous Prestressed Concrete Beams As Affected By Tendon Transformation and Untensioned Steel". Proceedings of the Institution of Civil Engineering. London, 1955.

11. MORICE, P.B. and LEWIS, H.E. "Prestressed Continuous Beams and Frames". Proceedings of the American Society of Civil Engineering, Volume 82. September, 1956.

12. MORICE, P.B. "The Analysis of Prestressed Concrete Structures and the Application of Recent Research". Proceedings of the Institution of Civil Engineering, Volume 6. March, 1957.

13. MORICE, P.B. and COLLEY, J. "Prestressed Concrete, Theory and Practice". Sir Isaac Pitman and Sons Limited. London, 1958.

14. MULLINS, HOWARD. "The Self-Anchored Suspension Bridge". Engineering News - Record. January 9th, 1936.

15. NEVILLE, A.M. "Properties of Concrete". Sir Isaac Pitman and Sons Limited. London, 1963.

16. NOWERA, M.A.H. "A Study of Suspended Prestressed Concrete Bridges". MSc Thesis. Southampton University, Southampton, 1984.

17. PUGSLEY, ALFRED. "The Theory of Suspension Bridges". Edward Arnold Limited. London, 1957.

18. REYNOLDS, C.E. and STEEDMAN, J.C. "Reinforced Concrete Designers's Handbook". 9th Edition. Cement and Concrete Association. London, 1981.

19. SELBERG, ARNE. "Design of Suspension Bridges". Trondheim. 1946.

20. STEINMAN, D.B. "A Practical Treatise on Suspension Bridges". John Wiley and Sons Inc. New York, 1929.

21. STEINMAN, D.B. "A Generalized Deflection Theory". Transactions of the American Society of Civil Engineering. 1935.

22. TOMS, A.H. "Experiments on the Stability of the Self Anchored Suspension Bridges". Journal of the Institution of Civil Engineering. 1938.

23. TIMOSHENKO, S. and WAY, S. "Suspension Bridges with a Continuous Stiffening Truss". Publication of the International Association for Bridge and Structural Engineering, 2, pp 452. 1934.

24. TIMOSHENKO, S. "Strength of Materials", Part I. 2nd Edition, D. Van Nostrand Company Inc. New York, 1940.

25. TIMOSHENKO, S.P. "The Stiffness of Suspension Bridges". "Collected papers of S.P. TIMOSHENKO". McGraw-Hill. New York, 1953.

26. TIMOSHENKO, S.P. "Theory of Suspension Bridges". "Collected papers of S.P. TIMOSHENKO". McGraw-Hill. New York, 1953.

27. TIMOSHENKO, S. "Strength of Materials", Part II. 3rd Edition, D. Van Nostrand Company Inc. New York, 1956.

28. TIMOSHENKO, S.P. and YOUNG, D.H. "Theory of Structures". 2nd Edition, McGraw-Hill. London, 1965.

29. VANDEPITTE, D. "Self-Anchored Suspension Bridges with Prestressed Unreinforced Concrete Stiffening Girders". International Conference on Prestressed Concrete. Gent, Belgium, 1951.

30. VANDEPITTE, D. "Maximum Span Lengths for Highway Deck Bridges with Multiple Simply Supported Prestressed Concrete Girders". International Conference on Prestressed Concrete. Gent, Belgium, 1951.

31. VANDEPITTE, D. "Recent Prestressed Concrete Constructions in Belguim". Lecture organized by the Prestressed Concrete Development Group and held at the Institution of Civil Engineering. London, December, 1956.

32. VANDEPITTE, DANIEL. C.C. "Prestressed Concrete Suspension Bridges". Proceedings of the International Conference on Prestressed Concrete. San Francisco, U.S.A., 1957.

33. VANDEPITTE, D. "De Berkening Van Voorgespannen Beton". En Inzonderheid De Begnoting Van Hit Voorspannings. Gent, Belgium, April 1959. (English Translation).

34. VANDEPITTE, DANIEL. C.C. "Prestressed Concrete Suspension Bridges and the Influence of Time Effects on the Magnitude of the Prestressing Force". Transport-Communications Monthly Review. London, December, 1961.

35. VANDEPITTE, D. "Design for a Prestressed Concrete Suspension Bridge (Not Constructed) over the Scheldlt River at Antwerp". (Translated Version). Part of an International Bid for the Design of a Bridge over the Scheldlt River at Antwerp, Belgium. Cement and Concrete Assocation. London, December, 1956.

36. VANDEPITTE, D. "Self-Anchored Prestressed Concrete Suspension Bridges with Parabolic Cables". Symposium on Suspension Bridges, Paper 38. Lisbon, November 1966.

37. VEZOUSKA,T.J. "Field Inspection of Grouted Post-tensioning Tendons". Post-tensioning Institute, pp16. Glenview, Illinois, March, 1977.

BIBLIOGRAPHY

1. ALLEN, A.H. "An Introduction to Prestressed Concrete". 2nd Edition, Cement and Concrete Association. London, 1981.

2. American Concrete Institute, ACI 318 - 63. Building Code Requirement for Reinforced and Prestressed Concrete, pp 144. Detroit, June, 1963.

3. BAKER, A.L.L. "Further Research in Reinforced Concrete, and its Application to Ultimate Load Design". Proc. of the A.S.C.E., Part 3, Vol 2, No 2, pp 269 - 310. August, 1953.

4. BILLETT, D.F. and APPLETON, J.H. "Flexural Strength of Presressed Concrete Beams". Journal of the American Concrete Institute, Vol 25, No 10, pp 387 - 854. June, 1954.

5. BLEICH, F. "The Mathematical Theory of Vibrations in Suspension Bridges". Washington Dept. of Commerce. Columbia, USA, 1978.

6. BOECKER, H.C. and JAMES, E.C. "Design and Construction of Prestressed Concrete Suspension Cable Anchorages". P.C.I. Journal June, 1967.

7. British Standard Institution. CP115. "The Structural Use of Prestressed Concrete in Buildings". pp 44. London, 1959.

8. BROTTON, D.M. "A General Computer Programme for the Solution of Suspension Bridge Problems". The Structural Engineer, Vol 44, pp 161 - 167. May. 1966.

9. BURDETTE, E.G. and GOODPASTURE, D.W. "Test to Failure of a Prestressed Concrete Bridge". P.C.I. Journal. June, 1974.

10. CHEN, WAI-FAH and ATSUTA, TOSHIO. "Theory of Beam-Columns", Volume 1. McGraw-Hill. New York, 1976.

11. COATS, R.C., COUTIE, M.G. and KONG, F.K. "Structural Analysis". 2nd Edition, Nelson. Hong Kong, 1981.

12. DUDRA, J. "Design and Construction of Hudson Hope Bridge". P.C.I. Journal. April, 1966.

13. EL-BEHAIRY, S. "Reinforced Concrete Design Handbook". 3rd Edition AIN-SHAMS University. Cairo, 1977.

14. FUKUDA, T. "Analysis of Multi-span Suspension Bridges". Journal of the Structure Division, A.S.C.E. Vol 93, ST3, proc, paper 5261, pp 63 - 86. June, 1967.

15. GARDNER, R.P.H. "The Behaviour of Prestressed Concrete I - Beams Under Combined Bending and Tension Stresses". Cement and Concrete Association. February, 1960.

16. GUYON, Y. "Development and Research in Prestressed Concrete Continuous Structures". Societe des Ingenieurs Civils de France British Section, pp 43. London, 1952.

17. HORNE, M.R. "Plastic Theory of Structures". 2nd Edition, Pergamon Press. Oxford, 1979.

18. IRVINE, H.M. "Maximum Hanger Loads in Suspension Bridges". New Zealand Engineering Society, Vol 27, Part 8, pp 258 - 262. 1972.

19. JANISZEUSKI, T. "Suspender Tension Method for Bridge Analysis". Journal of the Structural Division, A.S.C.E., Vol 93, ST5, Proc. Paper 5541, pp 63 - 86. October, 1967.

20. JEFFREY, A. "Mathematics for Engineers and Scientists". Nelson. London, 1969.

21. JENNINGS, A. "Approximate Analysis of a Single-Span Suspension Bridge Using Stress Energy". The Structure Engineering, Vol 48, No 5, pp 281 - 285. May, 1970.

22. JENNINGS, A. and MAIRS, J.E. "Static Analysis of Suspension Bridges". Proc. of the A.S.C.E., No 11, pp 2433 - 2454. November, 1972.

23. MAIRS, J.E. "Inclined Hangers for Suspension Bridges". Ph.D. Thesis Presented to the Queens University of Belfast, Northern Ireland. 1970.

24. MEDEARIS, K. "Numerical-Computer Methods for Engineers and Physical Scientists". K.M.A. Research. Denver, Fort Collins, Colorado, 1974.

25. MELAND, J. and STEINMAN, D.B. "Theory of Arches and Suspension Bridges". McGraw-Hill. New York, 1913.

26. MOY, S.S.J. "Plastic Methods for Steel and Concrete Structures". The Macmillan Press Ltd. London, 1981.

27. MUSCATI, S.A.H.A. "A Theoretical Study of the Fatigue Cumulative Damage Analysis of Reinforced Concrete Beams". Ph.D Theses Presented to Southampton University, 1986.

28. O'BRIEN, W.T. and FRANCIS, A.J. "Cable Movements Under Two-Dimensional Loads". Proc. of the A.S.C.E., Vol 90, ST3, pp 89 - 123. June, 1964.

29. PRIESTER, G.C. "Application of Trigonometric Series to Cable Stress Analysis in Suspension Bridges". Ann Arbor. Michigan, 1929.

30. PUGSLEY, A.G. "The Gravity Stiffness of a Suspension Bridge Cable". Quarterly Journal of Mechanics and Applied Mathematics, Vol 5. 5. 1952.

31. REYNOLDS, G .C. "Shear Provisions for Prestressed Concrete in the Draft Unified Code". Cement and Concrete Association. December 1969.

32. SAAFAN, S.A. "Theoretical Analysis of Suspension Bridges". Proc. of the A.S.C.E., ST4, Paper 4885. August, 1966.

33. SATO, M and MATSUSHITA, H. "The Hayahi - No - Mine Prestressed Bridge". P.C.I. Journal. March, 1976.

34. SELBERG, A. "Suspension Bridges with Cables Fastened to the Stiffening Girders at the Centre of the Bridge". A Conference on Suspension Bridges. New York, 1951.

35. SPENCER, A.J.M., PARKER, D.F. and others. "Engineering Mathematics". Volume 1 and 2. Van Nostrand Reinhold Company Ltd., New York, 1977.

36. SPILLER, J. W. "The Deflections of Suspension Bridges". The Institution of Civil Engineers. London, 1923.

37. Standard Association of Australia. SAA Code for Prestressed Concrete. Sydney, 1964.

38. STEINMAIN, D. B. "General Deflection Theory for Suspension Bridges. A.S.C.E. June, 1964.

39. VA DEPITTE, D. "Le Pont Suspender A Poutres De Rigidite en Beton, Precontraintes par les Cables Porleurs". Annales Travaux Publics de Belgique, pp 33 - 60. September, 1955 (English translation).

40. WEST, H.H. "Initial-Value Discrete Suspension Bridge Analysis". Int. J. Solids Structures, Vol 9, pp 1087 - 1105. 1973.

41. WOUDE, F.V. "Analysis of Suspension Bridges using Energy Principles". The Structural Engineer, No 4, Vol 54, pp 121 - 131. April, 1976

Appendices (1 - 15)

of Chapter 1

APPENDIX 1

1. The Determination of the Exact Length of the Cable

From the shown element, it is obvious that the exact length of the cable S can be evaluated from the following expression:

$$S = \int_{o}^{\ell} \left[1 + \left(\frac{dy}{dx} \right)^2 \right]^{1/2} dx \qquad \text{(i)}$$

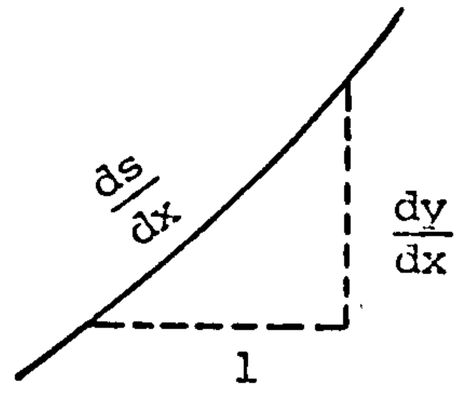

where:

$$\frac{dy}{dx} = F' + \frac{8n}{\ell} x \qquad \text{(Equation (2.9)).}$$

To solve this integration let:

$$\xi = F' + \frac{8n}{\ell} x \qquad \text{where } \xi \text{ is a variable,}$$

Hence, $\frac{d\xi}{dx} = \frac{8n}{\ell}$

and at $x = o$ $\quad \xi = F'$

$x = \ell$ $\quad \xi = F' + 8n$

Thus, substituting into equation (i), we obtain the simplified integration:

$$S = \frac{\ell}{8n} \int_{F'}^{F'+8n} [1+\xi^2]^{1/2} \, dx \qquad \text{(ii)}$$

This integration can be solved by substituting:

$$\xi = \sinh \phi$$

and $\quad d\xi = \cosh \phi \, d\phi \qquad$ where ϕ is another variable.

Thus, equation (ii) becomes:

$$S = \frac{\ell}{8n} \int \cosh^2 \phi \, d\phi$$

which yields,

$$S = \frac{\ell}{16n} \left[\phi + \frac{1}{2} \sinh 2\phi \right] \qquad \text{(iii)}$$

but $\phi = \sinh^{-1}\xi$

and $\frac{1}{2}\sinh 2\phi = \sinh\phi\cosh\phi = \xi\,[1+\xi^2]^{1/2}$

Thus, expression (iii) becomes,

$$S = \frac{\ell}{16n}\left[\sinh^{-1}\xi + \xi\,[1+\xi^2]^{1/2}\right]_{F'}^{F'+8n}$$

$$S = \frac{\ell}{16n}\left[\sinh^{-1}(F'+8n) - \sinh^{-1}F' + (F'+8n)[1+(F'+8n)^2]^{1/2} - F'[1+F'^2]^{1/2}\right] .$$

But $\sinh^{-1}\xi = \ln\,[\xi + [1+\xi^2]^{1/2}]$

Thus, the final expression for the exact cable length, in the left hand span, is:

$$S = \frac{\ell}{16n}\left[\ln\left(\frac{(F'+8n) + [1+(F'+8n)^2]^{1/2}}{F' + [1+F'^2]^{1/2}}\right) + (F'+8n)\,[1+(F'+8n)^2]^{1/2} - F'\,[1+F'^2]^{1/2}\right]$$

where F' and $(F'+8n)$ are the cable slopes at its ends ($x = o, \ell$). A similar procedure can be used for the determination of the exact cable length in the right hand span.

APPENDIX 2

2. The Determination of the Approximate Cable Length by Series Expansions

We know that the exact length of the cable has been expressed in terms of the slopes at its ends. We also know that the cable curves for suspension bridges are usually flat, due to the long spans with respect to the height of their towers, and consequently their slopes are small. Therefore, we can express the cable length in terms of series expansions. To do so, we have from Maclaurin's formula of expansions the well known expansion:

$$x\,[1+x^2]^{1/2} = x + \frac{x^3}{2} - \frac{x^5}{8} + \frac{x^7}{16}$$

However, the expansion for $\ln\,[x+(1+x^2)^{1/2}]$, or $\sinh^{-1}x$, is needed and therefore it has to be calculated from first principle. The general form for Maclaurin's expansion is:

$$y = y_o + xy_o' + \frac{x^2}{2!}\,y_o'' + \frac{x^3}{3!}\,y_o''' + \ldots\ldots\ldots + \frac{x^n}{n!}\,y_o^n$$

where the primes denote the derivative with respect to x and the subscript o denotes at x = o.

Hence we have:

$y = \sinh^{-1}x$	$y_o = o$
$y' = \frac{1}{(1+x^2)^{1/2}}$	$y_o' = +1$
$y'' = \frac{-x}{(1+x^2)^{3/2}}$	$y_o'' = o$
$y''' = \frac{(2x^2-1)}{(1+x^2)^{5/2}}$	$y_o''' = -1$
$y^{iv} = \frac{3x\,(3-2x^2)}{(1+x^2)^{7/2}}$	$y_o^{iv} = o$
$y^{v} = \frac{(9-72x^2+24x^4)}{(1+x^2)^{9/2}}$	$y_o^{v} = +9$

$$y^{vi} = \frac{-15x[15-40x^2+8x^4]}{(1+x^2)^{11/2}} \qquad y_o^{vi} = 0$$

$$y^{vii} = \frac{720x^6-5400x^4+4050x^2-225}{(1+x^2)^{13/2}} \qquad y_o^{vii} = -225$$

Substituting into the general equation for Maclaurin's expansion we obtain:

$$\sinh^{-1}x = \ln [x+ (1+x^2)^{1/2}] = x - \frac{x^3}{6} + \frac{3}{40} x^5 - \frac{5}{112} x^7$$

Hence, by substituting into Equation (2.14a) by these expansion using only 3 terms, we have:

$$S = \frac{\ell}{16n} \left[(F'+8n) - (F'+8n)^3 + \frac{3}{40} (F'+8n)^5 + (F'+8n) + \frac{(F'+8n)^3}{2} - \frac{(F'+8n)^5}{8}\right.$$

$$\left. - F' + \frac{F'^3}{6} - \frac{3}{40} F'^5 - F' - \frac{F'^3}{2} + \frac{F'^5}{8} \right]$$

$$S = \frac{\ell}{16n} \left[16n + \frac{1}{3} [(F'+8n)^3 - F'^3] - \frac{1}{20} [(F'+8n)^5 - F'^5] \right]$$

$$S = \ell \left[1 + \frac{F'^2}{2} + 4nF' + \frac{32}{3} n^2 - \frac{F'^4}{8} - 2nF'^3 - 16n^2F'^2 - 64n^3F' - \frac{512}{5} n^4 \right]$$

Rearranging this expression, we obtain

$$S = \ell \left[1 + \frac{1}{2} (F'+4n)^2 + \frac{8}{3} n^2 - \frac{1}{8} (F'+4n)^4 - 4n^2F'^2 - 32n^3F' - \frac{352}{5} n^4 \right]$$

$$S = \ell \left[1 + \frac{8}{3} n^2 - \frac{32}{5} n^4 + \frac{(F'+4n)^2}{8} [4-32n^2 - (F'+4n)^2] \right]$$

which finally gives the approximate length of the cable at the left hand span to be:

$$S = \ell \left[1 + \frac{8}{3} n^2 (5-12n^2) + \frac{(F'+4n)^2}{8} [4-32n^2 - (F'+4n)^2] \right]$$

A similar approach can be adopted to determine the approximate length of the cable for the right hand span.

APPENDIX 3

3. The Determination of the Exact Relationship Between the Changes in the Span and Cable Lengths

Starting with the expression:

$$\Delta S = \frac{\partial S}{\partial \ell} (\pm \Delta \ell) \qquad \text{(i)}$$

we have:

$$\frac{\partial S}{\partial \ell} = \frac{\partial}{\partial \ell} \left[\frac{\ell}{16n} \left[\sinh^{-1}(F+8n) - \sinh^{-1}F + (F+8n)[1+(F+8n)^2]^{1/2} - F\,[1+F^2]^{1/2} \right] \right]$$

$$\text{where} \quad F = \frac{h+a-4f}{\ell} \quad \text{and} \quad n = \frac{f}{\ell}$$

which yields:

$$\frac{\partial S}{\partial \ell} = \frac{\ell}{16n} \left[\frac{\frac{d(F+8n)}{d\ell}}{[1+(F+8n)^2]^{1/2}} - \frac{\frac{dF}{d\ell}}{[1+F^2]^{1/2}} + \frac{(F+8n)^2}{[1+(F+8n)^2]^{1/2}} \frac{d(F+8n)}{d\ell} \right.$$

$$\left. + [1+(F+8n)^2]^{1/2} \frac{d(F+8n)}{d\ell} - \frac{F^2}{[1+F^2]^{1/2}} \frac{dF}{d\ell} - [1+F^2]^{1/2} \frac{dF}{d\ell} \right]$$

$$+ \frac{1}{8n} \left[\sinh^{-1}(F+8n) - \sinh^{-1}F + (F+8n)\,[1+(F+8n)^2]^{1/2} - F\,[1+F^2]^{1/2} \right]$$

$$\frac{\partial S}{\partial \ell} = \frac{\ell}{8n} \left[[1+(F+8n)^2]^{1/2} \frac{d(F+8n)}{d\ell} - [1+F^2]^{1/2} \frac{dF}{d\ell} \right] + \frac{1}{8n} \left[\sinh^{-1}(F+8n) - \right.$$

$$\left. \sinh^{-1}F + (F+8n)\,[1+(F+8n)^2]^{1/2} - F\,[1+F^2]^{1/2} \right]$$

$$\frac{\partial S}{\partial \ell} = \frac{1}{8n} \left[\sinh^{-1}(F+8n) - \sinh^{-1}F + [1+(F+8n)^2]^{1/2} \left[\ell \frac{d(F+8n)}{d\ell} + (F+8n) \right] \right.$$

$$\left. - [1+F^2]^{1/2} \left[\ell \frac{dF}{d\ell} + F \right] \right] \qquad \text{(ii)}$$

But:

$$\ell \frac{d(F+8n)}{d\ell} = \ell \frac{d}{d\ell}\left[\frac{h+a+4f}{\ell}\right] = -\frac{h+a+4f}{\ell} = -(F+8n)$$

$$\ell \frac{dF}{d\ell} = \ell \frac{d}{d\ell}\left[\frac{h+a-4f}{\ell}\right] = -\frac{h+a-4f}{\ell} = -F$$

Substituting by these values into expression (ii) gives:

$$\frac{\partial S}{\partial \ell} = \frac{1}{8n} \ln\left[\frac{(F+8n)+\left[1+(F+8n)^2\right]^{1/2}}{F+\left[1+F^2\right]^{1/2}}\right] \qquad \text{(iii)}$$

Hence, from equation (i) we have the final relationship between $\Delta\ell$ and ΔS as follows:

$$\Delta S = \frac{(\pm\Delta\ell)}{8n} \ln\left[\frac{(F+8n)+\left[1+(F+8n)^2\right]^{1/2}}{F+\left[1+F^2\right]^{1/2}}\right] \qquad \text{(iv)}$$

A similar procedure can be undertaken to determine the exact relationship between the changes in the span and cable lengths for the right hand span.

APPENDIX 4

4. The Determination of the Approximate Relationship Between the Changes in the Span and Cable Lengths

From Appendix 2, we have the approximate length of the cable:

$$S = \ell \left[1 + \frac{8}{3} n^2 - \frac{32}{5} n^4 + \frac{(F+4n)^2}{8} [4-32n^2 (F+4n)^2]\right]$$

Hence,

$$\frac{\partial S}{\partial \ell} = \ell \left[- \frac{16}{3} \frac{n^2}{\ell} + \frac{128}{5} \frac{n^4}{\ell} + \frac{(F+4n)^2}{8} \left[64 \frac{n^2}{\ell} + 2 \frac{(F+4n)^2}{\ell}\right] - \frac{(F+4n)^2}{4\ell}\right.$$

$$\left. [4-32n^2 - (F+4n)^2]\right] + 1 + \frac{8}{3} n^2 - \frac{32}{5} n^4 + \frac{(F+4n)^2}{8} [4-32n^2 - (F+4n)^2]$$

$$\frac{\partial S}{\partial \ell} = 1 - \frac{8}{3} n^2 + \frac{96}{5} n^4 - \frac{(F+4n)^2}{8} [4-32n^2 - (F+4n)^2 - 64n^2 - 2 (F+4n)^2]$$

Thus, substituting into expression (i) Appendix 3, we obtain:

$$\Delta S = \left[1 - \frac{8}{15} n^2 (5-36n^2) - \frac{(F+4n)^2}{8} [4-96n^2 - 3 (F+4n)^2]\right] (\pm \Delta \ell)$$

A similar procedure can be applied for the right hand span.

APPENDIX 5

5. The Determination of the Exact Relationship Between the Changes in the Span Length and the Cable Sag

The derivative of cable exact length equation with respect to the cable sag f is:

$$\frac{\partial S}{\partial f} = \frac{\ell}{16n}\left[\frac{\frac{d(F+8n)}{df}}{[1+(F+8n)^2]^{1/2}} - \frac{\frac{dF}{df}}{[1+F^2]^{1/2}} + \frac{(F+8n)^2}{[1+(F+8n)^2]^{1/2}}\frac{d(F+8n)}{df}\right.$$

$$\left. + [1+(F+8n)^2]^{1/2}\ \frac{d(F+8n)}{df} - \frac{F^2}{[1+F^2]^{1/2}}\ \frac{dF}{df} - [1+F^2]^{1/2}\frac{dF}{df}\right]$$

$$-\frac{1}{16n^2}\left[\sinh^{-1}(F+8n) - \sinh^{-1}F + (F+8n)\,[1+(F+8n)^2]^{1/2} - F\,[1+F^2]^{1/2}\right]$$

which yields:

$$\frac{\partial S}{\partial f} = \frac{\ell}{8n}\left[\,[1+(F+8n)^2]^{1/2}\ \frac{d(F+8n)}{df} - [1+F^2]^{1/2}\frac{dF}{df}\,\right] - \frac{1}{16n^2}\left[\,\sinh^{-1}\,(F+8n)\right.$$

$$\left. - \sinh^{-1}F + (F+8n)\,[1+(F+8n)^2]^{1/2} - F\,[1+F^2]^{1/2}\,\right]$$

But, we have:

$$\frac{d(F+8n)}{df} = \frac{d}{df}\left(\frac{h+a+4f}{\ell}\right) = +\frac{4}{\ell}$$

$$\frac{dF}{df} = \frac{d}{df}\left(\frac{h+a-4f}{\ell}\right) = -\frac{4}{\ell}$$

Substituting these values into the above expression gives:

$$\frac{\partial S}{\partial f} = -\frac{1}{16n^2}\left[\sinh^{-1}(F+8n) - \sinh^{-1}F + [1+(F+8n)^2]^{1/2}[F+8n-8n] - [1+F^2]^{1/2}[F+8n]\right]$$

$$\frac{\partial S}{\partial f} = \frac{-1}{16n^2}\left[\ln\left(\frac{(F+8n)+\,[1+(F+8n)^2]^{1/2}}{F+\,[1+F^2]^{1/2}}\right) + F\,[1+(F+8n)^2]^{1/2} - (F+8n)\,[1+F^2]^{1/2}\right]$$

Substituting this expression into the basic formula:

$$\Delta f = \frac{\partial S/\partial \ell}{\partial S/\partial f} \; (\pm \Delta \ell)$$

which yields:

$$\Delta f = \frac{2n}{\left[\left[\dfrac{(F+8n)\;[1+F^2]^{1/2} - F\;[1+(F+8n)^2]^{1/2}}{\left[\dfrac{(F+8n) + [1+(F+8n)^2]^{1/2}}{F + [1 + F^2]^{1/2}}\right]}\right] - 1\right]} \; (\pm \Delta \ell)$$

A similar procedure can be employed for the right hand span.

APPENDIX 6

6. The Approximate Relationship Between the Changes in the Span Length and the Cable Sag

The derivative of the cable approximate length equation with respect to the cable sag f is:

$$\frac{\partial S}{\partial f} = \frac{\partial}{\partial f}\left[\ell\left[1 + \frac{8}{15}n^2(5-12n^2) + \frac{(F+4n)^2}{8}[4-32n^2-(F+4n)^2]\right]\right]$$

$$\frac{\partial S}{\partial f} = \ell\left[\frac{16}{3}\frac{n}{\ell} - \frac{128}{5}\frac{n^3}{\ell} - 8\frac{n}{\ell}(F+4n)^2\right]$$

where; $\frac{d(F+4n)}{df} = \frac{d}{df}\left(\frac{h+a}{\ell}\right) = o$

$$\frac{\partial S}{\partial f} = \frac{8}{15}n\left[5\left[2-3(F+4n)^2\right] - 48n^2\right]$$

We then substitute into the basic formula:

$$\Delta f = \frac{\partial S/\partial \ell}{\partial S/\partial f}(\pm \Delta \ell)$$

which gives:

$$\Delta f = \frac{(\pm \Delta \ell)}{64\ n}\left[\frac{[120-64\ n^2[5-36\ n^2] - 15(F+4n)^2[4-96\ n^2 - 3(F+4n)^2]]}{[5\ [2-3(F+4n)^2] - 48\ n^2]}\right]$$

A similar approach can be adopted for the right hand span.

APPENDIX 7

7. The Determination of the Exact Relationship Between the Changes in the Tower Height and the Cable Length

The exact cable length equation is:

$$S = \frac{\ell}{16n}\left[\sinh^{-1}(F+8n) - \sinh^{-1}F + (F+8n)\,[1+(F+8n)^2]^{1/2} - F\,[1+F^2]^{1/2}\right]$$

Hence, the derivative with respect to the tower height is:

$$\frac{\partial S}{\partial h} = \frac{\ell}{16n}\left[\frac{\frac{d(F+8n)}{dh}}{[1+(F+8n)^2]^{1/2}} + \frac{(F+8n)^2}{[1+(F+8n)^2]^{1/2}}\,\frac{d(F+8n)}{dh} + [1+(F+8n)^2]^{1/2}\right.$$

$$\left.\frac{d(F+8n)}{dh} - \frac{\frac{dF}{dh}}{[1+F^2]^{1/2}} - \frac{F^2}{[1+F^2]^{1/2}}\,\frac{dF}{dh} - [1+F^2]^{1/2}\,\frac{dF}{dh}\right]$$

But,

$$\frac{d(F+8n)}{dh} = \frac{dF}{dh} = \frac{1}{\ell}$$

and the basic formula is:

$$\Delta S = \frac{\partial S}{\partial h}\,(\pm\,\Delta h)$$

Thus, the final expression for ΔS is:

$$\Delta S = \frac{(\pm\,\Delta h)}{8n}\left[\,[1+(F+8n)^2]^{1/2} - [1+F^2]^{1/2}\,\right]$$

A similar procedure can be followed for the right hand span.

APPENDIX 8

8. The Determination of the Relationship Between the Changes in the Cable Tension and Length

From the figure, it is clear that:

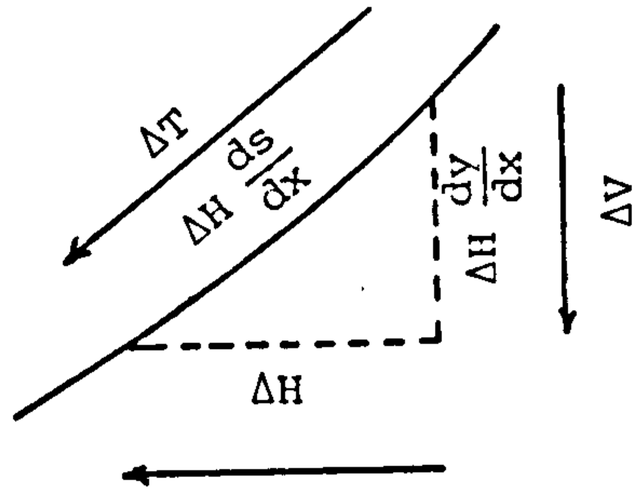

$$\Delta T = \Delta H \frac{ds}{dx}$$

and, $\quad \text{strain} = \frac{\text{stress}}{E_c}$

$$\frac{\Delta S}{ds} = \frac{\Delta T}{A_c E_c} = \frac{\Delta H}{A_c E_c} \frac{ds}{dx}$$

Hence, we have for the left hand span:

$$\Delta S = \frac{\Delta H}{A_c E_c} \int_0^{\ell} \left(\frac{ds}{dx} \right)^2 dx$$

But

$$\left(\frac{ds}{dx} \right)^2 = 1 + \left(\frac{dy}{dx} \right)^2$$

$$\left(\frac{ds}{dx} \right)^2 = 1 + F^2 + \frac{16n}{\ell} F x + \frac{64\ n^2}{\ell^2} x^2$$

Thus;

$$\Delta S = \frac{\Delta H}{A_c E_c} \int_0^{\ell} \left[(1+F^2) + \frac{16n}{\ell} F x + \frac{64\ n^2}{\ell^2} x^2 \right] dx$$

$$\Delta S = \frac{\Delta H}{A_c E_c} \left[(1+F^2)\ x + \frac{8n}{\ell} F x^2 + \frac{64}{3} \frac{n^2}{\ell^2} x^3 \right]_0^{\ell}$$

$$\Delta S = \frac{\Delta H \ell}{A_c E_c} \left[1 + F\ (F+8n) + \frac{64}{3} n^2 \right]$$

A similar expression can be written for the right hand span, hence the total change in the cable tension corresponding to the elastic deformation of the cable is the algebraic sum of the expressions for the two spans, which gives:

$$\Delta H = \frac{A_c E_c}{\ell} \left[\frac{\Delta S}{\left[1+F(F+8n) + \frac{64}{3} n^2 \right]} + \frac{\Delta S_1}{\lambda \left[1+F_1\ (F_1+8n_1) + \frac{64}{3} n_1^2 \right]} \right]$$

APPENDIX 9

9. The Determination of the Term δ_{bm}

$$\delta_{bm} = \sum \int \frac{m_x^2}{EI} dx$$

Hence,

$$\delta_{bm} = \frac{1}{EI} \left[\int_0^{\ell} m_x^2 \, dx + \int_0^{\ell_1} m_{x1}^2 \, dx \right]$$

where m_x and m_{x1} are given in Equations (2.42). Thus, we have:

$$\int_0^{\ell} m_x^2 \, dx = \int_0^{\ell} \left[\frac{4f}{\ell^2} (\ell x - x^2) - (\bar{m}+a) \frac{x}{\ell} + a \right]^2 dx$$

$$= \int_0^{\ell} \left[\frac{16f^2}{\ell^4} (\ell^2 x^2 - 2\ell x^3 + x^4) + (\bar{m}+a)^2 \frac{x^2}{\ell^2} + a^2 - \frac{8f}{\ell^3} (\bar{m}+a) \right.$$

$$\left. (\ell x^2 - x^3) + \frac{8f}{\ell^2} a (\ell x - x^2) - 2a (\bar{m}+a) \frac{x}{\ell} \right] dx$$

$$= \left[\frac{16f^2}{\ell^4} \left(\frac{\ell^2 x^3}{3} - \frac{\ell x^4}{2} + \frac{x^5}{5} \right) + (\bar{m}+a)^2 \frac{x^3}{3\ell^2} + a^2 x - \frac{8f}{\ell^3} (\bar{m}+a) \right.$$

$$\left. \left(\frac{\ell x^3}{3} - \frac{x^4}{4} \right) + \frac{8f}{\ell^2} a \left(\frac{\ell x^2}{2} - \frac{x^3}{3} \right) - a (\bar{m}+a) \frac{x^2}{\ell} \right]_0^{\ell}$$

$$= \ell \left[\frac{8}{15} f^2 + \frac{1}{3} (\bar{m}^2 + 2\bar{m}a + a^2) + a^2 - \frac{2}{3} f (\bar{m}+a) + \frac{4}{3} fa - a(\bar{m}+a) \right]$$

$$\int_0^{\ell} m_x^2 \, dx = \frac{\ell}{3} \left[\frac{8}{5} f^2 + 2 fa + a^2 + (\bar{m}^2 - \bar{m}a - 2f\bar{m}) \right]$$

Similarly, for the right hand span:

$$\int_0^{\ell_1} m_{x1}^2 \, dx = \frac{\ell_1}{3} \left[\frac{8}{5} f_1^2 + 2 f_1 a + a^2 + (\bar{m}^2 - \bar{m}a - 2f_1\bar{m}) \right]$$

Hence, by summing these expressions, we have:

$$\sum \int \frac{m^2 x}{EI}\, dx = \frac{\ell}{3EI}\left[\frac{8}{5} f^2 + \frac{8}{5}\lambda f_1^2 + 2fa + 2\lambda f_1 a + a^2 + \lambda a^2 + \bar{m}(\bar{m}-a) + \lambda\,\bar{m}(\bar{m}-a) - 2f\bar{m} - 2\lambda f_1 \bar{m}\right]$$

$$= \frac{\ell}{3EI}\left[\frac{8}{5} f^2\,(1+\omega^2\lambda^5) - 2f\,(\bar{m}-a)\,(1+\omega\lambda^3) + (1+\lambda)\,[a^2+\bar{m}(\bar{m}-a)]\right]$$

where $f_1 = \omega\,\lambda^2 f$ (Equation (2.6))

Hence, knowing that $e = \frac{1+\omega\lambda^3}{1+\lambda}$ where e is a constant, we find:

$$\sum \int \frac{m^2 x}{EI}\, dx = \frac{\ell}{3EI}\left[\frac{8}{5} f^2\,(1+\omega^2\lambda^5) + (1+\lambda)\,[a^2 + (\bar{m}-a)\,(\bar{m}-2fe)]\right]$$

Substituting by $\bar{m} = fe + \frac{a}{2}$ gives:

$$\delta_{bm} = \frac{\ell}{3EI}\,(1+\lambda)\left[\frac{8}{5} f^2\,\frac{(1+\omega^2\lambda^5)}{(1+\lambda)} + a^2 - \left(fe - \frac{a}{2}\right)^2\right]$$

From which, we arrive to the final expression for δ_{bm}:

$$\delta_{bm} = \frac{\ell(1+\lambda)}{3\,EI}\left[\frac{8}{5} f^2\,\frac{(1+\omega^2\lambda^5)}{(1+\lambda)} - (fe - \frac{3}{2}\,a)\,(fe + \frac{a}{2})\right] .$$

APPENDIX 10

10. The Determination of the Exact Expression for the Term δ_c

We know that:

$$\delta_c = \frac{1}{A_c E_c} \sum \int \left(\frac{ds}{dx} \right)^3 dx$$

and:

$$\int_o^{\ell} \left(\frac{ds}{dx} \right)^3 dx = \int_o^{\ell} \left[1 + \left(\frac{dy}{dx} \right)^2 \right]^{3/2} dx \qquad \text{(i)}$$

where $\frac{dy}{dx} = F + \frac{8n}{\ell} x$

Hence, to determine this integration, we use a similar approach to that used in Appendix 1 as follows:

let $\xi = \frac{dy}{dx} = F + \frac{8n}{\ell} x$

hence $dx = \frac{\ell}{8n} d\xi$ where ξ is a variable.

Thus, we find at $x = o$ $\xi = F$

$x = \ell$ $\xi = F+8n$

Substituting by these quantities, equation (i) becomes:

$$\int_o^{\ell} \left(\frac{ds}{dx} \right)^3 dx = \frac{\ell}{8n} \int_F^{F+8n} \left[1 + \xi^2 \right]^{3/2} d\xi \qquad \text{(ii)}$$

To solve this simplified integration,

let $\xi = \sinh \phi$ $d\xi = \cosh \phi \, d\phi$

and substitute in equation (ii), we give the following more simplified integration:

$$\int_o^{\ell} \left(\frac{ds}{dx} \right)^3 dx = \frac{\ell}{8n} \int \cosh^4 \phi \, d\phi \qquad \text{(iii)}$$

But $\cosh^2\phi = \frac{1}{2}\,[1+\cosh 2\phi]$

$$\cosh^4\phi = \frac{1}{4}\,[1+ 2\cosh 2\phi + \cosh^2 2\phi]$$

$$= \frac{1}{4}\,\left[1+ 2\cosh 2\phi + \frac{1}{2}\,[1 + \cosh 4\phi]\right]$$

$$\cosh^4\phi = \frac{1}{8}\,\left[3 + 4\cosh 2\phi + \cosh 4\phi\right]$$

Thus, substituting into the equation (iii), we find:

$$\int_0^{\ell} \left(\frac{ds}{dx}\right)^3 dx = \frac{\ell}{64n}\,\left[3\phi + 2\sinh 2\phi + \frac{1}{4}\sinh 4\phi\right]$$

$$= \frac{\ell}{64n}\,\left[3\phi + \frac{\sinh 2\phi}{2}\,(4 + \cosh 2\phi)\right]$$

$$= \frac{\ell}{64n}\,\left[3\phi + \frac{\sinh 2\phi}{2}\,(4 + 2\cosh^2\phi - 1)\right]$$

$$= \frac{\ell}{64n}\,\left[3\phi + \sinh\phi\ \text{cash}\ \phi\ (5+2\sinh^2\phi)\right]$$

$$\int_0^{\ell} \left(\frac{ds}{dx}\right)^3 dx = \frac{\ell}{64n}\,\left[3\phi + \sinh\phi\,[1 + \sinh^2\phi]^{1/2}\,(5+2\sinh^2\phi)\right] \quad \text{(iv)}$$

Hence, substituting by ϕ in terms of ξ into the above equation gives:

$$\int_0^{\ell} \left(\frac{ds}{dx}\right)^3 dx = \frac{\ell}{64n}\,\left[3\sinh^{-1}\xi + \xi\,[1+\xi^2]^{1/2}(5+2\xi^2)\right]_F^{F+8n}$$

$$= \frac{\ell}{64n}\,\left[3\left(\sinh^{-1}(F+8n) - \sinh^{-1}F\right) + (F+8n)\,[1+(F+8n)^2]^{1/2}\right.$$

$$\left.[5+2(F+8n)^2] - F\,[1+F^2]^{1/2}(5+2F^2)\right]$$

Similarly for the right hand span the expression for $\int_0^{\ell_1} \left(\frac{ds_1}{dx_1}\right)^3 dx_1$ can be written. Consequently, the final expression for δ_c is obtained by summing the two expressions as follows:

$$\delta_c = \frac{\ell}{64nA_cE_c}\left[3\ \ln\left(\frac{F+8n+[1+(F+8n)^2]^{1/2}}{F+[1+F^2]^{1/2}}\right) + (F+8n)\ [1+(F+8n)^2]^{1/2}[5+2(F+8n)^2]\right.$$

$$- F\ [1+F^2]^{1/2}(5+2F^2) + \frac{1}{\omega}\left[3\ \ln\left(\frac{(F_1+8n_1)+[1+(F_1+8n_1^2)^{1/2}]}{F_1+[1+F_1^2]^{1/2}}\right)\right.$$

$$\left.\left.+ (F_1+8n_1)\ [1+(F_1+8n_1)^2]^{1/2}\ [5+2\ (F_1+8n_1)^2] - F_1\ [1+F_1^2]^{1/2}(5+2F_1^2)\right]\right]$$

where $\dfrac{\ell_1 n}{\ell\ n_1} = \dfrac{\lambda^2 f}{\omega\ \lambda^2 f} = \dfrac{1}{\omega}$

and $\omega = \dfrac{W_1}{W}$

APPENDIX 11

11. The Determination of the Approximate Expression for the Term δ_c

By virtue of Maclaurin's formulae for expansions, see Appendix 2, the series expansion of the following expression is:

$$3\sinh^{-1}x + x\,[1+x^2]^{1/2}(5+2x^2) = 3\left[x - \frac{x^3}{6} + \frac{3}{40}x^5\right] + (5+2x^2)\left[x + \frac{x^2}{2} - \frac{x^3}{8}\right]$$

$$= 8x + 4x^3 + \frac{3}{5}x^5 - \frac{x^7}{4}$$

where x^7 can be ignored. Hence, substituting in the expression for the left hand span:

$$\int_0^{\ell}\left(\frac{ds}{dx}\right)^3 dx = \frac{\ell}{64n}\left[8\,(F+8n) + 4(F+8n)^3 + \frac{3}{5}(F+8n)^5 - 8F - 4F^3 - \frac{3}{5}F^5\right]$$

$$= \frac{\ell}{64n}\left[64n + 32n\,(3F^2 + 24nF + 64n) + \frac{24}{5}n\,(5F^4 + 80nF^3 + 640\,n^2F^2 + 2560\,n^3F + 4096\,n^4)\right]$$

$$= \ell\left[1 + \frac{3}{2}(F+4n)^2 + 8n^2 + \frac{3}{8}(F+4n)^4 + 12n^2F^2 + 96n^3F + \frac{1056}{5}n^4\right]$$

$$= \ell\left[1 + \frac{3}{2}(F+4n)^2 + 8n^2 + \frac{3}{8}(F+4n)^4 + 12n^2\,(F^2 + 8nF + 16n^2) + \frac{96}{5}n^4\right]$$

$$\int_0^{\ell}\left(\frac{ds}{dx}\right)^3 dx = \ell\left[1 + \frac{3}{8}(F+4n)^2\left[4 + 32n^2 + (F+4n)^2\right] + \frac{8}{5}n^2\,(5 + 12n^2)\right]$$

Similarly, for the right hand span cable, we have:

$$\int_0^{\ell_1} \left(\frac{ds_1}{dx_1} \right)^3 dx_1 = \ell_1 \left[1 + \frac{3}{8} (F_1+4n_1)^2 \left[4 + 32n_1^2 + (F_1+4n_1)^2 \right] + \frac{8}{5} n_1^2 \right.$$

$$\left. (5+12n_1^2) \right]$$

By summing the two expressions and considering:

$$\lambda = \frac{\ell_1}{\ell} \quad , \quad \frac{(F_1+4n_1)}{(F+4n)} = \frac{1}{\lambda} \quad \text{and} \quad \frac{n_1}{n} = \omega\lambda$$

we arrive to the final approximate formulae for the term δ_c:

$$\delta_c = \frac{\ell}{A_c E_c} \left[(1+\lambda) + \frac{3}{8} \frac{(F+4n)^2}{\lambda^3} \left[4\lambda^2 (1+\lambda) + 32\lambda^3 n^2 (1+\omega^2\lambda) \right.\right.$$

$$\left.\left. + (F+4n)^2 (1+\lambda^3) \right] + \frac{8}{5} n^2 \left[5 (1+\omega^2\lambda^3) + 12n^2 (1+\omega^4\lambda^5) \right] \right]$$

APPENDIX 12

12. The Determination of the Discrepancy Δ for a General Case of Loading

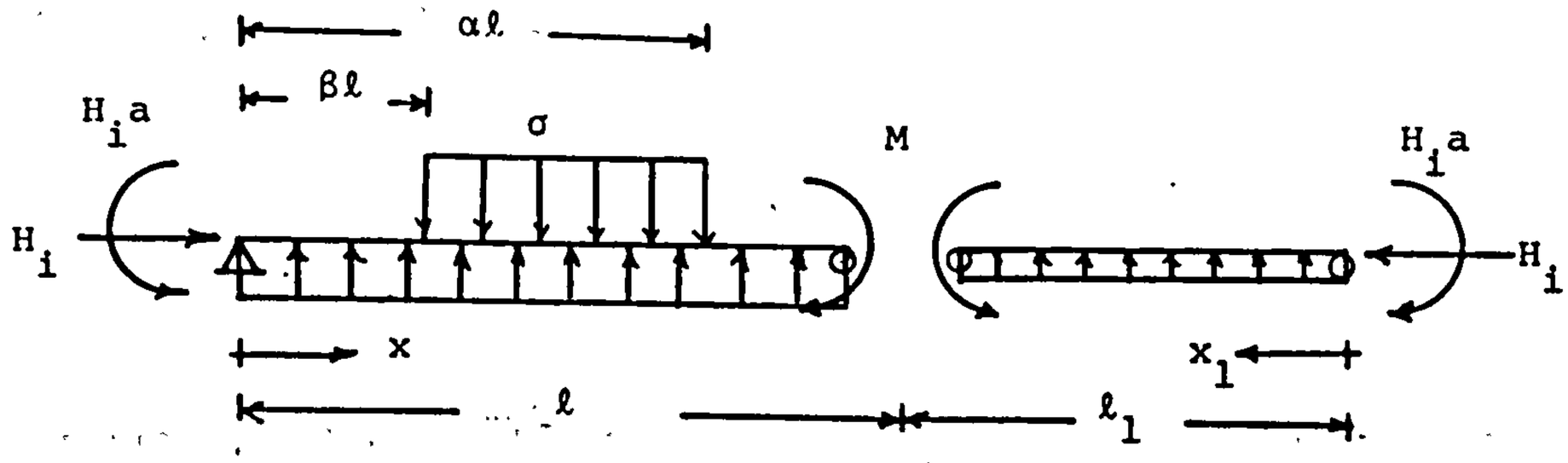

The above figure shows the forces applied on the suspended beam when separated from the main cable. Because of the complexity of the shown case of loading, the general loading σ will be studied separately from the other applied loads. Then, the different equations will be superimposed to determine the final value of the moment at the intermediate support M

and the gap Δ, $= -\sum \int \frac{M_x \, m_x}{EI} dx$.

1. For the General Load σ

The bending moments produced by σ in the left hand span can be evaluated from the following equations, (1):

$$M_{x(1)\sigma} = - H_i \eta_{1\sigma} - \frac{\sigma \ell}{2} (\alpha-\beta) [2- (\alpha+\beta)] x \qquad 0 \leqslant x \leqslant \beta\ell$$

$$M_{x(2)\sigma} = - H_i \eta_{2\sigma} - \frac{\sigma \ell}{2} (\alpha-\beta) [2- (\alpha+\beta)] x + \frac{\sigma}{2} (x-\beta\ell)^2 \qquad \beta\ell \leqslant x \leqslant \alpha\ell$$

$$M_{x(3)\sigma} = - H_i \eta_{3\sigma} - \frac{\sigma \ell}{2} (\alpha-\beta) [2- (\alpha+\beta)] x + \frac{\sigma \ell}{2} (\alpha-\beta) [2x-\ell (\alpha+\beta)]$$

$$\alpha\ell \leqslant x \leqslant \ell$$

where H_i is the initial prestressing force.

Hence, knowing that $M_x = EI \frac{d^2\eta}{dx^2}$, we obtain the following equations:

$$\frac{d^2\eta_{1\sigma}}{d_2x^2} + \mu_i^2 \eta_{1\sigma} = -\frac{\sigma l}{2EI}(\alpha-\beta)[2-(\alpha+\beta)]x \qquad o \leqslant x \leqslant \beta l$$

$$\frac{d^2\eta_{2\sigma}}{d\,x^2} + \mu_i^2 \eta_{2\sigma} = -\frac{\sigma l}{2EI}(\alpha-\beta)[2-(\alpha+\beta)]x + \frac{\sigma}{2EI}(x-\beta l)^2 \qquad \beta l \leqslant x \leqslant \alpha l$$

$$\frac{d^2\eta_{3\sigma}}{d\,x^2} + \mu_i^2 \eta_{3\sigma} = -\frac{\sigma l}{2EI}(\alpha-\beta)[2-(\alpha+\beta)]x + \frac{\sigma l}{2EI}(\alpha-\beta)[2x-l(\alpha+\beta)]$$

$$\alpha l \leqslant x \leqslant l$$

where $\mu_i^2 = \frac{H_i}{EI}$

The solution of these differential equations consists of two parts as follows:

General Solution = Complementary function + particular integral

Thus, to determine the first part of the general solution, we consider the left side of the equations alone and substitute $\eta_{C.F} = A' e^{ax}$ where A' and a are constants, (1). Thus, we have:

$$a^2 A' e^{ax} + \mu_i^2 A' e^{ax} = o$$

$$A' e^{ax}[a^2 + \mu_i^2] = o \qquad A' e^{ax} \neq o$$

Thus, $a = \pm i \mu_i$

Hence,

$$\eta_{C.F} = A_1' e^{i\mu_i x} + A_2' e^{-i\mu_i x}$$

$$= A_1' (\cos \mu_i x + i \sin \mu_i x) + A_1^2 (\cos \mu_i x - i \sin \mu_i x)$$

$$= [i (A_1' - A_2')] \sin \mu_i x + [A_1' + A_2'] \cos \mu_i x$$

$$\eta_{C.F} = A \sin \mu_i x + B \cos \mu_i x$$

Where A and B are constants to be evaluated from the boundary conditions. Obviously, different constants must be used for each of the three equations.

To determine the second part of the general solution, we substitute $\eta_{p.I} = A_1'' x^2 + A_2'' x + A_3''$ into each of the three equations which gives for the first equation:

$$2 A_1'' + \mu_i^2 [A_1'' x^2 + A_2'' x + A_3''] = - \frac{\sigma \ell}{2EI} (\alpha-\beta) [2-(\alpha+\beta)] x$$

By comparing the coefficients of x^2, x and absolute term on both sides of the equation, we determine the constants A_1'', A_2'' and A_3'' as follows:

$$A_1'' = o$$

$$A_2'' = - \frac{\sigma \ell}{2H_i} (\alpha-\beta) [2-(\alpha+\beta)]$$

$$A_3'' = o$$

And the general solution for the first equation is

$$\eta_{1\sigma} = A \sin \mu_i x + B \cos \mu_i x - \frac{\sigma \ell}{2H_i} (\alpha-\beta) [2-(\alpha+\beta)] x \qquad o \leqslant x \leqslant \beta\ell$$

Similarly, for the other two equations:

$$\eta_{2\sigma} = C \sin \mu_i x + D \cos \mu_i x - \frac{\sigma \ell}{2H_i} (\alpha-\beta) [2-(\alpha+\beta)] x + \frac{\sigma}{2H_i} (x-\beta\ell)^2 - \frac{\sigma}{\mu_i^2 H_i}$$

$$\beta\ell \leqslant x \leqslant \alpha\ell$$

$$\eta_{3\sigma} = E \sin \mu_i x + F \cos \mu_i x - \frac{\sigma \ell}{2H_i} (\alpha-\beta) [2-(\alpha+\beta)] x + \frac{\sigma \ell}{2H_i} (\alpha-\beta) [2x-\ell (\alpha+\beta)]$$

$$\alpha\ell \leqslant x \leqslant \ell$$

Where the constants A, B, C, D, E and F can be determined by considering the boundary conditions as follows:

a. at $x = o$ $\quad \eta_{1\sigma} = o$

b. at $x = \beta\ell$ $\quad \eta_{1\sigma} = \eta_{2\sigma}$

c. at $x = \beta\ell$ $\quad \frac{d\eta_{1\sigma}}{dx} = \frac{d\eta_{2\sigma}}{dx}$

d. at $x = \alpha\ell$ $\quad \eta_{2\sigma} = \eta_{3\sigma}$

e. at $x = \alpha\ell$ $\quad \frac{d\eta_{2\sigma}}{dx} = \frac{d\eta_{3\sigma}}{dx}$

f. at $x = \ell$ $\quad \eta_{3\sigma} = o$

} which gives 6 equations in 6 unknowns as follows.

a. at $x = o$ $\quad \eta_{1\sigma} = o$

$$B = o$$

b. at $x = \beta\ell$ $\quad \eta_{1\sigma} = \eta_{2\sigma}$

From which, we arrive to the equation:

$$A \sin \mu_i \beta\ell = C \sin \mu_i \beta\ell + D \cos \mu_i \beta\ell - \frac{\sigma}{\mu_i^2 H_i} \qquad (i)$$

c. at $x = \beta\ell$ $\quad \frac{d\eta_{1\sigma}}{dx} = \frac{d\eta_{2\sigma}}{dx}$

which yields;

$$A \cos \mu_i \beta\ell = C \cos \mu_i \beta\ell - D \sin \mu_i \beta\ell \qquad (ii)$$

From equations (i) and (ii)

$$D = \frac{\sigma}{\mu_i^2 H_i} \cos \mu_i \beta\ell \qquad (iii)$$

d. at $x = \alpha\ell$ $\quad \eta_{2\sigma} = \eta_{3\sigma}$

$$C \sin \mu_i \alpha\ell + D \cos \mu_i \alpha\ell - \frac{\sigma}{\mu_i^2 H_i} = E \sin \mu_i \alpha\ell + F \cos \mu_i \alpha\ell \qquad (iv)$$

e. at $x = \alpha\ell$ $\quad \frac{d\eta_{2\sigma}}{dx} = \frac{d\eta_{3\sigma}}{dx}$

$$C \cos \mu_i \alpha \ell + D \sin \mu_i \alpha \ell = E \cos \mu_i \alpha \ell - F \sin \mu_i \alpha \ell \qquad \text{(v)}$$

From equations (iv) and (v)

$$F = \frac{\sigma}{\mu_i^2 H_i} (\cos \mu_i \beta \ell - \cos \mu_i \alpha \ell) \qquad \text{(vi)}$$

f. at $x = \ell$ $\eta_{3\sigma} = o$ and from Equation (iv)

$$E = - \frac{\sigma}{\mu_i^2 H_1} \frac{\cos \mu_i \ell}{\sin \mu_i \ell} (\cos \mu_i \beta \ell - \cos \mu_i \alpha \ell) \qquad \text{(vii)}$$

Substituting in Equation (v)

$$C = \frac{\sigma}{\mu_i^2 H_i} \frac{1}{\sin \mu_i \ell} [\cos \mu_i \ell(1-\alpha) - \cos \mu_i \ell \cos \mu_i \beta \ell] \qquad \text{(viii)}$$

Substituting in Equations (i) by Equations (viii) and (iii)

$$A = \frac{\sigma}{\mu_i^2 H_i} \frac{1}{\sin \mu_i \ell} [\cos \mu_i \ell(1-\alpha) - \cos \mu_i \ell(1-\beta)] \qquad \text{(ix)}$$

Substituting from Equations (i), (iii), (vi), (vii), (viii) and (ix) into the deflection equations we obtain:-

$$\eta_{1\sigma} = \frac{\sigma}{\mu_i^2 H_i} \left[[\cos \mu_i \ell(1-\alpha) - \cos \mu_i \ell(1-\beta)] \frac{\sin \mu_i x}{\sin \mu_i \ell} - \frac{\mu_i^2 \ell^2}{2} (\alpha-\beta)[2-(\alpha+\beta)] \frac{x}{\ell} \right] \qquad o \leqslant x \leqslant \beta\ell$$

$$\eta_{2\sigma} = \frac{\sigma}{\mu_i^2 H_i} \left[\cos \mu_i \ell(1-\alpha) \frac{\sin \mu_i x}{\sin \mu_i \ell} + \cos \mu_i \beta \ell \frac{\sin \mu_i (\ell-x)}{\sin \mu_i \ell} - 1 - \frac{\mu_i^2 \ell^2}{2} \left[(\alpha-\beta)[2-(\alpha+\beta)] \frac{x}{\ell} - \left(\frac{x}{\ell} - \beta \right)^2 \right] \right] \qquad \beta\ell \leqslant x \leqslant \alpha\ell$$

$$\eta_{3\sigma} = \frac{\sigma}{\mu_i^2 H_i} \left[(\cos \mu_i \beta \ell - \cos \mu_i \alpha \ell) \frac{\sin \mu_i (\ell-x)}{\sin \mu_i \ell} - \frac{\mu_i^2 \ell^2}{2} (\alpha^2-\beta^2) \left(1 - \frac{x}{\ell}\right) \right] \qquad \alpha\ell \leqslant x \leqslant \ell$$

2. For the Upward Distributed Forces (yW and yW_1)

For the Left Hand Span

The deflection equation can be directly obtained by substituting, $\sigma = -yW$, $\alpha = 1$ and $\beta = o$ in the deflection equation for the general loading at the region $\beta\ell \leqslant x \leqslant \alpha\ell$ which gives:

$$\eta_w = \frac{-yW}{\mu_i^2 H_i}\left[\frac{\sin \mu_i x}{\sin \mu_i \ell} + \frac{\sin \mu_i(\ell-x)}{\sin \mu_i \ell} - 1 - \frac{\mu_i^2 x}{2}(\ell-x)\right] \quad o \leqslant x \leqslant \ell$$

Similarly for the right hand span,

$$\eta_{1w} = \frac{-yW_1}{\mu_i^2 H_i}\left[\frac{\sin \mu_i x_1}{\sin \mu_i \ell_1} + \frac{\sin \mu_i(\ell_1-x_1)}{\sin \mu_i \ell_1} - 1 - \frac{\mu_i^2 x_1}{2}(\ell_1-x_1)\right]$$

$$o \leqslant x_1 \leqslant \ell_1$$

3. For the Applied Moments (M and $H_i a$)

Starting with the Left Hand Span, we have:

$$M_{xm} = -H_i \eta_m + H_i a\left(1 - \frac{x}{\ell}\right) + M\frac{x}{\ell} \qquad o \leqslant x \leqslant \ell$$

by substituting $M_{xm} = EI\dfrac{d^2\eta_m}{dx^2}$ and carrying out the aforementioned procedure, we obtain:

$$\eta_m = A \sin \mu_i x + B \cos \mu_i x + \frac{M}{H_i}\frac{x}{\ell} + a\left(1 - \frac{x}{\ell}\right)$$

where by using the boundary conditions, $\eta_m = o$ at $x = o, \ell$, we arrive to the final expression for the deflections produced by the applied bending moments:

$$\eta_m = \frac{M}{H_i}\left[\frac{x}{\ell} - \frac{\sin \mu_i x}{\sin \mu_i \ell}\right] + a\left[1 - \left(\frac{x}{\ell} + \frac{\sin \mu_i(\ell-x)}{\sin \mu_i \ell}\right)\right] \quad o \leqslant x \leqslant \ell$$

Similarly, for the right hand span:

$$\eta_{1m} = \frac{M}{H_i}\left(\frac{x_1}{\ell_1} - \frac{\sin \mu_i x_1}{\sin \mu_i \ell_1}\right) + a\left[1 - \left(\frac{x_1}{\ell_1} + \frac{\sin \mu_i(\ell_1 - x_1)}{\sin \mu_i \ell_1}\right)\right]$$

$$o \leqslant x_1 \leqslant \ell_1$$

Thus, the final deflection equations for the case of loading shown in the figure for the left hand span:

$$(\eta)_1 = \eta_m + \eta_{1\sigma} + \eta_w \qquad o \leqslant x \leqslant \beta\ell$$

$$(\eta)_2 = \eta_m + \eta_{2\sigma} + \eta_w \qquad \beta\ell \leqslant x \leqslant \alpha\ell$$

$$(\eta)_3 = \eta_m + \eta_{3\sigma} + \eta_w \qquad \alpha\ell \leqslant x \leqslant \ell$$

and for the right hand span:

$$(\eta_1) = \eta_{1m} + \eta_{1w} \qquad o \leqslant x_1 \leqslant \ell_1$$

The bending moment at the intermediate support M can then be computed by taking advantage of the equal slope to the left and right of the intermediate support. Hence, we have:

$$\frac{d(\eta)_3}{dx}\ (\text{at } x = \ell) = -\frac{d(\eta_1)}{dx}\ (\text{at } x_1 = \ell_1)$$

$$\frac{d(\eta)_3}{dx} = \frac{d\eta_m}{dx} + \frac{d\eta_{3\sigma}}{dx} + \frac{d\eta_w}{dx} = -\frac{d(\eta_1)}{dx_1} = -\frac{d\eta_{1m}}{dx} - \frac{d\eta_{1w}}{dx}$$

$$\frac{d\eta_m}{dx} = \frac{M}{H_i}\left(\frac{1}{\ell} - \mu_i \frac{\cos \mu_i x}{\sin \mu_i \ell}\right) + a\left(-\frac{1}{\ell} + \mu_i \frac{\cos \mu_i(\ell - x)}{\sin \mu_i \ell}\right)$$

<u>at $x = \ell$</u>

$$\frac{d\eta_m}{dx} = \frac{M}{H_i}\ \frac{1}{\ell}\left(1 - \frac{\mu_i \ell}{\tan \mu_i \ell}\right) + a\,\frac{1}{\ell}\left(\frac{\mu_i \ell}{\sin \mu_i \ell} - 1\right)$$

Similarly <u>at $x = \ell_1$</u>

$$\frac{d\eta_{1m}}{dx} = \frac{M}{H_i}\ \frac{1}{\ell_1}\left(1 - \frac{\mu_i \ell_1}{\tan \mu_i \ell_1}\right) + a\,\frac{1}{\ell_1}\left(\frac{\mu_i \ell_1}{\sin \mu_i \ell_1} - 1\right)$$

For the upward distributed load, we have for the left hand span:

$$\frac{d\eta_w}{dx} = \frac{-yW}{\mu_i^2 H_i}\left[\frac{\mu_i \cos \mu_i x}{\sin \mu_i \ell} - \mu_i \frac{\cos \mu_i(\ell-x)}{\sin \mu_i \ell} - \frac{\mu_i^2}{2}(\ell-2x)\right]$$

<u>at $x = \ell$</u>

$$\frac{d\eta_w}{dx} = \frac{-yW}{H_i}\ \frac{\ell}{2}\left[\frac{-2}{\mu_i \ell \sin \mu_i \ell}\ (1 - \cos \mu_i \ell) + 1\right]$$

$$= \frac{yW}{2H_i}\ \ell\left[\frac{\tan \frac{\mu_i \ell}{2}}{\frac{\mu_i \ell}{2}} - 1\right]$$

Similarly, for the right hand span at <u>$x = \ell_1$</u>:

$$\frac{d\eta_{1w}}{dx_1} = \frac{yW}{2H_i}\ \ell_1\left[\frac{\tan \frac{\mu_i \ell_1}{2}}{\frac{\mu_i \ell_1}{2}} - 1\right]$$

For the applied live loading σ, we have:

$$\frac{d\ \eta_{3\sigma}}{dx} = -\frac{\sigma}{\mu_i^2 H_i}\left[\frac{-\mu_i \cos \mu_i(\ell-x)}{\sin \mu_i \ell}(\cos \mu_i \beta\ell - \cos \mu_i \alpha\ell) + \frac{\mu^2 \ell}{2}(\alpha^2-\beta^2)\right]$$

<u>at $x = \ell$</u>

$$\frac{d\ \eta_{3\sigma}}{dx} = -\frac{\sigma\ell}{2H_i}\left[\frac{2\ (\cos \mu_i \beta\ell - \cos \mu_i \alpha\ell)}{\mu_i \ell \sin \mu_i \ell} - (\alpha^2-\beta^2)\right]$$

Hence, by substituting in the equation for the equal slope on both sides of the intermediate support, we obtain:

$$\frac{M}{H_i}\phi_i + a\,\nu_i - \frac{\sigma\ell}{2\ H_i}\left[\frac{2\ (\cos \mu_i \beta\ell - \cos \mu_i \alpha\ell)}{\mu_i \ell \sin \mu_i \ell} - (\alpha^2-\beta^2)\right] + \frac{yW}{2\ H_i}\theta_i$$

$$= -\frac{M}{H_i}\phi_{1i} - a\,\nu_{1i} - \frac{yW_1}{2\ H_i}\theta_1$$

which yields;

$$M = -H_i a \frac{(\nu_i+\nu_{1i})}{(\phi_i+\phi_{1i})} + \frac{\sigma\ell}{2(\phi_i+\phi_{1i})}\left[\frac{2\ (\cos \mu_i \beta\ell - \cos \mu_i \alpha\ell)}{\mu_i \ell \sin \mu_i \ell} - (\alpha^2-\beta^2)\right] - \frac{yW}{2}$$

$$\frac{(\theta_i + \omega\theta_{1i})}{(\phi_i + \phi_{1i})}$$

where,

$$\nu_i = \frac{1}{\ell}\left[\frac{\mu_i \ell}{\sin \mu_i \ell} - 1\right] \qquad \nu_{1i} = \frac{1}{\ell_1}\left[\frac{\mu_i \ell_1}{\sin \mu_i \ell_1} - 1\right],$$

$$\phi_i = \frac{1}{\ell}\left[1 - \frac{\mu_i \ell}{\tan \mu_i \ell}\right] \qquad \phi_{1i} = \frac{1}{\ell_1}\left[1 - \frac{\mu_i \ell_1}{\tan \mu_i \ell_1}\right],$$

$$\theta_i = \ell\left[\frac{\tan \frac{\mu_i \ell}{2}}{\frac{\mu_i \ell}{2}} - 1\right] \qquad \theta_{1i} = \ell_1\left[\frac{\tan \frac{\mu_i \ell_1}{2}}{\frac{\mu_i \ell_1}{2}} - 1\right],$$

and where $\omega = \frac{W_1}{W}$ & $\mu_i^2 = \frac{H_i}{EI}$

Having found M, the next step is to calculate Δ as follows,

$$\Delta = -\sum \int \frac{M_x m_x}{EI} dx = \frac{-1}{EI}\left[\int_0^{\ell} M_x m_x dx + \int_0^{\ell_1} M_{x1} m_{x1} dx_1\right]$$

For simplicity, these integrations can be performed separately for each load, as before, where: (Equations (2.42))

$$m_x = -\left[\frac{4f}{\ell^2} x^2 + \frac{1}{\ell}\left[(fe + \frac{3}{2} a) - 4f\right] x - a\right] \qquad o \leqslant x \leqslant \ell$$

$$m_{x1} = -\left[\frac{4f_1}{\ell^2} x_1^2 + \frac{1}{\ell_1}\left[(fe + \frac{3}{2} a) - 4f_1\right] x_1 - a\right] \qquad o \leqslant x \leqslant \ell_1$$

1. <u>For the applied live loading σ</u>

From the deflection equations, the bending moment equations can be obtained by making use of the following relationship;

$$M_x = EI \frac{d^2\eta}{dx^2}$$

which yields:

$$M_{x(1)\sigma} = -\frac{\sigma}{\mu_i^2}\left[\cos \mu_i \ell(1-\alpha) - \cos \mu_i \ell(1-\beta)\right] \frac{\sin \mu_i x}{\sin \mu_i \ell} \qquad o \leqslant x \leqslant \beta\ell$$

$$M_{x(2)\sigma} = -\frac{\sigma}{\mu_i^2}\left[\cos \mu_i \ell(1-\alpha) \frac{\sin \mu_i x}{\sin \mu_i \ell} + \cos \mu_i \beta\ell \frac{\sin \mu_i(\ell-x)}{\sin \mu_i \ell} - 1\right]$$

$$\beta\ell \leqslant x \leqslant \alpha\ell$$

$$M_{x(3)\sigma} = -\frac{\sigma}{\mu_i^2}\left[\cos \mu_i \beta\ell - \cos \mu_i \alpha\ell\right] \frac{\sin \mu_i(\ell-x)}{\sin \mu_i \ell} \qquad \alpha\ell \leqslant x \leqslant \ell$$

Hence, $\int_o^{\ell} \frac{M_x\, m_x}{EI}\, dx = \frac{1}{EI}\left[\int_o^{\beta\ell} M_{x(1)\sigma}\, m_x\, dx + \int_{\beta\ell}^{\alpha\ell} M_{x(2)\sigma}\, m_x\, dx + \int_{\alpha\ell}^{\ell} M_{x(3)\sigma}\, m_x\, dx\right]$

Thus,

$$\int_o^{\ell} \frac{M_x\, m_x}{EI}\, dx = -\frac{\sigma}{H_i}\left[\cos \mu_i \ell(1-\alpha) \int_o^{\alpha\ell} m_x \frac{\sin \mu_i x}{\sin \mu_i \ell}\, dx - \cos \mu_i \ell(1-\beta) \int_o^{\beta\ell} m_x \frac{\sin \mu_i x}{\sin \mu_i \ell}\, dx + \cos \mu_i \beta\ell \int_{\beta\ell}^{\ell} m_x \frac{\sin \mu_i(\ell-x)}{\sin \mu_i \ell}\, dx - \cos \mu_i \alpha\ell \int_{\alpha\ell}^{\ell} m_x \frac{\sin \mu_i(\ell-x)}{\sin \mu_i \ell}\, dx - \int_{\beta\ell}^{\alpha\ell} m_x\, dx\right]$$

Bearing in mind that:

$$\int_a^b x^2 \sin \mu_i x\, dx = \frac{-1}{\mu_i}\left[x^2 \cos \mu_i x - \frac{2x}{\mu_i} \sin \mu_i x - \frac{2}{\mu_i^2} \cos \mu_i x\right]_a^b$$

$$\int_a^b x \sin \mu_i x\, dx = \frac{-1}{\mu_i}\left[x \cos \mu_i x - \frac{\sin \mu_i x}{\mu_i}\right]_a^b$$

$$\int_a^b x^2 \sin \mu_i(\ell-x)dx = \frac{1}{\mu_i}\left[x^2 \cos \mu_i(\ell-x) + \frac{2x}{\mu_i} \sin \mu_i(\ell-x) - \frac{2}{\mu^2} \cos \mu_i(\ell-x)\right]_a^b$$

$$\int_a^b x \sin \mu_i(\ell-x)\, dx = \frac{1}{\mu_i}\left[x \cos \mu_i(\ell-x) + \frac{\sin \mu_i(\ell-x)}{\mu_i}\right]_a^b$$

The above integration can be divided into the following:

$$\int_o^{\ell} \frac{M_x\, m_x}{EI}\, dx = -\frac{\sigma}{H_i}\left[I_1 + I_2 + I_3 + I_4 + I_5\right]$$

where I_1, I_2, I_3, I_4 and I_5 can easily be found as:-

$$I_1 = \frac{\cos \mu_i \ell(1-\alpha)}{\mu_i \sin \mu_i \ell}\left[\frac{4f}{\ell^2}\left(\alpha^2\ell^2 \cos \mu_i\alpha\ell - \frac{2\alpha\ell}{\mu_i}\sin \mu_i\alpha\ell - \frac{2}{\mu_i^2}\cos \mu_i\alpha\ell + \frac{2}{\mu_i^2}\right)\right.$$

$$\left. + \frac{1}{\ell}\left[\left(fe + \frac{3}{2}a\right) - 4f\right]\left(\alpha\ell \cos \mu_i\alpha\ell - \frac{\sin \mu_i\alpha\ell}{\mu_i}\right) - a\left(\cos \mu_i\alpha\ell - 1\right)\right]$$

$$I_2 = -\frac{\cos \mu_i \ell(1-\beta)}{\mu_i \sin \mu_i \ell}\left[\frac{4f}{\ell^2}\left(\beta^2\ell^2 \cos \mu_i\beta\ell - \frac{2\beta\ell}{\mu_i}\sin \mu_i\beta\ell - \frac{2}{\mu_i^2}\cos \mu_i\beta\ell + \frac{2}{\mu_i^2}\right)\right.$$

$$\left. + \frac{1}{\ell}\left[\left(fe + \frac{3}{2}a\right) - 4f\right]\left(\beta\ell \cos \mu_i\beta\ell - \frac{\sin \mu_i\beta\ell}{\mu_i}\right) - a\left(\cos \mu_i\beta\ell - 1\right)\right]$$

$$I_3 = -\frac{\cos \mu_i\beta\ell}{\mu_i \sin \mu_i\ell}\left[\frac{4f}{\ell^2}\left(\ell^2 - \frac{2}{\mu_i^2} - \beta^2\ell^2 \cos \mu_i\ell(1-\beta) - \frac{2\beta\ell}{\mu_i}\sin \mu_i\ell(1-\beta)\right.\right.$$

$$\left. + \frac{2}{\mu_i^2}\cos \mu_i\ell(1-\beta)\right) + \frac{1}{\ell}\left[\left(fe + \frac{3}{2}a\right) - 4f\right]\left(\ell - \beta\ell \cos \mu_i\ell(1-\beta)\right.$$

$$\left.\left. - \frac{\sin \mu_i\ell(1-\beta)}{\mu_i}\right) - a\left(1 - \cos \mu_i\ell(1-\beta)\right)\right]$$

$$I_4 = \frac{\cos \mu_i\alpha\ell}{\mu_i \sin \mu_i\ell}\left[\frac{4f}{\ell^2}\left[\ell^2 - \frac{2}{\mu_i^2} - \alpha^2\ell^2 \cos \mu_i\ell(1-\alpha) - \frac{2\alpha\ell}{\mu_i}\sin \mu_i\ell(1-\alpha)\right.\right.$$

$$\left. + \frac{2}{\mu_i^2}\cos \mu_i\ell(1-\alpha)\right] + \frac{1}{\ell}\left[\left(fe + \frac{3}{2}a\right) - 4f\right]\left(\ell - \alpha\ell \cos \mu_i\ell(1-\alpha)\right.$$

$$\left.\left. - \frac{\sin \mu_i\ell(1-\alpha)}{\mu_i}\right) - a\left(1 - \cos \mu_i\ell(1-\alpha)\right)\right]$$

$$\dot{I}_5 = \frac{4}{3} f\ell\ (\alpha^3-\beta^3) + \frac{\ell}{2}\left[\frac{3}{2} a - f(4-e)\right]\ (\alpha^2-\beta^2) - a\ell\ (\alpha-\beta)$$

By collecting the different terms, the gap, $\Delta\sigma$, due to the live load alone can be determined as:

$$\Delta_\sigma = \frac{\sigma_\ell}{H_i}\left[\left(\frac{8f}{\mu_i^2\ \ell^2} + a\right)\left[\frac{(\sin\frac{\mu_i\ell}{2}(1-2\beta) - \sin\frac{\mu_i\ell}{2}(1-2\alpha))}{\mu_i\ell\cos\frac{\mu_i\ell}{2}} - (\alpha-\beta)\right]\right.$$

$$- \frac{2}{3} f\ [\alpha^2(3-2\alpha) - \beta^2(3-2\beta)] - (fe + \frac{3}{2} a)\left[\frac{(\cos\mu_i\beta\ell - \cos\mu_i\alpha\ell)}{\mu_i\ell\sin\mu_i\ell}\right.$$

$$\left.\left. - \frac{1}{2}\ (\alpha^2-\beta^2)\right]\right]$$

2. <u>For the upward uniformly distributed load</u>

The gap it produces, Δ_w, can be directly evaluated for the left hand span when substituting $\sigma = -yW$, $\alpha = 1$ and $\beta = o$ into the above expression, which gives:

$$\Delta_w = + \frac{yW}{12\ H_i}\left[\ 2f\ [4\ell + 3\theta_i(e - \frac{16}{\mu_i^2\ \ell^2})] - 3a\ \theta_i\ \right]$$

Similarly <u>for the right hand span</u>:

$$\dot{\Delta}_{w1} = - \frac{yW_1}{12\ H_i}\left[\ 2f_1\ [4\ell_1 + 3\theta_{1i}(\frac{e}{\omega\lambda^2} - \frac{16}{\mu^2\ \ell^2})] - 3a\ \theta_{1i}\ \right]$$

Knowing that $f_1 = \omega\lambda^2 f$ and $\omega = \frac{W_1}{W}$, the sum of the previous two equations can be written as:

$$\Delta_{w+w1} = + \frac{yW}{12\ H_i}\left[\ 2f\ [4\ell\ (1+\omega^2\lambda^3) + 3e\ (\theta_i+\omega\theta_{1i}) - \frac{48}{\mu_i^2\ \ell^2}\right.$$

$$\left.(\theta_i+\omega^2\theta_{1i})] - 3a\ (\theta_i+\omega\theta_{1i})\ \right]$$

3. <u>For the bending moments,</u> we have for the left hand span:

$$M_{xm} = EI \frac{d^2\eta_m}{dx^2} = M \frac{\sin \mu_i x}{\sin \mu_i \ell} + H_i a \frac{\sin \mu_i (\ell - x)}{\sin \mu_i \ell}$$

Hence, integrating this equation multiplied by the equation for m_x over the entire length of the <u>left hand span</u> yields:

$$\Delta_m = + \frac{M}{EI} \left[\frac{4f}{\ell^2} \int_0^\ell x^2 \frac{\sin \mu_i x}{\sin \mu_i \ell} dx + \frac{1}{\ell} \left[\frac{3}{2} a - f(4-e) \right] \int_0^\ell x \frac{\sin \mu_i x}{\sin \mu_i \ell} dx \right.$$

$$\left. - a \int_0^\ell \frac{\sin \mu_i x}{\sin \mu_i \ell} dx \right] + \mu_i^2 a \left[\frac{4f}{\ell^2} \int_0^\ell x^2 \frac{\sin \mu_i (\ell - x)}{\sin \mu_i \ell} dx + \frac{1}{\ell} \right.$$

$$\left. \left[\frac{3}{2} a - f(4-e) \right] \int_0^\ell x \frac{\sin \mu_i (\ell - x)}{\sin \mu_i \ell} dx - a \int_0^\ell \frac{\sin \mu_i (\ell - x)}{\sin \mu_i \ell} dx \right]$$

knowing that,

$$\int_0^\ell x^2 \frac{\sin \mu_i x}{\sin \mu_i \ell} dx = - \frac{1}{\mu_i^2} (\theta_i - \phi_i \ell^2)$$

$$\int_0^\ell x \frac{\sin \mu_i x}{\sin \mu_i \ell} dx = \frac{\phi_i \ell}{\mu_i^2}$$

$$\int_0^\ell \frac{\sin \mu_i x}{\sin \mu_i \ell} dx = \frac{1}{2} (\theta_i + \ell)$$

$$\int_0^\ell x^2 \frac{\sin \mu_i (\ell - x)}{\sin \mu_i \ell} dx = - \frac{1}{\mu_i^2} (\theta_i - \nu_i \ell^2)$$

$$\int_0^\ell x \frac{\sin \mu_i (\ell - x)}{\sin \mu_i \ell} dx = \frac{\nu_i \ell}{\mu_i^2}$$

$$\int_0^{\ell} \frac{\sin \mu_i(\ell-x)}{\sin \mu_i \ell}\, dx = \frac{1}{2} \quad (\theta_i + \ell)$$

We arrive to the final result as:

$$\Delta_m = -\frac{M}{H_i}\left[\frac{4f}{\ell^2}\left(\theta_i - \frac{\phi_i \ell^2}{4} e\right) + \frac{a}{2}\left[\mu_i^2\,(\theta_i+\ell) - 3\phi_i\right]\right] - a\left[\frac{4f}{\ell^2}\left(\theta_i - \frac{\nu_i \ell^2}{4} e\right) + \frac{a}{2}\left[\mu_i^2\,(\theta_i+\ell) - 3\nu_i\right]\right]$$

Similarly, <u>for the right hand span</u>;

$$\Delta_{1m} = -\frac{M}{H_i}\left[\frac{4f_1}{\ell_1^2}\left(\theta_{1i} - \frac{\phi_{1i}\ell^2}{4\omega} e\right) + \frac{a}{2}\left[\mu_i^2\,(\theta_{1i}+\ell_1) - 3\phi_{1i}\right]\right]$$

$$- a\left[\frac{4f_1}{\ell_1^2}\left(\theta_{1i} - \frac{\nu_{1i}\ell^2}{4\omega} e\right) + \frac{a}{2}\left[\mu_i^2\,(\phi_{1i}+\ell_1) - 3\nu_{1i}\right]\right]$$

Thus, the total value of these integrations for both spans is:

$$\Delta_{m+1m} = -\frac{M}{H_i}\left[\frac{4f}{\ell^2}\left[(\theta_i+\omega\theta_{1i}) - (\phi_i+\phi_{1i})\frac{\ell^2 e}{4}\right] + \frac{a}{2}\left[\mu_i^2\left[\ell(1+\lambda)\right.\right.\right.$$

$$\left.\left.\left. + (\theta_i+\theta_{1i})\right] - 3(\phi_i+\phi_{1i})\right]\right] - a\left[\frac{4f}{\ell^2}\left[(\theta_i+\omega\theta_{1i}) - (\nu_i+\nu_{1i})\right.\right.$$

$$\left.\left.\frac{\ell^2 e}{4}\right] + \frac{a}{2}\left[\mu_i^2\left[\ell(1+\lambda) + (\theta_i+\theta_{1i})\right] - 3\,(\nu_i+\nu_{1i})\right]\right]$$

Substituting for the value of M we have:

$$\Delta_{m+1m} = -\left[-a\,(\nu_i+\nu_{1i}) + \frac{\sigma\ell}{H_i}\left[\frac{(\cos \mu_i\beta\ell - \cos \mu_i\alpha\ell)}{\mu_i \ell \sin \mu_i \ell} - \frac{1}{2}(\alpha^2-\beta^2)\right]\right.$$

$$\left. - \frac{yW}{2H_i}(\theta_i+\omega\theta_{1i})\right]\left[\frac{4f}{\ell^2}\left[\frac{(\theta_i+\omega\theta_{1i})}{(\phi_i+\phi_{1i})} - \frac{\ell^2 e}{4}\right] + \frac{a}{2}\right.$$

$$\left[\mu_i^2 \frac{[\ell(1+\lambda) + (\theta_i+\theta_{1i})]}{(\phi_i+\phi_{1i})} - 3\right]\Bigg] - a\left[\frac{4f}{\ell^2}\left[(\theta_i+\omega\theta_{1i}) - (\nu_i+\nu_{1i})\right.\right.$$

$$\left.\left.\frac{\ell^2 e}{4}\right] + \frac{a}{2}\left[\mu_i^2\,[\ell(1+\lambda) + (\theta_i+\theta_{1i})] - 3\,(\nu_i+\nu_{1i})\right]\right]$$

Hence, the final value of the gap Δ can be obtained as:

$$\Delta = \Delta_\sigma + \Delta_{w+w1} + \Delta_{m+1m}$$

From which we obtain:-

$$\Delta = -\frac{a}{2}\left[1 - \frac{(\nu_i+\nu_{1i})}{(\phi_i+\phi_{1i})}\right]\left[\frac{8f}{\ell^2}(\theta_i+\omega\theta_{1i}) + a\,\mu_i^2\,[\ell(1+\lambda) + (\theta_i+\theta_{1i})]\right]$$

$$+ \frac{\sigma\ell}{H_i}\left[\left(\frac{8f}{\mu_i^2\,\ell^2} + a\right)\left[\frac{[\sin\frac{\mu_i\ell}{2}(1-2\beta) - \sin\frac{\mu_i\ell}{2}(1-2\alpha)]}{\mu_i\ell\cos\frac{\mu_i\ell}{2}} - (\alpha-\beta)\right] - \frac{2}{3}f\right.$$

$$[\alpha^2(3-2\alpha) - \beta^2(3-2\beta)] - \frac{\mu_i^2}{2}\frac{(\theta_i+\omega\theta_{1i})}{(\phi_i+\phi_{1i})}\left(\frac{8f}{\mu_i^2\,\ell^2} + a\frac{[\ell(1+i\lambda) + (\theta_i+\theta_{1i})]}{(\theta_i+\omega\theta_{1i})}\right)$$

$$\left(\frac{(\cos\mu_i\beta\ell - \cos\mu_i\alpha\ell)}{\mu_i\ell\sin\mu_i\ell} - \frac{1}{2}(\alpha^2-\beta^2)\right)\Bigg] - \frac{\gamma W}{H_i}\left[\frac{8f}{\ell^2}\left(\frac{1}{\mu_i^2}(\theta_i+\omega^2\theta_{1i})\right.\right.$$

$$\left.\left.- \frac{(\theta_i+\omega\theta_{1i})^2}{4(\phi_i+\phi_{1i})} - \frac{\ell^3}{12}(1+\omega^2\lambda^3)\right) + a\,(\theta_i+\omega\theta_{1i})\left(1 - \frac{\mu_i^2}{4}\frac{[\ell(1+\lambda)+(\theta_i+\theta_{1i})]}{(\phi_i+\phi_{1i})}\right)\right]$$

The same expression can be used to determine the gap Δ for virtually all types of loading. Thus, for a continuous uniformly distributed load σ covering the left hand span, we substitute $\alpha = 1$, $\beta = o$ into this expression which gives:

$$\Delta_\sigma = \frac{\sigma\ell}{H_i}\left[\left(\frac{8f}{\mu_i^2\,\ell^2} + a\right)\left(\frac{\tan\frac{\mu_i\ell}{2}}{\frac{\mu_i\ell}{2}} - 1\right) - \frac{2}{3}f - \frac{\mu_i^2}{4}\frac{(\theta_i+\omega\theta_{1i})}{(\phi_i+\phi_{1i})}\left(\frac{8f}{\mu_i^2\,\ell^2} + a\right.\right.$$

$$\frac{[\ell(1+\lambda) + (\theta_i+\theta_{1i})}{(\phi_i+\omega\phi_{1i})} \Big] \left[\frac{\tan \frac{\mu_i \ell}{2}}{\frac{\mu_i \ell}{2}} - 1 \right] \Bigg]$$

$$\Delta_\sigma = \frac{\sigma}{H_i} \left[\left[\frac{8f}{\mu_i^2 \ell^2} + a \right] \theta_i - \frac{2}{3} f\ell - \frac{\mu_i^2}{4} \quad \theta_i \frac{(\theta_i+\omega\theta_{1i})}{(\phi_i+\phi_{1i})} \left[\frac{8f}{\mu_i^2 \ell^2} + a \right. \right.$$

$$\left. \left. \frac{[\ell(1+\lambda)+(\theta_i+\theta_{1i})]}{(\phi_i+\omega\phi_{1i})} \right] \right]$$

and the final value of Δ can be computed as follows:

$$\Delta = -\frac{a}{2} \left[1 - \frac{(\nu_i+\nu_{1i})}{(\phi_i+\phi_{1i})} \right] \left[\frac{8f}{\ell^2} (\theta_i+\omega\theta_{1i}) + a\,\mu_i^2 [\ell(1+\lambda) + (\theta_i+\theta_{1i})] \right]$$

$$+ \frac{\sigma}{H_i} \left[\frac{8f}{\ell^2} \left[\frac{\theta_i}{\mu_i^2} \left[1 - \frac{\mu_i^2}{4} \frac{(\theta_i+\omega\theta_{1i})}{(\phi_i+\phi_{1i})} \right] - \frac{\ell^3}{12} \right] + a\,\theta_i \left[1 - \frac{\mu_i^2}{4} \right. \right.$$

$$\left. \left. \frac{[\ell(1+\lambda) + (\theta_i+\theta_{1i})]}{(\phi_i+\phi_{1i})} \right] \right] - \frac{yW}{H_i} \left[\frac{8f}{\ell^2} \left[\frac{1}{\mu_i^2} (\theta_i+\omega^2\theta_{1i}) - \frac{(\theta_i+\omega\theta_{1i})^2}{4(\phi_i+\phi_{1i})} - \frac{\ell^3}{12} \right. \right.$$

$$\left. \left. (1+\omega^2\lambda^3) \right] + a\,(\theta_i+\omega\theta_{1i}) \left[1 - \frac{\mu_i^2}{4} \quad \frac{[\ell(1+\lambda) + (\theta_i+\theta_{1i})]}{(\phi_i+\phi_{1i})} \right] \right]$$

For a concentrated load, P, applied in the left hand span, we substitute $\alpha = t+\varepsilon$, $\beta = t-\varepsilon$ and $P = 2\sigma\ell\varepsilon$ where ε is a very small quantity as shown in the figure.

Thus, we have for the gap Δ_σ:

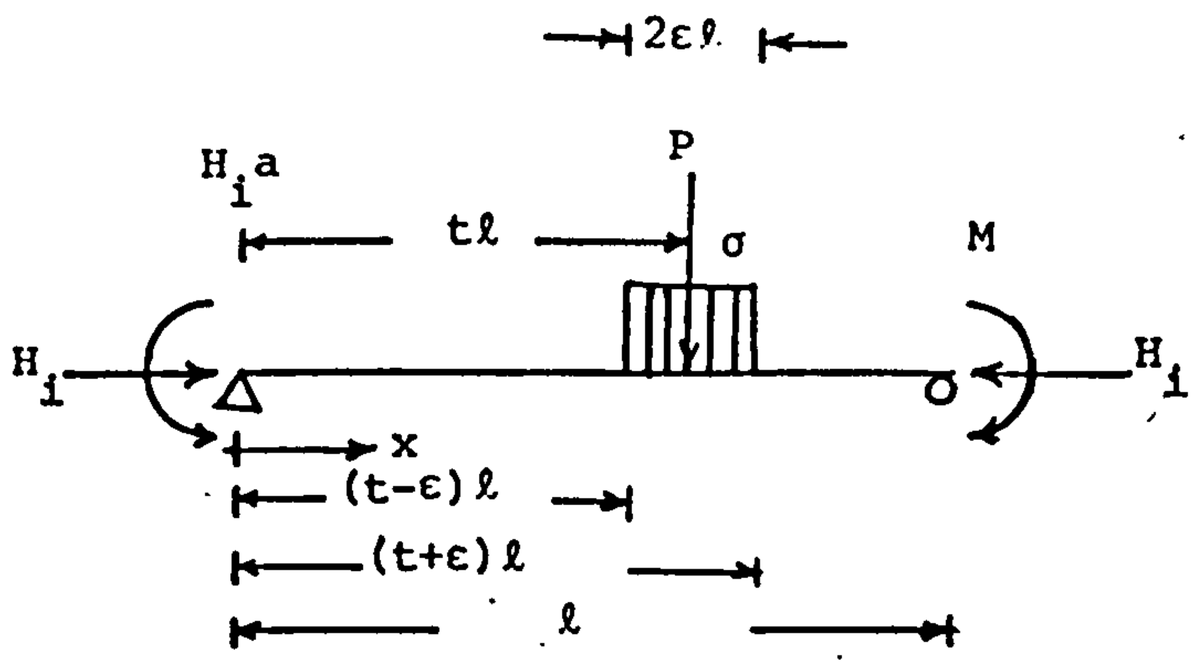

$$\Delta_\sigma = \frac{\sigma\ell}{H_i}\left[\left(\frac{8f}{\mu_i^2\,\ell^2}+a\right)\left(\frac{\sin\frac{\mu_i\ell}{2}[(1-2t)+2\varepsilon]-\sin\frac{\mu_i\ell}{2}[(1-2t)-2\varepsilon]}{\mu_i\ell\ \cos\frac{\mu_i\ell}{2}}-2\varepsilon\right)\right.$$

$$-8ft\varepsilon\,(1-t)-\frac{\mu_i^2}{2}\frac{(\theta_i+\omega\theta_{1i})}{(\phi_i+\phi_{1i})}\left(\frac{8f}{\mu_i^2\,\ell^2}+a\,\frac{[\ell(1+\lambda)+(\theta_i+\theta_{1i})}{(\theta_i+\omega\theta_{1i})}\right)$$

$$\left.\left[\frac{\cos\mu_i\ell(t-\varepsilon)-\cos\mu_i\ell(t+\varepsilon)}{\mu_i\ell\,\sin\mu_i\ell}-2t\varepsilon\right]\right]$$

$$\Delta_\sigma = \frac{2\sigma\ell\varepsilon}{H_i}\left[\left(\frac{8f}{\mu_i^2\,\ell^2}+a\right)\left(\frac{\cos\frac{\mu_i\ell}{2}(1-2t)}{\cos\frac{\mu_i\ell}{2}}-1\right)-4ft\,(1-t)-\frac{\mu_i^2}{2}\frac{(\theta_i+\omega\theta_{1i})}{(\phi_i+\phi_{1i})}\right.$$

$$\left.\left(\frac{8f}{\mu_i^2\,\ell^2}+a\,\frac{[\ell(1+\lambda)+(\theta_i+\theta_{1i})}{(\theta_i+\omega\theta_{1i})}\right)\left(\frac{\sin\mu_i t\ell}{\sin\mu_i\ell}-t\right)\right]$$

where $\sin\mu_i\varepsilon\ell = \mu_i\varepsilon\ell$ and ε^3 is ignored.

Hence, the final value for Δ can be found as:-

$$\Delta = -\frac{a}{2}\left[1-\frac{(\nu_i+\nu_{1i})}{(\phi_i+\phi_{1i})}\right]\left[\frac{8f}{\ell^2}(\theta_i+\omega\theta_{1i})+a\,\mu_i^2\,[\ell(1+\lambda)+(\theta_i+\theta_{1i})]\right]$$

$$+ \frac{2P}{H_i}\left[\frac{\sin\frac{\mu_i t\ell}{2}\sin\frac{\mu_i \ell}{2}(1-t)}{\cos\frac{\mu_i \ell}{2}}\left(\frac{8f}{\mu_i^2\ell^2}+a\right) - 2ft(1-t) - \frac{\mu_i^2}{4}\frac{(\theta_i+\omega\theta_{1i})}{(\phi_i+\phi_{1i})}\right.$$

$$\left.\left(\frac{8f}{\mu_i^2\ell^2}+a\frac{[\ell(1+\lambda)+(\theta_i+\theta_{1i})]}{(\theta_i+\omega\theta_{1i})}\right)\left(\frac{\sin\mu_i t\ell}{\sin\mu_i\ell}-t\right)\right] - \frac{yW}{H_i}\left[\frac{8f}{\ell^2}\left(\frac{1}{\mu_i^2}\right.\right.$$

$$(\theta_i+\omega^2\theta_{1i}) - \frac{(\theta_i+\omega\theta_{1i})^2}{4(\phi_i+\phi_{1i})} - \frac{\ell^3}{12}(1+\omega^2\lambda^3)\Big] + a(\theta_i+\omega\theta_{1i})\left[1-\frac{\mu_i^2}{4}\right.$$

$$\left.\left.\left.\frac{[\ell(1+\lambda)+(\theta_i+\theta_{1i})]}{(\phi_i+\phi_{1i})}\right)\right]\right]$$

Similarly, Δ can be calculated for loads applied in the right hand span.

APPENDIX 13

13. The Determination of the Term $\sum \frac{W}{H_w} \int \eta dx$ for a General Case of Loading

From Appendix 12, we have the deflection equations for a general case of loading as, (see figure in the preceding appendix)

$$\eta = \left[\frac{M}{H} \left(\frac{x}{\ell} - \frac{\sin \mu x}{\sin \mu \ell} \right) + a \left[1 - \left(\frac{x}{\ell} + \frac{\sin \mu(\ell - x)}{\sin \mu \ell} \right) \right] - \frac{W(y+\rho)}{\mu^2 H} \left[\frac{\sin \mu x}{\sin \mu \ell} + \frac{\sin \mu(\ell - x)}{\sin \mu \ell} - 1 - \frac{\mu^2 x}{2} (\ell - x) \right] \right]_{0 \leq x \leq \ell}$$

$$+ \frac{\sigma}{\mu^2 H} \left[\left([\cos \mu \ell(1-\alpha) - \cos \mu \ell(1-\beta)] \frac{\sin \mu x}{\sin \mu \ell} - \frac{\mu^2 \ell^2}{2} (\alpha - \beta) [2 - (\alpha + \beta)] \frac{x}{\ell} \right)_{0 \leq x \leq \beta \ell} + \left(\cos \mu \ell(1-\alpha) \frac{\sin \mu x}{\sin \mu \ell} \right.\right.$$

$$\left. + \cos \mu \beta \ell \frac{\sin \mu(\ell - x)}{\sin \mu \ell} - 1 - \frac{\mu^2 \ell^2}{2} \left[(\alpha - \beta)[2 - (\alpha + \beta)] \frac{x}{\ell} - \left(\frac{x}{\ell} - \beta \right)^2 \right] \right)_{\beta \ell \leq x \leq \alpha \ell}$$

$$\left. + \left[(\cos \mu \beta \ell - \cos \mu \alpha \ell) \frac{\sin \mu(\ell - x)}{\sin \mu \ell} - \frac{\mu^2 \ell^2}{2} (\alpha^2 - \beta^2) \left(1 - \frac{x}{\ell} \right) \right]_{\alpha \ell \leq x \leq \ell} \right]$$

for the left hand span and for the right hand span we have;

$$\eta_1 = \frac{M}{H} \left(\frac{x_1}{\ell_1} - \frac{\sin \mu x_1}{\sin \mu \ell_1} \right) - \frac{W_1(y+\rho)}{\mu^2 H} \left[\frac{\sin \mu x_1}{\sin \mu \ell_1} + \frac{\sin \mu(\ell_1 - x_1)}{\sin \mu \ell_1} - 1 \right.$$

$$\left. - \frac{\mu^2 x}{2} (\ell - x) \right] + a \left[1 - \left(\frac{x_1}{\ell_1} + \frac{\sin \mu(\ell_1 - x_1)}{\sin \mu \ell_1} \right) \right] \qquad 0 \leq x \leq \ell \qquad 1$$

Thus, we have for the left hand span;

$$\int_0^{\ell} \eta dx = I_1 + I_2 + I_3 + I_4 + I_5 + I_6$$

where,

$$I_1 = \frac{M}{H}\int_0^{\ell} \left(\frac{x}{\ell} - \frac{\sin \mu x}{\sin \mu \ell} \right) dx = \frac{M}{H} \left(\frac{\ell}{2} - \frac{(1-\cos \mu \ell)}{\mu \sin \mu \ell} \right)$$

$$I_1 = - \frac{M}{H} \frac{\theta}{2}$$

where $$\theta = \ell \left[\frac{\tan \frac{\mu \ell}{2}}{\frac{\mu \ell}{2}} - 1 \right]$$

$$I_2 = a\int_0^{\ell} \left[1 - \left(\frac{x}{\ell} + \frac{\sin \mu(\ell-x)}{\sin \mu \ell} \right) \right] dx = a \left[\ell - \frac{\ell}{2} - \frac{(1 - \cos \mu \ell)}{\mu \sin \mu \ell} \right]$$

$$I_2 = - a \frac{\theta}{2}$$

$$I_3 = - \frac{W (y+\rho)}{\mu^2 H}\int_0^{\ell} \left[\frac{\sin \mu x}{\sin \mu \ell} + \frac{\sin \mu(\ell-x)}{\sin \mu \ell} - 1 - \frac{\mu^2 x}{2} (\ell-x) \right] dx$$

$$I_3 = - \frac{W (y+\rho)}{\mu^2 H} \left[\frac{2 (1-\cos \mu \ell)}{\mu \sin \mu \ell} - \ell - \frac{\mu^2 \ell^3}{12} \right]$$

$$I_3 = - \frac{W (y+\rho)}{\mu^2 H} \left[\theta - \frac{\mu^2 \ell^3}{12} \right]$$

$$I_4 = \frac{\sigma}{\mu^2 H}\int_0^{\beta \ell} \left[\frac{[\cos \mu \ell(1-\alpha) - \cos \mu \ell(1-\beta)]}{\sin \mu \ell} \sin \mu x - \frac{\mu^2 \ell^2}{2} (\alpha-\beta)[2-(\alpha+\beta)] \frac{x}{\ell} \right] dx$$

$$I_4 = \frac{\sigma}{\mu^2 H} \left[\frac{[\cos \mu \ell(1-\alpha) - \cos \mu \ell(1-\beta)]}{\sin \mu \ell} (1 - \cos \mu \beta \ell) - \frac{\mu^2 \beta^2}{4} \ell^3 (\alpha-\beta)[2-(\alpha+\beta)] \right]$$

$$I_5 = \frac{\sigma}{\mu^2 H}\int_{\beta \ell}^{\alpha \ell} \left[\frac{\cos \mu \ell(1-\alpha)}{\sin \mu \ell} \sin \mu x + \frac{\cos \mu \beta \ell}{\sin \mu \ell} \sin \mu(\ell-x) - 1 - \frac{\mu^2 \ell^2}{2} \right.$$

$$\left. [(\alpha-\beta)[2-(\alpha+\beta)] \frac{x}{\ell} - \frac{x^2}{\ell^2} + \frac{2\beta x}{\ell} - \beta^2] \right] dx$$

$$I_5 = \frac{\sigma}{\mu^2 H} \left[\frac{[\cos \mu \ell(1-\alpha)[\cos \mu \beta \ell - \cos \mu \alpha \ell] + \cos \mu \beta \ell \, [\cos \mu \ell(1-\alpha) - \cos \mu \ell(1-\beta)]}{\mu \sin \mu \ell} \right.$$

$$- \ell(\alpha-\beta)] - \frac{\mu^2\ell^3}{4}\left[(\alpha^2-\beta^2)(\alpha-\beta)[2-(\alpha+\beta)] - \frac{2}{3}(\alpha^3-\beta^3) + 2\beta(\alpha^2-\beta^2) - 2\beta^2(\alpha-\beta)\right]\Bigg]$$

$$I_6 = \frac{\sigma}{\mu^2 H}\int_{\alpha\ell}^{\ell}\left[(\cos\mu\beta\ell - \cos\mu\alpha\ell)\frac{\sin\mu(\ell-x)}{\sin\mu\ell} - \frac{\mu^2\ell^2}{2}(\alpha^2-\beta^2)(1-\frac{x}{\ell})\right]dx$$

$$I_6 = \frac{\sigma}{\mu^2 H}\left[\frac{(\cos\mu\beta\ell - \cos\mu\alpha\ell)(1-\cos\mu\ell(1-\alpha))}{\mu\sin\mu\ell} - \frac{\mu^2\ell^2}{4}(\alpha^2-\beta^2)(1-2\alpha+\alpha^2)\right]$$

$$I_4 + I_5 + I_6 = \frac{\sigma}{\mu^2 H}\left[\frac{\cos\mu\ell(1-\alpha) - \cos\mu\alpha\ell - \cos\mu\ell(1-\beta) + \cos\mu\beta\ell}{\mu\sin\mu\ell} - \ell(\alpha-\beta)\right.$$

$$\left. - \frac{\mu^2\ell^3}{12}\left[\alpha^2(3-2\alpha) - \beta^2(3-2\beta)\right]\right]$$

Hence, the total value of the deflection integration for <u>the left hand span</u> is:

$$\int_0^{\ell}\eta dx = \frac{\sigma\ell}{H}\left[\frac{1}{\mu^2}\left[\frac{[\sin\frac{\mu\ell}{2}(1-2\beta) - \sin\frac{\mu\ell}{2}(1-2\alpha)]}{\mu\ell\cos\frac{\mu\ell}{2}} - (\alpha-\beta)\right] - \frac{\ell^2}{12}\right.\right.$$

$$\left.\left.[\alpha^2(3-2\alpha) - \beta^2(3-2\beta)]\right] - \frac{M}{H}\frac{\theta}{2} - a\frac{\theta}{2} - \frac{W(y+\rho)}{\mu^2 H}\left[\theta - \frac{\mu^2\ell^3}{12}\right]\right.$$

Similarly, we have for the <u>right hand span</u>;

$$\int_0^{\ell_1}\eta_1 dx = -\frac{M}{H}\frac{\theta_1}{2} - a\frac{\theta_1}{2} - \frac{W_1(y+\rho)}{\mu^2 H}\left[\theta_1 - \frac{\mu^2\ell_1^3}{12}\right]$$

Hence $$\sum\frac{W}{H_w}\int\eta dx = \frac{W}{H_w}\left[\int_0^{\ell}\eta dx + \omega\int_0^{\ell_1}\eta_1 dx_1\right]$$

$$\sum\frac{W}{H_w}\int\eta dx = \frac{W}{H_w}\left[\frac{\sigma\ell}{H}\left[\frac{1}{\mu^2}\left[\frac{[\sin\frac{\mu\ell}{2}(1-2\beta) - \sin\frac{\mu\ell}{2}(1-2\alpha)]}{\mu\ell\cos\frac{\mu\ell}{2}} - (\alpha-\beta)\right] - \frac{\ell^2}{12}\right.\right.\right.$$

$$\left[\alpha^2\ (3-2\alpha) - \beta^2\ (3-2\beta)\right] - \frac{M}{2H}\ (\theta+\omega\theta_1) - \frac{a}{2}\ (\theta+\omega\theta_1) - \frac{W}{H}\ (y+\rho)$$

$$\left[\frac{1}{\mu^2}\ (\theta+\omega^2\theta_1) - \frac{\ell^3}{12}\ (1+\omega^2\lambda^3)\right]$$

But from Appendix 12 we have;

$$\frac{M}{2H} = -\frac{a}{2}\frac{(\nu+\nu_1)}{(\phi+\phi_1)} + \frac{\sigma\ell}{4H}\frac{1}{(\phi+\phi_1)}\left[\frac{2(\cos\mu\beta\ell - \cos\mu\alpha\ell)}{\mu\ell\sin\mu\ell} - (\alpha^2-\beta^2)\right]$$

$$- \frac{W\ (y+\rho)}{4H}\frac{(\theta+\omega\theta_1)}{(\phi+\phi_1)}$$

Hence, the final value of $\sum \frac{W}{H_w}\int \eta dx$ can be obtained with less labour than expected as follows:

$$\sum \frac{W}{H_w}\int \eta dx = \frac{W}{H_w}\left[-\frac{a}{2}\ (\theta+\omega\theta_1)\left[1 - \frac{(\nu+\nu_1)}{(\phi+\phi_1)}\right] + \frac{\sigma\ell}{H}\left[\frac{1}{\mu^2}\right.\right.$$

$$\left[\frac{\left[\sin\frac{\mu\ell}{2}(1-2\beta) - \sin\frac{\mu\ell}{2}(1-2\alpha)\right]}{\mu\ell\cos\frac{\mu\ell}{2}} - (\alpha-\beta)\right] - \frac{\ell^2}{12}\left[\alpha^2(3-2\alpha)\right.$$

$$\left.\left.\left. - \beta^2(3-2\beta)\right] - \frac{(\theta+\omega\theta_1)}{4\ (\phi+\phi_1)}\left[\frac{2\ (\cos\mu\beta\ell - \cos\mu\alpha\ell)}{\mu\ell\sin\mu\ell} - (\alpha^2-\beta^2)\right]\right]\right.$$

$$\left. - \frac{W(y+\rho)}{H}\left[\frac{1}{\mu^2}\ (\theta+\omega^2\theta_1) - \frac{(\theta+\omega\theta_1)^2}{4\ (\phi+\phi_1)} - \frac{\ell^3}{12}\ (1+\omega^2\lambda^3)\right]\right]$$

From this expression, $\sum \frac{W}{H_w}\int \eta dx$ can be found for a continuous unifromly distributed load σ applied in the left hand span by substituting α = 1 and β = o, which gives:

$$\sum \frac{W}{H_w} \int \eta dx = \frac{W}{H_w} \left[- \frac{a}{2} (\theta+\omega\theta_1) \left[1 - \frac{(\nu+\nu_1)}{(\phi+\phi_1)} \right] + \frac{\sigma \ell}{H} \left[\frac{1}{\mu^2} \left[\frac{\tan \frac{\mu\ell}{2}}{\frac{\mu\ell}{2}} - 1 \right] \right. \right.$$

$$\left. \left. - \frac{\ell^2}{12} - \frac{(\theta+\omega\theta_1)}{4\ (\phi+\phi_1)} \left[\frac{\tan \frac{\mu\ell}{2}}{\frac{\mu\ell}{2}} - 1 \right] \right] - \frac{W}{H} (\gamma+\rho) \left[\frac{1}{\mu^2} (\theta+\omega^2\theta_1) \right. \right.$$

$$\left. \left. - \frac{(\theta+\omega\theta_1)^2}{4\ (\phi+\phi_1)} - \frac{\ell^3}{12} (1+\omega^2\lambda^3) \right] \right]$$

$$\sum \frac{W}{H_w} \int \eta dx = \frac{W}{H_w} \left[- \frac{a}{2} (\theta+\omega\theta_1) \left[1 - \frac{(\nu+\nu_1)}{(\phi+\phi_1)} \right] + \frac{\sigma}{H} \left[\frac{\theta}{\mu^2} \left(1 - \frac{\mu^2}{4} \frac{(\theta+\omega\theta_1)}{(\phi+\phi_1)} \right) \right. \right.$$

$$\left. \left. - \frac{\ell^3}{12} \right] - \frac{W}{H} (\gamma+\rho) \left[\frac{1}{\mu^2} (\theta+\omega^2\theta_1) - \frac{(\theta+\omega\theta_1)^2}{4\ (\phi+\phi_1)} - \frac{\ell^3}{12} (1+\omega^2\lambda^3) \right] \right]$$

For a concentrated load similar procedure to that used in Appendix 12 can be adopted by substituting $\beta = t-\varepsilon$, $\alpha = t + \varepsilon$ and $P = 2\sigma\ell\varepsilon$ into the general expression, we have for the first term: (see figure at the end of Appendix 12)

$$\frac{\sin \frac{\mu\ell}{2}(1-2\beta) - \sin \frac{\mu\ell}{2}(1-2\alpha)}{\mu\ell \cos \frac{\mu\ell}{2}} - (\alpha-\beta) = \frac{\sin \frac{\mu\ell}{2}[(1-2t)+2\varepsilon] - \sin \frac{\mu\ell}{2}[(1-2t)-2\varepsilon]}{\mu\ell \cos \frac{\mu\ell}{2}} - 2\varepsilon$$

$$\frac{\sin\frac{\mu\ell}{2}(1-2t)\ \cos\mu\ell\varepsilon + \sin\mu\ell\varepsilon\ \cos\frac{\mu\ell}{2}(1-2t) - \sin\frac{\mu\ell}{2}(1-2t)\ \cos\mu\ell\varepsilon + \sin\mu\ell\varepsilon\ \cos\frac{\mu\ell}{2}(1-2t)}{\mu\ell \cos \frac{\mu\ell}{2}} - 2\varepsilon$$

where ε is a very small quantity, Hence:

$\sin \mu\ell\varepsilon = \mu\ell\varepsilon$

Thus, we have the final value of this term;

$$2\varepsilon \left[\frac{\cos \frac{\mu\ell}{2}(1-2t)}{\cos \frac{\mu\ell}{2}} - 1 \right] = 4\varepsilon \frac{\sin \frac{\mu t\ell}{2} \sin \frac{\mu\ell}{2}(1-t)}{\cos \frac{\mu\ell}{2}}$$

For the second term we have,

$$\frac{\ell^2}{12}\left[\alpha^2(3-2\alpha) - \beta^2\,(3-2\beta)\right] = \frac{\ell^2}{12}\left[12t\varepsilon - 12t^2\varepsilon - 4\varepsilon^3\right]$$

ignoring ε^3, the final value is,

$$= \frac{\ell^2}{4}\,4\varepsilon t\,[1-t]$$

For the third term, we have:

$$\frac{2\,(\cos\mu\beta\ell - \cos\mu\alpha\ell)}{\mu\ell\,\sin\mu\ell} - (\alpha^2-\beta^2) = \frac{2\,[\cos\mu\ell(t-\varepsilon) - \cos\mu\ell(t+\varepsilon)]}{\mu\ell\,\sin\mu\ell} - 4t\varepsilon$$

$$\frac{2(\cos\mu t\ell\,\cos\mu\ell\varepsilon + \sin\mu t\ell\,\sin\mu\ell\varepsilon - \cos\mu t\ell\,\cos\mu\ell\varepsilon + \sin\mu\ell\varepsilon\,\sin\mu t\ell)}{\mu\ell\,\sin\mu\ell} - 4t\varepsilon$$

$$= 4\varepsilon\left[\frac{\sin\mu t\ell}{\sin\mu\ell} - t\right]$$

And the final value for $\sum \frac{W}{H_w}\int \eta dx$ for a concentrated load applied in the left hand span becomes:

$$\sum \frac{W}{H_w}\int \eta dx = \frac{W}{H_w}\left[-\frac{a}{2}\,(\theta+\omega\theta_1)\left[1 - \frac{(\nu+\nu_1)}{(\phi+\phi_1)}\right] + \frac{2P}{H}\left[\frac{\sin\frac{\mu t\ell}{2}\,\sin\frac{\mu\ell}{2}(1-t)}{\cos\frac{\mu\ell}{2}}\right.\right.$$

$$\left. - \frac{t\ell^2}{4}\,(1-t) - \frac{(\theta+\omega\theta_1)}{(\phi+\phi_1)}\left[\frac{\sin\mu t\ell}{\sin\mu\ell} - t\right]\right] - \frac{W}{H}\,(\gamma+\rho)\left[\frac{1}{\mu^2}\right.$$

$$\left.\left.(\theta+\omega^2\theta_1) - \frac{(\theta+\omega\theta_1)^2}{4\,(\phi+\phi_1)} - \frac{\ell^3}{12}\,(1+\omega^2\lambda^3)\right]\right]$$

A similar procedure can be adopted to find $\sum \frac{W}{H_w}\int \eta dx$ for loads applied in the right hand span.

APPENDIX 14

14. The Determination of the Error $\frac{1}{2} \sum \int \eta'^2 dx$

The difficulty of calculating $\sum \frac{1}{2} \int \eta'^2 dx$ for a general case of loading arises from having three equations for the deflections covering the whole left hand span length, Appendix 12, as follows:

$$EI \frac{d^2\eta_{1\sigma}}{dx^2} + H \eta_{1\sigma} = - \frac{\sigma l}{2} (\alpha-\beta) [2-(\alpha+\beta)]x \qquad 0 \leqslant x \leqslant \beta l$$

$$EI \frac{d^2\eta_{2\sigma}}{dx^2} + H \eta_{2\sigma} = - \frac{\sigma l}{2} (\alpha-\beta) [2-(\alpha+\beta)]x + \frac{\sigma}{2} [x-\beta l]^2 \qquad \beta l \leqslant x \leqslant \alpha l$$

$$EI \frac{d^2\eta_{3\sigma}}{dx^2} + H \eta_{3\sigma} = - \frac{\sigma l}{2} (\alpha-\beta) [2-(\alpha+\beta)]x + \frac{\sigma l}{2} (\alpha-\beta)[2x-l(\alpha+\beta)] \qquad \alpha l \leqslant x \leqslant l$$

The right hand side of these equations can be represented for the whole span length l by using trigonometric series in the form $\sum b_m \sin \frac{m\pi x}{l}$ where:

$$\sum_{m=1}^{\infty} b_m \sin \frac{m\pi x}{l} = b_1 \sin \frac{\pi x}{l} + b_2 \sin \frac{2\pi x}{l} + \ldots.$$

where, b_m can be calculated as:

$$b_m = \frac{2}{l} \left[- \frac{\sigma l}{2} (\alpha-\beta)[2-(\alpha+\beta)] \left[\int_0^{\beta l} x \sin \frac{m\pi x}{l} dx + \int_{\beta l}^{\alpha l} x \sin \frac{m\pi x}{l} dx \right.\right.$$

$$\left. + \int_{\alpha l}^{l} x \sin \frac{m\pi x}{l} dx \right] + \frac{\sigma}{2} \int_{\beta l}^{\alpha l} (x^2 - 2\beta l x + \beta^2 l^2) \sin \frac{m\pi x}{l} dx$$

$$\left. + \frac{\sigma l}{2} (\alpha-\beta) \int_{\alpha l}^{l} [2x - l(\alpha+\beta)] \sin \frac{m\pi x}{l} dx \right]$$

$$b_m = \frac{2}{l} \left[- \frac{\sigma l}{2} (\alpha-\beta)[2-(\alpha+\beta)] \int_0^{l} x \sin \frac{m\pi x}{l} dx + \frac{\sigma}{2} \left[\int_{\beta l}^{\alpha l} x^2 \sin \frac{m\pi x}{l} dx \right.\right.$$

$$\left. - 2 \beta l \int_{\beta l}^{\alpha l} x \sin \frac{m\pi x}{l} dx + \beta^2 l^2 \int_{\beta l}^{\alpha l} \sin \frac{m\pi x}{l} dx \right] + \frac{\sigma l}{2} (\alpha-\beta) \left[2 \int_{\alpha l}^{l} x \sin \frac{m\pi x}{l} dx \right.$$

$$- \ell(\alpha-\beta) \int_{\alpha\ell}^{\ell} \sin \frac{m\pi x}{\ell}\, dx] \Big]$$

Bearing in mind that:

$$\int_a^b x^2 \sin \frac{m\pi x}{\ell}\, dx = - \frac{\ell}{m\pi} \Big[x^2 \cos \frac{m\pi x}{\ell} - \frac{2x\ell}{m\pi} \sin \frac{m\pi x}{\ell} - \frac{2\ell^2}{m^2\pi^2} \cos \frac{m\pi x}{\ell} \Big]_a^b$$

$$\int_a^b x \sin \frac{m\pi x}{\ell}\, dx = - \frac{\ell}{m\pi} \Big[x \cos \frac{m\pi x}{\ell} - \frac{\ell}{m\pi} \sin \frac{m\pi x}{\ell} \Big]_a^b$$

$$\int_a^b \sin \frac{m\pi x}{\ell}\, dx = - \frac{\ell}{m\pi} \Big[\cos \frac{m\pi x}{\ell} \Big]_a^b$$

and $\sin m\pi = o$

$$b_m = \frac{\sigma\ell^2}{m\pi} \Big[(\alpha-\beta) \big[\cos m\pi - (\alpha+\beta) \cos m\pi - 2 \cos m\pi + 2\alpha \cos m\pi\alpha$$

$$- \frac{2}{m\pi} \sin m\pi\alpha + (\alpha+\beta) \cos m\pi - \alpha \cos m\pi\alpha - \beta \cos m\pi\alpha\big] - \alpha^2 \cos m\pi\alpha$$

$$+ \frac{2\alpha}{m\pi} \sin m\pi\alpha + \frac{2}{m^2\pi^2} (\cos m\pi\alpha - \cos m\pi\beta) + \beta^2 \cos m\pi\beta - \frac{2\beta}{m\pi} \sin m\pi\beta$$

$$+ 2\alpha\beta \cos m\pi\alpha - \frac{2\beta}{m\pi} \sin m\pi\alpha - 2\beta^2 \cos m\pi\beta + \frac{2\beta}{m\pi} \sin m\pi\beta - \beta^2 \cos m\pi\alpha$$

$$+ \beta^2 \cos m\pi\beta \Big]$$

$$b_m = \frac{\sigma\ell^2}{m\pi} \Big[\alpha^2 \cos m\pi\alpha - \alpha\beta \cos m\pi\alpha - \frac{2\alpha}{m\pi} \sin m\pi\alpha + \frac{2\beta}{m\pi} \sin m\pi\alpha - \alpha\beta \cos m\pi\alpha$$

$$+ \beta^2 \cos m\pi\alpha - \alpha^2 \cos m\pi\alpha + \frac{2\alpha}{m\pi} \sin m\pi\alpha + \frac{2}{m^2\pi^2} (\cos m\pi\alpha - \cos m\pi\beta) + 2\alpha\beta$$

$$\cos m\pi\alpha - \frac{2\beta}{m\pi} \sin m\pi\alpha - \beta^2 \cos m\pi\alpha \Big]$$

$$b_m = - \frac{2\sigma\ell^2}{m^3\pi^3} (\cos m\pi\beta - \cos m\pi\alpha)$$

Hence, we have:

$$EI \frac{d^2\eta_\sigma}{dx^2} + H\,\eta_\sigma = \sum_{m=1}^{\infty} b_m \sin \frac{m\pi x}{\ell}$$

The solution for this differential equation will be assumed as:

$$\eta_\sigma = \sum_{m=1}^{\infty} a_m \sin \frac{m\pi x}{\ell}.$$

Clearly, this solution satisfies the condition $\eta_\sigma = o$ at $x = o, \ell$. Hence, substituting this solution in the above equation we have:-

$$EI \frac{m^2\pi^2}{\ell^2} \sum_{m=1}^{\infty} a_m \sin \frac{m\pi x}{\ell} + H \sum_{m=1}^{\infty} a_m \sin \frac{m\pi x}{\ell} = \sum_{m=1}^{\infty} b_m \sin \frac{m\pi x}{\ell}$$

which yields:

$$- \frac{EI}{\ell^2} (m^2\pi^2 - \mu^2\ell^2) \sum_{m=1}^{\infty} a_m \sin \frac{m\pi x}{\ell} = \sum_{m=1}^{\infty} b_m \sin \frac{m\pi x}{\ell}$$

Hence, by equating the coefficients of $\sin \frac{m\pi x}{\ell}$, for each value of m, on both sides of the equation we have:-

$$a_m = \frac{-\ell^2 b_m}{EI\,(m^2\pi^2 - \mu^2\ell^2)}$$

and the final value for the deflection becomes:

$$\eta_\sigma = \frac{2\,\sigma\ell^4}{\pi^3\,EI} \sum_{m=1}^{\infty} \frac{(\cos m\pi\beta - \cos m\pi\alpha)}{m^3[m^2\pi^2 - \mu^2\ell^2]} \sin \frac{m\pi x}{\ell} \qquad o \leqslant x \leqslant \ell$$

Substituting this equation into the total expression for the deflection and taking the first derivative, we have:-

$$\eta' = \left[\frac{M}{\ell H} \left[1 - \mu\ell \frac{\cos \mu x}{\sin \mu\ell} \right] - \frac{a}{\ell} \left[1 - \mu\ell \frac{\cos \mu(\ell - x)}{\sin \mu\ell} \right] - \frac{W(y+\rho)}{\mu H} \left[\frac{\cos \mu x}{\sin \mu\ell} - \frac{\cos \mu(\ell - x)}{\sin \mu\ell} - \frac{\mu}{2} (\ell - 2x) \right] \right] + \frac{2\sigma\ell^3}{\pi^2 IE} \sum_{m=1}^{\infty} \frac{(\cos m\pi\beta - \cos m\pi\alpha)}{m^2[m^2\pi^2 - \mu^2\ell^2]} \cos \frac{m\pi x}{\ell}$$

$$o \leqslant x \leqslant \ell$$

for the left hand span and,

$$\eta_1' = \left[\frac{M}{\ell_1 H} \left[1 - \mu\ell_1 \frac{\cos \mu x_1}{\sin \mu\ell_1} \right] - \frac{a}{\ell_1} \left[1 - \mu\ell_1 \frac{\cos \mu(\ell_1 - x_1)}{\sin \mu\ell_1} \right] - \frac{W_1(y+\rho}{\mu H} \left[\frac{\cos \mu x_1}{\sin \mu\ell_1} \right. \right.$$

$$\left. \left. - \frac{\cos \mu(\ell_1 - x_1)}{\sin \mu\ell_1} - \frac{\mu}{2} (\ell_1 - 2x_1) \right] \right] \qquad o \leqslant x_1 \leqslant \ell_1$$

for the right hand span where,

$$M = - Ha \frac{(\nu+\nu_1)}{(\phi+\phi_1)} + \frac{\sigma\ell}{2(\phi+\phi_1)} \left[\frac{2[\cos \mu\beta\ell - \cos \mu\alpha\ell]}{\mu\ell \sin \mu\ell} - (\alpha^2 - \beta^2) \right] - \frac{W}{2} (y+\rho) \frac{(\theta+\omega\theta_1)}{(\phi+\phi_1)}$$

Hence, to calculate $\frac{1}{2} \sum \int \eta'^2 \, dx$, we have for the left hand span

$$\frac{1}{2} \int_o^{\ell} \eta'^2 \, dx = I_1 + I_2 + I_3$$

where,

$$I_1 = \frac{1}{2} \int_o^{\ell} \left[\frac{M^2}{\ell^2 H^2} \left(1 - \mu\ell \frac{\cos \mu x}{\sin \mu\ell} \right)^2 + \frac{a^2}{\ell^2} \left(1 - \mu\ell \frac{\cos \mu(\ell - x)}{\sin \mu\ell} \right)^2 + \frac{W^2(y+\rho)^2}{\mu^2 H^2} \right.$$

$$\left[\frac{\cos \mu x}{\sin \mu\ell} - \frac{\cos \mu(\ell - x)}{\sin \mu\ell} - \frac{\mu}{2} (\ell - 2x) \right]^2 - \frac{2Ma}{\ell^2 H} \left[1 - \mu\ell \frac{\cos \mu x}{\sin \mu\ell} \right] \left[1 - \mu\ell \right.$$

$$\left. \frac{\cos \mu(\ell - x)}{\sin \mu\ell} \right] - \frac{2W(y+\rho) M}{\mu\ell H^2} \left[1 - \mu\ell \frac{\cos \mu x}{\sin \mu\ell} \right] \left[\frac{\cos \mu x}{\sin \mu\ell} - \frac{\cos \mu(\ell - x)}{\sin \mu\ell} \right.$$

$$\left. - \frac{\mu}{2} (\ell - 2x) \right] + \frac{2W(y+\rho)}{\mu\ell H} a \left[1 - \mu\ell \frac{\cos \mu(\ell - x)}{\sin \mu\ell} \right] \left[\frac{\cos \mu x}{\sin \mu\ell} - \frac{\cos \mu(\ell - x)}{\sin \mu\ell} \right.$$

$$\left. \left. - \frac{\mu}{2} (\ell - 2x) \right] \right] dx$$

Bearing in mind that:

$$\int_o^{\ell} \left[1 - \mu\ell \frac{\cos \mu x}{\sin \mu\ell} \right]^2 dx = \int_o^{\ell} \left[1 - \mu\ell \frac{\cos \mu(\ell - x)}{\sin \mu\ell} \right]^2 dx = \frac{\ell^2}{2} \left[\nu(2+\nu\ell) - \phi \right]$$

$$\int_0^{\ell} \left[\frac{\cos \mu x}{\sin \mu \ell} - \frac{\cos \mu(\ell-x)}{\sin \mu \ell} - \frac{\mu}{2} (\ell-2x) \right]^2 dx = \frac{1}{12} \left[6\nu\ell \ (\ell+\theta) - 24\theta + \mu^2 \ell^3\right]$$

$$\int_0^{\ell} \left[1 - \mu\ell \frac{\cos \mu x}{\sin \mu \ell}\right] \left[1 - \mu\ell \frac{\cos \mu(\ell-x)}{\sin \mu \ell}\right] dx = \frac{\ell^2}{2} \left[\phi(1+\nu\ell) - 2\nu\right]$$

$$\int_0^{\ell} \left[1 - \mu\ell \frac{\cos \mu x}{\sin \mu \ell}\right] \left[\frac{\cos \mu x}{\sin \mu \ell} - \frac{\cos \mu(\ell-x)}{\sin \mu \ell} - \frac{\mu}{2} (\ell-2x)\right] dx = -\int_0^{\ell} \left[1 - \mu\ell \right.$$

$$\left. \frac{\cos \mu(\ell-x)}{\sin \mu \ell}\right]\left[\frac{\cos \mu x}{\sin \mu \ell} - \frac{\cos \mu(\ell-x)}{\sin \mu \ell} - \frac{\mu}{2} (\ell-2x)\right] dx = \frac{\mu\ell}{4} \left[\nu\ell \ (\ell+\theta) - 2\theta\right]$$

where:

$$\nu = \frac{1}{\ell} \left[\frac{\mu\ell}{\sin \mu\ell} - 1\right], \qquad \nu_1 = \frac{1}{\ell_1} \left[\frac{\mu\ell_1}{\sin \mu\ell_1} - 1\right]$$

$$\phi = \frac{1}{\ell} \left[1 - \frac{\mu\ell}{\tan \mu\ell}\right], \qquad \phi_1 = \frac{1}{\ell_1} \left[1 - \frac{\mu\ell_1}{\tan \mu\ell_1}\right]$$

$$\theta = \ell \left[\frac{\tan \frac{\mu\ell}{2}}{\frac{\mu\ell}{2}} - 1\right], \qquad \theta_1 = \ell_1 \left[\frac{\tan \frac{\mu\ell_1}{2}}{\frac{\mu\ell_1}{2}} - 1\right]$$

and where $\mu^2 = \frac{H}{EI}$.

Thus, the final value for I_1 becomes;

$$I_1 = \frac{1}{4} \left[\frac{M^2}{H^2} + a^2\right] \left[\nu(2+\nu\ell) - \phi\right] + \frac{W(y+\rho)}{4\ H^2} (M + Ha) \left[\nu\ell \ (\ell+\theta) - 2\theta\right] + \frac{Ma}{2H}$$

$$\left[\phi \ (1+\nu\ell) - 2\nu\right] + \frac{W^2(y+\rho)^2}{24\ \mu^2\ H^2} \left[6\nu\ell \ (\ell+\theta) - 24\theta + \mu^2\ell^3\right]$$

Similarly for the right hand span we have;

$$\frac{1}{2} \int_0^{\ell_1} \eta_1'^2 \, dx_1 = \frac{1}{4} \left(\frac{M^2}{H^2} + a^2\right) \left[\nu_1 \ (2+\nu_1\ell_1) - \phi_1\right] + \frac{W_1(y+\rho)}{4\ H^2} (M+Ha) \left[\nu_1\ell_1\right.$$

$$(\ell_1+\theta_1) - 2\theta_1] + \frac{Ma}{2H}\,[\phi_1(1+\nu_1\ell_1 - 2\nu_1] + \frac{W_1^2\,(y+\rho)}{24\,\mu^2\,H^2}\,[6\nu_1\ell_1$$

$$(\ell_1+\theta_1) - 24\,\theta_1 + \mu^2\ell_1^3\,]$$

For the second integration of the left hand span, I_2, we have:

$$I_2 = \frac{2\,\sigma\ell^3}{\pi^2\,EI}\sum_{m=1}^{\infty}\frac{(\cos m\pi\beta - \cos m\pi\alpha)}{m^2\,[m^2\pi^2 - \mu^2\ell^2]}\int_0^{\ell}\Bigg[\frac{M}{\ell H}\Big[\cos\frac{m\pi x}{\ell} - \mu\ell\,\frac{\cos\mu x}{\sin\mu\ell}\cos\frac{m\pi x}{\ell}\Big]$$

$$-\frac{a}{\ell}\Big[\cos\frac{m\pi x}{\ell} - \mu\ell\,\frac{\cos\mu(\ell-x)}{\sin\mu\ell}\cos\frac{m\pi x}{\ell}\Big] - \frac{W(y+\rho)}{\mu H}\Big[\frac{\cos\mu x}{\sin\mu\ell}\cos\frac{m\pi x}{\ell}$$

$$-\frac{\cos\mu(\ell-x)}{\sin\mu\ell}\cos\frac{m\pi x}{\ell} - \frac{\mu}{2}\Big[\ell\cos\frac{m\pi x}{\ell} - 2x\cos\frac{m\pi x}{\ell}\Big]\Bigg]\,dx$$

Bearing in mind that:

$$\int_0^{\ell}\cos\frac{m\pi x}{\ell} = 0$$

$$\int_0^{\ell}\frac{\cos\mu x}{\sin\mu\ell}\cos\frac{m\pi x}{\ell}\,dx = -\mu\ell^2\,\frac{\cos m\pi}{[m^2\pi^2 - \mu^2\ell^2]}$$

$$\int_0^{\ell}\frac{\cos\mu(\ell-x)}{\sin\mu\ell}\cos\frac{m\pi x}{\ell}\,dx = -\frac{\mu\ell^2}{[m^2\pi^2 - \mu^2\ell^2]}$$

$$\int_0^{\ell}x\cos\frac{m\pi x}{\ell}\,dx = -\frac{\ell^2}{m^2\pi^2}\,(1 - \cos m\pi)$$

Thus, the final value of I_2 can be found as;

$$I_2 = \frac{2\,\sigma\ell^5}{\pi^2\,E^2I^2}\sum_{m=1}^{\infty}\frac{(\cos m\pi\beta - \cos m\pi\alpha)}{m^2[m^2\pi^2 - \mu^2\ell^2]^2}\Big[M\cos m\pi - Ha - \frac{W(y+\rho)}{m^2\pi^2}\,\ell^2\,(1-\cos m\pi)\Big]$$

Finally,

$$I_3 = \frac{2\,\sigma^2\ell^6}{\pi^4\,E^2I^2}\sum_{m=1}^{\infty}\frac{(\cos m\pi\beta - \cos m\pi\alpha)^2}{m^4[m^2\pi^2 - \mu^2\ell^2]^2}\int_0^{\ell}\cos^2\frac{m\pi x}{\ell}\,dx$$

but

$$\int_0^{\ell} \cos^2 \frac{m\pi x}{\ell}\, dx = \frac{\ell}{2}$$

hence;

$$I_3 = \frac{\sigma^2 \ell^7}{\pi^4 E^2 I^2} \sum_{m=1}^{\infty} \frac{(\cos m\pi\beta - \cos m\pi\alpha)^2}{m^4 [m^2\pi^2 - \mu^2\ell^2]^2}$$

And the total value of the error $\left[\frac{1}{2} \sum \int \eta'^2\, dx \right]$ for both spans becomes,

$$\frac{1}{2} \sum \int \eta'^2\, dx = \frac{1}{4} \left(\frac{M^2}{H^2} + a^2 \right) [2 (\nu+\nu_1) + \ell (\nu^2+\lambda \nu_1^2) - (\phi+\phi_1)] + \frac{Ma}{2H}$$

$$[-2 (\nu+\nu_1) + \ell (\phi\nu + \lambda\phi_1\nu_1) + (\phi+\phi_1)] + \frac{W(\gamma+\rho)}{4H^2} (M+Ha)$$

$$[\nu\ell(\ell+\theta) + \omega\nu_1\ell_1(\ell_1+\theta_1) - 2(\theta+\omega\theta_1)] + \frac{W^2(\gamma+\rho)^2}{24\ \mu^2H^2} [6\ \nu\ell(\ell+\theta)$$

$$+ 6\ \omega^2\nu_1\ell_1\ (\ell_1+\theta_1) - 24\ (\theta+\omega^2\theta_1) + \mu^2\ell^3\ (1+\omega^2\lambda^3)] + \frac{2\ \overset{5}{\sigma}\ell}{\pi^2\ E^2I^2}$$

$$\sum_{m=1}^{\infty} \frac{(\cos m\pi\beta - \cos m\pi\alpha)}{m^2\ [m^2\pi^2 - \mu^2\ell^2]^2} \left[(-1)^m M - Ha - \frac{2W\ (\gamma+\rho)\ell^2}{m^2\ \pi^2} \sin^2 \frac{m\pi}{2} + \right.$$

$$\left. \frac{\sigma\ell^2}{2\ m^2\pi^2} (\cos m\pi\beta - \cos m\pi\alpha) \right]$$

where

$$M = - Ha \frac{(\nu+\nu_1)}{(\phi+\phi_1)} + \frac{\sigma\ell}{2(\phi+\phi_1)} \left[\frac{2(\cos \mu\beta\ell - \cos \mu\alpha\ell)}{\mu\ell \sin \mu\ell} - (\alpha^2-\beta^2) \right] - \frac{W}{2} (\gamma+\rho) \frac{(\theta+\omega\theta_1)}{(\phi+\phi_1)}$$

For a continuous uniformly distributed load, we can find $\left[\frac{1}{2} \sum \int \eta'^2\, dx \right]$

by substituting $\alpha = 1$ and $\beta = o$ in the general expression. Hence, we obtain:

$$\frac{1}{2} \sum \int \eta'^2 \, dx = \frac{1}{4} \left(\frac{M^2}{H^2} + a^2 \right) \left[2 (\nu+\nu_1) + \ell (\nu^2+\lambda \nu_1^2) - (\phi+\phi_1) \right] + \frac{Ma}{2H}$$

$$\left[-2 (\nu+\nu_1) + \ell (\phi\nu + \lambda\nu_1\phi_1) + (\phi+\phi_1) \right] + \frac{W(y+\rho)}{4H^2} (M+Ha)$$

$$\left[\nu\ell(\ell+\theta) + \omega\nu_1\ell_1(\ell_1+\theta_1) - 2(\theta+\omega\theta_1) \right] + \frac{W^2(y+\rho)^2}{24 \mu^2 H^2} \left[6 \nu\ell(\ell+\theta) + \right.$$

$$\left. 6 \omega^2\nu_1\ell_1(\ell_1+\theta_1) - 24 (\theta+\omega^2\theta_1) + \mu^2\ell^3(1+\omega^2\lambda^3) \right] + \frac{4 \sigma\ell^5}{\pi^2 E^2 I^2}$$

$$\sum_{m=1,3,5..}^{\infty} \frac{1}{m^2 \left[m^2\pi^2 - \mu^2\ell^2 \right]^2} \left[- M-Ha + \frac{\ell^2}{m^2\pi^2} \left[\sigma - 2W(y+\rho) \right] \right]$$

where $M = - Ha \frac{(\nu+\nu_1)}{(\phi+\phi_1)} + \frac{\sigma\theta}{2(\phi+\phi_1)} - \frac{W}{2} (y+\rho) \frac{(\theta+\omega\theta_1)}{(\phi+\phi_1)}$

For a concentrated load P, the aforementioned procedure in Appendix 12 can be used herein. Thus, substituting by $\beta = t-\varepsilon$, $\alpha = t+\varepsilon$, and $P = 2\sigma\ell\varepsilon$, we have:

$$\frac{1}{2} \sum \int \eta'^2 \, dx = \frac{1}{4} \left(\frac{M^2}{H^2} + a^2 \right) \left[2 (\nu+\nu_1) + \ell (\nu^2+\lambda \nu_1^2) - (\phi+\phi_1) \right] + \frac{Ma}{2H}$$

$$\left[-2 (\nu+\nu_1) + \ell (\phi\nu + \lambda\phi_1\nu_1) + (\phi+\phi_1) \right] + \frac{W(y+\rho)}{4H^2} (M+Ha)$$

$$\left[\nu\ell(\ell+\theta) + \omega\nu_1\ell_1(\ell_1+\theta_1) - 2(\theta+\omega\theta_1) \right] + \frac{W^2(y+\rho)^2}{24 \mu^2 H^2} \left[6 \nu\ell(\ell+\theta) \right.$$

$$\left. +6 \omega^2\nu_1\ell_1(\ell_1+\theta_1) - 24 (\theta+\omega^2\theta_1) + \mu^2\ell^3(1+\omega^2\lambda^3) \right] + \frac{2 P\ell^4}{\pi E^2 I^2}$$

$$\sum_{m=1}^{\infty} \frac{\sin m\pi t}{m \left[m^2\pi^2 - \mu^2\ell^2 \right]^2} \left[(-1)^m M-Ha - \frac{2W (y+\rho)\ell^2}{m^2\pi^2} \sin^2 \frac{m\pi}{2} \right.$$

$$\left. + \frac{P\ell}{2m\pi} \sin m\pi t \right]$$

where $M = - Ha \frac{(\nu+\nu_1)}{(\phi+\phi_1)} + \frac{P}{(\phi+\phi_1)} \left[\frac{\sin \mu t\ell}{\sin \mu\ell} - t \right] - \frac{W}{2} (y+\rho) \frac{(\theta+\omega\theta_1)}{(\phi+\phi_1)}$

Similarly, the error $\left[\frac{1}{2} \sum \int \eta'^2 \, dx \right]$ can be calculated when live loads are applied in the right hand span.

APPENDIX 15

15. The Determination of the Maximum Suspender Load

The shear forces equations for maximum upward distributed suspender forces, including the dead loads, are as from formulae (2.79) and (2.85):

$$Q_{smax} = - \frac{W(1+y+\rho_{max})}{\mu \sin \mu\ell} \left[\cos \mu x \left[1 - \frac{\mu^2}{2} \frac{(\theta+\omega\theta_1)}{(\phi+\phi_1)} \right] - \cos \mu(\ell-x) \right]$$

$$o \leqslant x \leqslant \ell$$

$$Q_{s1max} = - \frac{W_1(1+y+\rho_{max})}{\mu \sin \mu\ell_1} \left[\cos \mu x_1 \left[1 - \frac{\mu^2}{2\omega} \frac{(\theta+\omega\theta_1)}{(\phi+\phi_1)} \right] - \cos \mu(\ell_1-x_1) \right]$$

$$o \leqslant x_1 \leqslant \ell_1$$

From these equations the suspender load can initially be found by using the basic relationships as shown:

$$q'_{smax} = - \frac{dQ_{smax}}{dx} = - \frac{W(1+y+\rho_{max})}{\sin \mu\ell} \left[\sin \mu x \left[1 - \frac{\mu^2}{2} \frac{(\theta+\omega\theta_1)}{(\phi+\phi_1)} \right] + \sin \mu(\ell-x) \right]$$

$$q'_{s1max} = - \frac{dQ_{s1max}}{dx} = - \frac{W_1(1+y+\rho_{max})}{\sin \mu\ell} \left[\sin \mu x \left[1 - \frac{\mu^2}{2\omega} \frac{(\theta+\omega\theta_1)}{(\phi+\phi_1)} \right] + \sin \mu(\ell_1-x_1) \right]$$

However, these loads are not uniformly distributed and therefore, they do not comply with the basic assumptions stated in Section 2.1. Consequently, this non-uniform load must be approximated to a uniform load as follows:

$$q_{smax} = \frac{1}{\ell} \int_o^{\ell} q'_{smax} \, dx = - \frac{1}{\ell} \left[Q_{smax} \right]_o^{\ell}$$

Similarly,

$$q_{s1max} = \frac{1}{\ell_1}\int_{\circ}^{\ell_1} q'_{s1max}\, dx = -\frac{1}{\ell_1}\left[\, Q_{s1max}\,\right]_{\circ}^{\ell_1}$$

Hence, for the left hand span, we have:

$$q_{smax} = +\frac{W(1+y+\rho_{max})}{\mu \sin \mu\ell}\left[(\cos\,\mu\ell - 1)\left\{1 - \frac{\mu^2}{2}\frac{(\theta+\omega\theta_1)}{(\phi+\phi_1)}\right\} - (1 - \cos\mu\ell)\right]$$

$$= -W\,(1+y+\rho_{max})\,\frac{\tan\frac{\mu\ell}{2}}{\mu\ell}\left[\,2 - \frac{\mu^2}{2}\frac{(\theta+\omega\theta_1)}{(\phi+\phi_1)}\,\right]$$

$$q_{smax} = -W\,(1+y+\rho_{max})\,(1+\frac{\theta}{\ell})\left[1 - \frac{\mu^2}{4}\frac{(\theta+\omega\theta_1)}{(\phi+\phi_1)}\,\right]$$

Similarly for the right hand span:

$$q_{s1max} = -W_1\,(1+y+\rho_{max})\,(1+\frac{\theta_1}{\ell_1}\,)\left[1 - \frac{\mu^2}{4\omega}\frac{(\theta+\omega\theta_1)}{(\phi+\phi_1)}\,\right]$$

Appendices (16 - 23)

of Chapter 3

APPENDIX 16

16. The Determination of the Approximate Free Ungrouted Length of the Cable

From Appendix 2, we have:

$$\ln\left[x+\left(1+x^2\right)^{1/2}\right] = x - \frac{x^3}{6} + \frac{3}{40}x^5 - \frac{5}{117}x^7$$

$$x\left[1+x^2\right]^{1/2} = x + \frac{x^3}{2} - \frac{x^5}{8} + \frac{x^7}{16}$$

Substituting into equation (3.3), using only 2 terms:

$$S_f = \frac{\ell}{16n}\left[(F+8n) - \frac{1}{6}(F+8n)^3 + (F+8n) + \frac{1}{2}(F+8n)^3 - C + \frac{1}{6}C^3 - C - \frac{1}{2}C^3\right]$$

$$S_f = \frac{\ell}{16n}\left[(F+8n)\left[2 + \frac{1}{3}(F+8n)^2\right] - C\left[2+\frac{1}{3}C^2\right]\right]$$

which finally gives:

$$S_f = \frac{\ell}{48n}\left[(F+8n)\left[6+(F+8n)^2\right] - C\left[6+C^2\right]\right]$$

Similarly, the approximate length of the free ungrouted cable in the right hand span can be obtained.

APPENDIX 17

17. The Determination of the Approximate Relationship Between the Changes in the Span and Cable Lengths

The basic relationship is:

$$\Delta S_f = \frac{\partial S_f}{\partial \ell} \quad (\pm \Delta \ell)$$

Hence, from the preceding appendix, we have:

$$\frac{\partial S_f}{\partial \ell} = \frac{\ell}{48n}\left[\frac{-(F+8n)}{\ell}\left[6 + 3(F+8n)^2\right] + \frac{C}{\ell}\left[6 + 3C^2\right]\right] + \frac{1}{24n}\left[(F+8n)\right.$$

$$\left.\left[6 + (F+8n)^2\right] - C\left[6 + C^2\right]\right]$$

$$= \frac{1}{48n}\left[(F+8n)\left[6 - (F+8n)^2\right] - C\left[6-C^2\right]\right]$$

Hence,

$$\Delta S_f = \frac{(\pm \Delta \ell)}{48n}\left[(F+8n)\left[6 - (F+8n)^2\right] - C\left[6-C^2\right]\right]$$

A similar approach can be adopted for the right hand span.

APPENDIX 18

18. The Determination of the Approximate Relationship Between the Changes in the Span Length and the Cable Sag

From Appendix 5, the exact value of the derivative of the free cable length with respect to its sag $\frac{\partial S_f}{\partial f}$ can directly be found by replacing F by C which gives,

$$\frac{\partial S_g}{\partial f} = \frac{-1}{16n^2}\left[\ln\left(\frac{[(F+8n)+[1+(F+8n)^2]^{1/2}}{C+[1+C^2]^{1/2}}\right) + C\,[1+(F+8n)^2]^{1/2} - (F+8n)[1+C^2]^{1/2}\right]$$

For small values of the slopes at the ends of the free ungrouted cable, (F+8n) and (C), this formula can be approximated by using Maclaurin's expansions shown in Appendix 2. Thus we have, when using two terms of the expansion:

$$\frac{\partial S_f}{\partial f} = \frac{-1}{16n^2}\left[(F+8n) - \frac{1}{6}(F+8n)^3 - C + \frac{1}{6}C^3 + C\left[1 + \frac{1}{2}(F+8n)^2\right]\right.$$

$$\left. - (F+8n)\left[1 + \frac{1}{2}C^2\right]\right]$$

$$= \frac{+1}{16n^2}\left[\frac{1}{6}\left[(F+8n)^3 - C^3\right] - \frac{1}{2}C(F+8n)\left[(F+8n) - C\right]\right]$$

which finally gives:

$$\frac{\partial S_f}{\partial f} = \frac{1}{96n^2}\left[(F+8n)^3 - C^3 - 3C(F+8n)\left[(F+8n) - C\right]\right]$$

To determine the relationship between Δf and $(\pm \Delta \ell)$ we have, similarly to Appendix 5:

$$\frac{\partial S_f}{\partial f}\Delta f = \frac{\partial S_f}{\partial \ell}(\pm \Delta \ell)$$

Substituting from the preceding appendix by the value of $\frac{\partial S_f}{\partial \ell}$ we obtain:

$$\Delta f = 2n \frac{[(F+8n)[6-(F+8n)^2]-C[6-C^2]]}{[(F+8n)^3 - C^3 - 3C\ (F+8n)[(F+8n) - C]]} \quad (\pm \Delta \ell)$$

A similar approach can be adopted to find the approximate relationship between Δf_1 and $(\mp \Delta \ell)$ for the right hand span.

APPENDIX 19

19. The Determination of the Relationship Between the Changes in the Cable Length and Tension

From Appendix 8, we know:

$$\text{strain} = \frac{\text{stress}}{E_c}$$

$$\frac{\Delta S}{ds} = \frac{\Delta T}{A_c E_c} = \frac{\Delta H}{A_c E_c} \quad \frac{ds}{dx}$$

Thus,

$$\Delta S = \frac{\Delta H}{A_c E_c} \quad \frac{ds^2}{dx}$$

Integrating this equation over the free ungrouted part of the left hand span cable;

$$\Delta S_f = \frac{\Delta H}{A_c E_c} \int_{g\ell}^{\ell} \left(\frac{ds}{dx} \right)^2 dx$$

But $$\left(\frac{ds}{dx} \right)^2 = 1 + \left(\frac{dy}{dx} \right)^2$$

and $$\frac{dy}{dx} = F + \frac{8n}{\ell} \quad x$$

Thus, we have:

$$\Delta S_f = \frac{\Delta H}{A_c E_c} \int_{g\ell}^{\ell} \left[(1+F^2) + \frac{16n}{\ell} F x + 64 \frac{n^2}{\ell^2} x^2 \right] dx$$

$$= \frac{\Delta H}{A_c E_c} \left[(1+F^2) x + 8 \frac{n}{\ell} F x^2 + \frac{64}{3} \frac{n^2}{\ell^2} x^3 \right]_{g\ell}^{\ell}$$

$$= \frac{\Delta H \ell}{A_c E_c} \left[(1+F^2)(1-g) + 8nF(1-g^2) + \frac{64}{3} n^2 (1-g^3) \right]$$

$$= \frac{\Delta H \ell}{A_c E_c} \left[(1-g)[1+F^2+ 8nF (1+g)] + \frac{64}{3} n^2 (1-g^3) \right]$$

$$\Delta S_f = \frac{\Delta H \ell}{A_c E_c} \left[(1-g)\ [1+F\ (C + 8n)] + \frac{64}{3}\ n^2\ (1-g^3)\right]$$

Similarly, for the right hand span free ungrouted cable, we have:

$$\Delta S_{f1} = \frac{\Delta H \ell_1}{A_c E_c} \left[(1-g_1)\ [1+F_1(C_1+8n_1)] + \frac{64}{3}\ n_1^2\ (1-g_1^3)\right]$$

Hence, the total value of the change in the tension ΔH corresponding to changes in the cable length in both spans can be obtained from the following expression:

$$\Delta H = \frac{A_c E_c}{\ell}\left[\frac{\Delta S_f}{\left[(1-g)[1+F(C+8n)]+\frac{64}{3}\ n^2(1-g^3)\right]} + \frac{\Delta S_{f1}}{\lambda\left[(1-g_1)[1+F_1(C_1+8n_1)]+\frac{64}{3}\ n_1^2(1-g_1^3)\right]}\right]$$

APPENDIX 20

20. The Determination of the Approximate Value of the Term δ_{cf}

$$3 \ln [x+ (1+x^2)^{1/2}] + x [1+x^2]^{1/2} (5+2x^2) = 8x + 4x^3 + \frac{3}{5} x^5 - \frac{1}{4} x^7$$

Substituting into Equation (3.19), using only 2 terms of this expansion, we have:

$$\delta_{cf} = \frac{\ell}{64_n A_c E_c} \left[8 (F+8n) + 4(F+8n)^3 - 8C - 4C^3 + \frac{1}{\omega} \left[8 (F_1+8n_1) + 4 (F_1+8n_1)^3 - 8C_1 - 4C_1^3 \right] \right]$$

which yields:

$$\delta_{cf} = \frac{\ell}{16_n A_c E_c} \left[(F+8n) [2+ (F+8n)^2] - C[2+C^2] + \frac{1}{\omega} \left[(F_1+8n_1) [2+ (F_1+8n_1)^2] - C_1 [2 +C_1^2]\right]\right]$$

APPENDIX 21

21. The Determination of the Term $\left[\sum \frac{W}{H_w} \int \eta dx \right]$ for the first group of Forces

1. The two upward continuous uniformly distributed loads γW and γW_1

From Appendix 13, the term $\left[\sum \frac{W}{H_w} \int \eta \, dx \right]$ can directly be obtained for the two upward continuously uniformly distributed forces γW and γW_1 as follows:

$$\sum \frac{w}{H_w} \int \eta dx = \frac{w}{H_w} \left[\frac{-\gamma W}{H} \left[\frac{1}{\mu^2} (\theta+\omega^2\theta_1) - \frac{(\theta+\omega\theta_1)^2}{4(\phi+\phi_1)} - \frac{\ell^3}{12} (1+\omega^2\lambda^3) \right] \right]$$

2. The two upward partially distributed loads ρW and ρW_1

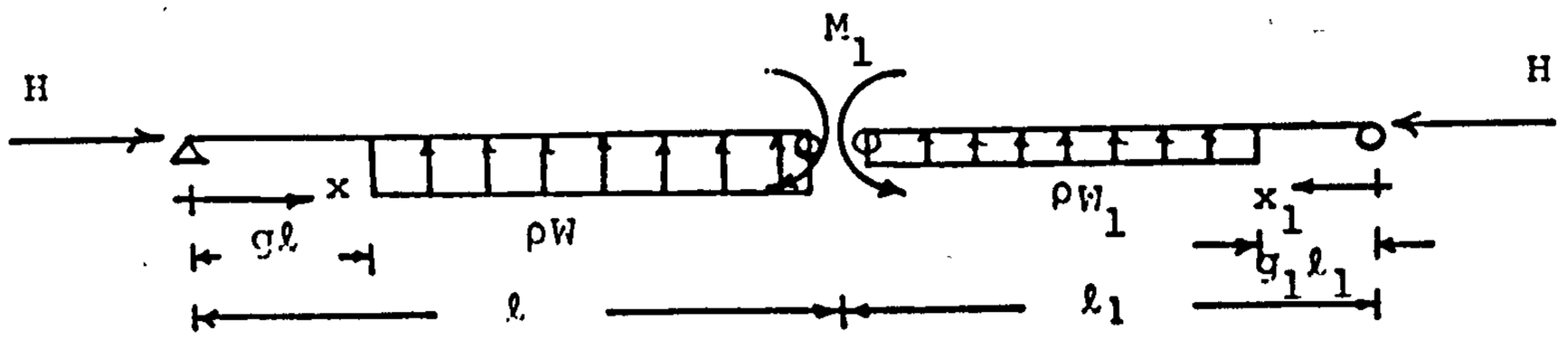

For the two upward partially distributed forces ρW and ρW_1, see the figure, the deflection equations can be written by substituting $\alpha = 1$ and $\beta = g$ and replacing σ by $-\rho W$ in the deflection equations for a general form of loading, see Appendix 12. Hence, we have for the left hand span:

$$\eta_1 = \frac{M_1}{H} \left[\frac{x}{\ell} - \frac{\sin \mu x}{\sin \mu \ell} \right] - \frac{\rho W}{\mu^2 H} \left[[1 - \cos \mu \ell (1-g)] \frac{\sin \mu x}{\sin \mu \ell} - \frac{\mu^2 \ell^2}{2} \right.$$

$$(1-g)^2 \frac{x}{\ell} \Bigg] \qquad o \leqslant x \leqslant g\ell$$

$$\eta_2 = \frac{M_1}{H}\left[\frac{x}{\ell} - \frac{\sin \mu x}{\sin \mu \ell}\right] - \frac{\rho W}{\mu^2 H}\left[\frac{\sin \mu x}{\sin \mu \ell} + \cos \mu g\ell \frac{\sin \mu(\ell-x)}{\sin \mu \ell} - 1 - \frac{\mu^2 \ell^2}{2}\right.$$

$$\left[(1-g)^2 \frac{x}{\ell} - (\frac{x}{\ell} - g)^2\right]\Bigg] \qquad g\ell \leqslant x \leqslant \ell$$

Similar equations can be written for the right hand span. Hence, to calculate the moment M at the intermediate support, we will take advantage of the equal slope at both sides of this support. Thus, for the left hand span:

$$\frac{d\eta_2}{dx} = \frac{M_1}{H}\phi + \frac{\rho W}{2H}\theta_g$$

Similarly, for the right hand span:

$$\frac{d\eta_{21}}{dx_1} = \frac{M_1}{H_1}\phi_1 + \frac{\rho W_1}{2H}\theta_{g1}$$

where $\phi = \frac{1}{\ell}\left[1 - \frac{\mu\ell}{\tan \mu\ell}\right]$ and $\phi_1 = \frac{1}{\ell_1}\left[1 - \frac{\mu\ell_1}{\tan \mu\ell_1}\right]$

and $\theta_g = \ell\left[\frac{(\cos \mu g\ell - \cos \mu\ell)}{\frac{\mu\ell}{2} \sin \mu\ell} - (1 - g^2)\right]$

and $\theta_{g1} = \ell\left[\frac{(\cos \mu g_1 \ell_1 - \cos \mu\ell_1)}{\frac{\mu\ell_1}{2} \sin \mu\ell_1} - (1 - g_1^2)\right]$

It is worth noting that g and $g_1 = 0$, become equal to θ_1 and θ

where $\theta = \ell\left[\frac{\tan \frac{\mu\ell}{2}}{\frac{\mu\ell}{2}} - 1\right]$ and $\theta_1 = \ell_1\left[\frac{\tan \frac{\mu\ell_1}{2}}{\frac{\mu\ell_1}{2}} - 1\right]$

Thus, $\frac{d\eta_2}{dx} = -\frac{d\eta_{21}}{dx_1}$

which yields:

$$M_1 = - \frac{\rho W}{2} \frac{(\theta_g + \omega\theta_{g1})}{(\phi+\phi_1)}$$

where $\omega = \frac{W_1}{W}$

Hence, for the left hand span:

$$\int_0^{\ell} \eta \, dx = \frac{M_1}{H} \int_0^{\ell} \left[\frac{x}{\ell} - \frac{\sin \mu x}{\sin \mu \ell} \right] dx - \frac{\rho W}{\mu^2 H} \left[\int_0^{g\ell} \left[[1 - \cos \mu\ell(1-g)] \frac{\sin \mu x}{\sin \mu \ell} \right.\right.$$

$$\left. - \frac{\mu^2 \ell^2}{2} (1-g)^2 \frac{x}{\ell} \right] dx + \int_{g\ell}^{\ell} \left[\frac{\sin \mu x}{\sin \mu \ell} + \cos \mu g \ell \frac{\sin \mu(\ell-x)}{\sin \mu \ell} \right.$$

$$\left.\left. - 1 - \frac{\mu^2 \ell^2}{2} \left[(1-g)^2 \frac{x}{\ell} - \left(\frac{x}{\ell} - g \right)^2 \right] \right] dx \right]$$

which gives:

$$\int_0^{\ell} \eta \, dx = - \frac{M_1}{H} \frac{\theta}{2} - \frac{\rho W}{H} \ell \left[\frac{1}{\mu^2} \left[\frac{\cos \frac{\mu g \ell}{2} \sin \frac{\mu \ell}{2}(1-g)}{\frac{\mu \ell}{2} \cos \frac{\mu \ell}{2}} - (1-g) \right] - \frac{\ell^2}{12} \right.$$

$$\left. \left[1 - g^2 (3-2g) \right] \right]$$

Similarly, for the right hand span;

$$\int_0^{\ell_1} \eta_1 \, dx_1 = - \frac{M_1}{H} \frac{\theta_1}{2} - \frac{\rho W_1}{H} \ell_1 \left[\frac{1}{\mu^2} \left[\frac{\cos \frac{\mu g_1 \ell_1}{2} \sin \frac{\mu \ell_1}{2}(1-g_1)}{\frac{\mu \ell_1}{2} \cos \frac{\mu \ell_1}{2}} - (1-g_1) \right] \right.$$

$$\left. - \frac{\ell_1^2}{12} [1 - g_1^2 (3-2g_1)] \right]$$

but we know:

$$\sum \frac{W}{H_w} \int \eta dx = \frac{W}{H_w} \left[\int_0^{\ell} \eta dx + \omega \int_0^{\ell_1} \eta_1 dx_1 \right]$$

which yields when substituting for M_1:

$$\sum \frac{W}{H_w} \int \eta dx = \frac{W}{H_w} \left[- \frac{\rho W}{H} \left[- (\theta+\omega\theta_1) \frac{(\theta_g+\omega\theta_{g1})}{4(\phi+\phi_1)} + \frac{\ell}{\mu^2} \left[\frac{\cos \frac{\mu g \ell}{2} \sin \frac{\mu \ell}{2}(1-g)}{\frac{\mu\ell}{2} \cos \frac{\mu\ell}{2}} \right.\right.\right.$$

$$\left. - (1-g) + \omega^2\lambda \left[\frac{\cos \frac{\mu g_1 \ell_1}{2} \sin \frac{\mu \ell_1}{2}(1-g_1)}{\frac{\mu\ell_1}{2} \cos \frac{\mu\ell_1}{2}} - (1-g_1) \right] \right]$$

$$\left. - \frac{\ell^3}{12} [1 - g^2(3-2g)] - \frac{\omega^2 \ell_1^3}{12} [1 - g_1^2(3-2g_1)] \right] \Bigg]$$

3. For the two upward concentrated forces $C H_p$ and $C_1 H_p$

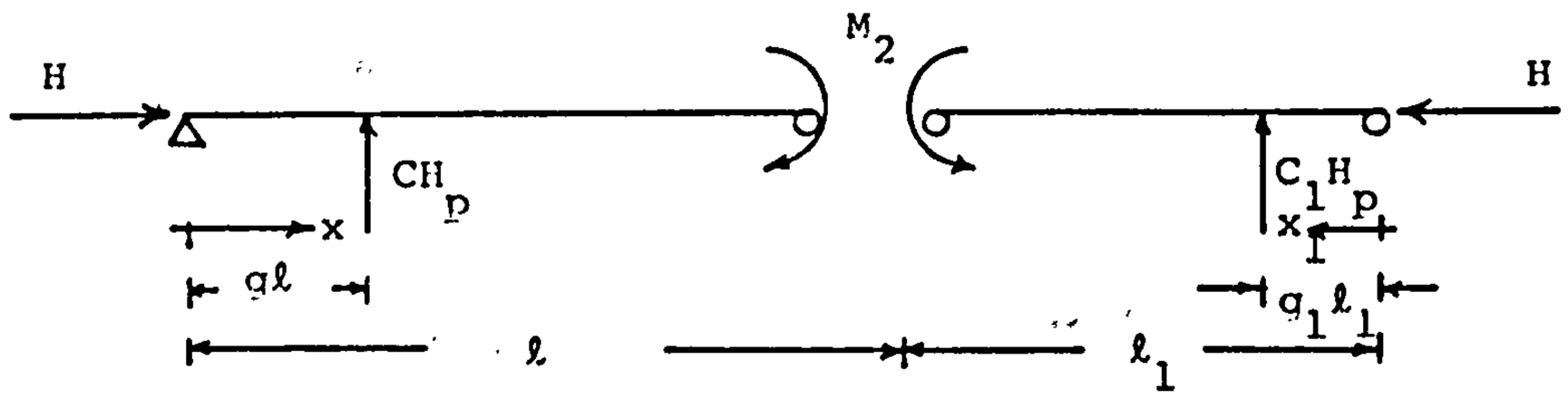

For the two upward concentrated forces $C H_p$ and $C_1 H_p$, which are the vertical components of the increase in the cable tension T_p, we have, [see Equation (3.2)]:

$$C = F + 8ng$$

$$C_1 + F_1 + 8n_1g_1$$

Thus, by substituting $\alpha = t+\varepsilon$ and $\beta = t-\varepsilon$ and replaceing $2\sigma\ell\varepsilon$ by $-CH_p$ for the left hand span and then taking the limit for this expression when $\varepsilon = o$ (see end of Appendix 12). We have the deflection equaitons for the left hand span:

$$\eta_1 = \frac{M_2}{H} \left[\frac{x}{\ell} - \frac{\sin \mu x}{\sin \mu\ell} \right] - \frac{CH_p}{\mu H} \left[\frac{\sin \mu\ell(1-g)}{\sin \mu\ell} \sin \mu x - \mu x (1-g) \right] \quad o \leqslant x \leqslant g\ell$$

$$\eta_2 = \frac{M_2}{H}\left[\frac{x}{\ell} - \frac{\sin \mu x}{\sin \mu \ell}\right] - \frac{CH_p}{\mu H}\left[\frac{\sin \mu g\ell}{\sin \mu \ell} \sin \mu(\ell-x) - \mu g\,(\ell-x)\right] \quad g\ell \leq x \leq \ell$$

Similar equations can be written for the right hand span. Hence, the slope at the left of the intermediate support can be computed as follows:

$$\frac{d\eta_2}{dx} = \frac{M_2}{H}\phi + \frac{CH_p}{H}\left[\frac{\sin \mu g\ell}{\sin \mu \ell} - g\right]$$

Similarly for the slope at the right of the intermediate support,

$$\frac{d\eta_{21}}{dx_1} = \frac{M_2}{H}\phi_1 + \frac{C_1 H_p}{H}\left[\frac{\sin \mu g_1 \ell_1}{\sin \mu \ell_1} - g_1\right]$$

Thus, the condition of the equal slopes is:

$$\frac{d\eta_2}{dx} = -\frac{d\eta_{21}}{dx_1}$$

which yields,

$$M_2 = -\frac{H_p}{(\phi+\phi_1)}\left[C\left(\frac{\sin \mu g\ell}{\sin \mu \ell} - g\right) + C_1\left(\frac{\sin \mu g_1 \ell_1}{\sin \mu \ell_1} - g_1\right)\right]$$

Hence; the deflection integration for the left hand span:

$$\int_0^{\ell} \eta\, dx = \frac{M_2}{H}\int_0^{\ell}\left[\frac{x}{\ell} - \frac{\sin \mu x}{\sin \mu \ell}\right] dx - \frac{CH_p}{\mu H}\left[\int_0^{g\ell}\left[\frac{\sin \mu \ell(1-g)}{\sin \mu \ell} \sin \mu x - \mu x\,(1-g)\right] dx + \int_{g\ell}^{\ell}\left[\frac{\sin \mu g\ell}{\sin \mu \ell} \sin \mu(\ell-x) - \mu g(\ell-x)\right] dx\right]$$

which gives:

$$\int_0^{\ell} \eta\, dx = -\frac{M_2}{H}\frac{\theta}{2} - \frac{CH_p}{\mu^2 H}\left[\frac{2 \sin \frac{\mu g\ell}{2} \sin \frac{\mu \ell}{2}(1-g)}{\cos \frac{\mu \ell}{2}} - \frac{\mu^2 \ell^2}{2} g\,(1-g)\right]$$

Similarly, for the right hand span;

$$\int_0^{\ell_1} \eta_1 \, dx_1 = -\frac{M_2}{H}\frac{\theta_1}{2} - \frac{C_1 H_p}{\mu^2 H}\left[\frac{2\sin\frac{\mu g_1 \ell_1}{2}\ \sin\frac{\mu\ell_1}{2}(1-g_1)}{\cos\frac{\mu\ell_1}{2}} - \frac{\mu^2\ell_1^2}{2} g_1(1-g_1)\right]$$

Hence, the total value of the term $\left(\sum \frac{W}{H_w}\int \eta dx\right)$ is:

$$\sum \frac{W}{H_w}\int \eta dx = \frac{W}{H_w}\left[\frac{H_p}{H}\frac{(\theta+\omega\theta_1)}{2(\phi+\phi_1)}\left[C\left[\frac{\sin\mu g\ell}{\sin\mu\ell} - g\right] + C_1\left[\frac{\sin\mu g_1\ell_1}{\sin\mu\ell_1} - g_1\right]\right]\right.$$

$$- \frac{H_p}{\mu^2 H}\left[C\left[\frac{2\sin\frac{\mu g\ell}{2}\ \sin\frac{\mu\ell}{2}(1-g)}{\cos\frac{\mu\ell}{2}} - \frac{\mu^2\ell^2}{2} g\,(1-g)\right]\right.$$

$$\left.\left. + \omega C_1\left[\frac{2\sin\frac{\mu g_1\ell_1}{2}\ \sin\frac{\mu\ell_1}{2}(1-g_1)}{\cos\frac{\mu\ell_1}{2}} - \frac{\mu^2\ell_1^2}{2} g_1\,(1-g_1)\right]\right]\right]$$

4. For the two concentrated moments, $H_p Z_1$

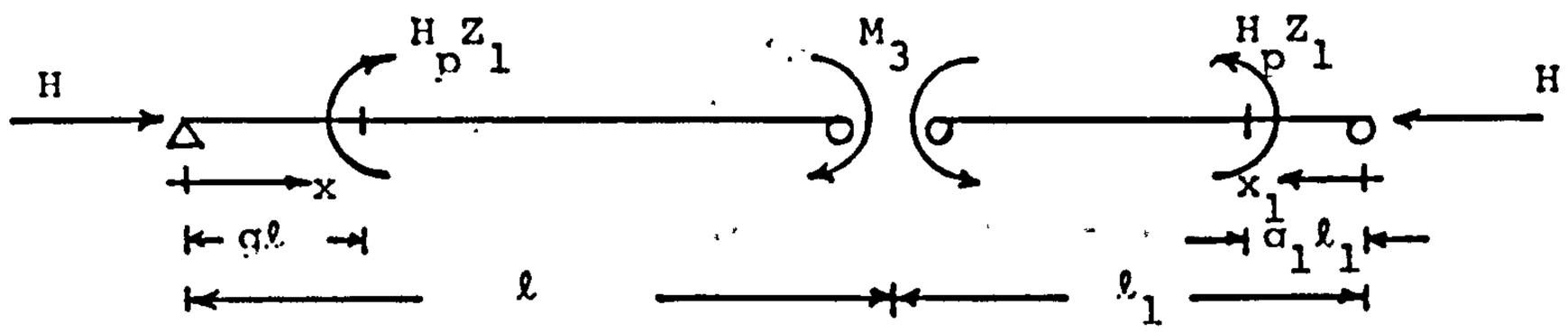

For the concentrated moments, $H_p Z_1$, the bending moment equations for the left hand span are:

$$M_x = EI\frac{d^2\eta_1}{dx^2} = -H\eta_1 + H_p Z_1\frac{x}{\ell} + M_3\frac{x}{\ell} \qquad 0 \leqslant x \leqslant g\ell$$

$$M_x = EI\frac{d^2\eta_2}{dx^2} = -H\eta_2 - \frac{H_p Z_1}{\ell}(\ell - x) + M_3\frac{x}{\ell} \qquad g\ell \leqslant x \leqslant \ell$$

which gives;

$$\frac{d^2\eta_1}{dx^2} + \mu^2 \eta_1 = \frac{H_p Z_1}{EI} \frac{x}{\ell} + \frac{M_3}{EI} \frac{x}{\ell}$$

$$\frac{d^2\eta_2}{dx^2} + \mu^2 \eta_2 = - \frac{H_p Z_1}{EI} \frac{(\ell-x)}{\ell} + \frac{M_3}{EI} \frac{x}{\ell}$$

The solution for these equations can simply be found as follows (see Appendix 12):

$$\eta_1 = A \sin \mu x + B \cos \mu x + \frac{H_p Z_1}{H} \frac{x}{\ell} + \frac{M_3}{H} \frac{x}{\ell}$$

$$\eta_2 = C \sin \mu x + D \cos \mu x - \frac{H_p Z_1}{H} \frac{(\ell-x)}{\ell} + \frac{M_3}{H} \frac{x}{\ell}$$

The constants A, B, C, and D can be calculated from the following boundary conditions.

1. <u>at x = o</u> <u>$\eta_1 = o$</u> B = o

2. <u>at x = gℓ</u> <u>$\frac{d\eta_1}{dx} = \frac{d\eta_2}{dx}$</u>

$$A \cos \mu g\ell = C \cos \mu g\ell - D \sin \mu g\ell \qquad \text{(i)}$$

3. <u>at x = gℓ</u> <u>$\eta_1 = \eta_2$</u>

$$A \sin \mu g\ell = C \sin \mu g\ell + D \cos \mu g\ell - \frac{H_p Z_1}{H} \qquad \text{(ii)}$$

(<u>Equations (i) * sin $\mu g\ell$) - (Equation (ii) * cos $\mu g\ell$</u>)

$$D = \frac{H_p Z_1}{H} \cos \mu g\ell \qquad \text{(iii)}$$

4. <u>at x = ℓ</u> <u>$\eta_2 = o$</u>

$$C = - \frac{H_p Z_1}{H} \cos \mu g\ell \cot \mu\ell - \frac{M_3}{H} \operatorname{cosec} \mu\ell \qquad \text{(iv)}$$

Substituting from (iv) into (i)

$$A = - \frac{H_p Z_1}{H} \cos \mu g\ell \cot \mu\ell - \frac{M_3}{H} \operatorname{cosec} \mu\ell - \frac{H_p Z_1}{H} \sin \mu g\ell$$

$$A = \frac{-1}{\sin \mu\ell}\left[\frac{M_3}{H} + \frac{H_p Z_1}{H} \cos \mu\ell(1-g)\right] \qquad (v)$$

Hence, the deflection equations are:

$$\eta_1 = \frac{M_3}{H}\left[\frac{x}{\ell} - \frac{\sin \mu x}{\sin \mu\ell}\right] + \frac{H_p Z_1}{H}\left[\frac{x}{\ell} - \cos \mu\ell(1-g)\,\frac{\sin \mu x}{\sin \mu\ell}\right] \qquad o \leqslant x \leqslant g\ell$$

$$\eta_2 = \frac{M_3}{H}\left[\frac{x}{\ell} - \frac{\sin \mu x}{\sin \mu\ell}\right] + \frac{H_p Z_1}{H}\left[\frac{(\ell-x)}{\ell} - \cos \mu g\ell\,\frac{\sin \mu(\ell-x)}{\sin \mu\ell}\right] \qquad g\ell \leqslant x \leqslant \ell$$

Similar equations can be written for the right hand span. Thus, the slopes at both sides of the intermediate support are equal, where:

$$\frac{d\eta_2}{dx} = \frac{M_3}{H}\phi - \frac{H_p Z_1}{H}\nu_g$$

for the left hand span and similarly;

$$\frac{d\eta_{21}}{dx_1} = \frac{M_3}{H}\phi_1 - \frac{H_p Z_1}{H}\nu_{g1}$$

for the right hand span:

where $\nu_g = \frac{1}{\ell}\left[\frac{\mu\ell}{\sin \mu\ell} \cos \mu g\ell - 1\right]$,

and $\nu_{g1} = \frac{1}{\ell_1}\left[\frac{\mu\ell_1}{\sin \mu\ell_1} \cos \mu g_1\ell_1 - 1\right]$

It is worth noting that at g and $g_1 = o$, ν_g and ν_{g1} become equal to ν and

and ν_1 where:

$$\nu = \frac{1}{\ell}\left[\frac{\mu\ell}{\sin \mu\ell} - 1\right] \text{ and } \nu_1 = \frac{1}{\ell_1}\left[\frac{\mu\ell_1}{\sin \mu\ell_1} - 1\right].$$

Thus, $$\frac{d\eta_2}{dx} = -\frac{d\eta_{21}}{dx_1}$$

which yields:

$$M_3 = H_p Z_1 \frac{(\nu_g + \nu_{g1})}{(\phi+\phi_1)}$$

Thus, for the left hand span:

$$\int_0^{\ell} \eta \, dx = \frac{M_3}{H} \int_0^{\ell} \left[\frac{x}{\ell} - \frac{\sin \mu x}{\sin \mu \ell} \right] dx + \frac{H_p Z_1}{H} \left[\int_0^{g\ell} \left[\frac{x}{\ell} - \cos \mu \ell (1-g) \frac{\sin \mu x}{\sin \mu \ell} \right] dx \right.$$

$$\left. - \int_{g\ell}^{\ell} \left[\frac{(\ell - x)}{\ell} - \cos \mu g \ell \frac{\sin \mu (\ell - x)}{\sin \mu \ell} \right] dx \right]$$

which gives:

$$\int_0^{\ell} \eta \, dx = - \frac{M_3}{H} \frac{\theta}{2} - \frac{H_p Z_1}{2H} \ell \left[\frac{\sin \frac{\mu \ell}{2} (1-2g)}{\frac{\mu \ell}{2} \cos \frac{\mu \ell}{2}} - (1 - 2g) \right]$$

Similarly, for the right hand span:

$$\int_0^{\ell_1} \eta_1 \, dx_1 = - \frac{M_3}{H} \frac{\theta_1}{2} - \frac{H_p Z_1}{2H} \ell_1 \left[\frac{\sin \frac{\mu \ell_1}{2} (1-2g_1)}{\frac{\mu \ell_1}{2} \cos \frac{\mu \ell_1}{2}} - (1-2g_1) \right]$$

Hence, the total value of the term $\left[\sum \frac{W}{H_w} \int \eta dx \right]$ is:

$$\sum \frac{W}{H_w} \int \eta dx = \frac{W}{H_w} \left[\frac{H_p Z_1}{2H} \left[- (\theta + \omega \theta_1) \frac{(\nu_g + \nu_{g1})}{(\phi + \phi_1)} + \ell \left[\frac{\sin \frac{\mu \ell}{2} (1-2)}{\frac{\mu \ell}{2} \cos \frac{\mu \ell}{2}} - (1-2g) \right] \right. \right.$$

$$\left. \left. - \omega \ell_1 \left[\frac{\sin \frac{\mu \ell_1}{2} (1-2g_1)}{\frac{\mu \ell_1}{2} \cos \frac{\mu \ell_1}{2}} - (1-2g_1) \right] \right] \right]$$

5. The end moments, $H_i a$

For the end moments, $H_i a$, the term $\left[\sum \frac{W}{H_w} \int \eta dx \right]$ can be directly obtained from Appendix 13, or by substituting $g = g_1 = o$ in the above formula which gives:

$$\sum \frac{W}{H_w} \int \eta dx = \frac{W}{H_w} \left[- \frac{H_i a}{2H} (\theta + \omega \theta_1) \left[1 - \frac{(\nu + \nu_1)}{(\phi + \phi_1)} \right] \right]$$

Finally, the total value of the term $\left[\sum \frac{W}{H_w} \int \eta dx \right]$ for the first group of forces can be obtained as by adding the five expressions obtained for the five applied loading.

APPENDIX 22

22. The Determination of the Internal Forces Produced by the First Group of Forces

1. For yW and yW_1

For the two upward continuous uniformly distributed forces yW and yW_1, the deflection equations are: (see Appendix 12)

$$\eta = -\frac{yW}{\mu^2 H}\left[\frac{\sin \mu x}{\sin \mu \ell}\left[1 - \frac{\mu^2}{2}\frac{(\theta+\omega\theta_1)}{(\phi+\phi_1)}\right] + \frac{\sin \mu(\ell-x)}{\sin \mu \ell} - 1 - \frac{\mu^2}{2}\frac{x}{\ell}\left[\ell\,(\ell-x) - \frac{(\theta+\omega\theta_1)}{(\phi+\phi_1)}\right]\right] \qquad o \leqslant x \leqslant \ell$$

for the left hand span and similarly;

$$\eta_1 = -\frac{yW_1}{\mu^2 H}\left[\frac{\sin \mu x_1}{\sin \mu \ell_1}\left[1 - \frac{\mu^2}{2\omega}\frac{(\theta+\omega\theta_1)}{(\phi+\phi_1)}\right] + \frac{\sin \mu(\ell_1-x_1)}{\sin \mu \ell_1} - 1 - \frac{\mu^2}{2}\frac{x_1}{\ell_1}\left[\ell_1\,(\ell_1-x_1) - \frac{(\theta+\omega\theta_1)}{\omega(\phi+\phi_1)}\right]\right] \qquad o \leqslant x_1 \leqslant \ell_1$$

for the right hand span.

Hence, the bending moments equations can be obtained from the relationship:

$$M_x = EI\frac{d^2\eta}{dx^2} \qquad \text{and} \qquad M_{x1} = EI\frac{d^2\eta_1}{dx_1^2}$$

for left and right hand spans respectively, which yields:

$$M_x = \frac{yW}{\mu^2 \sin \mu \ell}\left[\sin \mu x\left[1 - \frac{\mu^2}{2}\frac{(\theta+\omega\theta_1)}{(\phi+\phi_1)}\right] + \sin \mu(\ell-x) - \sin \mu \ell\right] \qquad o \leqslant x \leqslant \ell$$

for the left hand span, and similarly:

$$M_{x1} = \frac{yW_1}{\mu^2 \sin \mu\ell_1}\left[\sin \mu x_1 \left[1 - \frac{\mu^2}{2\omega} \frac{(\theta+\omega\theta_1)}{(\phi+\phi_1)} \right] + \sin \mu(\ell_1-x_1) - \sin \mu\ell_1 \right]$$

$$o \leqslant x \leqslant \ell_1$$

for the right hand span. The shear forces equations can be evaluated from the relationships:

$$Q_x = -\frac{dM_x}{dx} \qquad \text{and} \qquad Q_{x1} = -\frac{dM_{x1}}{dx_1}$$

for left and right hand spans respectivley which yields:

$$Q_x = -\frac{yW}{\mu \sin \mu\ell}\left[\cos \mu x \left[1 - \frac{\mu^2}{2} \frac{(\theta+\omega\theta_1)}{(\phi+\phi_1)} \right] - \cos \mu(\ell-x) \right] \qquad o \leqslant x \leqslant \ell$$

for the left hand span, and similarly:

$$Q_{x1} = -\frac{yW_1}{\mu \sin \mu\ell_1}\left[\cos \mu x_1 \left[1 - \frac{\mu^2}{2\omega} \frac{(\theta+\omega\theta_1)}{(\phi+\phi_1)} \right] - \cos \mu(\ell_1-x_1) \right]$$

$$o \leqslant x_1 \leqslant \ell_1$$

2. For ρW and ρW_1

For the two upward partially distributed forces ρW and ρW_1, the deflection equations are: (see Appendix 21)

$$\eta_{(1)} = -\frac{\rho W}{\mu^2 H}\left[\frac{\sin \mu x}{\sin \mu\ell}\left[[1 - \cos \mu\ell(1-g)] - \frac{\mu^2}{2} \frac{(\theta_g+\omega\theta_{g1})}{(\phi+\phi_1)} \right] - \frac{\mu^2}{2} \frac{x}{\ell} \right.$$

$$\left. \left[\ell^2 (1-g)^2 - \frac{(\theta_g+\omega\theta_g)}{(\phi+\phi_1)} \right] \right] \qquad o \leqslant x \leqslant g\ell$$

$$\eta_{(2)} = -\frac{\rho W}{\mu^2 H}\left[\frac{\sin \mu x}{\sin \mu\ell}\left[[1 - \frac{\mu^2}{2} \frac{(\theta_g+\omega\theta_{g1})}{(\phi+\phi_1)} \right] + \cos \mu g\ell \frac{\sin \mu(\ell-x)}{\sin \mu\ell} - 1 - \frac{\mu^2}{2}\left[\frac{x}{\ell} \right.\right.\right.$$

$$\left.\left.\left. \left[\ell^2 (1-g)^2 - \frac{(\theta_g+\omega\theta_g)}{(\phi+\phi_1)} \right] - (x-g\ell)^2 \right] \right] \qquad g\ell \leqslant x \leqslant \ell$$

for the left hand span, and similarly:

$$\eta_{1(1)} = -\frac{\rho W_1}{\mu^2 H}\left[\frac{\sin \mu x_1}{\sin \mu \ell_1}\left[[1-\cos \mu \ell_1(1-g_1)] - \frac{\mu^2}{2\omega}\frac{(\theta_g+\omega\theta_{g1})}{(\phi+\phi_1)}\right] - \frac{\mu^2}{2}\frac{x_1}{\ell_1}\right.$$

$$\left.\left[\ell_1^2(1-g_1)^2 - \frac{(\theta_g+\omega\theta_{g1})}{\omega(\phi+\phi_1)}\right]\right] \qquad 0 \leq x_1 \leq g_1\ell_1$$

$$\eta_{1(2)} = -\frac{\rho W_1}{\mu^2 H}\left[\frac{\sin \mu x_1}{\sin \mu \ell_1}\left[[1-\frac{\mu^2}{2\omega}\frac{(\theta_g+\omega\theta_{g1})}{(\phi+\phi_1)}\right] + \cos \mu g_1\ell_1 \frac{\sin \mu(\ell_1-x_1)}{\sin \mu\ell_1} - 1 -\right.$$

$$\left.\frac{\mu^2}{2}\left[\frac{x_1}{\ell_1}\left[\ell_1^2(1-g_1)^2 - \frac{(\theta_g+\omega\theta_{g1})}{\omega(\phi+\phi_1)}\right] - (x-g\ell)^2\right]\right] \qquad g_1\ell_1 \leq x_1 \leq \ell_1$$

for the right hand span. The bending moment equations can be obtained from the aforementioned relationships which gives:

$$M_{x(1)} = +\frac{\rho W}{\mu^2}\frac{\sin \mu x}{\sin \mu \ell}\left[[1-\cos \mu\ell(1-g)] - \frac{\mu^2}{2}\frac{(\theta_g+\omega\theta_{g1})}{(\phi+\phi_1)}\right] \qquad 0 \leq x \leq g\ell$$

$$M_{x(2)} = +\frac{\rho W}{\mu^2 \sin \mu\ell}\left[\sin \mu x\left[1-\frac{\mu^2}{2}\frac{(\theta_g+\omega\theta_{g1})}{(\phi+\phi_1)}\right] + \cos \mu g\ell \sin \mu(\ell-x)\right.$$

$$\left. - \sin \mu\ell\right] \qquad g\ell \leq x \leq \ell$$

for the left hand span and similarly;

$$M_{x1(1)} = +\frac{\rho W_1}{\mu^2}\frac{\sin \mu x_1}{\sin \mu \ell_1}\left[[1-\cos \mu\ell_1(1-g_1)] - \frac{\mu^2}{2\omega}\frac{(\theta_g+\omega\theta_{g1})}{(\phi+\phi_1)}\right]$$

$$0 \leq x \leq g\ell_1 \quad 1\ 1$$

$$M_{x1(2)} = +\frac{\rho W_1}{\mu^2 \sin \mu\ell_1}\left[\sin \mu x_1\left[1-\frac{\mu^2}{2\omega}\frac{(\theta_g+\omega\theta_{g1})}{(\phi+\phi_1)}\right] + \cos \mu g_1\ell_1 \sin \mu(\ell_1-x_1)\right.$$

$$\left. - \sin \mu\ell_1\right] \qquad g_1\ell_1 \leq x_1 \leq \ell_1$$

for the right hand spans. The shear forces equations can be obtained for the left hand span, as before:

$$Q_{x(1)} = -\frac{\rho W}{\mu}\ \frac{\cos \mu x}{\sin \mu \ell}\left[\left[\ 1 - \cos \mu \ell(1-g)\ \right] - \frac{\mu^2}{2}\ \frac{(\theta_g + \omega\theta_{g1})}{(\phi+\phi_1)}\right] \qquad o \leqslant x \leqslant g\ell$$

$$Q_{x(2)} = -\frac{\rho W}{\mu \sin \mu \ell}\left[\cos \mu x\left[\ 1 - \frac{\mu^2}{2}\ \frac{(\theta_g + \omega\theta_{g1})}{(\phi+\phi_1)}\ \right] - \cos \mu g\ell \cos \mu(\ell - x)\ \right]$$

$$g\ell \leqslant x \leqslant \ell$$

Similarly, for the right hand span;

$$Q_{x1(1)} = -\frac{\rho W_1}{\mu}\ \frac{\cos \mu x_1}{\sin \mu \ell_1}\left[\left[\ 1 - \cos \mu \ell_1(1-g_1)\ \right] - \frac{\mu^2}{2\omega}\ \frac{(\theta_g + \omega\theta_{g1})}{(\phi+\phi_1)}\ \right] \quad o \leqslant x_1 \leqslant g_1\ell_1$$

$$Q_{x1(2)} = -\frac{\rho W_1}{\mu \sin \mu \ell_1}\left[\cos \mu x_1\left[\ 1 - \frac{\mu^2}{2\omega}\ \frac{(\theta_g + \omega\theta_{g1})}{(\phi+\phi_1)}\ \right] - \cos \mu g_1\ell_1 \cos \mu(\ell_1 - x_1)\right]$$

$$g_1\ell_1 \leqslant x_1 \leqslant \ell_1$$

3. For $C\ H_p$ and $C_1\ H_p$

For the upward concentrated forces $C\ H_p$ and $C_1\ H_p$, we have the deflection equations for the left hand span: (see Appendix 21)

$$\eta_{(1)} = -\frac{H_p}{H(\phi+\phi_1)}\left[\ C\left[\frac{\sin \mu g\ell}{\sin \mu \ell} - g\right] + C_1\left[\frac{\sin \mu g_1\ell_1}{\sin \mu \ell_1} - g_1\right]\right]\left[\frac{x}{\ell} - \frac{\sin \mu x}{\sin \mu \ell}\right]$$

$$-\frac{C\ H_p}{\mu H}\left[\ \sin \mu\ell(1-g)\ \frac{\sin \mu x}{\sin \mu \ell} - \mu x(1-g)\right] \qquad o \leqslant x \leqslant g\ell$$

$$\eta_{(2)} = -\frac{H_p}{H(\phi+\phi_1)}\left[\ C\left[\frac{\sin \mu g\ell}{\sin \mu \ell} - g\right] + C_1\left[\frac{\sin \mu g_1\ell_1}{\sin \mu \ell_1} - g_1\right]\right]\left[\frac{x}{\ell} - \frac{\sin \mu x}{\sin \mu \ell}\right]$$

$$-\frac{C\ H_p}{\mu H}\left[\frac{\sin \mu g\ell}{\sin \mu \ell}\ \sin \mu(\ell - x) - \mu g(\ell - x)\right] \qquad g\ell \leqslant x \leqslant \ell$$

Similarly, for the right hand span:

$$\eta_{1(1)} = -\frac{H_p}{H(\phi+\phi_1)}\left[\ C\left[\frac{\sin \mu g\ell}{\sin \mu \ell} - g\right] + C_1\left[\frac{\sin \mu g_1\ell_1}{\sin \mu \ell_1} - g_1\right]\right]\left[\frac{x_1}{\ell_1} - \frac{\sin \mu x_1}{\sin \mu \ell_1}\right]$$

$$- \frac{C_1 H_p}{\mu H} \left[\sin \mu \ell_1 (1-g_1) \frac{\sin \mu x_1}{\sin \mu \ell_1} - \mu x_1 (1-g_1) \right] \qquad o \leqslant x_1 \leqslant g_1 \ell_1$$

$$\eta_{1(2)} = - \frac{H_p}{H(\phi+\phi_1)} \left[C \left[\frac{\sin \mu g \ell}{\sin \mu \ell} - g \right] + C_1 \left[\frac{\sin \mu g_1 \ell_1}{\sin \mu \ell_1} - g_1 \right] \right] \left[\frac{x_1}{\ell_1} - \frac{\sin \mu x_1}{\sin \mu \ell_1} \right]$$

$$- \frac{C_1 H_p}{\mu H} \left[\frac{\sin \mu g_1 \ell_1}{\sin \mu \ell_1} \sin \mu (\ell_1 - x_1) - \mu g_1 (\ell_1 - x_1) \right] \qquad g_1 \ell_1 \leqslant x_1 \leqslant \ell_1$$

The bending moment equations for the left hand span are:

$$M_{x(1)} = - \frac{H_p}{(\phi+\phi_1)} \left[C \left[\frac{\sin \mu g \ell}{\sin \mu \ell} - g \right] + C_1 \left[\frac{\sin \mu g_1 \ell_1}{\sin \mu \ell_1} - g_1 \right] \right] \frac{\sin \mu x}{\sin \mu \ell}$$

$$+ \frac{C H_p}{\mu} \frac{\sin \mu \ell (1-g)}{\sin \mu \ell} \sin \mu x \Bigg] \qquad o \leqslant x \leqslant g\ell$$

$$M_{x(2)} = - \frac{H_p}{(\phi+\phi_1)} \left[C \left[\frac{\sin \mu g \ell}{\sin \mu \ell} - g \right] + C_1 \left[\frac{\sin \mu g_1 \ell_1}{\sin \mu \ell_1} - g_1 \right] \right] \frac{\sin \mu x}{\sin \mu \ell}$$

$$+ \frac{C H_p}{\mu} \frac{\sin \mu g \ell}{\sin \mu \ell} \sin \mu (\ell - x) \qquad g\ell \leqslant x \leqslant \ell$$

Similarly, for the right hand span;

$$M_{x1(1)} = - \frac{H_p}{(\phi+\phi_1)} \left[C \left[\frac{\sin \mu g \ell}{\sin \mu \ell} - g \right] + C_1 \left[\frac{\sin \mu g_1 \ell_1}{\sin \mu \ell_1} - g_1 \right] \right] \frac{\sin \mu x_1}{\sin \mu \ell_1}$$

$$+ \frac{C_1 H_p}{\mu} \frac{\sin \mu \ell_1 (1-g_1)}{\sin \mu \ell_1} \sin \mu x_1 \qquad o \leqslant x_1 \leqslant g_1 \ell_1$$

$$M_{x1(2)} = - \frac{H_p}{(\phi+\phi_1)} \left[C \left[\frac{\sin \mu g \ell}{\sin \mu \ell} - g \right] + C_1 \left[\frac{\sin \mu g_1 \ell_1}{\sin \mu \ell_1} - g_1 \right] \right] \frac{\sin \mu x_1}{\sin \mu \ell_1}$$

$$+ \frac{C_1 H_p}{\mu} \frac{\sin \mu g_1 \ell_1}{\sin \mu \ell_1} \sin \mu (\ell_1 - x_1) \qquad g_1 \ell_1 \leqslant x_1 \leqslant \ell_1$$

The shear forces equation can be determined for the left hand span:

$$Q_{x(1)} = + \mu \frac{H_p}{(\phi+\phi_1)} \left[C \left[\frac{\sin \mu g \ell}{\sin \mu \ell} - g \right] + C_1 \left[\frac{\sin \mu g_1 \ell_1}{\sin \mu \ell_1} - g_1 \right] \right] \frac{\cos \mu x}{\sin \mu \ell}$$

$$- C H_p \frac{\sin \mu \ell (1-g)}{\sin \mu \ell} \cos \mu x \qquad o \leqslant x \leqslant g\ell$$

$$Q_{x(2)} = + \mu \frac{H_p}{(\phi+\phi_1)} \left[C \left(\frac{\sin \mu g \ell}{\sin \mu \ell} - g \right) + C_1 \left(\frac{\sin \mu g_1 \ell_1}{\sin \mu \ell_1} - g_1 \right) \right] \frac{\cos \mu x}{\sin \mu \ell}$$

$$+ C H_p \frac{\sin \mu g \ell}{\sin \mu \ell} \cos \mu(\ell - x) \qquad g\ell \leqslant x \leqslant \ell$$

Similarly, for the right hand spans:

$$Q_{x1(1)} = + \mu \frac{H_p}{(\phi+\phi_1)} \left[C \left(\frac{\sin \mu g \ell}{\sin \mu \ell} - g \right) + C_1 \left(\frac{\sin \mu g_1 \ell_1}{\sin \mu \ell_1} - g_1 \right) \right] \frac{\cos \mu x_1}{\sin \mu \ell_1}$$

$$- C_1 H_p \frac{\sin \mu \ell_1 (1-g_1)}{\sin \mu \ell_1} \cos \mu x_1 \qquad o \leqslant x_1 \leqslant g_1 \ell_1$$

$$Q_{x1(2)} = + \mu \frac{H_p}{(\phi+\phi_1)} \left[C \left(\frac{\sin \mu g \ell}{\sin \mu \ell} - g \right) + C_1 \left(\frac{\sin \mu g_1 \ell_1}{\sin \mu \ell_1} - g_1 \right) \right] \frac{\cos \mu x_1}{\sin \mu \ell_1}$$

$$+ C_1 H_p \frac{\sin \mu g_1 \ell_1}{\sin \mu \ell_1} \cos \mu(\ell_1 - x_1) \qquad g_1 \ell_1 \leqslant x_1 \leqslant \ell_1$$

4. For the concentrated moments $H_p Z_1$

For the two concentrated moments, the deflection equations are: (see Appendix 21)

$$\eta_{(1)} = \frac{H_p Z_1}{H} \left[\frac{x}{\ell} \left(1 + \frac{(\nu_g + \nu_{g1})}{(\phi+\phi_1)} \right) - \frac{\sin \mu x}{\sin \mu \ell} \left(\cos \mu \ell (1-g) + \frac{(\nu_g + \nu_{g1})}{(\phi+\phi_1)} \right) \right]$$

$$o \leqslant x \leqslant g\ell$$

$$\eta_{(2)} = \frac{H_p Z_1}{H} \left[\frac{x}{\ell} \left(1 + \frac{(\nu_g + \nu_{g1})}{(\phi+\phi_1)} \right) - 1 - \frac{\sin \mu x}{\sin \mu \ell} \frac{(\nu_g + \nu_{g1})}{(\phi+\phi_1)} + \cos \mu g \ell \frac{\sin \mu(\ell - x)}{\sin \mu \ell} \right]$$

$$g\ell \leqslant x \leqslant \ell$$

for the left hand span and similarly;

$$\eta_{1(1)} = \frac{H_p Z_1}{H} \left[\frac{x_1}{\ell_1} \left(1 + \frac{(\nu_g + \nu_{g1})}{(\phi+\phi_1)} \right) - \frac{\sin \mu x_1}{\sin \mu \ell_1} \left(\cos \mu \ell_1 (1-g_1) + \frac{(\nu_g + \nu_{g1})}{(\phi+\phi_1)} \right) \right]$$

$$o \leqslant x_1 \leqslant g_1 \ell_1$$

$$\eta_{1(2)} = \frac{H_p Z_1}{H} \left[\frac{x_1}{\ell_1} \left(1 + \frac{(\nu_g + \nu_{g1})}{(\phi+\phi_1)} \right) - 1 - \frac{\sin \mu x_1}{\sin \mu \ell_1} \frac{(\nu_g + \nu_{g1})}{(\phi+\phi_1)} + \cos \mu g_1 \ell_1 \right.$$

$$\frac{\sin \mu(\ell_1 - x_1)}{\sin \mu \ell_1} \Bigg] \qquad g_1 \ell_1 \leq x_1 \leq \ell_1$$

for the right hand span.

The bending moment equations for the left hand span are:

$$M_{x(1)} = H_p Z_1 \frac{\sin \mu x}{\sin \mu \ell} \left[\cos \mu \ell (1-g) + \frac{(\nu_g + \nu_{g1})}{(\phi + \phi_1)} \right] \qquad o \leq x \leq g\ell$$

$$M_{x(2)} = \frac{H_p Z_1}{\sin \mu \ell} \left[\sin \mu x \frac{(\nu_g + \nu_{g1})}{(\phi + \phi_1)} - \cos \mu g \ell \sin \mu(\ell - x) \right] \qquad g\ell \leq x \leq \ell$$

and similarly for the right hand span;

$$M_{x1(1)} = H_p Z_1 \frac{\sin \mu x_1}{\sin \mu \ell_1} \left[\cos \mu \ell_1 (1-g_1) + \frac{(\nu_g + \nu_{g1})}{(\phi + \phi_1)} \right] \qquad o \leq x \leq g_1 \ell_1$$

$$M_{x1(2)} = \frac{H_p Z_1}{\sin \mu \ell_1} \left[\sin \mu x_1 \frac{(\nu_g + \nu_{g1})}{(\phi + \phi_1)} - \cos \mu g_1 \ell_1 \sin \mu(\ell_1 - x_1) \right]$$

$$g_1 \ell_1 \leq x_1 \leq \ell_1$$

The shear forces equations for the left hand span are:

$$Q_{x(1)} = - \mu H_p Z_1 \frac{\cos \mu x}{\sin \mu \ell} \left[\cos \mu \ell (1-g) + \frac{(\nu_g + \nu_{g1})}{(\phi + \phi_1)} \right] \qquad o \leq x \leq g\ell$$

$$Q_{x(2)} = - \mu \frac{H_p Z_1}{\sin \mu \ell} \left[\cos \mu x \frac{(\nu_g + \nu_{g1})}{(\phi + \phi_1)} + \cos \mu g \ell \cos \mu(\ell - x) \right] \qquad g\ell \leq x \leq \ell$$

and similarly for the right hand span, we have:

$$Q_{x1(1)} = - \mu H_p Z_1 \frac{\cos \mu x_1}{\sin \mu \ell_1} \left[\cos \mu \ell_1 (1-g_1) + \frac{(\nu_g + \nu_{g1})}{(\phi + \phi_1)} \right] \qquad o \leq x_1 \leq g_1 \ell_1$$

$$Q_{x1(2)} = - \mu \frac{H_p Z_1}{\sin \mu \ell_1} \left[\cos \mu x_1 \frac{(\nu_g + \nu_{g1})}{(\phi + \phi_1)} + \cos \mu g_1 \ell_1 \cos \mu(\ell_1 - x_1) \right]$$

$$g_1 \ell_1 \leq x_1 \leq \ell_1$$

5. For the end moments $H_i a$

For the end moments $H_i a$, the deflection equation for the left hand

span is, (see Appendix 12), or by substituting $g = g_1 = o$ in the above equation:

$$\eta = - \frac{H_i a}{H} \left[\frac{x}{\ell} + \frac{\sin \mu(\ell-x)}{\sin \mu\ell} + \frac{(\nu+\nu_1)}{(\phi+\phi_1)} \left[\frac{x}{\ell} - \frac{\sin \mu x}{\sin \mu\ell} \right] - 1 \right] \qquad o \leqslant x \leqslant \ell$$

and similarly for the right hand span:

$$\eta_1 = - \frac{H_i a}{H} \left[\frac{x_1}{\ell_1} + \frac{\sin \mu(\ell_1-x_1)}{\sin \mu\ell_1} + \frac{(\nu+\nu_1)}{(\phi+\phi_1)} \left[\frac{x_1}{\ell_1} - \frac{\sin \mu x_1}{\sin \mu\ell_1} \right] - 1 \right]$$

$$o \leqslant x_1 \leqslant \ell_1$$

The bending moment equation for the left hand span is found to be:

$$M_x = \frac{H_i a}{\sin \mu\ell} \left[\sin \mu(\ell-x) - \frac{(\nu+\nu_1)}{(\phi+\phi_1)} \sin \mu x \right] \qquad o \leqslant x \leqslant \ell$$

and similarly for the right hand span:

$$M_{x1} = \frac{H_i a}{\sin \mu\ell_1} \left[\sin \mu(\ell_1-x_1) - \frac{(\nu+\nu_1)}{(\phi+\phi_1)} \sin \mu x_1 \right] \qquad o \leqslant x_1 \leqslant \ell_1$$

The shear forces equation for the left hand span can be obtained as follows:

$$Q_x = + \frac{\mu H_i a}{\sin \mu\ell} \left[\cos \mu(\ell-x) + \frac{(\nu+\nu_1)}{(\phi+\phi_1)} \cos \mu x \right] \qquad o \leqslant x \leqslant \ell$$

and similarly for the right hand span:

$$Q_{x1} = + \frac{\mu H_i a}{\sin \mu\ell_1} \left[\cos \mu(\ell_1-x_1) + \frac{(\nu+\nu_1)}{(\phi+\phi_1)} \cos \mu x_1 \right] \qquad o \leqslant x_1 \leqslant \ell_1$$

where ν, ν_1 , ϕ, ϕ_1 , θ, θ_1 , θ_g , θ_{g1}, ν_g and ν_{g1} can be obtained from the preceding appendix.

Finally, the total values of the deflections, bending moments and shear forces of the first group of forces can be determined when superimposing the previous cases of loading as shown in Equations (3.27), (3.28) and (3.29).

APPENDIX 23

23. The Determination of the Maximum Suspender Load

The shear forces equations for the maximum upward distributed suspender forces, including the dead loads, are: (see Formulae (3.29))

$$Q_{s(1)max} = \frac{-W(1+y)}{\mu \sin \mu\ell}\left[\cos \mu x\left[1 - \frac{\mu^2}{2}\frac{(\theta+\omega\theta_1)}{(\phi+\phi_1)}\right] - \cos \mu(\ell-x)\right]$$

$$- \frac{\rho_{max}\, W}{\mu}\frac{\cos \mu x}{\sin \mu\ell}\left[1 - \cos \mu\ell(1-g) - \frac{\mu^2}{2}\frac{(\theta_g+\omega\theta_{g1})}{(\phi+\phi_1)}\right]$$

$$0 \leqslant x \leqslant g\ell$$

$$Q_{s(2)max} = -\frac{W(1+y)}{\mu \sin \mu\ell}\left[\cos \mu x\left[1 - \frac{\mu^2}{2}\frac{(\theta+\omega\theta_1)}{(\phi+\phi_1)}\right] - \cos \mu(\ell-x)\right]$$

$$- \frac{\rho_{max}\, W}{\mu \sin \mu\ell}\left[\cos \mu x\left[1 - \frac{\mu^2}{2}\frac{(\theta_g+\omega\theta_{g1})}{(\phi+\phi_1)}\right] - \cos \mu g\ell \cos \mu(\ell-x)\right]$$

$$g\ell \leqslant x \leqslant \ell$$

for the left hand span. Similar equations can be written for the right hand span.

Thus the maximum suspender load can be initially found from the relationship (see Equations (2.1)):

$$q'_{smax} = -\frac{dQ_{smax}}{dx}$$

which gives;

$$q'_{s(1)max} = -\frac{W(1+y)}{\sin \mu\ell}\left[\sin \mu x\left[1 - \frac{\mu^2}{2}\frac{(\theta+\omega\theta_1)}{(\phi+\phi_1)}\right] - \sin \mu(\ell-x)\right]$$

$$- \rho_{max}\, W \frac{\sin \mu x}{\sin \mu\ell}\left[1 - \cos \mu\ell(1-g) - \frac{\mu^2}{2}\frac{(\theta_g+\omega\theta_{g1})}{(\phi+\phi_1)}\right]$$

$$0 \leqslant x \leqslant g\ell$$

$$q'_{s(2)max} = - \frac{W\ (1+y)}{\sin\ \mu\ell} \left[\sin\ \mu x \left[1 - \frac{\mu^2}{2} \frac{(\theta+\omega\theta_1)}{(\phi+\phi_1)} \right] + \sin\ \mu(\ell-x) \right]$$

$$- \frac{\rho_{max}\ W}{\sin\ \mu\ell} \left[\sin\ \mu x \left[1 - \frac{\mu^2}{2} \frac{(\theta_g+\omega\theta_{g1})}{(\phi+\phi_1)} \right] + \cos\ \mu g\ell\ \sin\ \mu(\ell-x) \right]$$

$$g\ell \leqslant x \leqslant \ell$$

Similar equations can be written for the right hand span.

These load equations do not represent a uniformly distributed load and therefore, they do not comply with the basic assumptions stated in Section 2 .1. Hence, the above equations must be approximated to a uniformly distributed load. To achieve this, we use the mathematical approximation:

$$q_{smax} = \frac{1}{\ell} \int_0^{\ell} q'_{smax}\ dx = \frac{1}{\ell} \left[\int_0^{g\ell} q'_{s(1)max}\ dx + \int_{g\ell}^{\ell} q'_{s(2)max}\ dx \right]$$

$$= \frac{-1}{\ell} \left[\left[Q_{s(1)max} \right]_0^{g\ell} + \left[Q_{s(2)max} \right]_{g\ell}^{\ell} \right]$$

Thus, the final maximum suspender forces for the left hand span can be evaluated as follows:

$$q_{smax} = - W\ (1+y)\ (1+ \frac{\theta}{\ell}\ ) \left[1 - \frac{\mu^2}{4} \frac{(\theta+\omega\theta_1)}{(\phi+\phi_1)} \right] - \frac{\rho_{max} W}{2} \left[(1+ \frac{\theta}{\ell}\ ) \right.$$

$$\left. \left[1 - \frac{\mu^2}{2} \frac{(\theta_g+\omega\theta_{g1})}{(\phi+\phi_1)} \right] + \frac{\sin \frac{\mu\ell}{2} (1 - 2g)}{\frac{\mu\ell}{2} \cos \frac{\mu\ell}{2}} \right]$$

Similarly, for the right hand span:

$$q_{s1max} = - W_1\ (1+y)\ (1+ \frac{\theta}{\ell}\ ) \left[1 - \frac{\mu^2}{4\omega} \frac{(\theta+\omega\theta_1)}{(\phi+\phi_1)} \right] - \frac{\rho_{max}\ W_1}{2} \left[(1+ \frac{\theta_1}{\ell_1}) \left[1 - \right. \right.$$

$$\left. \left. \frac{\mu^2}{2\omega} \frac{(\theta_g+\omega\theta_{g1})}{(\phi+\phi_1)} \right] + \frac{\sin \frac{\mu\ell_1}{2} (1-2g_1)}{\frac{\mu\ell_1}{2} \cos \frac{\mu\ell_1}{2}} \right]$$

Appendices (24 - 27)

of Chapter 4

APPENDIX 24

24. The Determination of the Value and Position of the Force in the Concrete Stress Block when the Axis of Zero Strain Lies in the Web and the Strain at the Top Fibre of the Beam is Equal to the ultimate Plastic Strain

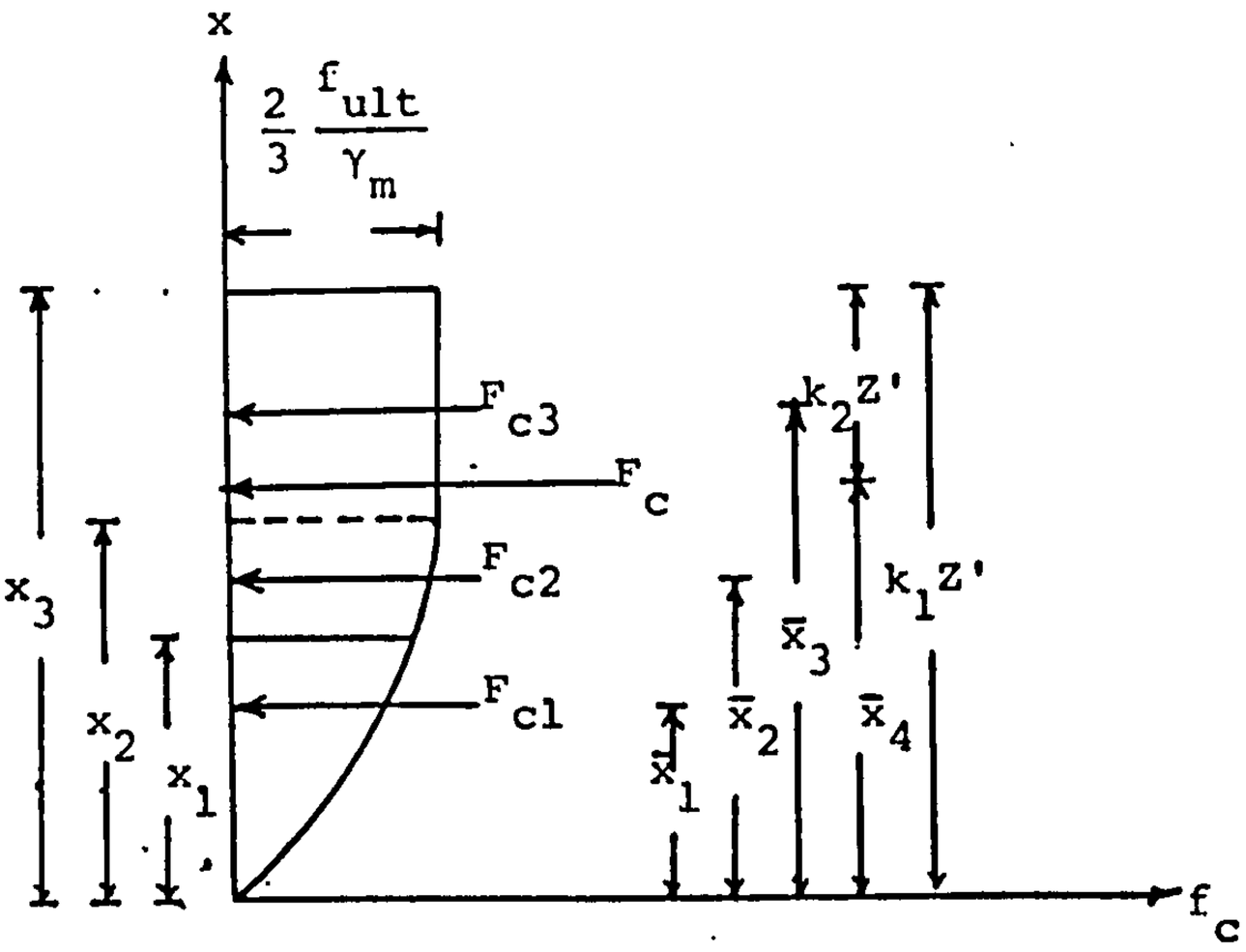

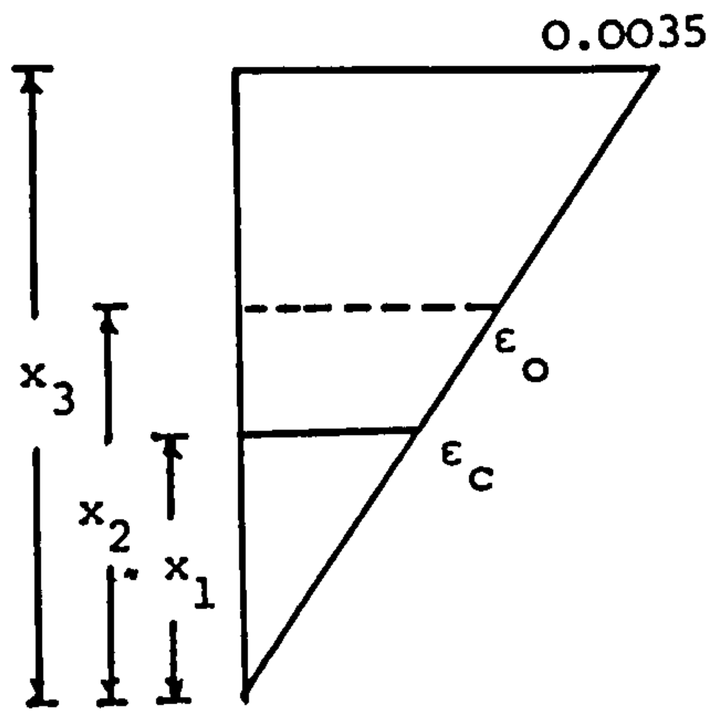

To determine the equation for the parabolic part of the stress block, we assume its equation to be of the following form:

$$f_c = \alpha_1 x^2 + \alpha_2 x + \alpha_3$$

where α_1, α_2 and α_3 are constants which can be evaluated from the following boundary conditions:

1. at $x = o$ $\quad f_c = o$ which gives $\alpha_3 = o$
2. at $x = x_2$ $\quad \frac{df_c}{dx} = o$ which yields:

$$2\alpha_1 x_2 + \alpha_2 = o$$

3. at $x = x_2$ $\qquad f_c = \frac{2}{3} \frac{f_{ult}}{\gamma_m}$ which gives:

$$\frac{2}{3} \frac{f_{ult}}{\gamma_m} = \alpha_1 x_2^2 - 2\alpha_1 x_2^2$$

$$\alpha_1 = -\frac{2}{3} \frac{f_{ult}}{\gamma_m x_2^2} \qquad \text{and } \alpha_2 = \frac{4}{3} \frac{f_{ult}}{\gamma_m x_2}$$

Thus, the equation for the parabolic part of the stress block can be written as follows:

$$f_c = \frac{2}{3} \frac{f_{ult}}{\gamma_m} \left[2 \frac{x}{x_2} - \frac{x^2}{x_2^2} \right] \qquad \text{(i)}$$

Hence, the area of the part bounded by $x = o$ and $x = x_1$ can be evaluated as follows:

$$A_1 = \int_o^{x_1} f_c dx = \frac{2}{9} \frac{f_{ult}}{\gamma_m} \frac{x_1^2}{x_2} \left[3 - \frac{x_1}{x_2}\right] \qquad \text{(ii)}$$

The total area of the parabolic part of the curve can be found as shown:

$$A = \int_o^{x_2} f_c dx = \frac{4}{9} \frac{f_{ult}}{\gamma_m} x_2$$

Hence, the area of the curve part bounded by $x = x_1$ and $x = x_2$ can be evaluated as follows:

$$A_2 = A - A_1$$

which gives,

$$A_2 = \frac{2}{3} \frac{f_{ult}}{\gamma_m} \frac{x_2}{3} \left[2 - \frac{x_1^2}{x_2^2} \left(3 - \frac{x_1}{x_2}\right)\right]$$

The area of the rectangular part of the stress block can be obtained as shown:

$$A_3 = \frac{2}{3} \frac{f_{ult}}{\gamma_m} (x_3 - x_2)$$

Thus, the total compressive force, F_c, of the concrete is:

$$F_c = F_{c1} + F_{c2} + F_{c3}$$

$$F_c = A_1 b + A_2 b_1 + A_3 b_1$$

Substituting for A_1, A_2 and A_3, we have:

$$F_c = \frac{2}{3} \frac{f_{ult}}{\gamma_m} \frac{bx_1^2}{3x_2} \left[3 - \frac{x_1}{x_2}\right] + \frac{2}{3} \frac{f_{ult}}{\gamma_m} \frac{b_1 x_2}{3} \left[2 - \frac{x_1^2}{x_2^2} \left(3 - \frac{x_1}{x_2}\right)\right]$$

$$+ \frac{2}{3} \frac{f_{ult}}{\gamma_m} b_1 (x_3 - x_2)$$

$$F_c = \frac{2}{3} \frac{f_{ult}}{\gamma_m} \frac{x_2}{3} \left[2 b_1 - (b_1 - b) \frac{x_1^2}{x_2^2} \left(3 - \frac{x_1}{x_2}\right) + 3b_1 \frac{x_3}{x_2} - 3b_1\right]$$

$$F_c = \frac{2}{9} \frac{f_{ult}}{\gamma_m} x_2 \left[b_1 \left(3 \frac{x_3}{x_2} - 1\right) - (b_1 - b) \frac{x_1^2}{x_2^2} \left(3 - \frac{x_1}{x_2}\right)\right]$$

but from figure (b), it is obvious that:

$$\frac{0.0035}{x_3} = \frac{\varepsilon_o}{x_2} = \frac{\varepsilon_c}{x_1}$$

which yields,

$$\frac{x_3}{x_2} = \frac{0.0035}{\varepsilon_o} \qquad x_2 = \frac{\varepsilon_o}{0.0035} x_3$$

$$\frac{x_1}{x_2} = \frac{\varepsilon_c}{\varepsilon_o}$$

but $x_3 = k_1 Z'$. Hence, substituting in the expression for F_c, we obtain:

$$F_c = \frac{2}{9} \frac{f_{ult}}{\gamma_m} k_1 Z' \left[b_1 \left(3 - \frac{\varepsilon_o}{0.0035}\right) - (b_1 - b) \frac{\varepsilon_c^2}{0.0035\ \varepsilon_o} \left(3 - \frac{\varepsilon_c}{\varepsilon_o}\right)\right]$$

The second term of the above equation can be written in another form

when knowing that:

$$\varepsilon_c = \frac{k_1 - z_3}{k_1} 0.0035$$

Thus, we have:

$$\frac{\varepsilon_c^2}{0.0035\ \varepsilon_o}\left(3 - \frac{\varepsilon_c}{\varepsilon_o}\right) = \frac{(k_1 - z_3)^2}{k_1^2}\frac{0.0035}{k_1}\left[3 - \frac{(k_1 - z_3)}{k_1}\frac{0.0035}{\varepsilon_o}\right]$$

$$= \frac{0.0035}{k_1^3\ \varepsilon_o}\left[\left(3 - \frac{0.0035}{\varepsilon_o}\right) k_1^3 - 3z_3\left(2 - \frac{0.0035}{\varepsilon_o}\right)k_1^2\right.$$

$$\left. + 3z_3^2\left(1 - \frac{0.0035}{\varepsilon_o}\right) k_1 + z_3^3\ \frac{0.0035}{\varepsilon_o}\right]$$

Consequently, the total value of F_c can be found as follows:

$$F_c = \frac{2}{9}\frac{f_{ult}}{\gamma_m}\frac{z'}{k_1^2}\frac{0.0035}{\varepsilon_o}\left[\left[b_1\frac{\varepsilon_o}{0.0035}\left(3 - \frac{\varepsilon_o}{0.0035}\right) - (b_1 - b)\left(3 - \frac{0.0035}{\varepsilon_o}\right)\right]k_1^3\right.$$

$$\left. + (b_1 - b)\left[3z_3\left(2 - \frac{0.0035}{\varepsilon_o}\right)k_1^2 - 3z_3^2\left(1 - \frac{0.0035}{\varepsilon_o}\right)k_1 - z_3^3\frac{0.0035}{\varepsilon_o}\right]\right]$$

The distance $\bar{x}_1$, see the figure, can be evaluated for the first area A_1 as follows:

$$\bar{x}_1 = \frac{\int_o^{x_1} f_c\ x dx}{A_1} = \frac{2}{3}\frac{f_{ult}}{\gamma_m A_1}\frac{x_1^3}{12\ x_2}\left(8 - \frac{3x_1}{x_2}\right)$$

Similarly, the distance $\bar{x}_2$ for the second area is:

$$\bar{x}_2 = \frac{\int_{x_1}^{x_2} f_c\ x dx}{A_2} = \frac{2}{3}\frac{f_{ult}}{\gamma_m A_2}\frac{x_2^3}{12}\left[5 - \frac{x_1^3}{x_2^3}\left(8 - 3\frac{x_1}{x_2}\right)\right]$$

and for the rectangular area, the distance $\bar{x}_3$ is:

$$\bar{x}_3 = \frac{1}{2}(x_3 + x_2)$$

Thus, the distance $\bar{x}_4$ can be obtained as follows: (see the figure)

$$F_c\ \bar{x}_4 = F_{c1}\ \bar{x}_1 + F_{c2}\ \bar{x}_2 + F_{c3}\ \bar{x}_3$$

$$F_c\,\bar{x}_4 = \frac{2}{3}\,\frac{f_{ult}}{\gamma_m}\,\frac{b x_1^3}{12\,x_2}\left(8 - 3\,\frac{x_1}{x_2}\right) + \frac{2}{3}\,\frac{f_{ult}}{\gamma_m}\,\frac{b_1\,x_2^2}{12}\left[5 - \frac{x_1^3}{x_2^3}\left(8 - 3\,\frac{x_1}{x_2}\right)\right]$$

$$+ \frac{2}{3}\,\frac{f_{ult}}{\gamma_m}\,\frac{b_1}{2}\,(x_3 + x_2)\,(x_3 - x_2)$$

$$F_c\,\bar{x}_4 = \frac{2}{3}\,\frac{f_{ult}}{\gamma_m}\,\frac{x_2^2}{12}\left[\,5\,b_1 - (b_1 - b)\,\frac{x_1^3}{x_2^3}\left(8 - 3\,\frac{x_1}{x_2}\right) + 6b_1\left(\frac{x_3^2}{x_2^2} - 1\right)\right]$$

$$F_c\,\bar{x}_4 = \frac{2}{3}\,\frac{f_{ult}}{\gamma_m}\,\frac{x_2^2}{12}\left[b_1\left(6\,\frac{x_3^2}{x_2^2} - 1\right) - (b_1 - b)\,\frac{x_1^3}{x_2^3}\left(8 - 3\,\frac{x_1}{x_2}\right)\right]$$

but F_c can be obtained as follows:

$$F_c = \frac{2}{3}\,\frac{f_{ult}}{\gamma_m}\,\frac{x_2}{3}\left[\,b_1\left(3\,\frac{x_3}{x_2} - 1\right) - (b_1 - b)\,\frac{x_1^2}{x_2^2}\left(3 - \frac{x_1}{x_2}\right)\right]$$

Hence, the final expression for $\bar{x}_4$ is:

$$\bar{x}_4 = \frac{x_2}{4}\;\frac{\left[b_1\left(6\,\frac{x_3^2}{x_2^2} - 1\right) - (b_1 - b)\,\frac{x_1^3}{x_2^3}\left(8 - 3\,\frac{x_1}{x_2}\right)\right]}{\left[b_1\left(3\,\frac{x_3}{x_2} - 1\right) - (b_1 - b)\,\frac{x_1^2}{x_2^2}\left(3 - \frac{x_1}{x_2}\right)\right]}$$

but $k_2 Z' = x_3 - \bar{x}_4$, see the figure, which yields:

$$k_2 Z' = \frac{x_3}{4}\left[4 - \frac{x_2}{x_3}\;\frac{\left[b_1\left(6\,\frac{x_3^2}{x_2^3} - 1\right) - (b_1 - b)\,\frac{x_1^3}{x_2^3}\left(8 - 3\,\frac{x_1}{x_2}\right)\right]}{\left[b_1\left(3\,\frac{x_3}{x_2} - 1\right) - (b_1 - b)\,\frac{x_1^2}{x_2^2}\left(3 - \frac{x_1}{x_2}\right)\right]}\right]$$

Rearranging the above expression, yields:

$$k_2 = \frac{k_1}{4} \frac{\left[b_1 \left(6 \frac{x_3}{x_2} + \frac{x_2}{x_3} - 4\right) + (b_1 - b) \frac{x_1^2}{x_2^2} \left[\frac{x_1}{x_3} \left(8 - 3 \frac{x_1}{x_2}\right) + 4 \frac{x_1}{x_2} - 12\right]\right]}{\left[b_1 \left(3 \frac{x_3}{x_2} - 1\right) - (b_1 - b) \frac{x_1^2}{x_2^2} \left(3 - \frac{x_1}{x_2}\right)\right]}$$

where $\frac{x_3}{x_2} = \frac{0.0035}{\varepsilon_o}$,

$\frac{x_1}{x_2} = \frac{\varepsilon_c}{\varepsilon_o}$,

and $\frac{x_1}{x_3} = \frac{\varepsilon_c}{0.0035}$

APPENDIX 25

25. The Determination of the Value and Position of the Force in the Concrete Stress Block when the Strain at the Bottom Fibre of the Beam is equal to the ultimate Plastic Strain

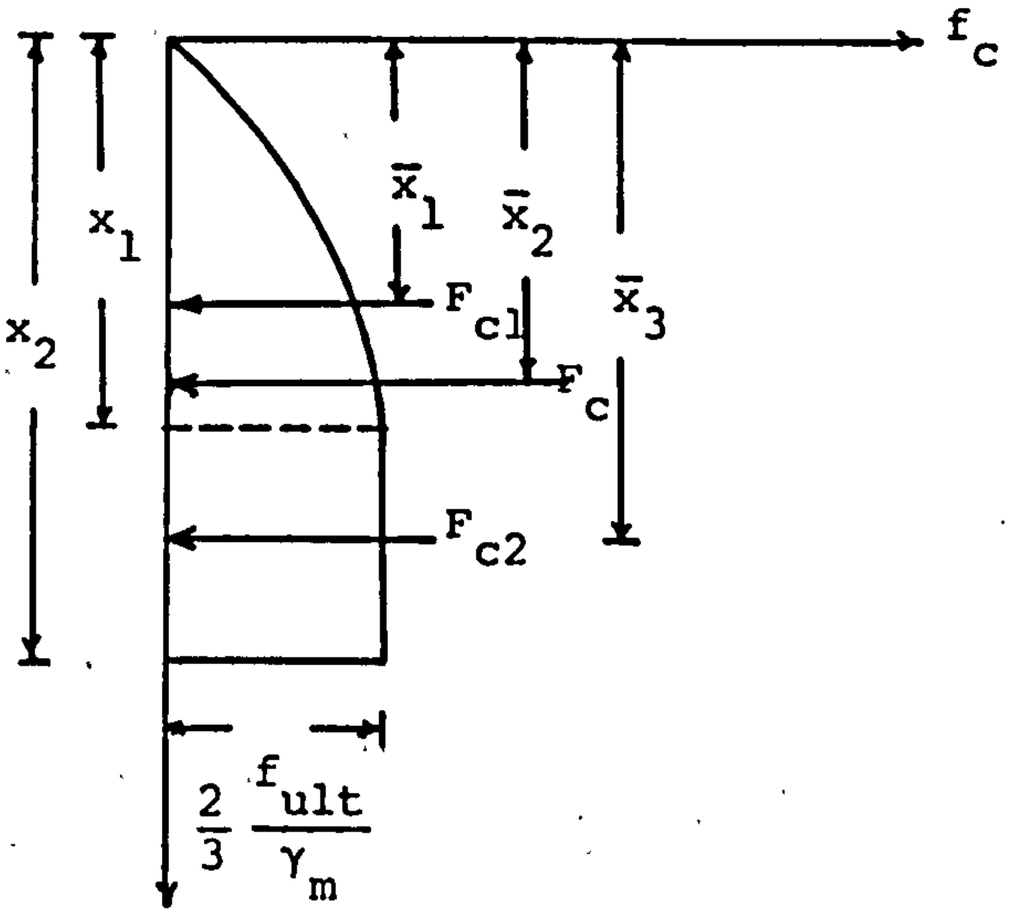

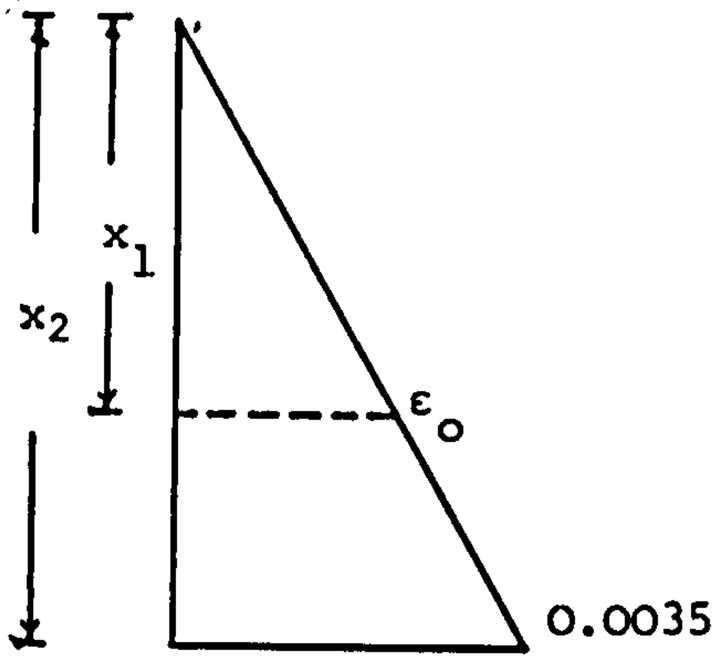

The equation for the parabolic part of the stress block curve can be determined, similarly to Appendix 24, as follows:

$$f_c = \frac{2}{3}\ \frac{f_{ult}}{\gamma_m}\ \left[2\ \frac{x}{x_1}\ -\ \frac{x^2}{x_1^2}\right]$$

Thus, the area of the parabolic part of the curve, A_1, is:

$$A_1 = \frac{4}{9}\ \frac{f_{ult}}{\gamma_m}\ x_1$$

The area of the rectangular part of the curve, A_2, is:

$$A_2 = \frac{2}{3} \frac{f_{ult}}{\gamma_m} (x_2 - x_1)$$

Thus, the total area A is found to be:

$$A = A_1 + A_2 = \frac{2}{3} \frac{f_{ult}}{\gamma_m} \frac{x_2}{3} (3 - \frac{x_1}{x_2})$$

$$\text{but } \frac{x_1}{x_2} = \frac{\varepsilon_o}{0.0035}$$

Hence, the total force, $F_c = A\ b$, can be determined as follows:

$$F_c = \frac{2}{3} \frac{f_{ult}}{\gamma_m} \frac{bx_2}{3} \left(3 - \frac{\varepsilon_o}{0.0035} \right)$$

$$\text{but } x_2 = Z - k_1 Z'$$

$$= Z'(z_4 - k_1)$$

Thus, the final expression for F_c is:

$$F_c = \frac{2}{9} \frac{f_{ult}}{\gamma_m} bZ' \left[3 - \frac{\varepsilon_o}{0.0035}\right][z_4 - k_1]$$

To evaluate the position of this force, we find the distance $\bar{x}_1$ for the parabolic area as follows:

$$\bar{x}_1 = \frac{\int_o^{x_1} f_c x\, dx}{A_1} = \frac{5}{18} \frac{f_{ult}}{\gamma_m} \frac{x_1^2}{A_1}$$

For the rectangular area, the distance $\bar{x}_2$ is directly found as follows:

$$\bar{x}_2 = \frac{1}{2} (x_1 + x_2)$$

Thus, to find the distance $\bar{x}_3$, in order to determine the point of application of the resultant force F_c, we have: (see the figure)

$$F_c \bar{x}_3 = F_{c1} \bar{x}_1 + F_{c2} \bar{x}_2$$

$$A \bar{x}_3 = A_1 \bar{x}_1 + A_2 \bar{x}_2$$

$$A\,\bar{x}_3 = \frac{5}{18}\,\frac{f_{ult}}{y_m}\,x_1^{\,2} + \frac{1}{3}\,\frac{f_{ult}}{y_m}\,(x_2^{\,2} - x_1^{\,2})$$

$$\bar{x}_3 = \frac{\frac{1}{18}\,\frac{f_{ult}}{y_m}\,x_2^{\,2}\,[6 - x_1^{\,2}/x_2^{\,2}]}{\frac{2}{9}\,\frac{f_{ult}}{y_m}\,x_2\,[3 - x_1/x_2]}$$

$$\bar{x}_3 = \frac{x_2}{4}\,\frac{[6 - x_1^{\,2}/x_2^{\,2}]}{[3 - x_1/x_2]}$$

but

$$k_2\,Z' = k_1 Z' + \bar{x}_3$$

and

$$x_2 = Z - k_1 Z'$$

Hence, we have:

$$k_2 Z' = k_1 Z' + \frac{Z'}{4}\,(z_4 - k_1)\,\frac{[6 - x_1^{\,2}/x_2^{\,2}]}{[3 - x_1/x_2]}$$

$$k_2 = \frac{1}{4\,[3 - x_1/x_2]}\,[4\,k_1\,[3 - x_1/x_2] + (z_4 - k_1)\,(6 - x_1^{\,2}/x_2^{\,2})]$$

which finally gives:

$$k_2 = \frac{\left[k_1\,[6 - \frac{x_1}{x_2}\,(4 - \frac{x_1}{x_2})] + z_4\,(6 - \frac{x_1^{\,2}}{x_2^{\,2}})\right]}{4\,[3 - \frac{x_1}{x_2}]}$$

where $\dfrac{x_1}{x_2} = \dfrac{\varepsilon_o}{0.0035}$

APPENDIX 26

26. The Determination of the Term $\sum \frac{W}{H_w} \int \eta \, dx$ for a General Case of Loading Applied on the Left Hand Span of an Ungrouted Prestressed Cable Suspended Beam after the Formation of its First Plastic Hinge

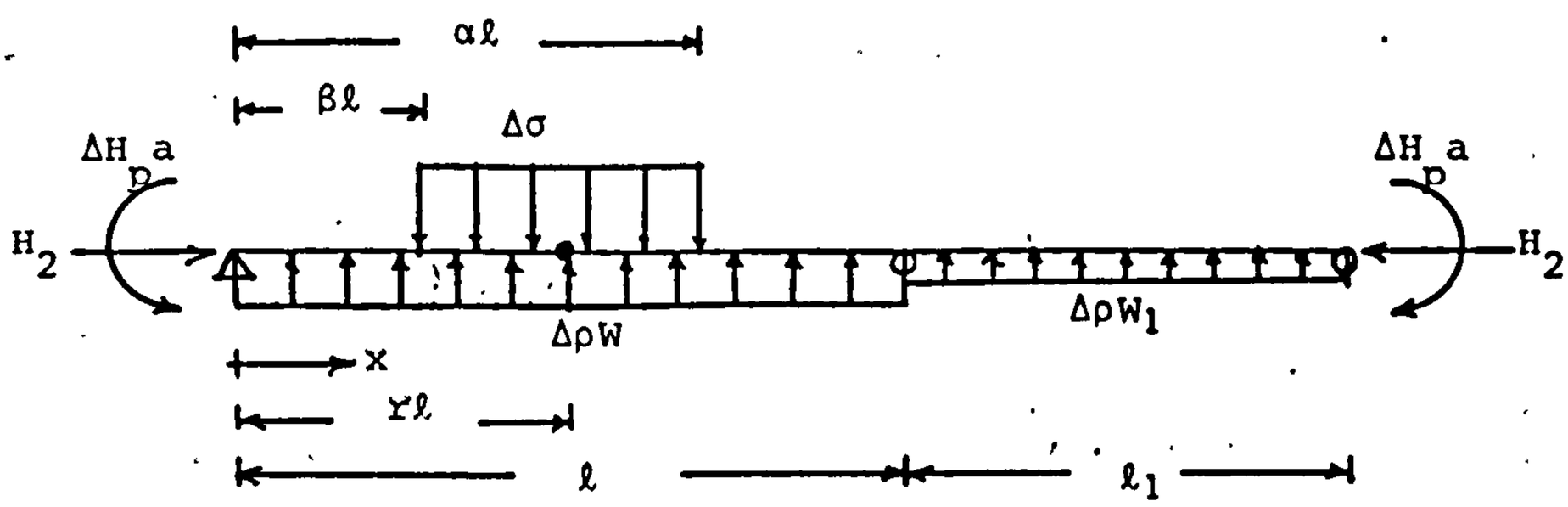

For simplicity, the case of loading shown in the figure will be divided into three cases of loading. The first, is the general loading $\Delta\sigma$ acting alone on the structure. Then, the second and third cases of loading are the upward uniformly distributed load and the end moments respectively. Thus, the final value of the term $\sum \frac{W}{H_w} \int \eta \, dx$ is obtained from the algebric sum of the terms found for the three cases of loading.

1. For the general loading $\Delta\sigma$

The deflection equations are obtained similarly to Appendix 12 as follows:

$$\eta_1 = A \sin \mu x + B \cos \mu x - \frac{\Delta\sigma \ell}{2rH_2} (r - \beta)^2 x \qquad 0 \leqslant x \leqslant \beta\ell$$

$$\eta_2 = C \sin \mu x + D \cos \mu x + \frac{\Delta\sigma \ell^2}{2 H_2} \left[\frac{x^2}{\ell^2} - \frac{x}{r\ell} (r^2+\beta^2) + \beta^2 - \frac{2}{\mu^2 \ell^2} \right]$$

$$\beta\ell \leqslant x \leqslant r\ell$$

$$\eta_3 = E \sin \mu x + F \cos \mu x + \frac{\Delta\sigma \ell^2}{2 H_2} \left[\frac{x^2}{\ell^2} - \frac{x}{r\ell} (r^2+\beta^2) + \beta^2 - \frac{2}{\mu^2 \ell^2} \right]$$

$$r\ell \leqslant x \leqslant \alpha\ell$$

$$\eta_4 = G \sin \mu x + I \cos \mu x + \frac{\Delta\sigma \ell^2}{2 H_2} \left[\left(2\alpha - r - \frac{\beta^2}{r}\right) \frac{x}{\ell} - (\alpha^2-\beta^2) \right]$$

$$\alpha\ell \leqslant x \leqslant \ell$$

$$\eta_5 = J \sin \mu x + K \cos \mu x + \frac{\Delta\sigma \ell^2}{2 \lambda H} \left[2\alpha - (\alpha^2-\beta^2) - \frac{1}{r} (r^2+\beta^2) \right] \left[1 + \lambda - \frac{x}{\ell} \right]$$

$$\ell \leqslant x \leqslant \ell+\ell_1$$

where $\mu^2 = \frac{H_2}{EI}$, $\lambda = \frac{\ell_1}{\ell}$

and where A, B, C, D, E, F, G, I, J and K are constants which are computed from the following boundary conditions:

1. at $x = o$ $\eta_1 = o$

2. at $x = \beta\ell$ $\frac{d\eta_1}{dx} = \frac{d\eta_2}{dx}$

3. at $x = \beta\ell$ $\eta_1 = \eta_2$

4. at $x = r\ell$ $\eta_2 = \eta_3$

5. at $x = \alpha\ell$ $\frac{d\eta_3}{dx} = \frac{d\eta_4}{dx}$

6. at $x = \alpha\ell$ $\eta_3 = \eta_4$

7. at $x = \ell$ $\eta_4 = o$

8. at $x = \ell$ $\frac{d\eta_4}{dx} = \frac{d\eta_5}{dx}$

9. at $x = \ell$ $\eta_5 = o$

10. at $x = \ell+\ell_1$ $\eta_5 = o$

which yields,

$$A = G + I \cot \mu r\ell + \frac{\Delta\sigma}{\mu^2 H_2} \left[\frac{\cos \mu\ell(\alpha-r) - \cos \mu\ell(r-\beta)}{\sin \mu r\ell} \right]$$

$$B = o$$

$$C = G + I \cot \mu r\ell + \frac{\Delta\sigma}{\mu^2 H_2} \left[\frac{\cos \mu\ell(\alpha-r) - \cos \mu\beta\ell \cos \mu r\ell}{\sin \mu r\ell} \right]$$

$$D = \frac{\Delta\sigma}{\mu^2 H_2} \cos \mu\beta\ell$$

$$E = G + \frac{\Delta\sigma}{\mu^2 H_2} \sin \mu\alpha\ell$$

$$F = I + \frac{\Delta\sigma}{\mu^2 H_2} \cos \mu\alpha\ell$$

$$G = \frac{\Delta\sigma\ell^2}{2 H_2} \left[\left[2\alpha - (\alpha^2-\beta^2) - \frac{1}{r} (r^2+\beta^2) \right] \left[\frac{\cos \mu\ell(1+\lambda)}{\sin \mu\ell_1} - \frac{(1+\lambda)}{\mu\ell_1} \cos \mu\ell \right] - \frac{(\alpha^2-\beta^2)}{\mu\ell} \right.$$

$$\left. \cos \mu\ell \right]$$

$$I = \frac{\Delta\sigma\ell^2}{2 H_2} \left[\left[2\alpha - (\alpha^2-\beta^2) - \frac{1}{r} (r^2+\beta^2) \right] \left[\frac{(1+\lambda)}{\mu\ell_1} \sin \mu\ell - \frac{\sin \mu\ell(1+\lambda)}{\sin \mu\ell_1} \right] + \frac{(\alpha^2-\beta^2)}{\mu\ell} \right.$$

$$\left. \sin \mu\ell \right]$$

$$J = \frac{\Delta\sigma\ell^2}{2 H_2} \frac{\cos \mu\ell(1+\lambda)}{\sin \mu\ell_1} \left[2\alpha - (\alpha^2-\beta^2) - \frac{1}{r} (r^2+\beta^2) \right]$$

$$K = - J \tan \mu\ell(1+\lambda)$$

Thus, the integration $\sum \frac{W}{H_w} \int \eta \, dx$ can be calculated as follows:

$$\sum \frac{W}{H_w} \int \eta \, dx = \frac{W}{H_w} \left[\int_{\circ}^{\beta\ell} \eta_1 dx + \int_{\beta\ell}^{r\ell} \eta_2 dx + \int_{r\ell}^{\alpha\ell} \eta_3 dx + \int_{\alpha\ell}^{\ell} \eta_4 dx + \omega \int_{\ell}^{\ell+\ell_1} \eta_5 dx \right]$$

This integration can be simplified to the following:

$$\sum \frac{W}{H_w} \int \eta \, dx = \frac{W}{H_w} \left[G \int_{\circ}^{\ell} \sin \mu x \, dx + I \left[\cot \mu r\ell \int_{\circ}^{r\ell} \sin \mu x \, dx + \int_{r\ell}^{\ell} \cos \mu x \, dx \right] \right.$$

$$= + \frac{\Delta\sigma}{\mu^2 H_2} \left[\frac{\cos \mu\ell(\alpha - r)}{\sin \mu r\ell} \int_{o}^{r\ell} \sin \mu x \, dx - \frac{\cos \mu\ell(r-\beta)}{\sin \mu r\ell} \int_{o}^{\beta\ell} \sin \mu x \, dx \right.$$

$$- \cos \mu\beta\ell \cot \mu r\ell \int_{\beta\ell}^{r\ell} \sin \mu x \, dx + \cos \mu\beta\ell \int_{\beta\ell}^{r\ell} \cos \mu x \, dx$$

$$\left. + \int_{r\ell}^{\alpha\ell} \cos \mu\ell(\alpha - \frac{x}{\ell}) \, dx \right] - \frac{\Delta\sigma\ell}{2rH_2} (r-\beta)^2 \int_{\circ}^{\beta\ell} x \, dx + \frac{\Delta\sigma\ell^2}{2 H_2} \int_{\beta\ell}^{\alpha\ell} \left[\frac{x^2}{\ell^2} \right.$$

$$- \frac{x}{r\ell} (r^2+\beta^2) + \beta^2 - \frac{2}{\mu^2\ell^2} \left. \right] dx + \frac{\Delta\sigma\ell^2}{2 H_2} \int_{\alpha\ell}^{\ell} \left[(2\alpha - r - \frac{\beta^2}{r}) \frac{x}{\ell} \right.$$

$$\left. - (\alpha^2-\beta^2) \right] dx - \frac{\omega J}{\cos \mu\ell(1+\lambda)} \int_{\ell}^{\ell+\ell_1} \sin \mu\ell(1+\lambda - \frac{x}{\ell}) \, dx + \frac{\omega \Delta\sigma\ell^2}{2\lambda H_2}$$

$$\left. \left[2\alpha - (\alpha^2-\beta^2) - \frac{1}{r} (r^2+\beta^2) \right] \int_{\ell}^{\ell+\ell_1} \left[1+\lambda - \frac{x}{\ell} \right] dx \right]$$

By working out these integrations and substituting for the values of G, I and J, the final value for the term $\sum \frac{W}{H_w} \int \eta \, dx$ is:

$$\sum \frac{W}{H_w} \int \eta \, dx = \frac{W}{H_w} \frac{\Delta\sigma\ell^2}{2\mu H_2} \left[\left[2\alpha - (\alpha^2-\beta^2) - \frac{1}{r} (r^2+\beta^2) \right] \right.$$

$$\left[\frac{\left[\cos \mu\ell(1+\lambda - \frac{r}{2}) - \cos \frac{\mu r\ell}{2} \left[\omega + (1-\omega) \cos \mu\ell_1 \right] \right]}{\sin \mu\ell_1 \cos \frac{\mu r\ell}{2}} + \frac{\mu\ell}{2} (1+\omega\lambda) \right]$$

$$\left. + \frac{2 \sin \frac{\mu\ell}{2} \sin \frac{\mu\ell}{2}(1-r)}{\mu\ell_1 \cos \frac{\mu r\ell}{2}} \left[(1+\lambda) \left[2\alpha - \frac{1}{r} (r^2+\beta^2) \right] - \lambda (\alpha^2-\beta^2) \right] \right]$$

$$- \frac{\mu\ell}{6}\left[\alpha^2(3-2\alpha) - \beta^2(3-2\beta)\right] + \frac{2}{\mu\ell}\left[\frac{\sin\frac{\mu\ell}{2}(2\alpha-r) - \sin\frac{\mu\ell}{2}(2\beta-r)}{\mu\ell\cos\frac{\mu r\ell}{2}} - (\alpha-\beta)\right]\Bigg] \qquad \text{(i)}$$

where $\mu^2 = \frac{H_2}{EI}$

and the expression for the moment at the intermediate support can be evaluated by substituting $x = \ell$ in the following expression:

$$M_{3(\Delta\sigma)} = EI\left(\frac{d^2\eta_4}{dx^2}\right)$$

which yields:

$$M_{3(\Delta\sigma)} = \frac{\Delta\sigma\ell^2}{2}\left[2\alpha - (\alpha^2-\beta^2) - \frac{1}{r}(r^2+\beta^2)\right] \qquad \text{(ii)}$$

2. For the continuous upward distributed forces $\Delta\rho W$ and $\Delta\rho W_1$

The deflection equations are obtained similarly to Appendix 12 as follows:

$$\eta_1 = A_1 \sin\mu x + B_1 \cos\mu x - \frac{\Delta\rho W}{2H_2}\left[x(x-r\ell) - \frac{2}{\mu^2}\right] \qquad 0 \leqslant x \leqslant r\ell$$

$$\eta_2 = C_1 \sin\mu x + D_1 \cos\mu x - \frac{\Delta\rho W}{2H_2}\left[x(x-r\ell) - \frac{2}{\mu^2}\right] \qquad r\ell \leqslant x \leqslant \ell$$

$$\eta_3 = E_1 \sin\mu x + F_1 \cos\mu x - \frac{\Delta\rho W\ell}{2\lambda H_2}\left[(1-r)[\ell(1+\lambda)-x] - \omega\lambda\left[(x-\ell)[(1+\lambda) - \frac{x}{\ell}] + \frac{2}{\mu^2\ell}\right]\right] \qquad \ell \leqslant x \leqslant \ell+\ell_1$$

where $\omega = \frac{W_1}{W}$ and $\mu^2 = \frac{H_2}{EI}$.

and where the constants A_1, B_1, C_1, D_1, E_1 and F_1 can be evaluted from the

following boundary conditions:

1. at $x = o$ $\qquad \eta_1 = o$

2. at $x = r\ell$ $\qquad \eta_1 = \eta_2$

3. at $x = \ell$ $\qquad \eta_2 = o$

4. at $x = \ell$ $\qquad \frac{d\eta_2}{dx} = \frac{d\eta_3}{dx}$

5. at $x = \ell$ $\qquad \eta_3 = o$

6. at $x = \ell + \ell_1$ $\qquad \eta_3 = o$

which yields,

$$A_1 = \frac{\Delta\rho W\ell^2}{2\,H_2}\left[(1-r)\,\frac{\sin\,\mu\ell(1+\lambda-r)}{\sin\,\mu\ell_1\,\sin\,\mu r\ell} + \frac{2}{\mu^2\ell^2}\,\frac{1}{\sin\,\mu r\ell}\left[2\,\sin\,\frac{\mu\ell}{2}\,\sin\,\frac{\mu\ell}{2}(1-2r)\right.\right.$$

$$\left.\left. + \omega\,\sin\,\mu\ell(1-r)\,\tan\,\frac{\mu\ell_1}{2}\right] - \frac{\sin\,\mu\ell(1-r)}{\mu\ell_1\,\sin\,\mu r\ell}\left[(1+\lambda)(1-r) + \lambda\,(1+\lambda)\right]\right]$$

$$B_1 = -\,\frac{\Delta\rho W}{\mu^2 H_2}$$

$$C_1 = -\,D_1\,\cot\,\mu\ell + \frac{\Delta\rho W\ell^2}{2\,H_2}\left[\,(1-r) - \frac{2}{\mu^2\ell^2}\,\right]\frac{1}{\sin\,\mu\ell}$$

$$D_1 = \frac{\Delta\rho W\ell^2}{2\,H_2}\left[\,(1-r)\,\frac{\sin\,\mu\ell(1+\lambda)}{\sin\,\mu\ell_1} - \frac{2}{\mu^2\ell^2}\left[\cos\,\mu\ell - \omega\,\sin\,\mu\ell\,\tan\,\frac{\mu\ell_1}{2}\,\right]\right.$$

$$\left. - \frac{\sin\,\mu\ell}{\mu\ell_1}\left[\,(1+\lambda)(1-r) + \lambda\,(1+\omega\lambda)\right]\right]$$

$$E_1 = -\,F_1\,\cot\,\mu\ell + \frac{\Delta\rho W\ell^2}{2\,H_2}\left[\,(1-r) - \frac{2\omega}{\mu^2\ell^2}\,\right]\frac{1}{\sin\,\mu\ell}$$

$$F_1 = \frac{\Delta\rho W\ell^2}{2\,H_2}\,\frac{\sin\,\mu\ell}{\sin\,\mu\ell_1}\left[\,(1-r)\,\frac{\sin\,\mu\ell(1+\lambda)}{\sin\,\mu\ell} - \frac{2\omega}{\mu^2\ell^2}\,\left[\,\frac{\sin\,\mu\ell(1+\lambda)}{\sin\,\mu\ell} - 1\right]\right]$$

Hence, the value of the integration $\sum \frac{W}{H_w} \int \eta\,dx$ can be calculated from the following expression:

$$\sum \frac{W}{H_w} \int \eta \, dx = \frac{W}{H_w} \left[\int_{o}^{r\ell} \eta_1 \, dx + \int_{r\ell}^{\ell} \eta_2 \, dx + \omega \int_{\ell}^{\ell+\ell_1} \eta_3 \, dx \right]$$

which finally gives:

$$\sum \frac{W}{H_w} \int \eta \, dx = \frac{W^2\ell^2}{2\mu H_2} \frac{\Delta\rho}{H_w} \left[\frac{(1-r)}{\sin \mu\ell_1} \left[\cos \mu\ell_1 - \frac{\cos \mu\ell(1-\lambda - \frac{r}{2})}{\cos \frac{\mu r\ell}{2}} \right] \right.$$

$$- \frac{4 \sin \frac{\mu\ell}{2}}{\mu^2\ell^2 \cos \frac{\mu r\ell}{2}} \left[\cos \mu\ell(1-r) - \omega \tan \frac{\mu\ell_1}{2} \sin \frac{\mu\ell}{2}(1-r) \right]$$

$$\frac{- 2 \sin \frac{\mu\ell}{2} \sin \frac{\mu\ell}{2}(1-r)}{\mu\ell_1 \cos \frac{\mu r\ell}{2}} \left[(1+\lambda)(1-r) + \lambda (1+\omega\lambda)\right] + \frac{\mu\ell}{6} \left[\frac{12}{\mu^2\ell^2} \right.$$

$$(1+\omega^2\lambda) + \omega\lambda \left[\omega\lambda^2 - 3(1-r)\right] - (2-3r)\left] + \omega \tan \frac{\mu\ell_1}{2} \left[(1-r) \right.\right.$$

$$\left.\left. - \frac{4\omega}{\mu^2\ell^2} \right]\right] \qquad \text{(iii)}$$

The bending moment at the intermediate support can be found when substituting $x = \ell$ in the following expression:

$$M_{3(\Delta\rho W)} = EI \left(\frac{d^2\eta_2}{dx^2} \right)$$

which gives:

$$M_{3(\Delta\rho W)} = - \frac{\Delta\rho W\ell^2}{2} (1-r) \qquad \text{(iv)}$$

3. For the end moments $\Delta H_p a$

The deflection equations can be determined similarly to Appendix 12, as follows:

$$\eta_1 = A_2 \sin \mu x + B_2 \cos \mu x + \frac{\Delta H_p a}{r\ell \, H_2} (r\ell - x) \qquad o \leqslant x \leqslant \ell$$

$$\eta_2 = C_2 \sin \mu x + D_2 \cos \mu x + \frac{\Delta H_p a}{r\ell \, H_2} (r\ell - x) \qquad r\ell \leqslant x \leqslant \ell$$

$$\eta_3 = E_2 \sin \mu x + F_2 \cos \mu x + \frac{\Delta H_p a}{r \ell_1 H_2} [x - \ell [1+\lambda(1-r)]] \qquad \ell \leqslant x \leqslant \ell+\ell_1$$

Thus, the constants A_2, B_2, C_2, D_2, E_2 and F_2 can be evaluated from the following boundary conditions:

1. at $x = o$ $\qquad \eta_1 = o$

2. at $x = r\ell$ $\qquad \eta_1 = \eta_2$

3. at $x = \ell$ $\qquad \eta_2 = o$

4. at $x = \ell$ $\qquad \frac{d\eta_2}{dx} = \frac{d\eta_3}{dx}$

5. at $x = \ell$ $\qquad \eta_3 = o$

6. at $x = \ell$ $\qquad \eta_3 = o$

which yields,

$$A_2 = - D_2 (\cot \mu\ell - \cos \mu r\ell) + \frac{\Delta H_p a}{H_2} \left[\cot \mu r\ell + \frac{(1-r)}{r \sin \mu\ell}\right]$$

$$B_2 = - \frac{\Delta H_p a}{H_2}$$

$$C_2 = - D \cot \mu\ell + \frac{\Delta H_p a}{H_2} \frac{(1-r)}{r \sin \mu\ell}$$

$$D_2 = \frac{\Delta H_p a}{r H_2} \left[\frac{\sin \mu\ell(1+\lambda)}{\sin \mu\ell_1} - r \frac{\cos \frac{\mu\ell}{2}(2+\lambda)}{\cos \frac{\mu\ell}{2}} - \frac{(1+\lambda)}{\mu\ell_1} \sin \mu\ell \right]$$

$$E_2 = - F_2 \cot \mu\ell + \frac{\Delta H_p a}{H_2} \frac{(1-r)}{r \sin \mu\ell}$$

$$F_2 = \frac{\Delta H_p a}{r H_2} \left[\frac{\sin \mu\ell(1+\lambda)}{\sin \mu\ell_1} - r \frac{\cos \frac{\mu\ell}{2}(2+\lambda)}{\cos \frac{\mu\ell_1}{2}} \right]$$

Hence, the value of the term $\sum \frac{W}{H_w} \int \eta \, dx$ can be evaluated from

the following expression:

$$\sum \frac{W}{H_w} \int \eta \, dx = \frac{W}{H_w} \left[\int_{o}^{r\ell} \eta_1 \, dx + \int_{r\ell}^{\ell} \eta_2 \, dx + \omega \int_{\ell}^{\ell+\ell_1} \eta_3 \, dx \right]$$

which yields:

$$\sum \frac{W}{H_w} \int \eta \, dx = \frac{W}{H_w} \frac{\Delta H_p a}{\mu r H_2} \left[\frac{2 \sin \frac{\mu\ell}{2}(1+2\lambda) \sin \frac{\mu\ell}{2}(1-r) + \sin \mu\ell_1 \sin \frac{\mu r\ell}{2}}{\sin \mu\ell_1 \cos \frac{\mu r\ell}{2}} \right.$$

$$- 2r \frac{\sin \frac{\mu\ell}{2} \cos \frac{\mu\ell}{2}(1+\lambda-r)}{\cos \frac{\mu\ell_1}{2} \cos \frac{\mu r\ell}{2}} - 2 \frac{(1+\lambda)}{\mu\ell_1} \frac{\sin \frac{\mu\ell}{2} \sin \frac{\mu\ell}{2}(1-r)}{\cos \frac{\mu r\ell}{2}}$$

$$\left. + (1-2r) \left[\omega \tan \frac{\mu\ell_1}{2} - \frac{\mu\ell}{2} (1+\omega\lambda) \right] \right] \qquad \text{(v)}$$

The moment at the intermediate support can be evaluated by substituting $x = \ell$ in the following expression:

$$M_{3(\Delta H_p a)} = EI \left(\frac{d^2 \eta_2}{dx^2} \right)$$

which yields:

$$M_{3(\Delta H_p a)} = - \Delta H_p a \frac{(1-r)}{r} \qquad \text{(vi)}$$

The total value of the term $\sum \frac{W}{H_w} \int \eta \, dx$ can then be evaluated by adding the Equations (i), (iii) and (v). Similarly the total value of the moment at the intermediate support can be found by adding equations (ii), (iv) and (vi).

Equations (i) and (ii) can be used for a concentrated load P when substituting $\Delta P = 2\Delta\sigma\ell\varepsilon$, $\alpha = t+\varepsilon$, $\beta = t-\varepsilon$ and $r = t$ where ε is a very small quantity as shown in the figure.

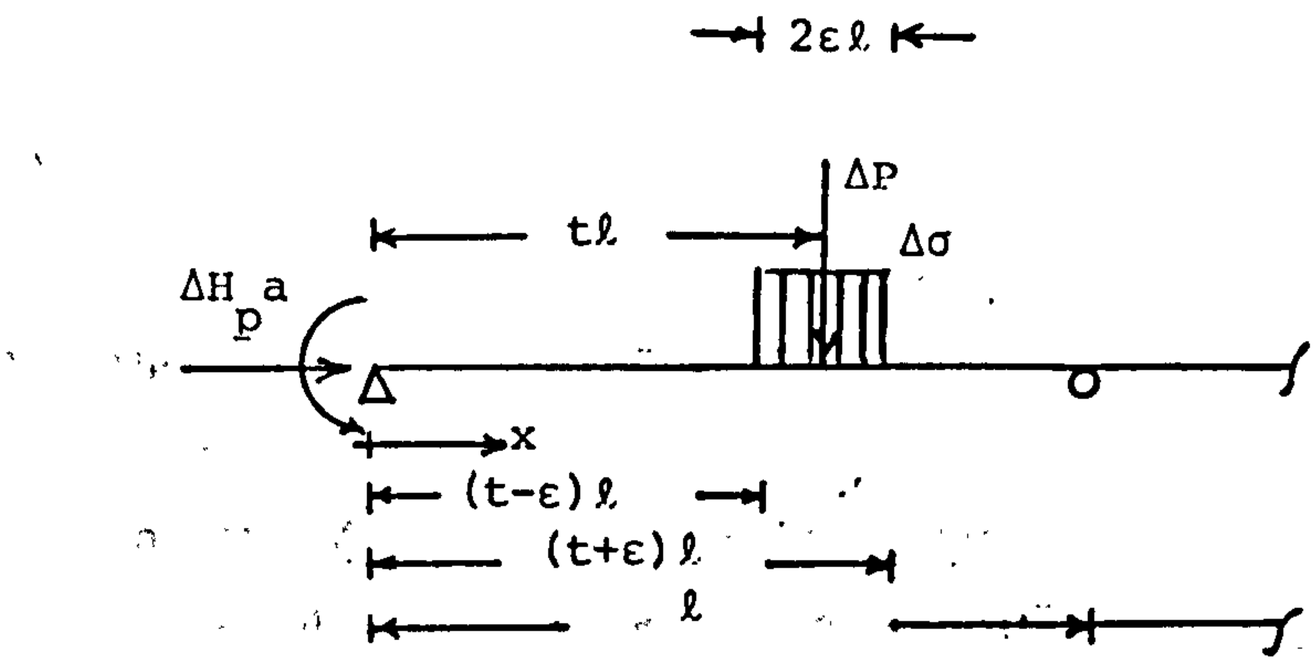

Hence, ignoring the high order terms of ε, we obtain the following:

$$2\alpha - (\alpha^2-\beta^2) - \frac{1}{r}(r^2+\beta^2) = 4\varepsilon(1-t)$$

$$(1+\lambda)\left[2\alpha - \frac{1}{r}(r^2+\beta^2)\right] - \lambda(\alpha^2-\beta^2) = 4\varepsilon\left[1+\lambda(1-t)\right]$$

$$\alpha^2(3-2\alpha) - \beta^2(3-2\beta) = 12t\varepsilon(1-t)$$

$$\frac{\sin\frac{\mu\ell}{2}(2\alpha-r) - \sin\frac{\mu\ell}{2}(2\beta-r)}{\mu\ell\cos\frac{\mu r\ell}{2}} - (\alpha-\beta) = o$$

and expressions (i) and (ii) become:

$$\sum\frac{W}{H_w}\int\eta\,dx = \frac{W}{H_w}\cdot\frac{\Delta P\ell}{\mu H_2}\left[(1-t)\left[\frac{\cos\mu\ell(1+\lambda-\frac{t}{2}) - \cos\frac{\mu t\ell}{2}\left[\omega+(1-\omega)\cos\mu\ell_1\right]}{\sin\mu\ell_1\cos\frac{\mu t\ell}{2}}\right.\right.$$

$$\left.\left. + \frac{\mu\ell}{2}(1+\omega\lambda)\right] + \frac{2[1+\lambda(1-t)]}{\mu\ell_2}\cdot\frac{\sin\frac{\mu\ell}{2}\sin\frac{\mu\ell}{2}(1-t)}{\cos\frac{\mu t\ell}{2}} - \frac{\mu t\ell}{2}(1-t)\right]$$

and;

$$M_{3(\Delta P)} = \Delta P\ell(1-t)$$

APPENDIX 27

27. The Determination of the Term $\sum \frac{W}{H_w} \int \eta \, dx$ for a General Case of Loading Applied in the Left Hand Span of a Grouted Prestressed Cable Suspended Beam after the Formation of its First Plastic Hinge

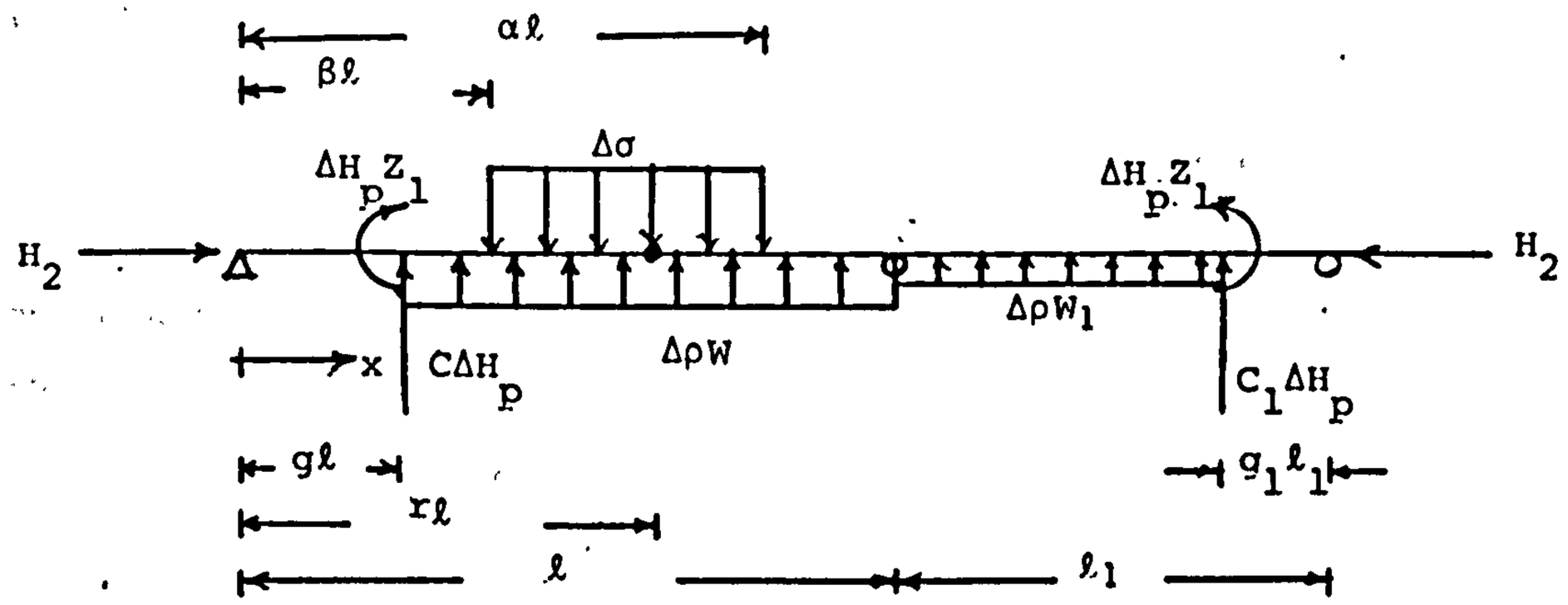

For simplicity, the shown case of loading is to be divided into four cases of loading to determine the term $\sum \frac{W}{H_w} \int \eta \, dx$. The first load to be considered is the general loading σ for which the term $\sum \frac{W}{H_w} \int \eta \, dx$ and the bending moment at the intermediate support $M_{3(\Delta\sigma)}$ can be obtained from Equations (i) and (ii) in Appendix 26.

2. For the two upward partial uniformly distributed forces $\Delta\rho W$ and $\Delta\rho W_1$

The deflection equations are obtained similarly to Appendix 12 as follows:

$$\eta_1 = A \sin \mu x + B \cos \mu x + \frac{\Delta\rho W \ell}{2rH_2} (r - g)^2 x \qquad 0 \leqslant x \leqslant g\ell$$

$$\eta_2 = C \sin \mu x + D \cos \mu x - \frac{\Delta\rho W}{2rH_2} \left[(x-r\ell)\ (rx - g^2\ell) - \frac{2r}{\mu^2}\right] \qquad g\ell \leqslant x \leqslant r\ell$$

$$\eta_3 = E \sin \mu x + F \cos \mu x - \frac{\Delta\rho W}{2rH_2} \left[(x-r\ell)\ (rx - g^2\ell) - \frac{2r}{\mu^2}\right] \qquad r\ell \leqslant x \leqslant \ell$$

$$\eta_4 = G \sin \mu x + I \cos \mu x - \frac{\Delta\rho W\ell}{2r\lambda H_2} \left[(1-r)\ (r-g^2)\ [\ell(1+\lambda) - x] - \omega r\lambda \right.$$

$$\left.\left[(x-\ell)\ [1+\lambda\ (1-g_1^2) - \frac{x}{\ell}\ ] + \frac{2}{\mu^2\ell}\right]\right] \qquad \ell \leqslant x \leqslant \ell+\ell_1(1-g_1)$$

$$\eta_5 = J \sin \mu x + K \cos \mu x - \frac{\Delta\rho W\ell}{2r\lambda H_2} \left[(1-r)\ (r-g^2) - \omega r\lambda^2\ (1-g_1)^2\right]$$

$$\left[\ \ell(1+\lambda) - x\ \right] \qquad \ell+\ell_1(1-g_1) \leqslant x \leqslant \ell+\ell_1$$

The constants A, B, C, D, E, F, G, I, J and K can be evaluated from the following boundary conditions:

1. at $x = o$ $\quad \eta_1 = o$

2. at $x = g\ell$ $\quad \eta_1 = \eta_2$

3. at $x = g\ell$ $\quad \frac{d\eta_1}{dx} = \frac{d\eta_2}{dx}$

4. at $x = r\ell$ $\quad \eta_2 = \eta_3$

5. at $x = \ell$ $\quad \eta_3 = o$

6. at $x = \ell$ $\quad \frac{d\eta_3}{dx} = \frac{d\eta_4}{dx}$

7. at $x = \ell$ $\quad \eta_4 = o$

8. at $x = \ell+\ell_1(1-g_1)$ $\quad \eta_4 = \eta_5$

9. at $x = \ell+\ell_1(1-g_1)$ $\quad \frac{d\eta_4}{dx} = \frac{d\eta_5}{dx}$

10. at $x = \ell + \ell_1$ $\quad \eta_5 = o$

which yields,

$$A = C + \frac{\Delta\rho W}{\mu^2 H_2} \sin \mu g \ell$$

$$B = o$$

$$C = \frac{\Delta\rho W \ell^2}{2r\ H_2} \left[(1-r)(r-g^2)\ \frac{\sin \mu\ell(1+\lambda-r)}{\sin \mu\ell_1 \sin \mu r\ell} + \frac{2r}{\mu^2\ell^2} \left[\cot \mu r\ell \cos \mu g\ell \right.\right.$$

$$- \frac{\cos \mu\ell(1-r)}{\sin \mu r\ell} + \omega \frac{\sin \mu\ell(1-r)}{\sin \mu\ell_1 \sin \mu r\ell} \left[\cos \mu g_1 \ell_1 - \cos \mu \ell_1\right]\right]$$

$$\left. - \frac{\sin \mu\ell(1-r)}{\mu\ell_1 \sin \mu r\ell} \left[(r-g^2)\ (1+\lambda-r) + r\lambda\ (1-r) + \omega r\lambda^2\ (1-g_1^2)\right]\right]$$

$$D = - \frac{\Delta\rho W}{\mu^2 H_2} \cos \mu g \ell$$

$$E = - F \cot \mu\ell + \frac{\Delta\rho W \ell^2}{2r\ H_2} \left[(1-r)\ (r-g^2) - \frac{2r}{\mu^2\ell^2} \right] \frac{1}{\sin \mu\ell}$$

$$F = \frac{\Delta\rho W \ell^2}{2r\ H_2} \left[(1-r)\ (r-g^2)\ \frac{\sin \mu\ell(1+\lambda)}{\sin \mu\ell_1} - \frac{2r}{\mu^2\ell^2} \left[\cos \mu\ell - \omega \frac{\sin \mu\ell}{\sin \mu\ell_1} \right.\right.$$

$$\left.\left. (\cos \mu g_1 \ell_1 - \cos \mu\ell)\right] - \frac{\sin \mu\ell}{\mu\ell_1} \left[(r-g^2)(1+\lambda-r) + r\lambda(1-r) + \omega r\lambda^2(1-g_1^2)\right]\right]$$

$$G = - I \cot \mu\ell + \frac{\Delta\rho W \ell^2}{2r\ H_2} \left[(1-r)\ (r-g^2) - \frac{2\omega r}{\mu^2\ell^2} \right] \frac{1}{\sin \mu\ell}$$

$$I = \frac{\Delta\rho W \ell^2}{2r\ H_2} \frac{\sin \mu\ell}{\sin \mu\ell_1} \left[(1-r)\ (r-g^2)\ \frac{\sin \mu\ell(1+\lambda)}{\sin \mu\ell} - \frac{2\omega r}{\mu^2\ell^2} \left[\frac{\sin \mu\ell(1+\lambda)}{\sin \mu\ell} \right.\right.$$

$$\left.\left. - \cos \mu g_1 \ell_1\right]\right]$$

$$J = - K \cot \mu\ell(1+\lambda)$$

$$K = \frac{\Delta\rho W \ell^2}{2r\ H_2} \frac{\sin \mu\ell(1+\lambda)}{\sin \mu\ell_1} \left[(1-r)\ (r-g^2) - \frac{2\omega r}{\mu^2\ell^2} \left[1 - \cos \mu\ell_1(1-g_1)\right]\right]$$

Thus, the integration $\sum \frac{W}{H_w} \int \eta\ dx$ can be evaluated from the following expression:

$$\sum \frac{W}{H_w} \int \eta \, dx = \frac{W}{H_w} \left[\int_{o}^{g\ell} \eta_1 dx + \int_{g\ell}^{r\ell} \eta_2 dx + \int_{r\ell}^{\ell} \eta_3 + \omega \left[\int_{\ell}^{\ell+\ell_1(1-g_1)} \eta_4 dx \right. \right.$$

$$\left. \left. + \int_{\ell+\ell_1(1-g_1)}^{\ell+\ell_1} \eta_5 dx \right] \right]$$

which yields:

$$\sum \frac{W}{H_w} \int \eta \, dx = \frac{W}{H_w} \frac{\Delta\rho W \ell^2}{2r\mu H_2} \left[\frac{(1-r)\ (r-g^2)}{\sin \mu\ell_1} \left[\cos \mu\ell_1 - \frac{\cos \mu\ell(1+\lambda - \frac{r}{2})}{\cos \frac{\mu r\ell}{2}} \right] \right.$$

$$- \frac{2r}{\mu^2\ell^2} \left[\frac{\sin \frac{\mu\ell}{2}(r-2g)}{\cos \frac{\mu r\ell}{2}} + \frac{\sin \frac{\mu\ell}{2}(2-r)}{\cos \frac{\mu r\ell}{2}} - 2\omega \frac{[\cos \mu g_1\ell_1 - \cos \mu\ell_1]}{\sin \mu\ell_1 \cos \frac{\mu r\ell}{2}} \sin \frac{\mu\ell}{2} \right.$$

$$\sin \frac{\mu\ell}{2}(1-r) + 2\omega^2 \left. \frac{\cos \frac{\mu g_1\ell_1}{2} \sin \frac{\mu\ell_1}{2}(1-g_1)}{\cos \frac{\mu\ell_1}{2}} \right] - \frac{2 \sin \frac{\mu\ell}{2} \sin \frac{\mu\ell}{2}(1-r)}{\mu\ell_1 \cos \frac{\mu r\ell}{2}}$$

$$\left[(r-g^2)\ (1+\lambda-r) + r\lambda\ (1-r) + \omega r\lambda^2(1-g_1^2) \right] + \frac{\mu\ell}{6} \left[\frac{12r}{\mu^2\ell^2} \left[(1-g) + \omega^2\lambda(1-g_1) \right] \right.$$

$$\left. + 3(1+\omega\lambda)(r^2+g^2) - r \left[2+3\omega\lambda + g^2[3(2+\omega\lambda) - 2g] - \omega^2\lambda^3 \left[1-3g_1^2 + 3g_1^3 \right] \right] \right]$$

$$\left. + \omega(1-r)(r-g^2) \tan \frac{\mu\ell_1}{2} \right] \qquad \text{(i)}$$

The moment at the intermediate support can be found from the following expression at $x = \ell$:

$$M_{3(\Delta\rho W)} = EI \left[\frac{d^2\eta_3}{dx^2} \right]$$

which yields:

$$M_{3(\Delta\rho W)} = - \frac{\Delta\rho W\ell^2}{2r} (1-r)(r-g^2) \qquad \text{(ii)}$$

It is worth noting that by substituting $g = g_1 = o$ in equations (i) and (ii), we can obtain equations (iii) and (iv) of Appendix 26, for continuous uniformly distributed loads.

3. For the two upward concentrated forces $C\Delta H_p$ and $C_1\Delta H_p$

The deflection equations are determined similarly to Appendix 12 as follows:

$$\eta_1 = A_1 \sin \mu x + B_1 \cos \mu x + \frac{C\ \Delta H_p}{r\ H_2} (r-g)x \qquad o \leqslant x \leqslant g\ell$$

$$\eta_2 = D_1 \sin \mu x + E_1 \cos \mu x - \frac{C\ \Delta H_p}{r\ H_2}\ g(x-r\ell) \qquad g\ell \leqslant x \leqslant \ell$$

$$\eta_3 = F_1 \sin \mu x + G_1 \cos \mu x - \frac{C\ \Delta H_p}{r\ H_2}\ g(x-r\ell) \qquad r\ell \leqslant x \leqslant \ell$$

$$\eta_4 = I_1 \sin \mu x + J_1 \cos \mu x - \frac{C\ \Delta H_p}{H_2}\ g\ \frac{(1-r)}{r}\ [\ell(1+\lambda) - x] + \frac{C_1\ \Delta H_p}{H_2}\ g_1\ (x-\ell)$$

$$\ell \leqslant x \leqslant \ell+\ell_1(1-g_1)$$

$$\eta_5 = K_1 \sin \mu x + L_1 \cos \mu x - \left[\frac{C\ \Delta H_p}{\lambda\ H_2}\ g\ \frac{(1-r)}{\Gamma} - \frac{C_1\ \Delta H_p}{H_2}\ (1-g_1) \right] [\ell(1+\lambda)-x]$$

$$\ell+\ell_1(1-g_1) \leqslant x \leqslant \ell+\ell_1$$

The constants A_1, B_1, C_1, D_1, E_1, F_1, G_1, I_1, J_1 and K_1 can be evaluted from the following boundary conditions:

1. at $x = o$ $\qquad \eta_1 = o$

2. at $x = g\ell$ $\qquad \eta_1 = \eta_2$

3. at $x = g\ell$ $\qquad \frac{d\eta_1}{dx} = \frac{d\eta_2}{dx}$

4. at $x = r\ell$ $\qquad \eta_2 = \eta_3$

5. at $x = \ell$ $\qquad \eta_3 = o$

6. at $x = \ell$ $\quad \dfrac{d\eta_3}{dx} = \dfrac{d\eta_4}{dx}$

7. at $x = \ell$ $\quad \eta_4 = o$

8. at $x = \ell+\ell_1(1-g_1)$ $\quad \eta_4 = \eta_5$

9. at $x = \ell+\ell_1(1-g_1)$ $\quad \dfrac{d\eta_4}{dx} = \dfrac{d\eta_5}{dx}$

10. at $x = \ell+\ell_1$ $\quad \eta_5 = o$

which yields,

$$A_1 = D_1 - \frac{C\ \Delta H_p}{\mu H_2} \cos \mu g \ell$$

$$B_1 = o$$

$$D_1 = \frac{C\ \Delta H_p}{\lambda r \mu H_2} \left[\frac{\mu g \ell_1}{\sin \mu \ell_1} (1-r) \frac{\sin \mu \ell(1+\lambda-r)}{\sin \mu r \ell} + \lambda r \sin \mu g \ell \cot \mu r \ell - g(1+\lambda-r) \right.$$

$$\left. \frac{\sin \mu \ell(1-r)}{\sin \mu r \ell} \right] + \frac{C_1\ \Delta H_p}{\mu H_2} \frac{\sin \mu \ell(1-r)}{\sin \mu \ell_1 \sin \mu r \ell} [\sin \mu g_1 \ell_1 - g_1 \sin \mu \ell_1]$$

$$E_1 = - \frac{C\ \Delta H_p}{\mu H_2} \sin \mu g \ell$$

$$F_1 = - G_1 \cot \mu \ell + \frac{C\ \Delta H_p}{\sin \mu \ell} g \ell \frac{(1-r)}{r_2 H}$$

$$G_1 = \frac{C\ \Delta H_p g}{\lambda r \mu H_2} \left[\frac{\mu \ell_1}{\sin \mu \ell_1} (1-r) \sin \mu \ell(1+\lambda) - (1+\lambda-r) \sin \mu \ell \right] + \frac{C_1\ \Delta H_p}{\mu\ H_2} \frac{\sin \mu \ell}{\sin \mu \ell_1}$$

$$[\sin \mu g_1 \ell_1 - g_1 \sin \mu \ell_1]$$

$$I_1 = - J_1 \cot \mu \ell + \frac{C\ \Delta H_p}{\sin \mu \ell} g \ell \frac{(1-r)}{r\ H_2}$$

$$J_1 = \frac{C\ \Delta H_p}{r\ H_2} g \ell (1-r) \frac{\sin \mu \ell(1+\lambda)}{\sin \mu \ell_1} + \frac{C_1\ \Delta H_p}{\mu\ H_2} \frac{\sin \mu g_1 \ell_1}{\sin \mu \ell_1} \sin \mu \ell$$

$$K_1 = - L_1 \cot \mu \ell(1+\lambda)$$

$$L_1 = \frac{\sin \mu\ell(1+\lambda)}{\sin \mu\ell_1} \left[\frac{C\Delta H_p}{H_2} g\ell \frac{(1-r)}{r} - \frac{C_1 \Delta H_p}{\mu H_2} \sin \mu\ell_1(1-g_1) \right]$$

Whence, the term $\sum \frac{W}{H_w} \int \eta \, dx$ can be evaluated as follows:

$$\sum \frac{W}{H_w} \int \eta \, dx = \frac{W}{H_w} \left[\int_{\circ}^{g\ell} \eta_1 dx + \int_{g\ell}^{r\ell} \eta_2 dx + \int_{r\ell}^{\ell} \eta_3 dx + \omega \left[\int_{\ell}^{\ell+\ell_1} \eta_4 dx + \int_{\ell+\ell_1}^{\ell+\ell_1(1-g_1)} \eta_5 dx \right] \right]$$

which yields:

$$\sum \frac{W}{H_w} \int \eta \, dx = \frac{W}{H_w} \frac{2\,\Delta H_p}{\mu^2 H_2} \left[C \left[\frac{\mu g\ell}{\sin \mu\ell_1} \frac{(1-r)}{2r} \left[(1-\omega) \cos \mu\ell_1 + \omega \left(1 - \frac{\mu\ell_1}{2} \right. \right. \right. \right.$$

$$\left. \left. \left. \left. \sin \mu\ell_1 \right) - \frac{\cos \mu\ell(1+\lambda - \frac{r}{2})}{\cos \frac{\mu r\ell}{2}} \right] - \frac{\sin \frac{\mu g\ell}{2} \sin \frac{\mu\ell}{2}(r-g)}{\cos \frac{\mu r\ell}{2}} - \frac{g}{\lambda r} (1+\lambda-r) \right. \right.$$

$$\left. \left. \frac{\sin \frac{\mu\ell}{2} \sin \frac{\mu\ell}{2}(1-r)}{\cos \frac{\mu r\ell}{2}} - \frac{\mu^2\ell^2}{4r} g\,[1-r(2-g)] \right] \right.$$

$$\left. + C_1 \left[\frac{\sin \frac{\mu\ell}{2} \sin \frac{\mu\ell}{2}(1-r)}{\sin \mu\ell_1 \cos \frac{\mu r\ell}{2}} \left(\sin \mu g_1 \ell_1 - g_1 \sin \mu\ell_1 \right) + \omega \frac{\mu^2\ell^2}{4} \right. \right.$$

$$\left. \left. g_1(1-g_1) - \omega \frac{\sin \frac{\mu g_1 \ell_1}{2}}{\cos \frac{\mu\ell_1}{2}} \sin \frac{\mu\ell_1}{2}(1-g_1) \right] \right] \qquad \text{(iii)}$$

The moment at the intermediate support can be determined by substituting $x = \ell$ in the following expression:

$$M_{3(C\Delta H_p)} = EI \left(\frac{d^2\eta_3}{dx^2} \right)$$

which yields,

$$M_{3(C\ \Delta H_p)} = - C\ \Delta H_p\ g\ell\ \frac{(1-r)}{r} \qquad \text{(iv)}$$

4. For the two concentrated moments $\Delta H_p Z_1$

The deflection equations can be written, similar to Appendix 12, as follows:

$$\eta_1 = A_2 \sin \mu x + B_2 \cos \mu x + \frac{\Delta H_p Z_1}{H_2}\ \frac{x}{r\ell} \qquad o \leqslant x \leqslant g\ell$$

$$\eta_2 = C_2 \sin \mu x + D_2 \cos \mu x + \frac{\Delta H_p Z_1}{H_2}\ \frac{(x-r\ell)}{r\ell} \qquad g\ell \leqslant x \leqslant r\ell$$

$$\eta_3 = E_2 \sin \mu x + F_2 \cos \mu x + \frac{\Delta H_p Z_1}{H_2}\ \frac{(x-r\ell)}{r\ell} \qquad r\ell \leqslant x \leqslant \ell$$

$$\eta_4 = G_2 \sin \mu x + I_2 \cos \mu x + \frac{\Delta H_p Z_1}{H_2}\ \frac{[\ell[1+\lambda(1-r)] - x]}{r\ell_1}$$

$$\ell \leqslant x\ \ell+\ell_1(1-g_1)$$

$$\eta_5 = J_2 \sin \mu x + K_2 \cos \mu x + \frac{\Delta H_p Z_1}{H_2}\ \frac{[\ell(1+\lambda) - x]}{r\ell_1}$$

$$\ell+\ell_1(1-g_1) \leqslant x \leqslant \ell+\ell_1$$

Hence, by using the aforementioned boundary conditions, the constants A_2, B_2, C_2, D_2, E_2, F_2, G_2, I_2, J_2 and K_2 can be evaluted as follows:

$$A_2 = C_2 - \frac{\Delta H_p Z_1}{H_2} \sin \mu g\ell$$

$$B_2 = o$$

$$C_2 = I_2\ \frac{\sin \mu\ell(1-r)}{\sin \mu\ell \sin \mu r\ell} + \frac{\Delta H_p Z_1}{H_2}\left[\ \frac{(1+\lambda)}{\mu r\ell_1}\ \frac{\sin \mu\ell(1-r)}{\sin \mu r\ell} - \frac{(1-r)}{r \sin \mu\ell}\right.$$

$$\left. - \cos \mu g\ell \cot \mu r\ell\ \right]$$

$$D_2 = \frac{\Delta H_p Z_1}{H_2} \cos \mu g\ell$$

$$E_2 = - F_2 \cot \mu\ell - \frac{\Delta H_p Z_1}{H_2} \cdot \frac{(1-r)}{r \sin \mu\ell}$$

$$F_2 = I_2 + \frac{\Delta H_p Z_1}{H_2} \frac{(1+\lambda)}{\mu r \ell_1} \sin \mu\ell_1$$

$$G_2 = - I_2 \cot \mu\ell - \frac{\Delta H_p Z_1}{H_2} \frac{(1-r)}{r \sin \mu\ell}$$

$$I_2 = - \frac{\Delta H_p Z_1}{H_2} \left[\frac{\sin \mu\ell \cos \mu g_1 \ell_1}{\sin \mu\ell_1} + \frac{(1-r)}{r} \frac{\sin \mu\ell(1+\lambda)}{\sin \mu\ell_1} \right]$$

$$J_2 = - K_2 \cot \mu\ell(1+\lambda)$$

$$K_2 = - \frac{\Delta H_p Z_1}{H_2} \frac{\sin \mu\ell(1+\lambda)}{\sin \mu\ell_1} \left[\cos \mu\ell_1(1-g_1) + \frac{(1-r)}{r} \right]$$

Whence, the term $\sum \frac{W}{H_w} \int \eta \, dx$ can be evaluated from the following expression:

$$\sum \frac{W}{H_w} \int \eta \, dx = \frac{W}{H_w} \left[\int_0^{g\ell} \eta_1 \, dx + \int_{g\ell}^{r\ell} \eta_2 \, dx + \int_{r\ell}^{\ell} \eta_3 \, dx + \omega \left[\int_{\ell}^{\ell+\ell_1(1-g_1)} \eta_4 \, dx + \int_{\ell+\ell_1(1-g_1)}^{\ell+\ell_1} \eta_5 \, dx \right] \right]$$

which yields:

$$\sum \frac{W}{H_w} \int \eta \, dx = \frac{W}{H_w} \frac{\Delta H_p Z_1}{\mu H_2} \left[\frac{2(1+\lambda)}{\mu r \ell_1} \frac{\sin \frac{\mu\ell}{2} \sin \frac{\mu\ell}{2}(1-r)}{\cos \frac{\mu r \ell}{2}} + \frac{\sin \frac{\mu\ell}{2}(r-2g)}{\cos \frac{\mu r \ell}{2}} \right.$$

$$\left. \frac{- 2 \sin \frac{\mu\ell}{2} \cos \mu g_1 \ell_1 \sin \frac{\mu\ell}{2}(1-r)}{\sin \mu\ell_1 \cos \frac{\mu r \ell}{2}} + \omega \frac{\sin \frac{\mu\ell_1}{2}(1-2g_1)}{\cos \frac{\mu\ell_1}{2}} \right.$$

$$\left. - \frac{(1-r)}{r} \frac{2 \sin \frac{\mu\ell}{2}(1+2\lambda) \sin \frac{\mu\ell}{2}(1-r) + \sin \mu\ell_1 \sin \frac{\mu r \ell}{2} + \omega \cos \frac{\mu r \ell}{2} (1-\cos \mu\ell_1)}{\sin \mu\ell_1 \cos \frac{\mu r \ell}{2}} \right]$$

$$+ \frac{\mu \ell}{2r} \left[[1-2r\ (1-g)] + \omega\lambda\ [1-2r\ (1-g_1)] \right] \Bigg] \qquad \text{(v)}$$

The moment at the intermediate can be determined when substituting $x = \ell$ in the following expression:

$$M_{3(\Delta H_p Z_1)} = EI \left(\frac{d^2 \eta_2}{dx^2} \right)$$

which yields:

$$M_{3(\Delta H_p Z_1)} = \Delta H_p Z_1 \ \frac{(1-r)}{r} \qquad \text{(vi)}$$

It is worth noting that by substituting $g = g_1 = o$ in the above equations, we can obtain equations (v) and (vi) of Appendix 26, for the end moments.

Appendix (28)

A general computer program

APPENDIX 28

28. The General Computer Program for the Analysis of Two-Span Prestressed Concrete Suspension Bridges

a. The Structure of the Program

The program has been written to analyse a two-span grouted prestressed concrete suspension bridge when a single general case of loading is applied on its left hand span. It comprises two major parts, the objective of the first part is to calculate the changes in the prestressing force, the bending moments, deflections and shear forces which result from the applied live loading. The second part is concerned with the calculation of failure loads of the bridge which are the first plastic hinge and the failure loads. In addition the program also calculates the loads at which the tensile reinforcement begins to yield at the first and second plastic hinges positions which are called the first and second yield loads (the procedure of the determination of these loads is the subject for a future paper by this writer).

The program at its present form is capable of analysing both grouted and ungrouted types of bridge when any form of loading is applied on either of its left or right hand span. This is due to the fact that almost all of the grouted bridge formulae are applicable to the ungrouted one when omitting the contribution of grout in these formulae, i.e. at $g = g_1 = o$. Furthermore, the computer is instructed to ignore the upward concentrated forces, CH_p and C_1H_p, as well as the concentrated moments, H_pZ_1, for the ungrouted type. In addition, the end moments, if any, are evaluated by using the initial prestressing force, i.e. H_ia, for the grouted case, or the total value of the prestressing force, i.e. Ha, for the ungrouted type. The computer carries out all of the above modifications automatically after the type of bridge has been specified interactively.

For the applied general form of loading, denoted V in the program, its position is given, in the input data, in the form of two ratios, A and B, of the span lengths which are denoted S and S_1 in the program, see the figure. The coordinates of the system are located at the left and right hand end supports.

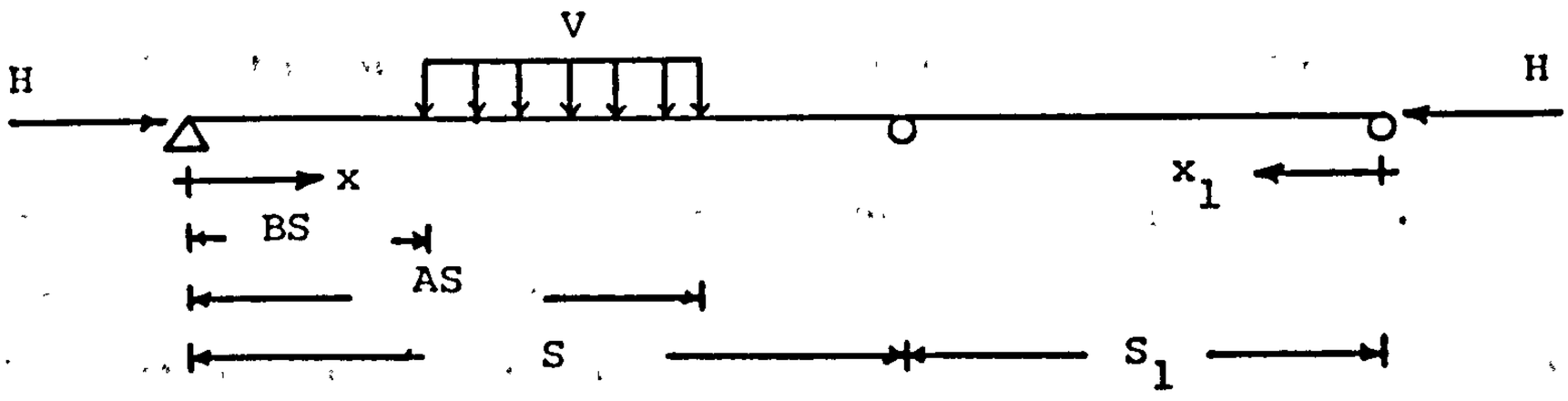

This form of loading can also be used as a continuous uniformly distributed load, when substituting A = 1 and B = o in the program. Moreover, a concentrated load, denoted WW in the program, which is applied at a distance ratio T with respect to either of the span lengths, can be transformed to the general loading form when substituting A = T + EPSL,

B = T - EPSL and $V = \frac{WW}{2\ EPSL\ S}$ where EPSL is a very small quantity, taken as 1×10^{-9} in the program. These transformations are performed automatically by the computer when it has been interactively informed of the type of loading applied on the structure.

As mentioned earlier, the program is capable of analysing the bridge for loads also applied in the right hand span. This is achieved when rotating the bridge by 180 degrees so that the load will act as if it was applied in the left hand span. The computer does this rotation automatically when it is interactively informed of the span where the live load is applied.

Having established the type of bridge as well as the type, magnitude and location of the applied live loading, the first stage of the program starts by the determination of the corresponding

change in the prestressing force, denoted is HP in the program. This is achieved by using Formulae (3.25) and carrying out the successive approximations procedure described in Section 2.5.3.3. Thus, HP is firstly assumed to be of a zero value, then, the right hand side of Formula (3.25) is calculated and compared with the value of HP. If the two values are not equal, the value of the right hand side is used as the starting value for another cycle of calculations. The whole procedure is repeated until both sides of the formula are equal and the final value of HP is obtained.

The following step is to determine the total prestressing force and find the bending moments for both spans of the structure by a straightforward substitution in the appropriate formulae given in Section 3.5.1. The values of the bending moments are calculated at the intervals which are specified in the input data as a ratio of the span lengths. For example, if the interval is given as 0.1, the program will evaluate the bending moments at every one tenth of both of the span lengths starting from the left and right end supports where the coordinates are located. Having found the bending moments, the value and position of the maximum bending moment, denoted as XM and XR in the program, are calculated by using Formulae (4.39) and (4.40).

Hence, the program proceeds to calculate the deflections and shear forces at the same previously given intervals for both span lengths. This is carried out by another straightforward substitution in the appropriate formulae specified in Section 3.5.1. Hence, the first stage of the program ends and the second stage starts by requesting the type and dimensions of the cross section of the beam as the program is capable of dealing with both T-shaped and rectangular shaped cross sections. The input data for this part of the program also includes information about the properties of the concrete and reinforcement, (see list of notations within the program).

Thus, the computer starts to calculate the ultimate moments of resistance, denoted as UM1 and UM2, for both cases when the top fibre of the beam lies in the compression and tension stress zone.

Moreover, it also calculates what is called the yield moments of resistance, denoted by YM1 and YM2, which is the moment at which the tensile reinforcement begins to yield, for the two mentioned cases (This is the subject for a future paper by the writer). It must be noted that the above values of the bending moments are obtained by using the initial prestressing force, denoted as HI in the program. Hence, by using the calculated value of the maximum bending moment, XM, the first plastic hinge and yield loads are initially found. Consequently, the corresponding changes in the prestressing force is evaluated as well as the total prestressing force. Hence, the computer is instructed to substitute this value in the expressions for the ultimate moments of resistance instead of the initial prestressing force. This results in more accurate values for the ultimate and yield moments of resistance and consequently the final first plastic hinge and first yield loads as well as the corresponding changes in the prestressing force are obtained. From this part of the program, it can be proved that the differences between the initial and final values of the first plastic hinge and first yield loads are almost negligible for most cases.

At this stage, the beam becomes a determinate structure and therefore the new formulae for the determination of the bending moments and the change in the prestressing force, denoted as DHP, are programmed. The main objective of the following part of the program is to calculate the load required to exceed the first plastic hinge load in order to cause the complete failure of the structure. This is carried out by firstly assuming the change in the prestressing force as zero and calculate the load, as specified in Equations (4.33) and (4.44). Whence, this value of the load is used to calculate DHP, from Formulae (4.32) or (4.42), and then compared with the assumed value. If they are not equal, another cycle of calculations starts by taking the change in the prestressing force equal to its calculated value. This procedure is repeated until two equal successive values for the change in the prestressing force and the load are obtained.

Having found the final value of DHP, it is added to the last obtained value for the total prestressing force, and the result is used to calculate the more accurate values for the ultimate and yield moments of resistance. Whence, the whole procedure of calculations is repeated once more to find the final change in the prestressing force as well as the load required to cause the failure of the structure. Then, the total values of the second yield and failure loads are computed as well as the total corresponding changes in the prestressing force. If the applied load was of a concentrated type, the computer automatically transforms the result back from the partial loading to the concentrated load form.

In the following part of this appendix, the structure of the program is clearly illustrated in the form of a flow chart.

b. The flow chart

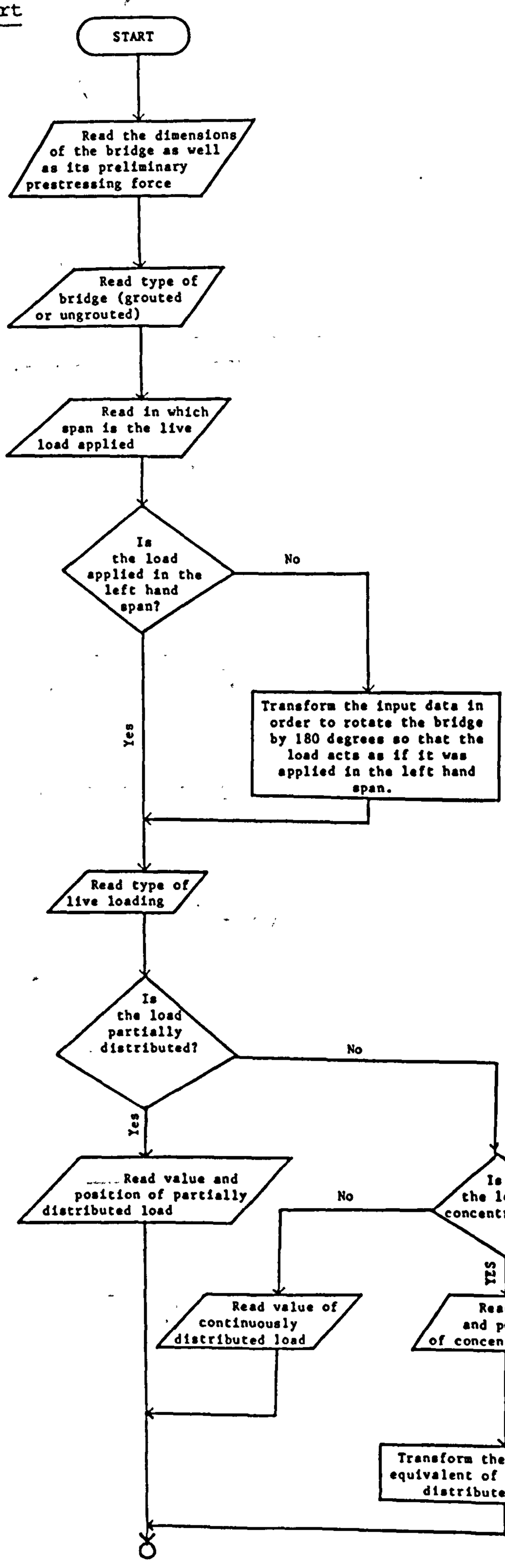

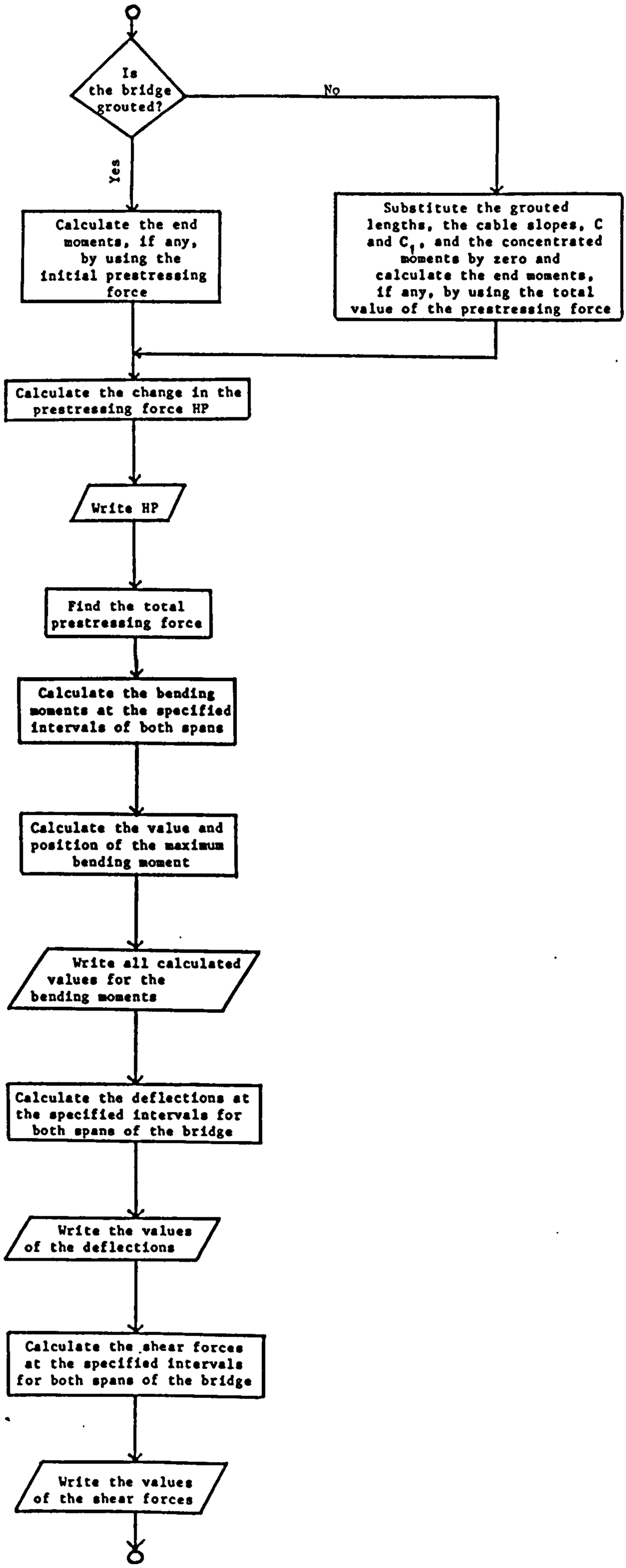
Is the bridge grouted?
No
Yes
Calculate the end moments, if any, by using the initial prestressing force
Substitute the grouted lengths, the cable slopes, C and C_1, and the concentrated moments by zero and calculate the end moments, if any, by using the total value of the prestressing force
Calculate the change in the prestressing force HP
Write HP
Find the total prestressing force
Calculate the bending moments at the specified intervals of both spans
Calculate the value and position of the maximum bending moment
Write all calculated values for the bending moments
Calculate the deflections at the specified intervals for both spans of the bridge
Write the values of the deflections
Calculate the shear forces at the specified intervals for both spans of the bridge
Write the values of the shear forces

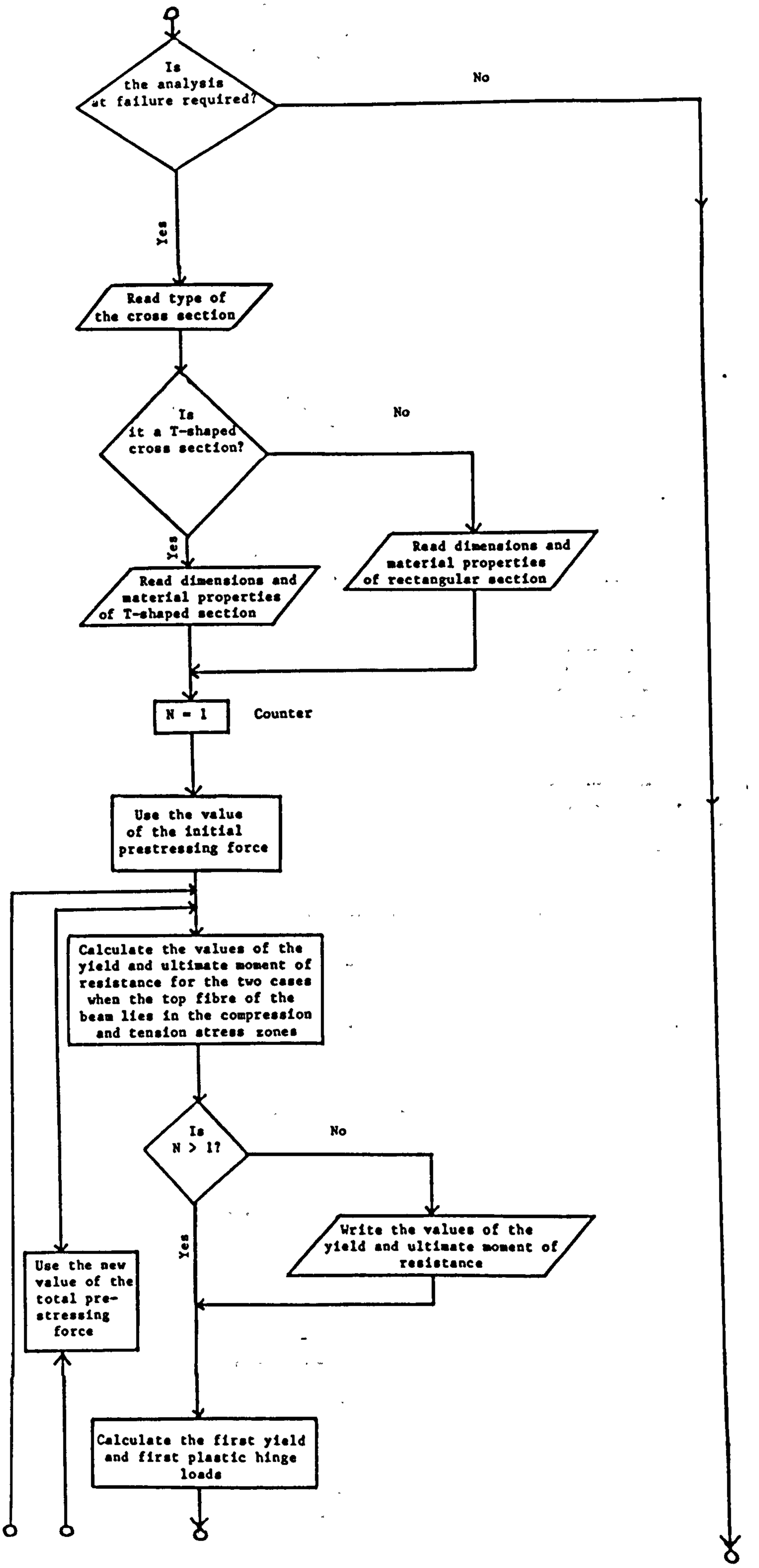
Is
the analysis
at failure required?
No
Yes
Read type of
the cross section
Is
it a T-shaped
cross section?
No
Yes
Read dimensions and
material properties
of T-shaped section
Read dimensions and
material properties
of rectangular section
N = 1
Counter
Use the value
of the initial
prestressing force
Calculate the values of the
yield and ultimate moment of
resistance for the two cases
when the top fibre of the
beam lies in the compression
and tension stress zones
Is
N > 1?
No
Yes
Write the values of the
yield and ultimate moment of
resistance
Use the new
value of the
total pre-
stressing
force
Calculate the first yield
and first plastic hinge
loads

Text cut off in original

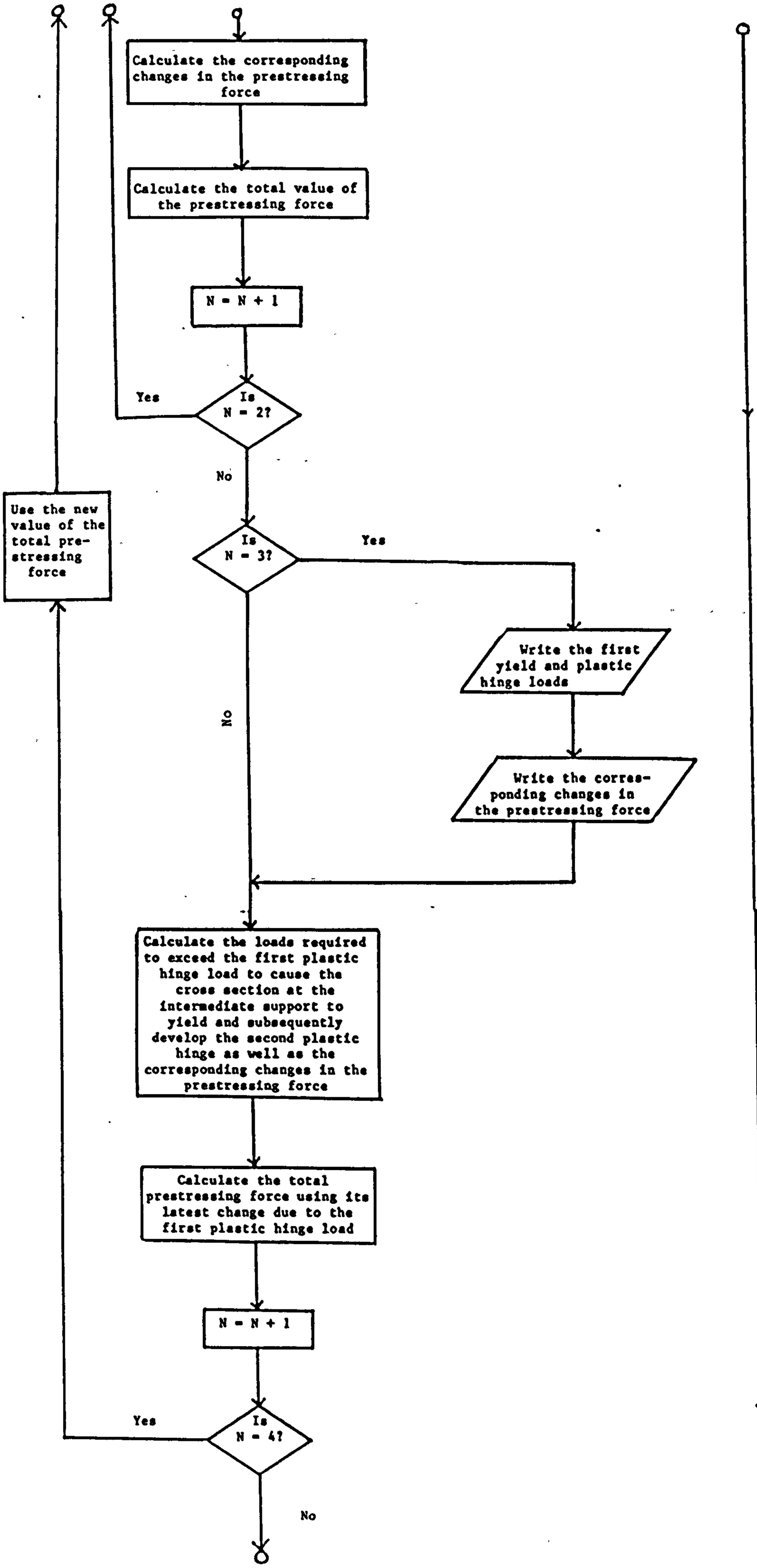
Calculate the corresponding changes in the prestressing force
Calculate the total value of the prestressing force
N = N + 1
Is N = 2?
Yes
No
Use the new value of the total pre-stressing force
Is N = 3?
Yes
No
Write the first yield and plastic hinge loads
Write the corres-ponding changes in the prestressing force
Calculate the loads required to exceed the first plastic hinge load to cause the cross section at the intermediate support to yield and subsequently develop the second plastic hinge as well as the corresponding changes in the prestressing force
Calculate the total prestressing force using its latest change due to the first plastic hinge load
N = N + 1
Is N = 4?
Yes
No

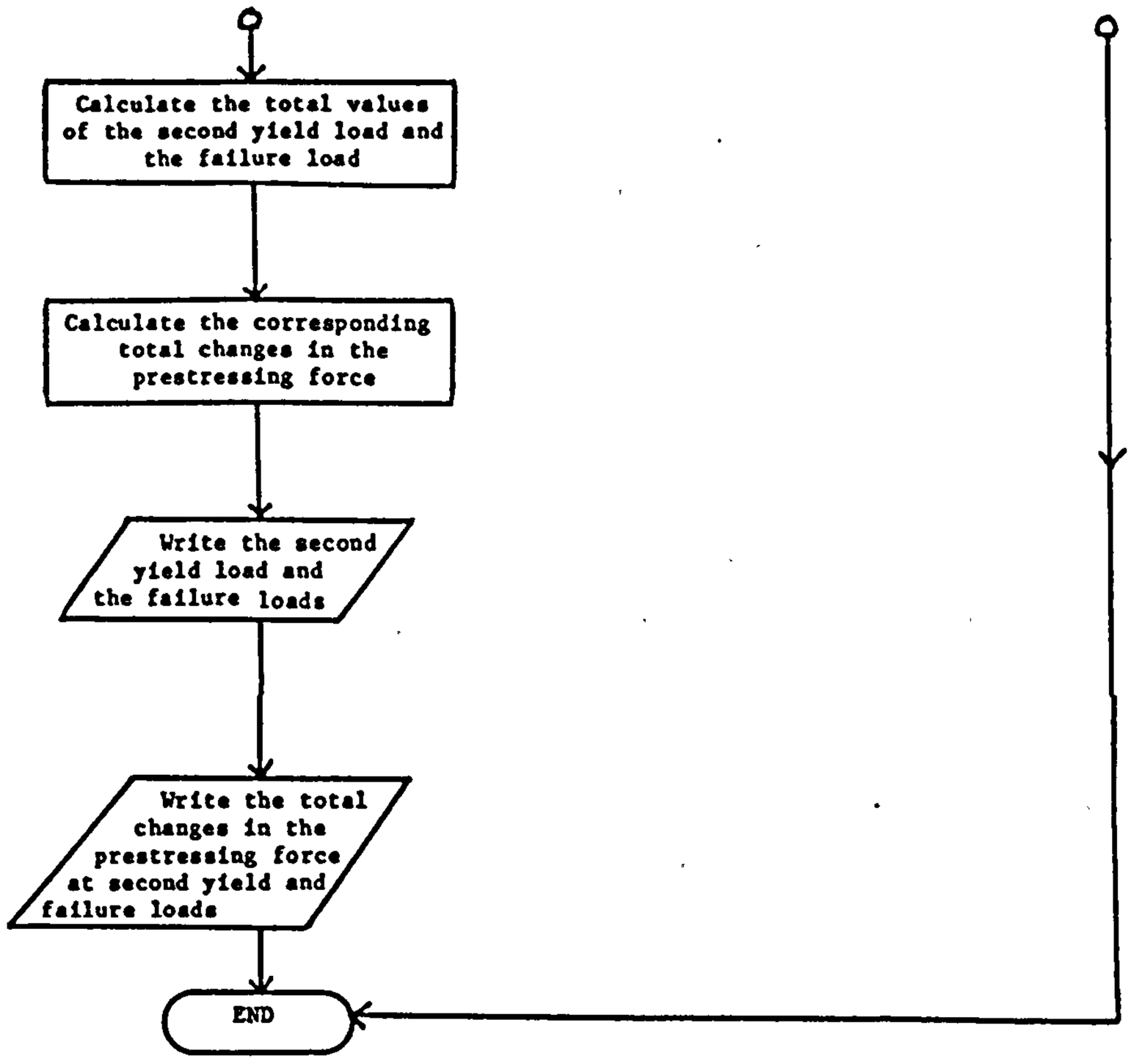
Calculate the total values of the second yield load and the failure load
Calculate the corresponding total changes in the prestressing force
Write the second yield load and the failure loads
Write the total changes in the prestressing force at second yield and failure loads
END

c. The Use of the Program

As mentioned earlier, the program is written to perform the elastic and plastic analyses for the bridge when a single loading is applied on either of its spans. However, it can also be used to carry out the elastic analysis when 'n' number of loads are applied on both spans of the bridge. This is carried out as we first run the program to perform the elastic analysis solely for the upward continuously distributed forces, yW and yW_1, and the end moments, if any, Ha or $H_i a$, with the live loads substituted zero. Hence, the program is to be run for 'n' times, according to the number of applied loads, to undertake the analysis for each load separately. Whence, the final results of the change in the prestressing force, the bending moments, the deflections and the shear forces can be obtained when finding the algebraic sum of these quantities for each load and subsequently subtract the results from those found earlier multiplied by (n - 1). The reason for this is that the upward forces, yW and yW_1, and the end moments, Ha or $H_i a$, only contribute once in the overall calculations and therefore, the extra forces they produce must be omitted as mentioned above.

The above procedure can not be used to perform the plastic analysis of the bridge due to the fact that the live loads may not necessarily increase by the same rate with respect to each other. Therefore, in order to check the stress state of the structure under any combination of live loads, the values of the maximum bending moment and the total prestressing force are obtained as mentioned earlier. Whence, the program is used to calculate the ultimate moment of resistance of the cross section of the beam, with the obtained total prestressing force, and is subsequently compared with the maximum bending moment. The significance of this comparison is that it enables the designer to check the safety of the structure for all possible case of loading when knowing how far the stresses in the structure are from the ultimate stresses.

d. The computer program

```
C     ************************************************************
C     * This is a general program for the analysis of two-span pre-*
C     * stressed concrete suspension bridges under any applied live*
C     * loading.The following notation is used within the program: *
C     *   S=The length of the left hand span (m).                  *
C     *  S1=The length of the right hand span (m).                 *
C     *   Z=The distance between the centre line of the suspended  *
C     *     beam and its top fibre (m).                            *
C     *  EC=The eccentricities at the ends of the suspended beam(m)*
C     *  HT=The height of the tower above the centre line of the   *
C     *     suspended beam (m).                                    *
C     *  HW=The preliminary value of the prestessing force (N).    *
C     *  ZE=The flexural rigidity of the suspended beam (N.sq m).  *
C     *  GA=The factor by which the preliminary prestessing force  *
C     *     has been increased to overcome the time effects as well*
C     *     as to adjust the initial prestessing force,for maximum *
C     *     efficiency.                                            *
C     *   W=The dead load of the suspended beam when added to the  *
C     *     weights of the main cable and the suspenders, in the   *
C     *     left hand span (N/m).                                  *
C     *  W1=The dead load of the suspended beam when added to the  *
C     *     weights of the main cable and the suspenders, in the   *
C     *     right hand span (N/m).                                 *
C     *  AC=The cross sectional area of the main cable (sq mm).    *
C     * ECA=Young's modulus of elasticity of the main cable(N/sqmm)*
C     *  TV=The intervals of the left and right hand span lengths  *
C     *     at which the bending moments,deflections and shear     *
C     *     forces are evaluated.i.e.if TV=0.1 the output will be  *
C     *     given at an interval of one tenth of either of the two *
C     *  HP=The change in the prestressing force corresponding to  *
C     *     the applied live loading (N).                          *
C     *  BM=The bending moments at the various positions of the    *
C     *     left hand span (N.m).                                  *
C     *  XM=The maximum bending moment which is usually located    *
C     *     in the span where the live load is applied (N.m).      *
C     *  XR=The position of the maximun bending moment as a ratio  *
C     *     of its distance from the end support to the span length*
C     * BM1=The bending moments at the various positions of the    *
C     *     right hand span (N.m).                                 *
C     *  DF=The deflections at the various positions of the left   *
C     *     hand span (m).                                         *
C     * DF1=The deflections at the various positions of the right  *
C     *     hand span (m).                                         *
C     *  SH=The shear forces at the various positions of the left  *
C     *     hand span (N).                                         *
C     * SH1=The shear forces at the various positions of the right *
C     *     hand span (N).                                         *
C     * BR1=The breadth of the flange of the T-shaped cross section*
C     *     (mm).                                                  *
C     *  BR=The breadth of the web for T-sec OR the breadth of the *
C     *     rectangular cross section (mm).                        *
C     *  DP=The thickness of the cross section of the beam (mm).   *
C     * EDP=The effective depth of the beam cross section (mm).    *
C     * DA1=The distance between the top fibre of the beam and the *
C     *     upper flange reinforcement for T.sec,OR,the top        *
C     *     reinforcement of the R.sec (mm).                       *
```

```
C     * DA2=The distance between the top fibre of the beam and the *
C     *     bottom flange reinforcement for T.sec,OR,the second    *
C     *     layer of reinforcement for the R.sec (mm).             *
C     *  FY=The yield stress of the reinforcement (N/sq mm).       *
C     * FUT=The cube strength of the concrete of the  beam (N/sqmm)*
C     *  ES=The modulus of elasticity for the reinforcement(N/sqmm)*
C     * AS1=The area of steel of the upper flange reinforcement    *
C     *     for T.sec,OR,the top reinforcement for R.sec (sq mm).  *
C     * AS2=The area of steel of the bottom flange reinforcement   *
C     *     for T.sec,OR,the second layer of reinforcement for     *
C     *     R.sec (sq mm).                                         *
C     * AS3=The area of steel of the main beam reinforcement(sq mm)*
C     * YM1=The yield moment for the cross section when the top    *
C     *     fibre lies in the compression stress zone (N. m).      *
C     * YM2=The yield moment for the cross section when the top    *
C     *     fibre lies in the tension stress zone (N.m).           *
C     * UM1=The ultimate moment of resistance for the cross section*
C     *     when the top fibre lies in the compression stress zone *
C     *     (N.m).                                                 *
C     * UM2=The ultimate moment of resistance for the cross section*
C     *     when the top fibre lies in the tesion stress zone(N.m).*
C     * YHP=The change in the prestressing force corresponding to  *
C     *     the first yield load (N).                              *
C     * UHP=The change in the prstressing force corresponding to   *
C     *     the first plastic hinge load (N).                      *
C     * HPTY=The total change in the prestressing force correspon- *
C     *      ding to the second yield load (N).                    *
C     * HPTU=The total change in the prestressing force correspon- *
C     *      ding to the failure load (N.m).                       *
C     * YV1=The first yield load (N).                              *
C     * UV1=The first plastic hinge load (N).                      *
C     * YV2=The second yield load (N).                             *
C     * UV2=The failure load (N).                                  *
C     ************************************************************

C     THE FIRST STAGE OF THE PROGRAM

      WRITE(6,2)
    2 FORMAT('ENTER S,S1,Z,EC,HT,HW,ZE,GA,W,W1,AC,ECA,TV')
      READ(5,*)S,S1,Z,EC,HT,HW,ZE,GA,W,W1,AC,ECA,TV

C     Learn the type of bridge (ungrouted/grouted) as well as
C     the type,position and value of the applied live loading

      WRITE(6,1000)
 1000 FORMAT('SPECIFY TYPE OF BRIDGE (UNGROUTED=1/GROUTED=2)')
      READ(5,*)ITYP
      WRITE(6,1001)
 1001 FORMAT('IN WHICH SPAN IS THE LOAD APPLIED?(L.SPAN=1/R.SPAN=2)')
      READ(5,*)ISPAN

C     For loads applied in the right hand span,the suspended
C     beam is rotated 180 degrees so that the live loading
C     acts as if it was applied in the left hand span

      IF(ISPAN.EQ.1)GO TO 1002
```

```
      SY=S
      WY=W
      S=S1
      S1=SY
      W=W1
      W1=WY
1002  WRITE(6,1003)
1003  FORMAT('SPECIFY TYPE OF LOADING (POINT=1/DISTRIBUTED=2)')
      READ(5,*)LTYP
      IF(LTYP.EQ.2)GO TO 1004
      WRITE(6,1005)
1005  FORMAT('ENTER VALUE AND POSITION OF POINT LOAD')
      READ(5,*)WW,T
      EPSL=0.000000001
      V=WW/(2*EPSL*S)
      A=T+EPSL
      B=T-EPSL
      GO TO 1010
1004  WRITE(6,1006)
1006  FORMAT('SPECIFY DISTRIBUTED LOAD (PARTIAL=1/CONTINUOUS=2)')
      READ(5,*)LDTYP
      IF(LDTYP.EQ.1)GO TO 1008
      WRITE(6,1007)
1007  FORMAT('ENTER VALUE OF DISTRIBUTED LOAD')
      READ(5,*)V
      A=1
      B=0
      GO TO 1010
 1008 WRITE(6,1009)
 1009 FORMAT('ENTER VALUE AND POSITION OF PARTIAL DIS.LOAD')
      READ(5,*)V,A,B
 1010 R=S1/S
      ACEC=AC*ECA
      F=(W*S**2)/(8*HW)
      R1=F/S
      R2=W1/W
      F1=R**2*R2*F
      FF=(HT+EC-(4*F))/S
      FF1=(HT+EC-(4*F1))/S1

C     Calculate the term which expresses the flexibility of
C     the main cable depending on the type of bridge

      IF(ITYP.EQ.1)GO TO 3
      IF(ITYP.EQ.2)GO TO 4
    3 Z=0
      G=0
      G1=0
      C=0
      C1=0
      E1=(FF+(4*R1))**2
      E2=(4*R**2*(1+R))+(32*R**3*R1**2*(1+(R*R2**2)))
      E3=(3/8)*(E1/R**3)*(E2+(E1*(1+R**3)))
      E4=(5*(1+(R**3*R2**2)))+(12*R1**2*(1+(R**5*R2**4)))
      E5=1+R+((8/5)*R1**2*E4)
      E=(S/ACEC)*(E3+E5)
```

```
      GO TO 5
    4 G=(SQRT(((FF/(8*R1))**2)+((Z+EC)/(4*F))))-(FF/(8*R1))
      G11=SQRT((((FF1*S1)/(8*F1))**2)+((Z+EC)/(4*F1)))
      G1=G11-((FF1*S1)/(8*F1))
      C=FF+(8*R1*G)
      C1=FF1+(8*R*R1*R2*G1)
      E1=(FF+(8*R1))*(2+((FF+(8*R1))**2))
      E2=(FF1+(8*R*R1*R2))*(2+((FF1+(8*R*R1*R2))**2))
      E3=(C*(2+C**2))+((1/R2)*C1*(2+C1**2))
      E=(S/(16*R1*ACEC))*(E1+((1/R2)*E2)-E3)
C     Evaluate the change in the prestressing force which is
C     developed as a result of the applied live loading and
C     carry out the necessary modifications according to the
C     specified type of bridge

    5 HP=0
      GO TO 6
    7 HP=HP1
    6 R3=HP/HW
      H=HW*(1+GA+R3)
      D=SQRT(H/ZE)
      DS=D*S
      DS1=D*S1
      DG=DS*G
      DG1=DS1*G1
      DSG=DS-DG
      DSG1=DS1-DG1
      DA=DS*A
      DB=DS*B
      DSA=DS-DA
      DSB=DS-DB
      FS=(1/S)*(1-(DS/TAN(DS)))
      FS1=(1/S1)*(1-(DS1/TAN(DS1)))
      CS=S*((TAN(DS/2)/(DS/2))-1)
      CS1=S1*((TAN(DS1/2)/(DS1/2))-1)
      FCS=(CS+(R2*CS1))/(FS+FS1)
      VS=(1/S)*((DS/SIN(DS))-1)
      VS1=(1/S1)*((DS1/SIN(DS1))-1)
      FVS=(VS+VS1)/(FS+FS1)
      CG=S*(((COS(DG)-COS(DS))/((DS/2)*SIN(DS)))-1+G**2)
      CG1=S1*(((COS(DG1)-COS(DS1))/((DS1/2)*SIN(DS1)))-1+G1**2)
      FCG=(CG+(R2*CG1))/(FS+FS1)
      VG=(1/S)*(((DS*COS(DG))/SIN(DS))-1)
      VG1=(1/S1)*(((DS1*COS(DG1))/SIN(DS1))-1)
      FVG=(VG+VG1)/(FS+FS1)
      Q11=((1/D**2)*(CS+(R2**2*CS1)))-((FCS**2/4)*(FS+FS1))
      Q1=(GA*(W/H))*(Q11-((S**3/12)*(1+(R**3*R2**2))))
      Q21=(S/D**2)*(((COS(DG/2)*SIN(DSG/2))/((DS/2)*COS(DS/2)))-1+G)
      Q22=((COS(DG1/2)*SIN(DSG1/2))/((DS1/2)*COS(DS1/2)))-1+G1
      Q23=(-1)*((CS+(R2*CS1))*(FCG/4))
      Q24=(1-(G**2*(3-(2*G))))+(R**3*R2**2*(1-(G1**2*(3-(2*G1)))))
      Q2=(R3*(W/H))*(Q21+(R2**2*(S1/D**2)*Q22)+Q23-((S**3/12)*Q24))
      Q31=((2*SIN(DG/2)*SIN((DS/2)-DG))/COS(DS/2))-((DS**2*G*(1-G))/2)
      Q32=((2*SIN(DG1/2)*SIN((DS1/2)-DG1))/COS(DS1/2))
      Q325=Q32-((DS1**2*G1*(1-G1))/2)
```

```
      Q33=(SIN(DG)/SIN(DS))-G
      Q34=(SIN(DG1)/SIN(DS1))-G1
      Q35=C*(Q31-(D**2*(FCS/2)*Q33))
      Q36=R2*C1*(Q325-(D**2*(FCS/2)*Q34))
      Q3=(HP/(D**2*H))*(Q35+Q36)
      Q41=(SIN((DS/2)-DG)/((DS/2)*COS(DS/2)))-1+(2*G)
      Q42=(SIN((DS1/2)-DG1)/((DS1/2)*COS(DS1/2)))-1+(2*G1)
      Q4=(-1)*((HP*Z)/(2*H))*((S*Q41)+(R2*S1*Q42)-(FCS*(VG+VG1)))
      IF(ITYP.EQ.1)GO TO 8
      IF(ITYP.EQ.2)GO TO 9
    8 Q5=(EC/2)*(CS+(R2*CS1))*(1-FVS)
      GO TO 10
    9 Q5=(HW/H)*(EC/2)*(1+GA)*(CS+(R2*CS1))*(1-FVS)
   10 Q=Q1+Q2+Q3+Q4+Q5
      Q61=((SIN((DS/2)-DB)-SIN((DS/2)-DA))/(DS*COS(DS/2)))-A+B
      Q62=(-1)*(S**2/12)*((3*A**2)-(2*A**3)-(3*B**2)+(2*B**3))
      Q63=((COS(DB)-COS(DA))/((DS/2)*SIN(DS)))-A**2+B**2
      Q6=(V*(S/H))*((Q61/D**2)+Q62-(FCS*(Q63/4)))
      HP1=(W/(E*HW))*(Q6-Q)
      IF(ABS((HP1-HP)/HP1).GT.0.00001)GO TO 7
      WRITE(6,11)HP1
   11 FORMAT('THE CHANGE IN THE CABLE TENSION= ',F10.5)
      WRITE(6,12)
   12 FORMAT('**********************************************')

C     Calculate the final values of the bending moments in the
C     span where the live loading is applied at the given
C     intervals of the span length and consider the necessary
C     alterations required according to the type of bridge

      IF(ISPAN.EQ.1)GO TO 131
      IF(ISPAN.EQ.2)GO TO 133
  131 WRITE(6,132)
  132 FORMAT('THE B.MOMENTS FOR THE LEFT HAND SPAN ARE')
      GO TO 135
  133 WRITE(6,134)
  134 FORMAT('THE B.MOMENTS FOR THE RIGHT HAND SPAN ARE')
  135 X=0
      GO TO 14
   15 X=X+(TV*S)
   14 SX=SIN(D*X)/SIN(DS)
      SX1=SIN(DS-(D*X))/SIN(DS)
      BM21=(SX*(1-((D**2/2)*FCS)))+SX1-1
      BM2=GA*W*(BM21/D**2)
      BM31=SX*(1-COS(DSG)-(D**2*(FCG/2)))
      BM3=R3*W*(BM31/D**2)
      BM41=(-1)*(HP/(FS+FS1))*((C*Q33)+(C1*Q34))
      BM4=SX*(BM41+(C*(HP/D)*SIN(DSG)))
      BM5=HP*Z*SX*(COS(DSG)+FVG)
      IF(ITYP.EQ.1)GO TO 16
      IF(ITYP.EQ.2)GO TO 17
   16 BM6=H*EC*(SX1-(FVS*SX))
      GO TO 18
   17 BM6=HW*(1+GA)*EC*(SX1-(FVS*SX))
   18 BM71=(SX*(1-((D**2/2)*FCG)))+(COS(DG)*SX1)-1
      BM7=R3*W*(BM71/D**2)
```

```
      BM8=(C*(HP/D)*SIN(DG)*SX1)+(BM41*SX)
      BM9=HP*Z*((SX*FVG)-(COS(DG)*SX1))
      BM10=BM2+BM3+BM4+BM5+BM6
      BM11=BM2+BM7+BM8+BM9+BM6
      BMV11=(D**2*(S/2)*Q63)/(FS+FS1)
      BMV1=(-1)*(V/D**2)*SX*(COS(DSA)-COS(DSB)-BMV11)
      BMV21=(SX*COS(DSA))+(SX1*COS(DB))-1-(SX*BMV11)
      BMV2=(-1)*(V/D**2)*BMV21
      BMV31=((COS(DB)-COS(DA))*SX1)-(BMV11*SX)
      BMV3=(-1)*(V/D**2)*BMV31
      IF(G.LE.B)GO TO 19
      IF(G.GT.B.AND.G.LE.A)GO TO 24
      IF(G.GT.A)GO TO 29
   19 IF(X.LE.(G*S))GO TO 20
      IF(X.GT.(G*S).AND.X.LE.(B*S))GO TO 21
      IF(X.GT.(B*S).AND.X.LE.(A*S))GO TO 22
      IF(X.GT.(A*S))GO TO 23
   20 BM=BM10+BMV1
      GO TO 34
   21 BM=BM11+BMV1
      GO TO 34
   22 BM=BM11+BMV2
      GO TO 34
   23 BM=BM11+BMV3
      GO TO 34
   24 IF(X.LE.(B*S))GO TO 25
      IF(X.GT.(B*S).AND.X.LE.(G*S))GO TO 26
      IF(X.GT.(G*S).AND.X.LE.(A*S))GO TO 27
      IF(X.GT.(A*S))GO TO 28
   25 BM=BM10+BMV1
      GO TO 34
   26 BM=BM10+BMV2
      GO TO 34
   27 BM=BM11+BMV2
      GO TO 34
   28 BM=BM11+BMV3
      GO TO 34
   29 IF(X.LE.(B*S))GO TO 30
      IF(X.GT.(B*S).AND.X.LE.(A*S))GO TO 31
      IF(X.GT.(A*S).AND.X.LE.(G*S))GO TO 32
      IF(X.GT.(G*S))GO TO 33
   30 BM=BM10+BMV1
      GO TO 34
   31 BM=BM10+BMV2
      GO TO 34
   32 BM=BM10+BMV3
      GO TO 34
   33 BM=BM11+BMV3
   34 IF(ISPAN.EQ.1)GO TO 341
      IF(ISPAN.EQ.2)GO TO 343
  341 WRITE(6,342)X,BM
  342 FORMAT('AT X=',F8.3,' B.M=',F15.5)
      GO TO 345
  343 WRITE(6,344)X,BM
  344 FORMAT('AT X1=',F8.3,' B.M=',F15.5)
  345 IF(X.LE.((1-TV)*S))GO TO 15
```

```
C     Determine the value and position of the maximum bending
C     moment in the span where the live loading is applied
C     taking into account the type of bridge

      XX11=(V*(COS(DSA)-BMV11))-(W*(GA+R3))
      XX12=W*D**2*((GA*FCS)+(R3*FCG))
      XX13=((-1)*BM41*D**2)-(D**2*HP*Z*FVG)
      XX14=(V*COS(DB))-(W*(GA+(R3*COS(DG))))
      XX15=(D**2*HP*Z)-(D*C*HP*SIN(DG))
      IF(ITYP.EQ.1)GO TO 355
      IF(ITYP.EQ.2)GO TO 356
  355 XX16=H*EC*D**2*FVS
      XX17=(-1)*D**2*H*EC
      GO TO 357
  356 XX16=HW*(1+GA)*EC*D**2*FVS
      XX17=(-1)*D**2*HW*(1+GA)*EC
  357 XX1=XX11+XX12+XX13+XX16
      XX2=(XX14+XX15+XX17)*SIN(DS)
      XX3=(XX1/XX2)-(1/TAN(DS))
      XR=(1/DS)*ATAN(XX3)
      XX=XR*S
      IF(ISPAN.EQ.1)GO TO 331
      IF(ISPAN.EQ.2)GO TO 333
  331 WRITE(6,332)XX
  332 FORMAT('THE MAX.B.M. IS AT X=',F8.3,' FROM THE L.H.SUPPORT')
      GO TO 335
  333 WRITE(6,334)XX
  334 FORMAT('THE MAX.B.M. IS AT X1=',F8.3,' FROM THE R.H.SUPPORT')
  335 SXX=SIN(D*XX)/SIN(DS)
      SXX1=SIN(DS-(D*XX))/SIN(DS)
      XM21=(SXX*(1-((D**2/2)*FCS)))+SXX1-1
      XM2=GA*W*(XM21/D**2)
      XM31=(SXX*(1-((D**2/2)*FCG)))+(COS(DG)*SXX1)-1
      XM3=R3*W*(XM31/D**2)
      XM4=(C*(HP/D)*SIN(DG)*SXX1)+(BM41*SXX)
      XM5=HP*Z*((SXX*FVG)-(COS(DG)*SXX1))
      IF(ITYP.EQ.1)GO TO 359
      IF(ITYP.EQ.2)GO TO 360
  359 XM6=H*EC*(SXX1-(FVS*SXX))
      GO TO 361
  360 XM6=HW*(1+GA)*EC*(SXX1-(FVS*SXX))
  361 XMV1=(SXX*COS(DSA))+(SXX1*COS(DB))-1-(SXX*BMV11)
      XMV=(-1)*(V/D**2)*XMV1
      XM=XM2+XM3+XM4+XM5+XM6+XMV
      IF(ISPAN.EQ.1)GO TO 336
      IF(ISPAN.EQ.2)GO TO 338
  336 WRITE(6,337)XM
  337 FORMAT('THE MAX.B.MOMENT AT L.H.SPAN=',F15.5)
      GO TO 340
  338 WRITE(6,339)XM
  339 FORMAT('THE MAX.B.MOMENT AT R.H.SPAN=',F15.5)

C     Evaluate the bending moment at the intermediate support
C     taking into account the specified type of bridge
```

```
340 XMI1=(-1)*((GA*W*(FCS/2))+(R3*W*(FCG/2))-BM41-(HP*Z*FVG))
    IF(ITYP.EQ.1)GO TO 209
    IF(ITYP.EQ.2)GO TO 210
209 XMI2=(-1)*H*EC*FVS
    GO TO 211
210 XMI2=(-1)*HW*(1+GA)*EC*FVS
211 XMI=XMI1+XMI2+(BMV11*(V/D**2))
    WRITE(6,226)
226 FORMAT('-----------------------------------------')
    WRITE(6,212)XMI
212 FORMAT('THE MOMENT AT THE INTERMEDIATE SUPPORT=',F15.5)
    WRITE(6,36)
 36 FORMAT('-----------------------------------------')

C     Calculate the final values of the bending moments in the
C     other span at the given intervals of the span length
C     according to the specified type of bridge

    IF(ISPAN.EQ.1)GO TO 371
    IF(ISPAN.EQ.2)GO TO 373
371 WRITE(6,372)
372 FORMAT('THE B.MOMENTS FOR THE RIGHT HAND SPAN ARE')
    GO TO 375
373 WRITE(6,374)
374 FORMAT('THE B.MOMENTS FOR THE LEFT HAND SPAN ARE')
375 X1=0
    GO TO 38
 39 X1=X1+(TV*S1)
 38 S1X=SIN(D*X1)/SIN(DS1)
    S1X1=SIN(DS1-(D*X1))/SIN(DS1)
    BM121=(S1X*(1-(D**2*(FCS/(2*R2)))))+S1X1-1
    BM12=GA*W1*(BM121/D**2)
    BM131=1-COS(DSG1)-(D**2*(FCG/(2*R2)))
    BM13=R3*W1*S1X*(BM131/D**2)
    BM141=C1*(HP/D)*SIN(DSG1)
    BM14=S1X*(BM141+BM41)
    BM15=HP*Z*S1X*(COS(DSG1)+FVG)
    IF(ITYP.EQ.1)GO TO 395
    IF(ITYP.EQ.2)GO TO 40
395 BM16=H*EC*(S1X1-(FVS*S1X))
    GO TO 41
 40 BM16=HW*(1+GA)*EC*(S1X1-(FVS*S1X))
 41 BM171=(S1X*(1-(D**2*(FCG/(2*R2)))))+(COS(DG1)*S1X1)-1
    BM17=R3*W1*(BM171/D**2)
    BM18=(C1*(HP/D)*SIN(DG1)*S1X1)+(BM41*S1X)
    BM19=HP*Z*((S1X*FVG)-(COS(DG1)*S1X1))
    BM20=BM12+BM13+BM14+BM15+BM16
    BM26=BM12+BM17+BM18+BM19+BM16
    BMV4=(V/D**2)*S1X*BMV11
    IF(X1.LE.(G1*S1))GO TO 42
    IF(X1.GT.(G1*S1))GO TO 43
42  BM1=BM20+BMV4
    GO TO 44
43  BM1=BM26+BMV4
44  IF(ISPAN.EQ.1)GO TO 441
    IF(ISPAN.EQ.2)GO TO 443
```

```
  441 WRITE(6,442)X1,BM1
  442 FORMAT('AT X1=',F8.3,' B.M.=',F15.5)
      GO TO 445
  443 WRITE(6,444)X1,BM1
  444 FORMAT('AT X=',F8.3,' B.M.=',F15.5)
  445 IF(X1.LE.((1-TV)*S1))GO TO 39
      WRITE(6,46)
   46 FORMAT('**********************************************')

C     Determine the final values of the deflections in the
C     span where the live loading is applied at the given
C     intervals of the span length according to the specified
C     type of bridge

      IF(ISPAN.EQ.1)GO TO 471
      IF(ISPAN.EQ.2)GO TO 473
  471 WRITE(6,472)
  472 FORMAT('THE DEFLECTIONS FOR THE LEFT HAND SPAN ARE')
      GO TO 475
  473 WRITE(6,474)
  474 FORMAT('THE DEFLECTIONS FOR THE RIGHT HAND SPAN ARE')
  475 X=0
      GO TO 48
   49 X=X+(TV*S)
   48 SX=SIN(D*X)/SIN(DS)
      SX1=SIN(DS-(D*X))/SIN(DS)
      DF21=1-(D**2*(FCS/2))
      DF22=(SX*DF21)+SX1-1
      DF23=DF22-(((D**2*X)/(2*S))*((S*(S-X))-FCS))
      DF2=(-1)*GA*(W/H)*(DF23/D**2)
      DF31=1-(D**2*(FCG/2))
      DF32=((D**2*X)/(2*S))*((S-(G*S))**2-FCG)
      DF33=SX*(DF31-COS(DSG))
      DF3=(-1)*R3*(W/(H*D**2))*(DF33-DF32)
      DF41=(BM41/H)*((X/S)-SX)
      DF42=(SX*SIN(DSG))-(D*X*(1-G))
      DF4=DF41-(C*(HP/H)*(DF42/D))
      DF5=(HP/H)*Z*(((X/S)*(1+FVG))-(SX*(COS(DSG)+FVG)))
      IF(ITYP.EQ.1)GO TO 50
      IF(ITYP.EQ.2)GO TO 51
   50 DF6=(-1)*EC*((X/S)+SX1+(FVS*((X/S)-SX))-1)
      GO TO 52
   51 DF6=(-1)*(HW/H)*(1+GA)*EC*((X/S)+SX1+(FVS*((X/S)-SX))-1)
   52 DF71=((-1)*DF32)+((D**2/2)*(X-(G*S))**2)
      DF7=(-1)*R3*(W/(H*D**2))*((SX*DF31)+(COS(DG)*SX1)-1+DF71)
      DF8=DF41-(C*(HP/(H*D))*((SIN(DG)*SX1)-(D*G*(S-X))))
      DF9=HP*(Z/H)*(((X/S)*(1+FVG))-1-(SX*FVG)+(COS(DG)*SX1))
      DF10=DF2+DF3+DF4+DF5+DF6
      DF11=DF2+DF7+DF8+DF9+DF6
      DFV11=((COS(DSA)-COS(DSB))*SX)+(BMV11*((X/S)-SX))
      DFV12=DS**2*(X/(2*S))*((2*(A-B))-A**2+B**2)
      DFV1=(V/(H*D**2))*(DFV11-DFV12)
      DFV21=(COS(DSA)*SX)+(COS(DB)*SX1)-1+(BMV11*((X/S)-SX))
      DFV22=DFV12-((DS**2/2)*((X/S)-B)**2)
      DFV2=(V/(H*D**2))*(DFV21-DFV22)
      DFV31=((COS(DB)-COS(DA))*SX1)+(BMV11*((X/S)-SX))
```

```
      DFV32=(DS**2/2)*(A**2-B**2)*(1-(X/S))
      DFV3=(V/(D**2*H))*(DFV31-DFV32)
      IF(G.LE.B)GO TO 53
      IF(G.GT.B.AND.G.LE.A)GO TO 58
      IF(G.GT.A)GO TO 63
   53 IF(X.LE.(G*S))GO TO 54
      IF(X.GT.(G*S).AND.X.LE.(B*S))GO TO 55
      IF(X.GT.(B*S).AND.X.LE.(A*S))GO TO 56
      IF(X.GT.(A*S))GO TO 57
   54 DF=DF10+DFV1
      GO TO 68
   55 DF=DF11+DFV1
      GO TO 68
   56 DF=DF11+DFV2
      GO TO 68
   57 DF=DF11+DFV3
      GO TO 68
   58 IF(X.LE.(B*S))GO TO 59
      IF(X.GT.(B*S).AND.X.LE.(G*S))GO TO 60
      IF(X.GT.(G*S).AND.X.LE.(A*S))GO TO 61
      IF(X.GT.(A*S))GO TO 62
   59 DF=DF10+DFV1
      GO TO 68
   60 DF=DF10+DFV2
      GO TO 68
   61 DF=DF11+DFV2
      GO TO 68
   62 DF=DF11+DFV3
      GO TO 68
   63 IF(X.LE.(B*S))GO TO 64
      IF(X.GT.(B*S).AND.X.LE.(A*S))GO TO 65
      IF(X.GT.(A*S).AND.X.LE.(G*S))GO TO 66
      IF(X.GT.(G*S))GO TO 67
   64 DF=DF10+DFV1
      GO TO 68
   65 DF=DF10+DFV2
      GO TO 68
   66 DF=DF10+DFV3
      GO TO 68
   67 DF=DF11+DFV3
   68 IF(ISPAN.EQ.1)GO TO 681
      IF(ISPAN.EQ.2)GO TO 683
  681 WRITE(6,682)X,DF
  682 FORMAT('AT X=',F5.3,' DF=',F8.5)
      GO TO 685
  683 WRITE(6,684)X,DF
  684 FORMAT('AT X1=',F5.3,' DF=',F8.5)
  685 IF(X.LE.((1-TV)*S))GO TO 49
      WRITE(6,70)
   70 FORMAT('-----------------------------------------')

C     Evaluate the final deflections in the other span at the
C     given intervals of the span length according to the
C     specified type of bridge

      IF(ISPAN.EQ.1)GO TO 711
```

```
      IF(ISPAN.EQ.2)GO TO 713
  711 WRITE(6,712)
  712 FORMAT('THE DEFLECTIONS FOR THE RIGHT HAND SPAN ARE')
      GO TO 715
  713 WRITE(6,714)
  714 FORMAT('THE DEFLECTIONS FOR THE LEFT HAND SPAN ARE')
  715 X1=0
      GO TO 72
   73 X1=X1+(TV*S1)
   72 S1X=SIN(D*X1)/SIN(DS1)
      S1X1=SIN(DS1-(D*X1))/SIN(DS1)
      DF215=1-(D**2*(FCS/(2*R2)))
      DF315=1-(D**2*(FCG/(2*R2)))
      DF121=(S1X*DF215)-(((D**2*X1)/(2*S1))*((S1*(S1-X1))-(FCS/R2)))
      DF12=(-1)*GA*(W1/H)*((DF121+S1X1-1)/D**2)
      DF131=S1X*(DF315-COS(DSG1))
      DF132=((D**2*X1)/(2*S1))*((S1-(G1*S1))**2-(FCG/R2))
      DF13=(-1)*R3*(W1/(H*D**2))*(DF131-DF132)
      DF141=(BM41/H)*((X1/S1)-S1X)
      DF14=DF141-((C1/D)*(HP/H)*((SIN(DSG1)*S1X)-(D*X1*(1-G1))))
      DF15=HP*(Z/H)*(((X1/S1)*(1+FVG))-(S1X*(COS(DSG1)+FVG)))
      IF(ITYP.EQ.1)GO TO 74
      IF(ITYP.EQ.2)GO TO 75
   74 DF16=(-1)*EC*((X1/S1)+S1X1+(FVS*((X1/S1)-S1X))-1)
      GO TO 76
   75 DF16=(-1)*(HW/H)*(1+GA)*EC*((X1/S1)+S1X1+(FVS*((X1/S1)-S1X))-1)
   76 DF171=(S1X*DF315)+(COS(DG1)*S1X1)-1
      DF172=DF132-((D**2/2)*(X1-(G1*S1))**2)
      DF17=(-1)*R3*(W1/(H*D**2))*(DF171-DF172)
      DF18=DF141-((C1/D)*(HP/H)*((SIN(DG1)*S1X1)-(D*G1*(S1-X1))))
      DF19=(HP/H)*Z*(((X1/S1)*(1+FVG))-1-(S1X*FVG)+(COS(DG1)*S1X1))
      DF20=DF12+DF13+DF14+DF15+DF16
      DF26=DF12+DF17+DF18+DF19+DF16
      DFV4=(V/(D**2*H))*BMV11*((X1/S1)-S1X)
      IF(X1.LE.(G1*S1))GO TO 77
      IF(X1.GT.(G1*S1))GO TO 78
   77 DF1=DF20+DFV4
      GO TO 79
   78 DF1=DF26+DFV4
   79 IF(ISPAN.EQ.1)GO TO 791
      IF(ISPAN.EQ.2)GO TO 793
  791 WRITE(6,792)X1,DF1
  792 FORMAT('AT X1=',F5.3,' DF=',F8.5)
      GO TO 795
  793 WRITE(6,794)X1,DF1
  794 FORMAT('AT X=',F5.3,' DF=',F8.5)
  795 IF(X1.LE.((1-TV)*S1))GO TO 73
      WRITE(6,81)
   81 FORMAT('**********************************************')

C     Determine the final values of the shear forces in the
C     span where the live loading is applied at the given
C     intervals of the span length according to the
C     specified type of bridge

      IF(ISPAN.EQ.1)GO TO 821
```

```
      IF(ISPAN.EQ.2)GO TO 823
  821 WRITE(6,822)
  822 FORMAT('THE SHEAR FORCES FOR THE LEFT HAND SPAN ARE')
      GO TO 825
  823 WRITE(6,824)
  824 FORMAT('THE SHEAR FORCES FOR THE RIGHT HAND SPAN ARE')
  825 X=0
      GO TO 83
   84 X=X+(TV*S)
   83 CX=COS(D*X)/SIN(DS)
      CX1=COS(DS-(D*X))/SIN(DS)
      SH2=(-1)*GA*(W/D)*((CX*DF21)-CX1)
      SH3=(-1)*R3*(W/D)*CX*(DF31-COS(DSG))
      SH4=((-1)*D*CX*BM41)-(C*HP*CX*SIN(DSG))
      SH5=(-1)*D*HP*Z*CX*(COS(DSG)+FVG)
      IF(ITYP.EQ.1)GO TO 85
      IF(ITYP.EQ.2)GO TO 86
   85 SH6=D*H*EC*(CX1+(FVS*CX))
      GO TO 87
   86 SH6=D*HW*(1+GA)*EC*(CX1+(FVS*CX))
   87 SH7=(-1)*R3*(W/D)*((CX*DF31)-(COS(DG)*CX1))
      SH8=((-1)*D*CX*BM41)+(C*HP*SIN(DG)*CX1)
      SH9=(-1)*D*HP*Z*((CX*FVG)+(COS(DG)*CX1))
      SH10=SH2+SH3+SH4+SH5+SH6
      SH11=SH2+SH7+SH8+SH9+SH6
      SHV1=(V/D)*CX*(COS(DSA)-COS(DSB)-BMV11)
      SHV2=(V/D)*((CX*COS(DSA))-(CX1*COS(DB))-(BMV11*CX))
      SHV3=(-1)*(V/D)*(((COS(DB)-COS(DA))*CX1)+(BMV11*CX))
      IF(G.LE.B)GO TO 88
      IF(G.GT.B.AND.G.LE.A)GO TO 93
      IF(G.GT.A)GO TO 98
   88 IF(X.LE.(G*S))GO TO 89
      IF(X.GT.(G*S).AND.X.LE.(B*S))GO TO 90
      IF(X.GT.(B*S).AND.X.LE.(A*S))GO TO 91
      IF(X.GT.(A*S))GO TO 92
   89 SH=SH10+SHV1
      GO TO 103
   90 SH=SH11+SHV1
      GO TO 103
   91 SH=SH11+SHV2
      GO TO 103
   92 SH=SH11+SHV3
      GO TO 103
   93 IF(X.LE.(B*S))GO TO 94
      IF(X.GT.(B*S).AND.X.LE.(G*S))GO TO 95
      IF(X.GT.(G*S).AND.X.LE.(A*S))GO TO 96
      IF(X.GT.(A*S))GO TO 97
   94 SH=SH10+SHV1
      GO TO 103
   95 SH=SH10+SHV2
      GO TO 103
   96 SH=SH11+SHV2
      GO TO 103
   97 SH=SH11+SHV3
      GO TO 103
   98 IF(X.LE.(B*S))GO TO 99
```

```
      IF(X.GT.(B*S).AND.X.LE.(A*S))GO TO 100
      IF(X.GT.(A*S).AND.X.LE.(G*S))GO TO 101
      IF(X.GT.(G*S))GO TO 102
   99 SH=SH10+SHV1
      GO TO 103
  100 SH=SH10+SHV2
      GO TO 103
  101 SH=SH10+SHV3
      GO TO 103
  102 SH=SH11+SHV3
  103 IF(ISPAN.EQ.1)GO TO 1031
      IF(ISPAN.EQ.2)GO TO 1033
 1031 WRITE(6,1032)X,SH
 1032 FORMAT('AT X=',F5.3,' S.F=',F15.5)
      GO TO 1035
 1033 WRITE(6,1034)X,SH
 1034 FORMAT('AT X1=',F5.3,' S.F=',F15.5)
 1035 IF(X.LE.((1-TV)*S))GO TO 84
      WRITE(6,105)
  105 FORMAT('-----------------------------------------')

C     Calculate the final values of the shear forces in the
C     other span at the given intervals of the span length
C     according to the specified type of bridge

      IF(ISPAN.EQ.1)GO TO 1061
      IF(ISPAN.EQ.2)GO TO 1063
 1061 WRITE(6,1062)
 1062 FORMAT('THE SHEAR FORCES FOR THE RIGHT HAND SPAN ARE')
      GO TO 1065
 1063 WRITE(6,1064)
 1064 FORMAT('THE SHEAR FORCES FOR THE LEFT HAND SPAN ARE')
 1065 X1=0
      GO TO 107
  108 X1=X1+(TV*S1)
  107 C1X=COS(D*X1)/SIN(DS1)
      C1X1=COS(DS1-(D*X1))/SIN(DS1)
      SH12=(-1)*GA*(W1/D)*((C1X*DF215)-C1X1)
      SH13=(-1)*R3*(W1/D)*C1X*(DF315-COS(DSG1))
      SH14=((-1)*D*C1X*BM41)-(C1*HP*C1X*SIN(DSG1))
      SH15=(-1)*HP*D*Z*C1X*(COS(DSG1)+FVG)
      IF(ITYP.EQ.1)GO TO 109
      IF(ITYP.EQ.2)GO TO 110
  109 SH16=D*H*EC*(C1X1+(FVS*C1X))
      GO TO 111
  110 SH16=D*HW*(1+GA)*EC*(C1X1+(FVS*C1X))
  111 SH17=(-1)*R3*(W1/D)*((C1X*DF315)-(COS(DG1)*C1X1))
      SH18=((-1)*D*C1X*BM41)+(C1*HP*SIN(DG1)*C1X1)
      SH19=(-1)*HP*D*Z*((C1X*FVG)+(COS(DG1)*C1X1))
      SH20=SH12+SH13+SH14+SH15+SH16
      SH26=SH12+SH17+SH18+SH19+SH16
      SHV4=(-1)*(V/D)*C1X*BMV11
      IF(X1.LE.(G1*S1))GO TO 112
      IF(X1.GT.(G1*S1))GO TO 113
  112 SH1=SH20+SHV4
      GO TO 114
```

```
 113 SH1=SH26+SHV4
 114 IF(ISPAN.EQ.1)GO TO 1141
     IF(ISPAN.EQ.2)GO TO 1143
1141 WRITE(6,1142)X1,SH1
1142 FORMAT('AT X1=',F5.3,' S.F=',F15.5)
     GO TO 1145
1143 WRITE(6,1144)X1,SH1
1144 FORMAT('AT X=',F5.3,' S.F=',F15.5)
1145 IF(X1.LE.((1-TV)*S1))GO TO 108
     WRITE(6,116)
 116 FORMAT('**************************************************')
C      THE SECOND STAGE OF THE PROGRAM

       WRITE(6,120)
  120 FORMAT('IS THE ANALYSIS FOR FAILURE REQUIRED?(YES=1/NO=2)')
       READ(5,*)IY
       IF(IY.EQ.2)GO TO 213

C      Learn the shape of the cross section of the suspended
C      beam (T-shaped/rectangular-shaped) and start the
C      procedure for the analysis at failure

       WRITE(6,227)
  227 FORMAT('WHAT SHAPE IS THE X.SEC. OF THE BEAM?(T.SEC=1/R.SEC=2)')
       READ(5,*)ISH
       IF(ISH.EQ.1)GO TO 228
       WRITE(6,229)
  229 FORMAT('ENTER BR,DP,EDP,DA1,DA2,FY,FUT,ES,AS1,AS2,AS3')
       READ(5,*)BR,DP,EDP,DA1,DA2,FY,FUT,ES,AS1,AS2,AS3
       BR1=BR
       FLT=0.0
       GO TO 230
  228 WRITE(6,121)
  121 FORMAT('ENTER BR1,BR,DP,EDP,DA1,DA2,FLT,FY,FUT,ES,AS1,AS2,AS3')
       READ(5,*)BR1,BR,DP,EDP,DA1,DA2,FLT,FY,FUT,ES,AS1,AS2,AS3

C      Calculate the yield moment of the cross section for the
C      case when the top fibre of the beam lies in the
C      compression stress zone

  230. Z1=DA1/EDP
       Z2=DA2/EDP
       Z3=FLT/EDP
       Z4=DP/EDP
       EPY=FY/ES
       EPO=SQRT(FUT)/4703.224
       RE=EPY/EPO
       R4=0.17094*(FUT/FY)*EDP
       DP11=(EDP/2)*(((BR1-BR)*Z3**2)+(BR*Z4**2))
       DP1=DP11/(((BR1-BR)*Z3)+(BR*Z4))
       N=1
       GO TO 606
  707 HI=HI+UHP
       N=N+1
       GO TO 909
```

```
808 HI=HI+DHP
    N=N+1
    GO TO 909
606 HI=HW*(1+GA)
909 R5=HI/FY
    T11=RE*R4*BR
    T1=(-1)*T11*(3+RE)
    T211=(3*T11)-AS1-AS2-AS3
    T2=T211-(3*RE*R4*Z3*(2+RE)*(BR1-BR))-R5
    T311=(AS1*(1+Z1))+(AS2*(1+Z2))+(2*AS3)+(2*R5)
    T3=T311+(3*RE*R4*Z3*(BR1-BR)*(2+(Z3*(1+RE))))
    T41=(AS1*Z1)+(AS2*Z2)+AS3+R5
    T4=T41+(R4*RE*Z3**2*(BR1-BR)*(3+(Z3*RE)))
    T5=T1*(BR1/BR)
    T6=(3*T11*(BR1/BR))-AS1-AS2-AS3-R5
    T71=R4*BR1*(3+(1/RE))
    T7=T71+(R4*RE*(BR1-BR)*(3+RE))
    T81=((-3)*R4*BR1*(2+(1/RE)))-AS1-AS2-AS3-R5
    T8=T81-(3*R4*RE*(BR1-BR)*(1+(Z3*(2+RE))))
    T91=T311+(3*R4*BR1*(1+(1/RE)))+(2*R5)
    T9=T91+(3*R4*RE*Z3*(BR1-BR)*(2+(Z3*(1+RE))))
    T101=((R4/RE)*BR1)+T41
    T10=T101+(R4*RE*Z3**2*(BR1-BR)*(3+(Z3*RE)))
    TT1=(SQRT(T3**2+(4*T2*T4))-T3)/(2*T2)
    GO TO 123
122 TT1=TT13
123 TT11=(T1*TT1**3)+(T2*TT1**2)+(T3*TT1)-T4
    TT12=(3*T1*TT1**2)+(2*T2*TT1)+T3
    TT13=TT1-(TT11/TT12)
    IF(ABS((TT1-TT13)/TT13).GT.0.00001)GO TO 122
    EPC=(TT1/(1-TT1))*EPY
    EPC1=((TT1-Z3)/(1-TT1))*EPY
    EPCO=EPC/EPO
    EPCO1=EPC1/EPO
    EPCC=EPC1/EPC
    FC11=(-1)*BR*(3+RE)*TT1**3
    FC12=3*(BR-((BR1-BR)*Z3*(2+RE)))*TT1**2
    FC13=3*Z3*(BR1-BR)*(2+(Z3*(1+RE)))*TT1
    FC14=Z3**2*(BR1-BR)*(3+(Z3*RE))
    FC=R4*FY*(RE/(1-TT1)**2)*(FC11+FC12+FC13-FC14)
    TT21=(-1)*(BR1-BR)*EPCC**2
    TT22=TT21*(12-(4*EPCO)-(8*EPCC)+(3*EPCO1*EPCC))
    TT23=(BR1*(4-EPCO))+TT22
    TT24=(BR1*(3-EPCO))+(TT21*(3-EPCO1))
    TT2=(TT1/4)*(TT23/TT24)
    IF(TT1.GT.Z3.AND.EPC.LE.EPO)GO TO 1330
    IF(TT1.LE.Z3.AND.EPC.LE.EPO)GO TO 124
    IF(TT1.GT.Z3.AND.EPC.GT.EPO)GO TO 127
    IF(TT1.LE.Z3.AND.EPC.GT.EPO)GO TO 1300
124 TT1=(SQRT(T311**2+(4*T6*T41))-T311)/(2*T6)
    GO TO 126
125 TT1=TT13
126 TT11=(T5*TT1**3)+(T6*TT1**2)+(T311*TT1)-T41
    TT12=(3*T5*TT1**2)+(2*T6*TT1)+T311
    TT13=TT1-(TT11/TT12)
    IF(ABS((TT1-TT13)/TT13).GT.0.0001)GO TO 125
```

```
      EPC=(TT1/(1-TT1))*EPY
      EPC1=((TT1-Z3)/(1-TT1))*EPY
      EPCO=EPC/EPO
      FC11=RE*TT1**2*(3-((3+RE)*TT1))
      FC=R4*FY*(BR1/(1-TT1)**2)*FC11
      TT2=(TT1/4)*((4-EPCO)/(3-EPCO))
      GO TO 1330
  127 TT1=(SQRT(T9**2+(4*T8*T10))-T9)/(2*T8)
      GO TO 129
  128 TT1=TT13
  129 TT11=(T7*TT1**3)+(T8*TT1**2)+(T9*TT1)-T10
      TT12=(3*T7*TT1**2)+(2*T8*TT1)+T9
      TT13=TT1-(TT11/TT12)
      IF(ABS((TT1-TT13)/TT13).GT.0.0001)GO TO 128
      EPC=(TT1/(1-TT1))*EPY
      EPC1=((TT1-Z3)/(1-TT1))*EPY
      EPCO=EPC/EPO
      EPCO1=EPC1/EPO
      EPCC=EPC1/EPC
      FC11=(((BR1/RE)*(3+(1/RE)))+((BR1-BR)*(3+RE)))*TT1**3
      FC12=(((BR1/RE)*(2+(1/RE)))+((BR1-BR)*(1+(Z3*(2+RE)))))*TT1**2
      FC13=3*(((BR1/RE)*(1+(1/RE)))+((BR1-BR)*Z3*(2+(Z3*(1+RE)))))*TT1
      FC14=(BR1/RE**2)+(Z3**2*(BR1-BR)*(3+(Z3*RE)))
      FC=R4*FY*(RE/(1-TT1)**2)*(FC11-(3*FC12)+FC13-FC14)
      TT21=(BR1-BR)*EPCO1**2
      TT22=BR1*((6*EPCO)+(1/EPCO)-4)
      TT23=TT21*((EPCC*(8-(3*EPCO1)))+(4*EPCO1)-12)
      TT24=(BR1*((3-EPCO)-1))+(TT21*(3-EPCO1))
      TT2=(TT1/4)*((TT22+TT23)/TT24)
      GO TO 1330
 1300 TT1=(SQRT(T91**2+(4*T81*T101))-T91)/(2*T81)
      GO TO 1320
 1310 TT1=TT13
 1320 TT11=(T71*TT1**3)+(T81*TT1**2)+(T91*TT1)-T101
      TT12=(3*T71*TT1**2)+(2*T81*TT1)+T91
      TT13=TT1-(TT11/TT12)
      IF(ABS((TT1-TT13)/TT13).GT.0.0001)GO TO 1310
      EPC=(TT1/(1-TT1))*EPY
      EPCO=EPC/EPO
      FC11=((3+(1/RE))*TT1**3)-(3*(2+(1/RE))*TT1**2)
      FC12=(3*(1+(1/RE))*TT1)-(1/RE)
      FC=R4*FY*(BR1/(1-TT1)**2)*(FC11+FC12)
      TT2=(TT1/4)*(((6*EPCO)+(1/EPCO)-4)/((3*EPCO)-1))
 1330 FS1=((TT1-Z1)/(1-TT1))*FY*AS1
      FS2=((TT1-Z2)/(1-TT1))*FY*AS2
      YM11=((FC*EDP*(1-TT2))+(FS1*EDP*(1-Z1))+(FS2*EDP*(1-Z2)))*0.001
      YM1=YM11-(R5*FY*(EDP-DP1)*0.001)

C     Calculate the yield moment of the cross section for the
C     case when the top fibre of the beam lies in the tension
C     stress zone

      T110=R4*BR*RE*(3+RE)
      T121=AS1+AS2+AS3+R5
      T12=((-3)*R4*BR*RE*(Z1+(Z4*(2+RE))))-T121
      T131=3*R4*BR*RE*Z4*((2*Z1)+(Z4*(1+RE)))
```

```
      T13=T131+(2*Z1*AS1)+(AS2*(Z1+Z2))+(AS3*(1+Z1))+(2*Z1*R5)
      T14=(R4*BR*Z4**2*RE*((3*Z1)+(Z4*RE)))+(Z1*T41)+(R5*Z1*(Z1-1))
      T15=(-1)*R4*BR*(3+(1/RE))-R5
      T16=(R4*BR*((3*Z4)+(Z1*(3+(2/RE)))))-T121
      T17=(R4*BR*Z1*((3*Z4)+(Z1/RE)))-T41
      TT30=T16**2+(4*T15*T17)
      TT3=(SQRT(TT30)+T16)/((-2)*T15)
      GO TO 1360
 1350 TT3=TT33
 1360 TT31=(T110*TT3**3)+(T12*TT3**2)+(T13*TT3)-T14
      TT32=(3*T110*TT3**2)+(2*T12*TT3)+T13
      TT33=TT3-(TT31/TT32)
      IF(ABS((TT3-TT33)/TT33).GT.0.0001)GO TO 1350
      EPC=((Z4-TT3)/(TT3-Z1))*EPY
      EPCO=EPC/EPO
      FC21=((3+RE)*TT3**3)-(3*TT3**2*(Z1+(Z4*(2+RE))))
      FC22=(3*Z4*((2*Z1)+(Z4*(1+RE)))*TT3)-(Z4**2*((3*Z1)+(Z4*RE)))
      FC1=R4*FY*(BR/(TT3-Z1)**2)*RE*(FC21+FC22)
      TT41=(TT3*(4-EPCO))+(Z4*(8-(3*EPCO)))
      TT4=TT41/(12-(4*EPCO))
      IF(EPC.LE.EPO)GO TO 137
      TT30=T16**2+(4*T15*T17)
      TT3=(SQRT(TT30)+T16)/((-2)*T15)
      EPC=((Z4-TT3)/(TT3-Z1))*EPY
      EPOC=EPO/EPC
      FC1=R4*FY*BR*((3*Z4)+(Z1/RE)-(TT3*(3+(1/RE))))
      TT41=(TT3*(6-(EPOC*(4-EPOC))))+(Z4*(6-EPOC**2))
      TT4=TT41/(12-(4*EPOC))
  137 FS3=((1-TT3)/(TT3-Z1))*FY*AS3
      FS4=((TT3-Z2)/(TT3-Z1))*FY*AS2
      YM21=(FC1*EDP*(TT4-Z1))+(FS3*EDP*(1-Z1))-(FS4*EDP*(Z2-Z1))
      YM2=(YM21-(R5*FY*(DP1-DA1)))*0.001

C     Determine the ultimat moment of resistance of the cross
C     section when the top fibre of the beam lies in the
C     compressin stress zone

      T181=R4*FY*BR1*(285.714/ES)*(3-(EPO*285.714))
      T18=T181-(R4*(FY/(ES*EPO))*(BR1-BR)*(3-(0.0035/EPO)))
      T191=AS1+AS2-(285.714*EPY*(R5+AS3))
      T19=(3*R4*(FY/(EPO*ES))*Z3*(BR1-BR)*(2-(0.0035/EPO)))+T191
      T201=(AS1*Z1)+(AS2*Z2)
      T202=3*R4*FY*(Z3**2/(EPO*ES))*(BR1-BR)*(1-(0.0035/EPO))
      T20=((-1)*T201)-T202
      T21=R4*FY*(Z3**3/(ES*EPO**2))*(BR1-BR)*0.0035
      TT5=(SQRT(T19**2-(4*T18*T20))-T19)/(2*T18)
      GO TO 140
  139 TT5=TT53
  140 TT51=(T18*TT5**3)+(T19*TT5**2)+(T20*TT5)-T21
      TT52=(3*T18*TT5**2)+(2*T19*TT5)+T20
      TT53=TT5-(TT51/TT52)
      IF(ABS((TT5-TT53)/TT53).GT.0.0001)GO TO 139
      EPC1=((TT5-Z3)/TT5)*0.0035
      EPCO1=EPC1/EPO
      FC31=BR1*EPO*285.714*(3-(285.714*EPO))
      FC32=(FC31-((BR1-BR)*(3-(0.0035/EPO))))*TT5**3
```

```
      FC33=(3*Z3*(2-(0.0035/EPO))*TT5**2)-((Z3**3/EPO)*0.0035)
      FC34=(BR1-BR)*(FC33-(3*Z3**2*(1-(0.0035/EPO))*TT5))
      FC2=R4*(FY/TT5**2)*(0.0035/EPO)*(FC32+FC34)
      TT61=(BR1-BR)*EPCO1**2
      TT62=BR1*((0.021/EPO)+(285.714*EPO)-4)
      TT63=TT61*((EPC1*285.714*(8-(3*EPCO1)))+(4*EPCO1)-12)
      TT64=(BR1*((0.0105/EPO)-1))-(TT61*(3-EPCO1))
      TT6=(TT5/4)*((TT62+TT63)/TT64)
      IF(TT5.GT.Z3)GO TO 141
      TT5=(SQRT(T191**2+(4*T181*T201))-T191)/(2*T181)
      FC2=R4*FY*TT5*BR1*(3-(285.714*EPO))
      TT61=((0.021/EPO)+(285.714*EPO)-4)/((0.0105/EPO)-1)
      TT6=(TT5/4)*TT61
  141 FS5=((TT5-Z1)/TT5)*0.0035*ES*AS1
      FS6=((TT5-Z2)/TT5)*0.0035*ES*AS2
      UM11=((FC2*EDP*(1-TT6))+(FS5*EDP*(1-Z1))+(FS6*EDP*(1-Z2)))*0.001
      UM1=UM11-(R5*FY*(EDP-DP1)*0.001)

C     Determine the ultimate moment of resistance of the cross
C     section when the top fibre of the beam lies in the
C     tension stress zone

      T22=R4*FY*BR*(3-(285.714*EPO))
      T231=(-2)*R4*FY*Z4*BR*(3-(285.714*EPO))+(R5*FY)
      T23=T231+(0.0035*ES*((AS1*EPY*285.714)-AS2-AS3))
      T241=R4*FY*BR*Z4**2*(3-(EPO/0.0035))-(Z4*R5*FY)
      T24=T241-(0.0035*ES*((AS1*EPY*285.714*Z4)-(AS2*Z2)-AS3))
      TT7=(((-1)*T23)-SQRT(T23**2-(4*T22*T24)))/(2*T22)
      FS7=((TT7-Z2)/(Z4-TT7))*0.0035*ES
      IF(FS7.LE.FY)GO TO 143
      T23=(T231/FY)+(AS1+AS2-(AS3*(0.0035/EPY)))
      T24=(T241/FY)-(((AS1+AS2)*Z4)-(AS3*(0.0035/EPY)))
      T25=T22/FY
      TT7=(((-1)*T23)-SQRT(T23**2-(4*T25*T24)))/(2*T25)
      FS7=FY
  143 FC3=R4*FY*BR*(3-(285.714*EPO))*(Z4-TT7)
      FS8=((1-TT7)/(Z4-TT7))*0.0035*ES*AS3
      TT81=TT7*(6-(285.714*EPO*(4-(285.714*EPO))))
      TT82=Z4*(6-((EPO*285.714)**2))
      TT8=(TT81+TT82)/(12-(1142.857*EPO))
      UM21=(FC3*EDP*(TT8-Z1))+(FS8*EDP*(1-Z1))-(R5*FY*(DP1-DA1))
      UM2=(UM21-(FS7*AS2*EDP*(Z2-Z1)))*0.001
      IF(N.GT.1)GO TO 234
      IF(ISH.EQ.1)GO TO 231
      WRITE(6,232)YM1
  232 FORMAT('THE Y.MOMENT (TOP FIBRE IN C.S.ZONE)=',F15.5)
      WRITE(6,235)YM2
  235 FORMAT('THE Y.MOMENT (TOP FIBRE IN T.S.ZONE)=',F15.5)
      WRITE(6,238)UM1
  238 FORMAT('THE ULT.M.RESISTANCE (TOP FIBRE IN C.S.ZONE)=',F15.5)
      WRITE(6,241)UM2
  241 FORMAT('THE ULT.M.RESISTANCE (TOP FIBRE IN T.S.ZONE)=',F15.5)
      GO TO 242
  231 WRITE(6,1340)YM1
 1340 FORMAT('THE Y.MOMENT (FLANGE IN C.S.ZONE)=',F15.5)
      WRITE(6,138)YM2
```

```
  138 FORMAT('THE Y.MOMENT (FLANGE IN T.S.ZONE)=',F15.5)
      WRITE(6,142)UM1
  142 FORMAT('THE ULT.M.RESISTANCE (FLANGE IN C.S.ZONE)=',F15.5)
      WRITE(6,144)UM2
  144 FORMAT('THE ULT.M.RESISTANCE (FLANGE IN T.S.ZONE)=',F15.5)
  242 WRITE(6,243)
  243 FORMAT('**********************************************')

C     Calculate the first yield load and the first plastic
C     hinge load

  234 YV1=ABS((YM1*V)/XM)
      UV1=ABS((UM1*V)/XM)
      UMI=(ABS(UM1/XM))*XMI

C     Evaluate the changes in the prestressing forse which
C     are generated as a result of the first yield load
C     and the first plastic hinge load

      YHP=(ABS(YM1/XM))*HP1
      UHP=(ABS(UM1/XM))*HP1
      IF(N.LT.2)GO TO 707
      IF(N.EQ.3)GO TO 999
      WRITE(6,221)YHP
  221 FORMAT('THE CHANGE IN THE CABLE TEN. AT FIRST Y.LOAD=',F15.5)
      WRITE(6,215)UHP
  215 FORMAT('THE CHANGE IN THE CABLE TEN. AT FIRST P.H.LOAD=',F15.5)
  999 H1=(HW*(1+GA))+UHP
      A11=S**2*((2*A)-A**2+B**2-((1/XR)*(XR**2+B**2)))
      A12=(W*S**2*(XR-G**2))+(2*HW*((C*G*S)-Z))
      A1=((1-XR)/(XR*HW))*(A11/A12)
      GO TO 223
  222 A2=(2*(UM2-UMI))/A11
      GO TO 224
  223 A2=(2*(YM2-UMI))/A11

C     Determine the changes in the prestressing force and the
C     loads exceeding the first plastic hinge load in order
C     to yield the tensile reinforcement at the intermediate
C     support and subsequently cause the second plastic and the
C     complete failure of the suspended beam

  224 DHP=0
      GO TO 201
  200 DHP=DHP1
  201 DV=(A1*DHP)+A2
      UR=DHP/HW
      H2=H1+DHP
      UD=SQRT(H2/ZE)
      UDS=UD*S
      UDS1=UD*S1
      UDG=UDS*G
      UDG1=UDS1*G1
      UDSG=UDS-UDG
      UDSG1=UDS1-UDG1
      UDX=UDS*(XR/2)
```

```
      UDSX=(UDS/2)-UDX
      UDR=UDS*(1+R-(XR/2))
      ZZ11=COS(UDR)-(COS(UDX)*(R2+((1-R2)*COS(UDS1))))
      ZZ12=(ZZ11/(SIN(UDS1)*COS(UDX)))+((UDS/2)*(1+(R*R2)))
      ZZ13=ZZ12*(A11/S**2)
      ZZ14=(2*SIN(UDS/2)*SIN(UDSX))/(UDS1*COS(UDX))
      ZZ15=ZZ14*(((1+R)*((2*A)-XR-(B**2/XR)))-(R*(A**2-B**2)))
      ZZ16=(-1)*(UDS/6)*((3*A**2)-(2*A**3)-(3*B**2)+(2*B**3))
      ZZ17=(SIN((UDS*A)-UDX)-SIN((UDS*B)-UDX))/(UDS*COS(UDX))
      ZZ18=(2/UDS)*(ZZ17-A+B)
      ZZ1=((DV*S**2)/(2*UD*H2))*(ZZ13+ZZ15+ZZ16+ZZ18)
      ZZ21=(1-XR)*((XR-G**2)/SIN(UDS1))*(COS(UDS1)-(COS(UDR)/COS(UDX)))
            ZZ22=SIN(UDX-UDG)+SIN(UDS-UDX)
            ZZ23=2*R2**2*COS(UDG1/2)*SIN(UDSG1/2)*(COS(UDX)/COS(UDS1))
            ZZ24=(COS(UDG1)-COS(UDS1))*(SIN(UDS/2)/SIN(UDS1))*SIN(UDSX)
            ZZ25=(-2)*(XR/(UDS**2*COS(UDX)))*(ZZ22+ZZ23+((-2)*R2*ZZ24))
            ZZ26=((-2)*SIN(UDS/2)*SIN(UDSX))/(UDS1*COS(UDX))
            ZZ27=((XR-G**2)*(1+R-XR))+(R*XR*(1-XR))+(R**2*R2*XR*(1-G1**2))
            ZZ28=ZZ26*ZZ27
            ZZ29=((12*XR)/UDS**2)*(1-G+(R2**2*R*(1-G1)))
            ZZ30=2+(3*R*R2)+(G**2*(6+(3*R*R2)-(2*G)))
            ZZ31=ZZ30-(R**3*R2**2*(1-(3*G1**2)+(2*G1**3)))
            ZZ32=(3*(1+(R*R2))*(XR**2+G**2))-(XR*ZZ31)
            ZZ33=(UDS/6)*(ZZ29+ZZ32)
            ZZ34=R2*(1-XR)*(XR-G**2)*TAN(UDS1/2)
            ZZ2=((UR*W*S**2)/(2*XR*UD*H2))*(ZZ21+ZZ25+ZZ28+ZZ33+ZZ34)
            ZZ35=(R2*(1-((UDS1/2)*SIN(UDS1))))-(COS(UDR)/COS(UDX))
            ZZ36=(UDG/SIN(UDS1))*((1-XR)/(2*XR))*(ZZ35+((1-R2)*COS(UDS1)))
            ZZ37=SIN(UDG/2)*SIN(UDX-(UDG/2))
            ZZ38=(G/(R*XR))*(1+R-XR)*SIN(UDS/2)*SIN(UDSX)
            ZZ39=UDS**2*(G/(4*XR))*COS(UDX)*(1-(XR*(2-G)))
            ZZ40=C*(ZZ36-((1/COS(UDX))*(ZZ37+ZZ38+ZZ39)))
            ZZ41=SIN(UDS/2)*SIN(UDSX)*(SIN(UDG1)-(G1*SIN(UDS1)))
            ZZ42=(ZZ41/(SIN(UDS1)*COS(UDX)))+(R2*UDS1**2*(G1/4)*(1-G1))
            ZZ43=(-1)*R2*SIN(UDG1/2)*(SIN(UDSG1/2)/COS(UDS1/2))
            ZZ44=C1*(ZZ42+ZZ43)
            ZZ3=((2*DHP)/(UD**2*H2))*(ZZ40+ZZ44)
            IF(ITYP.EQ.1)GO TO 202
            IF(ITYP.EQ.2)GO TO 203
        202 ZZ45=(2*SIN((UDS/2)+UDS1)*(SIN(UDSX)/SIN(UDS1)))+SIN(UDX)
            ZZ46=(-2)*XR*(SIN(UDS/2)/COS(UDS1/2))*COS((UDS/2)*(1+R-XR))
            ZZ47=(-2)*((1+R)/UDS1)*SIN(UDS/2)*SIN(UDSX)
            ZZ48=(1-(2*XR))*((R2*TAN(UDS1/2))-((UDS/2)*(1+(R*R2))))*COS(UDX)
            ZZ4=((DHP*EC)/(UD*XR*H2))*((ZZ45+ZZ46+ZZ47+ZZ48)/COS(UDX))
            GO TO 204
        203 ZZ45=2*((1+R)/(UDS1*XR))*SIN(UDS/2)*SIN(UDSX)
            ZZ46=SIN(UDX-UDG)+(R2*SIN((UDS1/2)-UDG1)*(COS(UDX)/COS(UDS1/2)))
            ZZ47=(-2)*SIN(UDS/2)*COS(UDG1)*(SIN(UDSX)/SIN(UDS1))
            ZZ48=(2*SIN((UDS/2)+UDS1)*SIN(UDSX))+(SIN(UDS1)*SIN(UDX))
            ZZ49=ZZ48+(R2*COS(UDX)*(1-COS(UDS1)))
            ZZ50=((XR-1)/(XR*SIN(UDS1)))*ZZ49
            ZZ51=1-(2*XR*(1-G))+(R*R2*(1-(2*XR*(1-G1))))
            ZZ52=(UDS*COS(UDX)*ZZ51)/(2*XR)
            ZZ4=((DHP*Z)/(UD*H2*COS(UDX)))*(ZZ45+ZZ46+ZZ47+ZZ50+ZZ52)
        204 ZZ5=ZZ1+ZZ2+ZZ3+ZZ4
```

```
      DHP1=(W/(E*HW))*ZZ5
      IF(ABS((DHP1-DHP)/DHP1).GT.0.0001)GO TO 200
      IF(A2.GT.((2*(YM2-UMI))/A11))GO TO 225

C     Calculate the total values of the second yield and the
C     failure loads

      YDV=DV
      YDHP=DHP1
      GO TO 222

C     Determine the total values of the changes in the
C     prestressing force corresponding to the second
C     yield and failure loads

  225 IF(N.LT.3)GO TO 808
      HPTY=UHP+YDHP
      HPTU=UHP+DHP1
      YV2=UV1+YDV
      UV2=UV1+DV
      WRITE(6,205)HPTY
  205 FORMAT('THE TOTAL CHANGE IN CABLE TEN. AT SECOND Y.LOAD=',F15.5)
      WRITE(6,207)HPTU
  207 FORMAT('THE TOTAL CHANGE IN CABLE TEN. AT FAILURE=',F15.5)
      WRITE(6,244)
  244 FORMAT('************************************************')

C     For concentrated loads,transform the obtained results
C     of the partially distributed second yield and failure
C     loads back to the point load form

      IF(LTYP.EQ.1)GO TO 216
      WRITE(6,145)YV1
  145 FORMAT('THE FIRST Y.LOAD=',F15.5)
      WRITE(6,146)UV1
  146 FORMAT('THE FIRST P.H.LOAD=',F15.5)
      WRITE(6,206)YV2
  206 FORMAT('THE SECOND Y.LOAD=',F15.5)
      WRITE(6,208)UV2
  208 FORMAT('THE FAILURE LOAD=',F15.5)
      GO TO 245
  216 YWW1=2*YV1*S*EPSL
      UWW1=2*UV1*S*EPSL
      YWW2=2*YV2*S*EPSL
      UWW2=2*UV2*S*EPSL
      WRITE(6,217)YWW1
  217 FORMAT('THE FIRST Y.LOAD=',F15.5)
      WRITE(6,218)UWW1
  218 FORMAT('THE FIRST PLASTIC HINGE LOAD=',F15.5)
      WRITE(6,219)YWW2
  219 FORMAT('THE SECOND Y.LOAD=',F15.5)
      WRITE(6,220)UWW2
  220 FORMAT('THE FAILURE LOAD=',F15.5)
  245 WRITE(6,246)
  246 FORMAT('************************************************')
  213 STOP
      END
```